LEABHARLANN CHOLÁISTE NA TRÍONÓIDE, BAILE ÁTHA CLIATH | TRINITY COLLEGE LIBRARY DUBLIN
Ollscoil Átha Cliath | The University of Dublin

Terms and Conditions of Use of Digitised Theses from Trinity College Library Dublin

Copyright statement

All material supplied by Trinity College Library is protected by copyright (under the Copyright and Related Rights Act, 2000 as amended) and other relevant Intellectual Property Rights. By accessing and using a Digitised Thesis from Trinity College Library you acknowledge that all Intellectual Property Rights in any Works supplied are the sole and exclusive property of the copyright and/or other IPR holder. Specific copyright holders may not be explicitly identified. Use of materials from other sources within a thesis should not be construed as a claim over them.

A non-exclusive, non-transferable licence is hereby granted to those using or reproducing, in whole or in part, the material for valid purposes, providing the copyright owners are acknowledged using the normal conventions. Where specific permission to use material is required, this is identified and such permission must be sought from the copyright holder or agency cited.

Liability statement

By using a Digitised Thesis, I accept that Trinity College Dublin bears no legal responsibility for the accuracy, legality or comprehensiveness of materials contained within the thesis, and that Trinity College Dublin accepts no liability for indirect, consequential, or incidental, damages or losses arising from use of the thesis for whatever reason. Information located in a thesis may be subject to specific use constraints, details of which may not be explicitly described. It is the responsibility of potential and actual users to be aware of such constraints and to abide by them. By making use of material from a digitised thesis, you accept these copyright and disclaimer provisions. Where it is brought to the attention of Trinity College Library that there may be a breach of copyright or other restraint, it is the policy to withdraw or take down access to a thesis while the issue is being resolved.

Access Agreement

By using a Digitised Thesis from Trinity College Library you are bound by the following Terms & Conditions. Please read them carefully.

I have read and I understand the following statement: All material supplied via a Digitised Thesis from Trinity College Library is protected by copyright and other intellectual property rights, and duplication or sale of all or part of any of a thesis is not permitted, except that material may be duplicated by you for your research use or for educational purposes in electronic or print form providing the copyright owners are acknowledged using the normal conventions. You must obtain permission for any other use. Electronic or print copies may not be offered, whether for sale or otherwise to anyone. This copy has been supplied on the understanding that it is copyright material and that no quotation from the thesis may be published without proper acknowledgement.

THE INFLUENCE OF DRUG PHYSICOCHEMICAL PROPERTIES ON RELEASE FROM THERMORESPONSIVE "SMART" HYDROGELS

by

David C. Coughlan, B.Sc. (Pharm.), M.P.S.I.

being a thesis submitted for the degree of

Doctor of Philosophy
in Pharmaceutics

at

University of Dublin
Trinity College

under the direction and supervision of

Professor O.I. Corrigan, B.Sc. (Pharm.), M.A., Ph.D., F.T.C.D., F.P.S.I.

November 2004

TRINITY COLLEGE
0 5 MAY 2005
LIBRARY DUBLIN
THOSIS
7578

DECLARATION

This thesis is submitted by the undersigned to the University of Dublin for examination for the degree of Doctor of Philosophy. It has not been submitted as an exercise for a degree at any other university. I carried out all the practical work except where duly acknowledged. I wrote this manuscript with the aid of editorial advice from Professor O.I. Corrigan. I agree that the library may lend or copy this thesis upon request.

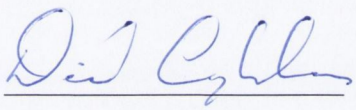

David C. Coughlan

To my parents

SUMMARY

Thermoresponsive hydrogels are a class of "smart" or "environmentally sensitive" systems with potential for controlling the release of a drug in response to a specific stimulus. Previous research in the area of thermoresponsive drug delivery did not examine the effect of the chosen drug on the release pattern obtained. The potential use of thermoresponsive poly(N-isopropylacrylamide) hydrogels was evaluated in the present thesis by using a range of model drugs with different physicochemical properties. The characteristics of the drugs used and their effects on the "smart" behaviour of thermoresponsive hydrogels were investigated.

Drug release profiles were examined above and below the phase transition temperature of the hydrogels. The drug release mechanism during the hydrogel swelling period was approximately diffusion controlled, with some contribution from the swelling process. The swelling process had a greater effect on the release mechanism of the smaller model drugs. It was shown that it was possible to alter the mechanism (from Fickian to non-Fickian) and release rate of a drug by changing the drug loading or the crosslinking content of the hydrogel, where the swelling characteristics and therefore pore size of the hydrogel was affected.

An increase in temperature resulted in a decrease in both the rate and extent of hydrogel swelling, with an effective reversal of thermal control of drug release. The extent of thermal control depended on the physicochemical properties of the model drug used. The loaded drug was shown to influence the rate of swelling of the hydrogel, depending on drug solubility, binding ability or the osmotic effect exerted. The resulting release rates of the drugs were dependent on the swelling state of the hydrogel and the relationship between pore size and drug molecular size in solution. The system examined was particularly useful at preventing the release of model drugs of molecular diameter >10Å.

The rate of swelling also affected the extent of deswelling/contraction on switching the external temperature during pulsatile release studies. The ability to predict the pulse of drug release caused by hydrogel contraction was shown by knowledge of the hydrogel

swelling and deswelling rates, drug solubility and the existence of a drug molecular size gradient within the loaded gel.

The chemical nature of the chosen drug was important in thermoresponsive drug delivery systems. Binding was shown between the benzoates and the linear polymer by DSC, transmittance measurements, FTIR and phase solubility techniques. Direct binding isotherms were also established with the crosslinked system, where the benzoates significantly affected the swelling of the hydrogel. The binding was hydrophobic in nature between the polymer isopropyl group and the benzene ring/ester side chain of the benzoate and the effect was clarified in terms of the influence of the binding on the position of the phase transition temperature of the polymer/hydrogel. Molecular modelling, in conjunction with the techniques mentioned above, confirmed the importance of the alkyl side chain of the esters in the binding process and suggested two different benzoate-polymer binding orientations depending on the functional groups present on the drug molecule.

The benzoate-polymer binding was sufficient to control the rate of swelling of all the hydrogels examined and a new type of swelling front was discussed. The effect of binding was to slow the release rate directly as well as slowing the rate indirectly by controlling the effective pore size and volume of media available for diffusion. Drug binding, as well as the effect of swelling, was shown to cause deviations from a Fickian diffusional release mechanism. The hydrophobic binding process discussed significantly affected the thermoresponsive nature of the hydrogels with consequences for hydrogel swelling and the rate of drug release.

The current thesis therefore highlighted the role played by the drug in controlling the release characteristics from thermoresponsive "smart" hydrogels. Drug physicochemical properties such as solubility, size and chemical nature were of particular importance.

TABLE OF CONTENTS

Acknowledgements i

Presentations and publications associated with this thesis ii

Abbreviations and symbols iii

Origin and scope of the thesis vi

INTRODUCTION

Chapter 1 ~ Thermoresponsive 'Smart' Drug Delivery Systems

1.1 Introduction 1

1.2 Smart polymers 2

1.2.1 pH 2

1.2.2 Temperature 3

1.2.2.1 Types of thermoresponsive polymers 3

1.2.2.2 Mechanism of thermo responsiveness 5

1.2.3 Light 6

1.2.4 Electric 7

1.2.5 Biomolecule sensitive hydrogels 7

1.2.6 Others 8

1.2.7 Use of smart polymers 9

1.3 Poly (N-isopropylacrylamide) 9

1.3.1 Synthesis 9

1.3.2 Altering the LCST 11

1.3.3 Positive and negative thermosensitivity 12

1.3.4 Drug delivery systems 13

1.3.4.1 Linear poly(N-isopropylacrylamide) 13

1.3.4.2 Poly(N-isopropylacrylamide) membranes 13

1.3.4.3 Incorporation of PNIPA in coating 14

1.3.4.4 Surface grafting of thermoresponsive polymers 14

1.3.4.5 Interpenetrating networks 14

1.3.5 Effect of additives on transition temperature 15

1.3.5.1 Inorganic salt 15

1.3.5.2 Surfactants 16

1.4 Other thermoresponsive polymers 16

1.4.1 Poly(vinylmethylether) 16
1.4.2 Miscellaneous 16
1.4.3 Positive temperature dependent gels 17
1.5 Potential uses of thermoresponsive drug delivery systems 17
1.5.1 Constant temperature 18
1.5.2 Changing temperature 18
1.5.2.1 Pulsed release modulated by external temperature 19
1.5.2.2 Pulsed release auto regulated by change in body temperature 20

Chapter 2 ~ Hydrogel Swelling/Deswelling Kinetics and Drug Release Mechanisms

2.1 Introduction 21
2.2 Drug dissolution and diffusion 21
2.3 Drug release from swellable devices 26
2.3.1 Diffusion and hydrogel swelling 26
2.3.2 Drug release from hydrogels 29
2.3.2.1 Mechanism of release 31
2.3.2.2 Effect of drug molecular size 32
2.3.2.3 Effect of drug loading 32
2.4 Swelling and drug release from PNIPA hydrogels 33
2.4.1 Hydrogel loading 33
2.4.2 Swelling/deswelling kinetics and drug release from thermoresponsive hydrogels 35
2.4.2.1 PNIPA hydrogels containing hydrophobic comonomers 35
2.4.2.2 Homogeneous PNIPA hydrogels 37
2.4.2.3 PNIPA hydrogels containing hydrophilic comonomers 38
2.4.3 Positive thermosensitive release 38
2.4.3.1 Diffusion area regulated mechanism 39
2.4.3.2 Matrix pumping 39
2.4.3.3 Positive thermosensitive hydrogels 39

EXPERIMENTAL

Chapter 3 ~ Materials and Methods

3.1 Materials 40

3.2 Methods of synthesis 42

3.2.1 Hydrogel 42

3.2.2 Linear polymer 42

3.3 Methods of characterisation 42

3.3.1 Gel permeation chromatography 42

3.3.2 Glass transition temperature (Tg) 43

3.3.3 Phase transition temperature (LCST) 43

3.3.3.1 DSC ($LCST_d$) 43

3.3.3.2 Transmittance measurements ($LCST_t$) 43

3.3.4 Drug solubility studies 44

3.3.5 X-Ray Diffraction 44

3.3.6 Swelling studies 44

3.3.7 Pore size distribution determination 45

3.3.7.1 Scanning electron microscopy 45

3.3.7.2 Nitrogen desorption isotherms 46

3.3.7.3 Solute exclusion technique 46

3.3.8 Preparation of polymer/drug co-precipitate blends 47

3.3.9 Fourier transform infrared spectroscopy (FTIR) 47

3.3.10 Binding studies 48

3.3.10.1 Binding isotherm 48

3.3.10.2 Phase solubility study 48

3.3.11 Density determination 48

3.3.12 Melting point determination 48

3.3.13 Calculation of solubility parameter 49

3.4 Drug loading and release 50

3.4.1 Drug loading 50

3.4.2 Model drug assays 50

3.4.3 Drug release studies 50

3.4.4 Dissolution studies on pure drug discs 51

3.5 Mathematical modelling 51

3.6 Molecular modelling 52

3.6.1 Molecular size simulation 52

3.6.2 Construction of simulations and equilibration procedures 52
3.6.3 Production runs and analysis 53
3.7 Statistical significance testing 53

RESULTS AND DISCUSSION

Chapter 4 ~ Polymer, Hydrogel and Model Drug Characterisation

4.1 Introduction 54
4.2 Linear polymer characterisation 54
4.2.1 Molecular weight 54
4.2.2 Lower Critical Solution Temperature 55
4.2.2.1 DSC 55
4.2.2.2 Transmittance 57
4.2.3 Fourier transform infrared spectroscopy 58
4.3 Model drug characterisation 59
4.3.1 Physicochemical properties 59
4.3.2 Fourier transform infrared spectroscopy 67
4.4 Hydrogel characterisation 70
4.4.1 Equilibrium swelling studies 71
4.4.2 Phase transition temperature 75
4.4.3 Swelling kinetics 77
4.4.4 Swelling/deswelling kinetics 80
4.4.5 Pore Size Distribution 83
4.4.5.1 Scanning Electron Microscopy 84
4.4.5.2 Nitrogen desorption 88
4.4.5.3 Solute exclusion technique 90

Chapter 5 ~ Effect of Drug Physicochemical Properties on Swelling/Deswelling Kinetics and Pulsatile Drug Release from PNIPA-H1

5.1 Introduction 94
5.2 Influence of model drugs on swelling/deswelling 95
5.2.1 Hydrophobic drugs 97
5.2.2 Hydrophilic drugs 98

5.3 Pulsatile drug release 100
5.3.1 Hydrophobic drugs 100
5.3.2 Hydrophilic drugs 105
5.4 Conclusions 110

Chapter 6 ~ A Study of Poly(N-isopropylacrylamide)-Drug Interactions

6.1 Introduction 111
6.2 Benzoates 112
6.2.1 Hydrogel 112
6.2.1.1 Equilibrium Swelling 112
6.2.1.2 Binding Isotherm 115
6.2.2 Linear polymer 117
6.2.2.1 X-Ray analysis 117
6.2.2.2 Glass transition temperature 119
6.2.2.3 FTIR spectroscopy 120
6.2.2.4 Phase transition temperature 122
6.2.2.5 Phase solubility study 126
6.3 Diltiazem 130
6.3.1 Hydrogel 130
6.3.2 Linear polymer 131
6.3.2.1 X-Ray analysis 131
6.3.2.2 Glass transition temperature 132
6.3.2.3 FTIR spectroscopy 133
6.3.2.4 Phase transition temperature 134
6.4 Vitamin B12 (Cyanocobalamin) 136
6.4.1 Hydrogel 136
6.4.2 Linear polymer 136
6.4.2.1 X-Ray analysis 137
6.4.2.2 Glass transition temperature 137
6.4.2.3 FTIR spectroscopy 138
6.4.2.4 Phase transition temperature 138
6.5 Dextrans 139
6.5.1 Hydrogel 139
6.5.2 Linear polymer 140
6.5.2.1 X-Ray analysis 140
6.5.2.2 Glass transition temperature 141

6.5.2.3 FTIR spectroscopy 141
6.5.2.4 Phase transition temperature 142
6.6 Conclusions 145

Chapter 7 ~ An Evaluation of the Role of Temperature in Controlled Release from PNIPA-H1

7.1 Introduction 147
7.2 Effect of temperature on drug dissolution 147
7.2.1 Hydrophobic drugs 147
7.2.2 Hydrophilic drugs 149
7.3 Influence of drug physicochemical properties on hydrogel swelling rate 149
7.3.1 Hydrophobic drugs 151
7.3.2 Hydrophilic drugs 154
7.4 Model drug release 154
7.4.1 Hydrophobic drugs 154
7.4.2 Hydrophilic drugs 160
7.5 Influence of drug loading on swelling/release 165
7.5.1 Benzoic Acid 165
7.5.2 Sodium Benzoate 169
7.6 Conclusions 173

Chapter 8 ~ An Investigation into the Effect of Crosslinking Content on Release from PNIPA Hydrogels

8.1 Introduction 174
8.2 Swelling 174
8.3 Drug Release 180
8.4 Conclusions 187

Chapter 9 ~ Molecular Modelling of Poly(N-isopropylacrylamide) and Drug-Polymer Interactions

9.1 Introduction 189
9.2 PNIPA-water systems 190

9.2.1 Simulation of transition temperatures 190
9.2.2 Diffusivity 192
9.2.3 Bonding interactions 194
9.3 Polymer-benzoate-water systems 199
9.3.1 Simulation of transition temperatures 199
9.3.2 Diffusivity 202
9.3.3 Bonding interactions 204
9.4 Conclusions 211

Chapter 10 ~ General Discussion

10.1 Introduction 212
10.2 Swelling and release studies 212
10.2.1 Hydrogel swelling and diffusional drug release 212
10.2.2 Hydrogel contraction and drug pulse 215
10.2.3 Effect of drug-polymer binding 216
10.3 Molecular modelling 222
10.4 Conclusions 223
10.5 Future Work 225

References 226

Appendices

Appendix I Calibration Curves 250
Appendix II Glass Transition Temperature (Tg) of Drug-Polymer Co-Precipitate Blends 251
Appendix III FTIR Spectra of Drug-Polymer Co-Precipitate Blends 257
Appendix IV Phase Transition Temperature (LCST) Measurements 263
Appendix V Molecular Modelling Software Input Files from Accelrys' Materials Studio® Version 2.1.5 273
Appendix VI Binding Isotherm 277
Appendix VII Dissolution of Pure Drug Discs 278

ACKNOWLEDGEMENTS

I would like to sincerely thank Professor Owen Corrigan for his patience, support and advice during the course of my research and in the preparation of this thesis.

I am grateful to Trinity College for providing me with a postgraduate award and travel funding as well as to Enterprise Ireland for their financial support. I would also like to thank Fujitsu Siemens Computers for their sponsorship of the Ussher Scholarship.

I would like to acknowledge Dr. John Walsh for the use of his spectrofluorimeter and the other academic staff within the School for use of equipment and for answering any queries. I would like to thank the executive and technical staff of the School of Pharmacy, in particular Pat Quinlan and Brian Canning for their many moments of assistance.

To Neal Leddy for his hard work and assistance on SEM and nitrogen physisorption. Also to Jenny Melia from Materials Ireland Polymer Research Centre for her help and advice.

To ex-final year students, Fran Quilty and Denise O'Brien, for their hard work and contribution to this thesis.

A big thank you to my fellow postgrads over the past three years in the School in particular Adam, Rob, Anthony, Fiona B, Fiona Ní, Cora, Lene, Gill, Ojas, Karl, Deirdre C, Deirdre D, Lidia, Emma, Mark, Katie, Almaith, Alecia, Helena and all the others. In particular, special mention goes to Rob and Lidia for their technical help and advice and to Alecia, Emma, Cora, Fiona Ní and Katie for their endless proof reading.

A special thanks to Cora for all her loving support and advice!

Finally, I would like to thank all my family for their encouragement and support…no doubt happy that my student days are over!

PRESENTATIONS/PUBLICATIONS ASSOCIATED WITH THIS THESIS

Poster presentations:

Effect of drug physicochemical properties on thermally controlled release from poly(N-isopropylacrylamide) based hydrogels. D.C. Coughlan, F.P. Quilty, J.M. Melia and O.I. Corrigan, *30th International Controlled Release Society*, Glasgow, Scotland, July 2003.

Relationship between drug molecular size and the magnitude of the drug pulse resulting from temperature induced contraction of a thermosensitive hydrogel, D.C. Coughlan, F.P. Quilty and O.I. Corrigan, *International Meeting on Pharmaceutics, Biopharmaceutics and Pharmaceutical Technology*, Nuremberg, Germany, March 2004.

Oral Presentations:

Thermoresponsive "smart" polymers for drug delivery, D.C. Coughlan, F.P. Quilty and O.I. Corrigan, *25th Annual Joint Research Seminar*, Trinity College Dublin, March 2003.

Thermoresponsive poly(N-isopropylacrylamide) 'smart' polymers for pulsed drug delivery, D.C. Coughlan and O.I. Corrigan, *Socrates Intensive Programme: "Innovative therapeutics: from molecules to drugs"*. Kings College London, June 2003.

Publication:

Effect of drug physicochemical properties on swelling/deswelling kinetics and pulsatile drug release from thermoresponsive poly(N-isopropylacrylamide) hydrogels. D.C. Coughlan, F.P. Quilty and O.I. Corrigan. *J. Cont. Rel.* 98, 1 (2004) 97-114.

ABBREVIATIONS AND SYMBOLS

ρ	Density
δ	Solubility parameter
μm	Micrometer
±	Plus or minus
™	Trademark
~	Approximately
°	Degree
°C	Degree Centigrade
Å	Angstrom
AA	Acrylic acid
AAm	Acrylamide
APS	Ammonium Persulfate
APy	N-acryloylpyrrolidine
AUC	Area under the curve
BA	Benzoic Acid
BMA	Butyl methacrylate
CD	Coefficient of determination
cm	Centimetre
cm^{-1}	Frequency
D	Diffusion coefficient
D4	Dextran MW~4,000
D10	Dextran MW~10,000
D40	Dextran MW~40,000
D70	Dextran MW~70,000
DB	Diltiazem Base
DHCl	Diltiazem HCl
DMA	N,N'-dimethylacrylamide
DSC	Differential scanning calorimetry
F	Fractional drug release
FITC	Fluorescein isothiocyanate
FTIR	Fourier transform infrared spectroscopy
g	Gram
g/l	Grams per litre
GPC	Gel permeation chromatography
h	Hour

H_2O	Water
HCl	Hydrochloric acid
IPN	Interpenetrating network
J	Joule
K	Degree Kelvin
k_c	Cube root dissolution rate constant
k_d	Diffusional release rate constant
k_{MC}	Maximum contraction rate
k_s	Swelling rate constant
k_{ss}	Quasi-steady state release rate constant
l	Litre
LCST	Lower critical solution temperature
$LCST_d$	LCST as determined by DSC measurements
$LCST_t$	LCST as determined by transmittance measurements
$LCST_s$	LCST as determined by swelling measurements
M	Moles per litre
MBA	N, N' methylenebisacrylamide
mg	Milligram
MHB	Methyl 4-hydroxybenzoate
min	Minute
ml	Millilitre
mm	Millimetre
mM	Millimolar
mmol	Millimole
mol	Mole
m.p.	Melting point
MW	Molecular weight
n	Diffusional exponent
n	Number of replicates
NaB	Sodium Benzoate
NaCl	Sodium chloride
NIPA	N-isopropylacrylamide
nm	Nanometre
PB	Phosphate Buffer pH 6.8, Sorensons (isotonic)
ps	Picosecond
PEO	Poly(ethylene oxide)
pH	Minus log of hydrogen ion concentration

pHEMA	Poly(2-hydroxyethyl methacrylate)
PHB	Propyl 4-hydroxybenzoate
pKa	Dissociation exponent for a weak acid
PNIPA	Poly(N-isopropylacrylamide)
PNIPA-H	PNIPA hydrogel
PNIPA-H1	PNIPA hydrogel containing 1.15mol % MBA
PNIPA-H2	PNIPA hydrogel containing 2.22mol % MBA
PNIPA-H3	PNIPA hydrogel containing 5.68mol % MBA
PNIPA-H4	PNIPA hydrogel containing 11.17mol % MBA
PNIPA-L	Linear Poly(N-isopropylacrylamide)
PPO	Poly(propylene oxide)
PVA	Poly(vinyl alcohol)
PVME	Poly(vinyl methylether)
R^2	correlation coefficient
RMA	Alkyl methacrylate
r.p.m.	Revolutions per minute
s	Second
s.d.	Standard deviation
S	Fraction swelling
S.R.	Swelling ratio
SEM	Scanning Electron Microscopy
t	Time
T	Temperature
TEMED	N,N,N',N' Tetramethylenediamine
Tg	Glass transition temperature
UCST	Upper critical solution temperature
UV	Ultra violet
VB	Vitamin B12
vs.	Versus
v/v	Volume per volume
w/v	Weight per volume
w/w	Weight per weight
XRD	X-ray diffraction

ORIGIN AND SCOPE

Poly(N-isopropylacrylamide) (PNIPA) based hydrogels possess a lower critical solution temperature (LCST) which allows them to swell below this temperature and shrink/deswell above this temperature. The sharp phase transition of PNIPA near to body temperature has made this polymer the focus of research as a thermoresponsive "smart" drug delivery system.

Much of the research to date on thermoresponsive hydrogels for drug delivery has focused on control of the physical properties of the hydrogel such as the phase transition temperature (Yoshida *et al.,* 1994b), the rate of swelling/deswelling (Wu *et al.*, 1992; Yoshida *et al.*, 1995), the biodegradability of the system (Kim *et al.*, 2000; Lowe *et al.*, 2003) or the development of systems where the on-phase is at the higher temperature (Yoshida *et al.,* 1994a; Zhang *et al.*, 2002; Gutowska *et al.*, 1997; Shin *et al.*, 2001). A single model drug was often chosen in these cases to examine the suitability of the prepared system.

The majority of studies examining drug release from thermoresponsive systems have been carried out by Okano and co-workers on heterogeneous PNIPA hydrogels containing butyl methacrylate (BMA) as a hydrophobic comonomer and using the model drug indomethacin (Bae *et al.,* 1987, 1991b; Okano *et al.,* 1990; Yoshida *et al.*, 1991a, 1991b, 1992, 1994a). *'On-off'* release profiles of indomethacin have been described in response to a stepwise temperature change (Bae *et al.,* 1987; Okano *et al.,* 1990; Yoshida *et al.,* 1991b). Pulsatile release was explained by the formation of a dense, less permeable surface layer of gel, described as a "skin-type barrier" which was attributed to the presence of the BMA (Yoshida *et al.*, 1991b). Some other authors have subsequently also used indomethacin as a model drug for pulsatile release studies (Gutowska et al., 1997; Shin et al., 2001), sometimes when PNIPA was copolymerised with hydrophilic comonomers (D'Emanuele and Dinarvand, 1995; Dinarvand and D'Emanuele, 1995). Other drugs used in release studies from thermoresponsive systems examined include insulin (Okano *et al.,* 1990), heparin (Gutowska, *et al.*, 1992) and 5-fluorouracil (Zhang *et al.*, 2002). The studies mentioned did not examine the influence of the chosen drug on hydrogel swelling or drug release properties.

The aim of the present work was to explore the influence of the chosen drug on the ability to thermally control release from a homogeneous PNIPA hydrogel. In order to extend our understanding of the mechanisms of swelling and release from PNIPA hydrogels, the following objectives were defined:

- To analyse the extent to which the chosen drug influences the swelling/deswelling kinetics of the system, the size of the drug pulse seen following hydrogel contraction and the ability of the system to turn "off" drug release.

- To investigate potential drug-polymer interactions.

- To examine drug release mechanisms from the hydrogel at a particular temperature and to determine the effect of varying the drug type, drug loading and percentage crosslinker in the hydrogel.

In addition, a molecular modelling study was carried out on PNIPA using a commercial molecular modelling software package (Accelrys' Materials Studio® Version 2.1.5) with the following aims:

- To simulate the thermoresponsive nature of the polymer for comparison with experimental data.

- To simulate and examine potential interactions between PNIPA and selected drugs.

CHAPTER 1

Thermoresponsive 'Smart' Drug Delivery Systems

1.1 INTRODUCTION

Polymers are large molecules, naturally occurring or synthetic, made of a linked series of repeating monomer units. A hydrogel is a water-swollen network of hydrophilic polymers (Peppas, 1986). The three dimensional structure of a hydrogel is maintained by crosslinking of the polymer chains. Crosslinking is usually in the form of covalent bonds but may also be formed by hydrogen bonding, van der Waals interactions or physical entanglement of the polymer chains (Qui and Park, 2001).

The physical properties of a particular hydrogel will depend on the monomer(s) present as well as the nature and extent of the crosslinker. The mechanical and physical properties of the hydrogel are readily altered by the addition of comonomers or modification of the crosslinker. These adjustable properties may potentially offer many advantages in the use of hydrogels as drug delivery systems. In the present context, some hydrogels can also change their gel structure in response to external stimuli. This is the class of smart/intelligent or environmentally sensitive hydrogels (Kost and Langer, 1991; Qui and Park, 2001).

Smart polymers are polymers that can undergo a conformational change in response to an external stimulus. Such stimuli can be described as physical or chemical stimuli; physical stimuli include temperature, electric field, solvent composition, light, pressure, ultrasound or magnetic field while chemical stimuli include pH, ions or specific molecules such as antigens or glucose/insulin (Hoffman, 1997). When smart polymers are crosslinked, a smart hydrogel is formed which retains the stimulus responsive property of the polymer. A stimuli sensitive hydrogel can thus change its structure and physical properties in response to corresponding external stimuli. Such a physical change in the system can potentially be used to control the rate and extent of drug release.

Traditional drug delivery systems have been developed which can maintain the drug in the desired therapeutic range with a fewer number of doses. This can help to optimise therapy and to increase patient compliance. In many situations, such constant release profiles may not be desirable e.g. insulin for diabetes mellitus, antiarrhythmics for heart rhythm disorders, gastric acid inhibitors for ulcer control, nitrates for angina pectoris, selective B-blockage, birth control, general hormone replacement, immunization and cancer chemotherapy (Kost and Langer 1991, 1992). In these cases, metabolic or disease requirements determine how much drug is needed, at what time and at what site in the body it is needed.

With a smart or responsive drug delivery system, the device can potentially sense a signal caused by the disease or some malfunction and then act to release the drug in direct response (ideally judging the magnitude of the signal). Such drug delivery systems could also react to an externally

applied stimulus (e.g. increase or decrease of temperature) to turn on or off drug release. Both of these situations result in a pulsatile drug delivery pattern (Hoffman, 1987; Kost and Langer, 1991; Ichikawa and Fukumori, 1997; Bromberg and Ron, 1998; Qui and Park, 2001). Such a pattern of drug release is useful in increasing the effectiveness of drug therapy while reducing the treatment cost of the medication. It can also help to minimise the side effects of the drug on the patient.

Pulsed or pulsatile drug delivery involves the release of a drug from a drug delivery system at a specific rate for a definite time period immediately after a predetermined off-release period. Intelligent drug delivery systems such as self-regulating or auto-feedback drug release systems may be achieved by the utilization of stimuli responsive polymers or hydrogels. In using hydrogels in pulsatile drug delivery, the hydrogel ideally swells and collapses with changes in environmental conditions, reversibly capable of accommodating and preventing diffusion of the drug. In addition, smart hydrogels may have the ability to physically protect the drug from a hostile environment until the stimulus is applied e.g. low pH/ presence of enzymes. As a result they may be able to protect a protein's native structure and conformation (Bromberg and Ron, 1998). Targeting of the smart system to, and retention at, the drug absorption site may also be possible (Qui and Park, 2001).

1.2 SMART POLYMERS

The use of a stimulus as a means of controlling the rate and extent of drug release is not a completely new area of research. Enteric coating, as reviewed by Dittgen *et al.* (1997), is an established method of bypassing the stomach and only allowing release of an active substance when reaching the relatively alkaline pH of the small intestine. There are only a few commercially successful hydrogel based drug delivery systems (non-stimuli responsive), most of which are over-the-counter dressings and surgical aids e.g. Aquatrix II™ a chitosan-PVP hydrogel (Gupta *et al.*, 2002). Stimuli responsive hydrogels as drug delivery systems are mainly in the experimental stage. Some brief aspects of the various potential stimuli are discussed in this section.

1.2.1 pH

The pH range of fluids in various segments of the gastrointestinal tract has been utilised as a stimulus for drug release. Enteric coating uses commercially available non-crosslinked acrylic polymers that can only dissolve in the alkaline environment of the small intestine while remaining insoluble in the acidic environment of the stomach (Dittgen *et al.*, 1997). pH sensitive polymers and hydrogels were investigated as potential smart drug delivery devices (Siegel *et al.*, 1988; Patel and Amiji, 1996; Akala *et al.*, 1998; Ranjha and Doelker, 1999; Markland *et al.*, 1999). These

hydrogels contain acidic (e.g. carboxylic) or basic (e.g. ammonium salts) groups in the polymer backbone. Polyacidic hydrogels will swell to a greater extent with increasing pH, since the acidic groups will become more ionised. The opposite holds true for polybasic hydrogels, since the ionisation of the basic groups will increase with decreasing pH. Drug release from such devices will display release rates that are pH dependent (Gupta *et al.,* 2002; Kost and Langer, 1991; Qui and Park, 2001). For example, Siegel *et al.* (1988) showed an increased release rate of caffeine in acidic environments using a methylmethacrylate/ N,N-dimethylamino-ethylmethacrylate hydrogel. Ranjha and Doelker (1999) only showed significant release of betamethasone and proxyphylline above pH 5.5 from poly(methylacrylate-co-methacrylic acid) and above pH 6.5 from poly(ethyl acrylate-co-methacrylic acid) hydrogels. The latter system was proposed for improved site-specific delivery to the colon. Hydrogels, which are pH sensitive and potentially biodegradable, have also been prepared (Akala *et al.*, 1998; Markland *et al.*, 1999). Markland *et al.* (1999) synthesised a polypeptide pH sensitive hydrogel and examined the release of lysozyme while the hydrogel of Akala *et al.* (1998) contained aromatic azo bonds that are degradable by the azoreductase activity in the colon.

1.2.2 Temperature

The majority of temperature sensitive polymers have a Lower Critical Solution Temperature (LCST). While most substances increase their water solubility as temperature increases, polymers with a LCST decrease their water-solubility above this critical temperature. These polymers are soluble below their LCST and precipitate out when heated above the LCST. Such a phase transition can potentially be used in controlled or pulsatile drug delivery.

1.2.2.1 Types of thermoresponsive polymers

There are numerous different types of polymers that are thought to show a LCST in water. Table 1.1 shows a list of such polymers

Table 1.1: Polymers showing an LCST in water (Jeong *et al.*, 2002).

Polymer	LCST (°C)	Polymer	LCST (°C)
Poly (N-isopropylacrylamide)	~32	Poly (siloxyethylene glycol)	10-60
Poly (vinyl methyl ether)	~40	Poly (silamine)	~37
Poly (N-vinylcaprolactam)	~30	Methylcellulose	~80
Poly (propylene glycol)	~50	Hydroxypropylcellulose	~55
Poly (methacrylic acid)	~75	Polyphosphazene derivatives	33-100
Poly (vinyl methyl oxazolidone)	~65		

The most extensively studied thermosensitive polymers in drug delivery are those which show an aqueous phase transition around body temperature (~37°C) e.g. poly (N-isopropylacrylamide) (PNIPA) (Fig. 1.1). Thermoresponsive drug delivery systems usually involve the use of the

corresponding crosslinked polymer or hydrogel. This gives a system that can be conveniently loaded with drug. These thermoresponsive hydrogels can be classified into those that are covalently crosslinked and those that are non-covalently crosslinked.

Covalently crosslinked thermoresponsive hydrogels are formed from the chemical crosslinking of temperature sensitive polymer chains. Poly(N-isopropylacrylamide) (PNIPA) (Fig. 1.1) and related compounds are probably the most extensively studied of this class e.g. Hoffman *et al.* (1986); Bae *et al.* (1987) and Makino *et al.* (2001). Poly(vinyl methyl ether) (Fig. 1.1) also has a phase transition near to body temperature (Horne *et al.*, 1971; Jeong *et al.*, 2002).

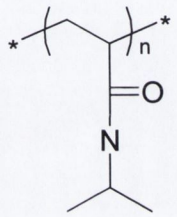

Poly(N-isopropylacrylamide)

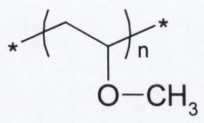

Poly(vinyl methyl ether)

Fig. 1.1: Structure of repeating units of poly(N-isopropylacrylamide) and poly(vinyl methyl ether)

Hydrogels made from these monomers are hydrophilic and swell below the LCST, but on increasing temperature above the LCST they hydrophobically collapse and aggregate, resulting in the hydrogel returning to a shrunken state with an abrupt collapse in volume. This phase transition is reversible on changing temperature around the LCST and can potentially be used to control the release of a drug substance from the system.

If the polymer chains in hydrogels are not covalently crosslinked, certain temperature sensitive systems may undergo a sol-gel phase transition, instead of swelling-deswelling transition. Block copolymers like poly(ethylene oxide)-poly(propylene oxide (PEO-PPO) (Pluronics®, Poloxamers®, Tetronics®) possess an inverse temperature sensitive property based on a sol-gel phase conversion around body temperature (Fig. 1.2).

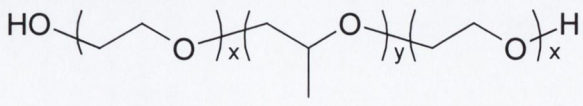

PEO-PPO-PEO

Fig.1.2: Structure of a poly(ethylene oxide)-poly(propylene oxide) (PEO-PPO-PEO) block copolymer (e.g. Pluronic® F68 where x=76 and y=29 (Bromberg and Ron, 1998)).

In the case of these thermoreversible gels, a hydrogel is formed by placing/injecting the polymer solution (with loaded drug) into a 37°C aqueous environment. Jeong *et al.* (1997) incorporated a biodegradable segment of poly(L-lactic acid) into the block copolymer to give a partially biodegradable system. Such a system is liquid at room temperature but gels near body temperature and so is suitable as a sustained release subcutaneous injection.

1.2.2.2 Mechanism of thermo responsiveness

The temperature sensitive phenomenon is thought to be due to a change in polymer-polymer and polymer-water interactions at different temperatures as illustrated in Fig. 1.3.

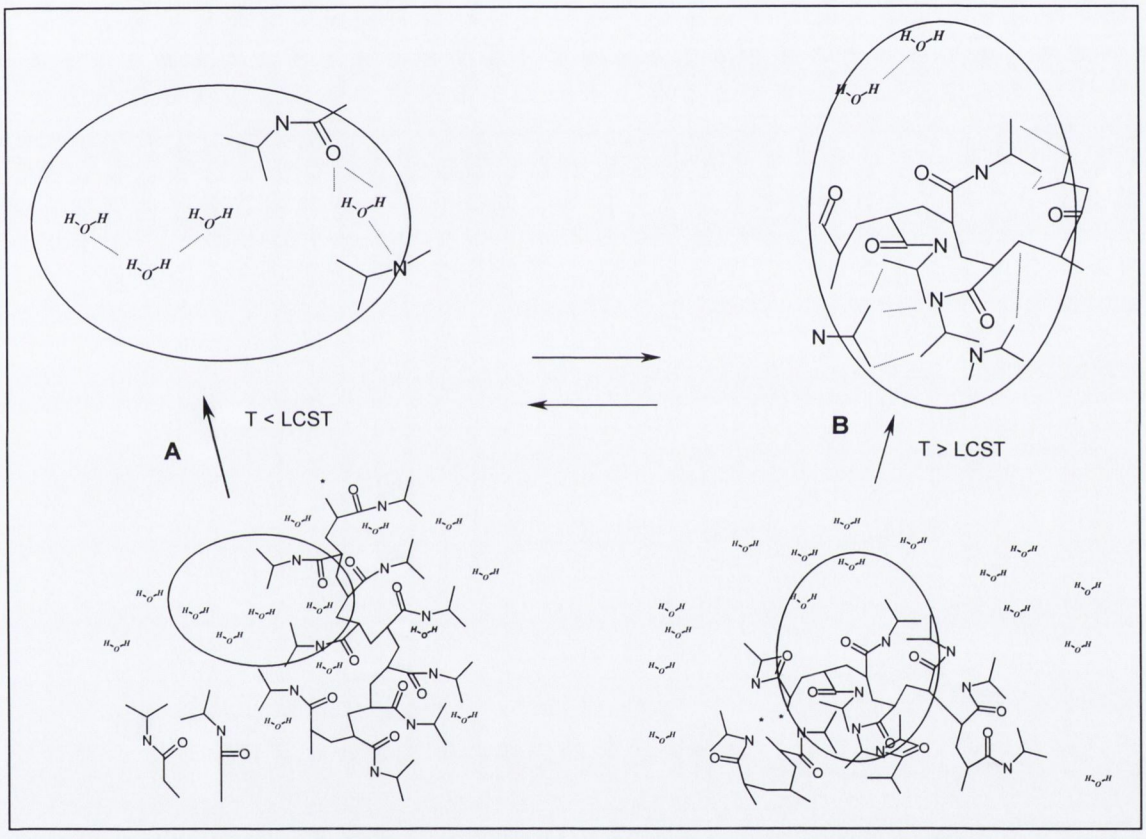

Fig 1.3: A proposed mechanism of thermoresponsive change in linear poly(N-isopropylacrylamide). Below the LCST hydrogen bonding occurs (dashed lines) between the polymer and water molecules (A), which disturbs the normal hydrogen bonded structure of water. Above the LCST, hydrophobic interactions among hydrophobic segments become strengthened (B) resulting in polymer precipitation.

Much work on this phase transition has been carried out using linear polymers of N-isopropylacrylamide (Schild, 1992). Linear poly (N-isopropylacrylamide) chains in dilute aqueous solution below the LCST appear to exist as isolated, flexible but extended coils (Schild, 1992). Hydrogen bonding is thought to dominate, in particular between the hydrophilic segments of the polymer chain and the water molecules (Qui and Park, 2001) (Fig. 1.3A). The polymer in solution

may be surrounded by a protective hydration sheath where the normal structure of water is disturbed due to polymer-water interactions (Ataman, 1987). At the LCST, individual polymer chains appear to collapse as hydrophobic interactions among hydrophobic segments become strengthened while hydrogen bonding becomes weaker (Fig. 1.3B). Theoretical models have shown that the LCST phenomenon results only from the changes in preference for hydrogen bonding, but it is thought that there is an element of the hydrophobic effect as well (Schild, 1992).

Ataman (1987) described the LCST as the sudden dissolution of the molecules' protective hydration sheath, thereby exposing the hydrophobic character of the polymer and causing its precipitation. In the case of a hydrogel, this phenomenon results in a hydrophilic swollen hydrogel below the LCST. Above this temperature, shrinkage of the hydrogel occurs due to hydrophobic interactions and interpolymer chain association.

The use of thermoresponsive polymers and hydrogels in drug delivery will be dealt with in more detail in sections 1.3 to 1.5 and in the next chapter.

1.2.3 Light

Light sensitive hydrogels can be separated into ultraviolet (UV)-sensitive and visible light sensitive hydrogels. UV-sensitive hydrogels are synthesised by introducing a leuco derivative molecule, bis(4-dimethylamino)phenylmethyl leucocyanide, into the polymer network (Mamada *et al.*, 1990). Light induced swelling occurs due to an increase in osmotic pressure within the gel due to the appearance of cyanide ions formed by UV irradiation (Fig 1.4).

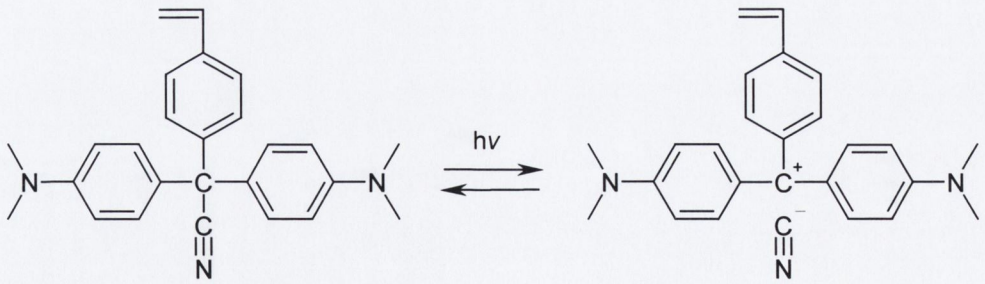

Fig. 1.4: Structure of leuco derivative molecule bis(4-(dimethylamino)phenyl)(4-vinylphenyl)methylleucocyanide

Visible light sensitive hydrogels were prepared by introducing a light-sensitive chromophore (e.g. trisodium salt of copper chlorophyllin) to PNIPA hydrogels (Suzuki *et al.*, 1990). The chromophore absorbs light, which is dissipated locally as heat. This in turn alters the swelling

behaviour of the thermosensitive PNIPA. The swelling of PNIPA can also be directly influenced by the formation of a temperature gradient due to a CO_2 laser infrared beam (Zhang *et al.*, 1995). Yui *et al.* (1993) examined the potential application of a visible light responsive hydrogel for temporal drug delivery. They examined the response of crosslinked hyaluronic acid hydrogels that undergo photosensitised degradation in the presence of methylene blue.

1.2.4 Electric

Hydrogels sensitive to electric currents are made of polyelectrolytes, which undergo shrinking or swelling in the presence of an applied electric field. They are essentially pH-sensitive hydrogels that are able to convert chemical energy to mechanical energy. Application of an electric field across a hydrated polyelectrolyte gives rise to a net force on the space charge in the fluid phase, which contains an excess of counter-ions over co-ions. This force is transferred to the solvent, resulting in electro-osmotic fluid flow relative to the solid membrane matrix (Grodzinsky and Grimshaw, 1990). The flow ceased when the current was shut off and reversed direction when the direction of current was reversed. Various authors have shown pulsatile release of drugs such as edrophonium chloride and hydrocortisone (Kown *et al.*, 1991) or insulin (Sawahata *et al.*, 1990). A similar mechanism to that described has been used in the field of iontophoresis for localised drug delivery to muscles and joints (Tyle, 1986; Banga and Chien, 1988) or for potential systemic drug delivery (Okabe *et al.*, 1986; Siddiqui *et al.*, 1987).

1.2.5 Biomolecule sensitive hydrogels

Hydrogels that undergo swelling changes in response to specific biomolecules have potential as self-regulated drug delivery systems (Miyata *et al.*, 2002). Biomolecules could include glucose, enzymes or antigens. Glucose sensitive hydrogels are being investigated as self regulated insulin delivery systems. Three main types currently exist. Glucose oxidase-loaded hydrogels (e.g. Ito *et al.*, 1989; Hassan *et al.*, 1997) combine glucose oxidase with pH sensitive hydrogels. The glucose oxidase converts glucose to gluconic acid, lowering the pH in the hydrogel and influencing the swelling of the hydrogel and thus release of insulin. The second type of glucose sensitive hydrogel involves the glucose binding protein Concanavalin A (Con A) (Brownlee and Cerami, 1979; Seminoff *et al.*, 1989; Kim *et al.*, 1990). A stable, biologically active glycosylated insulin derivative able to form a complex with Con A is synthesised. This derivative competes with glucose for binding to Con A and so the release of the insulin derivative is dependent on blood glucose levels. The third type of glucose sensitive hydrogel contains phenylboronic acid moieties (Kitano *et al.*, 1992). Phenylboronic acid and its derivatives form complexes with polyol compounds, such as glucose in aqueous solution as shown in Fig 1.5. This complex can be

dissociated in the presence of a competing polyol compound, which is able to form a stronger complex. Poly(vinyl alcohol) (PVA) competes with glucose for binding to phenylboronic acid.

The PVA can act as a crosslinker when complexed, while the glucose is monofunctional. As the glucose concentration increases, the crosslinking density of the gel decreases and the gel swells/erodes to release more insulin.

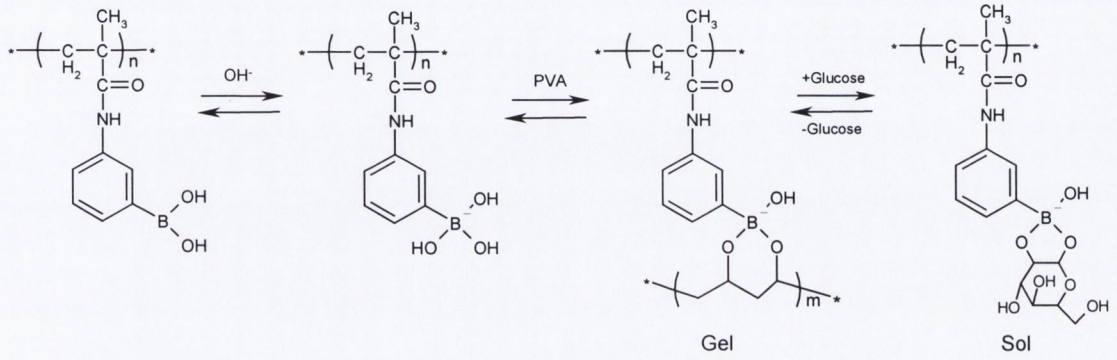

Fig. 1.5: Sol-gel phase transition of a phenylborate polymer. At alkaline pH, phenylborate polymer interacts with PVA to form a gel. Glucose replaces PVA to induce a transition from the gel to the sol phase.

Other types of biomolecular responsive hydrogels include biodegradable hydrogels that can undergo swelling changes in response to enzymes such as azoreductase (Akala *et al.,* 1998) or dextranases (Hovgaard *et al.,* 1995). These could potentially be used in oral drug delivery to target the colon. Antigen sensitive hydrogels have also recently been synthesised (Miyata *et al.,* 1999). The hydrogel swells in the presence of a free antigen because the intra-chain antigen-antibody binding can be dissociated by exchange of the grafted antigen for free antigen. In the absence of a free antigen, the hydrogel shrinks.

1.2.6 Others

Other smart drug delivery stimuli involving hydrogels include the use of a magnetic field (Kost *et al.,* 1987; Saslawski *et al.,* 1988), ultrasound (Miyazaki *et al.,* 1985; Kost and Langer, 1990), pressure (Zhong *et al.,* 1996) or radiation (Juodkazis *et al.,* 2000)

Kost *et al.* (1987) magnetically enhanced insulin release in diabetic rats using a polymer matrix containing insulin and magnetic beads. The release rate from such systems is influenced by

magnetic field properties and the mechanical properties of the polymer matrix (Saslawski *et al.*, 1988).

Miyazaki *et al.* (1985) and Kost and Langer (1990) used ultrasound to modulate the release rate from bioerodible and non-erodible polymers, including hydrogels. The ultrasound may cause an increase in temperature in the delivery system, which may facilitate drug diffusion from the system (Miyazaki *et al.*, 1985).

Zhong *et al.* (1996) found that the phase transition of temperature sensitive gels was pressure dependent, with potential implications for the degree of swelling.

Juodkazis *et al.* (2000) recently reported reversible phase transitions in polymer gels induced by radiation. The volume phase transitions were attributed to the radiation rather than local heating.

1.2.7 Uses of smart polymers

Apart from their potential use in drug delivery, smart polymers are being investigated for use in other areas. Smart polymers could function as biomimetic actuators as they are capable of converting chemical energy (e.g. pH change) into mechanical energy (e.g. change in shape). Such a transforming property is exhibited by living organisms and has applications in the design of artificial organs (e.g. muscles) or machines (Kajiwara and Ross-Murphy, 1992; Osada *et al.*, 1992). In a similar way, smart polymers could act as chemical valves or be used in the immobilization of enzymes and cells (Dong and Hoffmann, 1986).

1.3 POLY(N-ISOPROPYLACRYLAMIDE)

Poly(N-isopropylacrylamide) has a LCST near body temperature (Table 1.1) and so has been the interest of much research in the area of thermoresponsive drug delivery.

1.3.1 Synthesis

Poly(N-isopropylacrylamide) has been synthesised by using a variety of techniques (Schild, 1992) including redox initiation in aqueous media, free radical initiation of organic solutions, ionic polymerisations and synthesis by radiation.

Whether one polymerises in aqueous or organic solutions has been shown to affect the properties of the linear polymer (Schild, 1992). The most widely used techniques for hydrogel synthesis in the

drug delivery field are redox initiation in aqueous media e.g. Hoffman *et al.* (1986), Okano *et al.* (1990) Andersson *et al.* (1997), Makino *et al.* (2001) or free radical initiation in organic solutions e.g. Bae *et al.* (1987, 1991b), Okano *et al.* (1990), Yoshida *et al.* (1991a, 1991b, 1992, 1994a) and Gutowska *et al.* (1992).

Redox initiation in aqueous media provides a simple and convenient method of hydrogel synthesis. A typical reaction uses ammonium persulfate as the initiator and either sodium metabisulfite (Andersson *et al.,* 1997), or N,N,N',N'-tetramethylethylenediamine (TEMED) (Hoffman *et al.,* 1986; Okano *et al.,* 1990) as the accelerator. N,N'-methylenebisacrylamide is used as the crosslinker in these reactions with a typical reaction scheme shown in Fig 1.6.

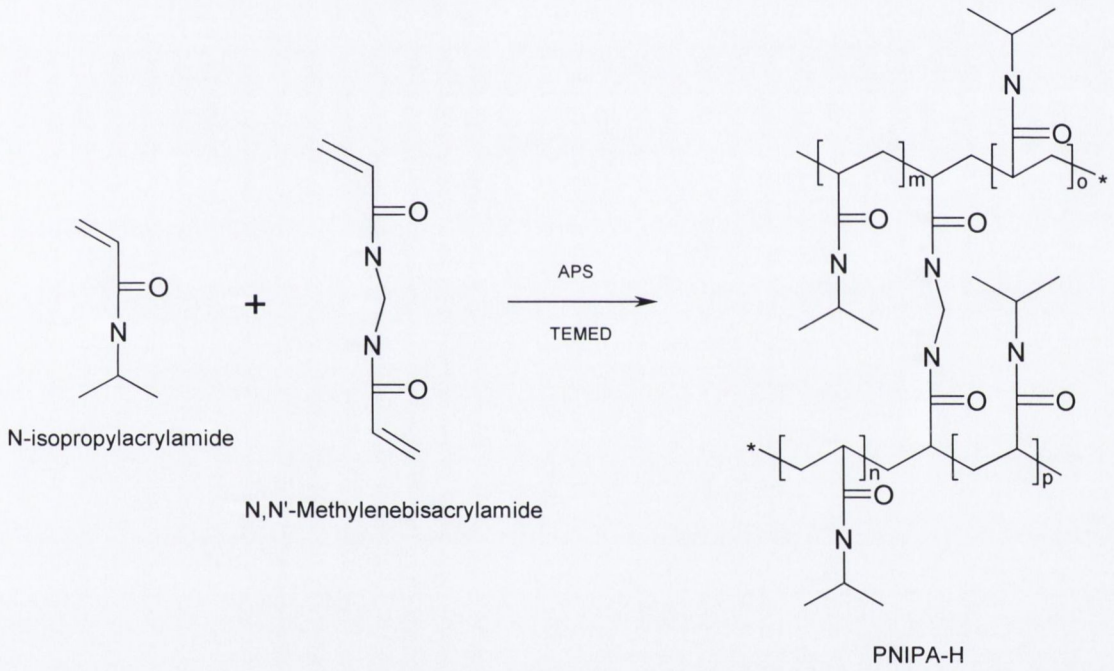

Fig. 1.6: Synthesis of an aqueous based poly(N-isopropylacrylamide) hydrogel (PNIPA-H). The reaction is initiated using ammonium persulfate (APS) and propagated with tetramethylethylenediamine (TEMED). Value of integers (m,n,o,p) depend on crosslinking density.

Free radical initiation in organic solution has been the main method used in hydrogel synthesis for drug delivery studies. The addition of hydrophobic comonomers such as butyl methacrylate necessitates the use of an organic solvent such as 1,4-dioxane to be used as a diluent. A typical reaction uses an initiator such as azo-bis-isobutyronitrile (AIBN) e.g. Gutowska *et al.* (1992) or t-butyl peroxyoctanoate (BPO) e.g. Bae *et al.* (1987). Ethylene glycol dimethacrylate is generally used as the crosslinker in these dioxane based reactions.

Bae *et al.* (1991a, 1991b) showed that a hydrogel synthesised in 1,4 dioxane showed a higher swelling level before collapse point, a lower gel collapse point and a lower swelling level after gel collapse than a similar system synthesised in aqueous media. Different crosslinking densities were however used, which may account for much of the difference.

1.3.2 Altering the LCST

Okano *et al.* (1990) studied the relationship between alkyl group lengths in crosslinked poly (N,N'-alkyl substituted acrylamides) and their aqueous swelling as a function of temperature. They found that a more pronounced deswelling or gel collapse with temperature increase followed the trend shown in Fig. 1.7.

The thermosensitivity of swelling was shown to be due to a delicate hydrophilic/hydrophobic balance of polymer chains and was affected by the size, configuration and mobility of alkyl side groups.

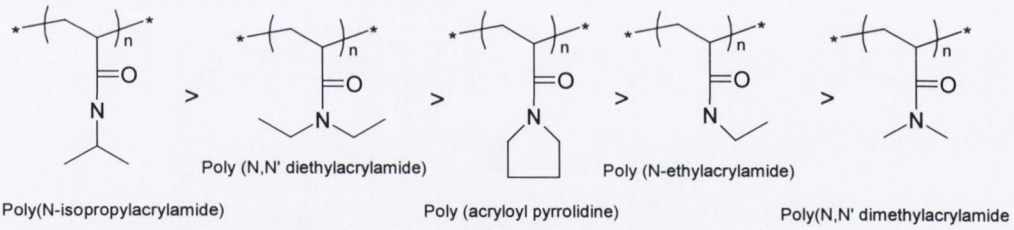

Fig. 1.7: Series of poly(N,N'-alkyl substituted acrylamides) in order of magnitude of gel collapse on increasing the temperature.

It has also been shown that the phase transition temperature (LCST) and equilibrium-swelling ratio of a N-isopropylacrylamide polymer can be modified by the introduction of hydrophilic or hydrophobic comonomers (Beltran *et al.*, 1991; Feil *et al.*, 1993; Yoshida *et al.*, 1994b). The hydrophilic or hydrophobic nature of the comonomer was relative to the original monomer.

The addition of hydrophilic comonomers such as acrylic acid, acrylamide or N,N'dimethylacrylamide (Fig. 1.8) can elevate the LCST of the hydrogel as well as increase the gel swelling levels.

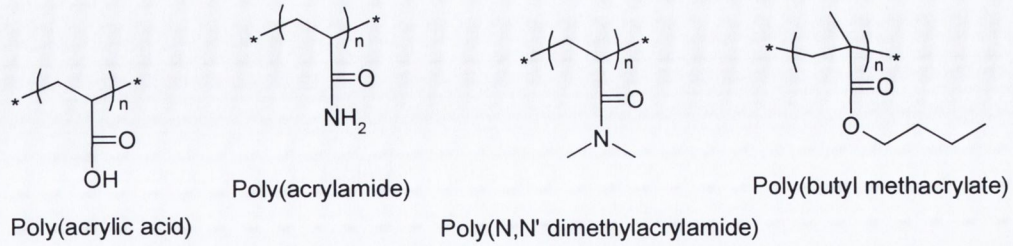

Poly(acrylic acid) Poly(acrylamide) Poly(N,N' dimethylacrylamide) Poly(butyl methacrylate)

Fig. 1.8: Some possible comonomers for polymerisation with NIPA

A hydrophobic comonomer such as butylmethacrylate (Fig. 1.8) can lower the gel collapse temperature as well as lowering the equilibrium swelling ratio. Yoshida *et al.* (1994b) showed that as the length of the alkyl side chain of the comonomer increased, the phase transition tended to shift to an even lower temperature and lead to a smaller equilibrium swelling ratio. They also showed that the thermosensitivity of these hydrogels was affected by the comonomers, including preventing the formation of a dense shrunken state at higher temperatures.

The equilibrium-swelling ratio of such hydrogels was also dependent on the pH of the media in the case of ionisable comonomers such as acrylic acid or acrylamide (Beltran *et al.,* 1991; Dong and Hoffman, 1991).

1.3.3 Positive and negative thermosensitivity

Most thermosensitive systems, including the linear and crosslinked polymers in Table 1.1, exhibit a LCST and thus show negative temperature dependency (Yoshida *et al.,* 1994c). Negative thermosensitivity can be described as decreased swelling at increased temperature. This means the systems are hydrophilic and swell at temperatures below the LCST and they become insoluble or shrink above this temperature. In drug delivery terms, this generally results in what is referred to as *negative thermosensitive release* i.e. faster drug release at the lower temperature where increased swelling and thus diffusion can occur.

Other polymeric systems can show an Upper Critical Solution Temperature (UCST) where the systems precipitate or shrink in water below this critical temperature. Such a hydrogel system would swell at high temperature, showing positive temperature dependency. Little is known about hydrogels with UCST (see section 1.4.3) but in theory they would result in *positive thermosensitive release* i.e. faster drug release at higher temperature.

Negative thermosensitive release is defined here as a higher rate of release of a drug on decreasing the temperature of the system as compared to the release profile at the higher temperature.

Positive thermosensitive release is defined here as a higher rate of release of a drug on increasing the temperature of the system as compared to the release profile at the lower temperature.

1.3.4 Drug delivery systems

Various authors have used thermoresponsive poly(N-isopropylacrylamide) based hydrogels to modify the release rate of model drugs by altering the external temperature. The types of systems used and the mechanisms of release will be described in chapter 2. The thermosensitivity of PNIPA has been utilised in other applications to control drug release and these are described in the current section.

1.3.4.1 Linear poly(N-isopropylacrylamide)

There have been a few studies which have investigated drug release from the linear poly(N-isopropylacrylamide) polymer. Ramkisoon-Ganorkar *et al.* (1999) showed that by altering the average molecular weight and polydispersity of linear polymers of NIPAA/butylmethacrylate-acrylic acid (85:5:10), the polymer dissolution rate and release rate of insulin could be modulated. Kim *et al.* (1994) synthesised linear pH/temperature sensitive polymers in the form of beads by precipitation of the polymer at the interface of cold aqueous solution droplets and warm oil phase. The beads were loaded with insulin and the subsequent release was influenced by temperature and pH.

1.3.4.2 Poly(N-isopropylacrylamide) membranes

The permeation rate of various solutes through PNIPA membranes could also be controlled by temperature. Ogata *et al.* (1995) showed that they could control the permeation of solutes of different molecular weight through a poly(vinyl alcohol)-PNIPA membrane by changing the temperature from 34°C to 45°C. They also found that the permeation of butyl alcohols through the slightly swollen membrane above the LCST depended on the hydrophobicity of the solutes.

Akerman *et al.* (1998) examined the effect of various temperatures on the flux of FITC-dextrans (MW 4,400–50,600) across NIPA-poly(vinylidene fluoride) membranes. They showed that the flux of bigger molecules was effectively controlled while the flux of smaller molecules was not controlled thermally even at a high degree of membrane grafting.

Okano *et al.* (1990) showed that the permeation of glucose and insulin across a poly(NIPA-co-butyl methacrylate) membrane (95:5) could be rapidly turned on and off in response to temperature

fluctuations between 20°C and 30°C. The temperature control was explained in this case by a surface response to temperature rather than bulk swelling change.

1.3.4.3 Incorporation of PNIPA within coating

Ichikawa and Fukumori (2000) designed a positive thermosensitive drug release microcapsule. Its thermosensitive coat was composed of ethylcellulose containing PNIPA hydrogel "particles". The release rate of the model drug (carbazochrome sodium sulfonate) increased on increasing temperature due to the shrinkage of the thermosensitive hydrogel particles within the coating of the microcapsule. The resultant voids in the coating facilitated diffusion of the drug from the core.

1.3.4.4 Surface grafting of thermoresponsive polymers

Okahata *et al.* (1986) prepared thermoresponsive microcapsules by grafting of PNIPA onto the surface of nylon microcapsules. Above the LCST, the release rate of sodium chloride and various dyes was significantly decreased due to the thermosensitive polymer being in the collapsed state at the surface of the microcapsules. At the lower temperature, the layer became loose and the release rate increased in a reversible fashion.

Several authors have also synthesised thermosensitive liposomes by adding thermosensitive polymers onto the liposomal membranes (Wu *et al.,* 1992b; Kono *et al.,* 1994, 1999). The liposome is stabilised by the highly hydrated polymer chains below its LCST. Above the LCST the dehydrated and contracted polymer chains cause destabilization of the liposome, an increase in hydrophobicity of the liposome surface, and/or exposure of the bare liposome surface (Kono, 2001). Kono *et al.* (1994) showed an enhanced release of calcein above 42°C with no release below 20°C.

1.3.4.5 Interpenetrating networks

Interpenetrating networks (IPNs) are formed when one crosslinked network is intertwined with another independent network. IPN's provide another way to alter the temperature dependence of swelling and the gel shrinkage of a PNIPA hydrogel.

Gutowska *et al.* (1994) synthesised IPNs of crosslinked PNIPA and linear poly(ether(urethane-urea). The IPNs showed greater mechanical strength and faster deswelling rates than the crosslinked PNIPA alone. The release of heparin was also studied at various temperatures. Bae *et al.* (1991b) and Okano *et al.* (1990) formed IPNs of poly(NIPA) and polytetramethylene ether glycol (PTMEG). On-off pulsatile release of indomethacin was shown. The content of PTMEG did not affect the transition temperature but did affect the overall hydrophobicilty and swelling of the system.

1.3.5 Effect of additives on transition temperature

Thermosensitive polymers with an LCST show a phase transition temperature as described in section 1.2.2. The transition temperature has been shown to be affected by various factors including the solvent used (Lee *et al.,* 2000) as well as the addition of salts and surfactants (Saito *et al.,* 1992; Eeckman *et al.,* 2001). The effect of model drugs on the polymer phase transition has not been investigated to date. The influence of salts and surfactants on the aqueous phase transition temperature is reviewed.

1.3.5.1 Inorganic salt

Studies by Horne *et al.* (1971) and Ataman (1987) examined the effect of electrolytes on aqueous colloidal dispersions of poly(vinyl methyl ether) and poly(ethylene oxide) respectively. Flocculation of such dispersions or a 'salting out' effect has been shown on the addition of electrolytes, although some salts induced a 'salting in' process e.g. tetra-alkyl ammonium salts. The 'salting out' process resulted in a decrease in the phase transition temperature of thermosensitive polymers while the 'salting in' process increased the transition temperature (Horne *et al.,* 1971; Saito *et al.,* 1992; Eeckman *et al.,* 2001).

The inorganic ions are not thought to be adsorbed into the polymer network but still affect the phase transition behaviour (Saito *et al.,* 1992). Hydrogen bonding plays an important role in the phase transition of thermosensitive polymers as described in section 1.2.2.2 and disruption of this hydrogen bonding will alter the phase transition. In solution, an extended hydration sheath may surround polymers where water is more structured (Section 1.2.2.2). Aqueous salt solutions have been shown to consist of three regions (Ataman, 1987): region (A) permanently associated with the ion; region (B) consisting of water molecules partially ordered by the electric field of region A; and region (C) consisting of the normal hydrogen bonded water structure. Certain ions can destroy the hydrogen-bonded structure of water with the proportion of (B) in a given salt solution being a measure of the ability of the ion to destroy water structure. These salts have the ability to break the hydration layer around PNIPA chains. Aqueous salt solutions alter the water structure in the polymer hydration sheath and cause changes in the interactions between the polymer and the water. An increase in the hydrophobic character of PNIPA chains results, which consequently lowers the phase transition. Ataman (1987) showed that salting out ions destructure the hydration sheath while salting in ions strengthen it.

Eeckman *et al.* (2001) showed that both the valence and size of the anion play an important role in the salting out process in respect of PNIPA polymers. Anions were classified on a molar

concentration basis in accordance with the Hoffmeister series in respect of salting out effectiveness:

$$PO_4^{3-} > HPO_4^{2-} > SO_4^{2-} > OH^- > H_2PO_4^- > HCO_3^- > F^- > CH_3COO^- > Cl^- > Br^- > I^-$$

When the molecular weight of the salt was used instead of molar concentration the ranking was:

$$OH^- > F^- > PO_4^{3-} > SO_4^{2-} > HPO_4^{2-} > H_2PO_4^- > HCO_3^- > CH_3COO^- > Cl^- > Br^- > I^-$$

The effect of the cation on the transition temperature of PNIPA was insignificant (Saito *et al.*, 1992).

1.3.5.2 Surfactants

Surfactants can also cause a decrease or increase in the LCST of PNIPA depending on the hydrophobic chain length and the surfactant concentration (Eeckman *et al.*, 2001, Schild and Tirrell, 1991). This behaviour has been characterised as the sum of two antagonistic phenomena, i.e. a salting out effect due to the anionic character of the free surfactant molecules and a conversion of the originally hydrophobic polymer into a more hydrophilic complex by bonding of the long aliphatic hydrocarbon chains of the surfactants with the polymer hydrophobic segments (Eeckman *et al.*, 2001). In contrast with the salt effect, it has been suggested that these surfactants may bind to the polymer (Schild and Tirrell, 1991; Saito *et al.*, 1992; Eeckman *et al.*, 2001).

1.4 OTHER THERMORESPONSIVE POLYMERS

1.4.1 Poly(vinyl methylether)

Poly(vinyl methylether) (PVME) (Fig. 1.1) also has a LCST near physiological temperature (Horne *et al.*, 1971; Jeong *et al.*, 2002). Horne *et al.* (1971) examined the linear polymer and the influence of various salts and surfactants on the transition temperature. Thermoresponsive gels of PVME were synthesised by crosslinking or by γ-irradiation of the linear polymer (e.g. Kabra *et al.*, 1992). The studies mentioned did not examine drug release from PVME systems.

1.4.2 Miscellaneous

The presence of a LCST appears to be due to a delicate hydrophilic/hydrophobic balance within the polymer and the temperature of the experiment (section 1.3.2). Several publications present the synthesis of new polymers that display the LCST phenomenon (Yoshida *et al.*, 1989, 1991c; Lin *et*

al., 1998; Lee *et al.,* 1998; Lau and Wu, 1999; Tachibana *et al.,* 2003). Pulsatile drug release was shown from the thermoresponsive acryloyl-L-proline methylester hydrogels (Miyajima *et al.,* 1993). A higher release rate was presented over the interval at 30°C compared to a lower release rate at 0°C and was attributed to the shrinkage of the gel. Lau and Wu (1999) presented the synthesis of a thermally sensitive and biocompatible poly(N-vinylcaprolactam). Some of the more recent thermosensitive polymers may also potentially be biodegradable and include poly(amino acids) polymers (Tachibana *et al.,* 2003) and lactose based hydrogels (Lin *et al.,* 1997). Other authors, in an attempt to synthesise biodegradable thermoresponsive hydrogels based on PNIPA, have incorporated biodegradable crosslinkers (Kurisawa *et al.,* 1998; Oh *et al.,* 1999) or biodegradable comonomers such as poly(lactic acid) (Kim *et al.*, 2000).

1.4.3 Positive temperature dependent gels

Hydrogels with an upper critical solution temperature would swell at high temperatures and remain deswollen at lower temperatures. Less is known about hydrogels with an UCST. Katono *et al.* (1991) showed positive temperature dependence of swelling with IPNs of poly (acrylamide/butyl methacrylate) and polyacrylic acid. The transition temperature shifted to higher temperature with increasing butylmethacrylate content and pulsatile release of ketoprofen was examined. The presence of the UCST was attributed to a hydrogen bonded complex formation between poly(acrylic acid) and poly(acrylamide). The same group (Sasase *et al.,* 1992) have also attempted to increase the UCST towards body temperature by altering the comonomers. Aoki *et al.* (1996) synthesised polymeric hydrogels from 6-(acryloyloxymethyl)uracil which exhibited a more shrunken state at the lower temperature and showed positive thermosensitive release of ketoprofen. The UCST was again designed using a pair of polymers that showed attractive polymer-polymer interactions such as complex formation via hydrogen bonding.

1.5 POTENTIAL USES OF THERMORESPONSIVE DRUG DELIVERY SYSTEMS

Thermoresponsive polymeric systems undergo reversible volume phase transition or gel-sol phase transitions upon changes in environmental conditions. This phase transition can potentially be modified to respond to only small temperature change as described in section 1.3.2. In drug delivery there is the potential to modulate drug release through temperature control of the device. This would result in an alteration of the release rate or switching on or off the release. Such pulsatile release may be required to match physiological needs or to respond to an external stimulus. Potential uses of such systems, at temperatures above and below the LCST of the polymer/hydrogel, are described in the following section.

1.5.1 Constant temperature

In conventional drug delivery, the drug concentration in the blood rises when the drug is taken, then peaks and declines. Multiple doses at specified intervals may then be required to keep the drug at a therapeutic plasma level, above an ineffective level but below a toxic level. This led to the development of constant rate drug delivery systems. Such controlled release devices, which are available commercially, can maintain the drug within a given effective therapeutic range with the administration of fewer doses. These drug delivery devices can also localise delivery to a particular area of the body, preserve medications that are rapidly destroyed by the body and help improve compliance.

As a constant drug delivery device at body temperature (37°C), the properties of thermosensitive hydrogels could be tailored to match the desired release profile. If the LCST of the system is above body temperature, the hydrogel will swell and the rate and degree of swelling can be controlled by the monomers and crosslinker. If the LCST of the system is below this temperature, no swelling or a lower level of swelling will occur. The non-crosslinked linear polymer would also dissolve or precipitate depending on the LCST relative to body temperature. Uludag *et al.* (2001), for example, engineered PNIPA polymers for delivery of therapeutic proteins to improve their therapeutic efficacy.

A fully or partially swollen thermoresponsive hydrogel with a LCST lower than body temperature could potentially be used for storage of the active agent. Administration at body temperature would result in hydrogel contraction with a resulting drug pulse.

Linear and crosslinked thermoresponsive systems are also being investigated for use in controlled release ophthalmic drops (Hoffman *et al.*, 1995; Hsiue *et al.*, 2002, 2003). Drugs such as timolol maleate (Hoffman *et al.*, 1995) and epinephrine (Hsiue *et al.*, 2002, 2003) were loaded at room temperature and administered at eye temperature (34°C >LCST). The linear system precipitated as a colloid/nanoparticle soft film after contacting the surface of the cornea and significant extended release and prolonged clinical efficacy was observed (Hsiue *et al.*, 2002, 2003).

1.5.2 Changing temperature

The use of thermoresponsive systems in the above situations involved only one temperature upon administration of the drug delivery device. There is also the potential to utilise more than one temperature in order to optimise the drug release. Such situations can be divided into externally controlled pulsed release and self-regulated pulse release using thermoresponsive hydrogels.

1.5.2.1 Pulse release modulated by external temperature

External heat or cold sources may be used to alter the temperature of the drug delivery system, thereby increasing or decreasing the drug release rate. Subdermal implants are a possible method of controlling the swelling state of an implanted hydrogel and the subsequent release rate. Such an implant could be useful in patients where frequent but non-continuous drug release is desirable.

The use of local heat along with a thermoresponsive system is also attracting attention as an active way of targeting solid tumors (Meyer *et al.,* 2001; Weidner, 2001; Chilkoti, 2002; Yokoyama, 2003). Attaching cytotoxic agents to soluble polymers is known to improve drug pharmacokinetics and accumulation at the tumor site due to passive targeting (Weidner, 2001). Hyperthermia is also known to preferentially increase the permeability of tumor vasculature compared to normal vasculature. Combining a soluble thermoresponsive polymer with local heat administration may synergistically enhance the delivery of drugs to tumors (Meyer *et al.,* 2001; Weidner, 2001). Meyer *et al.* (2001) used thermoresponsive systems to target solid tumors. Thermally responsive polymers were synthesised with an LCST of 40°C and they were found to selectively accumulate in the solid tumor, which was maintained above physiological temperature by externally applied, focused hyperthermia (42°C). Using a slightly different concept of thermal targeting, Yokoyama *et al.* (2003) combined local hyperthermia caused by ultrasound with thermoresponsive polymeric micelles containing the drug to target solid tumors. In this case, contraction of the thermoresponsive polymer on the outside of the micelle allowed the drug to selectively diffuse out from the core in the vicinity of the tumor.

Linear thermoresponsive polymers have recently been proposed as carriers for DNA delivery (Hinrichs *et al.,* 1999; Kurisawa *et al.,* 2000; Alexander *et al.,* 2004). Non-viral vectors such as cationic lipids are low in transfection efficiency in comparison to viral vectors. Polymeric carrier systems are an alternative. Cationic lipids and polymeric carrier systems must fulfil two requirements simultaneously: (i) complex formation for cell uptake and prevention of DNA degradation and (ii) complex dissociation for transcription by RNA polymerase (Kurisawa *et al.,* 2000). Since these are opposite phenomena, an intelligent thermoresponsive system was used with complex formation above the LCST (for cell entry) and dissociation below the LCST (for transcription). Kurisawa *et al.,* (2000) showed enhanced reporter gene expression by lowering the incubation temperature.

Smart hydrogels such as thermoresponsive hydrogels can also potentially be used for flow control in drug delivery devices (Eddington and Beebe, 2004). The hydrogel in its swollen state prevents the flow of media from the device and therefore the drug release. In the shrunken state, diffusion of the drug from the device can take place.

1.5.2.2 Pulse release auto-regulated by change in body temperature

There is also the potential to make use of body temperature to activate a thermoresponsive drug delivery system. Actual body temperature depends on the site in body. There are normal fluctuations in body temperature during each 24-hour period (circadian rhythm), being lowest in the morning before dawn and highest in the afternoon. There are also regional changes in temperature around the body due to altered flow to extremities e.g. stress. Other factors that affect body temperature include exercise, hormones, food intake and drug intake. Two potential systems exist. Firstly a system could respond to an increase in body temperature (hyperthermia) by releasing an antipyretic drug (e.g. paracetamol) to lower the temperature. Drug release would stop when the set temperature is reached. Possible causes of hyperthermia include fever (caused by microorganisms), febrile seizures, diseased states (e.g. inflammation, cancer, blood clots, connective tissue disorders, and central nervous system hemorrhage or stroke), menstrual cycle and drugs (e.g. ecstasy related hyperthermia, antidepressants and antibiotics like vancomycin). In cases such as febrile seizures antipyretic prophylaxis may be difficult, as seizures may have already occurred by the time a febrile illness is identified. A "smart" system could potentially respond instantaneously to the slight rise in body temperature.

A second potential system could respond to a decrease in body temperature by release of a stimulant drug (e.g. immunostimulant drug if immunocompromised) or a potential drug to help the body recover its normal homeostatic state. The elderly, sick, frail and immunocompromised are particularly susceptible to hypothermia. It can also occur postoperatively and can be a serious side effect of some drugs e.g. antipsychotics such as chlorpromazine

CHAPTER 2

Hydrogel Swelling/Deswelling Kinetics and Drug Release Mechanisms

2.1 INTRODUCTION

In swellable drug delivery systems such as hydrogels, the dissolution medium or penetrant surrounding the controlled release device diffuses into the polymer meshwork resulting in swelling of the system. The entrapped drug can then dissolve and diffuse out of the system into the bulk media. Section 2.2 briefly describes the processes of drug dissolution and diffusion relevant to the present work. This is followed (section 2.3) by the examination of diffusion in terms of swelling and drug release from hydrogels. Section 2.4 examines the specific case of swelling of, and drug release from, thermoresponsive hydrogels.

2.2 DRUG DISSOLUTION AND DIFFUSION

Diffusion is defined as a process by which matter is transported from one part of a system to another as a result of random molecular motions (Crank, 1975). The flow of molecules through a barrier such as a polymeric membrane can occur by molecular diffusion/permeation through a non-porous medium or by diffusion through solvent filled pores of a membrane. The former depends on dissolution of the permeating molecules in the bulk membrane while the latter is influenced by the relative sizes of the penetrating molecules and the diameter of the pores (Martin, 1993).

In transport studies across membranes, the steady state flux is governed by Fick's first law of diffusion, which states that the rate of transfer of diffusing substance per unit area (J) is proportional to the concentration gradient:

$$J = -D \frac{\delta C}{\delta x}$$

Equation 2.1

Where

D = the diffusion coefficient of the penetrant

C = the concentration of the penetrant

x = the distance of movement perpendicular to the surface of the barrier

The negative sign signifies that diffusion occurs in a direction opposite to that of increasing concentration. The chemical nature of the diffusant as well as temperature, pressure and solvent values can affect D values.

Fick's second law examines the rate of change of diffusant concentration at a point in the system. It states that a change in concentration with time in a particular region is proportional to the change in the concentration gradient at that point in the system (Martin, 1993):

$$\frac{\delta C}{\delta t} = D\frac{\delta^2 c}{\delta x^2}$$

Equation 2.2

Dissolution is the process by which a solid dissolves and enters into solution. The dissolution process can be diffusion controlled, surface reaction controlled or a function of both processes. Diffusion controlled dissolution is the norm in most cases of dissolution of solids in liquids. In this case, the liberation of the solute molecules at the interface is much faster than the diffusion of the solute from the interfacial boundary to the body of the solution.

Nernst and Brunner (1904) developed a diffusion controlled dissolution model or film theory, which postulated the existence of an aqueous diffusion layer or stagnant liquid film at the surface of the solid undergoing dissolution. They applied Fick's first law of diffusion (Equation 2.1) and developed equation 2.3a to describe the dissolution process at steady state:

$$\frac{dC}{dt} = \frac{DA}{Vh}(C_s - C_t)$$

Equation 2.3a

$$\frac{dC}{dt} = \frac{DA}{Vh} C_s$$

Equation 2.3b

Where:

dC/dt = rate of change of concentration with respect to time

C_s = saturation solubility of the solid

C_t = concentration of the solute in the bulk solution at time t

D = Diffusion coefficient

A = Surface Area

V = Volume of dissolution medium

h = diffusion layer thickness

Equation 2.3a interpreted the dissolution of a solid as a diffusion controlled process in which dissolution of the solid at the interface occurs in a thin stagnant layer around the particle of thickness, *h*. The rate-determining step of diffusion then occurs from this boundary layer to the bulk media where rapid mixing occurs.

When the concentration of solute in the bulk solution is much less than drug solubility, sink conditions occur and C_t becomes negligible compared to C_s. In such cases, equation 2.3a can be written as equation 2.3b.

Hixson and Crowell (1931) modified the above equations to develop an equation that expresses the rate of dissolution of uniformly sized particles based on the cube root of the weight of the particles:

$$w_o^{1/3} - w^{1/3} = kt$$

Equation 2.4a

Where

w_o = initial powder weight

w = powder weight at time t

k = the cube root dissolution rate constant, approximated by: $k' N^{1/3} \frac{DC_s}{\delta}$ (Costa and Lobo, 2001)

N = number of particles

k' = constant relating to the surface, shape and density of the particles

D = diffusion coefficient

C_s = solubility at equilibrium temperature

δ = diffusion layer thickness

This is known as the Hixson-Crowell cubic root law where k is the cube root dissolution rate constant.

Since the fraction dissolved $F = \frac{w_o - w}{w_o}$ $(0 \leq F \leq 1)$, then equation 2.4a can be expressed as (Rost and Quist, 2003):

$$F = 1 - \left(1 - \frac{kt}{w_o^{1/3}}\right)^3$$

Equation 2.4b

Equation 2.4b gives the fraction dissolved of a number of identical particles, each having the initial weight w_o and can be used for the non-linear fitting of the cube root law to dissolution profiles (Rost and Quist, 2003).

Diffusion controlled drug delivery systems can be divided into two main classes: reservoir devices and matrix devices. Reservoir devices are characterised by a core of drug, the reservoir, surrounded by a polymeric membrane. The nature of the drug and membrane determines the release of drug from the system with the diffusion process described by Fick's laws of diffusion.

A matrix device consists of a drug dispersed homogeneously throughout a matrix. In unsaturated systems such as topical creams and ointments, the drug is dissolved in the aqueous phase and must diffuse out of the system. Higuchi (1962) showed that such release obeyed Fick's second law (Equation 2.2) and that the release of drug in solution from a single surface of a homogenous ointment could be described by equation 2.5a

$$Q = 2C_o\left(\frac{Dt}{\pi}\right)^{1/2}$$

Equation 2.5a

Where:

Q = Amount of drug released per unit surface area

D = Diffusion coefficient of the drug in the matrix

C_o = Initial concentration of drug in the ointment

t = time

This equation holds for a homogenous phase where the fraction released is less than about 30%. Desai *et al.* (1965) modified the equation to describe drug release from a heterogeneous phase (Equation 2.5b):

$$Q = 2\varepsilon C_o\left(\frac{Dt}{\tau\pi}\right)^{1/2}$$

Equation 2.5b

Where:

ε = the porosity of the matrix

τ = the tortuosity of the capillary system

Higuchi (1961) also examined the release of drug from a saturated system and proposed equation 2.6a for the release from planar matrix systems:

$$Q = [D(2C_o\text{-}C_s)\, C_s t]^{1/2}$$

Equation 2.6a

$$Q = (2C_o D C_s t)^{1/2}$$

Equation 2.6b

$$\frac{dQ}{dt} = (C_o D C_s / 2t)^{1/2}$$

Equation 2.6c

Where:

C_o = Total amount of drug in unit volume of matrix

C_s = Solubility of drug in polymeric matrix

The drug in the outside layer is thus dissolved first and can diffuse out. In a non-swellable system, this process continues with the interface between the bulk solution and the solid drug moving towards the interior of the system. If C_o is a lot greater than C_s, as is often the case, then equation 2.6a can be reduced to Equation 2.6b. The amount of drug released is thus proportional to the square root of time. The rate of release (dQ/dt) can be derived from equation 2.6b to give equation 2.6c. The rate of release can therefore be altered by the total concentration of drug available (C_o) and by increasing or decreasing the drugs solubility (C_s) in the polymer by complexation.

The release of a solid drug from a granular matrix involves the simultaneous penetration of the surrounding liquid, dissolution of drug, and leaching out of the drug through interstitial channels. This leads to a diffusional equation that takes into account the volume and length of opening in the matrix:

$$Q = \left(\frac{D\varepsilon}{\tau}(2C_o - \varepsilon C_s)C_s t\right)^{1/2}$$

Equation 2.7

For the purpose of data treatment, all of these equations can be reduced to:

$$Q = kt^{1/2}$$

Equation 2.8

A plot of the amount of drug released versus the square root of time will be linear if the release of the drug from the matrix is diffusion controlled. If this is the case, then one may control the release of drug from a homogeneous matrix system by varying the initial concentration of drug in the matrix, the porosity or tortuosity of the matrix or the solubility of the drug.

2.3 DRUG RELEASE FROM SWELLABLE DEVICES

The release of a drug substance from a dehydrated (glassy) hydrogel matrix involves several interrelated steps as reviewed by Colombo (1993):

a) Absorption of penetrating media with subsequent swelling of the hydrogel matrix. Thermodynamic compatibility between the solvent (usually aqueous based) and the hydrogel is important for swelling to occur.
b) Dissolution of the contained drug substance.
c) Counter current diffusion of the solute out of the system.

A complicated process results, where drug diffusion is coupled to the swelling kinetics of the system. Much of the work on drug release from swellable hydrophilic systems described below has been performed using crosslinked systems such as poly(2-hydroxyethyl methacrylate) (pHEMA) and copolymers (e.g. Korsmeyer and Peppas, 1984; Lee, 1985; Brannon-Peppas and Peppas, 1989; Shah, 1991; Lee and Kim, 1991; Brazel and Peppas, 1999a,1999b), other hydrogels such as poly(vinyl alcohol) (e.g. Brazel and Peppas, 1999a, 1999b; Mandal, 2000) or using swellable hydrophilic polymer matrices such as hydroxypropyl methylcellulose (HPMC) (Panomsuk *et al.*, 1995; Siepmann *et al.*, 1999).

2.3.1 Diffusion and hydrogel swelling

Hydrogel swelling occurs due to diffusion of the penetrant molecules into the polymer matrix. Crank (1975) proposed that three successive steps occurred in the swelling of a gel from its dry state: (1) diffusion of water molecules into the polymer network, (2) relaxation of polymer chains with hydration, and (3) expansion of the polymer network into the surrounding bulk water medium with hydration. The swelling behaviour thus depends on which step becomes rate determining. Three classes of diffusion processes were distinguished according to the relative rate of diffusion and polymer relaxation:

- Case I or Fickian diffusion
- Case II diffusion
- Non-fickian or anomalous diffusion

In Case I, or Fickian diffusion, relaxation of polymer chains does not occur throughout the whole process and the water diffusion process becomes the dominant factor. In this case, water uptake behaviour can be described by the diffusion equation (Fick's second law, equation 2.2). A square root of time relationship results. Crank (1975) proposed the following equation, for diffusion in a plane sheet (i.e. where the diffusing substance enters through the plane faces and a negligible amount through the edges):

$$\frac{W_{H2O}(t)}{W_{H2O}(\infty)} = 4\left(\frac{Dt}{\pi l^2}\right)^{1/2}$$

$$\text{For } 0 \leq \frac{W_{H2O}(t)}{W_{H2O}(\infty)} \leq 0.6$$

Equation 2.9a

Where

D = diffusivity of water in the polymer

l = membrane thickness

$W_{H2O}(t)$ = total amount of water absorbed by the membrane at time t

$W_{H2O}(\infty)$ = total amount of water absorbed by the membrane at the equilibrium state ($t = \infty$)

In this case, the amount of absorbed solvent is proportional to the square root of time.

Case II is the other extreme, in which the diffusion process is very fast compared to the relaxation process. The controlling step is the velocity of the advancing front, which forms the boundary between a swollen gel and a glassy core. The relaxation process becomes the rate-determining step when the diffusion rate is much faster than the relaxation rate. This results in a clear interface between the completely swollen region at the surface side and an internal glassy core. The interface moves into the interior as the solvent uptake proceeds. The absorption rate could be expressed by the following equation for a slab-shaped polymer matrix:

$$\frac{W_{H2O}(t)}{W_{H2O}(\infty)} = \left(\frac{2k_o}{C_o l}\right)t$$

Equation 2.9b

Where:

k_o = the relaxation constant

C_o = equilibrium concentration of solvent in polymer

In this case, the amount of absorbed solvent was proportional to time. Case I and Case II are both simple cases in the sense that the behaviour of each can be described in terms of a single parameter. Case I systems are controlled by the diffusion coefficient. In Case II, the parameter is the constant velocity of an advancing front, which is the boundary between swollen gel and glassy core. Non-Fickian or anomalous diffusion describes situations where the diffusion rate of solvent molecules is comparable with the relaxation rate of polymer chains. These systems lie between cases I and II and the amount sorbed versus time curve can be represented by a power law relation with an exponent between 0.5 and 1.0. Two or more parameters are needed to describe the interacting diffusion and relaxation effects.

Polymers can be described as being in a rubbery or a glassy state. The essential distinction between these two states is that polymers in the rubbery state respond rapidly to changes in their condition while properties of a glassy polymer tend to be time-dependent e.g. a stress may be slow to decay after a glassy polymer has been stretched while the stress is reversed almost immediately with a rubbery polymer. Glassy polymers generally exhibit 'anomalous' or 'non-Fickian' behaviour especially when the penetrant causes excessive swelling of the polymer (Crank, 1975). Diffusion is generally Fickian for rubbery polymers. The polymer chains in such rubbery polymers are thought to adjust so quickly to the presence of the penetrant that they do not cause diffusion anomalies.

Swelling ratios have been used to characterise the swelling of hydrogels. The swelling ratio (S.R.) is the weight of the absorbed water per weight of dried polymer disc and has been defined in several ways (Equation 2.10 A-C). For example Yoshida *et al.* (1991b) and Hoffman *et al.* (1986) used equation 2.10A to characterise hydrogel swelling; Okano *et al.* (1990) used equation 2.10B while Gutowska *et al.* (1992) and Mandal (2000) used equation 2.10C.

$$\text{S.R. (A)} = \frac{W_s}{W_d}, \qquad \text{S.R. (B)} = \frac{W_s + W_d}{W_d}, \qquad \text{S.R. (C)} = \frac{W_s - W_d}{W_d}$$

Equation 2.10

where

W_s = weight of the swollen membrane at time t

W_d = weight of the dried disc

In each case, the swelling ratio produces a value for the actual swelling of the hydrogel relative to its original dry weight.

2.3.2 Drug release from hydrogels

As shown above, the swelling of hydrogels is governed by the relative rate of penetrant diffusion and polymer relaxation. In a drug loaded hydrogel matrix, the diffusion of the drug substance from the system is coupled to this process. Fig 2.1(i and ii) shows a schematic of the hydrogel swelling process and concomitant drug release. An initially glassy hydrogel (B), containing solid drug (D), is placed in an aqueous solvent (A) at time zero (Fig 2.1(i)) (from Davidson and Peppas, 1986; Grassi et al., 1998; Brazel and Peppas, 2000)

The penetrant (A) diffuses into the polymer network causing a depression in the glass transition temperature of the polymer, eventually reaching a high enough concentration to cause the polymer region to swell and become rubbery (Brazel and Peppas, 2000). Several moving boundaries result (Fig 2.1(ii)). The swelling front (S) separates the glassy portion of the system from the rubbery one, and moves towards the glassy core. At the same time, the polymer/penetrant interface (S') moves outwards displacing the penetrant medium. The drug present (D) dissolves and diffuses out across the gel layer. A diffusion front (not shown in Fig. 2.1(ii)) may separate the regions of undissolved and dissolved drug, and follows the swelling front in its motion. A drug concentration well below its solubility threshold in the penetrant will cause the swelling front (S) and diffusion front to coincide (Grassi et al., 1998). The rate of diffusion of the drug out of the system is dependent both on the rate of penetrant uptake by the system and the rate of diffusion of the drug through the rubbery layer (Davidson and Peppas, 1986).

A theoretical concentration profile of both the solvent and the solute during the swelling-controlled release process are also shown in Fig 2.1 (iii and iv). Water concentration in the rubbery region increases with distance from the centre of the system (Fig 2.1(iii)). A corresponding drug concentration gradient would exist in this rubbery region and would depend on properties of the drug (Fig. 2.1(iv)). Sink conditions are assumed in the bulk region.

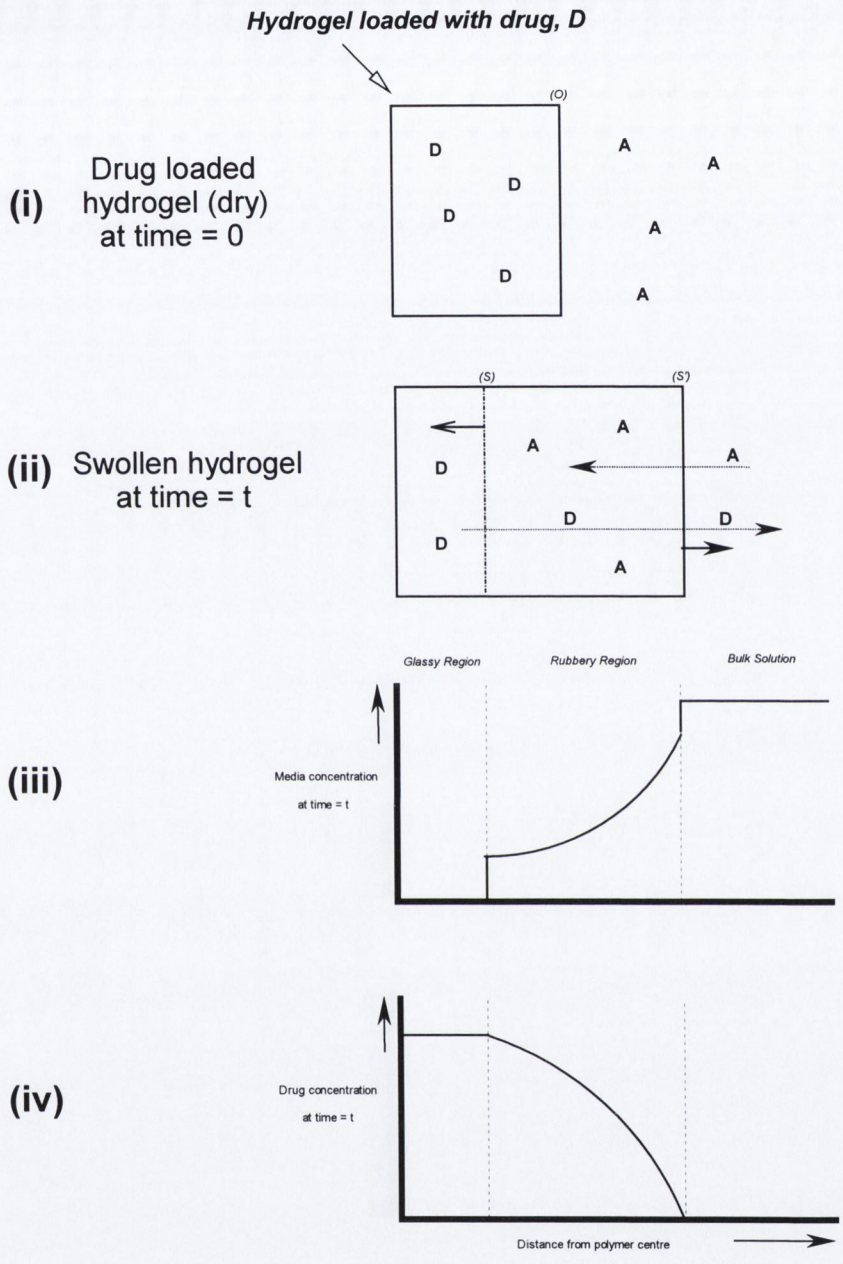

Fig. 2.1: Schematic of desolvated hydrogel containing drug **D**, placed into aqueous medium, **A** (i) at time zero and (ii) after time, *t*. Also shown are theoretical concentration profiles at time *t* of (iii) water during the swelling controlled release process where the glassy/rubbery front still exists and of (iv) drug (**D**) during the swelling controlled release process

[Only one surface is exposed to aqueous media for clarity. Boundaries: ***(S)*** swelling front/drug diffusion front between drug core and rubbery hydrated hydrogel, ***(O)*** original polymer/penetrant interface at T=0, ***(S')*** interface between rubbery hydrogel and bulk solution]

Release from swellable hydrogels has been generally described by the following empirical equation (Ritger and Peppas, 1987b):

$$F = kt^n$$

Equation 2.11

Where:

F = fractional drug release (or fraction swelling)

t = time

k = kinetic constant characteristic of system

n = exponent

Equation 2.11 is frequently used in describing the relative importance of Fickian (n = 0.5) and Case II (n = 1.0) transport in drug release. The same equation is often used to describe the swelling process. For n = 0.5 the solvent diffusion or drug release follows a Fickian diffusion mechanism. For n > 0.5, non-Fickian or anomalous diffusion behaviour is generally observed. The special case of n = 1.0 gives rise to a Case II transport mechanism, resulting in zero-order drug release. Equation 2.11 is useful in the analysis of Fickian and non-Fickian diffusional release from non-swellable (Ritger and Peppas, 1987a) and swellable (Ritger and Peppas, 1987b) polymeric devices.

Higuchi's diffusional equation (Equation 2.5a) can be expressed in terms of the fraction released (F) from a dosage form

$$F = kt^{1/2}$$

Equation 2.12

This is the specific case of equation 2.11 where solvent uptake or solute release can mainly be described as a diffusional process.

2.3.2.1 Mechanism of release

The release of drug substances from hydrogels swollen to their equilibrium state varied with the square root of time according to Fick's law. Katime *et al.* (2001) showed Fickian release of theophylline and aminophylline from swollen acrylic acid/n-alkyl methacrylate hydrogels.

The swelling and release of drugs from an initially dehydrated, but swellable device, has been shown to follow mechanisms ranging from Fickian to Case II through to super Case II, where the diffusion exponent n > 1.0.

Fickian swelling and release from initially dried hydrogels can depend on the polymers and drugs used. Mandal (2000) showed Fickian release of miconazole from several PVA hydrogels. Katime *et al.* (2001) showed approximately Fickian release of theophylline from dried acrylic acid/n-alkyl methacrylate hydrogels while release of aminophylline was non-Fickian, in comparison to the Fickian release of both drugs from the swollen membrane as detailed above.

The existence of some molecular relaxation process in addition to diffusion is believed to be responsible for the non-Fickian behaviour. Swelling of pHEMA and its copolymers has been shown to be non-Fickian (Korsmeyer and Peppas, 1984). Korsmeyer and Peppas (1984) demonstrated quasi-zero order release of theophylline from initially dry hydrogels depending on the co-polymer composition and sample thickness. Zero-order release of drug has been shown (Ritger and Peppas, 1987b; Lee, 1985) when the drug penetrant front moved at a constant rate into the matrix, with drug release controlled by penetration of the media. The release mechanism was also affected by drug molecular size and drug loading as described below.

2.3.2.2 Effect of drug molecular size

In addition to the effect of swelling kinetics on drug release, the drug molecular size has also been shown to affect the mechanism of release from swellable systems. Vyavahare *et al.* (1990) reported zero-order release of benzoic acid from glassy pHEMA, whereas release of a bulkier theophylline was shown to follow anomalous kinetics. The same group (Shah *et al.*, 1991) subsequently modified pHEMA to make it pH dependent [poly(HEMA-co-4-carboxy styrene)] and reported zero-order release of theophylline at pH 11. The change in release mechanism resulting in zero-order release was attributed to an increase in the diffusivity of the active ingredient due to the enhanced swelling at pH 11, rather than Case II transport controlled penetration of the medium.

2.3.2.3 Effect of drug loading

Lee (1985) examined the effect of thiamine hydrochloride and diclofenac sodium on penetration of solvent and drug diffusion fronts into pHEMA beads. The water-soluble thiamine HCl altered both the swelling osmotic pressure and the associated time-dependent relaxation of the hydrogel network during the simultaneous absorption of water and desorption of drug. An increased drug loading resulted in a change in the relative importance of the diffusion process versus the polymer relaxation as a function of drug loading. The fractional release and solvent front penetration displayed more Fickian-like behaviour as the water-soluble drug loading level increased.

Drug precipitation was observed with higher loadings of diclofenac sodium. In addition, a second slow moving front was seen separating the precipitated phase from the clear swollen region. Lee (1985) subsequently suggested that the solvent penetration front proceeded much faster than the

drug diffusion front because of relatively low drug solubility and the associated slow rate of dissolution. It was suggested that the opaque drug core might mask the rapid solvent penetration.

Lee and Kim (1991) also reported that the initial swelling front penetration into pHEMA was observed to exhibit more Fickian-like character as drug loading increased. This was attributed to a change in relative importance of the diffusion process versus the polymer relaxation as a function of drug loading. A double front formation, namely a swelling front and a drug dissolution front, was reported for diclofenac sodium but not observed with the more soluble oxprenolol hydrochloride.

2.4 SWELLING AND DRUG RELEASE FROM PNIPA HYDROGELS

The mechanism of release from thermoresponsive hydrogels is further complicated due to the effect of temperature on the swelling of the hydrogel and on the diffusion coefficient of the drug. Several different models of drug delivery from thermoresponsive hydrogels have been proposed in the literature (Hoffman, 1987; Yoshida *et al.,* 1994; Bromberg and Ron, 1998). These models are illustrated in Fig. 2.2 (i and ii) and are examined in the following sections.

2.4.1 Hydrogel loading

The most widely used method of hydrogel drug loading is that illustrated in Fig. 2.2(i)A where the preformed purified gel is allowed to swell in a drug-containing solution (e.g. Bae *et al.,* 1987; Gutowska *et al.,* 1992; Yoshida *et al.,* 1994a). The solvent can subsequently be removed (Fig. 2.2(i)C). The exclusion of large molecules, larger than the mesh size of the swollen hydrogel, is a limitation of this approach although non-aqueous solvents can be used to enhance swelling. Another drug loading technique involves mixing the drug with the appropriate monomer, crosslinker and initiator solution, which is then allowed to polymerise, entrapping the drug within the formed matrix (Kim *et al.,* 1992). This technique of loading may cause a side reaction or denaturation of the drug/protein and purification of the system of reaction reagents is also an issue. Gehrke *et al.* (1995) used another loading technique involving the partitioning of proteins into the gel phase.

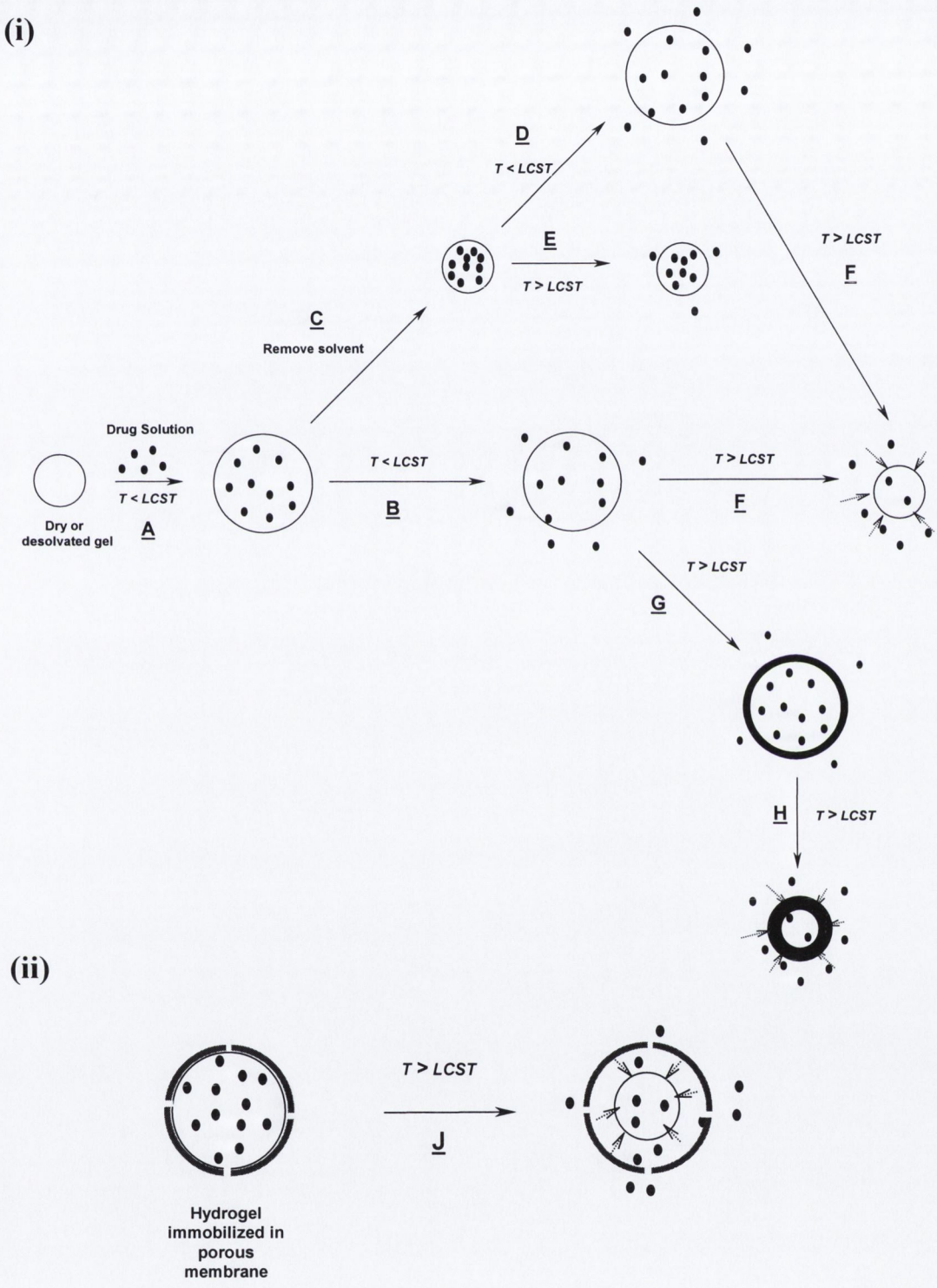

Fig. 2.2: Schematic of the various drug release concepts from thermoresponsive hydrogels as proposed in the literature. Each step, designated by a letter, is described in the text. The temperature is set at either above (T>LCST) or below (T<LCST) the LCST of the hydrogel.
(i) hydrogel alone, (ii) hydrogel immobilised in a porous membrane.
(→) indicates hydrogel deswelling or squeezing effect.

2.4.2 Swelling/deswelling kinetics and drug release from thermoresponsive hydrogels

Drug release from these systems can occur during the swelling of the hydrogel, either above (Fig 2.2(i)E) or below (Fig. 2.2(i)B/D) the LCST or in the deswelling/shrinking process on temperature "switch" (Fig. 2.2(i) F/G/H/J). A desolvated or partially swollen hydrogel can swell at a temperature below the LCST, resulting in diffusion of the drug from the system (Fig 2.2(i)B/D). The degree of swelling is time and temperature dependent but is also dependent on the comonomers present and the degree of crosslinking. If the hydrogel system is desolvated or already in a collapsed state and at a temperature above the LCST, swelling and drug diffusion may or may not occur depending on the comonomers present and on the degree of crosslinking (Fig 2.2(i)E).

Several different mechanisms of drug release, ranging from Fickian to Case II have been shown in a variety of thermoresponsive hydrogels. The hydrogels used in these studies can be divided into three main types (all containing a crosslinker). The first type is N-isopropylacrylamide (NIPA) copolymerised with a hydrophobic comonomer such as an alkyl methacrylate (Bae *et al.*, 1987; Yoshida *et al.*, 1991,1994b; Okano *et al.*, 1990; Gutowska, *et al.*, 1992). The second type is pure PNIPA (Hoffman *et al.*, 1986; Andersson *et al.*, 1997; Makino *et al.*, 2001; Wu *et al.*, 2003; Zhang *et al.*, 2002). The third type is NIPA copolymerised with a hydrophilic comonomer (Yoshida *et al.*, 1994a, 1994b; D'Emanuele and Dinarvand, 1995; Dinarvand and D'Emanuele, 1995). In cases where PNIPA is copolymerised with another monomer, the hydrogel can be described as heterogeneous.

2.4.2.1 PNIPA hydrogels containing hydrophobic comonomers

Much of the work to date involving drug release from thermoresponsive systems has been carried out on heterogeneous PNIPA hydrogels using an alkyl methacrylate (RMA) like butyl methacrylate (BMA) as a hydrophobic comonomer [Bae *et al.*, 1987, 1991b; Okano *et al.*, 1990; Yoshida *et al.*, 1991a, 1991b, 1992, 1994a]. The addition of this comonomer, shown in Fig. 1.8, has the effect of

- decreasing the phase transition of the system (Yoshida *et al.*, 1994b)
- increasing the mechanical strength of the hydrogel (Bae *et al.*, 1987),
- forming an "enhanced skin type layer" by collapsing of the long chain hydrophobic comonomers on the surface of the hydrogel on increasing temperature (e.g. Yoshida *et al.*, 1994b) (Fig 2.2(i) G/H).

Yoshida *et al.* (1991a) used a monolithic device to show zero-order release of indomethacin. Conditions of high drug loading in polymer matrices of poly(NIPA-co-RMA) gave approximately

zero-order release patterns. Okuyama *et al.* (1993) and Yoshida *et al.* (1994a) showed that swelling of a poly(NIPA-co-BMA) hydrogel from the dried state was proportional to the square root of time above the phase transition temperature. Two further swelling profiles were obtained below the LCST, attributed to the influence of polymer relaxation processes. At 20°C, swelling increased linearly with time due to Case II transport mechanisms. At 10°C, a sigmoidal swelling pattern was observed. The difference in the swelling patterns below the LCST was attributed to different constraining forces for swelling. The release mechanism of indomethacin followed the swelling patterns, being zero-order at 20°C and sigmoidal at 10°C.

Okano and co-workers (Bae *et al.,* 1987, 1991b; Okano *et al.,* 1990; Yoshida *et al.*, 1991a, 1991b, 1992, 1994a; Okuyama *et al.* 1993) have generally concentrated on the release of the model drug indomethacin from the system. The release of other model drugs from NIPAA-co-RMA systems included heparin (Gutowska *et al.,* 1992) and insulin (Okano *et al.,* 1990).

Co-polymerisation of PNIPA with an alkyl methacrylate appeared to result in the reversible formation of an "enhanced dense surface layer" in response to stepwise temperature change. This dense skin layer may be used in surface-regulated "on-off" release while the core remains swollen (Fig 2.2(i)G). Gradual gel deswelling can also occur (Fig, 2.2(i)H). The surface skin layer is then thought to stop drug release from the polymer matrix. 'On-off' release profiles of indomethacin have been described in response to a stepwise temperature change [Bae *et al.,* 1987; Okano *et al.,* 1990; Yoshida *et al.,* 1991b]. The temperatures chosen were below and above the LCST, namely 20°C/25°C and 30°C. Pulsatile release was explained by the formation of a dense, less permeable surface layer of gel, described as an "enhanced skin-type barrier". The length of the alkyl side chain was shown to control the thickness and density of the surface skin layer (Yoshida *et al.,* 1994b).

It has also been suggested that the properties of the skin-type barrier are influenced by the temperature difference between the initial and final medium and the presence of a hydrophilic drug within the hydrogel (Gutowska *et al.,* 1992). The rate of deswelling depended on the temperature of the initial equilibrium, with control of the release rate from a swollen hydrogel possible by optimising the initial loading temperature.

While the off phase above has been attributed to the presence of the enhanced skin layer caused by the RMA, all thermoresponsive hydrogels, including homogenous PNIPA hydrogels or those modified with a hydrophilic comonomer, would be expected to form a relatively dense surface layer in the initial stages of shrinkage (Hoffman, 1986). This "skin layer" consists of hydrophobically collapsed polymer chains to the outside of the swollen hydrogel when it is placed

into a medium above its LCST. The contraction/deswelling process would then move towards the inside of the hydrogel at a rate dependent on the magnitude of temperature switch and the properties of the comonomers. When fully deswollen, the whole system would take on the properties of the hydrophobically collapsed polymer.

Some attempts have also been made in the literature to theoretically characterise contraction/deswelling and drug release profile in thermoresponsive hydrogels. Yoshida *et al.* (1992) studied the drug release profile during the shrinking process of poly(NIPA-co-RMA) gels. They created a drug release model for the shrinking process using a tortuous pore model and simulated four decreasing patterns of release rate for different induction patterns of pressure. Colombo *et al.* (1996) modelled the phase transition and sorption/desorption kinetics in several thermosensitive hydrogels using thermodynamic phase equilibrium models.

2.4.2.2 Homogeneous PNIPA hydrogels

Studies by Andersson *et al.* (1997) and Makino *et al.* (2001) using homogeneous PNIPA examined drug release at temperatures either side of the LCST. Andersson *et al.* (1997) studied the effective diffusion coefficients of glucose and insulin at various temperatures from the equilibrated hydrogel at that temperature as illustrated in Fig 2.2(i)B/E. Their results showed an increased resistance for diffusion inside the gel at higher temperatures, due to a lower degree of hydrogel swelling at that temperature. The network was shown to have a considerable effect on insulin which has a MW ~5,800. The effect of higher temperature on diffusion of the much smaller glucose was more important. They concluded that for small molecules the effect of the network was negligible. Makino *et al.* (2001) examined the release of dibucaine HCl, sodium benzoate and theophylline at 25°C (Fig 2.2(i)D) and 40°C (Fig 2.2(i)E). Differences in release rates were attributed to electrostatic attractive or repulsive forces between the drugs and the polymer chains.

Hoffman *et al.* (1986) examined the release of Vitamin B12 (MW 1,350) and myoglobin (MW 16,890) on heating the loaded swollen hydrogel from 4°C to 50°C as illustrated in Fig 2.2(i)F. A complex release pattern occurred with an initial rapid release followed by a slower release. The release pattern was attributed to the increasing hydrostatic pressure within the hydrogel as it collapsed. They also showed that none of the hydrogels prepared were able to absorb chymotrypsin (MW25,000) and this was attributed to gel pore size at different temperatures.

Pulsatile "on-off" drug release from homogeneous PNIPA hydrogels has not been presented to date.

2.4.2.3 PNIPA hydrogels containing hydrophilic comonomers

Hydrophilic comonomers have been used to increase the phase transition temperature of PNIPA towards body temperature (Schild, 1992; Dinarvand and D'Emanuele, 1995; Yoshida *et al.*, 1994b) and/or to obtain a pH/temperature responsive systems (Brazel and Peppas, 1996; Gutowska *et al.*, 1997). Yoshida *et al.* (1994a, 1994b) described the incorporation of these comonomers as preventing the formation of the "skin type layer" which controlled the "off" phase as described in section 2.4.2.1. Yoshida *et al.* (1994a) incorporated hydrophilic acrylamide (AAm), N,N'-dimethylacrylamide (DMA) and N-acryloylpyrrolidine (APy) as comonomers. The LCST of the poly(NIPA-co-AAm) increased with increasing amount of AAm, but the thermosensitivity of the hydrogel diminished. An off phase was not achieved which was attributed to the hydrophilic AAm preventing formation of the dense shrunken state at higher temperatures. It was also suggested that the hydrophilic comonomer prevented the formation of the enhanced dense skin layer when BMA was also incorporated. Poly(DMA) and poly(APy) themselves showed negative temperature dependence of swelling and on-off drug release of indomethacin was shown using a poly(NIPA-co-DMA) hydrogel.

Some authors have combined the temperature sensitivity of NIPA with an ionic comonomer to give a pH and temperature responsive system. Brazel and Peppas (1996) attempted the pulsed release of heparin (molecular diameter ~30Å) and streptokinase (~55Å) by changing the pH and temperature. The hydrogels used were only capable of the pulsatile streptokinase release with the much smaller heparin molecule diffusing equally rapidly in the collapsed (mesh size ~ 100Å) and swollen (mesh size ~ 125Å) hydrogel states. Vakkalanka *et al.* (1996), using NIPA copolymerised with methacrylic acid or acrylic acid, also altered the release rate of streptokinase using pH and temperature. The ionic components resulted in increased swelling at high pH and thus an increase in release rate. Gutowska *et al.* (1997) utilised a cationic gel that would swell at low pH. The squeezing effect of the system on increasing pH (from stomach to intestine) caused an increase in release rate of dyphylline (diprophylline) from the enclosed hydrogel at 37°C.

With homogenous or hydrophilically-modified PNIPA hydrogels, a drug pulse on increasing temperature was also evident (Dinarvand and D'Emanuele, 1995; Brazel and Peppas, 1996; Zhang *et al.*, 2002). This drug pulse has been used as one way of obtaining positive thermosensitive release as illustrated in Fig 2.2(ii).

2.4.3 Positive thermosensitive release

PNIPA hydrogels swell below the LCST and shrink/deswell above the transition temperature, resulting in negative thermosensitive release of drug with a greater diffusion rate below the LCST.

Three main approaches have been suggested to achieve positive thermosensitivity (Ichikawa and Fukumori, 1997):

2.4.3.1 Diffusion area regulated mechanism

This approach involves the structural design of a device containing negatively thermosensitive hydrogels. A hydrogel immobilized within a porous membrane results in positive release as the swollen membrane blocks both diffusion and convective flow through the pores and allows permeation when collapsed (Fig. 2.2(ii)).

Diffusion of drug from the system is regulated in part by the size of the pores within the membrane. The ability of the system to squeeze drug out would also be important. Yoshida *et al.* (1994c) used a poly(NIPA-co-AAm) system enclosed within an impermeable capsule with a releasing orifice to demonstrate positive thermosensitive release of indomethacin. Zhang *et al.* (2002) showed positive release of 5-fluouracil from a hydrogel enclosed in a dialysis bag. Gutowska *et al.* (1997) used a poly (NIPA-co-acrylic acid) hydrogel to show positive thermosensitive release of acetaminophen.

2.4.3.2 Matrix pumping

This approach utilises the squeezing mechanism that occurs on increasing the temperature of negatively thermosensitive hydrogels. Yoshida *et al.* (1991c) utilised the thermoresponsive methacryloyl-L-proline/PEG no. 600 dimethacrylate gel. The swollen system had a large number of micropores, which did not disappear on increasing temperature. As a result the release rate of testosterone was enhanced at higher temperatures due to the matrix pumping function. In these systems it was difficult to obtain an off state. Miyajima *et al.* (1993) developed positive thermosensitive release systems based on hydrogel of acryloyl derivatives with pendant alpha-amino acids to show matrix pumping function.

Shin *et al.* (2001) developed interpenetrating networks of PNIPA and tailored nanoporous silica to obtain a sustained positive thermoresponsive drug release profile of indomethacin. It was proposed that on increasing temperature, the drug was squeezed into the porous channels and at the same time it opens the porous channels to the outside media. The drug then diffused out from these channels.

2.4.3.3 Positive thermoresponsive hydrogels

The positive temperature dependent gels as described in section 1.4.3 swell to a greater extent at higher temperatures and may therefore be useful for development of positive temperature dependent drug release.

CHAPTER 3

Materials and Methods

3.1 MATERIALS

Material (abbreviation)	*Supplier/Manufacturer*
Ammonium Persulfate (APS)	Aldrich
Benzoic Acid (BA)	Sigma
Benzoic Acid, Sodium Salt (NaB)	Sigma
Deionised Water	-----
Diltiazem HCl (DHCl)	Seloc
Diltiazem Base (DB)	Elan 17/04/1994
Dextran MW 10,200	Sigma
Dextran MW 43,000	Sigma
Dextran MW 68,800	Sigma
Disodium hydrogen phosphate dodecahydrate	Merck
Dimethylformamide (DMF)	Riedel-de Haën
Ethanol, 98%	Trinity Stores
FITC-Dextran MW 4,000	Sigma
FITC-Dextran MW 9,500	Sigma
FITC-Dextran MW 42,000	Sigma
FITC-Dextran MW 77,000	Sigma
Methyl 4-hydroxybenzoate (MHB)	Aldrich
N, N' methylenebisacrylamide (MBA)	Aldrich
N-isopropylacrylamide (NIPA)	Aldrich
Nitrogen Gas	Boc Gases
N,N,N',N' Tetramethylenediamine (TEMED)	Aldrich
Polystyrene standards (GPC)	Polymer Laboratories
Propyl 4-hydroxybenzoate (PHB)	Aldrich
Sodium Chloride	BDH
Sodium dihydrogen phosphate dihydrate	Merck
Vitamin B12 (VB12)	Sigma

Instrumentation

Waters 410 Differential Refractometer, Waters 510 pump

Mettler Toledo 821^e Differential Scanning Calorimeter (DSC)

Single Cell Peltier temperature controller (Thermo Electron Corporation, U.K.)

Siemens D500 Diffraktometer

Sotax AT7 USP paddle method dissolution bath

VirTis BenchTop 6K Freeze Dryer

Scanning Electron Microscopy (SEM) Hitachi S-35500

Nova 4200e Surface Area and Pore Size Analyser

Nicolet Magna-Infrared (IR) 560 Spectrometer

Helium pycnometer (Micromeritics AccuPyc 1330)

Cecil CE2020 Ultra Violet (UV) Spectrophotometer

Turner Quantech Digital Filter Fluorometer

Software

Imagetool for Windows ® Version 3.00

Cecil Dissolution Software Version 5.0

Micromath Scientist for Windows ® Version 1.0 (Micromath Scientific Software)

Accelrys' Materials Studio® Version 2.1.5

Minitab® statistical software Version 13.32

3.2 METHODS OF SYNTHESIS

3.2.1 Hydrogel

A series of PNIPA hydrogels (PNIPA-H) were prepared in a cylindrical plastic tube (internal diameter 15 mm) in distilled water at 20°C using TEMED (8.17 mol % based on monomer) and APS (1.91 mol %) as initiator and propagator respectively (Schild, 1992). Various percentages of MBA were used as the crosslinker [PNIPA-H1 (1.15 mol %), PNIPA-H2 (2.22 mol %), PNIPA-H3 (5.68 mol %), PNIPA-H4 (11.17 mol %)]. Nitrogen was bubbled through the solution for 15 minutes before the addition of the TEMED. The polymerisation mixture was left standing at room temperature for 1 hour to ensure that all the monomer had reacted. The prepared hydrogels were sliced into discs and cleaned by repeatedly swelling in water followed by heating to approximately 50°C. They were then filtered and dried in a vacuum oven at 50°C for 48 hours. The dried discs (50mg) had diameter 6mm and height ~1.5mm.

3.2.2 Linear polymer

A linear polymer (PNIPA-L) was synthesised in a similar manner to the hydrogels but without the crosslinker. After the polymerisation process, the solution obtained was heated above 50°C, the precipitated polymer collected by filtration, washed with hot water at ~50°C and then dissolved in cold water at room temperature. This process was repeated several times to purify the polymer. The collected polymer was then dried in a vacuum oven at 50°C for 48 hours.

3.3 METHODS OF CHARACTERISATION

3.3.1 Gel Permeation Chromatography

The molecular weights of batches of PNIPA-L were determined by gel permeation chromatography, using a method similar to that described by David *et al.* (2003). Solutions of the polymers and polystyrene standards (2mg/ml) were prepared in DMF and 100 µl was injected into a system consisting of a Waters Styragel® HR column, a Waters 510 pump and a Waters 410 Differential Refractometer (elution rate 1ml/min). The internal temperature was set at 40°C. Millennium® 2010 software was used to integrate the peaks. Samples were injected in triplicate and the elution time compared with the calibration curve given in Appendix IB.

3.3.2 Glass transition temperature (Tg)

All Differential Scanning Calorimetry (DSC) analysis was performed using a Mettler Toledo 821^e DSC. Temperature calibration was performed using an indium standard.

The glass transition temperatures (Tg) of PNIPA-L, PNIPA-H and the various drug/polymer co-precipitated blends were determined using 5-10mg dried samples run in an open pan i.e. a hermetically sealed aluminium pan with three vent holes pierced in the lid. All samples were initially heated to 180°C at 10°C/min, cooled to 25°C at 20°C/min followed by heating to 260°C at 10°C/min. The first heating cycle was to remove all residual moisture/solvent and erase the effect of previous thermal history. Each sample was analysed in duplicate and the glass transition temperature was taken as the midpoint of the inflection.

The Tg's of the crystalline drugs were determined (where appropriate) by melting the drug, followed by quench cooling in liquid nitrogen before scanning from –40°C to 260°C at 10°C/min.

3.3.3 Phase transition temperature (LCST)

3.3.3.1 DSC ($LCST_d$)

The LCST of PNIPA-L (1.4 %w/v solution, unless otherwise stated) was determined using an aqueous sample (30-40mg by weight) run in a sealed pan under nitrogen purge at a heating rate of 2°C/min (unless otherwise stated). Samples were scanned in the range of 25°C to 40°C. Various groups have defined the transition temperature as either the temperature of onset (e.g. Otake *et al.*, 1990) or as the peak temperature (e.g. Eeckman *et al.*, 2001). The phase transition in the current thesis was taken as the maximum of the endothermic transition peak (average of two measurements).

The effect of the drug substances on the transition temperature was investigated using a similar method by scanning the polymer solution (1.4 %w/v solution at 2°C/min) in the presence of various concentrations of the model drug. Samples (previously stored at 4°C) were maintained at 10°C for 5 minutes and then heated at a rate of 2°C/min to 35°C.

3.3.3.2 Transmittance measurements ($LCST_t$)

The LCST of the linear polymer (PNIPA-L) was measured by determining the turbidity of the polymer solution as a function of temperature (Eeckman *et al.*, 2001). The transmittance of a 1.4% w/v PNIPA-L solution in phosphate buffer pH 6.8 (Sorensons buffer, isotonic) (PB) (unless otherwise stated) was measured at 500nm with the temperature controlled by a Single Cell Peltier

temperature controller (Thermo Electron Corporation, U.K.). Solutions also containing a specified concentration of a model drug were examined. A magnetic flea stirrer was used to maintain agitation of the solutions during the heating process. The % transmittance of the solution was determined at specified temperature intervals, at a heating rate of ~0.5°C/min. Various authors have defined the LCST differently, usually as a % transmittance of the polymer solution during the heating process. Kohori *et al.* (1998) calculated the LCST as the "onset of turbidity"; Tachibana *et al.* (2003) as 90% transmittance; Aoki *et al.* (1998) and Wang *et al.* (2002) as 50% transmittance with Eeckman *et al.* (2001) calculating the transition as the "abscissa of the inflection point". The LCST of the PNIPA-L in the present work is defined as 50% transmittance of the polymer solution during the heating process.

3.3.4 Drug solubility studies

Solubility studies (Chiou and Kyle, 1979) were carried out at either 25°C or 37°C in a jacketed-water vessel containing PB. Excess drug was added and solutions were agitated using an overhead stirrer (Heidolph) at 300 r.p.m. The solution was then assayed in triplicate at appropriate time intervals until equilibrium solubility was reached.

3.3.5 X-Ray diffraction

X-ray powder diffraction patterns of the pure drugs, polymer (PNIPA-L) and drug-polymer co-precipitate blends were obtained using a Siemens D500 Diffraktometer. Samples were evaluated from 5-35 2Theta degrees, using a 1.00° dispersion split; a 1.00° scatter split and a 0.15° receiving split. The Cu anode X-ray tube was operated at 40kV and 30mA and diffraction patterns were recorded using nickel filtered kα radiation. All samples were mounted such that the surface of the sample was level with that of the holder.

3.3.6 Swelling studies

Hydrogel swelling over time and equilibrium swelling at a particular temperature was examined. All swelling studies were performed in PB unless otherwise specified. The hydrogels were dried in a vacuum oven at 50°C for 48 hours and weighed (W_d). To determine equilibrium swelling, the dry disc was then placed into an excess of the swelling media at a specific temperature and the disc was allowed to swell to equilibrium. Swelling studies over time were performed in 900ml PB in a USP paddle method dissolution bath (Sotax AT7). The swollen hydrogel was briefly removed from the media at certain time intervals and blotted with filter paper to remove any excess surface moisture before weighing. This procedure was performed in triplicate in each case. Swelling studies on drug-

loaded systems were carried out in an identical manner and the discs were transferred between identical baths maintained at either 25°C or 37°C for pulsatile swelling studies.

The phase transition temperature ($LCST_s$) was determined by decreasing the temperature of the media daily to allow equilibrium swelling at that particular temperature. The LCST was defined here (based on n = 3 measurements) as the temperature at which the hydrogel showed a statistically significant ($p < 0.05$) increase in swelling from the baseline value, the baseline being above the transition temperature.

The ability of the hydrogel (PNIPA-H1) to swell in the presence of the various drugs was also examined. The dried hydrogels (PNIPA-H1), previously weighed, were allowed to swell for 96 hours in 10ml of various concentrations of drug solution at 25°C. A plot of swelling ratio versus drug concentration showed the influence of the drug on the ability of the hydrogel to swell.

The swelling of the hydrogels was then examined using either the swelling ratio (S.R., Equation 3.1a) or the fraction swelling (S, Equation 3.1b):

$$\text{S.R.} = \frac{W_s - W_d}{W_d}$$

Equation 3.1a

$$\text{S} = \frac{W_s - W_d}{W_e - W_d}$$

Equation 3.1b

Where:

W_s = weight of hydrogel at time t

W_d = weight of dry disc

W_e = weight of swollen hydrogel at equilibrium (25°C)

3.3.7 Pore size distribution determination

3.3.7.1 Scanning electron microscope

The hydrogels were allowed to equilibrate for 96 hours at the specified temperature (25°C/37°C) in excess PB before flash-freezing using liquid nitrogen. The samples were then dried overnight using a VirTis BenchTop 6K Freeze Dryer. Samples were fractured, mounted on aluminium stubs and sputter coated with gold prior to examination on a SEM Hitachi S-35500.

Approximate pore sizes in the SEM scans were obtained using Imagetool for Windows ® Version 3.00. Fifty measurements were obtained at random on n = 3 SEM images (magnification X1000). A normal probability distribution was obtained using the average and standard deviation of the data (n = 150).

3.3.7.2 Nitrogen desorption isotherms

The freeze-dried samples obtained above were also used to determine the pore size distribution of the systems. The samples were outgassed at 100°C for 12 hours prior to use. Adsorption and desorption isotherms of nitrogen were measured at 273K using a Nova 4200e Surface Area and Pore Size Analyser. The pore size distribution curve was determined by Quantachrome NovaWin2 software from the desorption isotherm using the model proposed by Barrett, Joyner and Halenda (BJH). Using this technique, mesopore size estimations (NovaWin2, 2003) were obtained from:

$$r_p = \frac{-2\gamma V_m}{RT \ln(P/P_o)} + t$$

Equation 3.2

where

r_p is the radius of the pore

γ is the surface tension of nitrogen at its boiling point (8.85 ergs/cm^2 at 77K)

V_m is the molar volume of liquid nitrogen (34.7cm^3/mol)

R is the gas constant (8.314 X 10^7 ergs/deg/mol)

T is the boiling point of nitrogen (77K)

P/P_o is the relative pressure of nitrogen

t is the thickness of the adsorbed layer.

3.3.7.3 Solute exclusion technique

The pore size distribution of PNIPA-H1 was characterised by the solute exclusion technique (Lin *et al.*, 1987; Wu *et al.*, 1992) using a range of model drugs with various molecular weights (Table 4.4).

Hydrogel discs were dried for 48 hours in a vacuum oven at 50°C and weighed. The hydrogels were then equilibrated in excess PB at either 25°C or 37°C for 72 hours. The swollen hydrogels were weighed (V_t) and placed into drug solutions (5ml) of known concentration (DHCl 25µg/ml, VB 50µg/ml, Dextrans 0.1µg/ml) at either 25°C or 37°C. The systems were allowed to equilibrate for 7 days at the chosen temperature. The gels were then removed from the drug solution and placed in 5ml fresh PB at room temperature for a further 7 days before being assayed (C_e). The

results were compared to a control containing only the model drug maintained under the same conditions. The volume of pores accessible to each drug fraction (V, in ml) was then estimated from the following equation:

$$V = 5\left(\frac{C_e}{C_o}\right)$$

Equation 3.3a

Where

C_o = Initial concentration drug present (expressed in μg/ml) after equilibration of the gels

C_e = Drug concentration (μg/ml) after exhaustive extraction

The volume fraction of pores (VF) with sizes larger than the probing molecule is given by:

$$VF = \frac{V}{V_t}$$

Equation 3.3b

Where

V_t = total volume of media in the gels (ml).

3.3.8 Preparation of polymer/drug co-precipitate blends

A solvent casting method was used to prepare blends of PNIPA-L and the model drugs. Solutions (10% w/v) of the appropriate ratios of drug/polymer were prepared in water or ethanol. This solution was poured into a petri dish and dried under vacuum at room temperature. The prepared solutions were also used for FTIR analysis (section 3.3.9)

3.3.9 Fourier transform infrared spectroscopy (FTIR)

FTIR spectra of PNIPA-L/drug co-precipitate blends were obtained with a Nicolet Magna-IR 560 spectrometer using Zinc Selenide (ZnSe) salt plates (Specac Limited, U.K.). Thin films of the blends were obtained by placing 2-3 drops of the polymer/drug solution prepared in section 3.3.8 onto the plates. The plates were then dried under vacuum at room temperature for 48 hours. The spectra were obtained by averaging 64 scans in the spectral range 4000-400cm^{-1}.

3.3.10 Binding studies

3.3.10.1 Binding isotherm

The nature of the binding between the benzoates and PNIPA-H1 was investigated by the use of binding isotherms (Connors, 1987). Various drug solutions were prepared in either PB or 0.01M HCL (isotonic) (4ml, n = 3) and their absorbance was measured at the appropriate wavelength (Appendix I). PNIPA-H1, previously dried in a vacuum oven for 48 hours, was crushed and 100mg was added to the drug solution maintained at 37°C. After equilibration at 37°C for 24 hours, the samples were filtered through a 0.45μm filter and the absorbance of each solution was determined. An example of the effect of the presence of PNIPA-H1 on the absorbance of various solutions of MHB (in 0.01M HCl) is shown in Appendix VIA.

3.3.10.2 Phase solubility study

The type of phase solubility diagram between two interacting components was determined by complexation solubility analysis using the overhead stirrer solubility method (Corrigan and Stanley, 1981). Solutions (10mls) of the various concentrations of PNIPA-L were added to glass vials immersed in a water bath at 25°C (< LCST). After temperature equilibration, an excess of the drug in the solid state (400mg) was then added to the flasks and the contents were stirred at 300rpm using a glass stirrer. After 2 hours, a 5ml sample was removed, immediately filtered through 0.45μm filters and assayed by UV spectroscopy (Appendix IA). The readings obtained were compared to a control without drug to account for any background absorption.

3.3.11 Density determination

The density of the powdered model drugs and the linear polymer was determined using a helium pycnometer (Micromeritics AccuPyc 1330). Powder samples were previously dried at 40°C overnight in a vacuum oven.

3.3.12 Melting point determination

The melting points of the various crystalline drugs were determined by DSC in an open pan. 5-10mg of sample was heated at a rate of 10°C/min from 25°C to a suitable temperature above the melting point. The melting point was taken as the average onset of melting of three samples.

3.3.13 Calculation of solubility parameter

The solubility parameter is defined as the square root of cohesive energy density and is a measure of the interatomic/molecular interactions. Hansen's approach of partial solubility parameters (Van Krevelen, 1990) defines the solubility parameter as

$$\delta^2 = \delta_d^2 + \delta_h^2 + \delta_p^2$$

Equation 3.4

where δ is the total solubility parameter and $\delta_d, \delta_h, \delta_p$ refer to the contributions from the dispersive forces, hydrogen bonding and polar components respectively. The individual components are calculated using the group functional contributions given by the following equations:

$$\delta_d = \frac{\sum F_d}{V}$$

Equation 3.5a

$$\delta_p = \frac{\sqrt{\sum F_p^2}}{V}$$

Equation 3.5b

$$\delta_h = \sqrt{\frac{\sum E_h}{V}}$$

Equation 3.5c

where F_d, F_p and E_h refer to the functional group contributions to the dispersion, polar and hydrogen bonding components respectively and V is the total molar volume (Van Krevelen, 1990). The values of F_d, F_p and E_h of the functional groups were obtained from the values compiled by Van Krevelen and the total molar volume from the values of Fedors (Van Krevelen, 1990).

The values for sodium benzoate used were obtained from Bustamante *et al.* (2000) who used a modified extended Hansen method to determine the partial solubility parameters of sodium salts.

3.4 DRUG LOADING AND RELEASE

3.4.1 Drug loading

The dried hydrogel discs were loaded by sorption of an aqueous or ethanolic drug solution, followed by solvent removal in a dessicator at room temperature to entrap the drug molecules. Loading of NaB, BA, DHCl, DB, MHB and PHB was ~28% w/w based on dried hydrogel disc (20mg of drug), while that of VB12 was ~8 % w/w loading (4mg of drug) and the dextrans ~4% w/w loading (2mg of drug). Loading content was controlled by complete sorption of a known volume of drug solution (0.4mls) for 48 hours in a suitable glass vial before drying out.

3.4.2 Model drug assays

The dextrans were assayed by detection of a dextran probe (FITC-Dextran) incorporated within the bulk dextran. The concentration of FITC-Dextran released was measured at room temperature using a Turner Quantech Digital Filter Fluorometer at an excitation wavelength of 490nm and emission wavelength of 515nm (Dong *et al.*, 1994). A calibration curve was established for each of the fluorescent probes in the range 0-120ng/ml in PB.

The smaller model drugs were assayed by UV spectroscopy at an appropriate wavelength [BA, NaB (224nm), DB, DHCl (238nm), MHB, PHB (256nm), VB12 (362nm)].

3.4.3 Drug release studies

Drug release studies were carried out in 900ml PB at 25°C or 37°C in a USP paddle method dissolution bath (Sotax AT7, 50 r.p.m.). The loaded discs were maintained in the bath within a wire mesh, which allowed room for swelling/contraction of the hydrogel. In the case of pulsatile drug release, the discs were transferred between identical baths maintained at either 25°C or 37°C. Samples from the bath were taken using an automated dissolution apparatus consisting of an attached Cecil CE2020 Spectrophotometer and Cecil Dissolution Software Version 5. The software was programmed to take samples at appropriate intervals and assayed at the chosen wavelength (section 3.4.2). Alternatively, samples were manually withdrawn from the bath. A 5.0ml sample was withdrawn at appropriate intervals from the same position in the bath. Each sample was replaced with an equal volume of fresh media, which was maintained at the same temperature as the bulk media. Samples were filtered through a 0.45μm filter and analysed.

Results from the release studies were expressed as the cumulative amount of drug (mg, ng or fraction drug loading) plotted against time. The profiles are the average of three determinations with the error bars indicating the standard deviation of these values.

Pulsed release experiments were performed in a similar way. Discs were transferred between 900ml baths maintained at the specified temperature.

3.4.4 Dissolution studies on pure drug discs

Pure drug discs were prepared by compressing 100mg of drug under 2 tonnes of pressure for 5 minutes in a 8mm punch and die set. The rate of dissolution was determined in 900ml PB at 25°C or 37°C in a USP paddle method dissolution bath (Sotax AT7, 50 r.p.m.) using an identical method to that described in the previous section (section 3.4.3)

3.5 MATHEMATICAL MODELLING

The experimental swelling and release data was fitted to the relevant mathematical model using the non-linear curve fitting program Micromath® Scientist™ for Windows™ Version 1.0 (Micromath® Scientific Software). The goodness of fit and suitability of a model was evaluated using the coefficient of determination (CD).

The CD is a measure of the fraction of the total variance accounted for by the model (Scientist Handbook, 1995). It is calculated using the formula

$$CD = \frac{\sum_{i=1}^{n} w_i \, (Y_{obs_i} - \overline{Y}_{obs})^2 - \sum_{i=1}^{n} w_i \, (Y_{obs_i} - Y_{cal_i})^2}{\sum_{i=1}^{n} w_i \, (Y_{obs_i} - \overline{Y}_{obs})^2}$$

Equation 3.6

where n is the number of points, w_i is the weight applied to each point and Y_{obs_i}, $\overline{Y}_{obs}$ and Y_{cal_i} are the observed data points, the weighted mean of the observed data and the model predicted data points, respectively.

3.6 MOLECULAR MODELLING

3.6.1 Molecular size simulation

Approximate molecular diameters of the model drugs in solution were determined using molecular modelling software (Accelrys' Materials Studio® Version 2.1.5). A series of dextrans were constructed using the polymer building functionality up to a molecular weight of 35,000. Model periodic systems were built using the Amorphous Cell Construction software containing a minimum of 100 water molecules per model drug. A Temperature Cycle Protocol from the Amorphous Cell (AC) module was then performed (default values) to equilibrate the cell. A typical input file for the software is given in Appendix V(A). The radius of gyration was estimated from an average of 10 configurations. A plot of the radius of gyration versus the molecular weight of dextran was used to obtain an estimate of the diameter of the dextrans in solution. A similar equilibration procedure was used to determine an approximate molecular diameter of the other model drugs.

3.6.2 Construction of simulations and equilibration procedures

Molecular dynamic simulations were carried out using Accelrys' Materials Studio® Version 2.1.5 using the COMPASS forcefield and a method similar to that used by Yoshioka *et al.* (2003). The Velocity Verlet algorithm was used for integration. Interaction between non-bonded atoms was represented in van der Waals and Coulombic terms. Summation for Coulomb interaction was carried out by the Ewald approach (Ewald accuracy of 0.01, update width of 1.00, dielectric value of 1.0000). Summation method for van der Waals interactions was group based (cutoff of 9.50 Å, spline width of 1.00 Å, buffer width of 0.50 Å). A polymer of NIPA was constructed (20mer) along with model benzoate and water molecules. Periodic cells containing the appropriate ratio of NIPA, water and drug molecules were then constructed at 500K (3 configurations) using the Amorphous Cell Construction software with minimisation procedures using the Steepest Descents and Conjugate Gradients (5000 steps). A typical input file for the software is given in Appendix V(B).

In order to examine the effect of temperature on the density of the systems, isothermal-isobaric (NPT) molecular dynamic simulations were carried out for the constructed systems at a pressure of 0.1MPa using the Discover Dynamics Software. Temperature and pressure were controlled by the Anderson procedure. A series of simulations with descending temperatures starting at 500K were run. NPT simulations at each temperature ran for 50ps with a step size of 1fs. The periodic cells were cooled at a rate of 10K/50ps with subsequent simulation started from the final configuration

obtained at the preceding temperature. NPT simulations for a single temperature took approximately 1 hour with the simulation repeated for the 3 configurations produced by the Amorphous Cell Construction. A typical input file for the software is given in Appendix V(C). Density at each temperature was taken as the average density value between 25ps and 50ps.

Where density measurements were not performed, NPT simulations at each temperature (450K, 350K, 300K) ran for 250ps with a step size of 1fs.

3.6.3 Production runs and analysis

Subsequent production runs were performed on the configurations produced by the Amorphous Cell Construction using the equilibrated density values obtained by the NPT simulations above. Isothermal molecular dynamic simulations at a constant volume (NVT) were carried out with these configurations with simulation temperature controlled by the Nose thermostat. The duration of NVT simulation was 10^5 steps with a step size of 0.5fs (Yoshioka *et al.* 2003). The full trajectory was saved with a frame output every 100 steps. NVT simulation for a single temperature level took approximately 2 hours and a typical input file is shown in Appendix V(D).

In order to calculate approximate values for molecular diffusion, the mean square displacement (MSD) of the oxygen atoms in water (WO), polymer (PO) and drug (DO) where appropriate was calculated using the full trajectory file produced above. A typical input file for the software is given in Appendix V(E).

The radial distribution function (pair correlation function, g(r)) between various atoms of the polymer, water and benzoates described in the text was calculated. A typical input file for the software is given in Appendix V(F).

3.7 STATISTICAL SIGNIFICANCE TESTING

Statistical significance between two parameters was evaluated by an independent 2-sample t-test (0.05 probability level) using Minitab® statistical software version 13.32.

CHAPTER 4

Polymer, Hydrogel and Model Drug Characterisation

4.1 INTRODUCTION

The PNIPA hydrogels (PNIPA-H) used in the present study are characterised using their swelling properties, thermal properties and pore size distribution. In addition, the characterisation of non-crosslinked linear PNIPA polymers (PNIPA-L) is described in section 4.2. The model drugs used are also described in section 4.3.

4.2 LINEAR POLYMER CHARACTERISATION

There have been a limited number of studies in the literature that compared the characteristics of linear PNIPA chains and crosslinked PNIPA gels (Schild, 1992; Otake *et al.*, 1990). The characteristics of linear batches of PNIPA polymer (PNIPA-L), prepared as described in section 3.2.2, were examined here for comparison with the hydrogel. The prepared batches were characterised by determination of polymer molecular weight and by analysis of the phase transition phenomenon of the polymer in deionised water and phosphate buffer pH 6.8 (isotonic) (PB).

4.2.1 Molecular Weight

Three batches of PNIPA-L (designated as PNIPA-L1, PNIPA-L2 and PNIPA-L3) were synthesised and their molecular weights, as determined by gel permeation chromatography (GPC) (Section 3.3.1), are shown in Table 4.1.

Table 4.1: Comparison of properties of PNIPA-L batches

	PNIPA-L1	PNIPA-L2	PNIPA-L3
Molecular weight ($X10^6$)	1.41 ± 0.37	1.05 ± 0.32	1.30 ± 0.21
Glass transition temperature (°C)	140.89 ± 0.99	137.51 ± 0.09	140.88 ± 0.18
Phase Transition Temperature (LCST) (°C)	34.12 ± 0.04	34.09 ± 0.07	34.09 ± 0.06

There was no statistical difference ($p > 0.05$) between the molecular weight of the three batches. The measured values were consistent with the study of Eeckman *et al.* (2001) who used viscosity measurements to estimate the molecular weight of a similar PNIPA polymer as 1×10^6. The glass transition temperature (Tg) of each polymer was also determined at a heating rate of 10°C/min. Previous studies have shown that the Tg of a polymer is molecular weight dependent (Rosen, 1993). Increased molecular weight causes chain entanglement and decreases chain mobility, resulting in a higher Tg. The Tg of PNIPA-L2 was statistically lower ($p<0.05$) than the other batches. This result may indicate a slightly lower molecular weight polymer in this batch, which could not be differentiated using GPC. A possible reason for this molecular weight difference was temperature variation during synthesis of this polymer batch.

4.2.2 Lower Critical Solution Temperature

The lower critical solution temperatures (LCST) of the synthesised polymers were determined by DSC analysis and by measuring the transmittance of the polymer solution at various temperatures as described in section 3.3.3.

4.2.2.1 Differential Scanning Calorimetry

DSC analysis of a PNIPA-L solution resulted in a distinct endotherm at the lower critical solution temperature due to the precipitation of the polymer at that temperature (Fig. 4.1).

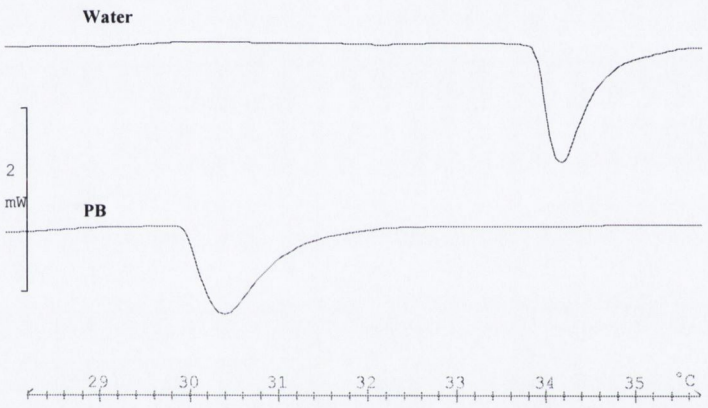

Fig. 4.1: DSC thermogram of a 1.4% w/v solution of PNIPA-L3 in deionised water (top) and phosphate buffer pH 6.8 (bottom) (Heating rate 2°C/min).

Schild and Tirrell (1990) reported a decrease in LCST with increasing polymer molecular weight in the range M_n=1.6 $X10^5$ to 5.4 $X10^3$. There was no significant difference ($p > 0.05$) in the phase transition temperatures between the three batches in the present study (Table 4.1).

The effect of altering the polymer concentration and heating rate on the phase transition temperature of the polymer in deionised water is shown in Fig. 1, Appendix IV. Endotherm characteristics, as measured by DSC, are given in Table 4.2.

Table 4.2: Influence of polymer concentration (at 2°C/min) and heating rates (using a 1.4%w/v solution) on DSC endotherm of PNIPA-L3 in deionised water.

Concentration PNIPA-L (% w/v)	Onset (°C)	Peak (°C) ($LCST_d$)	Peak width (°C)	Integral ($J\ g^{-1}$)	Enthalpy (kJ/mol NIPA)
0.5	33.90 ± 0.03	34.18 ± 0.04	1.20 ± 0.18	0.25 ± 0.04	5.54 ± 0.80
1.4	33.82 ± 0.05	34.09 ± 0.06	1.28 ± 0.08	0.65 ± 0.02	5.21 ± 0.17
3	33.70 ± 0.03	34.02 ± 0.04	1.83 ± 0.28	1.33 ± 0.09	5.00 ± 0.35
5	33.34 ± 0.42	33.91 ± 0.22	2.22 ± 0.08	2.34 ± 0.18	5.30 ± 0.41
10	33.50 ± 0.12	33.96 ± 0.00	2.26 ± 0.41	3.30 ± 1.62	3.72 ± 1.83
20	33.27 ± 0.12	33.96 ± 0.12	2.75 ± 0.35	5.69 ± 1.94	3.22 ± 1.10
Heating Rate (°C/min)	Onset (°C)	Peak (°C) ($LCST_d$)	Peak width (°C)	Integral ($J\ g^{-1}$)	Enthalpy (kJ/mol NIPA)
1	33.56 ± 0.01	33.80 ± 0.01	1.10 ± 0.01	0.62 ± 0.03	5.01 ± 0.23
2	33.82 ± 0.05	34.09 ± 0.06	1.28 ± 0.08	0.65 ± 0.02	5.21 ± 0.17
3	33.85 ± 0.14	34.29 ± 0.13	2.47 ± 0.07	0.69 ± 0.02	5.54 ± 0.17
4	33.85 ± 0.03	34.31 ± 0.01	3.40 ± 0.23	0.62 ± 0.01	5.01 ± 0.11
5	33.93 ± 0.03	34.44 ± 0.03	3.50 ± 0.07	0.71 ± 0.11	5.70 ± 0.86
6	34.05 ± 0.08	34.69 ± 0.16	3.88 ± 0.52	0.61 ± 0.04	4.89 ± 0.29

Apart from an increase in the viscosity of the prepared solution, the effect of increasing polymer concentration (Appendix IV, Fig. 1a) was to increase the peak width and height as well as decrease the transition onset and peak values (Table 4.2). The findings were in agreement with the study of Otake *et al.* (1990). In contrast, the study of Schild and Tirrell (1990) found that peak characteristics of the PNIPA endotherm were independent of concentration in the range 0.4-4.0mg/ml. As expected, the measured transition heat per gram of polymer solution varied with concentration and can be attributed (Schild, 1992) to the energy required to break hydrogen bonds between polymer and water molecules. The calculated enthalpy change per mol of N-isopropylacrylamide (NIPA) did not vary in the range 0.5-10mg/ml and averaged at about 5kJ/mol. This can be compared to a typical value of 6.3kJ/mol (Schild, 1992) for hydrogen bond interactions and an average value of 5.0kJ/mol obtained by Otake *et al.* (1990) for PNIPA-L solutions.

The heating rate also had an effect on the LCST endotherm. The effect of increasing the heating rate (Appendix IV, Fig. 1b) was to increase the transition onset and peak values (Table 4.2), in agreement with the study of Otake *et al.* (1990). The enthalpy change per mole of NIPA did not vary significantly although the width of the peak increased with increased heating rate.

From the results above, a higher concentration and/or a faster heating rate decreased the precision for the determination of the transition temperature and the heat change. A 1.4% w/v polymer solution was chosen for further study of the LCST phenomenon at a heating rate of 2°C/min, as used by Eeckman *et al.* (2001). The resulting endotherm was sharp with a narrow distribution (Fig. 4.1). This polymer solution was also of low viscosity. In the present study, the peak temperature was taken as the phase transition temperature, designated here as $LCST_d$.

Table 4.3: Phase transition temperature of 1.4%w/w PNIPA-L3 in water and PB as measured by DSC (section 4.2.2.1) and % transmittance (section 4.2.2.2)

	DSC					Transmittance
	Onset (°C)	Peak (°C) ($LCST_d$)	Peak width	Integral (J g^{-1})	Enthalpy (kJ/mol NIPA)	($LCST_t$)
Water	33.82 ± 0.05	34.09 ± 0.06	1.28 ± 0.08	0.65 ± 0.02	5.21 ± 0.17	32.80 ± 0.11
PB	29.50 ± 0.01	29.95 ± 0.04	2.07 ± 0.02	0.56 ± 0.07	4.53 ± 0.57	27.77 ± 0.09

Fig. 4.1 also shows the LCST of PNIPA-L3 in phosphate buffer pH 6.8 (PB). The phase transition decreased from 34.09°C in water to 29.95°C in PB (Table 4.3). The effect of the buffer salts was to decrease the phase transition temperature of PNIPA-L. Horne *et al.* (1971), Saito *et al.* (1992) and Eeckman *et al.* (2001) showed a similar decrease in the phase transition temperature of thermoresponsive polymers with various salt types; attributed to the ability of the salt anions to break the hydration layer around the polymer chains as described in section 1.3.5.1. Apart from a decrease in the peak position, the effect of the salts was to significantly increase the peak width (Table 4.3).

4.2.2.2 Transmittance

The phase transition temperature of PNIPA-L was also examined by measuring the transmittance of the polymer solution at 500nm at different temperatures. At temperatures below the LCST the solution remained clear, while at a certain temperature (cloud point, $LCST_t$) the polymer precipitated out of solution and the transmittance decreased dramatically (Fig 4.2). The LCST (Table 4.3) was defined as 50% transmittance of the polymer solution during the heating process.

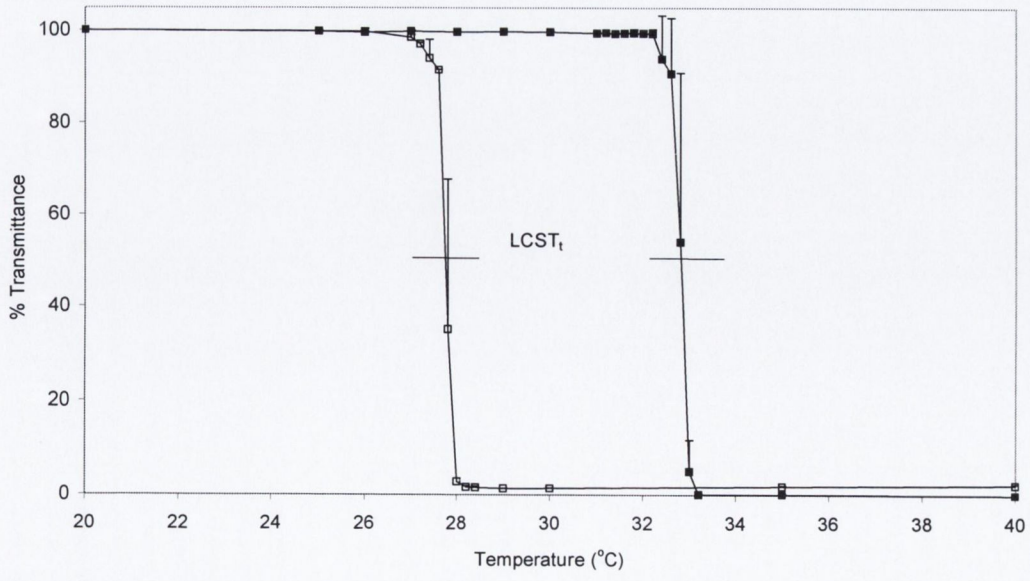

Fig. 4.2: Percentage transmittance of a 1.4% w/v solution of PNIPA-L3 in water (■) and PB (□) at various temperatures.

The phase transition temperature obtained in both water and PB was slightly lower than the values from DSC, defined as the maximum of the endothermic transition peak. This would suggest that transmittance is a more sensitive method for determining the LCST. The slower heating rate (~0.5°C/min) could be a contributing factor to the lower values obtained. In addition, the use of transmittance measurements is complicated by the rate of heat transfer in the larger volumes used as well as variations in precipitated aggregate sizes and settling of precipitates (Schild and Tirrell, 1990).

Transmittance measurements were therefore used in the current thesis in conjunction with DSC measurements for examination of the LCST phenomenon. The phosphate buffer salts had a similar effect on the LCST as was shown with DSC measurements (Table 4.3).

4.2.3 Fourier transform infrared (FTIR) spectroscopy

The FTIR spectrum of PNIPA-L obtained by the method described in section 3.3.9 is shown in Fig. 4.3.

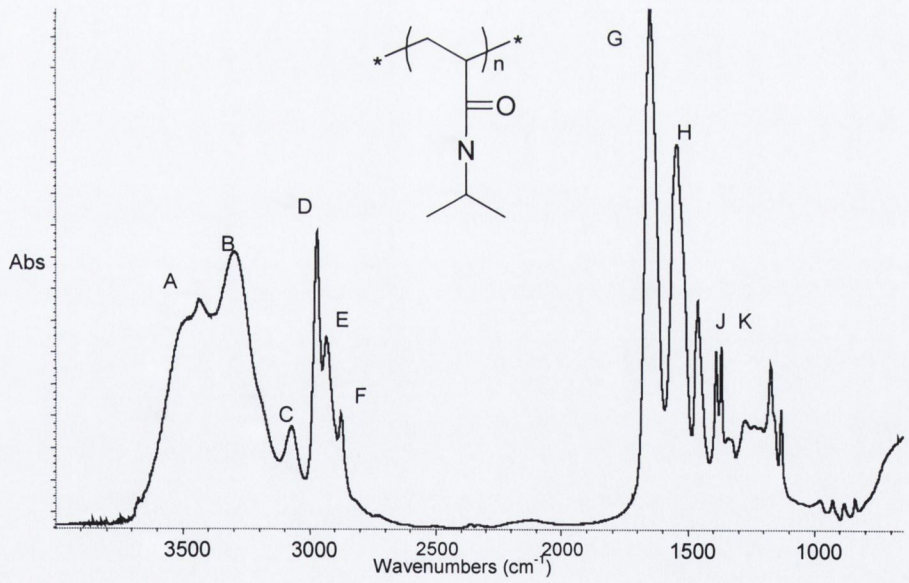

Fig 4.3: FTIR spectra of PNIPA-L. Relevant peaks are assigned by a letter in the text.

PNIPA contains distinct hydrophilic and hydrophobic constituents, resulting in the thermoresponsive nature of the polymer. The hydrophilic portion of PNIPA is the secondary amide group with characteristic peaks at 1647cm^{-1} (C=O stretch, G) and 1542cm^{-1} (Amide II, H) (Wang *et al.*, 2002). Non-cyclic monosubstituted amides usually exist with the NH and C=O bonds in the *trans* configuration, resulting in a hydrogen-bonded NH stretch near 3300cm^{-1}, with a weaker band

near 3100cm^{-1} (Lin-Vien *et al.,* 1991). The relevant functional groups in PNIPA appear at 3299cm^{-1} (B) and 3073cm^{-1} (C) respectively, with a broad and overlapping peak at 3438cm^{-1} (A) from bonded O-H groups due to the presence of water in the sample.

The hydrophobic portion of PNIPA consists of an alkane backbone and a side chain isopropyl group. The three peaks at 2971, 2933 and 2875cm^{-1} (D, E and F) are associated with symmetric and antisymmetric CH stretching of the polymer backbone (Gupta *et al.,* 2000) with possible contributions from the isopropyl group. The peaks at 1387cm^{-1} (J) and 1367cm^{-1} (K) correspond to the characteristic absorbance of the isopropyl group in PNIPA (Gupta and Khandekar, 2003; Liu *et al.,* 2004).

4.3 MODEL DRUG CHARACTERISATION

4.3.1 Physicochemical properties

The potential use of the thermoresponsive hydrogels were evaluated by using a range of model drugs with different physicochemical properties. The model drugs used are shown in Fig. 4.4 along with some physicochemical properties in Table 4.4.

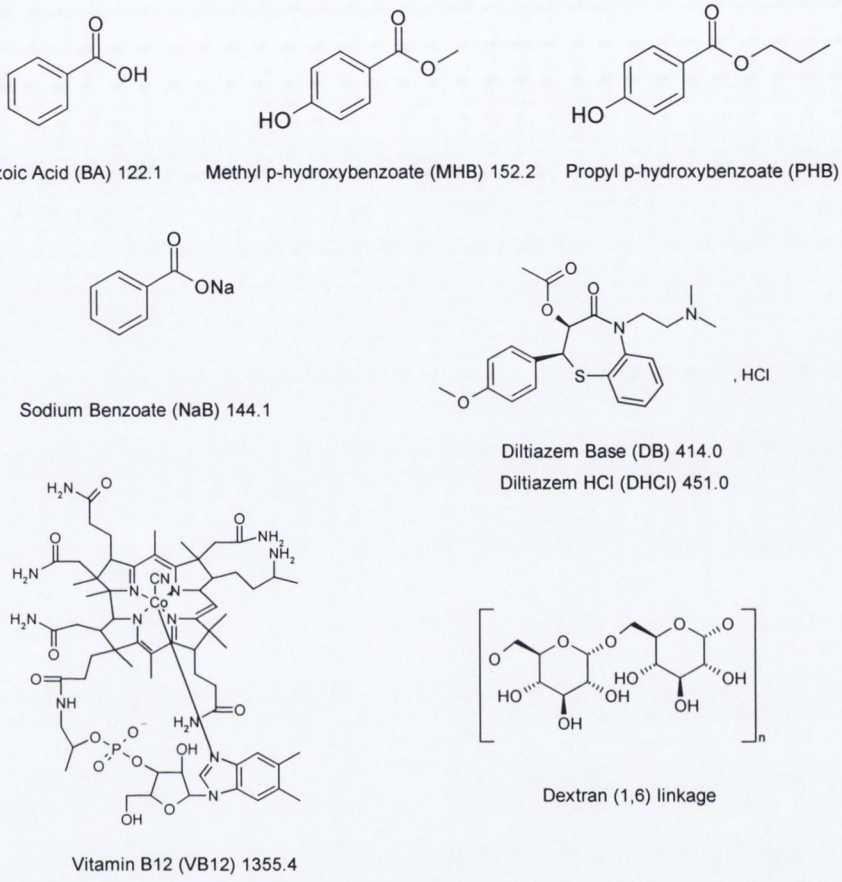

Fig. 4.4: Structure and molecular weight of model drugs used

Benzoic acid (and its sodium salt) and diltiazem base (and its hydrochloride salt) were used as model acidic and basic drugs respectively. The drugs were divided into a hydrophobic and hydrophilic series, the former reflecting solubility less than 10mg/ml i.e. "slightly soluble" according to the U.S.P. definition of solubility (United States Pharmacopoeia, 2000). Benzoic acid and its methyl and propyl esters gave a drug series with decreasing aqueous solubility. Diltiazem base also had similar solubility to the drugs in this hydrophobic series. Vitamin B12 and a range of dextrans (MW4000 to MW70000) were used as larger model drugs. These compounds, along with NaB and DHCl, made up the hydrophilic drug series. The model drugs used thus provided a series of probe molecules with different physicochemical properties, namely solubility, size (up to MW70,000) and chemical nature.

Table 4.4: Physicochemical properties of various model drugs

Model Drug	Molecular Weight	Solubility in PB (isotonic) at 25°C (g/l)	Solubility in PB (isotonic) at 37°C (g/l)	FITC label (mol/mol glucose) ($X10^3$)	Molecular diameter (25°C) in solution (Å)	
					Estimate 1[(b)]	Estimate 2[(c)]
Sodium Benzoate	144.1	380.35 ± 46.9	399.55 ± 16.60	---	---	4.22 ± 0.03
Benzoic Acid	122.1	7.87 ± 0.09	9.59 ± 0.48	---	---	4.22 ± 0.03
Methyl p-hydroxybenzoate	152.2	1.93 ± 0.15	4.19 ± 0.09	---	---	5.19 ± 0.05
Propyl p-hydroxybenzoate	180.2	0.37 ± 0.02	0.72 ± 0.02	---	---	6.09 ± 0.17
Diltiazem HCl	451.0	309.60 ± 7.85	549.34 ± 38.72	---	---	8.19 ± 0.16
Diltiazem Base	414.5	1.99 ± 0.03	3.43 ± 0.13	---	---	8.19 ± 0.16
Vitamin B12	1355.4	12.33 ± 0.12	21.37 ± 0.50	---	---	11.75 ± 0.14
Dextran MW 4,000	4300[(a)]	Very Soluble [(d)]	Very Soluble [(d)]	4.0	32.8	25.1
Dextran MW 10,000	10200[(a)]	Very Soluble [(d)]	Very Soluble [(d)]	0.5	48.7	38.3
Dextran MW 40,000	43000[(a)]	Very Soluble [(d)]	Very Soluble [(d)]	0.5	94.1	77.9
Dextran MW 70,000	68800[(a)]	Very Soluble [(d)]	Very Soluble [(d)]	0.65	116.7	98.3

[(a)]Molecular weight of bulk dextran as stated by Sigma-Aldrich

[(b)]Diameters estimated by interpolation of data given by Stone and Scallon (1968) for a series of dextran fractions

[(c)]Diameters estimated from radius of gyration by molecular modelling using Accelrys Materials Studio® software

[(d)] Martindale 1996

Approximate molecular diameters of the model drugs in solution were determined using molecular modelling software (Accelrys' Materials Studio® Version 2.1.5) as described in section 3.6.1. The radius of gyration is defined as the root mean square distance of the atoms in the molecule from their common centre of mass. The value produced gives a measure of the hydrodynamic radius of the molecule. The benzoates, diltiazem and vitamin B12 were constructed (n = 3) and equilibrated as described before determination of the radius of gyration (Table 4.4). Fig 4.4 shows molecular modelling images of a single configuration of selected model drugs.

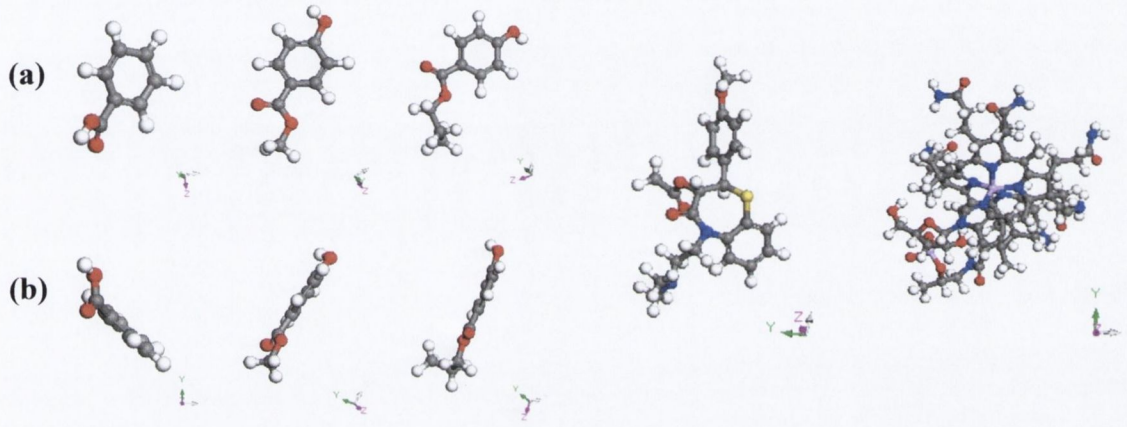

Fig 4.4: Molecular modelling images of (from left to right) benzoic acid, methyl p-hydroxybenzoate, propyl p-hydroxybenzoate, diltiazem and vitamin B12. The images of the benzoates are shown from two different perspectives, a and b. [carbon (grey), hydrogen (white), oxygen (red), nitrogen (blue), sulphur (yellow), cobalt (pink)]

The images of the benzoates in Fig. 4.4 revealed molecules that are approximately 2-dimensional in solution. A series of dextrans (Fig 4.5) of increasing molecular weight were also constructed and equilibrated.

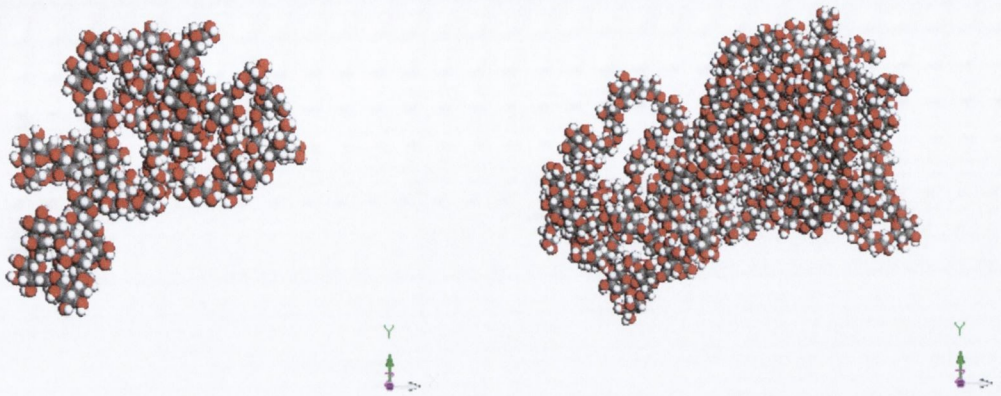

Fig 4.5: Molecular modelling images of Dextran MW10,000 (left) and Dextran MW30,000 (right) [carbon (grey), hydrogen (white), oxygen (red)].

The radius of gyration was then determined (n = 10) and plotted as shown in Fig 4.6. The values obtained were in close agreement with the calculated values of Stone and Scallan (1968) as shown. The diameters of the dextrans were then estimated from this plot and are given in Table 4.4

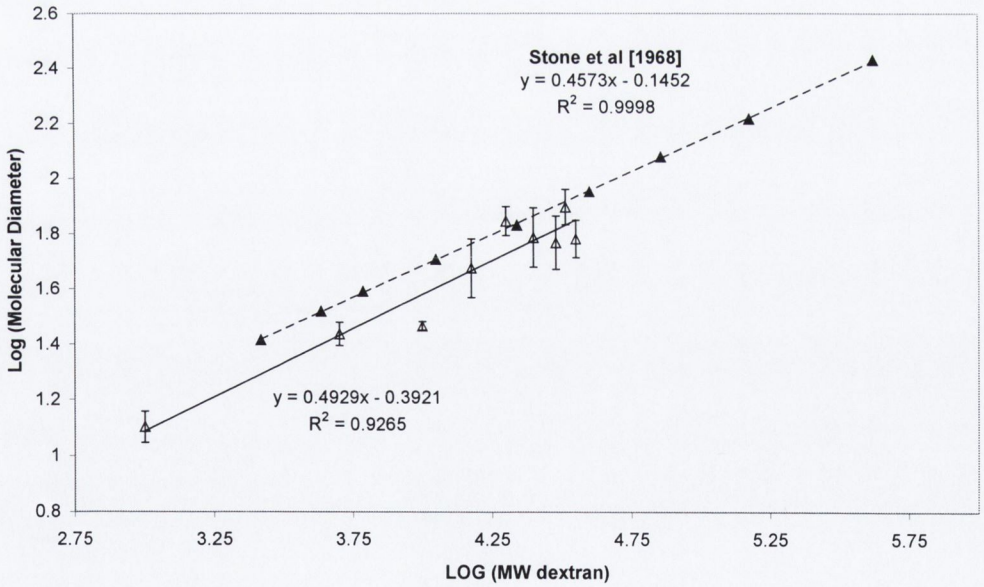

Fig. 4.6: Comparison of linear logarithmic relationships between dextran molecular diameter and molecular weight. Molecular modelling simulation (solid line, section 3.6.1) and literature value (dashed line).

Drug solubility was determined in PB as described in section 3.3.4. A rise in temperature was expected to increase the solubility of a solid in a liquid; in cases where the solid absorbed heat when it dissolved (Martin 1993, Chp. 10). In the present study, there was a linear relationship

between the solubility values at the two temperatures in the solubility range of 0 – 25 g/l (Fig. 4.7), with solubility increasing by a factor of ~1.6 with a temperature increase of 12°C.

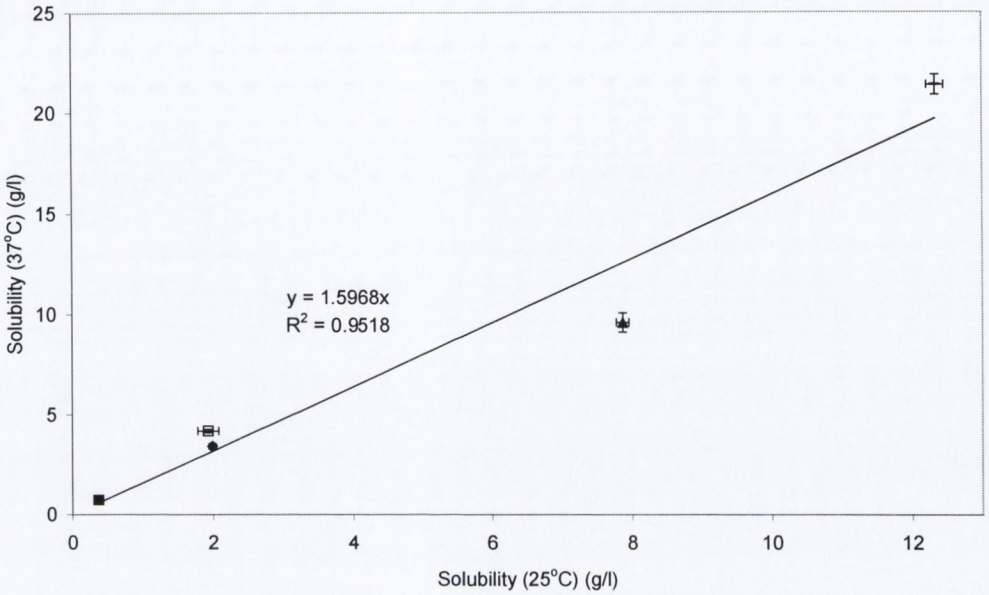

Fig. 4.7: Plot of equilibrium drug solubility at 25°C in PB against equilibrium drug solubility at 37°C in PB [BA (▲), MHB (□), PHB (■), DB (♦), VB12 (-)].

A similar increase in solubility was seen with DHCl (Table 4.4). No statistical difference in solubility ($p > 0.05$) was, however, apparent with NaB on raising the temperature from 25°C to 37°C.

Table 4.5 shows further properties of the model drugs used including melting point (section 3.3.12), glass transition temperatures (section 3.3.2), density (section 3.3.11) and estimated partial solubility parameters (section 3.3.13). Initial estimates of the Tg of the benzoates are given in Table 4.5 by using a Tm/Tg ratio of 0.70, where Tm is the melting point of the crystalline drug and the value of 0.70 is the average ratio obtained for similar low molecular weight compounds by Kerč and Stčič (1995). The estimated Tg values shown in Table 4.3 may be much higher than the actual values due to the tendency of these small molecular weight compounds to self-associate e.g. form dimers (Painter *et al.*, 1991).

The 75°C difference in Tg between diltiazem base and its sodium salt was identical to the difference shown by Tong and Zografi (1999) between indomethacin and its sodium salt. The change in Tg was attributed to the ionic interaction between the ions, leading to less molecular mobility in the salt form (Tong *et al.*, 2002). The ratio of T_g to melting temperature, T_m, was 0.48 and 0.32 for DH and DB respectively, lower than the range obtained for similar low molecular weight compounds by Kerč and Stčič (1995).

The partial solubility parameters of the model drugs were determined according to the method of Hoftyzer-Van Krevelen (Van Krevelen, 1990) (Table 4.5). The solubility parameters have previously been used to predict miscibility of drugs/excipients and polymers (Rowe, 1988; Hancock *et al.*, 1997; Greenhalgh *et al.,* 1999; Forster *et al.,* 2001; Nair *et al.*, 2001). This total solubility parameter is a measure of interatomic/molecular interactions and materials with similar solubility parameters will have similar intermolecular interactions, which will favour miscibility. The partial solubility parameters give an indication of the relative strengths of the various types of forces present including dispersion forces (δ_d), polar (δ_p) and hydrogen bonding (δ_H) (Van Krevelen, 1990). Compounds with similar values for δ are likely to be miscible ($\Delta\delta < 7.0$ $MPa^{1/2}$), while when $\Delta\delta$ is >10 $MPa^{1/2}$, the compounds are likely to be immiscible (Greenhalgh *et al.,* 1999).

The estimated solubility parameters of the benzoates are given in Table 4.5. BA and its esters were likely to be miscible with PNIPA, while NaB was likely to be immiscible due to differences in polar forces (δ_p). The total solubility parameter of VB12 predicted miscibility with PNIPA, although the partial solubility parameters revealed differences in polar forces between the VB12 and PNIPA. The total and partial solubility parameters of the dextrans were estimated using the value for one monomer unit of glucose. These values predicted immiscibility between the dextrans and PNIPA.

Table 4.5: Properties of PNIPA-L and various model drugs

	Melting temperature Tm (^{o}C)	Glass transition temperature Tg (^{o}C) [a]	Tg/Tm	Density (g cm^{-3})	Partial solubility parameters (MPa)$^{1/2}$ [b]			
					δ	δ_d	δ_p	δ_H
PNIPA-L	--	140.88 ± 0.18	--	1.0453 ± 0.0009	22.23	18.98	8.81	7.50
Sodium Benzoate	435.26 ± 0.33	305*	N/A	1.0734 ± 0.0002	35.87	16.28	29.19	13.04
Benzoic Acid	122.36 ± 0.01	86*	N/A	0.9337 ± 0.0003	22.44	19.62	4.35	10.01
Methyl p-hydroxybenzoate	125.66 ± 0.12	88*	N/A	0.9791 ± 0.0003	26.08	20.11	6.22	15.40
Propyl p-hydroxybenzoate	95.82 ± 0.39	67*	N/A	0.9073 ± 0.0005	24.16	19.37	4.85	13.59
Diltiazem HCl	212.48 ± 0.12	102.38 ± 0.12	0.48	0.8900 ± 0.0003	--	--	--	--
Diltiazem Base	87.17 ± 1.73	28.17 ± 0.10	0.32	0.8930 ± 0.0002	22.27	20.44	4.86	7.39
Vitamin B12	232.64 ± 1.04	85.88 ± 1.24	0.37	0.9660 ± 0.0004	24.58	20.55	0.14	13.48
Dextran MW 4,000	--	177.74 ± 2.98	--	0.8549 ± 0.0048	44.03	30.29	0.74	31.94
Dextran MW 10,000	--	209.22 ± 0.22	--	0.7371 ± 0.0024	44.03	30.29	0.74	31.94
Dextran MW 40,000	--	218.99 ± 0.17	--	0.7168 ± 0.0105	44.03	30.29	0.74	31.94
Dextran MW 70,000	--	221.40 ± 0.58	--	0.7325 ± 0.0122	44.03	30.29	0.74	31.94

[a] Tg of benzoates* estimated based on ratio Tg/Tm =0.70 (Kerč and Stčič, 1995). Tg of DB, DH and VB12 determined as described in section 3.3.2.

[b] The calculated partial solubility parameters were estimated using the Hoftzymer/Van Krevelen method and the molar volumes of Fedors (Van Krevelen, 1990) (section 3.3.13). The value for NaB was determined by Bustamante *et al.* (2000). Partial solubility parameters of the polymers were estimated using one monomer unit. The group contribution of the Cobalt atom was omitted from the estimated value of vitamin B12.

4.3.2 Fourier transform infrared spectroscopy

FTIR spectra of the model drugs were obtained as described in section 3.3.9. The FTIR spectra of the four benzoates are given in Fig. 4.8

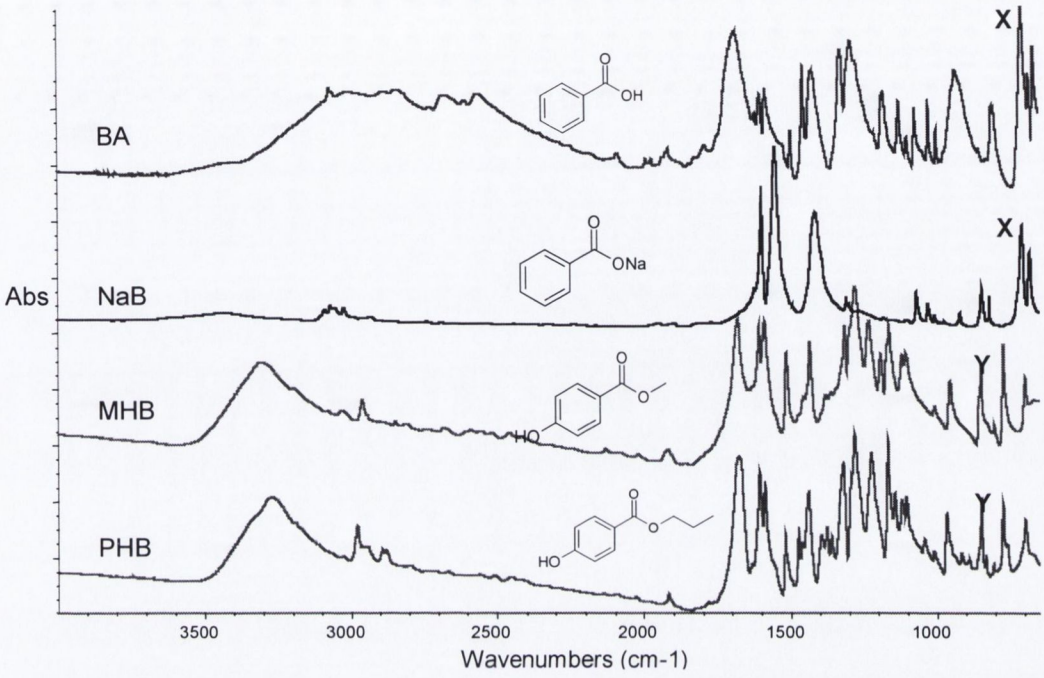

Fig 4.8: FTIR spectra of benzoates. From top to bottom: BA, NaB, MHB and PHB. Peaks marked X (707cm^{-1}) in BA and NaB and at Y (849cm^{-1}) in MHB and PHB are assigned to phenyl C-H out of plane bending.

The characteristic band corresponding to carbonyl stretching appeared at 1684cm^{-1} in the spectrum of BA with the bands at 1326cm^{-1} and 1291cm^{-1} due to coupled C-O stretching and O-H bending vibrations (Johnson and Rumon, 1965; Hayashi and Umemura, 1974; Gangakhedkar *et al.*, 1974). The peak at 934cm^{-1} has been assigned to a combination of OH out of plane vibrations and one of the out-of-plane vibrations of the benzene ring (Hayashi and Umemura, 1974). The band at 707cm^{-1} is due to phenyl C-H out of plane bending (Gangakhedkar *et al.*, 1974; Chen *et al.*, 2000). A peak at 707cm^{-1} also appears in the spectrum of NaB and can also be attributed to C-H out of plane bending. The bands at 1550cm^{-1} and 1413cm^{-1} in the NaB spectrum have been assigned to the stretching of the carbonyl anion group of NaB (Johnson and Rumon, 1965).

MHB and PHB, in addition to the presence of the ester groups, also contain a hydroxyl group in the para position. In the spectrum of MHB, OH stretching band appeared as a broad band around 3307cm^{-1}, sharp carbonyl stretching appeared at 1679cm^{-1} and C=C benzene ring stretching can be assigned to the peak at 1588cm^{-1} (Oguchi *et al.*, 2002; Owen *et al.*, 2003). With PHB, equivalent

bands to that of MHB were seen for OH stretching (3267cm^{-1}), carbonyl stretching (1677cm^{-1}) and C=C benzene ring stretching (1588cm^{-1}) while the peak at 2980cm^{-1} may be associated with C-H stretching of the propyl group (Owen *et al.*, 2003). A peak at approximately 849cm^{-1} is present in the spectrum of both MHB and PHB and can be assigned to phenyl C-H out of plane bending. There is also a peak at ~771cm^{-1} in both spectra which may be due to coupling of the –COO- group with the phenyl ring.

The FTIR spectra of diltiazem base and its hydrochloride salt are given in Fig. 4.9.

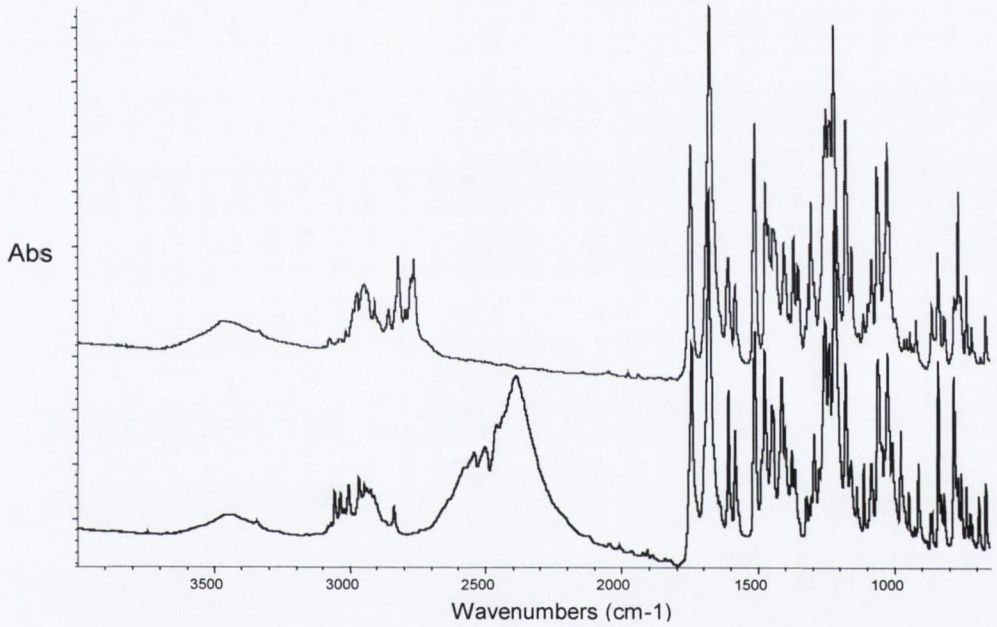

Fig 4.9: FTIR spectra of diltiazem base (top) and diltiazem HCl (bottom)

Bands associated with carbonyl stretching appeared at 1747cm^{-1}/1674cm^{-1} for DB and 1743cm^{-1} /1679cm^{-1} for DHCl (Kugita *et al.*, 1971; Tanaka *et al.*, 1992). The peaks around 3000cm^{-1} can be assigned to aliphatic and aromatic C-H stretching.

The FTIR spectra of vitamin B12 is given in Fig. 4.10. A broad band dominates the FTIR spectrum of VB12 with a maximum at 3384cm^{-1}. This can be attributed to the stretching vibrations of OH and NH groups, including the presence of water due to the hygroscopic nature of the compound. The broad band overlaps with peaks at ~3000cm^{-1} due to aliphatic and aromatic C-H stretching. A band corresponding to C=O stretch is at 1668cm^{-1}.

The FTIR spectra of the dextrans are given in Fig. 4.11. The characteristic stretching vibrations of the hydroxyl groups dominate the FTIR spectra of the dextrans with maximums at 3404-3430cm^{-1} and 1012-1018cm^{-1} (Wang *et al.*, 2002). The peak maximum observed at ~3400cm^{-1} showed a general linear increase with increased molecular weight and Tg (R^2= 0.8608) of the dextran (Table

4.3). This is similar to the study of Wolkers *et al.* (2004), where the OH stretching band of a series of amorphous carbohydrates shifted to higher wavelengths with increasing Tg. The observation was attributed to an increase in the average length of the hydrogen bonds with increasing Tg. Taylor and Zografi (1998) also showed that the extent of hydrogen bonding between several sugars and PVP was found to correlate inversely with the glass transition temperature of the sugar, with the tendency to hydrogen bond decreasing as the Tg increased.

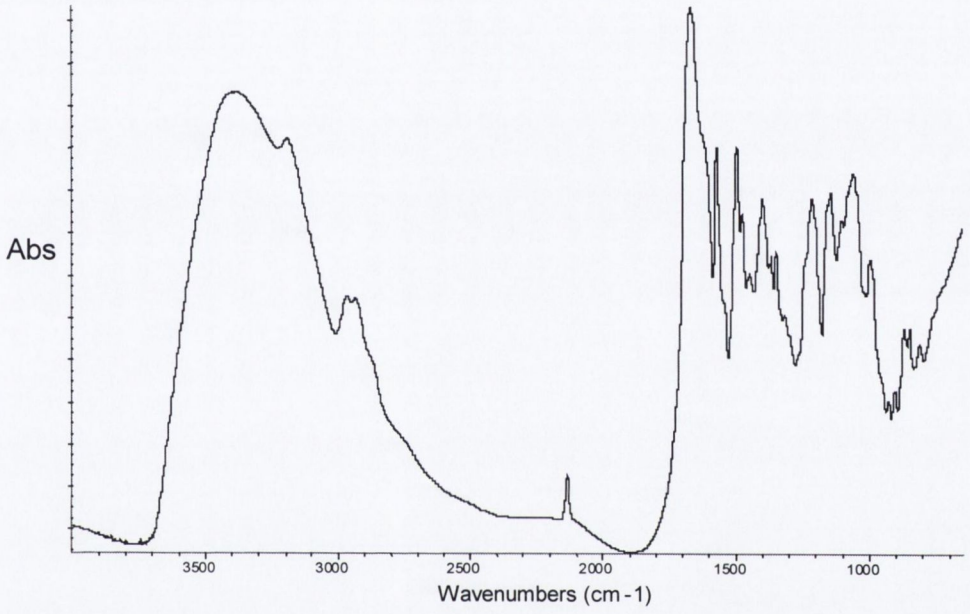

Fig 4.10: FTIR spectrum of vitamin B12

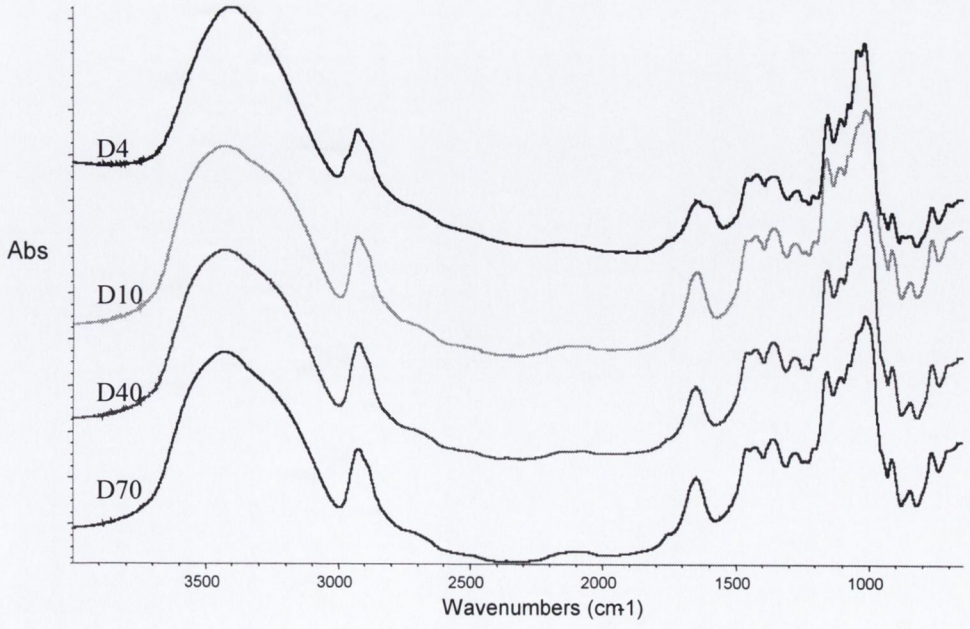

Fig 4.11: FTIR spectra of the dextrans: from top to bottom D4, D10, D40 and D70

4.4 HYDROGEL CHARACTERISATION

A series of poly(N-isopropylacrylamide)-based hydrogels (PNIPA-H) were synthesised as described in section 3.2.1, each with a different percentage cross linker. The percentage crosslinking and the measured glass transition temperature (Tg) (section 3.3.2) of the systems are given in Table 4.6.

Table 4.6: Percentage crosslinker and glass transition temperature of poly(N-isopropylacrylamide)-based hydrogels

	N,N'-methylenebisacrylamide (MBA)		Tg (°C)
	% w/w	mol %	
PNIPA-H1	1.56	1.15	143.1 ± 1.6
PNIPA-H2	3.00	2.22	148.1 ± 0.1
PNIPA-H3	7.58	5.68	157.3 ± 5.3
PNIPA-H4	14.63	11.17	170.8 ± 5.2

The level of crosslinking in a hydrogel is one of the most important factors that influences hydrogel swelling (Peppas, 1986). Omidian *et al.* (1998) also showed that the level of swelling was dependent on the type of crosslinker used as well as the type of monomer and method of polymerisation. The mechanical strength of the hydrogel can be improved by increasing the degree of crosslinking (Johnson *et al.*, 2004).

There was a direct linear relationship ($R^2 = 0.9923$) between the glass transition temperature of the hydrogels and the mol % crosslinker in the system (Fig. 4.12).

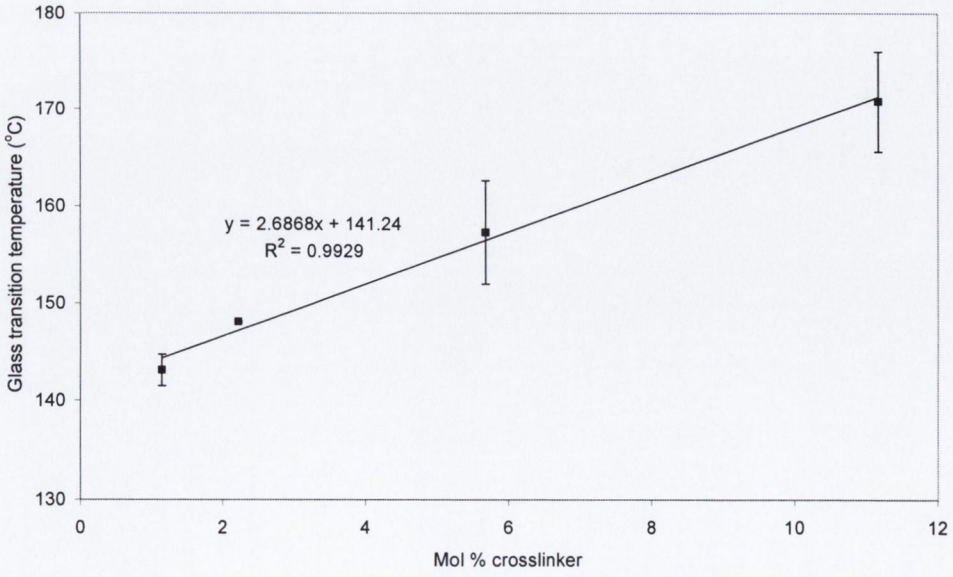

Fig. 4.12: Plot of hydrogel glass transition temperature (Tg) against mol % crosslinker in the hydrogel

Xiao and Zhou (2003) showed a similar increase in Tg of a PVA hydrogel with increasing crosslinking ratio. Crosslinking significantly lowers the mobility of the polymer chains, requiring a higher temperature to promote mobility, characterising the glass transition (Sousa *et al.*, 1998). An increase in the percentage crosslinker would lower this mobility further. Based on the linear correlation above, a theoretical Tg for an uncrosslinked system was obtained at approximately 140°C, comparing favourably with the Tg of the linear polymers shown in Table 4.1. The similarity in Tg between the crosslinked system and the linear polymer may indicate that the polymer chains in the crosslinked hydrogels have a similar molecular weight to the linear systems (~1.3 X 10^6 Da, Table 4.1). The Tg obtained for the prepared systems can be compared to values of 135.0°C (0.7mol% MBA, 20°C/min) and 111.5°C (2.0mol% MBA, 10°C/min) obtained by Sousa *et al.* (1998) and Erbil *et al.* (2004) respectively, using similar PNIPA hydrogels crosslinked with methylenebisacrylamide (MBA).

The hydrogels were further characterised based on their swelling properties, transition temperatures and pore size distributions. Absolute swelling and swelling over time at a particular temperature, along with the effect of stepwise temperature change on swelling of the hydrogels were examined.

4.4.1 Equilibrium swelling studies

The swelling of the hydrogels was characterised using either the swelling ratio (Equation 3.1a) or the fraction swelling (Equation 3.1b). The swelling ratio (Equation 3.1a) relates the weight of the swollen hydrogel at a particular time to the weight of the dried, desolvated hydrogel disc. Several different forms of this equation have been used in the literature as described in section 2.3.1. These equations give an indication of the absolute swelling level of a hydrogel, assuming that the dry weight is similar in each instance. The fraction swelling (Equation 3.1b) gives an indication of the relative level of media uptake at a particular time.

The equilibrium swelling of the PNIPA-H1 was examined over a range of temperatures in water and phosphate buffer pH 6.8 (PB) (Fig. 4.7). The phase transition temperature based on the swelling data ($LCST_s$) was defined in section 3.3.6. PNIPA-H1 showed a phase transition at 33°C in deionised water and this was decreased to 29°C by the buffer salts. The phase transition temperature in water was within the range (32°C to 34°C) reported by other authors for PNIPA hydrogels (Hoffman, 1987; Ichikawa and Fukumori, 1997; Schild, 1992). The influence of the buffer salts on the phase transition temperature of the hydrogel was similar to the salting out effect seen by Eeckman *et al.* (2001) on the LCST of PNIPA-L. There was also a relationship between the effect of the salts on the linear system, described using DSC and transmittance measurements, and the effect on PNIPA-H1, described using swelling measurements (Fig. 4.13)

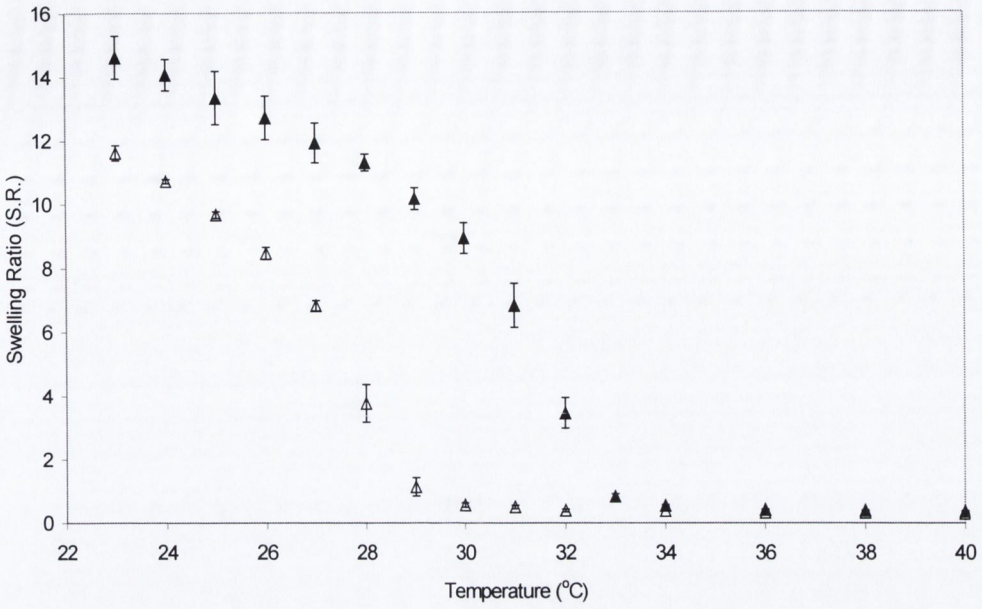

Fig. 4.13: Equilibrium swelling ratio (n = 3) of PNIPA-H1 at various temperatures in deionised water (▲) and PB (Δ).

The equilibrium swelling with temperature of the other hydrogels were examined in PB (Fig 4.14).

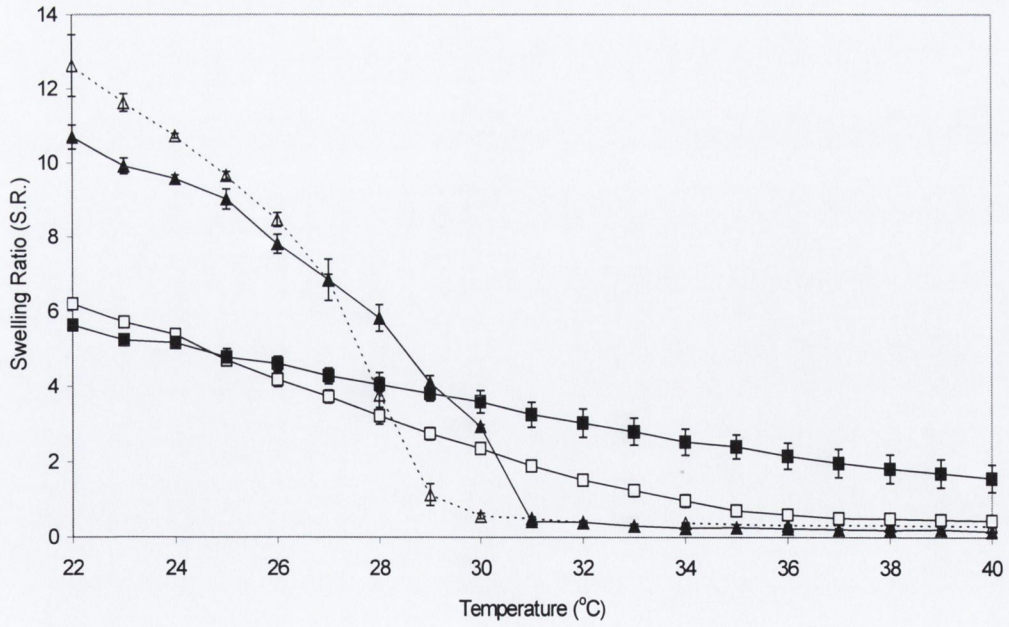

Fig. 4.14: Equilibrium swelling ratio (n=3) of PNIPA-H1 (------,Δ), PNIPA-H2 (▲), PNIPA-H3 (□), PNIPA-H4 (■) at various temperatures in PB.

PNIPA-H2 and PNIPA-H3 showed phase transitions of 31°C and 35°C respectively. PNIPA-H4 was the most highly crosslinked (11.17 mol%) and a distinct phase transition was not seen.

PNIPA-H4 showed a continuous swelling change over the temperature range studied, while the lower crosslinked hydrogels showed a discontinuous swelling change with temperature.

The equilibrium swelling of the above hydrogels at a temperature below (25°C) and above (37°C) the phase transition temperature was examined more closely (Fig 4.15).

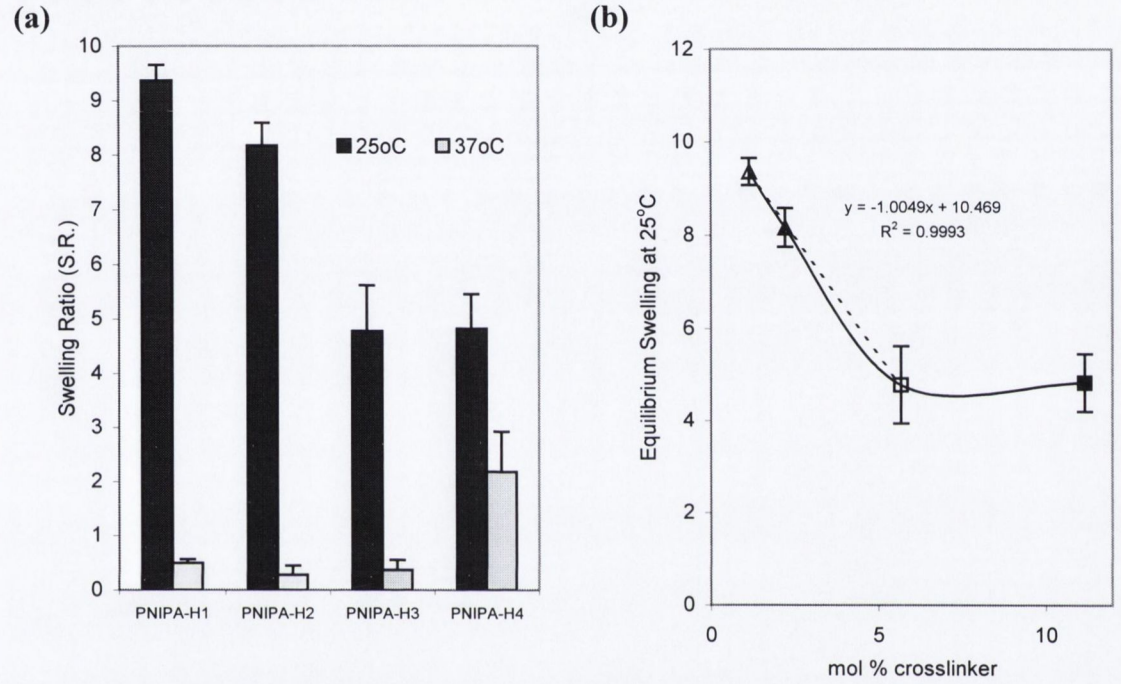

Fig. 4.15: (a) Equilibrium swelling ratio (n=9) of the hydrogels at 25°C and 37°C in PB (b) Relationship between equilibrium swelling ratio at 25°C and mol% crosslinker [PNIPA-H1 (Δ), PNIPA-H2 (▲), PNIPA-H3 (□), PNIPA-H4 (■)].

Below the LCST (25°C), the equilibrium swelling ratio of the hydrogels decreased as the percentage crosslinker increased, with a linear relationship (R^2 = 0.9993) seen for the first three hydrogels of the series (MBA ≤ 5.68 mol%) (Fig. 4.15b). There was no statistical difference ($p<0.05$) between PNIPA-H3 and PNIPA-H4 swelling levels at this temperature. This was expected from the swelling patterns in Fig. 4.14. With non-thermoresponsive hydrogels, several studies (Peppas, 1986; Canal and Peppas, 1989; Omidian *et al.,* 1998; Akala *et al.,* 1998; Kabiri *et al.,* 2003) have shown that as the percentage crosslinker present in the hydrogel increased, the equilibrium or steady state swelling ratio of the hydrogel decreased. Kabiri *et al.* (2003) found that a small change in crosslinker content at low crosslinker concentration range has large effects on water absorbency. On the other hand, they showed that dependency of swelling on crosslinker content was not as important at higher levels of crosslinker. The present study showed that at relatively high levels of crosslinking, the linear relationship between swelling and the level of crosslinking does not hold.

Above the LCST (37°C), only PNIPA-H4 showed a significant difference in swelling level, where a higher level of swelling was seen. Huglin and co-workers (Huglin *et al.*, 1997; Xue *et al.*, 2001), Xue and Hamley (2002) and Yilidiz *et al.* (2002) showed a decrease in the equilibrium swelling ratio with increasing crosslinker content below the LCST, while there was no difference above the LCST where the gels were in the collapsed state. The range of MBA crosslinker concentrations examined in these studies was 0.1-2.5 mol%. Ni and Zu (2004) showed a similar pattern with tetra (ethylene glycol) diacrylate as crosslinker. Huglin *et al.* (1997) showed that gels modified with hydrophilic co-monomers and which were in a partially swollen state above the LCST, also showed this trend. These studies did not show an increase in swelling ratio above the LCST as was seen here with PNIPA-H4. This effect is probably due to the influence of the water-soluble crosslinker on the hydrophilicity of the hydrogel, preventing a shrunken state at the temperatures examined.

The magnitude of swelling change between these two temperatures decreased with increasing percentage crosslinker, with a linear decrease with increasing mol% crosslinker for the first three hydrogels of the series (MBA $\leq$ 5.68 mol%; R^2=0.9997). The extent of crosslinking is thus controlling the equilibrium swellings at both temperatures when MBA $\leq$ 5.68 mol %. Yilidiz *et al.* (2002) also noted that the difference between the upper and lower plateau regions of the equilibrium-swelling curve decreased with increasing MBA concentration. In the case of PNIPA-H4, a second contributing factor to the swelling levels may be the chemical nature of the crosslinker in addition to the decreased influence of the thermoresponsive monomer (NIPA) in the system. This is investigated further in the next section (section 4.4.2).

The studies mentioned (Huglin *et al.*, 1997; Xue *et al.*, 2001; Xue and Hamley, 2002; Yilidiz *et al.*, 2002) also showed independence of the $LCST_S$ with crosslinker concentration. In contrast, Han *et al.* (2003) showed an increase in the LCST with increasing mole ratio (0.5-2 mol%) of crosslinker tetra ethylene glycol dimethacrylate. This was attributed to a combination of the increased hydrophilicity of the hydrogel and an increased "stiffness" of the hydrogel, which may prevent hydrophobic interactions. An apparent increase in the $LCST_S$ with increasing crosslinker content was seen in the present study. The influence of the crosslinker on the phase transition temperature was further investigated by Differential Scanning Calorimetry in the next section.

The effect of additives on the equilibrium swelling at 25°C was also examined. As shown above, the effect of the PB was to decrease the equilibrium swelling level at 25°C. Fig. 4.16 also shows the effect of 0.01M HCl on the equilibrium swelling levels.

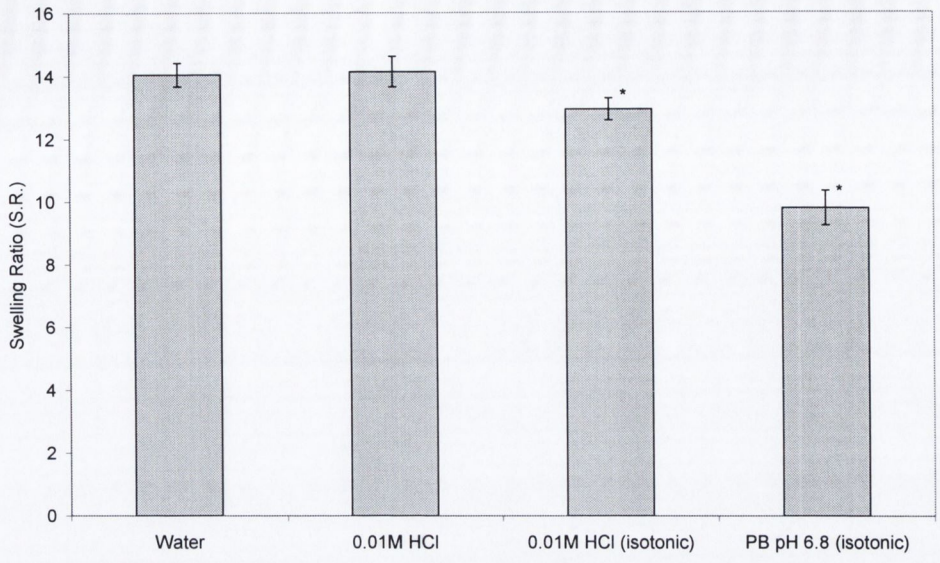

Fig. 4.16: Effect of additives on the equilibrium swelling level of PNIPA-H1 at 25°C (* indicated statistically significant, $p<0.05$, from water).

The presence of the acid alone did not significantly affect the swelling equilibrium compared with water, confirming the non-ionic nature of the hydrogels used. The addition of salt, however, caused a significant decrease ($p<0.05$) in the swelling level as shown. The decrease in the swelling levels can be attributed to a salting out effect, with the effectiveness of this salting out effect depending on the position of the anions present in the Hoffmeister series as described in Chapter 1 (section 1.3.5).

4.4.2 Phase transition temperature

The phase transition temperature of PNIPA hydrogels was determined by DSC analysis (Table 4.7). Examples of the LCST of the various hydrogels obtained in water are shown in Appendix IV, Fig. 2. In the case of the hydrogels, a sample of the swollen hydrogel (25°C) was scanned at 2°C/min in a sealed pan.

In both water ($R^2=0.8945$) and PB ($R^2=0.983$), there was a linear increase in the endotherm peak positions as the % MBA increased (Fig 4.17a). There was no pattern apparent with the onset of endotherm. The increase in the peak positions indicated that the chemical nature of the crosslinker had an effect on the phase transition temperature. An increase in the peak position of the order of 1.0-1.5°C was seen.

Table 4.7: Phase transition temperature (n=3) of PNIPA-H in water and PB

	DSC-**Water**				Swelling* ($LCST_s$)
	Onset (°C)	Peak (°C) ($LCST_d$)	Integral (J/g gel)	Integral (kJ/mol NIPA)	
PNIPA-H1	31.83 ± 0.36	33.00 ± 0.38	1.63 ± 0.12	2.48 ± 0.19	33
PNIPA-H2	31.09 ± 0.27	32.90 ± 0.29	1.61 ± 0.06	2.24 ± 0.08	N/A
PNIPA-H3	29.91 ± 0.52	33.88 ± 0.04	1.68 ± 0.21	1.41 ± 0.18	N/A
PNIPA-H4	32.47 ± 0.11	34.25 ± 0.04	0.29 ± 0.05	0.23 ± 0.04	N/A
	DSC-**PB**				Swelling* ($LCST_s$)
	Onset (°C)	Peak (°C) ($LCST_d$)	Integral (J/g gel)	Integral (kJ/mol NIPA)	
PNIPA-H1	28.64 ± 0.07	29.86 ± 0.18	1.88 ± 0.05	2.01 ± 0.05	29
PNIPA-H2	27.80 ± 0.23	30.21 ± 0.07	1.86 ± 0.04	1.76 ± 0.04	31
PNIPA-H3	28.52 ± 0.28	30.54 ± 0.10	0.61 ± 0.16	0.35 ± 0.09	35
PNIPA-H4	29.95 ± 0.18	31.39 ± 0.14	0.06 ± 0.04	0.03 ± 0.02	ND

*LCST as defined in section 3.3.6; ND: not detectable; N/A: data not available

The intercepts corresponding to an uncrosslinked system were at ~33°C and ~30°C in water and PB respectively, compared with values of 34.09 ± 0.06°C and 29.95 ± 0.04°C for the linear polymer (Table 4.3). There was no statistical difference between these values in PB ($p>0.05$) while the intercept for the gels was significantly lower ($p<0.05$) than the uncrosslinked system. Differences in molecular weight between the polymer and hydrogels and different polymer concentration used in analysing the systems could have contributed to the discrepancy.

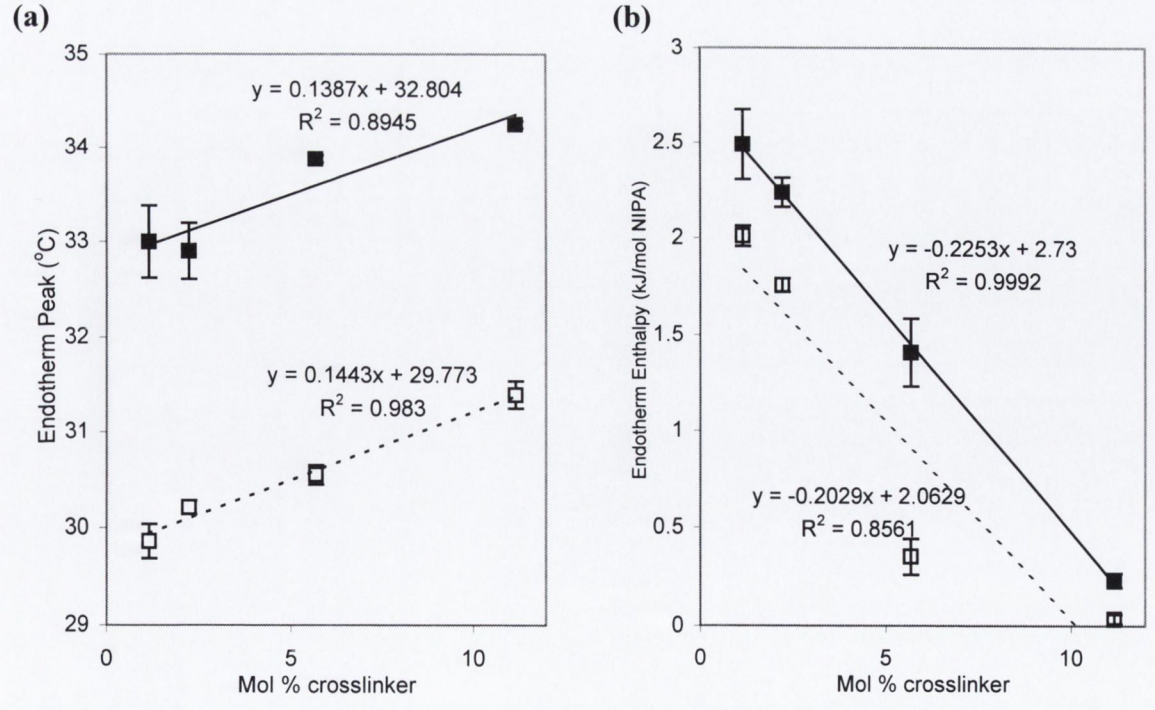

Fig. 4.17: Influence of % crosslinker (MBA) on (a) endotherm peak position and (b) enthalpy in water (solid line, ■) and PB (dashed line, □).

The integral indicates the magnitude of the transition as detected by DSC. When calculated per gram of gel, a significant decrease in the value was only seen with PNIPA-H4. However, when the level of swelling was taken into account, which factored in the actual sample size (excluding water), then a significant decrease in the endotherm value was seen with increasing crosslinker in both water (R^2=0.9992) and PB (R^2=0.8561) (Fig 4.17b). For enthalpy change, the intercept corresponding to an uncrosslinked system was at 2.73 and 2.06 kJ/mol NIPA in water and PB respectively, compared with and statistically different ($p<0.05$) to, 5.21 and 4.53 kJ/mol NIPA for the linear polymer (1.4%w/v and 2°C/min). Since enthalpy change was shown to be concentration independent (Table 4.2), this discrepancy can be attributed to the presence of the crosslinker (methylenebisacrylamide) which imparts a three-dimensional structure to the polymer chains; limiting the extent of hydrophobic/hydrophilic interactions that can occur. An increase in the percentage crosslinker also decreases the percentage of the thermoresponsive element (NIPA) present. The relationships shown in Fig 4.17 were for the most part parallel for water and PB, indicating a similar effect in both solvents.

The increase in peak position would suggest that the crosslinker increased the overall hydrophilicity of the system, also shown by the increase in $LCST_S$. The relatively small shift in peak position of $LCST_d$, however, does not account for the drastic change in the swelling of these systems as was described in section 4.4.1. An apparent increase in $LCST_S$ with increasing crosslinker content was seen in the present study. This result showed that a shift in $LCST_d$ was not the only contributing factor to swelling in these hydrogels. The chemical nature and extent of crosslinker was important. In addition, the percentage of the thermoresponsive monomers present in the hydrogel would also influence swelling. A decrease in peak enthalpy with increasing crosslinker was seen with the hydrogels (Fig 4.17a). The highly crosslinked PNIPA-H4 was only weakly thermoresponsive as a result. The consequences of this were a small continuous swelling change with temperature and a higher swelling ratio at higher temperatures (Figs 4.14 and 4.15).

4.4.3 Swelling kinetics

The presence of the different percentages of crosslinker not only influenced equilibrium swelling at a particular temperature, but also affected the rate of swelling at that temperature. The swelling rates of the hydrogel discs, initially in a dried out state, were examined over time at 25°C and 37°C (Fig. 4.18).

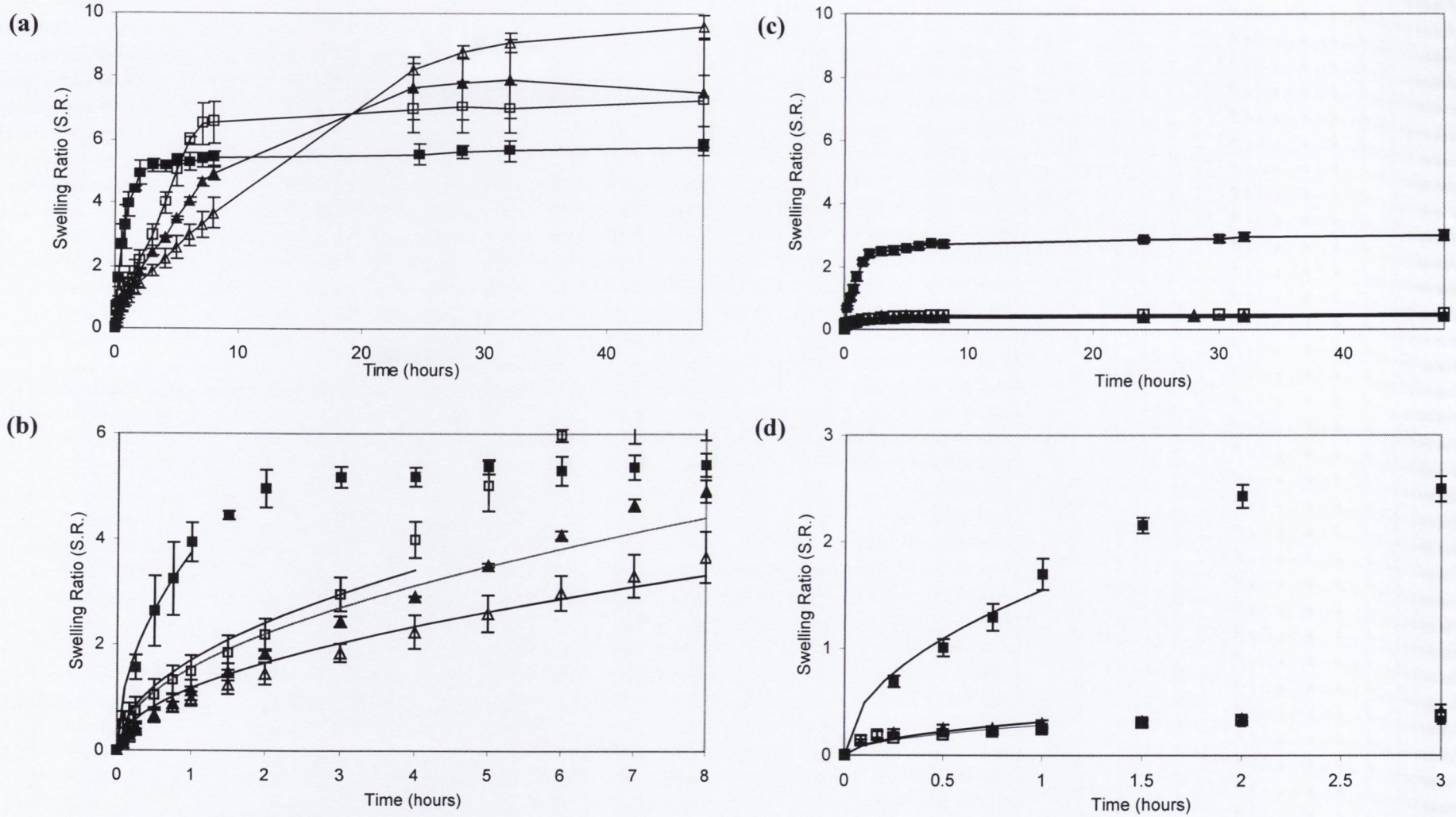

Fig. 4.18: Swelling Ratio of PNIPA-H1 (■), PNIPA-H2 (□), PNIPA-H3 (▲) and PNIPA-H4 (Δ) over 48 hours at (a) 25°C and (c) 37°C in PB. Also shown are early timeperiods (S.R. < 60% of equilibrium) at (b) 25°C and (d) 37°C fitted to the square root of time (Equation 2.12, *Higuchi*).

At 25°C (Fig. 4.18a), the swelling profiles (60% of equilibrium swelling) were found to be approximately proportional to the square root of time (Equation 2.12, *Higuchi*) (Table 4.8) where the rate constant, k_s, was approximated by $k_s = 2AC_o\left(\frac{D_{app}}{\pi}\right)^{0.5}$ for matrix diffusion (Higuchi, 1962).

A better fit was obtained in each case when the diffusional exponent (n) was allowed to vary (Table 4.8). Equilibrium swelling at 25°C took up to 48 hours to be reached, depending on the extent of crosslinking.

Table 4.8. Swelling rate constants k_s (Equation 2.12, *Higuchi*) at 25°C and 37°C with associated coefficient of determination (CD). Diffusional exponents, n, were estimated using Equation 2.11 (*Peppas*). Also shown are apparent diffusion coefficients (D_{app}) of water into the hydrogels estimated using the amount of media absorbed per unit surface area (Equation 2.5a).

25°C	k_{s25}	CD	D_{app} (X10^{-6})	n	CD
PNIPA-H1	19.568 ± 2.474	0.9762	1.437 ± 0.309	0.639 ± 0.008	0.9981
PNIPA-H2	25.987 ± 0.283	0.9490	2.701 ± 0.409	0.730 ± 0.081	0.9982
PNIPA-H3	28.441 ± 2.623	0.9390	2.295 ± 1.581	0.666 ± 0.198	0.9828
PNIPA-H4	62.550 ± 10.125	0.9734	14.062 ± 2.418	0.654 ± 0.105	0.9907
37°C	k_{s37}	CD		n	CD
PNIPA-H1	5.272 ± 0.471	0.9036	0.067 ± 0.002	0.260 ± 0.191	0.9883
PNIPA-H2	4.803 ± 0.142	0.8013	0.057 ± 0.004	0.250 ± 0.043	0.9736
PNIPA-H3	4.712 ± 0.178	0.8715	0.058 ± 0.005	0.203 ± 0.150	0.9546
PNIPA-H4	25.822 ± 2.099	0.9742	3.558 ± 0.588	0.679 ± 0.080	0.994

There was a linear relationship ($R^2 = 0.9164$) between the swelling rate constant k_{s25} and the mol% crosslinker present in the hydrogel (Fig. 4.19).

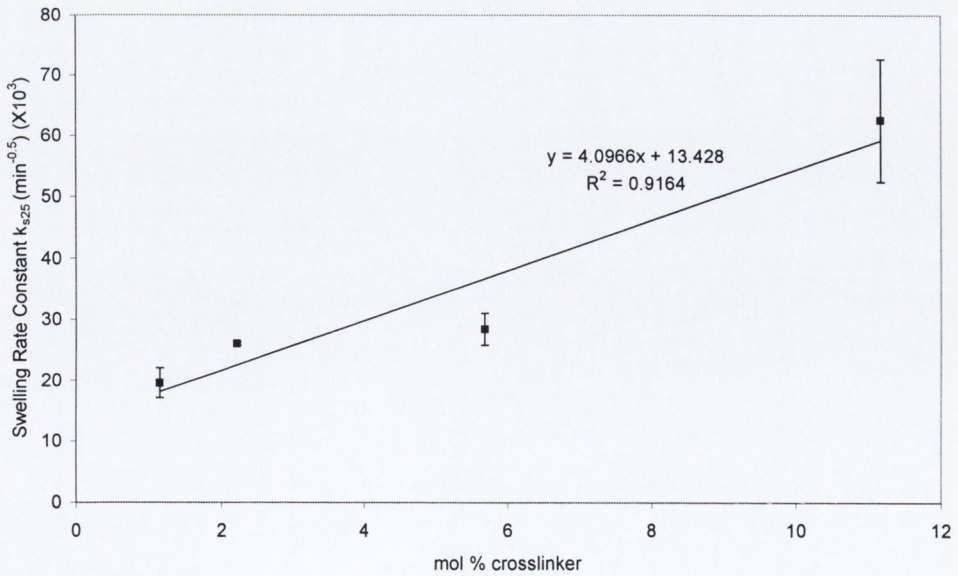

Fig. 4.19: Plot of swelling rate constants at 25°C (k_{s25}) against mol% crosslinker (MBA) in the hydrogel series.

The increase in swelling rate was consistent with reports by Omidian and co-workers (Omidian *et al.*, 1998; Kabiri *et al.*, 2003) who prepared non-thermoresponsive hydrogels and found an increase in the swelling rate with increasing concentration of crosslinker (MBA). The swelling rate increase was attributed to a longer gelation time at lower crosslinker (MBA) concentrations. In addition, they proposed that if the polymer network only acted as a barrier against diffusing water, less water molecules should diffuse in the highly crosslinked network. The opposite case occurs in a highly hydrophilic polymer, which attracts water instead of repelling them. As a result, they proposed that higher crosslinking density may cause a stronger thermodynamic force. The higher crosslinking density then resulted in an enhancement of swelling rate at the expense of decreasing ultimate swelling capacity.

Photographs of the swelling of PNIPA-H1 at various time points are shown in Fig. 4.20.

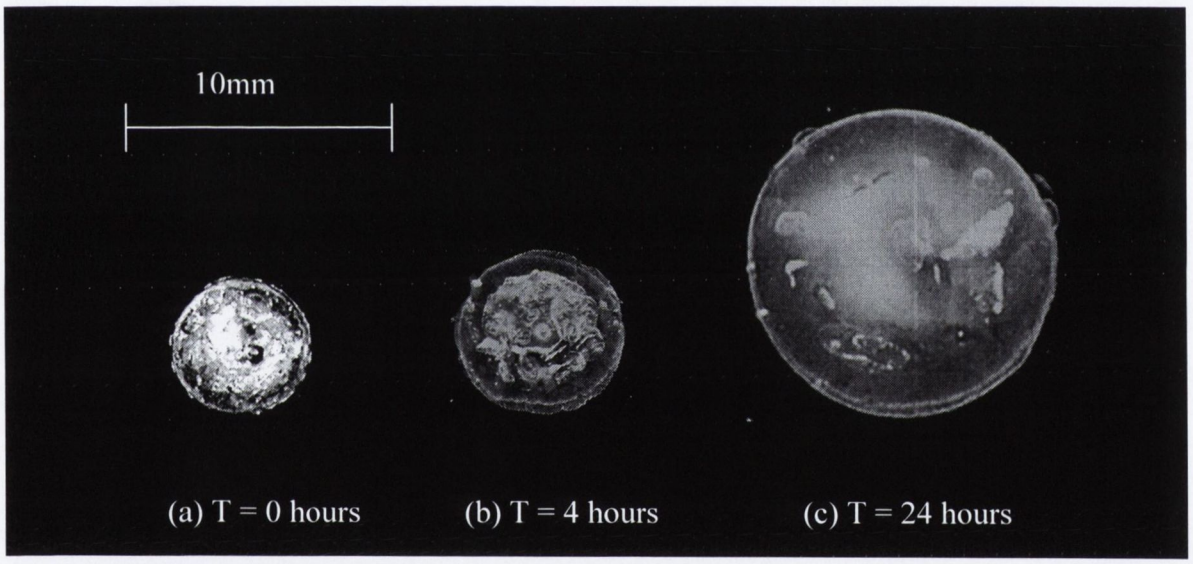

Fig. 4.20: Photographs of PNIPA-H1 hydrogel swelling at 25°C at various time points.

At 37°C (Fig. 4.18c), the diffusional exponents in the series PNIPA-H1 to PNIPA-H3 were <0.5, although reasonable fits were still obtained when plotted against the square root of time (Table 4.8). There was a dramatic decrease in the rate as well as the extent of swelling at 37°C compared to 25°C (Table 4.8). The equilibrium level of swelling at 37°C, defined here as the "equilibrium residual volume", was reached within about 3 hours for each hydrogel.

The apparent diffusion coefficient values of water (D_{app}) into the hydrogel at 25°C and 37°C were also given in Table 4.8. At 25°C, the values for the first three hydrogels in the series (H1 to H3) ranged from 1.4 X 10^{-6} cm^2/s to 2.3 X 10^{-6} cm^2/s. These values can be compared to diffusion coefficients of ~4 X 10^{-6} cm^2/s (Ashraf *et al.*, 1994; Panomsuk *et al.*, 1995) for hydration of various hydrophilic cellulose matrices at 37°C, or a water diffusion coefficient of 5.6 X 10^{-6} cm^2/s

in a fully swollen hydroxypropyl methylcellulose tablet (Siepmann *et al.*, 1999). These values are an order of magnitude slower than the diffusion coefficient into PNIPA-H4 (1.4 X 10^{-5} cm^2/s), which approached the self-diffusion coefficient of water at 25°C (~2.2 X 10^{-5} cm^2/s) (Angell *et al.*, 1976; Tyrrell and Harris 1984).

4.4.4 Swelling /deswelling kinetics

Fig. 4.21 shows the swelling and deswelling/contraction patterns of the unloaded hydrogel discs (in PB) on switching the temperature between 25°C and 37°C.

The swelling was found to be proportional to the square root of time during both 25°C swelling periods. The swelling rate constants (k_s) are given in Table 4.9 for both the 0 to 1 hour (k_s1) and the 4 to 7 hour (k_s2) swelling periods. The swelling rate constants did not significantly change ($p>0.05$) between the two periods of swelling.

Table 4.9: Swelling rate constants (k_s, based on swelling ratio) and maximum contraction rates (k_{MC}) for the two swelling–contraction cycles (Fig. 4.21(a))

Hydrogel	k_s1 $(min^{-0.5})(X10^3)$	k_s2 $(min^{-0.5})(X10^3)$	k_{MC1} $(min^{-1})(X10^2)$	k_{MC2} $(min^{-1})(X10^2)$
PNIPA-H1	16.249 ± 1.416	16.088 ± 1.834	13.570 ± 1.617	21.940 ± 1.198
PNIPA-H2	21.867 ± 2.586	27.631 ± 6.611	17.394 ± 1.651	55.453 ± 18.161
PNIPA-H3	24.034 ± 4.766	34.368 ± 11.573	9.586 ± 2.451	62.582 ± 4.037
PNIPA-H4	61.894 ± 12.311	84.892 ± 10.731	20.148 ± 7.293	29.764 ± 2.774

A temperature switch above the LCST of the polymer caused a rapid and sharp deswelling or contraction of the hydrogel with expulsion of the absorbed medium. The maximum contraction rate (k_{MC}, indicated in Fig. 4.21b) was dependent on the level of swelling prior to temperature switch, which was dependent on the duration of the swelling phase. The k_{MC} of the unloaded system was thus greater after the second (3 hour) period of swelling (k_{MC2}) than it was after the first period (1 hour, k_{MC1}). Following contraction, a residual volume was reached at 37°C. This residual volume had its own equilibrium value, shown as the equilibrium level in Fig. 4.18c for the various hydrogels. The equilibrium residual volume was only reached after the second contraction phase in the case of PNIPA-H1; indicating that the interior of the collapsed hydrogel was not fully hydrated during the first period at 37°C. For the other hydrogels, this equilibrium volume was reached in the first hour due to the faster rates of swelling.

(a)

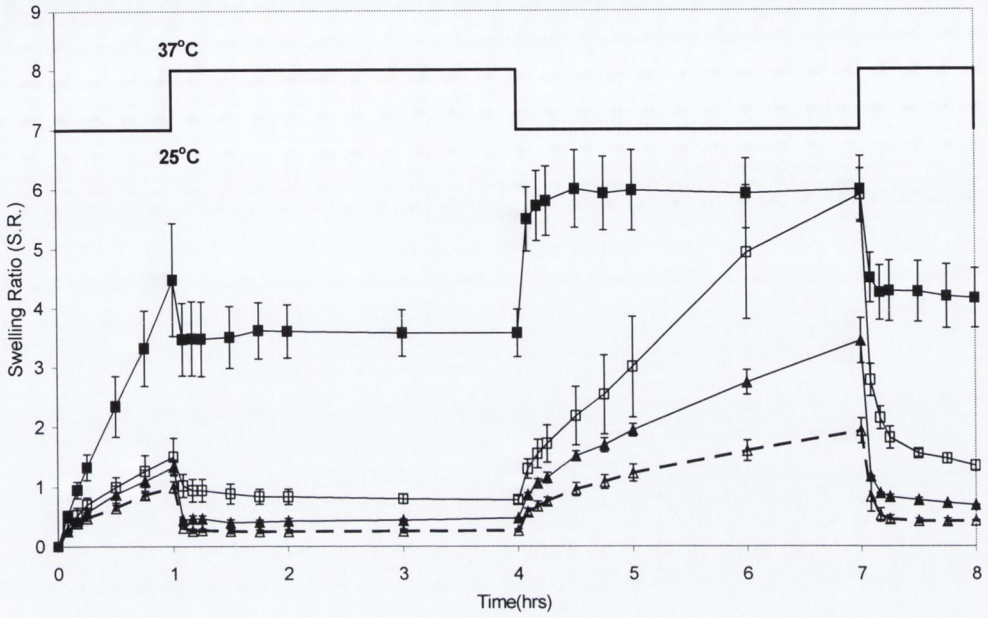

(b)

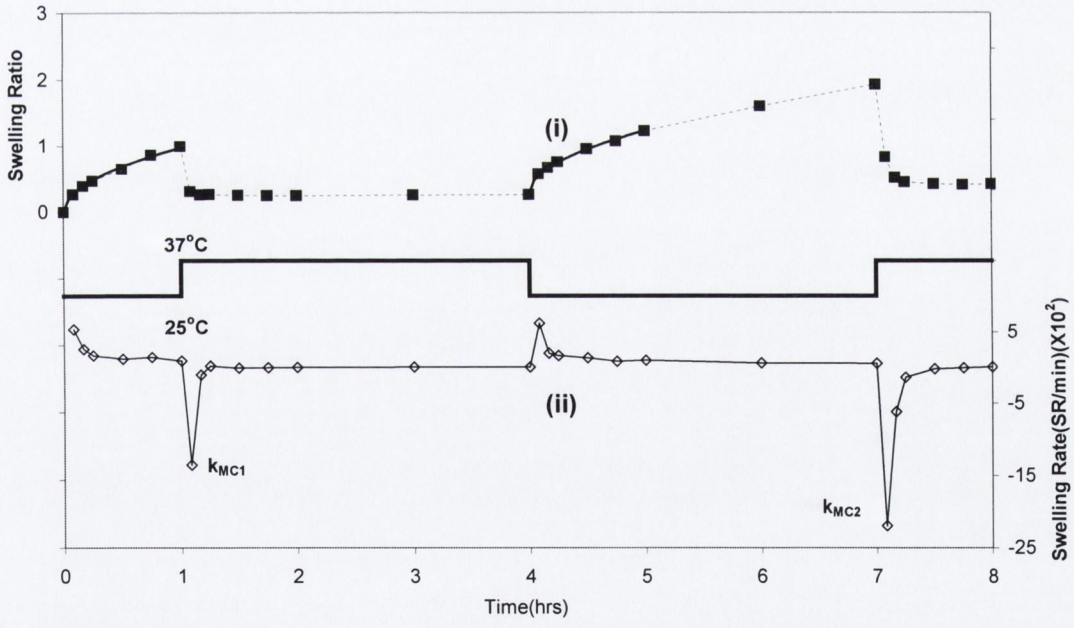

Fig. 4.21: Swelling-contraction cycle

(a) of PNIPA-H1 (Δ), PNIPA-H2 (▲), PNIPA-H3 (□) and PNIPA-H4 (■) on temperature switch between 25°C and 37°C.

(b) of PNIPA-H1 (i, ■)and corresponding contraction rate (ii, ◊) on temperature switch between 25°C and 37°C. Also shown are k_{MC1} and k_{MC2} along with first hour of swelling fitted to Equation 2.12 (*Higuchi*)

Temperature switch indicated by solid line.

There was a reasonable linear relationship (R^2=0.8960) between the k_{MC} of all the hydrogels and the resulting magnitude of contraction (Fig. 4.22a). This magnitude of contraction also correlated to the level of swelling prior to switch in the case of the first three hydrogels of the series (H1, H2 and H3, Fig. 4.22b). In the case of PNIPA-H4, a higher equilibrium residual volume at 37°C resulted in a smaller than expected magnitude of contraction than was observed with the other hydrogels.

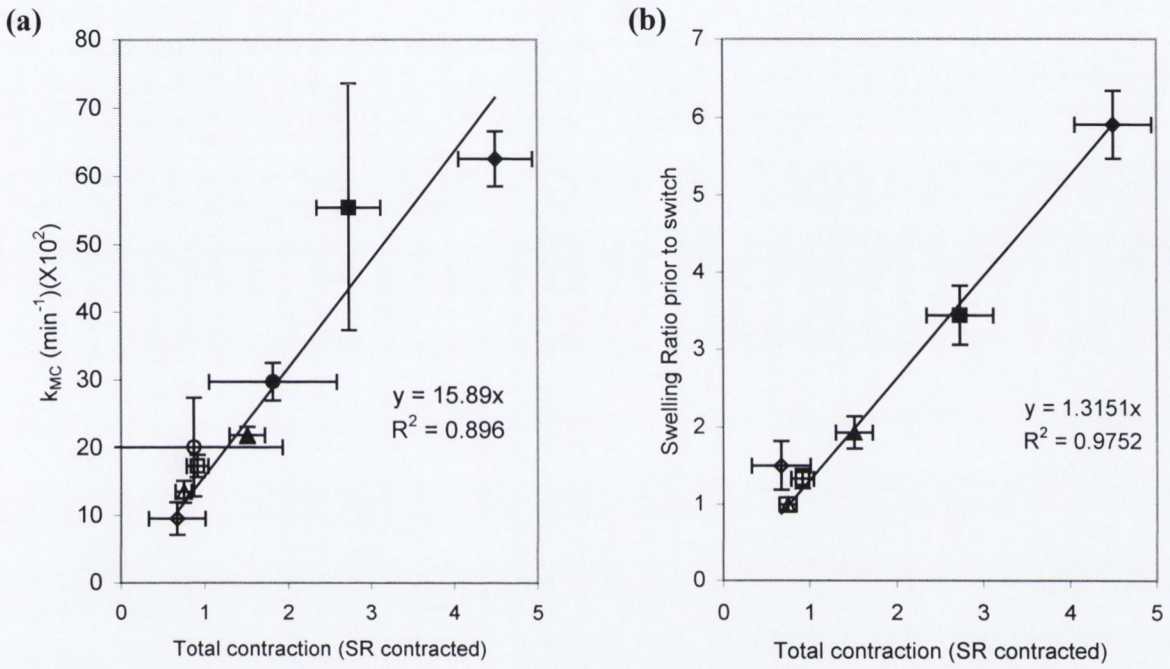

Fig. 4.22: Plot of relationship between (a) k_{MC} and magnitude of contraction and (b) swelling level prior to switch and magnitude of contraction [PNIPA-H1 (Δ/▲), PNIPA-H2 (□/■), PNIPA-H3 (◊/♦) and PNIPA-H4 (○/●)]. Data based on first period of swelling/deswelling (open symbols) and second period of swelling/deswelling (closed symbols).

4.4.5 Pore size distribution

Pore size can be defined here as the three-dimensional mesh size of polymer chain networks in the gel that contains aqueous fluid-filled pores and their interconnections. Pores were classified according to their sizes as described by IUPAC (International Union of Pure and Applied Chemistry). "Macropores" are pores with openings exceeding 500 Å in diameter. "Micropores" are pores with diameters less than 20 Å. "Mesopores" are pores of between 20 Å and 500 Å in diameter. Different methods of determining the mesh size or pore size distribution of hydrogels have previously been attempted. The pore size of the hydrogel can be examined in a swollen state by theoretical evaluation of the extent of swelling (Peppas and Wright, 1998; Canal and Peppas, 1989; am Ende *et al.*, 1995), solute exclusion technique (Lin *et al.*, 1987; Park and Hoffman, 1994; Walther *et al.*, 1995) or more recently thermoporosimetry (Ishikiriyama *et al.*, 1995; Iza *et al.*,

2000). Alternatively the gel can be dried (e.g. freeze drying) and examined in the solid state using techniques such as scanning electron microscopy (SEM) (Zhang and Peppas, 2002; Ying *et al.,* 2003; Sen *et al.,* 2003) or nitrogen physisorption techniques (Ishikiriyama *et al.,* 1995; Iza *et al.*, 2000; Zhang *et al.,* 2003).

In order to examine hydrogels in their "swollen" state, the sample can be flash frozen in liquid nitrogen and dried out under vacuum (freeze-drying). Scherer (1993) examined the process of freezing a liquid in the pores of a gel. This study showed that cracking and gel shrinkage occur during freezing. They estimated that pore sizes may be underestimated by ~30% for a typical silica gel, if water is the liquid in the pores. Ishikiriyama *et al.* (1995) showed that freeze-drying decreased the pore volume and peak radius of a poly(methyl methacrylate) membrane, although this effect was not seen with the other hydrogel membranes examined.

The present study examines the pore size of all four hydrogels by SEM and nitrogen desorption technique from a freeze-dried state at 25°C and 37°C. The results for PNIPA-H1 are compared to the values obtained by analysis of the same hydrogel at 25°C and 37°C using the solute exclusion technique.

4.4.5.1 Scanning Electron Microscopy

SEM is a solid-state method of examining the morphology of hydrogels, usually after a freeze-drying process (Zhang and Peppas, 2002; Ying *et al.,* 2003; Sen *et al.*, 2003). Gutowska *et al.* (1994) and Wu *et al.* (2003) used SEM to examine the porous structure of PNIPA gels. Zhang and Peppas (2002) examined the morphology of the PNIPA-poly(methacrylic acid) IPNs in their wet state by freezing the hydrogels in liquid nitrogen and examination by cryogenic SEM. A general decrease in pore size of their gels was observed on decreasing the pH and/or increasing the temperature in these studies. The present hydrogels were freeze-dried from an equilibrium swelling state at either 25°C (Fig. 4.23) or 37°C (Fig 4.24, Fig 4.25) and sputter coated with gold prior to examination on a SEM.

At 25°C (Fig 4.23), the influence of the percentage crosslinker on the pore size can be seen visually. Under the same magnification at 37°C (Fig 4.24), pores can only be seen with PNIPA-H3 and PNIPA-H4. The hydrogels in the series PNIPA-H1 to PNIPA-H3 were swollen to the same extent at this temperature (Fig. 4.15a), yet the morphology and macropore size was drastically different. PNIPA-H4 swelled to a greater extent at this temperature than the other hydrogels (Fig. 4.15a) and the resulting macropore size was greater, despite the higher percentage crosslinking. Smaller pores could also be seen when PNIPA-H1 and PNIPA-H2 were examined under higher magnification (Fig. 4.25).

(a) PNIPA-H1

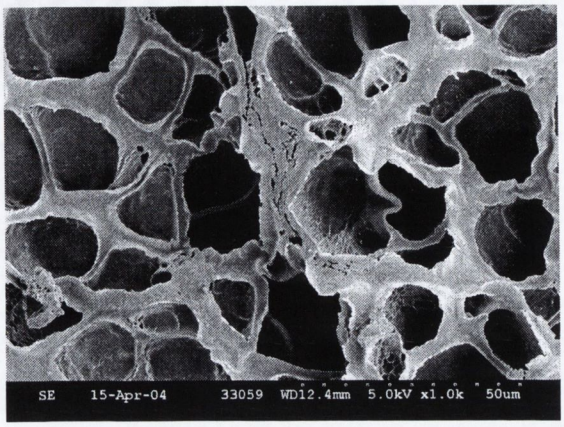

(b) PNIPA-H2

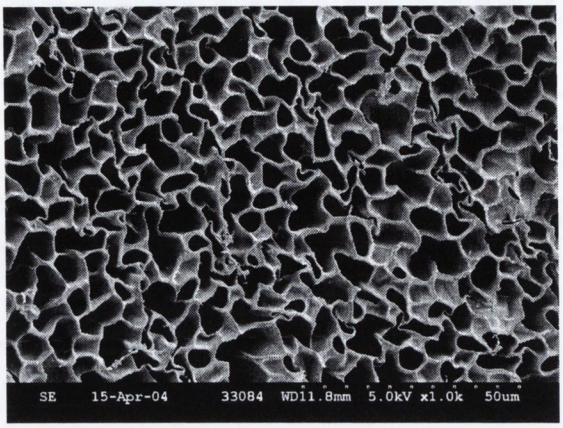

(c) PNIPA-H3

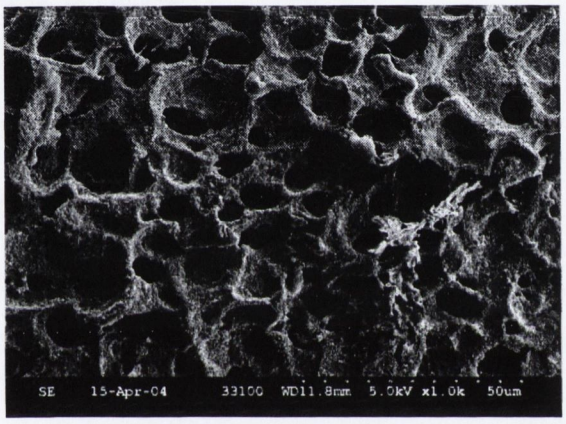

(d) PNIPA-H4

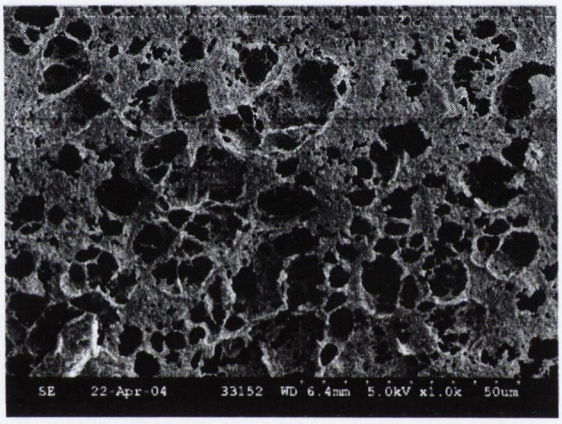

Fig 4.23: SEM (Magnification 1000X) of PNIPA hydrogels, freeze-dried from an equilibrium swollen state at 25°C in PB

In an attempt to quantify the size of the pores seen visually by SEM, approximate pore sizes in the SEM scans were obtained using computer software (Imagetool for Windows ® Version 3.00). Fifty measurements of cross-sectional diameters were obtained at random on SEM images (n = 3). A normal probability distribution was obtained using the average and standard deviation of the data (n=150) to give Fig 4.26.

Table 4.10: Hydrogel macropore size (mean ± s.d.) as determined by SEM. Also shown are the equilibrium level of swelling at 25°C and 37°C.

Hydrogel	Mol % crosslinker	25°C		37°C	
		Equilibrium Swelling (S.R.)	Observed pore size at 25°C (μm) (n=150)	Equilibrium Swelling (S.R.)	Observed pore size at 37°C (μm) (n=150)
PNIPA-H1	1.15	9.37 ± 0.29	11.837 ± 5.356	0.49 ± 0.07	ND
PNIPA-H2	2.22	8.17± 0.42	6.181 ± 2.783	0.28 ± 0.17	ND
PNIPA-H3	5.68	4.78 ± 0.84	5.093 ± 2.637	0.37 ± 0.18	3.593 ± 2.401
PNIPA-H4	11.17	4.82 ± 0.63	3.962 ± 1.648	2.17 ± 0.74	4.241 ± 2.651

(a) PNIPA-H1

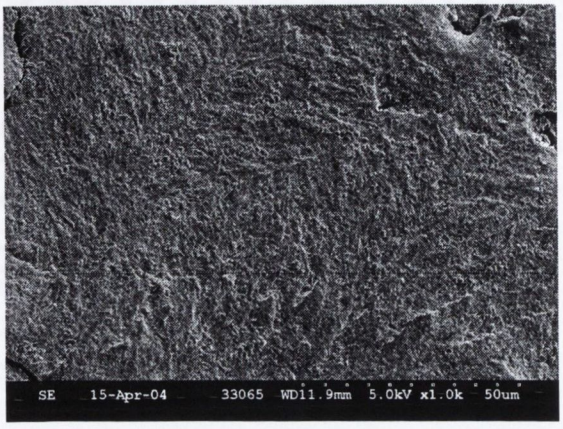

(b) PNIPA-H2

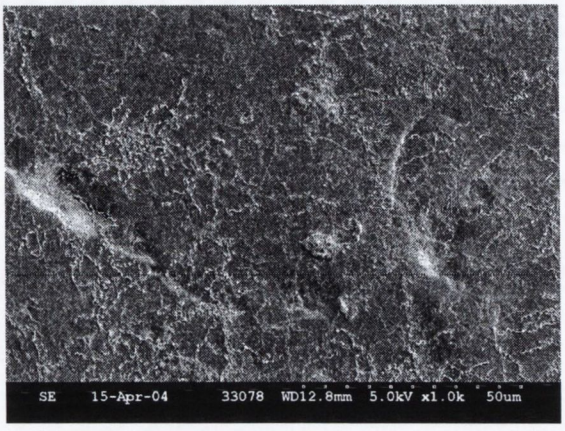

(c) PNIPA-H3

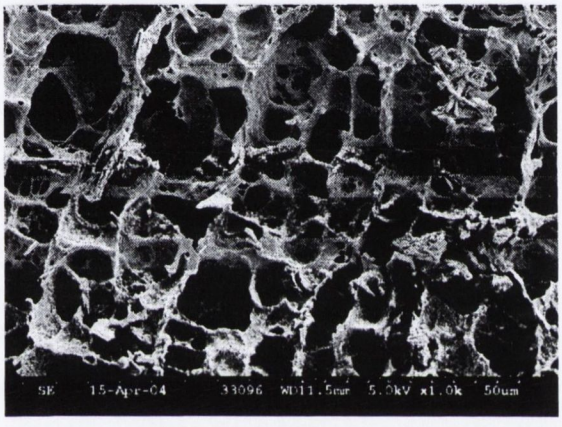

(d) PNIPA-H4

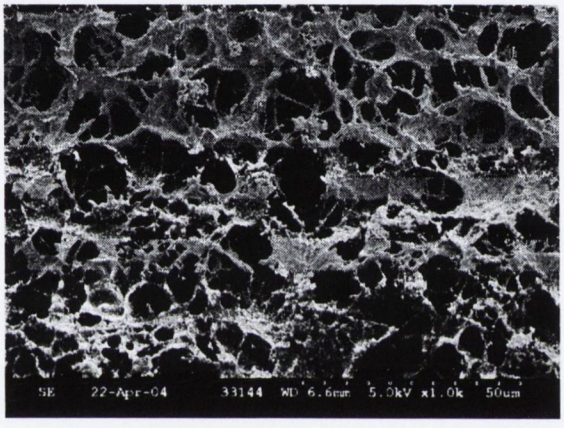

Fig 4.24: SEM (Magnification 1000X) of PNIPA hydrogels, freeze-dried from an equilibrium swollen state at 37°C in PB.

(a) PNIPA-H1

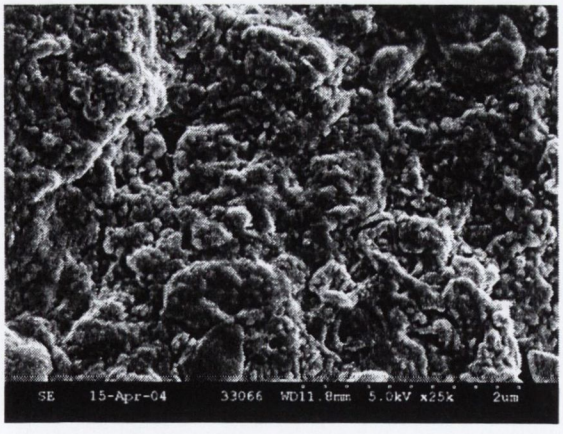

(b) PNIPA-H2



Fig 4.25: SEM (Magnification 25000X) of PNIPA hydrogels, freeze-dried from an equilibrium swollen state at 37°C in PB.

A large range of macropore sizes was observed using this technique at 25°C, with a general trend towards a decrease in the macropore size as the percentage crosslinker increased as shown in Fig. 4.26.

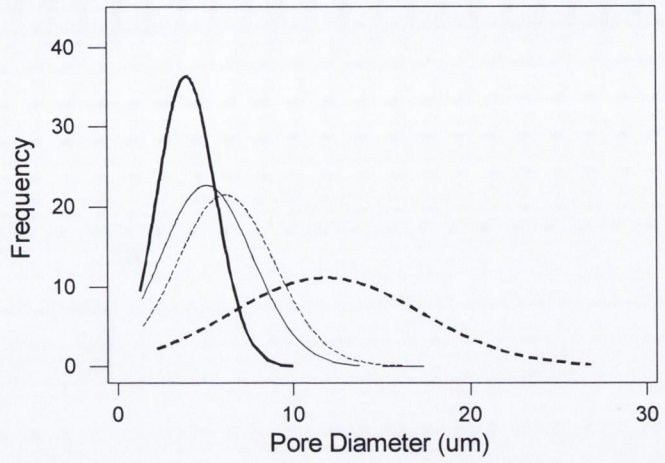

Fig 4.26: Normal pore size distribution curves of PNIPA hydrogels (total of n=150 measurements each, based on n=3 SEM images) at 25°C [PNIPA-H1 (bold-dashed curve), PNIPA-H2 (dashed curve), PNIPA-H3 (solid curve), PNIPA-H4 (bold-solid curve)]

At 37°C, the pores of PNIPA-H1 and PNIPA-H2 could not be quantified using SEM due to their smaller size at this temperature. The effect of increased temperature on PNIPA-H1, H2 and H3 was to decrease the observed pore size, although this decrease was not as pronounced with PNIPA-H4. The pore size difference observed between the two temperatures were not as significant for the more highly crosslinked hydrogels (PNIPA-H3 and H4), in qualitative agreement with the swelling study in Fig. 4.15a. The mean pore size at 37°C also showed a qualitative trend of increased size with increasing crosslinker in the series PNIPA-H2 to H4.

The SEM data was useful in examining the macropores of the gels in their swollen state. A trend towards a decrease in the mean pore size with increasing percentage crosslinker could be observed at 25°C, similar to trends previously reported with non-thermoresponsive hydrogels (e.g. Peppas and Lustig, 1985; am Ende *et al.,* 1995). A trend towards an increase in the mean pore size with increasing percentage crosslinker was observed at 37°C. PNIPA-H4 had a higher equilibrium swelling level at this temperature (Fig. 4.15a, Table 4.10) and a larger pore size was therefore expected. The level of swelling of PNIPA-H3 was not statistically different ($p > 0.05$, Table 4.10) from PNIPA-H1 and PNIPA-H2, yet the morphology was drastically different as observed by SEM. An apparent increase in pore size with increasing percentage crosslinker was therefore observed. As the percentage of non-thermoresponsive crosslinker methylenebisacrylamide (MBA) increased, the local pore size may have increased at 37°C due to the MBA remaining in a hydrophilic state, surrounded by the hydrophobically collapsed NIPA monomers. The higher level of crosslinking may therefore be acting in these systems to prevent complete hydrophobic collapse of the hydrogel. The presence of increasing amounts of MBA resulted in increasing local pore

sizes, even when differences were undetectable by gravimetric swelling measurements (Table 4.10). Park and Hoffman (1990) previously described a situation where PNIPA was copolymerised with acrylamide (AAm). In PNIPA-AAm gels they showed that two opposite forces were at work above the LCST i.e. thermal expansion mainly from AAm moieties and thermal shrinkage due to NIPA moieties. An increase in pore size resulted when the percentage AAm was increased. The non-thermoresponsive nature of the present crosslinker (MBA) therefore acted in the same way to increase pore size above the LCST, in contrast to an expected decrease in the pore size as previously described using non-thermoresponsive hydrogels (e.g. Peppas and Lustig, 1985; am Ende *et al.*, 1995).

4.4.5.2 Nitrogen Desorption

A desorption isotherm can be used to evaluate the pore size distribution of an adsorbent, with nitrogen being the most common adsorbate for pore size distribution measurements. The nitrogen desorption isotherm was obtained as described in section 3.3.7.2. Mesopore size calculations were made assuming cylindrical pore geometry using equation 3.2 (Barrett, Joyner, Hallenda (BJH) method). The pore size distributions obtained are shown in Fig. 4.27 for the four hydrogels at 25°C (solid lines) and at 37°C (dashed lines). Fig. 4.28 compares the distributions obtained using the four gels at 37°C. The pore volumes and radius calculated using the BJH method are given in Table 4.11.

The data obtained in Fig. 4.27 indicated the presence of mesopores (diameter range ~20Å to 500Å) in the hydrogels. A wide and continuous range of pores sizes were observed due to the random nature of the crosslinking process. The volume of pores increased towards the micropore end of the scale with a peak also seen around 200Å in the case of PNIPA-H4. There was a greater volume of these pores (Table 4.11) at 25°C than at 37°C as expected from the greater extent of swelling described in Fig.4.15a. The difference in pore volume between the two temperatures decreased as the percentage crosslinker increased (Table 4.11), also similar to the pattern shown in Fig. 4.15a with the swelling data.

Table 4.11: Pore volume and pore radius as determined for the four hydrogels using the BJH method of nitrogen desorption

Hydrogel	**25°C**		**37°C**	
	Pore Volume (cc/g)	**Average Pore Radius**	**Pore Volume (cc/g)**	**Average Pore Radius**
PNIPA-H1	0.49	15.63Å	0.01	16.95Å
PNIPA-H2	0.06	18.38Å	0.01	16.88Å
PNIPA-H3	0.04	16.91Å	0.02	15.60Å
PNIPA-H4	0.10	16.96Å	0.05	16.95Å

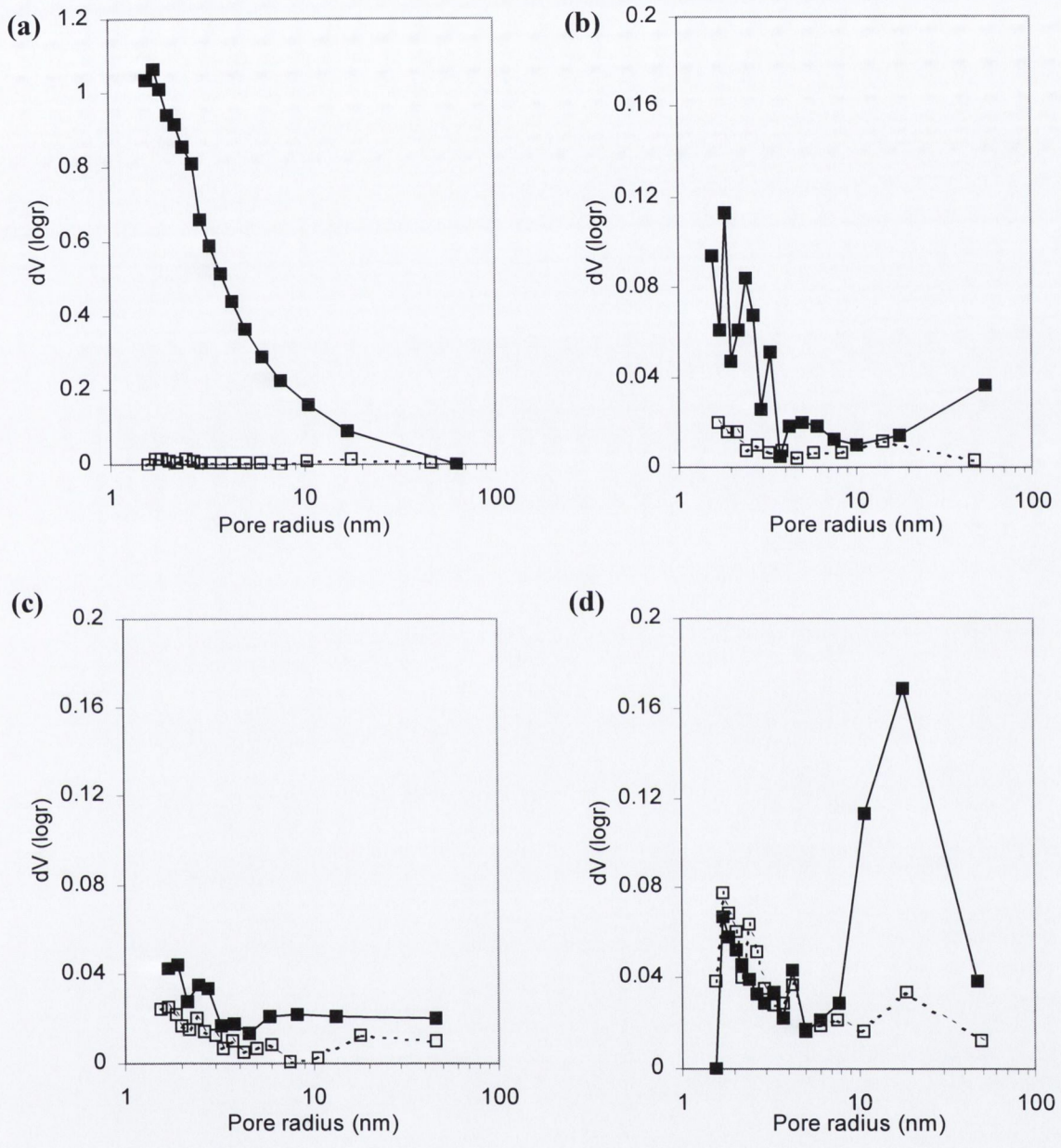

Fig. 4.27: Mesopore size distributions obtained using the BJH method from nitrogen desorption isotherms (a) PNIPA-H1 (b) PNIPA-H2 (c) PNIPA-H3 (d) PNIPA-H4. Hydrogels freeze-dried from an equilibrium swelling state at 25°C (solid lines) or 37°C (dashed lines).

Fig. 4.28 compares the pore size distributions at 37°C. At this temperature, there were a greater volume of mesopores in the range 10Å to 100Å as the percentage crosslinker increased, consistent with the qualitative increase in pore size seen with the SEM data (Fig. 4.24).

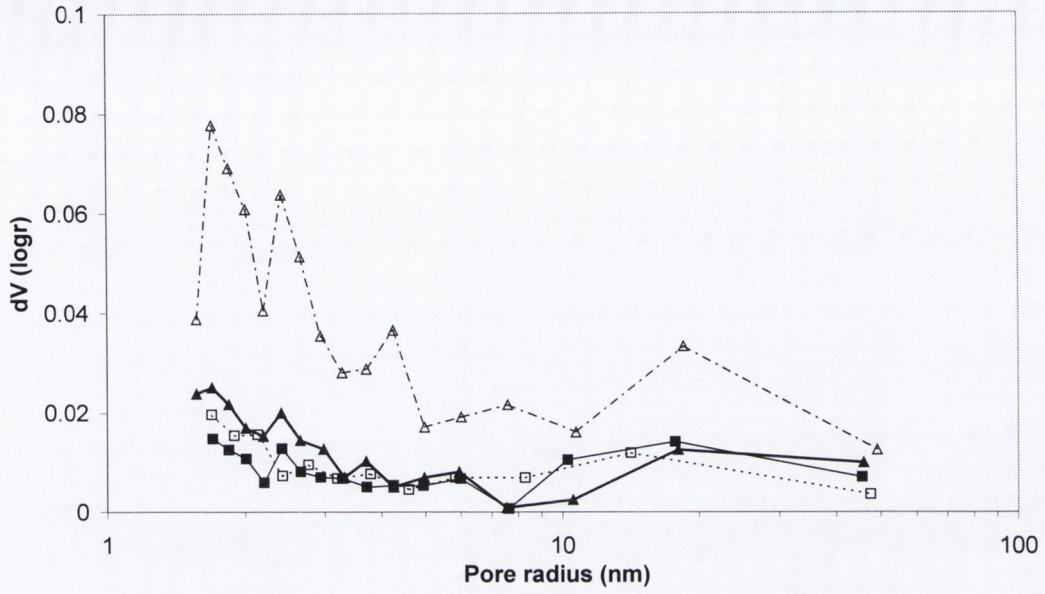

Fig. 4.28: Comparison of pore size distributions at 37°C of PNIPA-H1 (solid line, ■), PNIPA-H2 (dashed line, □), PNIPA-H3 (bold line, ▲), PNIPA-H4 (dash-dot line, Δ).

The mesopore size at 37°C therefore appears to increase with increasing crosslinker above the LCST, in qualitative agreement with the SEM results.

The average pore radii predicted by the BHJ method (Table 4.11) were at the lower end of the mesopore range (15Å to 18Å), although no trends were observed in the data with increasing crosslinker.

4.4.5.3 Solute exclusion technique

The pore size distribution of PNIPA-H1 was also characterised by a solute exclusion technique using a series of model probes of various sizes as described in section 3.3.7.3. This technique essentially involves measurement of the ability of each probe fraction to permeate from the bulk media into the equilibrated hydrogel at a given temperature. The principle of the solute exclusion technique for characterisation of pore size distribution of hydrogels is illustrated in Fig. 4.29.

The swollen hydrogel is immersed in a known volume of a solution containing a molecular probe. If all the water originally associated with the hydrogel is accessible to the probe molecules, it will all equilibrate with and dilute the solution (Case I). In case II, some of the pores are inaccessible to the larger molecules. This water is unavailable for dilution and the mixed solution will therefore be less diluted than in case I. When the probe molecule is so large that it cannot enter any pores of the hydrogel (Case III), the inaccessible water equals the total water for swelling of the hydrogel. By

using a series of molecules of increasing size, quantitative information can be obtained on the fractional pore volume as a function of maximum pore size.

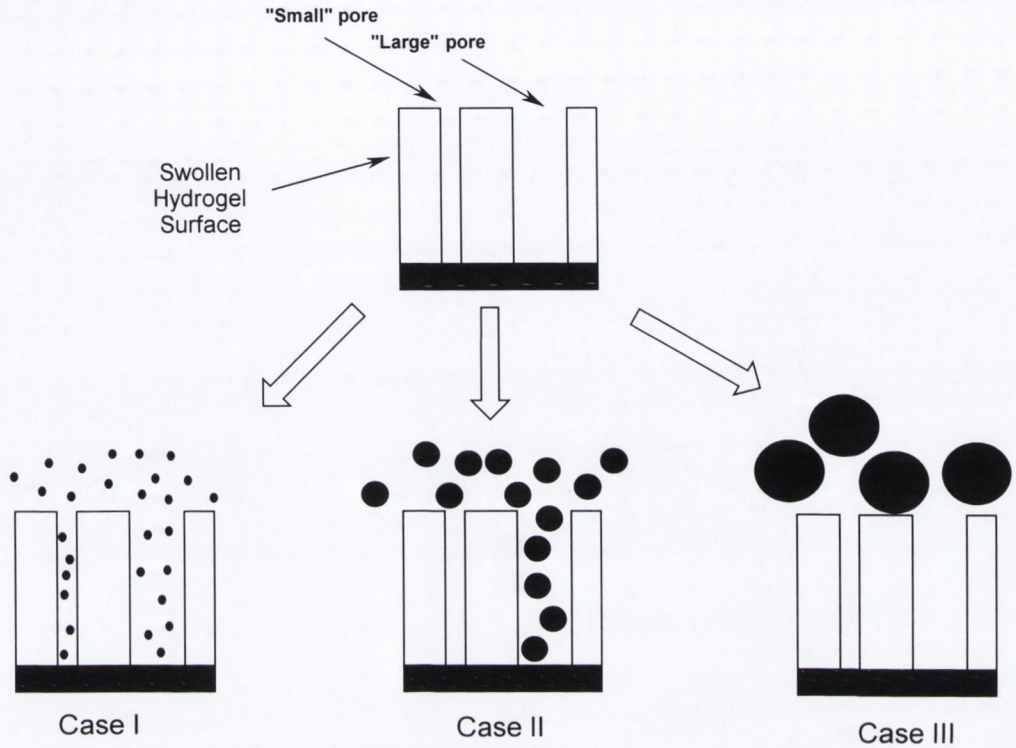

Fig. 4.29: Illustration of the principle of the solute exclusion technique for the measurement of pore size distribution of swollen hydrogels (Wu *et al.*, 1992a).

Assumptions in this experiment are that all the water in the gel is available to dissolve the drug molecules, the concentration of drug molecules in the total gel water is the same as that in the external bulk solution and that there are no interactions between the probe molecules and the polymer matrix. In addition it is assumed that the probe molecules are approximately spherical when in solution.

Fig. 4.30a shows the volume of pores in PNIPA-H1 accessible to each drug fraction above and below the LCST. The values at 37°C were lower than at 25°C since the hydrogel is in a collapsed state, resulting in smaller pore size and a lower volume of media present. At the lower temperature there is a much greater volume of pores available. When these volumes were taken into account, the volume fraction (VF) of pores with sizes larger than the probing molecules were examined (Fig. 4.30b/c and Table 4.12). At 25°C, the value of VF approaches 1.0 for DHCl (molecular diameter 8.19Å), VB12 (11.75Å) and D4 (25.1Å). This indicates that in the swollen state, these probe molecules are small enough to access almost all of the hydrogels pores, or conversely all the pores in the hydrogel at 25°C were large enough to accommodate these probe molecules. D10 (38.3Å),

D40 (77.9Å) and D70 (98.3Å) could access 70%, 40% and ~35% respectively of the available pores.

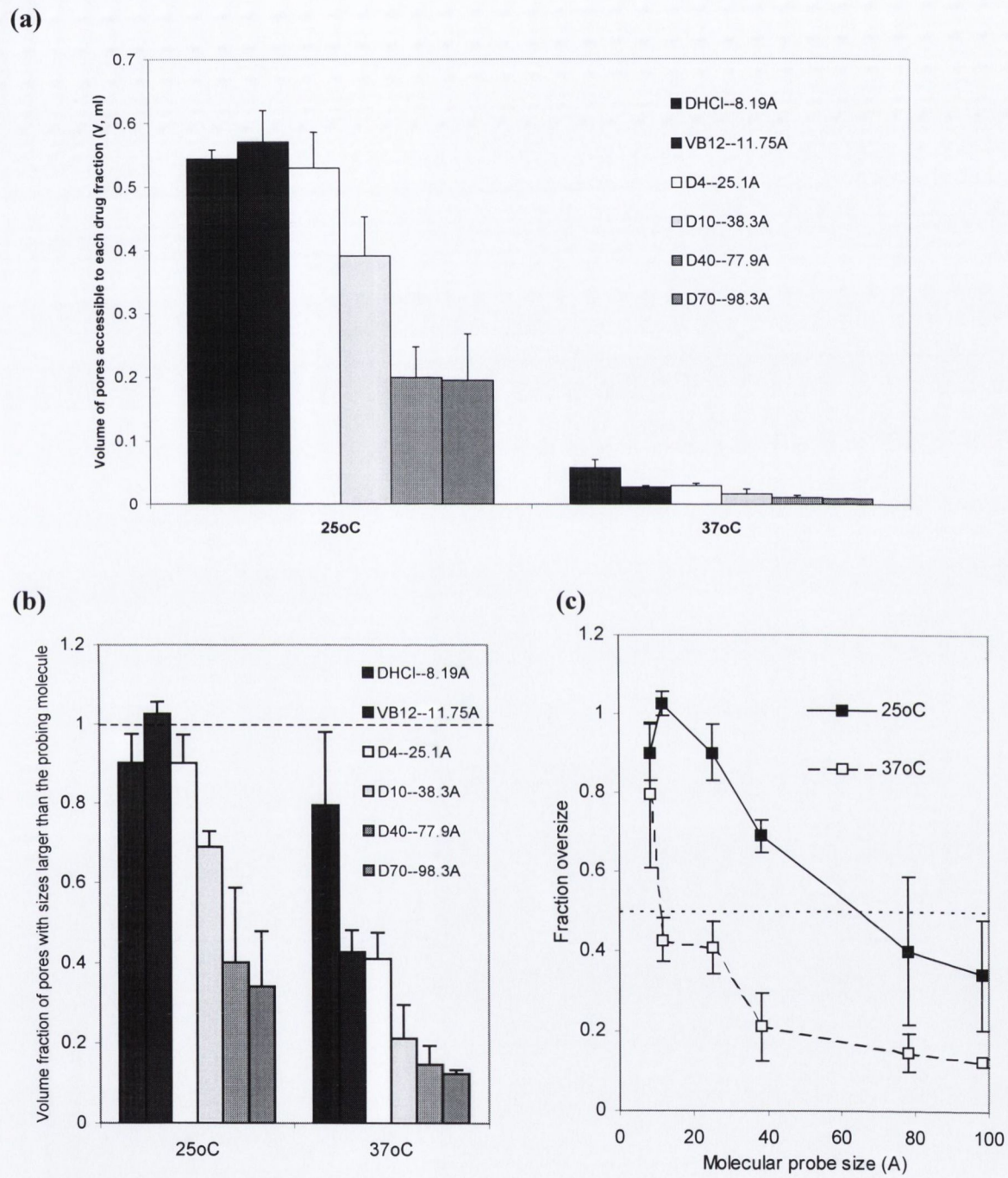

Fig. 4.30: Bar charts showing (a) the volume of pores of PNIPA-H1 (ml) accessible to each drug fraction at 25°C and 37°C (Eqn. 3.2) and (b) the volume fraction of pores with sizes larger than the probing molecule (Eqn. 3.3) (Dashed line in (b) indicates 100% of pores). Also given in (c) is fraction oversize with dashed line indicating 50% of pores with size larger than probing molecule.

At 37°C, when the hydrogel was in a collapsed state, DHCl and VB12 could access ~80% and 40% respectively of the available pores. The larger dextrans could only access between 10% and 20% of the available pores, assuming no polymer-drug interactions.

Table 4.12: Volume fraction (VF) of total media in PNIPA-H1 which is accessible to each probe molecule fraction

Probe molecule	**Molecular diameter (Å) (Table 4.4)**	**VF at 25°C**	**VF at 37°C**
DHCl	8.19	0.902 ± 0.073	0.794 ± 0.185
VB12	11.75	1.025 ± 0.030	0.427 ± 0.054
D4	25.1	0.900 ± 0.072	0.410 ± 0.065
D10	38.3	0.690 ± 0.040	0.212 ± 0.084
D40	77.9	0.401 ± 0.185	0.147 ± 0.047
D70	98.3	0.342 ± 0.137	0.124 ± 0.010

When the fraction of model probe accessible to 50% of the available pores was examined (Fig. 4.30c), an estimate for the average pore size was obtained: ~60Å at 25°C and ~10Å at 37°C.

This technique is therefore useful in examining the ability of the probe molecules to permeate the pores of the hydrogel in different swelling states. At 25°C, molecules of diameter greater than 25Å could not access all of the available pores. At 37°C, there were pores inaccessible to even the smallest (8Å) of the probes. The large probe molecules had difficulty in accessing the available pores even in the hydrogel with the largest pores at 25°C. This inaccessibility may be expected from the observed pore size distribution obtained by nitrogen desorption, where the presence of a high proportion of micropores (<20Å) was apparent from the data.

The methods used for determining the pore size distributions can be compared. SEM was useful in showing the effect of temperature and crosslinking on macropore size. Smaller pores could be seen by SEM under higher magnification (Fig. 4.25) and it was these pores that were shown by the desorption isotherms to be predominant in the hydrogels at both temperatures. The results at 25°C for PNIPA-H1 indicated that even in the highly swollen state there were still pores present at the lower end of the mesopore range and in the micropore range (< 20Å) for this lightly crosslinked hydrogel. It was these micropores in the molecular size range that were the limiting pores for the access of the larger probe molecules in the solute exclusion technique.

CHAPTER 5

Effect of Drug Physicochemical Properties on Swelling/Deswelling Kinetics and Pulsatile Drug Release from PNIPA-H1

5.1 INTRODUCTION

As outlined in Chapter 2, most of the studies to date examining thermoresponsive pulsatile drug release have concentrated on release of the hydrophobic drug indomethacin from heterogeneous PNIPA hydrogels using butyl methacrylate as a comonomer. Pulsatile release from such hydrogels has been explained by the formation of a dense, less permeable surface layer of gel formed on increasing temperature. This surface layer was described as a skin-type barrier caused by the presence of the alkyl side chain (Yoshida *et al.*, 1991, 1994b; Okano *et al.*, 1990; Gutowska *et al.*, 1992).

Some pulsatile release studies have also been performed using thermoresponsive systems where NIPA was copolymerised with a hydrophilic comonomer (Yoshida *et al.*, 1994a, 1994b; D'Emanuele and Dinarvand, 1995; Dinarvand and D'Emanuele, 1995). Such comonomers have been used to increase the phase transition temperature of PNIPA towards body temperature (Schild 1992; Yoshida *et al.*, 1994b). The incorporation of these comonomers may prevent the formation of this skin type layer (Yoshida *et al.*, 1994a, 1994b), which controlled the *off*-phase as described above. An *off*-phase was often difficult to show with the hydrogel-only systems (D'Emanuele and Dinarvand, 1995; Dinarvand and D'Emanuele, 1995), even if an alkyl methacrylate was also copolymerised in the hydrogel (Yoshida *et al.*, 1994b). In some cases this has been attributed to an "insufficiently dense skin layer" (Yoshida *et al.*, 1994b), with the relationship between drug size and hydrogel pore size not being considered. The influence of the skin layer on control of drug release may not be significant in such instances. The levels of equilibrium swelling at the chosen temperatures as well as the rate of swelling/deswelling of the hydrogel will be the determining factors that will control pore size and drug release from these systems. The influence of the chosen drug on the ability to thermally control release is therefore important and has not been examined in the above studies.

In homogeneous PNIPA hydrogels or hydrophilically-modified PNIPA hydrogels, a drug pulse on increasing temperature was also evident (Dinarvand and D'Emanuele, 1995; Zhang *et al.*, 2002). The drug pulse seen on temperature increase was used by several authors to develop systems where the *on*-phase was at the higher temperature (positive thermosensitive release, section 2.4.3.1) (Yoshida *et al.*, 1994c; Zhang *et al.*, 2002; Gutowska *et al.*, 1997; Shin *et al.*, 2001). Indomethacin was again the model drug of choice in these studies (Yoshida *et al.*, 1994c; Gutowska *et al.*, 1997; Shin *et al.*, 2001) except in the recent study of Zhang *et al.* (2002) who used 5-fluorouracil. The magnitude of the drug pulse influences the drug concentration gradient created across the membrane in these systems, which therefore affects the rate of drug diffusion on raising the

temperature. The effect of the loaded drug on the magnitude of this "pulse" was not considered in the studies mentioned.

The present chapter examines pulsatile release from a homogeneous PNIPA hydrogel, which is lightly crosslinked (1.15mol % crosslinker) (PNIPA-H1), where drug release is not affected by a hydrophobic comonomer as described above. The extent to which the chosen drug influences the pulsatile swelling of the system, the diffusional release of drug from the system, the size of the drug pulse seen following hydrogel contraction and the ability of the system to turn "*off*" drug release has been examined. The use of this thermoresponsive hydrogel in pulsatile drug delivery was evaluated by using a range of model probe molecules with different physicochemical properties, namely solubility, size (up to MW70,000) and chemical nature (Table 4.4). The hydrogels were loaded with drug (section 3.4.1) and swelling/deswelling (section 3.3.6) and pulsatile release studies (section 3.4.3) were performed as described.

5.2 INFLUENCE OF MODEL DRUGS ON SWELLING/DESWELLING

The model drugs used in the present study were described in Chapter 4. The relevant physiochemical properties of the drugs are summarised in Table 4.4. The drugs were divided into a hydrophobic and hydrophilic series as described.

The swelling and deswelling/contraction patterns of the unloaded PNIPA-H1 disc in PB on switching the temperature between 25°C and 37°C was shown in Fig. 4.20 along with the corresponding swelling and contraction rates. The swelling was found to be approximately proportional to the square root of time during both 25°C swelling periods (Equation 2.12, *Higuchi*). The swelling rate constants (k_s), calculated in this case based on the fraction swelling (Equation 3.1b), are given in Table 5.1 for both the 0 to 1 hour (k_s1) and the 4 to 7 hour (k_s2) swelling periods. The maximum contraction rate (k_{MC}), as described in section 4.4.4, is also given in Table 5.1 based on the fraction swelling data.

The swelling and contraction patterns of the drug-loaded discs are shown in Fig. 5.1 (a-d) along with the corresponding pattern for the unloaded hydrogel (shown as dashed line). The influence of the various drugs on this swelling-contraction pattern was also quantified using the swelling rate constants (k_s1, k_s2) and the maximum contraction rates (k_{MC1}, k_{MC2}) and the values obtained are shown in Table 5.1.

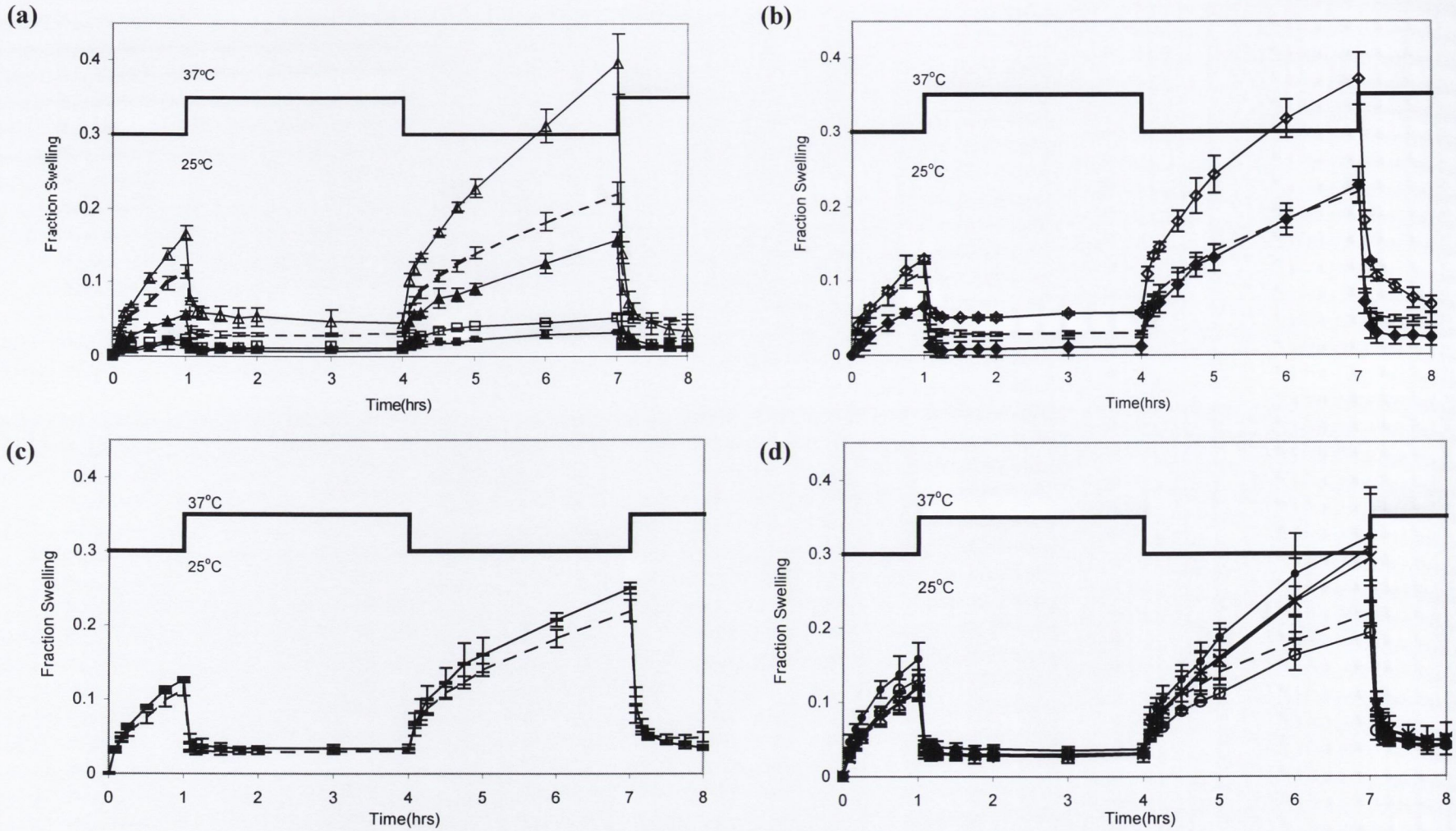

Fig. 5.1: Swelling-contraction of unloaded hydrogel disc (----) on temperature switch between 25°C and 37°C for comparison with drug loaded systems: (a) NaB (Δ), BA (▲), MHB (□), PHB (■), loading ~28% w/w (b) DHCl (◊), DB (♦) ~28% w/w (c) VB12 (—),~8% w/w (d) D4 (○), D10 (×), D40 (●), D70 (+), ~4% w/w.

Table 5.1: Swelling rate constants (k_s) and maximum contraction rates (k_{MC}) for the two swelling–contraction cycles (Fig. 5.1(a-d))

	k_s1 $(min^{-0.5})(X10^3)$	k_s2 $(min^{-0.5})(X10^3)$	k_{MC1} $(min^{-1})(X10^2)$	k_{MC2} $(min^{-1})(X10^2)$
Unloaded	1.853 ± 0.156	1.829 ± 0.112	1.542 ± 0.103	2.536 ± 0.505
BA	0.913 ± 0.068	1.446 ± 0.226	0.804 ± 0.197	2.441 ± 0.192
MHB	0.359 ± 0.028	0.529 ± 0.032	0.246 ± 0.052	0.732 ± 0.059
PHB	0.286 ± 0.076	0.219 ± 0.019	0.078 ± 0.085	0.401 ± 0.069
DB	1.021 ± 0.227	2.021 ± 0.100	1.040 ± 0.240	3.137 ± 0.169
NaB	2.596 ± 0.121	3.027 ± 0.285	1.800 ± 0.226	5.112 ± 0.962
DHCl	2.134 ± 0.129	3.018 ± 0.340	1.396 ± 0.161	3.801 ± 0.586
VB12	2.105 ± 0.015	2.123 ± 0.378	1.704 ± 0.177	3.160 ± 0.369
D4	2.109 ± 0.166	1.318 ± 0.012	1.891 ± 0.307	2.648 ± 0.306
D10	1.918 ± 0.278	2.036 ± 0.288	1.704 ± 0.083	3.959 ± 0.296
D40	2.656 ± 0.369	2.349 ± 0.268	2.220 ± 0.294	4.511 ± 1.044
D70	1.927 ± 0.297	2.072 ± 0.515	1.712 ± 0.277	4.432 ± 1.304

5.2.1 Hydrophobic drugs

The benzoate ester drug series and diltiazem base (DB) all have relatively low solubility in PB (Table 4.4). For the benzoate ester series (Fig. 5.1a), the effect of the drug was to decrease the rate of swelling of the hydrogel. The swelling rate of the hydrogel in the time period studied decreased as the solubility of loaded drug decreased. The dissolving drug front thus had a significant influence on the rate of hydrogel swelling. In the case of MHB and BA, the swelling rate during period 2 was significantly greater than that during period 1. This effect can be attributed to the diminishing influence of the drug over time on the ability of the outermost layer of the hydrogel to swell. The change in swelling rate is shown in Fig. 5.2a, which plots the swelling rate constant for swelling period 1 (k_s1) against the swelling rate constant for swelling period 2 (k_s2). Also shown in Fig. 5.2a is the data for the unloaded hydrogel as well as a 1:1 relationship between k_s1 and k_s2 (dashed line).

Diltiazem base (Fig 5.1b) slowed the rate of swelling during the period 1 but not during period 2. When these swelling constants (k_s1) were plotted against the solubility of the drug (Fig. 5.2b), a linear increase with solubility was observed for the benzoate series. DB deviated from the trend, suggesting that diltiazem influenced the swelling of the hydrogel different to that of the benzoate series. The effect of drug on the apparent diffusion coefficient of water (D_{app}) into the hydrogel at 25°C showed a similar, drug solubility dependent, pattern to that shown above. The effect of the loaded hydrophobic drug was to decrease D_{app}, ranging between a 3-fold decrease for DB (0.4 X 10^{-6} cm^2/s) to a 40-fold decrease for PHB (0.03 X 10^{-6} cm^2/s), compared to a value of 1.3 X 10^{-6} cm^2/s for the unloaded PNIPA-H1.

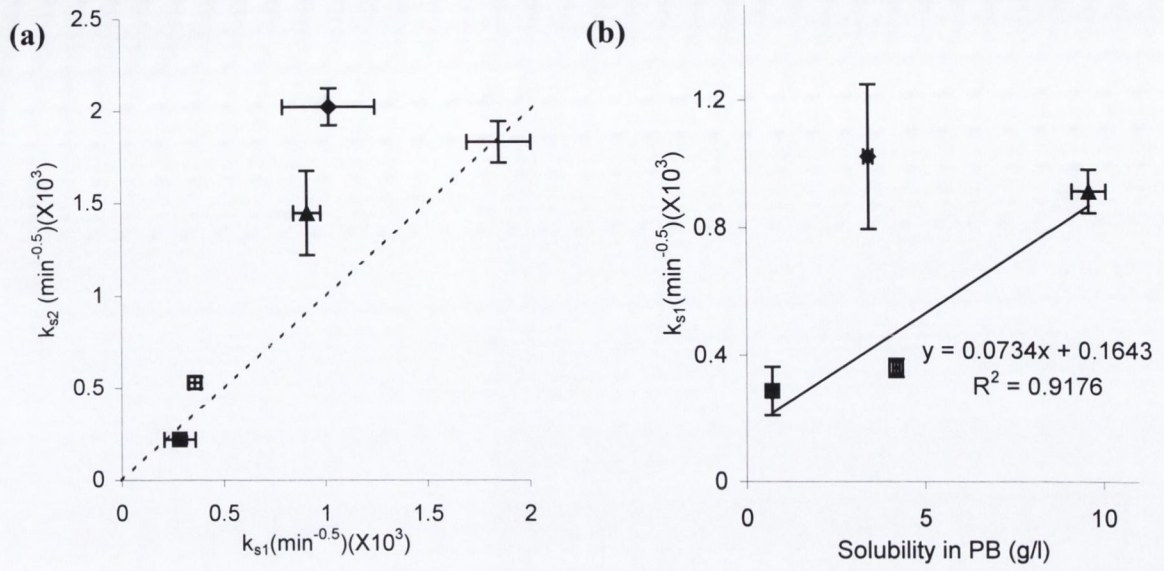

Fig. 5.2: Relationship between

(a) Swelling rate constants, k_s1 and k_s2, for hydrogel loaded with hydrophobic drugs. Also shown is a 1:1 relationship (dashed line) and data for unloaded hydrogel [BA (▲), MHB (□), PHB (■), DB (♦), Unloaded (+)].

(b) Swelling rate constant (k_s1) and drug solubility in PB [BA (▲), MHB (□), PHB (■), DB (♦)].

The residual volume was defined in Chapter 4 as the level of swelling at 37°C. The residual volume, following gel contraction at 37°C, was lowered by the presence of drug in the hydrogel, preventing the system from reaching its equilibrium level at 37°C in the time period studied.

The swelling level prior to temperature switch influenced the magnitude of contraction at the switch temperature, which in turn was shown from this series to depend on the hydrophilicity of the loaded drug. From Table 5.1, the more hydrophobic the drug within the benzoate series, the lower the swelling in a given time period, the smaller the magnitude and rate of contraction (k_{MC}).

5.2.2 Hydrophilic drugs

Loading of the hydrogel with hydrophilic drugs resulted in an increase in the rate of swelling of the hydrogel, contrasting with the decrease observed with the hydrophobic drugs. This effect was particularly apparent with NaB (Fig.5.1a) and DHCl (Fig.5.1b), which would exert the greatest osmotic effect of the hydrophilic drugs studied (5552 mosmol/L and 1774 mosmol/L concentrations respectively based on disc absorbing own weight in water), contrasting with the

isotonic buffer (~330 mosmol/L). The apparent diffusion coefficient of water (D_{app}) into the hydrogel increased to 2.7 X 10^{-6} cm^2/s for NaB and 1.8 X 10^{-6} cm^2/s for DHCl. VB12 (Fig 2c) and dextrans MW10,000, MW40,000 and MW70,000 (Fig. 5.1d) also increased the rate of swelling of the hydrogel. No molecular weight dependent pattern was evident for the dextrans.

The residual volume at 37°C following the first contraction period was similar or slightly increased by the presence of the hydrophilic drugs. The greater osmotic effect of NaB and DHCl caused a greater rate of swelling as indicated above and thus also resulted in faster hydration of the interior of the hydrogel, enabling the system to reach the equilibrium residual volume at 37°C faster than the unloaded hydrogel.

The increase in rate of swelling caused by these drugs resulted in a greater magnitude and rate of contraction (k_{MC}) (Table 5.1) on switching the temperature.

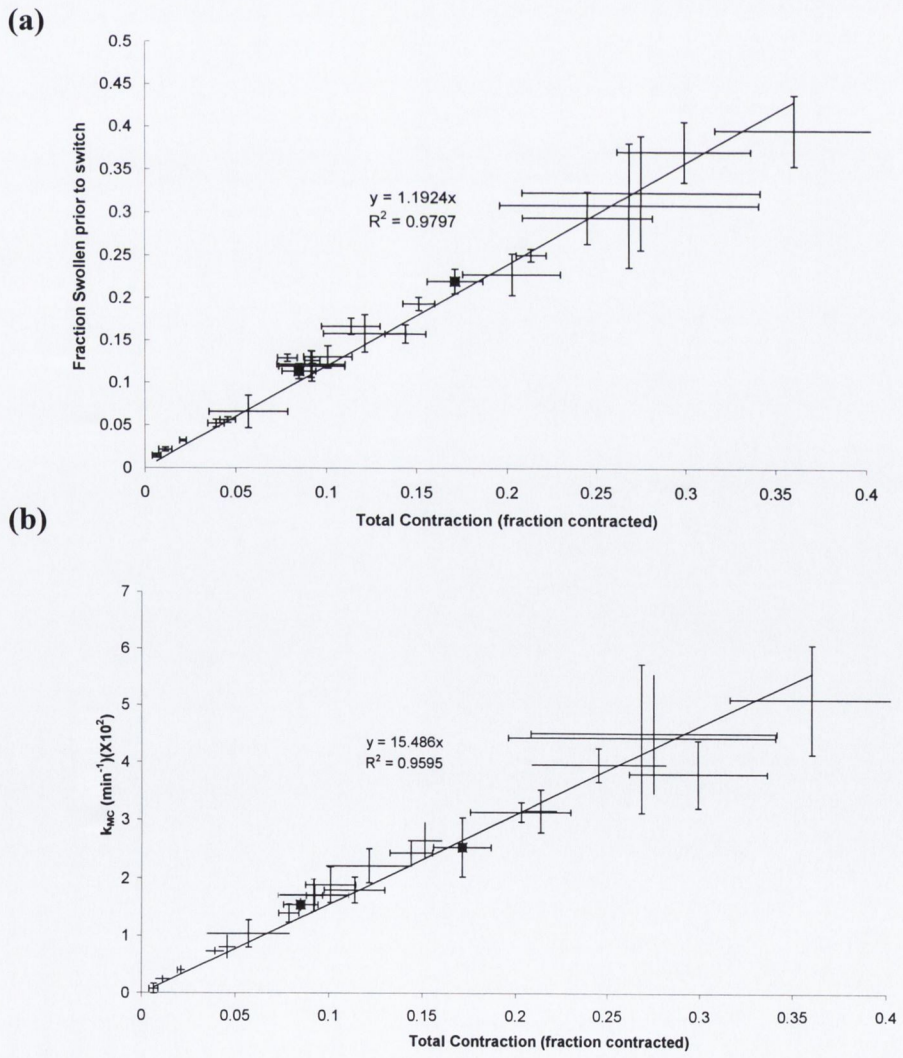

Fig. 5.3: Relationship between total magnitude of contraction and (a) fraction swollen prior to temperature switch and (b) maximum contraction rate (k_{MC}) [Unloaded (■)].

For all drugs examined, linear relationships existed between the total magnitude of contraction and both the level of swelling prior to switch (Fig. 5.3a) and the k_{MC} (Fig. 5.3b). The higher the swelling level attained, the greater the magnitude and rate of contraction. The hydrophobic drugs caused a decrease in swelling rate (lower k_s) and thus gave a lower magnitude and rate of contraction. The hydrophilic drugs increased the rate of swelling with a proportional greater magnitude and rate of contraction

Swelling and contraction cycles of thermoresponsive hydrogels were therefore shown to be strongly influenced by the physicochemical properties of the loaded drug. The magnitude and rate of contraction was dependent on the level of swelling prior to temperature switch. This in turn was dependent on the interval allowed for swelling but was also shown to be dependent on the drug hydrophilicity and chemical nature. The rate and level of swelling achieved, which affects pore size in the hydrogel, and the rate and magnitude of contraction, which may affect the magnitude of drug pulse, will have a significant influence on temperature controlled drug release from these systems.

5.3 PULSATILE DRUG RELEASE

The effect of a temperature switch between 25°C and 37°C on the rate of drug release from the hydrogel was examined.

5.3.1 Hydrophobic Drugs

The cumulative fraction released and corresponding release rate of benzoic acid and its esters on switching the external temperature is shown in Fig. 5.4.

Release of benzoic acid occurred at 25°C as the hydrogel swelled, allowing medium influx and thus drug diffusion. The fraction released in the first time period at 25°C was plotted against the square root of time (Equation 2.12, *Higuchi*), where the release rate constant (k_d) reflected matrix diffusion release (Table 5.2). As a first approximation, this equation gave a reasonable representation of release and allowed the use of k_d to compare the different systems. The release rate constants obtained were found to be proportional to the square root of drug solubility (Fig. 5.5a).

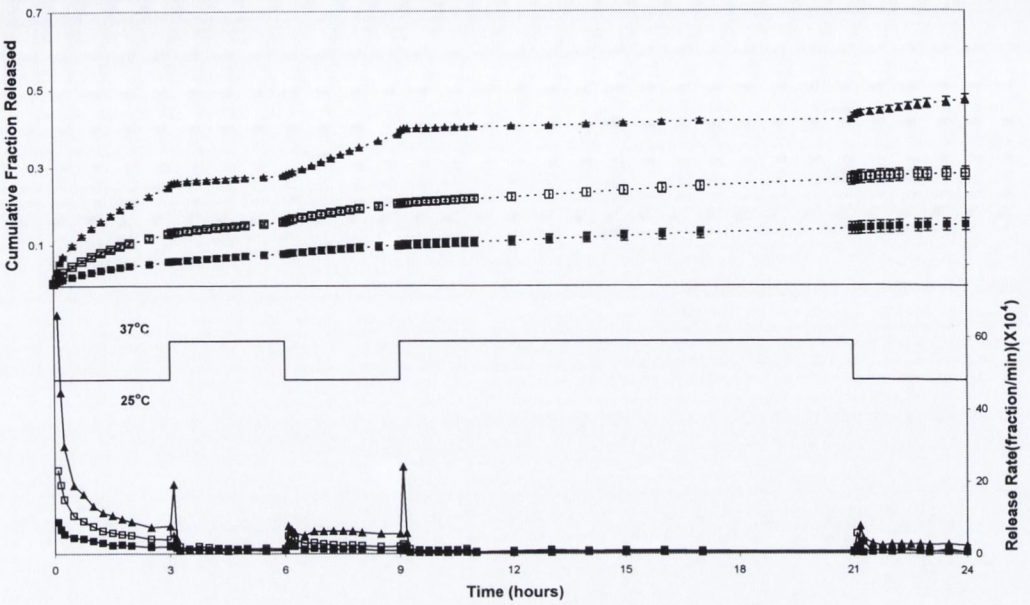

Fig. 5.4: Cumulative fraction released (top, dashed lines) and corresponding release rates (bottom, solid lines) of BA (▲), MHB (□) and PHB (■) on temperature switch between 25°C and 37°C.

Table 5.2: Release rate constant (k_d) at 25°C (Equation 2.12, *Higuchi*) and Area Under Release Rate Curves versus time (AUC) obtained on switching temperature to 37°C. Also given are the coefficients of determination associated with k_d. The diffusional exponents were obtained when release profiles at 25°C was fitted to Equation 2.11 (*Peppas*).

	Release rate constant (k_d) at 25°C ($min^{-0.5}$) (X 10^3) (Equation 2.12, *Higuchi*)	Coefficient of Determination (CD)	Diffusional Exponent (n) at 25°C (Equation 2.11, *Peppas*)	Area Under Release Rate Curve (AUC) (fraction) (X 10^2)
BA	2.386 ± 0.045	0.9984	0.518 ± 0.016	1.550 ± 0.112
MHB	1.207 ± 0.102	0.9859	0.596 ± 0.008	0.581 ± 0.198
PHB	0.503 ± 0.040	0.9720	0.646 ± 0.043	0.256 ± 0.073
DB	2.469 ± 0.158	0.9663	0.671 ± 0.019	2.209 ± 0.393
NaB	----	----	1.057 ± 0.291	----
DH	3.172 ± 0.032	0.9894	0.525 ± 0.066	11.652 ± 0.095
VB12	2.234 ± 0.031	0.9765	0.605 ± 0.062	14.884 ± 2.803
D4	3.129 ± 0.254	0.9937	0.545 ± 0.093	20.577 ± 2.878
D10	2.861 ± 0.098	0.9922	0.598 ± 0.052	44.586 ± 4.510
D40	4.774 ± 0.669	0.9491	0.275 ± 0.038	43.788 ± 6.309
D70	4.118 ± 0.810	0.9621	0.340 ± 0.135	60.805 ± 4.682

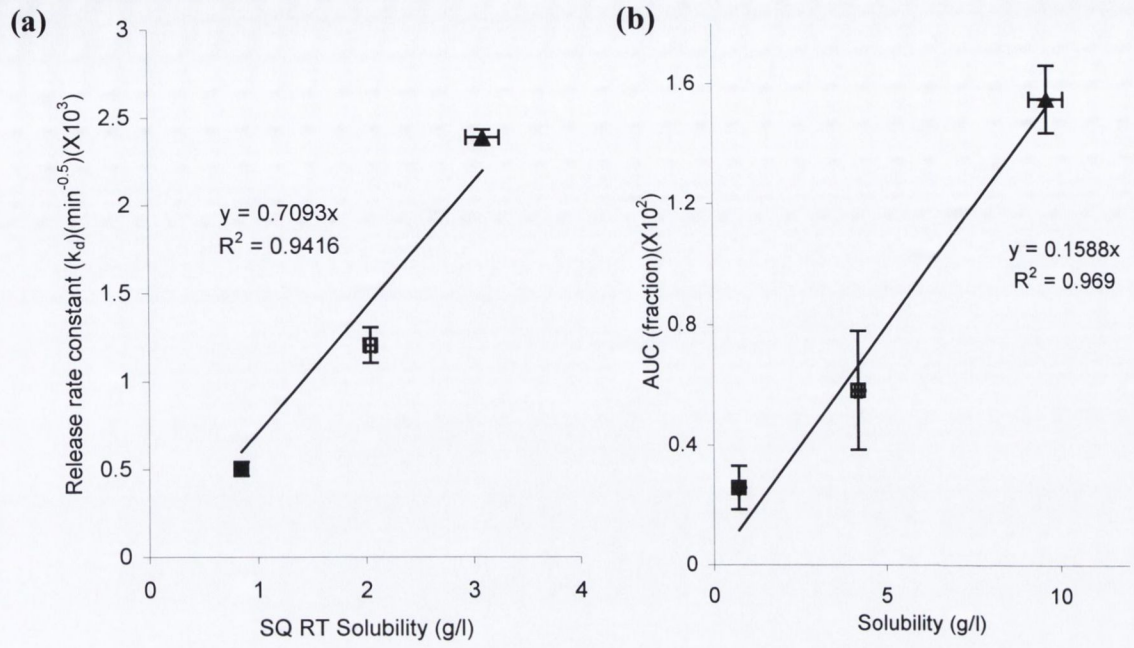

Fig. 5.5: Plot of (a) release rate constants at 25°C (k_d) against the square root of drug solubility and (b) Area Under the Release Rate Curve (AUC) against drug solubility [BA (▲), MHB (□) and PHB (■)].

A sharp pulse of drug release on increasing temperature was seen due to the collapse of the polymer chains above the LCST. In order to quantify the drug pulse seen on temperature increase, the area under the release rate curve (AUC) was calculated (Table 5.2). The AUC was found to be directly proportional to the drug solubility in the benzoate ester series (R^2=0.969, Fig. 5.5b). A direct relationship existed between k_d and AUC (Fig 5.6a), which indicated that the magnitude of the drug pulse was solubility dependent. This relationship suggested that the drug pulse was attributed to the presence of the dissolved drug in the swollen hydrogel region surrounding the drug core prior to temperature increase. Such drug was mechanically squeezed out from the system when the polymer chains collapsed. In addition to this, the solubility of the drug affected the magnitude of the hydrogel contraction as indicated by the relevant k_{MC} value. A linear relationship was found between the k_{MC} and the AUC (Fig. 5.6b), consistent with expulsion of the dissolved drug.

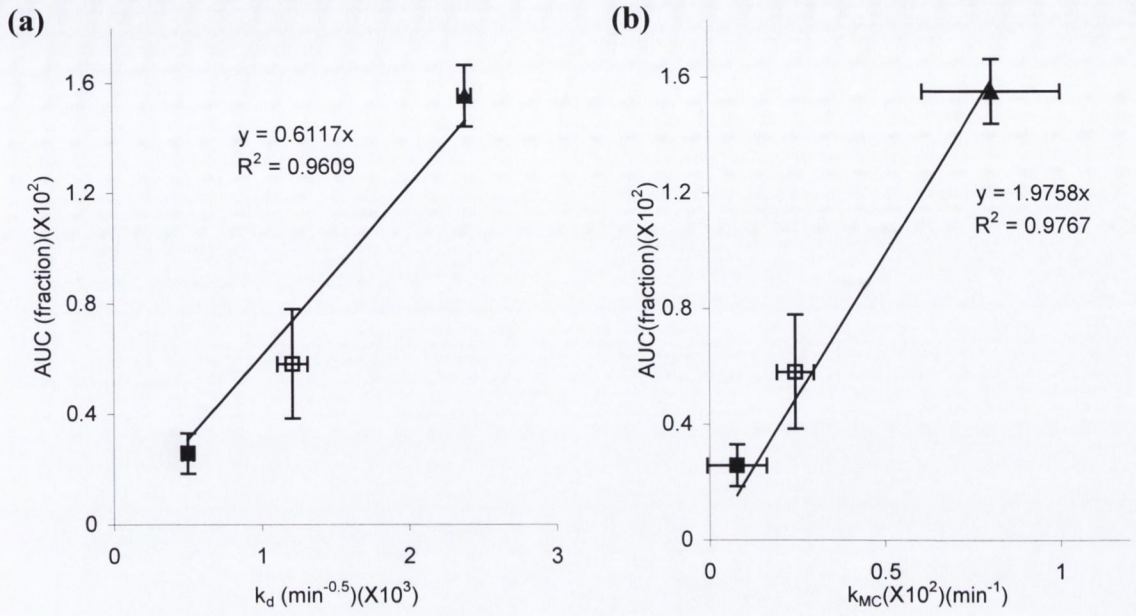

Fig. 5.6: Relationships between Area Under Release Rate Curve (AUC) and
(a) release rate constants (k_d) in the benzoate ester series
(b) maximum contraction rate (k_{MC}) in the benzoate ester series
[BA (▲), MHB (□), PHB (■)].

The fraction released (0-1 hour) at 25°C was also examined using Equation 2.11 (*Peppas*) to give the diffusional exponent (*n*), which gave an indication of the release mechanism (Ritger and Peppas, 1987b). This equation, requiring two parameters, gave a better fit to the data compared with Equation 2.12 (*Higuchi*) (Table 5.2). The deviation of the diffusional exponent from the square root of time reflects the contribution of swelling to the overall release mechanism. A decrease in the diffusional exponent (*n*) towards Fickian diffusion was observed as the solubility of the loaded benzoate increased (Table 5.2).

The temperature switch above the LCST slowed the diffusion-controlled release rate significantly. The change in the release rate was quantified by calculating a quasi-steady state release rate constant (k_{ss}) and this was used to compare diffusion-controlled release before and after the temperature switch, as opposed to the drug pulse release resulting from hydrogel contraction. The constant was defined as the average release rate at each temperature, excluding the first 30 minutes after the temperature switch. The proximity of this value to zero (within error bars) may be used to indicate the ability of the hydrogel to thermally shut off release. Fig.5.7 includes a bar chart of the k_{ss} of BA and PHB.

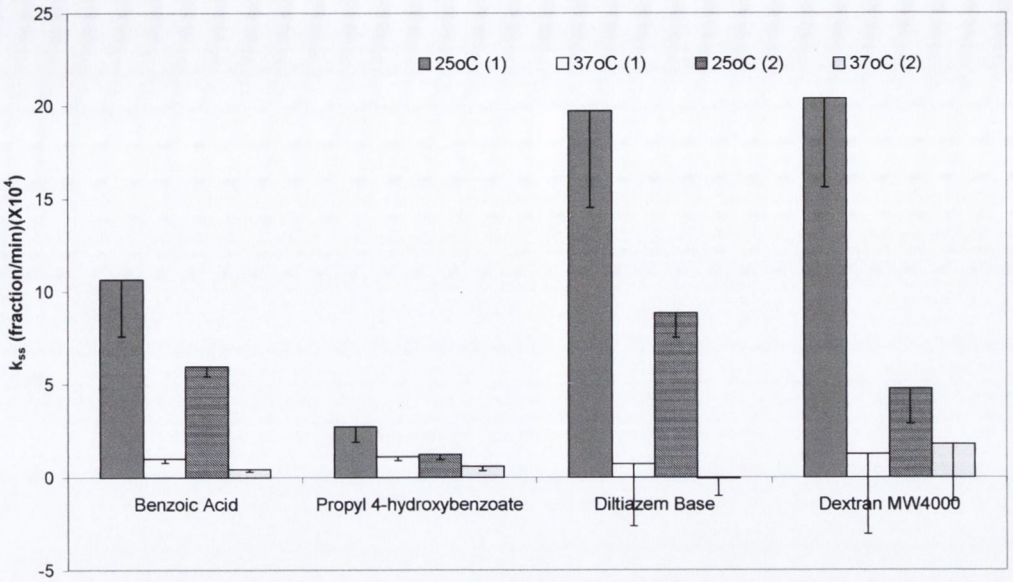

Fig. 5.7: Steady state release rate constant (k_{ss}) for selected drugs; defined as the average release rate at each temperature, excluding the first 30 minutes after the temperature switch.

A significant change in the release rate with temperature was seen with BA, although the release was not switched off at the higher temperature. As the solubility of the series of benzoate esters decreased, the ability of the hydrogel to thermally control the rate of drug release decreased (illustrated in Fig 5.7 between BA and PHB). This result can be compared to Fig. 5.1a where the swelling of the same systems was examined. Due to the slow rate of drug dissolution of the benzoate esters at 25°C, penetration of the swelling front into the disc was also retarded and was dependent on the drug front. The thickness of the collapsed layer over the drug core will also be dependent on the magnitude of the swollen layer present prior to collapse. In the case of PHB, a lower level of swelling of the hydrogel occurred prior to temperature increase. As a result the release rate continued at a similar level to that at the lower temperature due to a thin collapsed layer counteracted by the influence of the higher temperature on drug dissolution and diffusion.

The cumulative fraction released and corresponding release rate versus time of diltiazem base on switching the external temperature is shown in Fig. 5.8. Pulsatile "on-off" release was evident. Fig. 5.7 also includes the k_{ss} values of DB in each temperature phase where the error bars are seen to be in close proximity to, or crossing, the x-axis; indicating that release effectively stopped at that temperature. DB is a larger drug molecule than the benzoates (Table 4.4) and an "off" phase was achieved. With the smaller benzoates, a lower release rate simply occurred at the higher temperature.

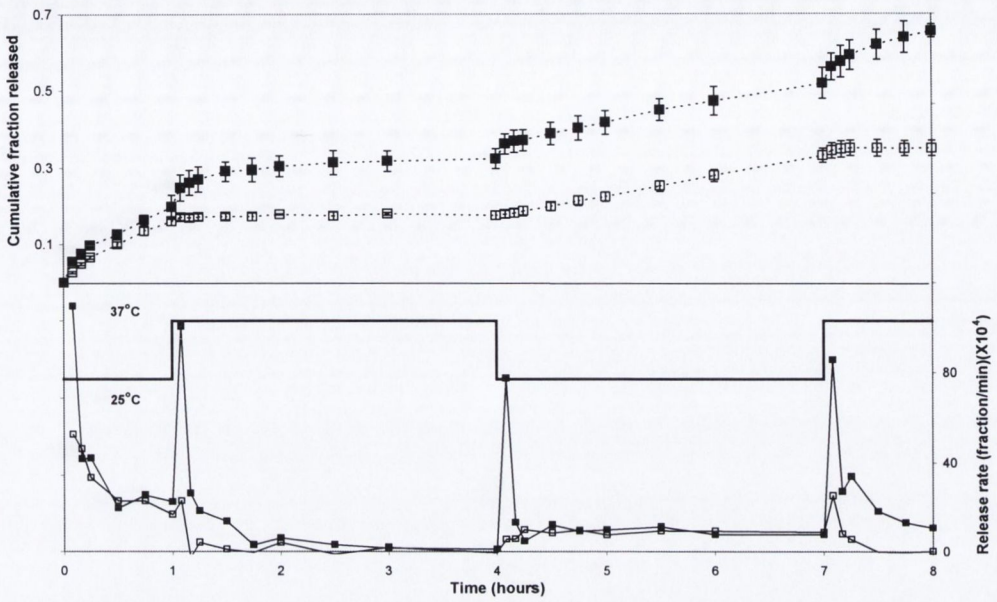

Fig. 5.8: Cumulative fraction released (top, dashed lines) and corresponding release rates (bottom, solid lines) of DHCl (■) and DB (□) on temperature switch between 25°C and 37°C.

For all the hydrophobic drugs, the release rate during subsequent 25°C periods was shown to be a continuation of the diffusion-controlled release seen in the first period. This resulted in the quasi steady state release rate when the temperature was decreased. The small apparent "pulse" of drug on lowering the temperature was not significant.

5.3.2 Hydrophilic drugs

The cumulative fraction released and corresponding release rate of sodium benzoate on switching the external temperature is shown in Fig. 5.9. The relatively high aqueous solubility and small molecular size of sodium benzoate, limiting the ability of the hydrogel system to retard release over long periods. A large pulse of drug was released on raising the temperature and the release rate subsequently slowed at this temperature. *"On-off"* release was not achieved.

A pulsatile *on-off* release was evident for the slightly larger but also highly soluble DHCl (Fig 5.8). A pulse of drug release was seen when the temperature was either increased or decreased. The greater pulse seen with DHCl than with DB on increasing temperature highlighted the influence of the solubility of the drug on the ability of the drug to dissolve and the hydrogel to swell (Fig. 5.1b), which in turn affected the magnitude of the contraction observed. The larger drug pulse was due to the greater amount of dissolved drug present at the time of hydrogel contraction and the greater magnitude of contraction.

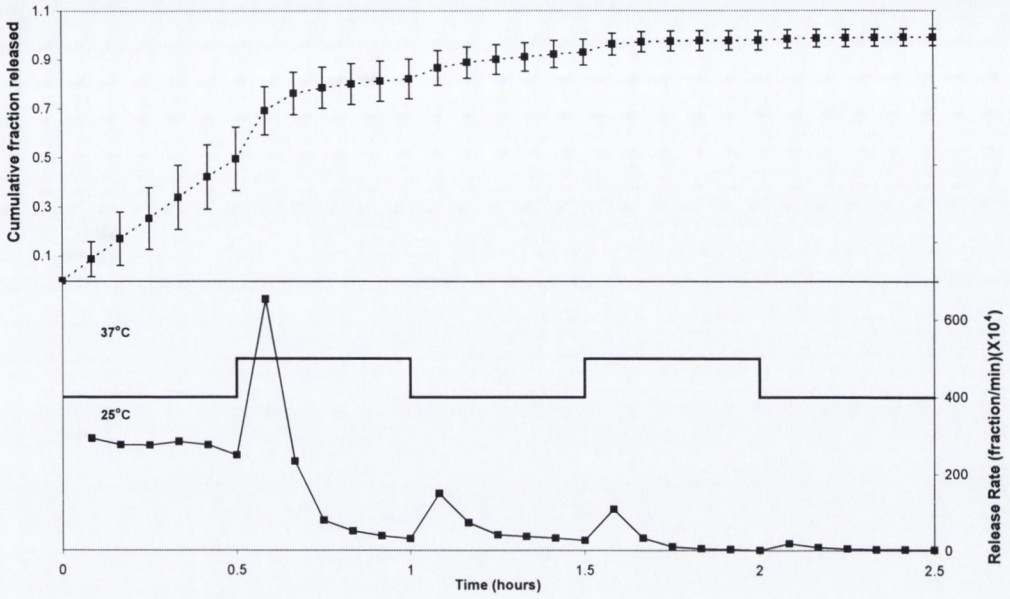

Fig. 5.9: Cumulative fraction released (top, dashed lines) and corresponding release rate (bottom, solid lines) of NaB

The cumulative fraction released and the corresponding release rate of VB12 on switching the external temperature is shown in Fig. 5.10. VB12 showed a similar pulsatile *"on-off"* release pattern to DHCl, with a drug pulse seen on increasing temperature.

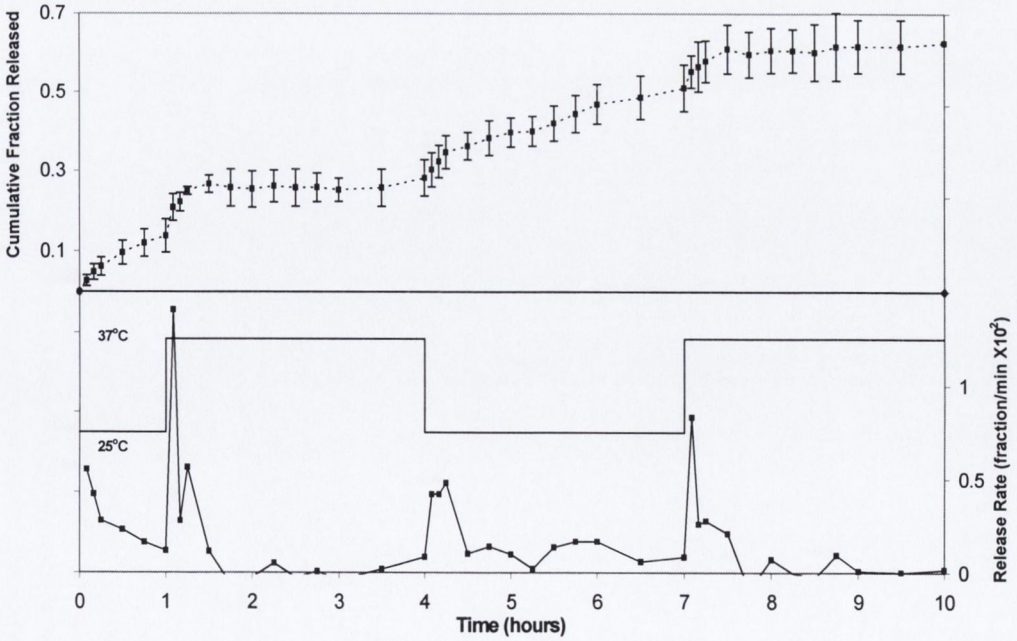

Fig. 5.10: Cumulative fraction released (top, dashed lines) and corresponding release rate (bottom, solid lines) of VB12

The cumulative fraction released and the corresponding release rate of a series of dextrans on switching the external temperature is shown in Fig. 5.11. A pulsatile on-off release pattern was evident in this series with the pattern of release varying with the molecular weight of the dextran. The *"on-off"* release of D4, compared to the hydrophobic drugs, is illustrated in Fig. 5.7. Release of these dextrans when the temperature was dropped and the system started to swell again was slower to resume compared to smaller hydrophilic drugs such as DHCl. This was consistent with a lower diffusion coefficient and greater hindrance to transport with the larger drug molecules. The magnitude of the drug pulses obtained relative to their slow rate of diffusion resulted in an effective positive thermosensitive system using a negative thermosensitive hydrogel, where the *"on"* phase was caused by the hydrogel contraction. This emerging pattern was seen as the molecular weight of the model drug increased and was particularly apparent with dextran MW70000.

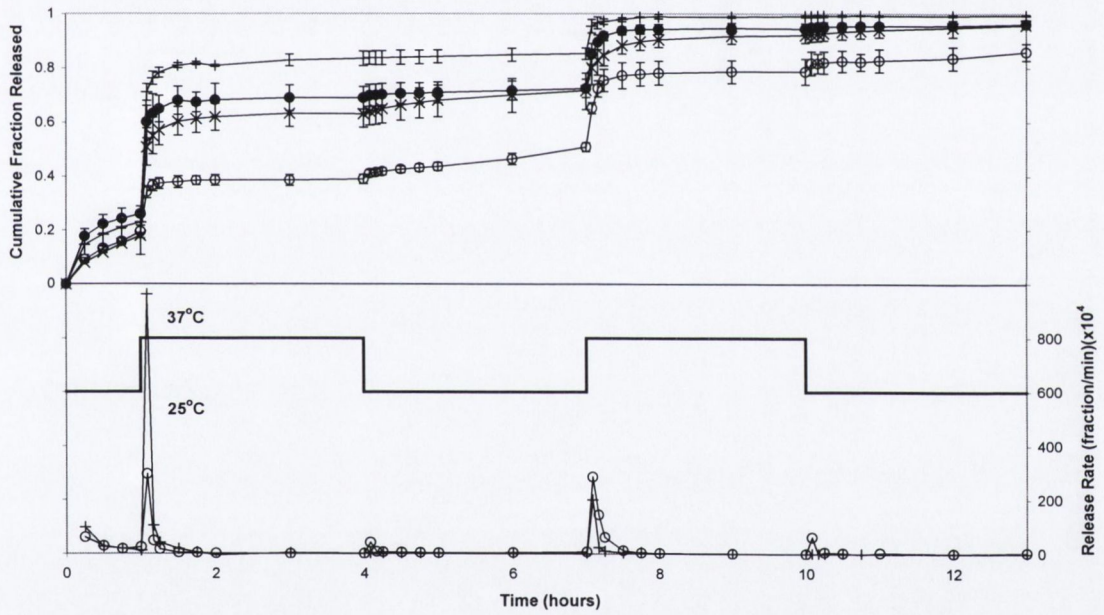

Fig. 5.11: Cumulative fraction released (top, dashed lines) and corresponding release rate (bottom, solid lines) of D4 (○), D10 (×), D40 (●) and D70 (+) on temperature switch between 25°C and 37°C. Release rates of D4 and D70 only shown in (b) for clarity.

In order to quantify the drug pulse seen on temperature increase, the area under the release rate curve (AUC) was calculated for the dextrans along with DHCl and VB12. From Table 5.2, it is clear that as the molecular weight of the series increased, a greater percentage of loading was expelled, ranging from ~11% in the case of DHCl to ~60% in the case of D70. The amount of drug pulsed out in proportion to the amount present was estimated by dividing the AUC by the loading remaining prior to the temperature switch. This parameter was plotted against drug molecular weight and radius of gyration. The latter was estimated using molecular modelling as described in section 3.6.1. The amount of drug expelled in the first pulse increased with drug molecular weight,

with this increase found to show a better linear relationship with drug molecular radius (R^2=0.908, Fig 5.12) than with molecular weight (R^2= 0.817).

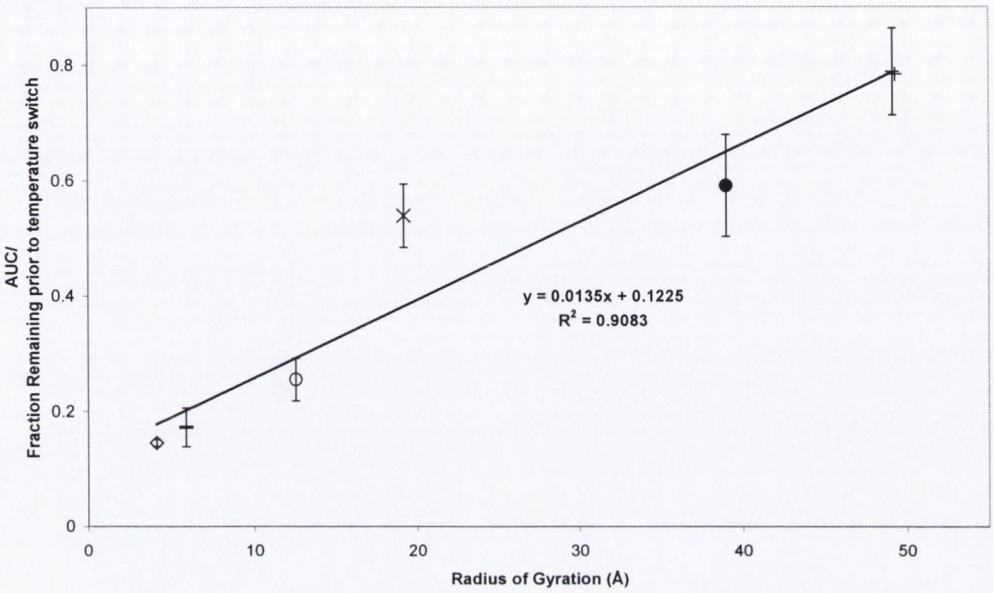

Fig. 5.12: Plot of adjusted AUC against the radius of gyration of a series of hydrophilic drugs [DHCl (◊), VB12 (—), D4 (○), D10 (×), D40 (●), D70 (+)].

From the swelling data (Section 5.2.2), all the hydrophilic drugs had a similar effect on hydrogel swelling; with similar volumes of media expelled from the systems as a result. Identical fractions of the dissolved drugs on a weight basis may have been expected to be expelled with this media, or a smaller proportion of larger drugs due to increased hindrance to transport as the hydrogel collapsed. The opposite effect was observed in the current study (Fig. 5.12).

A further study was carried out to investigate this effect. The hydrogels were loaded with identical volumes of the drug solutions for both 48 hours and 120 hours and placed directly into the release medium at 37°C, without drying out the gels. Hydrogel deswelling occurred immediately and the release profiles over the first hour are shown in Fig. 5.13a. The fraction released after 1 hour is shown in Fig. 5.13b.

There was no statistical difference ($p > 0.05$) at any of the time points between the systems loaded over 48 hours or 120 hours, indicating that the time period used for loading was sufficient. There was, however, a molecular size dependent pattern apparent, in particular between the DHCl and the larger dextrans. There was no significant difference between D4 and D70 fraction released after 1 hour, confirming that the drying process also contributed to the molecular size dependent drug

pulse. Both the loading of the drug and the subsequent drying procedure therefore caused the molecular size dependent profile in Fig. 5.12.

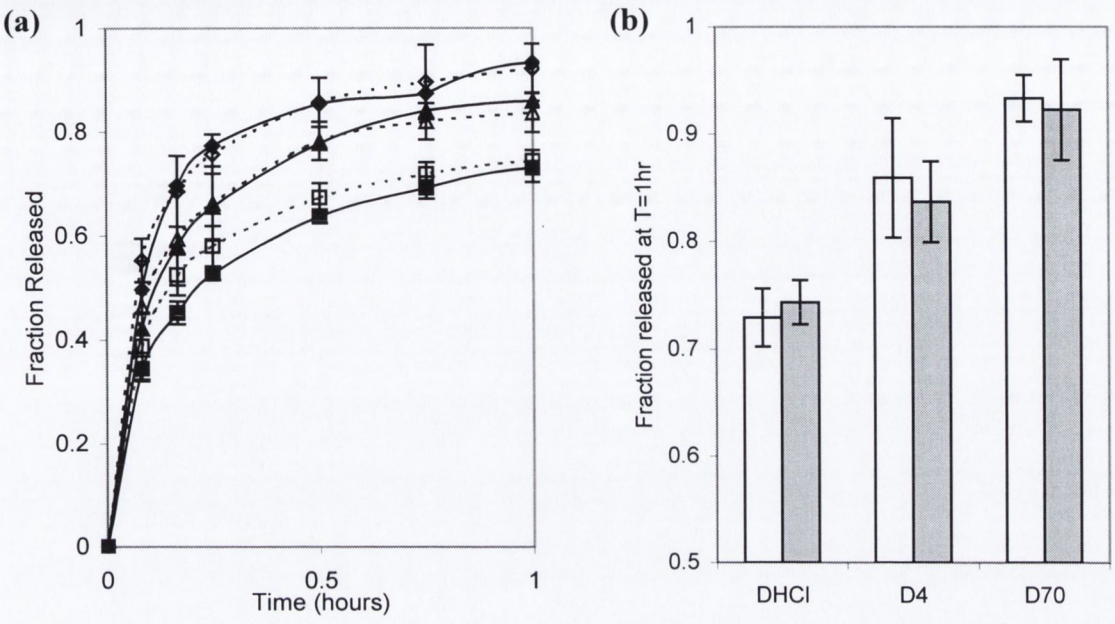

Fig. 5.13: (a) Release profiles obtained when swollen hydrogels loaded over 48hours (closed symbols, solid lines) or 120 hours (open symbols, dashed lines) were placed in release medium at 37°C [DHCl (■/□), D4 (▲/Δ), D70 (♦/◊)] (b) Fraction released at T=1 [loading time 48 hrs (white bars) and 120 hrs (grey bars)]

There was no statistical difference ($p>0.05$) between the magnitude of pulse of DHCl and that of VB12, with the effect apparent for the larger dextrans only. The larger molecules therefore appear to become preferentially entangled in the outer sections of the hydrogel during loading and particularly during drying, thus creating the molecular size dependent gradient. The effect during loading would be expected considering the inability of the dextrans at 25°C to permeate into all the available pores of the hydrogel as shown in the solute exclusion technique in Chapter 4 (Fig. 4.30b). Such an effect was then exaggerated during the drying process. A previous study by Yu and Grainger (1995) also attributed a burst release of insulin from several hydrogels to the incorporation of the insulin into the surface layers of the gels during the solvent sorption method of loading.

With the smaller hydrophilic drugs (DHCl, VB, D4), an apparent drug "pulse" was also seen on dropping the temperature. Diffusion of the smaller probe molecules within the collapsed hydrogel may occur during transfer to the lower temperature, resulting in a transient increase in the release rate. This did not occur with the hydrophobic drugs (section 5.3.1) due to their lower solubility.

5.4 CONCLUSIONS

The physiochemical properties of the chosen drug greatly influenced the swelling and contraction of PNIPA-H1 as well as the pattern of pulsatile drug release. In particular, drug solubility, size and chemical nature were shown to be of importance. The hydrogel swelling rate was decreased by the presence of hydrophobic drugs and may be increased by the osmotic influence of hydrophilic drug molecules. A temperature switch above the LCST of the hydrogel caused contraction/deswelling of the system, with the resulting magnitude and rate of hydrogel contraction proportional to the extent of swelling prior to temperature switch. Drug release at 25°C was approximately proportional to the square root of time for both the hydrophobic and hydrophilic drug series. Hydrogel contraction on temperature switch resulted in a drug pulse, which was solubility dependent for the hydrophobic benzoate series. The drug pulse was attributed to the presence of the dissolved drug in the swollen hydrogel region surrounding the drug core prior to temperature increase. Effectiveness of thermal control of hydrophobic drug release increased with increasing solubility, although on-off release was only shown with DB. The magnitude of the pulse of hydrophilic drug released on hydrogel contraction increased with molecular diameter, attributed to a molecular size dependent gradient formed during the loading/drying process. Pulsatile *'on-off'* drug release was shown with DHCl, VB12 and the various dextrans. An effective positive thermosensitive system using a negative thermosensitive hydrogel was seen with the higher molecular weight dextrans. This effect was caused by negligible diffusion in an expanding network below the LCST and a sharp drug pulse due to subsequent hydrogel contraction above the LCST.

The chemical nature of the chosen drug and possible interactions with PNIPA are examined in more detail in Chapter 6. The influence of this and other drug physicochemical properties on release characteristics is further explored in Chapter 7 in order to explain many of the trends described.

CHAPTER 6

A Study of Poly(N-isopropylacrylamide)-Drug Interactions

6.1 INTRODUCTION

Potential interactions between the model drugs used and poly(N-isopropylacrylamide) were investigated. The study in Chapter 5 indicated that the chemical nature of the drug may have influenced the swelling and release kinetics of the system, particularly in the case of the hydrophobic drugs. The model drugs (Table 4.4) were analysed under the following headings: benzoates, diltiazem, vitamin B12 and the dextrans. Interactions were examined using both a lightly crosslinked hydrogel (PNIPA-H1), which is in a solid state at all temperatures, and a linear polymer (PNIPA-L), which dissolves below the LCST and precipitates above the LCST. The linear polymer was used for convenience of analysis and comparisons were made with results from the hydrogel. The influence of the chemical nature of the crosslinker was considered negligible. The review paper of Schild (1992) compared literature studies on the linear PNIPA polymer and studies on the PNIPA gel. As an example, several authors have examined the influence of surfactants on the LCST of the linear polymer (Schild and Tirrell, 1991; Saito *et al.,* 1992; Eeckman *et al.,* 2001), while Kokufuta *et al.* (1993) showed a similar surfactant effect on PNIPA gel. The current study will examine the influence of the model drugs on both types of systems.

As mentioned in section 1.3.5, the phase transition temperature of PNIPA is affected by various factors including the solvent used (Lee *et al.,* 2000) as well as the addition of salts and surfactants (Saito *et al.,* 1992; Eeckman *et al.,* 2001). In the case of the surfactants, it was suggested that they might bind to the polymer (Schild and Tirrell, 1991; Saito *et al.,* 1992; Kokufuta *et al.*, 1993; Eeckman *et al.,* 2001), thereby altering the hydrophilic/hydrophobic balance of the polymer/hydrogel. Previous studies have not examined the influence of drug substances on PNIPA systems.

In the current chapter, the influence of various concentrations of each drug in solution (PB) on the equilibrium swelling level of PNIPA-H1 at 25°C was examined. Drug-hydrogel binding was then investigated where appropriate using a dried, crushed hydrogel at 37°C. Additional studies were also carried out on the linear polymer. Due to the ability of PNIPA-L to dissolve below the LCST, studies were performed using both an aqueous drug-polymer solution and a drug polymer blend formed by co-precipitation. DSC and transmittance studies were used to investigate the influence of the drugs on the LCST of a polymer solution. Phase solubility studies were also preformed where appropriate at 25°C (<LCST) to investigate binding. Drug-polymer co-precipitated blends were prepared as described in section 3.3.8. These co-precipitates were analysed by XRD, thermal analysis and FTIR. The results were then interpreted and comparison was made between the two distinct polymeric systems used.

6.2 BENZOATES

The influence of the benzoates on the hydrogel and on the polymer in aqueous solution was examined. In aqueous solutions, concentrations up to the solubility limit of the drug in the solvent at the experimental temperature were used. The benzoate/polymer co-precipitate blends were prepared from ethanolic solutions, except for the NaB blends that were prepared from aqueous solutions.

6.2.1 Hydrogel

The hydrogel (PNIPA-H1) is in a solid state at all temperatures, whether swollen (<LCST) or collapsed (>LCST). The influence of an excess volume of each benzoate solution on equilibrium swelling of PNIPA-H1 at 25°C was examined. Binding was also examined using the hydrogel at 37°C where swelling was minimal.

6.2.1.1 Equilibrium swelling

The equilibrium swelling ratios of PNIPA-H1 in various concentrations of the benzoate solutions in PB at 25°C (<LCST) are shown in Fig 6.1. Fig 6.1a also includes the equilibrium swelling ratio of PNIPA-H1 in various concentrations of BA at 25°C in 0.01M HCl (isotonic). The concentration of benzoate that caused a decrease in swelling by 50% was defined by a parameter, k_{H1} (Table 6.1). A second parameter, k_{H2}, was derived as the molar quantity of model drug required to inhibit hydrogel swelling.

The influence of BA on the swelling equilibrium is shown in Fig. 6.1a. The presence of BA in the PB did not affect the equilibrium swelling of PNIPA-H1 up to a concentration of ~0.035M. Above this value, a sharp drop in swelling occurred which was shown to correspond to a drop in the measured pH of the buffer towards the pKa of the acid (pKa BA = 4.20, Martin 1993). The pH drop resulted in an increase in the proportion of unionised species in the solution as calculated by the Henderson-Hasselbach equation (Martin, 1993) and shown by the dashed line in Fig. 6.1a. In 0.01M HCl, where BA was almost completely unionised, there was a significant decrease in equilibrium swelling at all concentrations of BA. In the concentration range studied, the effect of BA on swelling was therefore due to the unionised BA species.

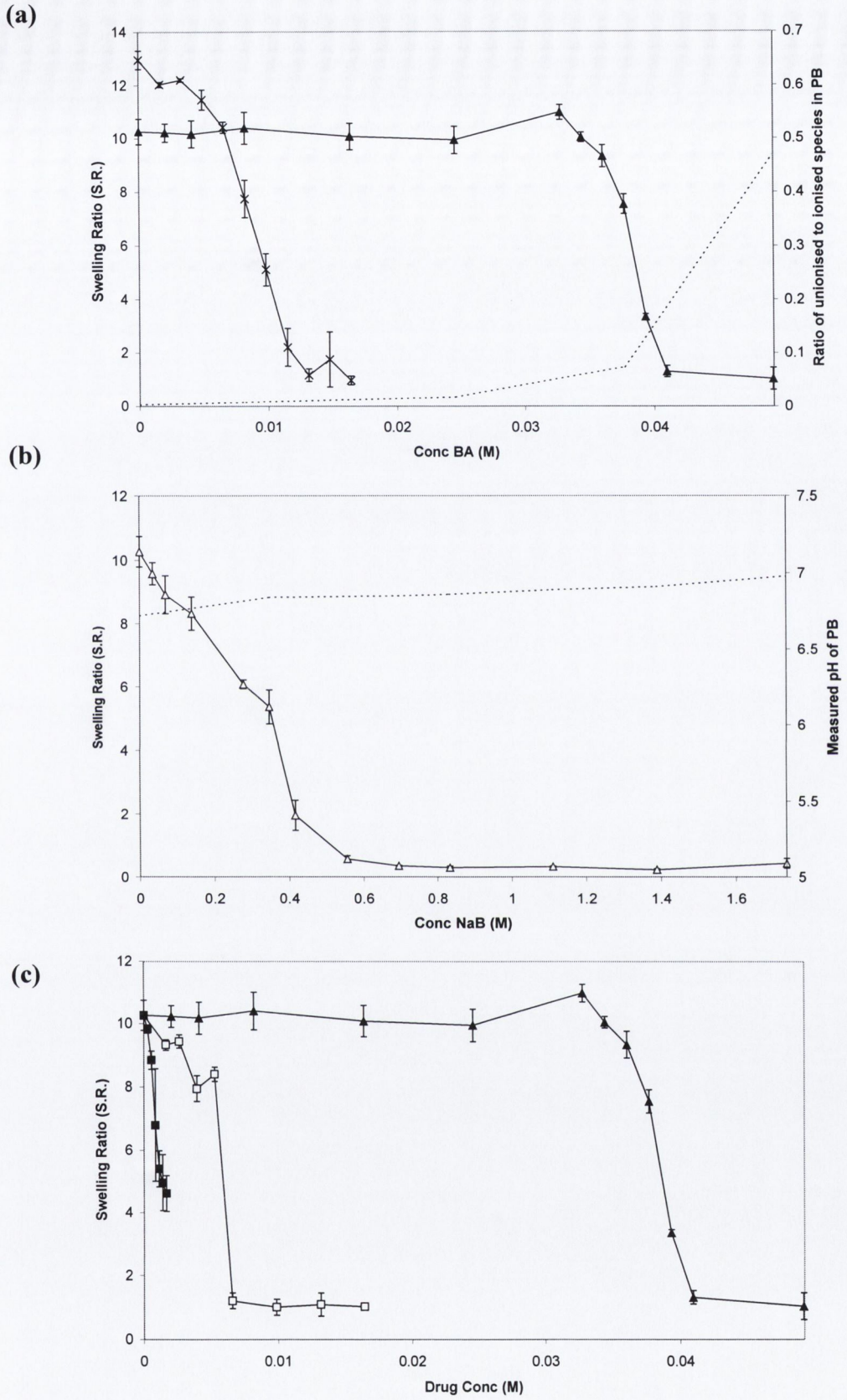

Fig 6.1: Equilibrium swelling ratios (n = 3; mean ± s.d) of PNIPA-H1 at 25°C in various concentrations of (a) BA in PB (▲) and in 0.01M HCl (X); (b) NaB (Δ) in PB and (c) BA (▲), MHB (□) and PHB (■) in PB. Also shown as dashed lines in (a) is the ratio of unionised to ionised species of BA in PB and in (b) is the measured pH of the PB solution.

Table 6.1: Drug concentration required to reduce swelling of PNIPA-H1 at 25°C in PB by 50% of initial value (k_{H1}) and binding constants calculated at 37°C (k_b). k_{H2} values estimate the number of moles of model drug per mole of NIPA required to inhibit swelling

	k_{H1} at 25°C		**k_{H2} (moles drug/mole NIPA in dry disc)**	**Binding constant (k_b) at 37°C, M^{-1} (X 10^2) (Eqn. 6.2; Appendix VIB)**
	g/l	**moles/l (M) (X 10^2)**		
BA	4.721 ± 0.004	3.867 ± 0.004	1.75	ND
	(1.093 ± 0.050)*	(0.895 ± 0.041)*	(0.41)	(0.54)*
NaB	50.839 ± 1.149	35.280 ± 0.797	15.97	--
MHB	0.894 ± 0.005	0.588 ± 0.003	0.27	3.53
				(2.63)*
PHB	0.230 ± 0.070	0.128 ± 0.039	0.06	9.20
				(33.89)*
DHCl	348.120 ± 20.517	77.188 ± 4.549	34.94	--
D10	57.244 ± 4.711	0.561 ± 0.046	0.25	--
D40	58.178 ± 8.949	0.135 ± 0.021	0.06	--
D70	62.445 ± 6.112	0.091 ± 0.009	0.04	--

*Values in brackets indicate experiment performed in 0.01M HCl.

ND = not detectable

Fig 6.1b shows the influence of the presence of NaB on the equilibrium swelling of PNIPA-H1 in PB at 25°C. NaB is ~40 times more soluble than BA in PB (Table 4.4) and the data shown cover a much wider range of concentrations. In the same concentration range as that in Fig 6.1a, there was no significant change in swelling of the PNIPA-H1 caused by NaB. The measured pH was ~6.8 and the weak acid present was in the ionised form in solution. At higher concentrations, there was a gradual decrease in the ability of the hydrogel to swell with the k_{H1} value being ~10 times greater than that of BA. The measured pH of the buffer is also shown in Fig. 6.1b and a slight increase in pH was seen with increasing concentration of NaB. The upward shift in pH was caused by the presence of free sodium ions acting as a strong base. The benzoic anion and the sodium cation remained the dominant species present. The presence of the benzoate anion may have a "salting out effect" on the thermoresponsive polymer, similar to that shown by Saito *et al.* (1992) and Eeckman *et al.* (2001) and described in section 1.3.5.1. The possibility of such an effect is further investigated in section 6.2.2.4.

The benzoate esters, although esterified at the acid group of BA, also contain a para hydroxyl group and pKa values of 8.37 and 8.36 have been reported for MHB and PHB respectively (Büchi *et al.*, 1971). MHB and PHB were, however, essentially unionised at pH 6.8 and the presence of the drug was shown to have no effect on the measured pH. There was a decrease in the k_{H1} value in PB as the length of the side chain group increased (Fig 6.1c, Table 6.1).

The unionised forms of the benzoates as well as the hydrophobicity of the ester side chain were significant factors in causing the observed, sharp collapse in equilibrium swelling at a temperature

below the LCST of the polymer. A more gradual deswelling was seen with the ionised form of benzoic acid at higher concentrations. Further studies were therefore carried out on the hydrogel (section 6.2.1.2) and on the linear polymer (section 6.2.2) to investigate these effects.

6.2.1.2 Binding Isotherm

To investigate potential adsorption or binding of the benzoates to PNIPA, spectroscopic studies were performed between solutions of the benzoates and PNIPA-H1 in a dried, crushed form as described in section 3.3.10.1. The amount of PNIPA-H1 was kept constant (25mg/ml) and the absorbance of various solutions of BA, MHB and PHB was determined before and after equilibration at 37°C, a temperature above the LCST of the hydrogel. At this temperature, minimal swelling of the hydrogel occurred.

Binding curves between the benzoates and PNIPA-H1 are shown in Fig. 6.2. Using this technique, binding was observed for MHB and PHB in PB while binding for all three benzoates in 0.01M HCl was apparent.

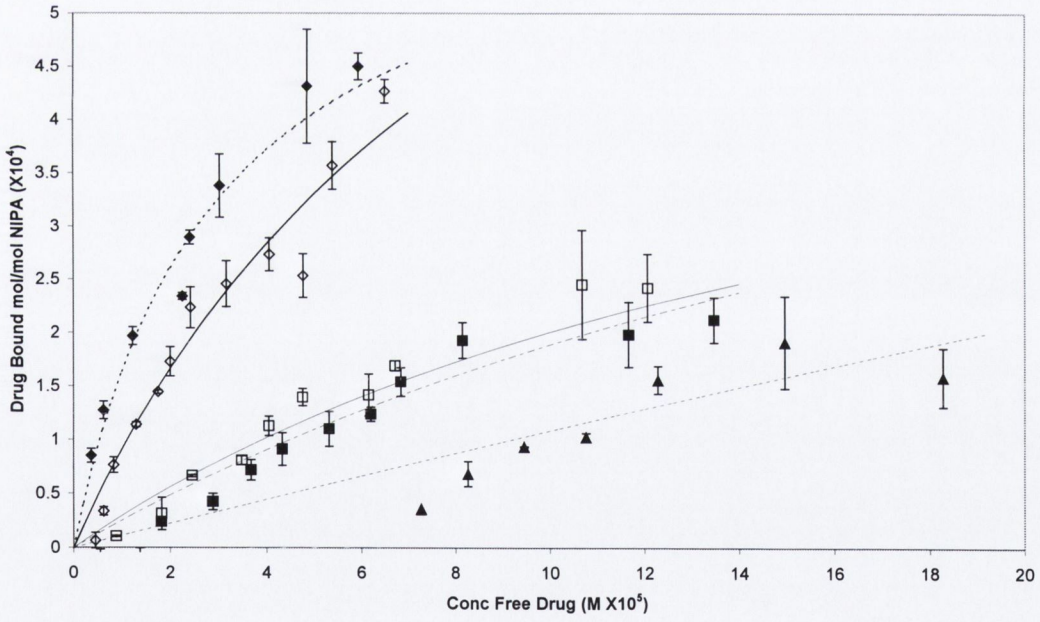

Fig 6.2: Binding curve plot of benzoates in PB (solid lines; open symbols: MHB (□), PHB (◊)] and in 0.01M HCl [dashed lines; closed symbols: BA (▲), MHB (■), PHB (♦)] (n = 3; mean ± s.d).

Binding between BA and PNIPA was apparent in the unionised form but could not be detected using this technique in PB. Binding increased with increasing hydrophobicity of the ester side chain. From this study, the benzoates appear to bind by hydrophobic interactions between the benzene ring/side chain ester and the hydrophobic groups of PNIPA. There was no difference

between the binding profiles of MHB in both solvents, while an increased k_b value was seen for PHB in the acidic medium.

The data presented in Fig. 6.2 was fitted by the Langmuir isotherm (Equation 6.1a):

$$y = \frac{y_{\max} k_b x}{1 + k_b x}$$

Equation 6.1a

where

y = mole of drug bound per mole polymer

x = the molar concentration of free drug

y_{max} = the maximum possible number of moles of drug bound per mole of polymer

k_b = constant

A double reciprocal plot of the Langmuir isotherm (Connors, 1987) gives equation 6.2, which was used to estimate the binding constant k_b, given in Table 6.1.

$$\frac{1}{y} = \frac{1}{y_{\max} k_b} * \frac{1}{x} + \frac{1}{y_{\max}}$$

Equation 6.1b

Based on the values in Table 6.1 in PB (for MHB and PHB) and in 0.01M HCl (for BA) (representing unionised form in each case), there was a linear relationship (Fig 6.3) between the binding constant (k_b) and the constant k_{H1}, consistent with drug-polymer binding being the cause of the drug dependent swelling profiles seen in Fig. 6.1a and Fig. 6.1c.

As the level of binding (k_b) increased, there was a corresponding decrease in the molar amount required to affect the hydrogel swelling (k_{H1}). The binding observed therefore lowered equilibrium swelling of the hydrogel at a given temperature. Reasons for this effect were investigated further using the linear polymer.

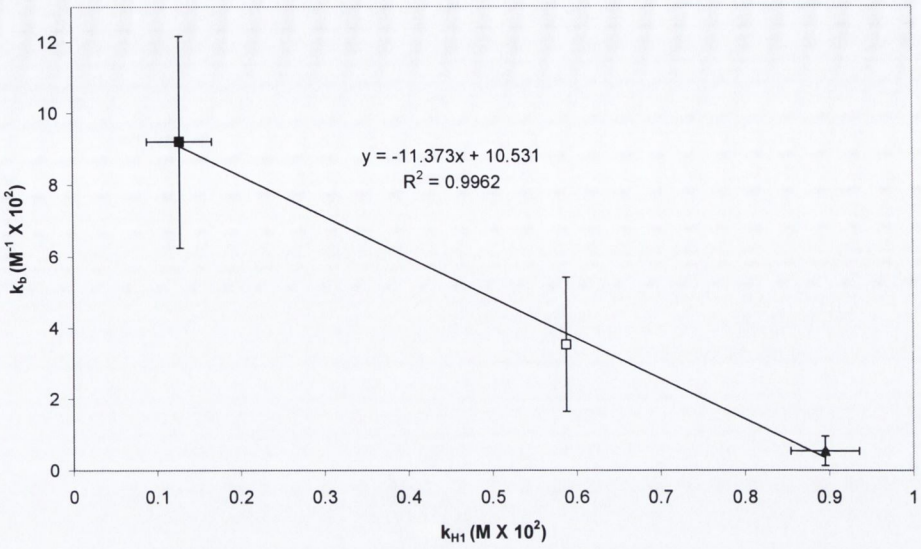

Fig. 6.3: Plot of k_{Hl} values against binding constants (k_b) [BA(▲), MHB (□), PHB (■)]. Values representing unionised form of drug were used: in 0.01M HCl for BA and in PB for PHB and MHB (Table 6.1).

6.2.2 Linear polymer

Studies on the hydrogel (PNIPA-H1) indicated binding between the benzoates and PNIPA. Drug-polymer interactions were further analysed using PNIPA-L in a solid state (co-precipitated blends) and in solution. The blends were analysed by XRD and FTIR as well as by determination of the glass transition temperature of the blends with various drug content. The influence of the drugs on the LCST of the polymer was analysed by DSC and transmittance measurements using an aqueous solution of the polymer. Phase solubility diagrams were also examined.

6.2.2.1 X-ray analysis

The amorphous nature of the polymer (PNIPA-L3) was apparent from the halo pattern and the absence of any sharp peaks. In contrast, benzoic acid and its esters were highly crystalline solids as shown by the sharp peaks in the XRD pattern. Sodium benzoate showed less intense peaks and can be described as semi-crystalline. The inhibitory effect of the polymer on drug crystallisation can be seen for each of the benzoates (Fig. 6.4). Miscibility between BA and its esters and PNIPA was expected based on the predicted solubility parameters (Table 4.5), while the solubility parameters of NaB (Table 4.5) suggested that such a drug-polymer blend would be immiscible. No crystalline peaks were observed at drug concentrations up to 20%w/w for NaB, 40%w/w for BA and 30%w/w for MHB and PHB. The inability of the polymer to prevent recrystallisation of NaB at lower concentrations than with the other benzoates was consistent with the estimated immiscibility as measured by the total solubility parameters.

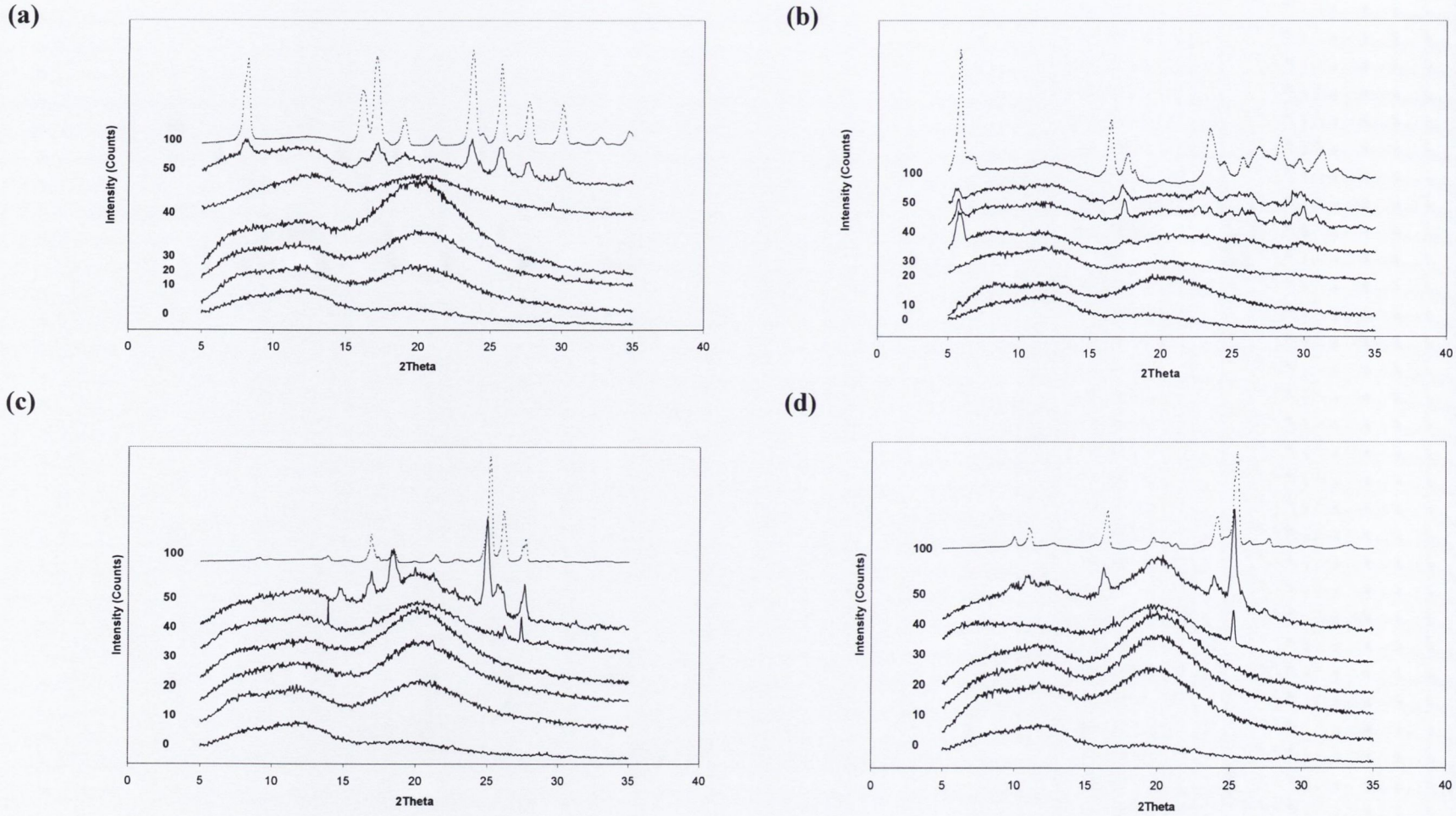

Fig 6.4: X-Ray diffraction patterns of drug/polymer co-precipitated blends (a) BA (b) NaB (c) MHB (d) PHB. From bottom to top: (i) pure polymer (0% drug) (ii) 10%w/w drug (iii) 20% drug (iv) 30% drug (v) 40% drug (vi) 50% drug (vii) 100% (pure) drug.

The ability of a polymer to prevent drug recrystallisation in a blend has previously been attributed to interactions of the drug with the polymer, resulting in a change in the molecular mobility of the drug, ultimately leading to an amorphous form of the drug (Yoshioka *et al.,* 1995). Where the crystal peaks can be seen, there was the possibility of two phases; a miscible amorphous drug-polymer phase and a second phase composed of only crystalline drug.

6.2.2.2 Glass transition temperature

The glass transition temperature (Tg) of an amorphous polymer or film is a property related to its permeability and mechanical properties. Interactions between co-precipitated drug and polymer can influence the Tg of the polymer-drug blend (Nair *et al.*, 2001). The influence of the benzoates on the Tg of the benzoate-PNIPA co-precipitated blends was examined as described in section 3.3.2. The Tg of the linear polymer used was 140.88°C (414.03K, PNIPA-L3). The glass transition temperature of the pure benzoates could not be determined experimentally due to rapid recrystallisation of the drug.

The Tg of the blends decreased as the proportion of the BA, MHB or PHB increased (Appendix II, Fig 1, 3 and 4). The Tg of the polymer may be expected to decrease in the presence of a small molecule due to the plasticising effect of the drug on the polymer (Okhamafe and York, 1989). The change in glass transition temperature of the fully amorphous blends as a function of molar percentage of drug present is presented in Fig. 6.5.

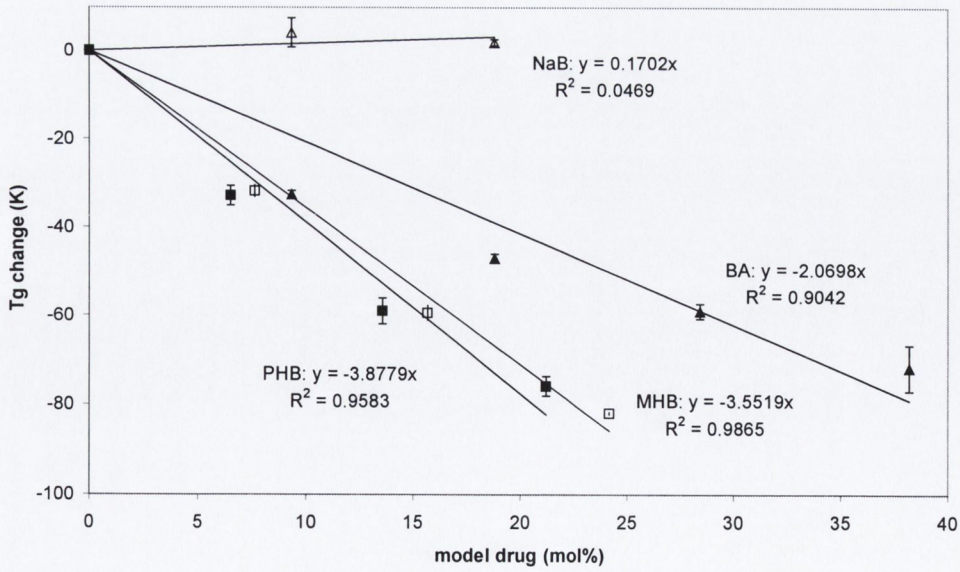

Fig 6.5: Effect of drug type on Tg change of drug/polymer co-precipitated blends [NaB (Δ), BA(▲) , MHB (□) and PHB (■)].

Previous studies on non-thermoresponsive polymers (Okhamafe and York, 1989; Gutierrez-Roca and McGinity, 1994; Nair *et al.,* 2001) have suggested a correlation between decreased drug molecular size and increased plasticising effect on the polymer due to increased access of the drug to the polymer chains. The opposite effect occurred in the present study as the plasticising effect increased as the molecular size of the benzoate series increased, quantified by the slope of the lines in Fig 6.5. More specifically, as the hydrophobicity of the series increased, the Tg decreased to a greater extent. The differences observed in depression of the Tg of the blends followed the same pattern as was shown with the binding constants (Table 6.1).

The Tg of the NaB-polymer blend did not change from that of the polymer, even in the presence of 50%w/w NaB (Appendix II, Fig 2). Immiscibility of NaB with the polymer, as predicted by the solubility parameter, may have resulted in a lack of interactions. The ionic form of BA was shown to prevent interactions with the hydrogel in section 6.2.1. Crystalline peaks in the XRD were also seen at the 20% w/w with NaB, a lower value than the other benzoates despite the salt only being semi-crystalline. The higher Tg of a salt form of a drug compared to the parent acid/base (Tong and Zografi, 1999) may also have contributed to the higher Tg value observed with the blend.

6.2.2.3 FTIR spectroscopy

Fourier transform infrared spectroscopy (FTIR) has been used both quantitatively and qualitatively to study the miscibility of polymer-drug blends (Nair *et al.*, 2001). The technique can provide information regarding any interactions of drug polymer blends at the molecular level. The FTIR spectrum in the absorbance mode of PNIPA and the benzoates were shown in Chapter 4 and the relevant peaks were assigned. FTIR of the various drug-polymer blends are shown in Appendix III, Figs 1-4. Due to the hydrophilic/hydrophobic nature of the polymer, potential interactions could involve non-polar dispersion forces with the carbon backbone/isopropyl group or hydrogen bond interactions with the hydrophilic amide group of the polymer.

Drug polymer interactions can be revealed by examination of wavelength shifts in the characteristic peak positions of either the drug or the polymer. Regions of the spectra where the peaks do not overlap are potentially useful. The characteristic peak position of the benzoates with increasing concentration of PNIPA was examined. The peak at $707cm^{-1}$ in the spectrum of BA and NaB was attributed to phenyl C-H out of plane bending (Gangakhedkar *et al.*, 1974; Chen *et al.,* 2000) (Peak **X**, Fig. 4.8). A linear increase in this peak position with increasing concentration of PNIPA in the blend was seen in the BA spectra (Fig 6.6a), suggesting the presence of hydrophobic interactions between the benzene ring of BA and the polymer. The presence of high NIPA concentrations did not appear to saturate the effect.

The peak at ~849cm^{-1} in the spectra of MHB and PHB (Peak **Y**, Fig. 4.8) were also attributed to phenyl C-H out of plane bending. An increase in the position of these peaks was seen with increasing concentration of PNIPA in the blend (Fig 6.6b), again suggesting the presence of hydrophobic interactions between the benzene ring of the esters and the polymer. There was a greater peak shift for PHB (Fig 6.6b), indicating that the propyl group in the side chain of the ester was involved in additional binding to the polymer, perhaps resulting in closer association between the polymer and the benzene group. The benzene ring peak shifts shown were stronger for BA, indicating that the effect may be only secondary in the binding process of MHB and PHB where the side chain ester also increased binding. The peak shift observed at the benzene ring site began to level off at approximately 50 mol% and 70 mol% PNIPA in the cases of PHB and MHB, suggesting approximate 1:1 and 0.5:1 benzoate:NIPA binding ratios respectively.

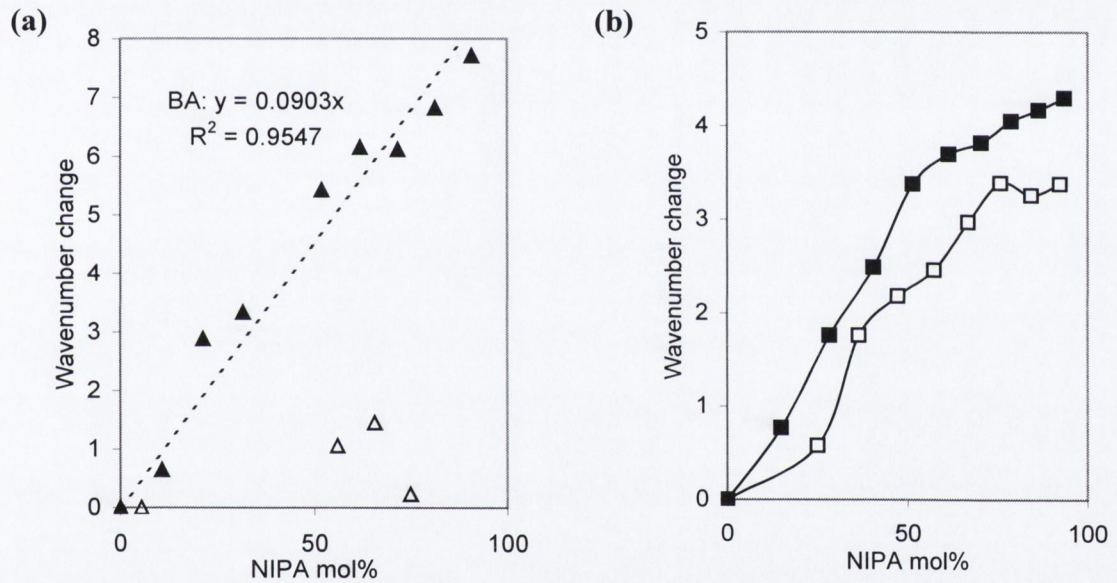

Fig 6.6: FTIR wavelength shifts of benzoate/polymer co-precipitated blends with increasing concentration of PNIPA-L: (a) wavelength change at 707cm^{-1} in spectrum of blends containing BA (▲) and NaB (Δ) (b) wavelength change at 849cm^{-1} in spectrum of blends containing MHB (□) and PHB (■). Both peaks assigned to phenyl C-H out of plane bending.

The peak at ~771cm^{-1} in the spectra of MHB and PHB may be due to coupling of the –COO- group with the phenyl ring. The presence of PNIPA also caused a weak upward peak shift for MHB (Appendix III, Fig. 4), possibly due to binding with the polymer amide group.

Binding of the benzoates studied appears to involve mainly non-polar dispersion forces of the benzene ring and the side chain ester with the hydrophobic groups of the polymer. There may also be some hydrogen bonding present. Ionisation of the acid appears to prevent the binding, as was shown in the studies with the hydrogel.

The polymer groups involved in the binding were examined by the characteristic polymer (PNIPA) peak positions (Fig 4.3) with increasing concentration of drug. The presence of BA caused a large increase in the peak position of peak B (hydrogen-bonded NH stretch), while a slight decrease was observed with NaB (Fig 6.7). Hydrogen bonding interactions would be indicated by a characteristic downward shift in the vibrational frequency of the polymer functional group involved in hydrogen bonding (Shamblin *et al.*, 1998) and may be present between PNIPA and sodium benzoate. The upward shift observed for BA may result from a decrease in the hydrogen-bonding tendency of the polymer caused by hydrophobic binding of BA. Comparisons with the esters could not be made due to peak overlap in this region due to the para hydroxy group stretching.

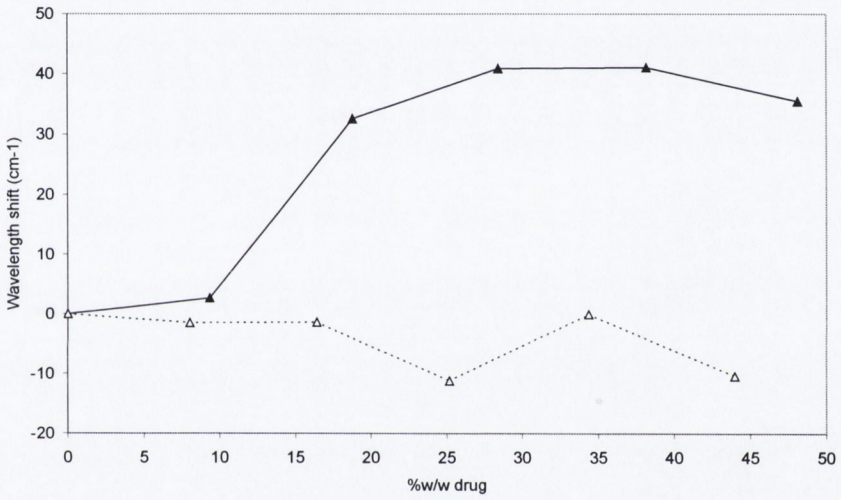

Fig 6.7: FTIR wavelength shifts of drug/polymer co-precipitated blends with increasing concentration of benzoate: BA (▲) and NaB (Δ).

An upward shift in peak H (Amide II) was also seen with increasing concentration of both BA and NaB although this may be attributed to peak overlap between the drug and polymer spectra.

There was significant peak overlap in the area of the backbone carbons (peaks D, E, F) and the isopropyl group (peaks J, K). These peaks are relatively weak and the functional groups are common making definite conclusions difficult using this technique as to the polymer groups of PNIPA involved in the hydrophobic binding mentioned above.

6.2.2.4 Phase transition temperature

The influence of various concentrations of the benzoates on the phase transition temperature (LCST) of PNIPA-L3 in PB (Appendix IV, Figs. 3-6) is shown in Fig. 6.8. The effect on the onset and peak values as measured by DSC and on the transmittance values was examined. Also shown are the endotherm integral values calculated per gram of polymer solution. The decrease in phase

transition temperature was quantified by the magnitude of the slope of the fitted lines in Fig. 6.8 (Table 6.2). The slopes were obtained by a best-fit line through the origin value and defined by a parameter, k_{LS}. A second value for BA was also calculated for the downward portion of the graph as shown in Fig. 6.8a. In each case the number of moles of benzoate per mole of NIPA required to decrease the LCST to 25°C was calculated (k_L) and shown in Table 6.2.

Table 6.2: Magnitude of change of LCST in PB caused by the presence of the benzoates as measured by the slope of the plots (k_{LS}) in Fig. 6.8. Also give is the number of moles of each benzoate per mole of NIPA required to reduce the LCST to 25°C (k_L).

	DSC Onset			**DSC Peak ($LCST_d$)**		
	k_{LS} (°C M^{-1})	**R^2**	**k_L moles/ mol NIPA**	**k_{LS} (°C M^{-1})**	**R^2**	**k_L moles/ mol NIPA**
NaB	-8.19 ± 0.01	0.9944	4.440	-8.11 ± 0.01	0.9972	4.936
BA	-58.95 ± 0.94	0.3623	0.590	-29.18 ± 1.58	0.3623	1.255
BA[(a)]	-389.20 ± 0.431	0.9340	0.373	-191.09 ± 2.59	0.9817	0.487
MHB	-631.34 ± 55.04	0.9593	0.058	-391.44 ± 8.71	0.9986	0.102
PHB	-953.13 ± 22.75	0.8392	0.038	-426.05 ± 10.92	0.8562	0.094
	% Transmittance ($LCST_t$)			**DSC Integral**		
	k_{LS} (°C M^{-1})	**R^2**	**k_L moles/ mol NIPA**	**Slope (J g^{-1} M^{-1})**	**R^2**	
NaB	-8.83 ± 0.11	0.9788	2.532	-0.08 ± 0.02	0.6079	
BA	-96.76 ± 3.53	0.4859	0.231	3.01 ± 0.54	0.5455	
BA[(a)]	-462.15 ± 4.31	0.9183	0.317	--	--	
MHB	-1064.35 ± 6.58	0.9783	0.021	-3.26 ± 1.33	0.0498*	
PHB	-3948.95 ± 313.03	0.9413	0.006	28.32 ± 16.38	-0.2735*	

All slopes calculated when fixed through origin value except for BA where slope[(a)] also calculated for downward portion as shown in Fig. 6.8a.

The presence of BA in PB up to a concentration of ~0.035M did not have an effect on the LCST of the polymer solution as shown in Fig. 6.8a. Above this concentration, the measured pH of the solution approached the pKa of BA (pKa = 4.2), similar to the pH change shown in Fig. 6.1a. The appearance of significant concentrations of the unionised form of BA caused a decrease in the LCST of the polymer. The same pattern was shown in Fig. 6.1a for equilibrium swelling of the hydrogel. Binding of the unionised benzoates to the hydrogel was shown to be the cause of the swelling pattern in section 6.3.1. Binding of the unionised form of BA to PNIPA was shown here to lower the LCST of the polymer. Swelling at 25°C was therefore affected when the LCST was lowered sufficiently near this temperature.

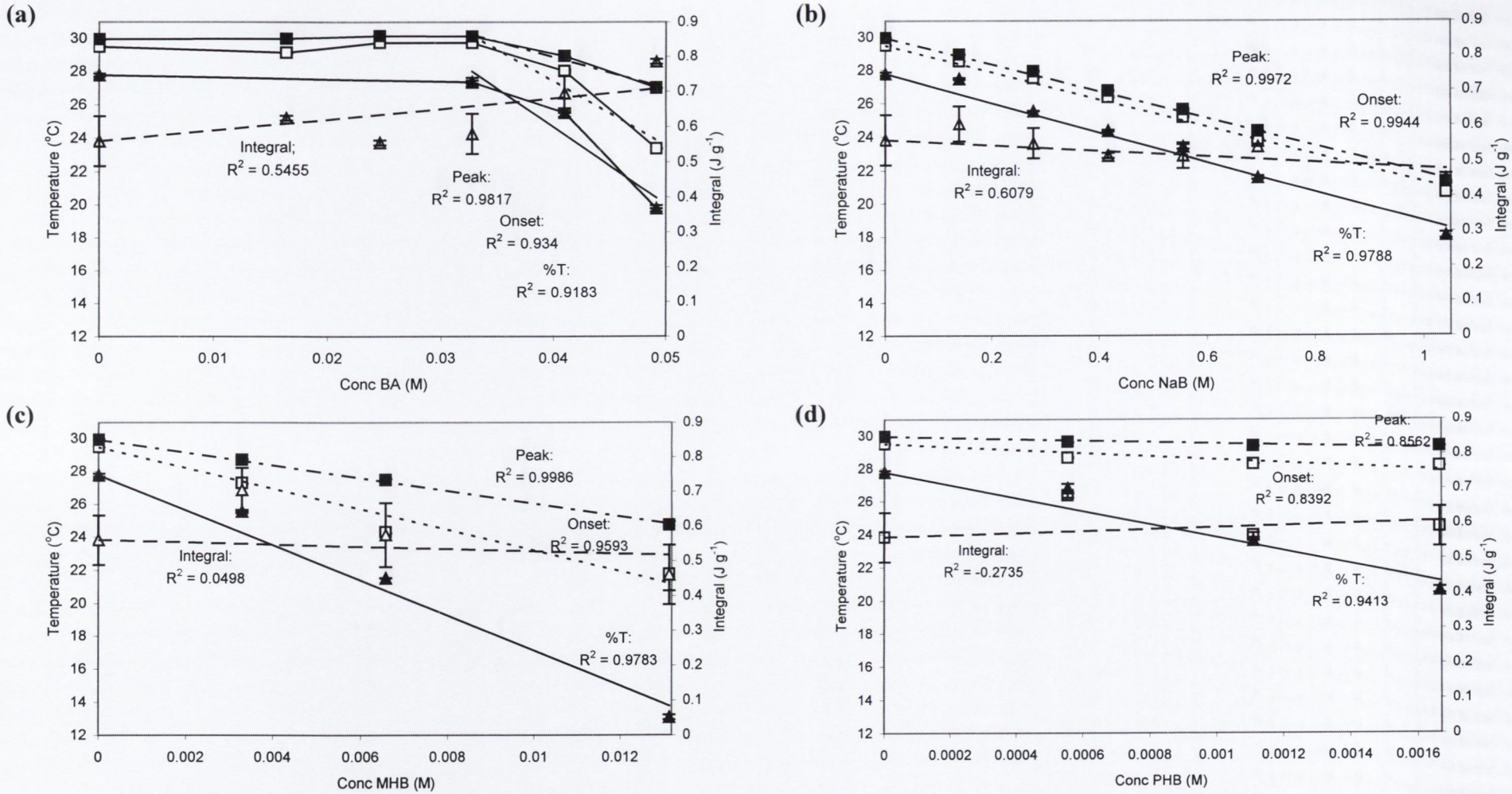

Fig. 6.8: Plot of endotherm peak (■), onset (□) and integral (Δ, secondary y axis) obtained by DSC of a 1.4% w/w solution of PNIPA-L3 containing various concentrations of (a) BA (b) NaB (c) MHB (d) PHB. Also shown are the $LCST_t$ values from the % transmittance study (▲) (Appendix IV, Fig 3-6), defined as 50% transmittance.

Binding of the ionised form of BA did not appear to be significant in the concentration range studied. The presence of sodium benzoate (Fig 6.8b) in the same concentration range as BA also did not affect the LCST, as this species exists in the ionised form at pH 6.8. At high concentrations, however, NaB caused a gradual decrease in the LCST of the polymer. The decrease in transition temperature as measured by endotherm onset, peak and transmittance values resulted in three approximately parallel lines as shown by the k_{LS} values (Table 6.2). The magnitude of the decrease in LCST, as measured by the k_L values, was ~10 times lower than the downward portion shown by BA. Since significant binding was not apparent, the effect seen on the LCST can be attributed to the large benzoic anion disrupting the hydrogen bonding between the polymer and the water molecules. Such a salting out effect required higher concentrations to be present and resulted in an increase in the hydrophobic nature of the polymer and a decrease in LCST, as shown previously by Eeckman *et al.* (2001) and Schild and Tirrell (1991) with various salts and small surfactants. Such effects may explain the swelling pattern of the hydrogel seen in Fig. 6.1b. An approximate 10-fold difference was also seen with either the k_{H1} or k_{H2} values between BA and NaB (Table 6.1). The salting out effect also lowered the phase transition temperature of the polymer chains and therefore the equilibrium swelling level of the hydrogel at a particular temperature.

Increasing the hydrophobic nature of the ester side chain resulted in sharper decrease in the LCST caused by greater binding affinity (Table 6.2). From the FTIR data, the benzoates associated with hydrophobic segments of the polymer, resulting in a more hydrophobic system and causing the phase transition to occur at a lower temperature. The values in Table 6.2 quantify the magnitude of the decrease in the phase transition with increasing benzoate concentration. The same pattern was observed whether the DSC peak or onset or the % transmittance values were used. The analytical method and/or heating rate used to determine the phase transition affected the temperature at which the LCST of the PNIPA-L was determined. A linear relationship (Fig. 6.9, $R^2 = 0.9988$) was shown between the peak k_{LS} values in Table 6.2 and the k_{H1} values in PB (Table 6.1) determined with the hydrogels, confirming the influence of the binding on the LCST and therefore on swelling. There was greater variability in the linear relationship determined using the onset value ($R^2 = 0.9387$) or the %T value ($R^2 = 0.5945$), due to greater variability in determining the LCST using these analytical measurements.

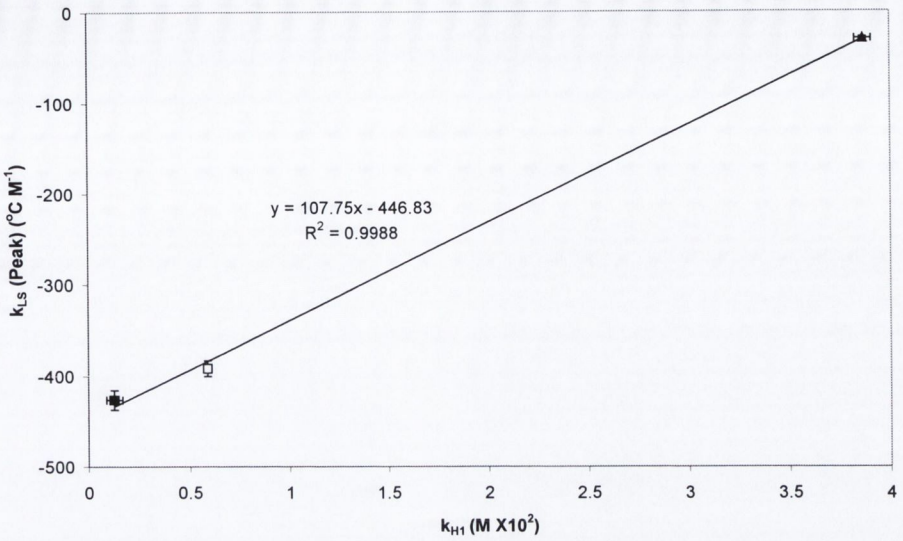

Fig. 6.9: Plot of k_{H1} values in PB (Table 6.1) against the change in the LCST in PB per unit concentration of benzoate (k_{LS}) (Table 6.3), using peak values ($LCST_d$): BA(▲) , MHB (□) and PHB (■)

Comparisons can also be made between the hydrogel k_{H2} values, which measure the number of moles required to theoretically prevent swelling at 25°C, and the k_L values, which are the number of moles necessary to decrease the LCST to 25°C. As the hydrophobicity of the ester series decreased, both the k_{H2} and the k_L values also decreased, in line with the decrease in the binding constant in Table 6.1. The k_{H2} and the k_L values for BA and the esters approximately correspond between the two systems, indicating that the effect of binding on the LCST caused the swelling patterns. The k_{H2} value for NaB was, however, significantly larger than the corresponding k_L value, indicating that the salting out effect on the LCST was not the only contributing factor to the swelling pattern. The very high concentrations of NaB may also have prevented solvation of the polymer chains due to competition for hydrogen bonding with the water molecules present. A statistically significant decrease ($p<0.05$) in the magnitude of the integral value was seen with NaB. At the high concentrations, NaB may interfere with the H-bonding ability of PNIPA in solution. In contrast there was a statistically significant increase ($p<0.05$) in the magnitude of the phase transition with increasing benzoic acid while there was no significant change ($p>0.05$) caused by the benzoate esters.

6.2.2.5 Phase solubility study

The type of phase solubility diagram obtained due to binding between the benzoates and PNIPA-L was determined by complexation solubility analysis (section 3.3.10.2).

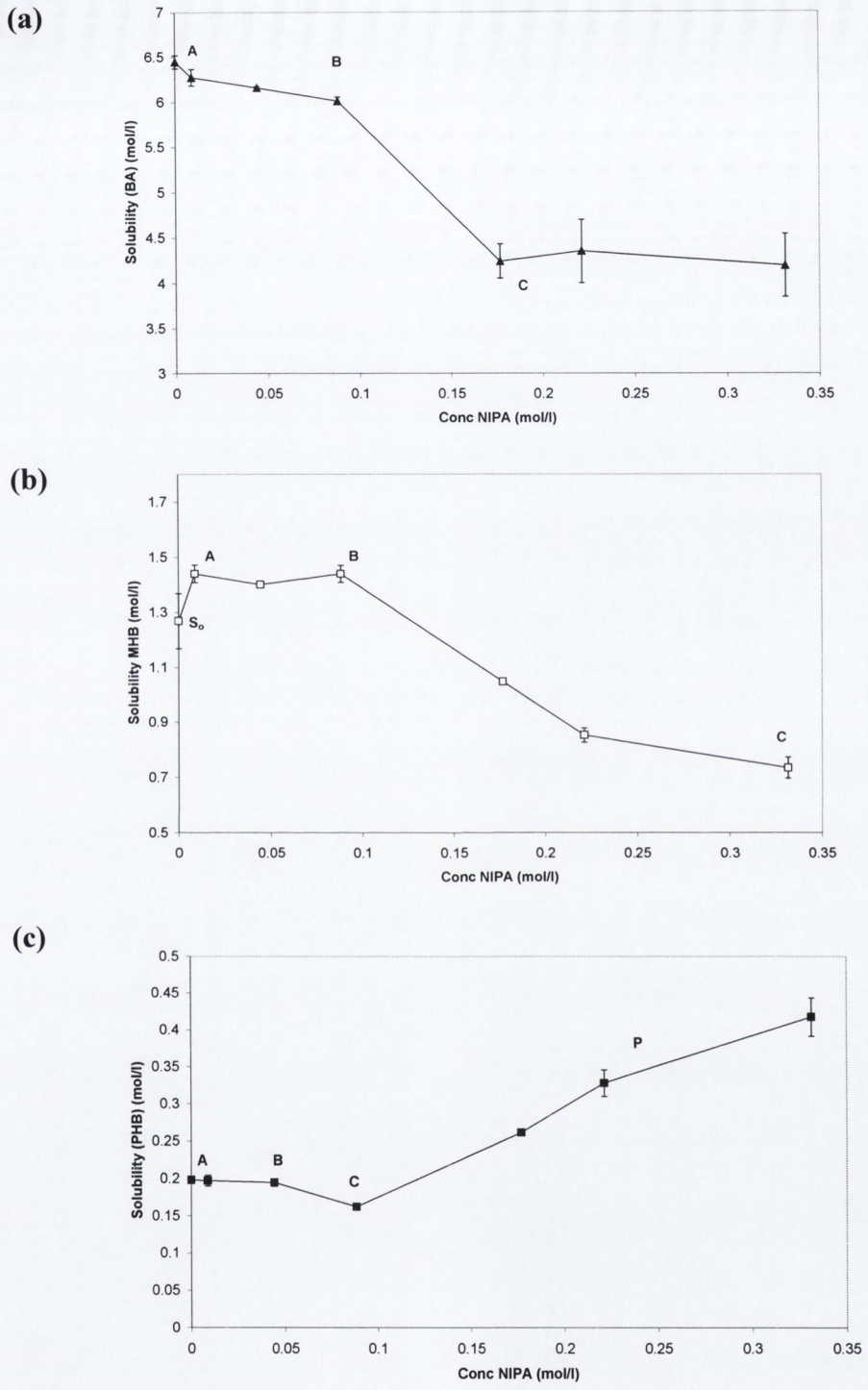

Fig 6.10: Phase diagrams showing the effect of PNIPA-L3 on the apparent solubility of (a) BA (b) MHB and (c) PHB at 25°C in PB (n = 3, mean ± s.d). Letters shown described in text.

Higuchi and Connors (1965) described two types of complexes that can form between substrate (S) and ligand (L). Type A phase diagrams show an apparent increase in the solubility of the substrate caused by the presence of component L. These phase diagrams therefore indicate the formation of

soluble complexes. Type B phase diagrams were observed in the present study (Fig 6.10a-c), which indicated the presence of insoluble complexes. A typical diagram is seen with MHB at 25°C in Fig 6.10b and was described by Higuchi and Connors (1965) as follows. From S_o to A, the apparent solubility of MHB is increased due to soluble complex formation between MHB and PNIPA-L (similar to a Type A diagram). At point A, however, the solubility limit of this complex is reached. Addition of further PNIPA-L resulted in formation of more complex, which must precipitate; the concentration of MHB thus remains constant by dissolution of free solid MHB. At point B all of the solid MHB has been consumed in this manner, and further addition of the substrate (PNIPA-L) resulted in depletion of MHB in the solution by complex formation and concomitant precipitation of the insoluble complex (B-C). The phase diagrams of BA (Fig 6.10a) and PHB (Fig. 6.10c) showed a similar pattern with no initial rise in solubility seen and a shorter plateau phase in the case of PHB. A subsequent increase in apparent solubility (P) after point C was also seen with all three systems and is shown in Fig 6.10c. Similar effects have previously been noted (Higuchi and Lach, 1954; Takayama *et al.,* 1977) and attributed to the formation of another complex species, which was more soluble than the one responsible for the descending portion of the curve.

In the present context, a soluble complex formed by hydrophobic binding between the benzoate and the polymer as shown by FTIR. The benzoate lowered the LCST of the polymer towards the temperature of the experiment (25°C), resulting in precipitation of the complex. Due to the presence of excess benzoate in the experiment, the soluble complex would not be expected to be observed, as was the case with BA (Fig 6.10a) and PHB (Fig. 6.10c).

An attempt was made to characterise the complexation phenomenon based on the phase solubility diagrams. Stoichiometric ratios can be estimated for Type B diagrams (Higuchi and Lach, 1954). A stoichiometric calculation is possible because if the analysis is true then the amount of PNIPA-L represented by the plateau is equal to that entering into the complex in this interval, and the corresponding amount of benzoate being converted to complex is equal to that present as free undissolved drug at point A (Higuchi and Lach, 1954). The estimated stoichiometric ratios and complex formulas are given in Table 6.3.

Table 6.3: Estimated stoichiometric ratios/complex formulas along with complex formation constants assuming a 1:1 ratio (K)

	Stoichiometric ratio (Benzoate:NIPA)	**Estimated complex formula**	**K**
BA	2.97:1	$(BA)_3(NIPA)$	49.31
MHB	2.83:1	$(MHB)_3(NIPA)$	13.82
PHB	4.98:1	$(PHB)_5(NIPA)$	140.65

Whether the stoichiometry is a valid reflection of the chemistry depends upon whether one or several complexes are formed; if more than one complex is contributing to the solubility behaviour at any region of the diagram, the stoichiometry may reflect contributions from all of the complexes (Higuchi and Connors, 1965).

Assuming that a single complex, S_mL_n, is responsible for the change in apparent solubility of S, the complex formation constant ($K_{m:n}$) is given by the following equation:

$$K_{m:n} = \frac{(S_m L_n)}{(S)^m (L)^n}$$

Equation 6.3

where

S_mL_n = the concentration of complex in the solution

S = the concentration of substrate in solution (representing the substance in excess)

K= the concentration of ligand in solution

At point X on the descending portion of Type B curves (coordinates L_xS_x) the following equations hold:

$$S_x = (S) + m(S_m L_n)$$

Equation 6.4a

$$L_x = (L) + n(S_m L_n)$$

Equation 6.4b

This gives an equation of the form:

$$K_{m:n} = \frac{S_D}{(S_x - mS_D)^m (L_x - nS_D)^n}$$

Equation 6.5

where S_D is the concentration of S where all free S has been removed from solution.

The complex formation constants assuming a 1:1 complex are given in Table 6.3.

Other possible reasons for the downward portions of the observed phase diagrams is the formation of a solid solution between the solid benzoate and the insoluble complex (Benzoate-PNIPA)

(Higuchi and Connors, 1965). This produces a phase diagram, which shows an immediate and progressive decrease in the apparent concentration of the benzoate (substrate). Havemeyer and Higuchi (1960) showed a progressive decrease in the apparent concentration of vitamin B12 in the presence of mercuric chloride. Other suggested reasons for the effect included a salting out effect or a medium effect upon the absorption spectrum (Havemeyer and Higuchi, 1960).

6.3 DILTIAZEM

6.3.1 Hydrogel

The influence of diltiazem base and its hydrochloride salt on the equilibrium swelling of PNIPA-H1 is shown in Fig. 6.11. The effect of DHCl was examined up to a higher concentration than DB due to its greater solubility in PB.

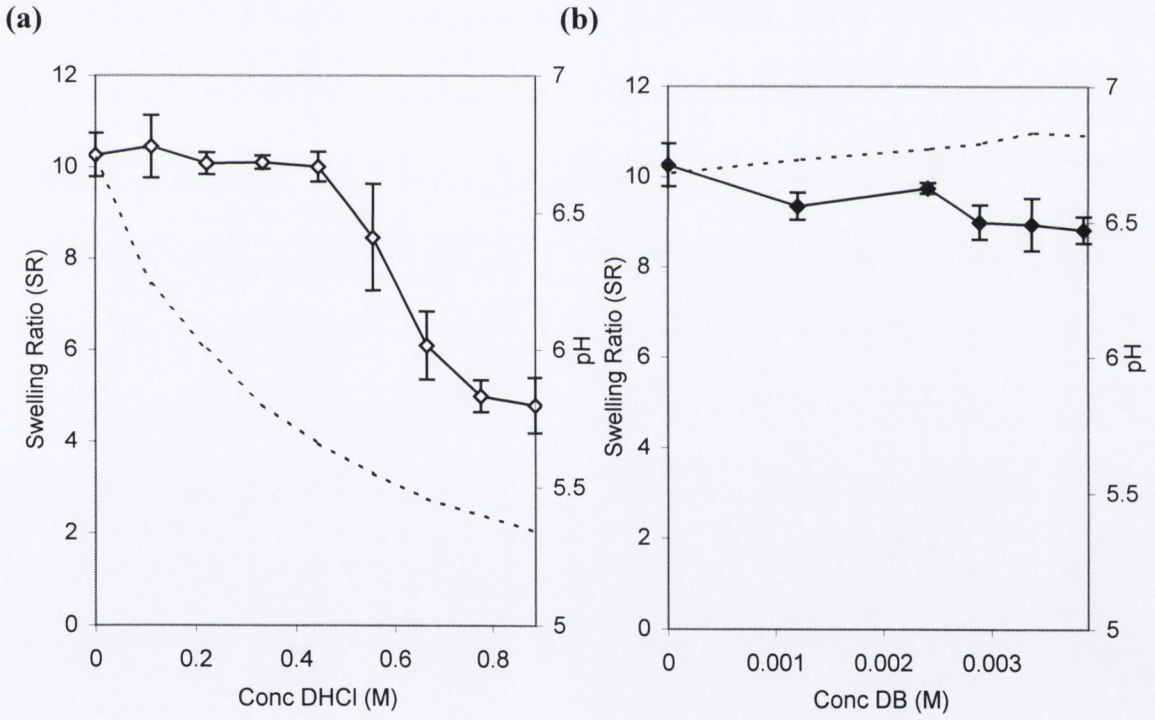

Fig 6.11: Equilibrium swelling ratios (n = 3; mean ± s.d.) of PNIPA-H1 in various concentrations of (a) DHCl and (b) DB in PB at 25°C. Also shown are measured pH values in PB pH 6.8 (dashed lines)

The presence of DHCl (Fig. 6.11a) did not affect the swelling of PNIPA-H1 until relatively high concentrations (>0.4M), resulting in a k_{H1} value of 0.77M (Table 6.1). There was a small decrease in the equilibrium swelling of the hydrogel in DB, although a k_{H1} value could not be detected. A drop in pH was also observed with increasing concentration of DHCl, although for both DHCl and DB the pH remained below the pKa of the base (pKa=8.91). The unionised species therefore

dominated. Possible diltiazem-PNIPA interactions were further investigated using the linear polymer.

6.3.2 Linear polymer

Studies on the hydrogel (PNIPA-H1) did not indicate a significant binding effect similar to that seen with the benzoates. Potential interactions were, however, further analysed using PNIPA-L in a solid state and in solution.

6.3.2.1 X-ray analysis

The inhibitory effect of the polymer on diltiazem crystallization, as shown by XRD, was apparent only at drug concentrations ≤20%w/w for both DB and DHCl (Fig. 6.12). Above these concentrations there was the possibility of two phases; a miscible amorphous phase and a second phase of only crystalline drug.

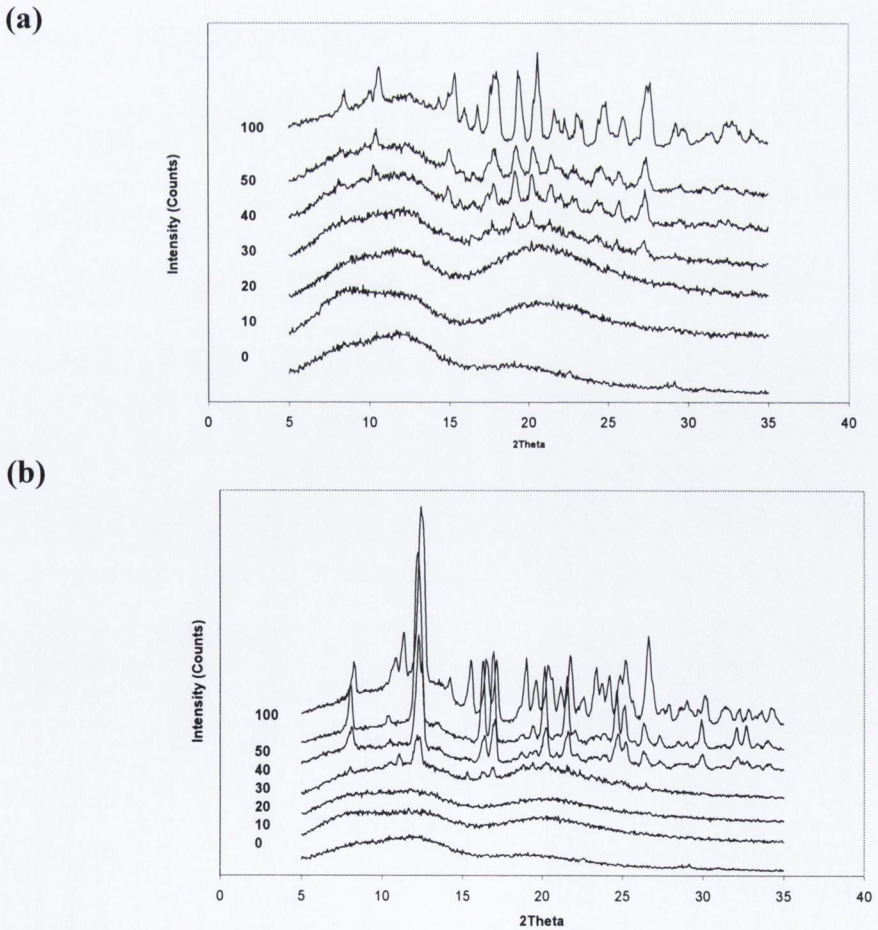

Fig 6.12: XRD pattern of drug/polymer co-precipitated blends containing various proportions of (a) DHCl (b) DB (0 to 100%w/w of diltiazem as indicated).

6.3.2.2 Glass transition temperature

Only one glass transition temperature was observed in the co-precipitated blends for both DHCl and DB (Appendix II, Fig. 5 and Fig. 6 respectively) and the average values obtained are shown in Fig. 6.13. In both cases, an initial decrease in the Tg was observed followed by a levelling off and a slight increase. Melting of DH in the blend could be seen at concentrations of 30% w/w and greater (Appendix II, Fig. 5), consistent with the observed crystallinity in the blend as shown by XRD. The melting transition is also shown in Fig. 6.13.

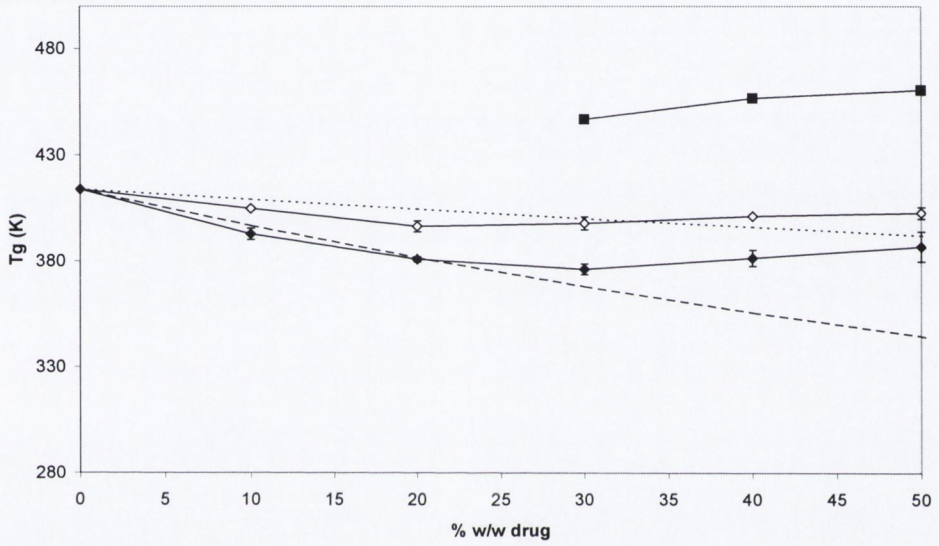

Fig 6.13: Tg values of drug/polymer co-precipitated blends with various compositions of DH (◊) or DB (♦). (Appendix II, Fig 5-6) Also shown is the observed melting transition of DH at certain blend compositions (■). Dashed line represents the predictions of the Gordon-Taylor equation.

Several empirical or semi-empirical equations have been used to predict the dependence of Tg on the composition of polymer blends. The commonly used Gordon Taylor equation is based on the additivity of free volumes of the individual components characteristic of ideal mixing and is given by the expression (Gordon and Taylor, 1952):

$$T_{g12} = \frac{w_1 T_{g1} + K w_2 T_{g2}}{w_1 + K w_2}$$

Equation 6.6

where T_{g12} is the glass transition temperature of the drug polymer blend. w_1, w_2, T_{g1} and T_{g2} are the weight fractions and glass transition temperatures (in Kelvin) of the drug and polymer respectively. The constant K, which is a measure of interaction between the components, can be approximated using the equation (Sihma and Boyer, 1962):

$$K \approx \frac{\rho_1 T_{g1}}{\rho_2 T_{g2}}$$

Equation 6.7

Where ρ_1 and ρ_2 refer to the true densities of the components. The parameters used are given in Chapter 4 (Table 4.5). The influence of blend composition on observed Tg is shown in Fig. 6.13 along with the predictions of the Gordon Taylor equation. The predictions of the Gordon-Taylor equation match the observed decrease in Tg of both drug–polymer blends over the range 0-30% w/w. This may indicate similar drug-polymer and drug-drug interactions (Nair *et al.*, 2001) or may be due to the plasticising effect of the drugs in increasing the free volume of the polymer at low concentrations. The presence of crystalline drug in the blend at concentrations of 30% w/w and greater increased the rigidity of polymer chain resulting in a levelling off and subsequent increase in the Tg.

The ability to predict the Tg of the blends in the presence of diltiazem does not suggest any major drug-polymer interactions.

6.3.2.3 FTIR spectroscopy

The FTIR spectrum of DH and DB were shown in Fig 4.9. The spectra of the various blends with PNIPA are given in Appendix III (Figs 5 and 6 respectively). The hydrogen-bonded NH stretch at 3299 cm^{-1} (B) and 3073 cm^{-1} (C) of PNIPA showed some peak shift to lower wavenumbers, particularly in the case of DH (Fig. 6.14), indicating hydrogen bonding between DH and PNIPA.

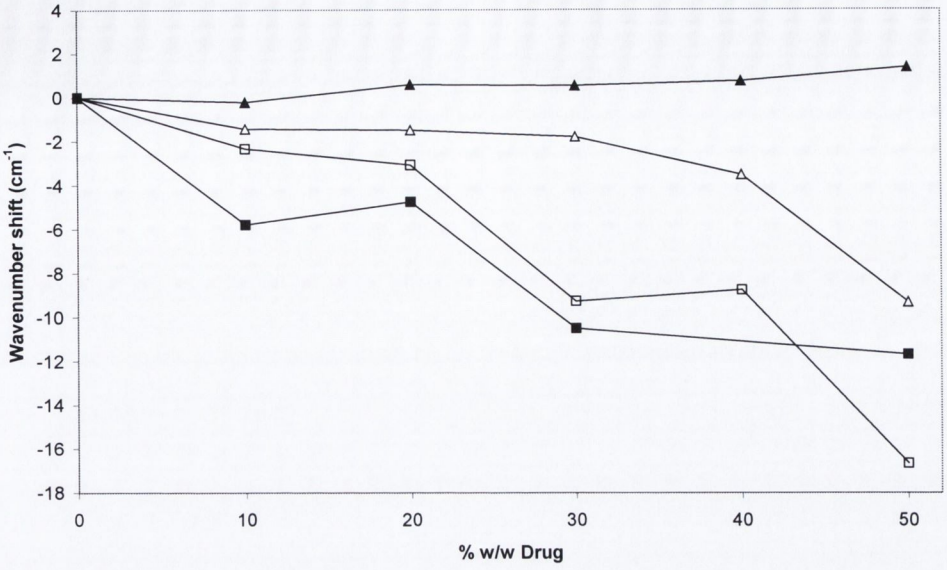

Fig 6.14: Change in wavenumber peak with increasing concentration of DH (■/□) or DB (▲/Δ). Peak B (3299cm^{-1}, closed symbols) and C (3073cm^{-1}, open symbols) of PNIPA correspond to hydrogen bonded N-H stretching on PNIPA.

There were no other significant peak shifts, with either the polymer or the model drugs, detectable by FTIR.

6.3.2.4 Phase transition temperature

The influence of various concentrations of DHCl and DB on the phase transition temperature of PNIPA-L3 (Appendix IV, Fig. 7-8) is shown in Fig. 6.15. Also shown are the endotherm integral values calculated per gram polymer solution. Neither DHCl (Fig 6.15a) nor DB (Fig 6.15b) significantly affected the position of the LCST as detected either by DSC or by % transmittance (shown by the horizontal lines). The presence of DB also did not affect the magnitude of the phase transition as measured by the integral value. The concentrations of DHCl used were much higher due to its higher aqueous solubility. As the concentration of DHCl added increased, the integral decreased (R^2= 0.8986), representing a decrease in the magnitude of the phase transition as detected by DSC (Fig 6.15a and Appendix IV, Fig 7). When extrapolated to a zero integral value, a concentration of ~0.89M DHCl was obtained, compared to the k_{HI} value of 0.77M for the hydrogel.

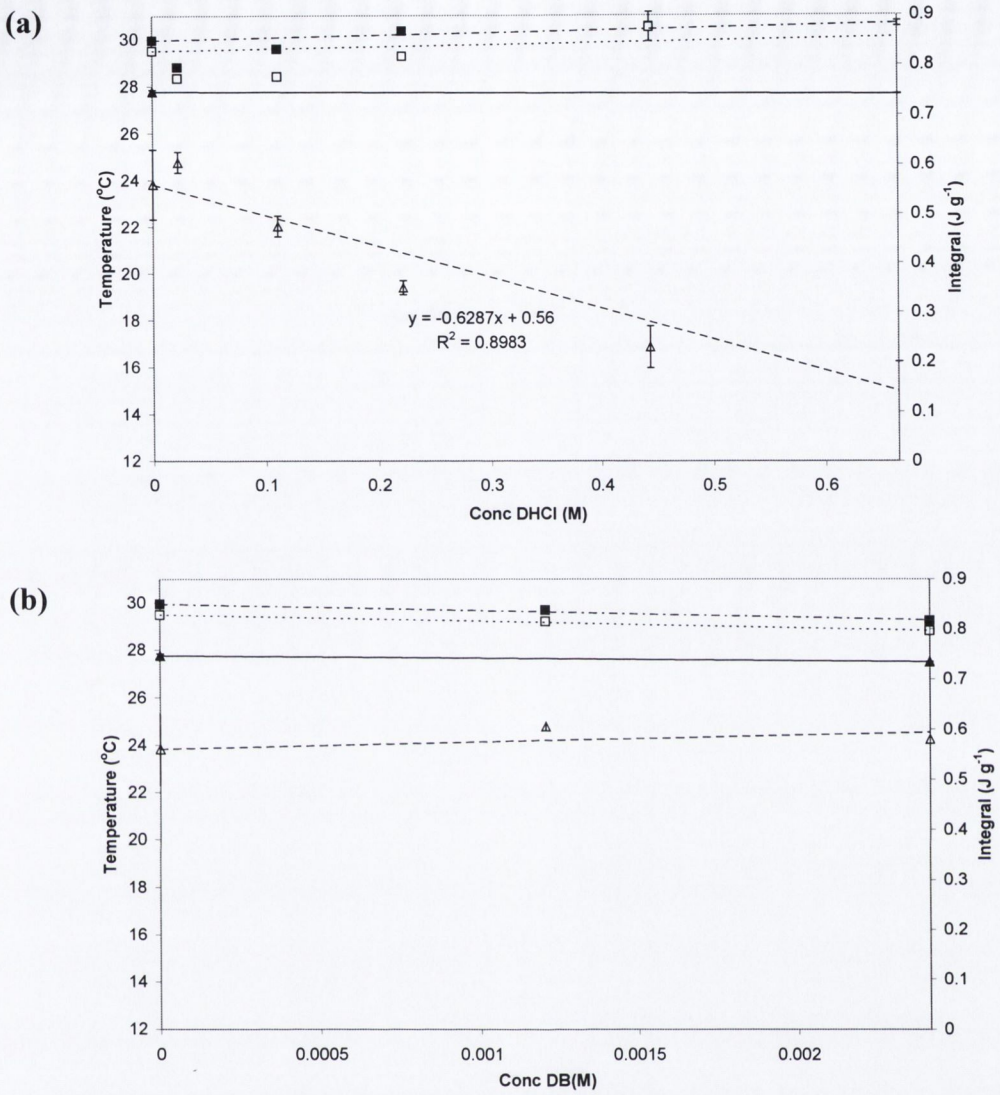

Fig. 6.15: Plot of endotherm peak (■), onset (□) and integral (Δ, secondary y axis) obtained by DSC of a 1.4% w/w solution of PNIPA-L3 containing various concentrations of (a) DHCl (b) DB. Also shown are the $LCST_t$ values from the % transmittance study (▲) (Appendix IV, Fig. 7-8), defined as 50% transmittance.

The effect of DHCl on the magnitude (as measured by the integral value) and position of the LCST can be compared with the effect of NaB on the LCST (Fig. 6.8b, Table 6.2) and on hydrogel equilibrium swelling at 25°C (Fig. 6.1b). In the case of NaB, both the size of the phase transition and the temperature at which it took place decreased with increasing concentration of salt added. The decrease in the position of the LCST was attributed to a salting out effect caused by the benzoate anion. The decrease in the magnitude of the transition may have been due to competition between the polymer and the high concentrations of drug for the available water molecules. Both of these factors resulted in the swelling profile observed (Fig. 6.1b). In the present case of DHCl, the salt had a greater effect than NaB on the magnitude of the phase transition, as shown by the greater slope. A salting out effect was not apparent, as there was no significant effect on the

position of the LCST. The decrease in the magnitude of the transition also appears to have been due to competition between the polymer and the drug for the available water molecules. Swelling of PNIPA-H1 in the presence of DHCl was unaffected up until relatively high concentrations as shown in Fig. 6.11a. The effect of very high concentrations of DHCl on the swelling of PNIPA-H1 can therefore be attributed to competition between the drug and the polymer for hydrogen bonding to the available water molecules.

6.4 VITAMIN B12 (CYANOCOBALAMIN)

6.4.1 Hydrogel

The influence of vitamin B12 (VB12) on the ability of PNIPA-H1 to swell at 25°C is shown in Fig. 6.16. There was a small statistically significant decrease ($p < 0.05$) in the equilibrium swelling in the range examined. A k_{H1} value was, however, not detectable. Further studies were performed using the linear polymer.

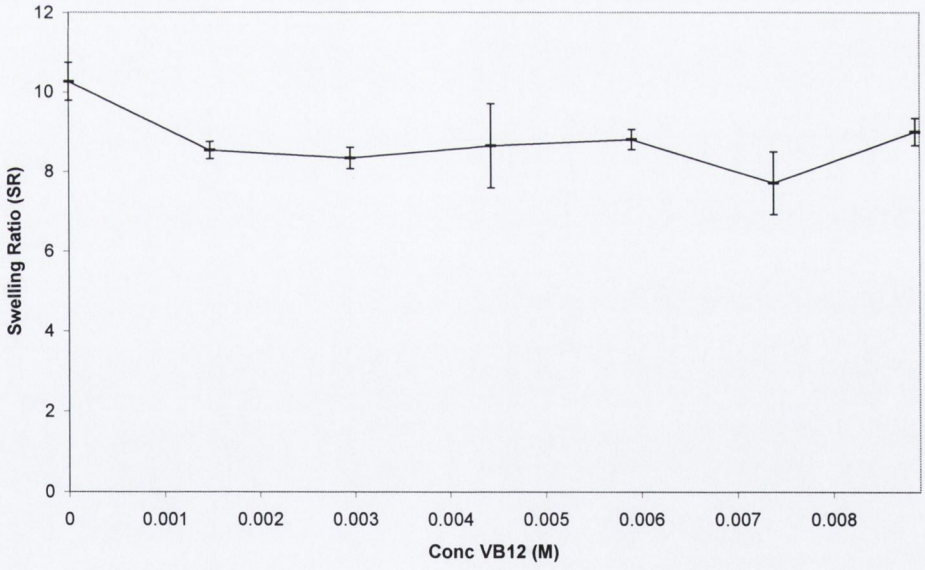

Fig 6.16: Equilibrium swelling ratio (n = 3; mean ± s.d) of PNIPA-H1 in various concentrations of vitamin B12 in PB at 25°C.

6.4.2 Linear polymer

6.4.2.1 X-ray analysis

Vitamin B12 was semi-crystalline in nature, illustrated by the halo pattern and the presence of some sharp peaks (Fig. 6.17). The inhibitory effect of the polymer on drug crystallization can be seen. The presence of the crystalline drug in the co-precipitated blend was only apparent at drug concentrations >30% w/w.

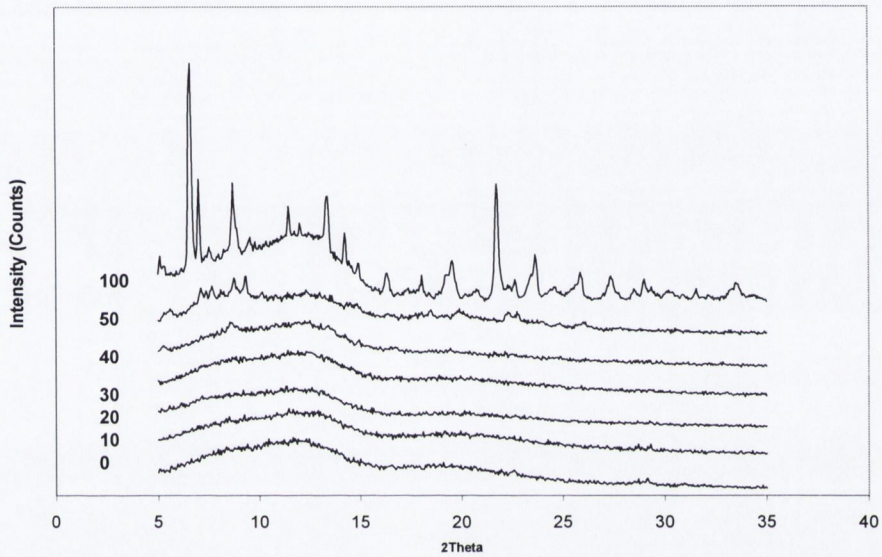

Fig. 6.17: XRD pattern of drug/polymer co-precipitated blends containing various proportions of VB12 (0-100%w/w as indicated).

6.4.2.2 Glass transition temperature

A glass transition temperature of ~89°C was obtained for vitamin B12 (Table 4.5). The effect of various concentrations of vitamin B12 on the glass transition of PNIPA-L3 is shown in Fig. 6.18 and Appendix II, Fig 7.

For all compositions, a single Tg was observed corresponding to that of the PNIPA-L3. In addition, a peak was also observed in each co-precipitated blend corresponding to the melting point of vitamin B12. This indicates that a crystalline phase was present even at 10% VB12 and was not detectable by XRD (Fig. 6.17).

The observed glass transition temperature was slightly greater than that predicted by the Gordon-Taylor equation (Fig. 6.18) due to the effect of the crystalline drug on the rigidity of the polymer chain.

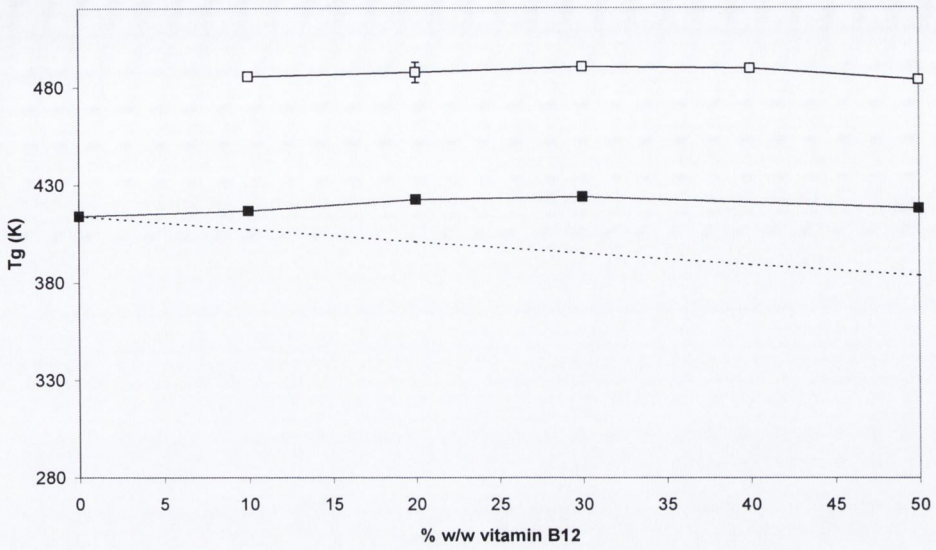

Fig. 6.18: Tg values of drug/polymer co-precipitated blends with various compositions of VB12 (■). Also shown is the observed melting transition (□). Dashed line represents the prediction of the Gordon-Taylor equation.

6.4.2.3 FTIR spectroscopy

Due to the chemical structure of VB12 containing several hydrophilic and hydrophobic groups, there was significant peak overlap with the FTIR spectrum of PNIPA-L (Appendix III). There were, however, no significant peak shifts apparent in PNIPA-L with increasing concentration of VB12.

6.4.2.4 Phase transition temperature

The influence of VB12 on the phase transition temperature (Appendix IV, Fig.9) was examined using DSC measurements (Fig. 6.19). Transmittance measurements could not be performed due to the non-transparency of VB12 in solution at 500nm. The presence of VB12 did not affect the magnitude or position of the phase transition temperature PNIPA-L in the concentration range studied.

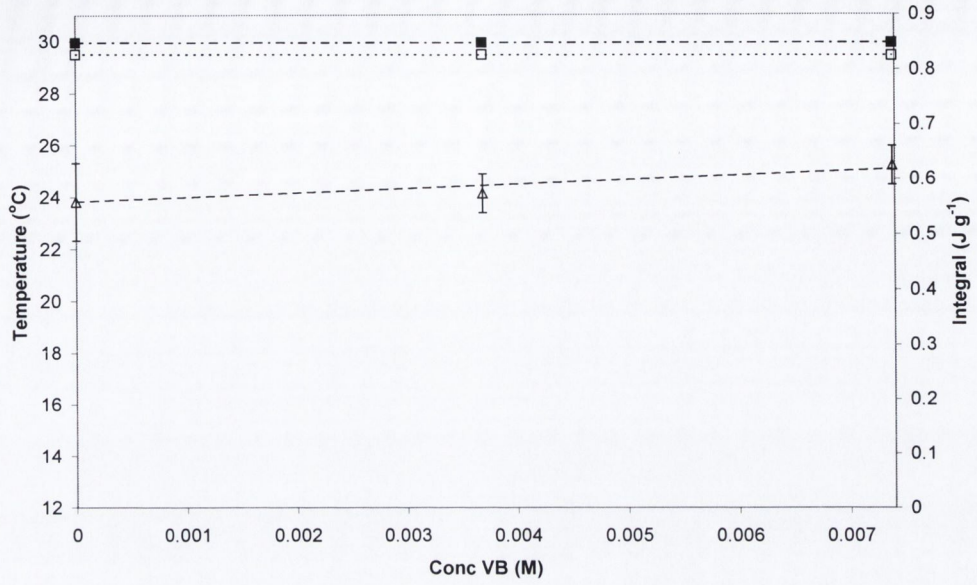

Fig. 6.19: Plot of endotherm peak (■), onset (□) and integral (Δ, secondary y axis) obtained by DSC of a 1.4% w/w solution of PNIPA-L3 containing various concentrations of VB12.

Studies with VB12 indicated no interactions with the polymer or the hydrogel of PNIPA.

6.5 DEXTRANS

6.5.1 Hydrogel

The equilibrium swelling ratio of PNIPA-H1 in various concentrations of the dextrans (D10, D40 and D70) on a weight basis (Fig. 6.20a) and on a molar basis (Fig. 6.20b) at 25°C is shown. As the concentrations of the dextrans increased, the equilibrium swelling of the hydrogel decreased. There was no molecular weight difference in the swelling depression when analysed on a weight basis (Fig. 6.20a).

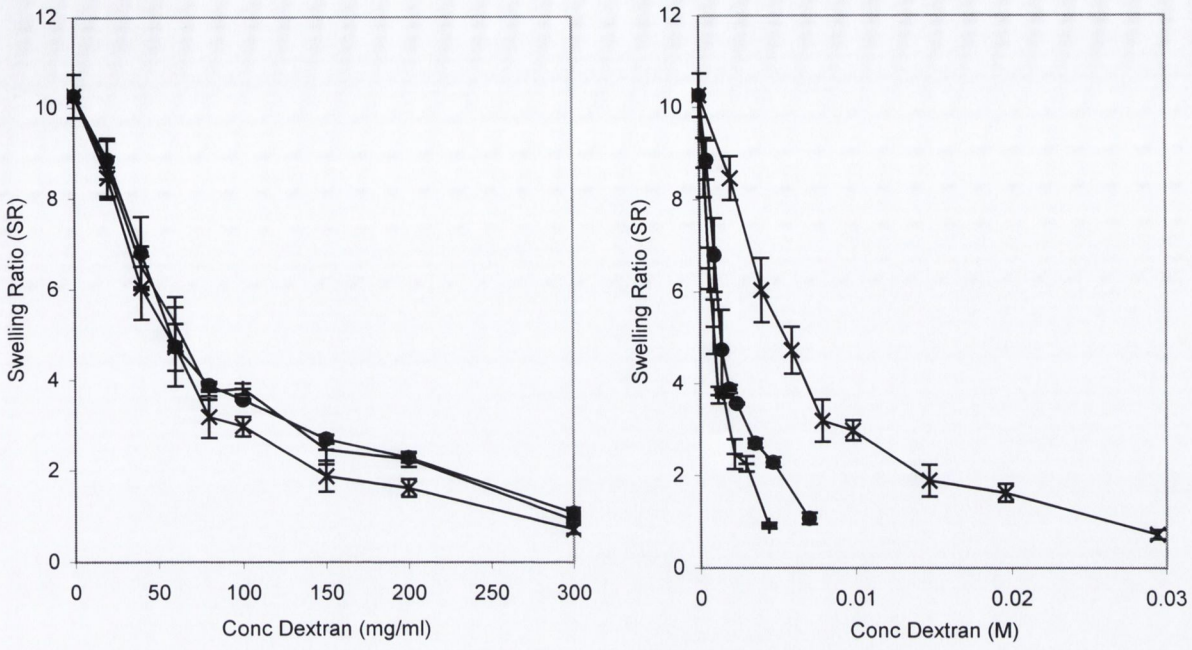

Fig 6.20: Equilibrium swelling ratios (n = 3; mean ± s.d) of PNIPA-H1 in various concentrations of D10 (x), D40 (o) or D70 (+) in PB at 25°C on (a) a weight basis (b) a molar basis

6.5.2 Linear polymer

6.5.2.1 X-ray analysis

The dextrans were all amorphous in nature and the resulting blends with PNIPA-L were also amorphous as expected (Fig. 6.21)

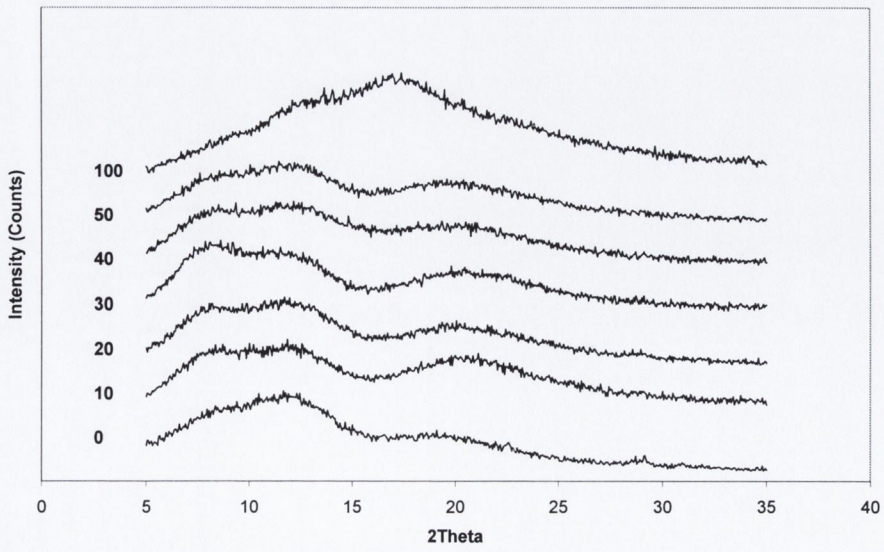

Fig. 6.21: XRD pattern of drug/polymer co-precipitated blends containing various proportions of D40 (0-100%w/w as indicated)

6.5.2.2 Glass transition temperature

There was a general increase in the Tg of the dextrans with increasing molecular weight as described in chapter 4 (Table 4.5). A single Tg, corresponding to the glass transition of PNIPA-L, was observed for all of the PNIPA-dextran blends examined (Fig. 6.22 and Appendix II, Fig. 8-11). A second Tg corresponding to the glass transition of the dextran was observed in some of the blends (Appendix II, Figs 8-11).

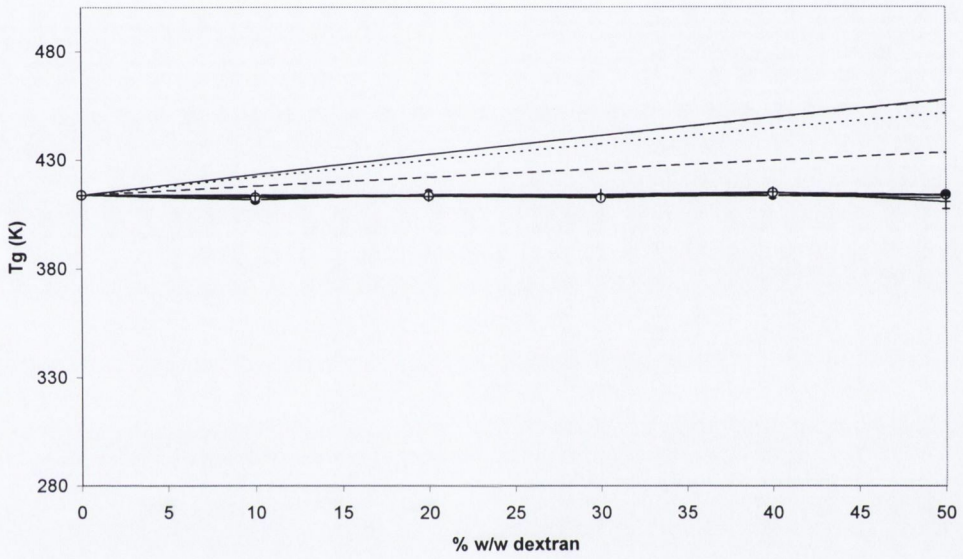

Fig. 6.22: Tg values of drug/polymer co-precipitated blends with various compositions of the dextrans. The straight lines (no symbols) represent the prediction of the Gordon-Taylor equation (– – –D4, ----D10, —— D40, —·— D70).

The presence of only one Tg value intermediate to that of the components has previously been used to establish miscibility of the components (Shamblin *et al.*, 1998; Taylor and Zografi, 1998). In this case, however, the Tg corresponded to that of the PNIPA-L with no observed effect from the dextrans. A constant Tg at all compositions has been attributed to a lack of interaction between the two components (Nair *et al.,* 2001). The Tg values were also lower than those predicted by the Gordon-Taylor model i.e. negative deviations from ideality were observed. A lower than expected Tg has previously been attributed to the drug and polymer binding less strongly with each other than with themselves (Painter *et al.*, 1991). These results are consistent with immiscibility of the highly hydrophilic dextrans with the polymer at the concentrations shown.

6.5.2.3 FTIR spectroscopy

Due to the hydrophilic nature of the dextran backbone, hydrogen-bonding could be a major factor governing the molecular interactions. Interactions could potentially occur between the amide

groups of PNIPA-L and the hydroxyl groups of the dextrans. Hydrogen bonding interactions with dextran would be indicated by a characteristic downward shift in the vibrational frequency of the polymer functional group involved in hydrogen bonding (Shamblin *et al.*, 1998). The FTIR spectra (Appendix III) do not show evidence for interactions between the components through hydrogen bonding. No trend was observed in the fluctuation of the peak at 1647cm^{-1}, assigned to the carbonylamide and N-H stretching of PNIPA. There were also no observed trends in the other peaks of PNIPA-L due to the presence of any of the four dextrans.

6.5.2.4 Phase transition temperature

The effect of the hydrophilic dextrans on the phase transition temperature of PNIPA-L3 was examined by DSC measurements and % transmittance (Appendix IV, Fig. 10-11). Solutions of the dextrans and PNIPA in PB were observed to separate over time, indicating the immiscibility of the two polymers in solution. The DSC endotherms of PNIPA-L3 in the presence of various concentrations of D40 are shown in Appendix IV, Fig 10; along with the transmittance measurements from the same systems. The values obtained for peak onset, maximum and integral are shown in Fig. 6.23 along with the apparent LCST as measured by % transmittance.

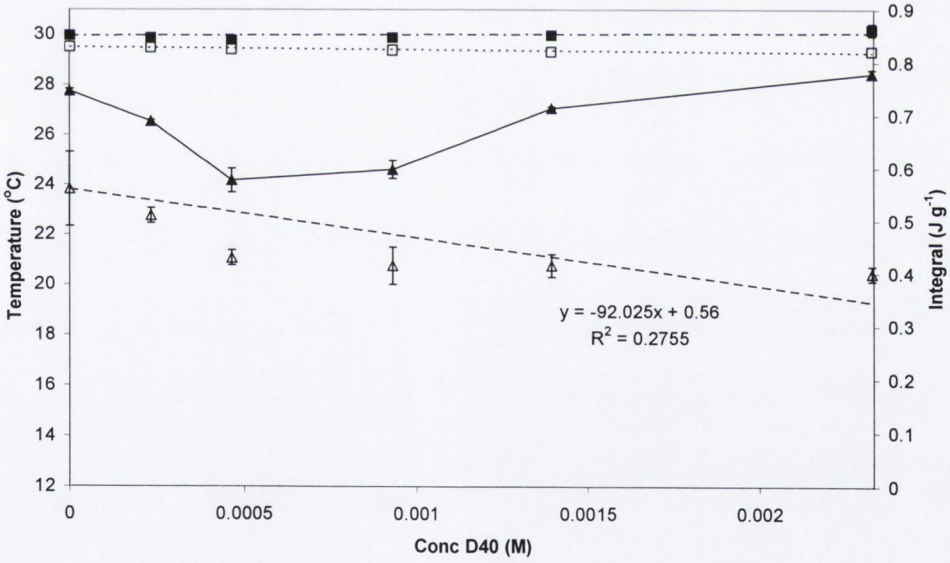

Fig. 6.23: Plot of endotherm peak (■), onset (□) and integral (Δ, secondary y axis) obtained by DSC of a 1.4% w/w solution of PNIPA-L3 containing various concentrations of D40. Also shown are the $LCST_t$ values from the % transmittance study (▲) (Appendix IV, Fig. 10), defined as 50% transmittance.

The position of the LCST, as measured by DSC, did not change as the concentration of D40 increased (Fig. 6.23). A similar effect was seen with the other dextrans (Fig. 11, Appendix IV). This was consistent with a lack of PNIPA-dextran interactions. A decrease in the integral was observed with increasing concentration of D40, corresponding to a decrease in the magnitude of the

phase transition. The magnitude of the decrease in the integral was independent of the dextran molecular weight on a weight basis (Fig. 6.24a). The influence of the dextrans on the magnitude of the LCST of PNIPA-L, as measured by the integral value, was therefore directly related to the number of glucose monomer units present. At dextran concentrations above 100 mg/ml, the phase transition was not detectable by DSC.

(a)

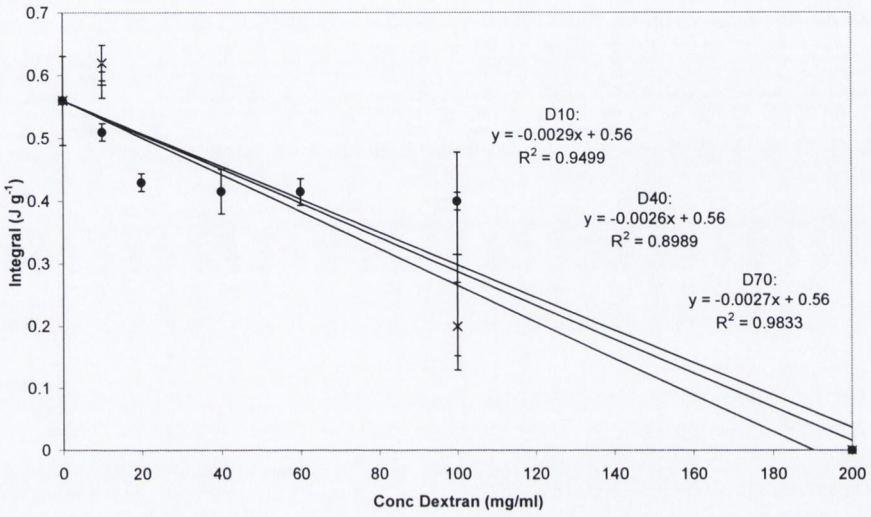

(b)

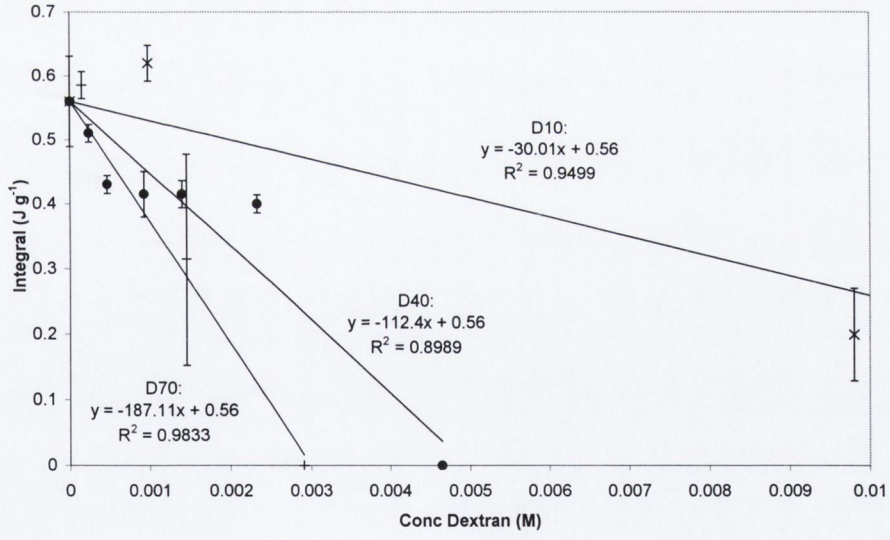

Fig 6.24: Influence of concentration of D10 (x), D40 (•) and D70 (+) on integral value of a 1.4%w/w solution of PNIPA-L3 (heating rate 2°C/min) (a) on weight basis, (b) on molar basis

On a molar basis, the magnitude of decrease in the integral increased with molecular weight (Fig. 6.24b). Table 6.4 calculates an integral constant (ki), defined as the molar concentration of the model drug per mole of NIPA required to decrease the integral to half its initial value. Also shown are the values for NaB and DH.

Table 6.4: Integral constants (ki) measuring the moles of model drug per mole NIPA required to decrease the integral to half its initial value. Also given are the k_{H1} values from Table 6.1 and the calculated k_{H1} values based on Fig. 6.24.

	Integral constant (k_i) (moles drug/mole NIPA)	**k_{H1} (Table 6.1) M (X 10^2)**	**Predicted value of k_{H1} based on dextran data**
NaB	28.78	35.280 ± 0.797	217.90
DH	3.56	77.188 ± 4.549	26.94
D10	0.075	0.561 ± 0.046	--
D40	0.020	0.135 ± 0.021	--
D70	0.012	0.091 ± 0.009	--

There was a direct linear relationship (R^2=0.999) between the k_i value and the k_{H1} value for the three dextrans examined (Fig. 6.25).

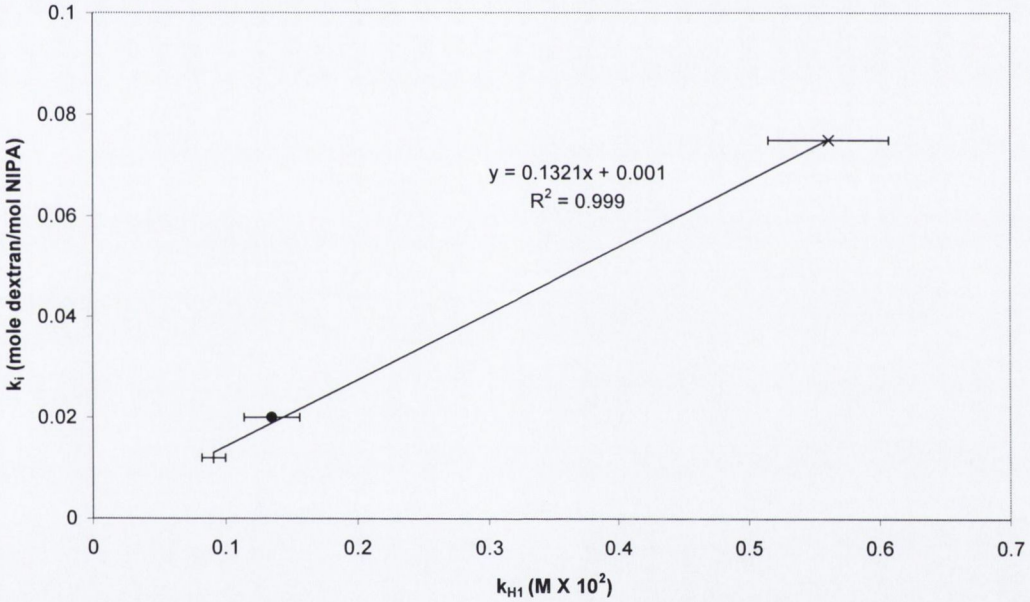

Fig. 6.25: Plot of integral constant (k_i) against k_{H1} value for D10 (x), D40 (•) and D70 (+).

Assuming binding does not occur, the integral value would be affected by the availability of hydrogen-bonding water molecules in solution. The presence of the highly hydrophilic dextrans diminished the hydrogen-bonding ability of PNIPA with water, decreasing the magnitude of the phase transition. High dextran concentrations sufficiently interfered with PNIPA-water hydrogen bonding to prevent any transition being detected. In the crosslinked system, hydrogen bonding is necessary for hydrogel swelling. The linear relationship shown in Fig. 6.25 therefore suggests that the dextrans compete with the polymer for hydrogen bonding with the available water molecules. Equilibrium swelling at 25°C was affected as a result with PNIPA-H1 unable to hydrogen bond, and therefore swell, in the presence of high concentrations of the dextrans (Fig. 6.20).

Based on the linear relationship, predictions for NaB and DH were also made (Table 6.4). Differences between the predicted and measured k_{HI} values for NaB and DH would be due to a combination of differences in hydrogen bonding ability with water and with the polymer and other interactions such as the salting out effect seen with NaB. The predicted value for NaB was of a different order of magnitude to the actual value, consistent with the presence of a secondary, salting out effect.

The phase transition as measured by transmittance showed an unusual pattern (Fig 6.23 and Appendix IV, Fig. 11). There was an apparent decrease in $LCST_t$ at low dextran concentrations followed by broadening of the transition over a wider temperature range, resulting in a subsequent increase in the transition temperature. This pattern may be explained by a separation of phases observed during the transmittance measurements due to the immiscibility of the dextran and the polymer. Separation occurred despite the presence of a magnetic flea stirrer in the solution during the heating process. At low dextran concentrations, the presence of the dextran may cause desolvation of the PNIPA and consequent precipitation. Such a decrease in the phase transition may be undetectable by DSC due to the presence of two distinct aqueous phases in the sample. The magnitude of the transition as measured by DSC was, however affected by the dextran due to competition with water molecules. At higher dextran concentrations, the transmittance measurements may only be examining the PNIPA-water phase where the transition, diminished by competition for the water molecules, occurs around the temperature of the control.

6.6 CONCLUSIONS

Potential interactions between the model drugs used and the linear polymer and the hydrogel were examined. The types of interactions found between the drugs and PNIPA can be divided into three types.

The first type was hydrophobic binding, evident between the unionised benzoates and PNIPA. The benzoate anion did not show a significant binding tendency. The binding was hydrophobic in nature and occurred between the carbon backbone/isopropyl side chain of PNIPA and the benzene ring/ester side chain of the benzoates. Binding increased with increasing hydrophobicity of the ester side chain. The consequence of the observed binding was to increase the hydrophobicity of the PNIPA, resulting in a decrease in the LCST of both the polymer and the hydrogel. Precipitation of the polymer, or shrinkage of the hydrogel, therefore occurred at a particular drug concentration when the extent of binding was sufficient to decrease the LCST to the temperature of the experiment.

The second type of interaction was a 'salting out' effect that occurred with PNIPA in the presence of NaB. Previous studies have shown (Eeckman *et al.*, 2001) that both the valence and size of the anion play an important role in the salting out process in respect of PNIPA polymers, with the effect of the cation not being significant. The benzoate anion appeared to cause this salting out effect as described in section 1.3.5. The salting out process on the LCST of the polymer was relatively weak compared to the effect of direct hydrophobic binding on the LCST due to the unionised benzoate.

While aqueous salt solutions are thought to alter the water structure in the polymer hydration sheath causing the salting out effect (section 1.3.5.1), a third type of 'indirect' interaction also occurred in the drug-hydrogel system. Relatively high concentrations of the highly water-soluble model drugs (NaB, DHCl and the dextrans) prevented swelling of the hydrogel, probably by competition with the hydrogel for the available water molecules. The magnitude of the phase transition as detected by DSC was also weakened as a result of the decrease in available water molecules.

The significance of these drug-polymer interactions will be discussed in the following chapters.

CHAPTER 7

An Evaluation of the Role of Temperature and Drug Properties in Controlled Release from PNIPA-H1

7.1 INTRODUCTION

The study in Chapter 5 revealed that drug physicochemical properties, in particular drug solubility, size and chemical nature, influenced the swelling/deswelling kinetics of, and pulsatile release from, PNIPA-H1. The present chapter examines these properties in more detail by study of the release of the same model drug series from PNIPA-H1 at either 25°C or 37°C over 48 hours. The effect of temperature on the rate of dissolution of pure drug discs was compared to the rate of media diffusion into, and drug diffusion out of, the drug-loaded hydrogels at these two temperatures. The swelling and release profiles are also examined in relation to hydrogel pore size (Chapter 4), drug-polymer interactions (Chapter 6) and drug loading.

7.2 EFFECT OF TEMPERATURE ON DRUG DISSOLUTION

Solubility of the model drugs examined, with the exception of NaB, increased by a factor of ~1.6 with a temperature increase of 12°C (from 25°C to 37°C) as shown in Fig. 4.7. The influence of temperature on the rate of dissolution of the pure drug substances was investigated. Pure drug discs (100mg) were prepared as described in section 3.4.4 and dissolution studies (n = 3) were carried out in 900ml PB at 25°C and at 37°C. The dissolution profiles obtained are shown in Appendix VII and were fitted to the Hixson-Crowell cube root law (Equation 2.4b) to give the dissolution rate constants (k_c) shown in Table 7.1. An estimate of the ratio between the dissolution rate constant at 37°C (k_{c37}) and the constant at 25°C (k_{c25}) is also given in Table 7.1.

Table 7.1: Cube root dissolution rate constants (k_c, Equation 2.4b) at 25°C (k_{c25}) and 37°C (k_{c37}) and associated coefficients of determination (CD).

	25°C			37°C			k_{c37}: k_{c25}
	Solubility in PB (mg/ml)	k_{c25} (min^{-1})($X10^3$)	CD	Solubility in PB (mg/ml)	k_{c37} (min^{-1})($X10^3$)	CD	
NaB	380.35 ± 46.9	59.350 ± 0.870	0.9967	399.55 ± 16.6	57.133 ± 9.122	0.9925	1.0:1
BA	7.87 ± 0.09	0.978 ± 0.123	0.9826	9.59 ± 0.48	1.946 ± 0.559	0.9954	2.0:1
MHB	1.93 ± 0.15	0.403 ± 0.099	0.9984	4.19 ± 0.09	0.762 ± 0.116	0.9868	1.9:1
PHB	0.37 ± 0.02	0.043 ± 0.005	0.9949	0.72 ± 0.02	0.103 ± 0.035	0.9968	2.4:1
DHCl	309.60 ± 7.85	39.361 ± 9.852	0.9961	549.34 ± 38.72	55.962 ± 6.237	0.9988	1.4:1
DB	1.99 ± 0.03	0.083 ± 0.003	0.9743	3.43 ± 0.13	0.115 ± 0.007	0.9943	1.4:1
VB12	12.33 ± 0.12	1.615 ± 0.349	0.9958	21.37 ± 0.50	2.186 ± 0.202	0.9991	1.4:1
D4	Very soluble*	50.222 ± 19.038	0.9971	Very soluble*	41.781 ± 8.917	0.9942	0.8:1
D10	Very soluble*	14.772 ± 1.373	0.9931	Very soluble*	24.359 ± 2.495	0.9975	1.6:1
D40	Very soluble*	7.447 ± 0.320	0.9910	Very soluble*	11.287 ± 1.275	0.9937	1.5:1
D70	Very soluble*	6.915 ± 0.092	0.9925	Very soluble*	8.8339 ± 1.135	0.9922	1.3:1

*Martindale 1996

The rate of dissolution (k_c) at a given temperature was dependent on drug solubility and molecular size.

7.2.1. Hydrophobic drugs

As the solubility of the benzoate ester series increased, the dissolution rate constants at both temperatures increased in proportion as shown in Fig. 7.1a (25°C) and Fig. 7.1b (37°C).

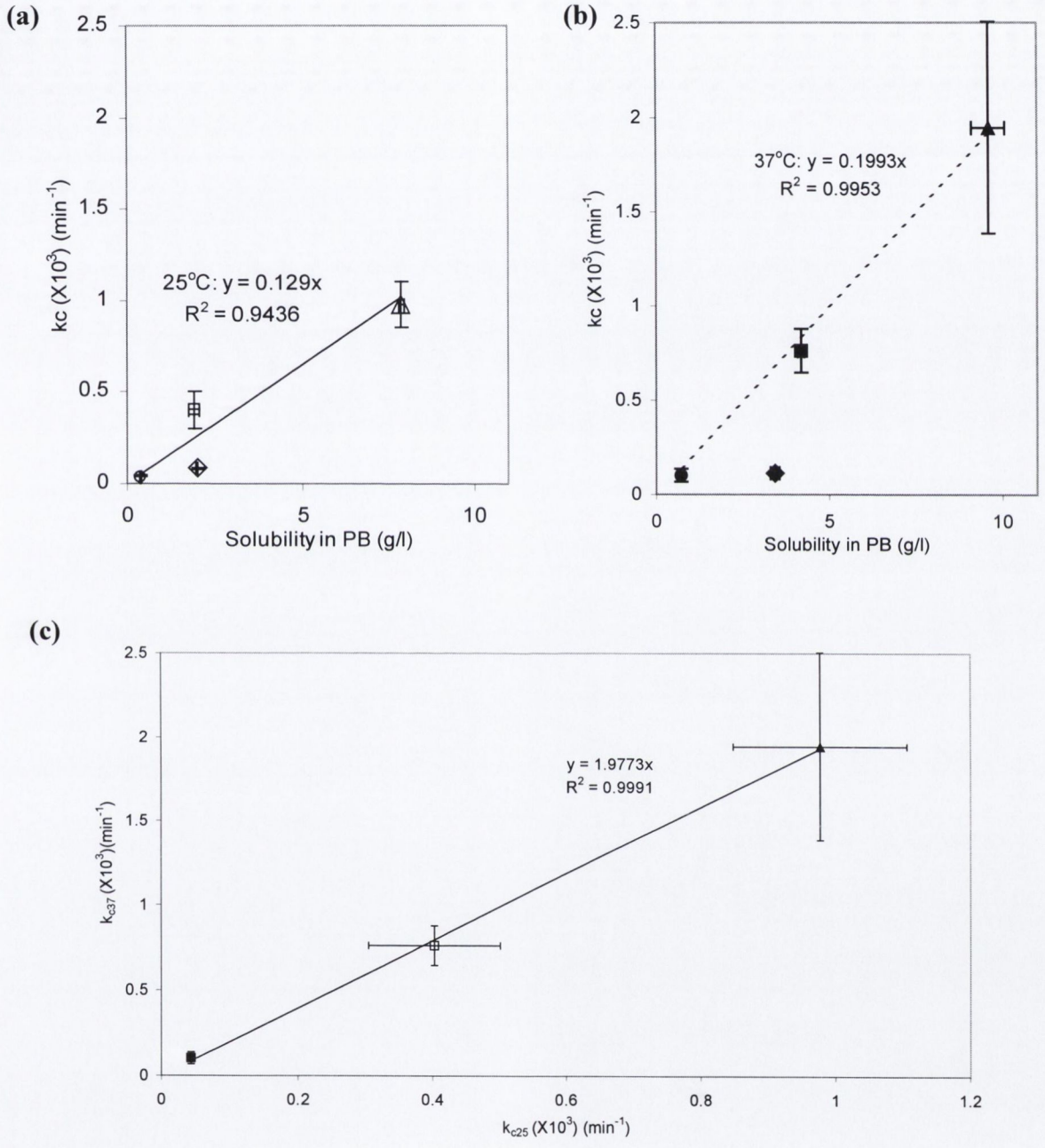

Fig. 7.1: Plot of benzoate dissolution rate constants (k_{c25} and k_{c37}) against corresponding drug solubility in PB at (a) 25°C (open symbols) and (b) 37°C (closed symbols). Linear fits represent benzoate series at 25°C (solid line) and 37°C (dashed line). [BA(▲/Δ), MHB (□/■), PHB (●/○)]. Also shown are corresponding values for DB (♦/◊).

(c) Plot of dissolution rate constant at 37°C (k_{c37}) against dissolution rate constant at 25°C (k_{c25}) for the benzoate ester series [BA(▲), MHB (□), PHB (■)].

The difference in dissolution rates obtained within the benzoate series could not be adequately accounted for by differences in molecular weight using the Stokes-Einstein equation (Martin, 1993; Chp. 15). Different inter- and intra- molecular interactions in any given benzoate would affect the diffusion coefficients of these small molecules. The values for DB are also shown in Fig. 7.1a/b for comparison. DB had a lower dissolution rate than predicted from the benzoate series, attributable to its larger molecular weight.

A linear relationship was apparent between the benzoate constants k_{c37} and k_{c25} (Fig. 7.1c). An approximate 2-fold increase in dissolution rate of pure drug was obtained with the benzoate ester series on increasing the temperature from 25°C to 37°C.

7.2.2 Hydrophilic drugs

The dissolution rate of the hydrophilic drugs was more rapid than for the hydrophobic series as expected due to their higher aqueous solubility (Table 7.1). Within the dextran series, there was a significant decrease ($p < 0.05$) in dissolution rate with increasing molecular weight of the dextrans at both temperatures (Fig. 7.2). The decrease in dissolution rate/diffusion with increasing size in the series D10 to D70 was accounted for by molecular weight difference using the Stokes-Einstein equation (Martin, 1993; Chp. 15).

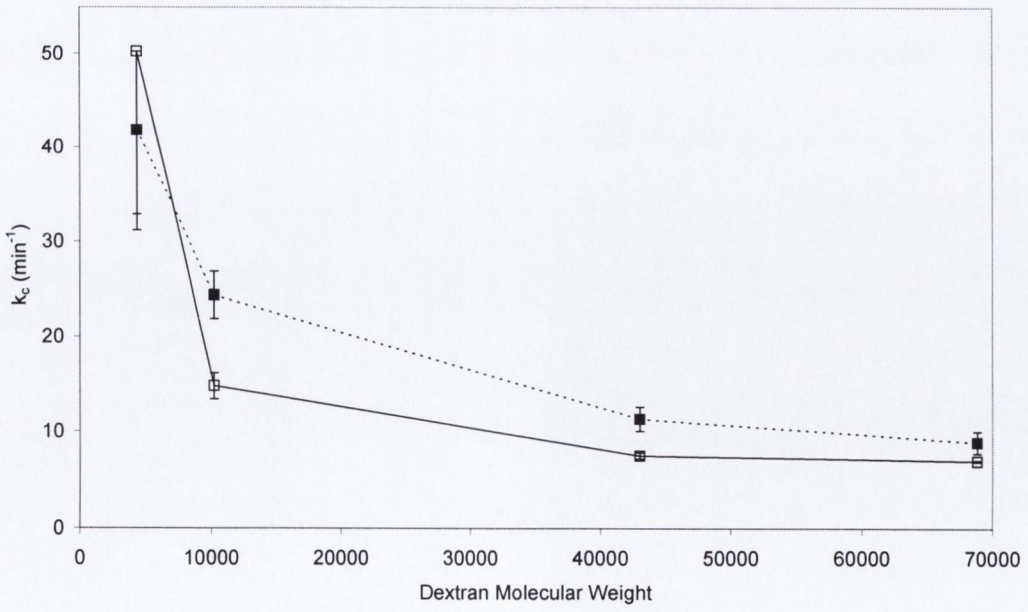

Fig. 7.2: Plot of dissolution rate constants (k_c) against dextran molecular weight at 37°C (dashed line) and at 25°C (solid line).

There was no significant change detectable ($p > 0.05$) in the rate of dissolution of NaB and D4 on temperature increase from 25°C to 37°C. While the benzoates showed a two-fold increase in

dissolution rate on increasing the temperature, the rate constants of the other model drugs increased by approximately 1.4 times (Table 7.1).

7.3 INFLUENCE OF DRUG PHYSICOCHEMICAL PROPERTIES ON HYDROGEL SWELLING RATE

The influence of the loaded drug on the swelling rate of PNIPA-H1 at 25°C and 37°C was examined. The swelling profiles of PNIPA-H1 in the presence of the various drug substances are shown in Fig. 7.3 at 25°C (Fig. 7.3a) and 37°C (Fig. 7.3b). The swelling profiles are presented based on the fraction swelling, where equilibrium swelling is at 25°C (Equation 3.1b). In Chapter 6, the influence of the various model drugs on equilibrium PNIPA-H1 swelling at 25°C was examined. The drug loadings (up to 28.6%w/w, 20mg drug) and the volume of media (900ml) used in the present swelling/release experiments did not significantly affect the equilibrium swelling of PNIPA-H1 at 25°C. The effect of the drugs on the swelling rate at both temperatures and the equilibrium residual volume at 37°C is examined in the current section.

The swelling profiles were plotted against the square root of time to examine the influence of the drugs on the swelling rate. The swelling rate constants obtained are given in Table 7.2 along with apparent diffusion coefficients of water uptake calculated using Equation 2.5a. Drug physicochemical properties played a significant role in the hydrogel swelling rate at both temperatures. The drugs were divided into hydrophobic and hydrophilic groups as described in section 4.3.1 to examine their influence on swelling.

Table 7.2: Swelling rate constants (k_s) at both 25°C and 37°C based on fraction swelling (equilibrium at 25°C) and associated coefficients of determination (CD). Also shown are apparent diffusion coefficients of water estimated using the amount of media absorbed per unit surface area (Equation 2.5a).

	k_s25 $(min^{-0.5})(X10^3)$	CD	D_{app} $(cm^2/s)(X10^{-6})$	k_s37 $(min^{-0.5})(X10^3)$	CD	D_{app} $(cm^2/s)(X10^{-6})$
Unloaded	2.047 ± 0.268	0.9762	1.437 ± 0.309	0.456 ± 0.009	0.9036	0.067 ± 0.002
BA	1.029 ± 0.059	0.9721	0.299 ± 0.030	0.194 ± 0.048	0.6060	0.011 ± 0.005
MHB	0.420 ± 0.014	0.9688	0.061 ± 0.018	0.185 ± 0.012	0.8303	0.009 ± 0.001
PHB	0.244 ± 0.023	0.7043	0.021 ± 0.004	0.188 ± 0.005	0.3634	0.010 ± 0.001
DB	1.453 ± 0.129	0.9746	0.720 ± 0.058	0.287 ± 0.042	0.7755	0.024 ± 0.008
NaB	3.341 ± 0.108	0.9903	3.754 ± 0.301	1.369 ± 0.118	0.9254	0.500 ± 0.074
DHCl	2.337 ± 0.100	0.9932	1.965 ± 0.097	1.349 ± 0.086	0.9921	0.516 ± 0.072
VB12	2.523 ± 0.221	0.9969	2.411 ± 0.207	0.697 ± 0.242	0.7826	0.153 ± 0.101
D4	2.325 ± 0.484	0.9927	1.941 ± 0.238	0.624 ± 0.084	0.9571	0.122 ± 0.030
D10	2.608 ± 0.067	0.9891	2.057 ± 0.112	0.503 ± 0.109	0.6557	0.081 ± 0.033
D40	2.430 ± 0.386	0.9861	2.227 ± 0.435	0.502 ± 0.223	0.8505	0.088 ± 0.077
D70	2.620 ± 0.098	0.9915	2.185 ± 0.367	0.407 ± 0.071	0.9136	0.052 ± 0.017

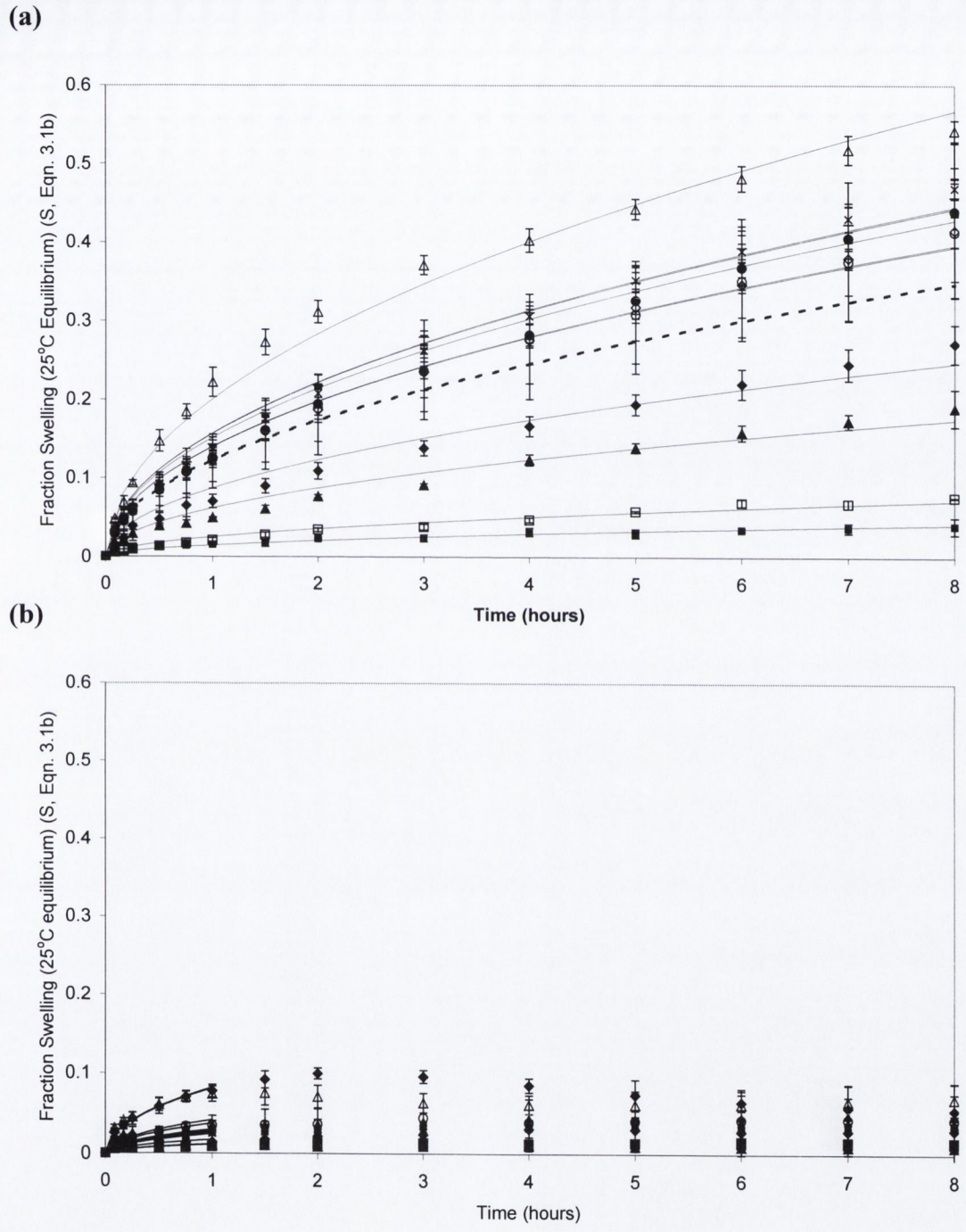

Fig. 7.3: Swelling of PNIPA-H1 over time at (a) 25°C and (b) 37°C loaded with model drugs [NaB (Δ), BA(▲), MHB (□) , PHB (■), DH (◊), DB (♦), VB (-), D4 (○), D10 (x), D40 (●) D70 (+)]. Also shown is data fitted to Equation 2.12 (*Higuchi*).

7.3.1 Hydrophobic Drugs

The influence of the hydrophobic drugs on PNIPA-H1 swelling rate at 25°C was similar to the previous swelling/deswelling study in Chapter 5 (section 5.2). For the benzoate ester series, the effect of the drug decreased the rate of swelling of the hydrogel. The swelling rate was dependent on the solubility of the loaded drug in this series as shown in Fig. 7.4a. DB also slowed the rate of swelling with deviation from the trend in Fig. 7.4a. A similar deviation from the trend was seen with DB when the swelling rate constant at 25°C (k_{s25}) was plotted against the dissolution rate constant at 25°C (k_{c25}) (Fig. 7.4b). The effect of the drug on the apparent diffusion coefficient of water into the hydrogel at 25°C showed a similar, drug solubility dependent, pattern.

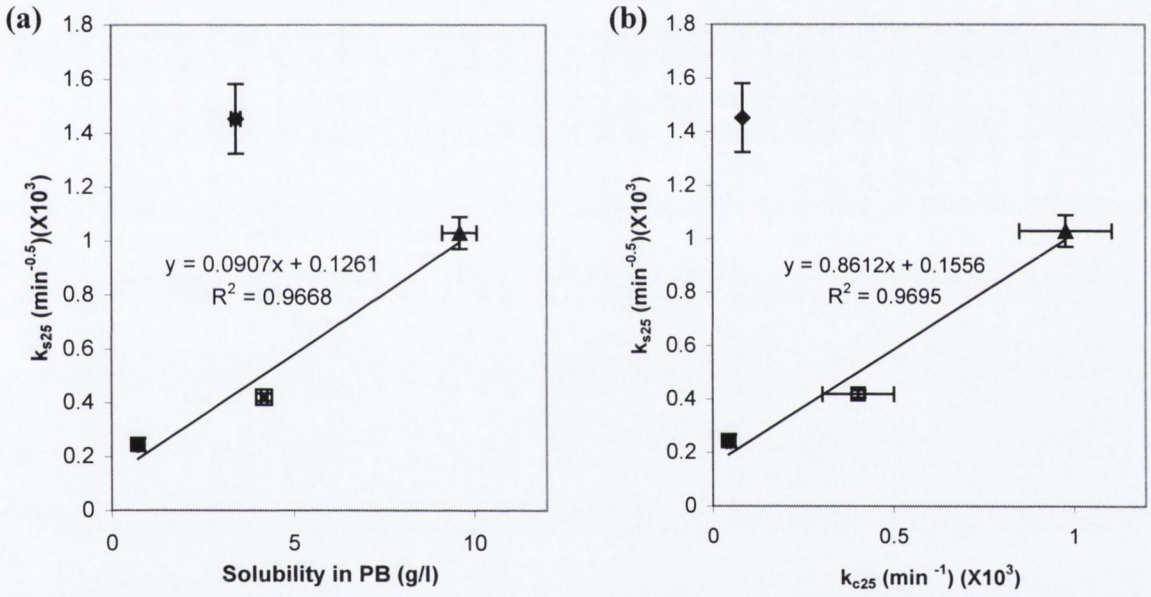

Fig. 7.4: Relationship in the benzoate series between swelling rate constant (k_{s25}) and

(a) drug solubility in PB

(b) cube root dissolution rate constant (k_{c25})

Also shown are corresponding values for DB [BA(▲), MHB (□) , PHB (■),DB (♦)].

The study of Yoshida *et al.* (1991a) also showed that the presence of a hydrophobic drug, indomethacin, suppressed the swelling rate of hydrophilic polymeric matrices. The decrease in the swelling rate was attributed to the solute effect of the hydrophobic drug. A decrease in the swelling rate was similarly seen in the present study with DB. No significant diltiazem-PNIPA interactions were described in section 6.3. The decrease in swelling rate can be attributed to a separation of the diffusion front and swelling front during the swelling process (section 2.3.2), therefore slowing the rate of swelling. The pulsatile swelling study in Chapter 5 showed that the swelling rate was unaffected during the second swelling cycle by DB (section 5.2), confirming that the decrease in

swelling rate was solely due to the presence of a diffusion front and the dissolved drug had no significant effect on swelling.

As described in the previous section, pure DB had a lower dissolution rate than predicted from the benzoate series (Fig. 7.1a/b), attributable to its larger molecular weight. Fig 7.4a/b, however, showed the benzoate loaded hydrogels had a lower rate of swelling than the DB loaded hydrogel. If hydrophobic drug solubility and/or the rate of drug dissolution/diffusion linked to drug size were the factors controlling the rate of swelling of the loaded hydrogel, then DB should have slowed the swelling to an extent lower than that predicted from the benzoate series. The effect of the benzoate series was, therefore, lower than would be expected due to the effect of binding of the benzoates to the polymer as described in section 6.2, therefore slowing the swelling rate further than expected. The benzoates also lowered the swelling rate during the second swelling cycle as described in section 5.2 consistent with the binding effect of the dissolved drug.

At 37°C, the rate of swelling of the hydrogel was significantly decreased ($p < 0.05$) in the presence of the hydrophobic drugs, although no difference ($p > 0.05$) between the individual benzoates was shown (Table 7.2). There was a dramatic decrease in the apparent diffusion coefficient of water at 37°C, despite the increase in temperature.

The drug loadings used and the volume of swelling media (900ml) meant that the drugs examined did not affect the equilibrium swelling levels at 25°C. The level of swelling at 37°C, defined in Chapter 4 as the residual volume, however, appeared to be influenced by the loaded drug in the time period studied. Fig 7.5 shows the residual volume levels after 8 hours at 37°C (grey bars) and after 48 hours at 37°C (white bars), for comparison with the unloaded system, which has reached an equilibrium residual volume within 3 hours (section 4.4.3).

The residual volume was lower after 8 hours in the presence of the hydrophobic drugs. After 48 hours, the hydrogels loaded with DB had recovered to their equilibrium level, with no statistical difference from the unloaded hydrogel ($p>0.05$). The benzoates, however, prevented such an equilibrium being reached at this temperature in the time period studied due to polymer binding.

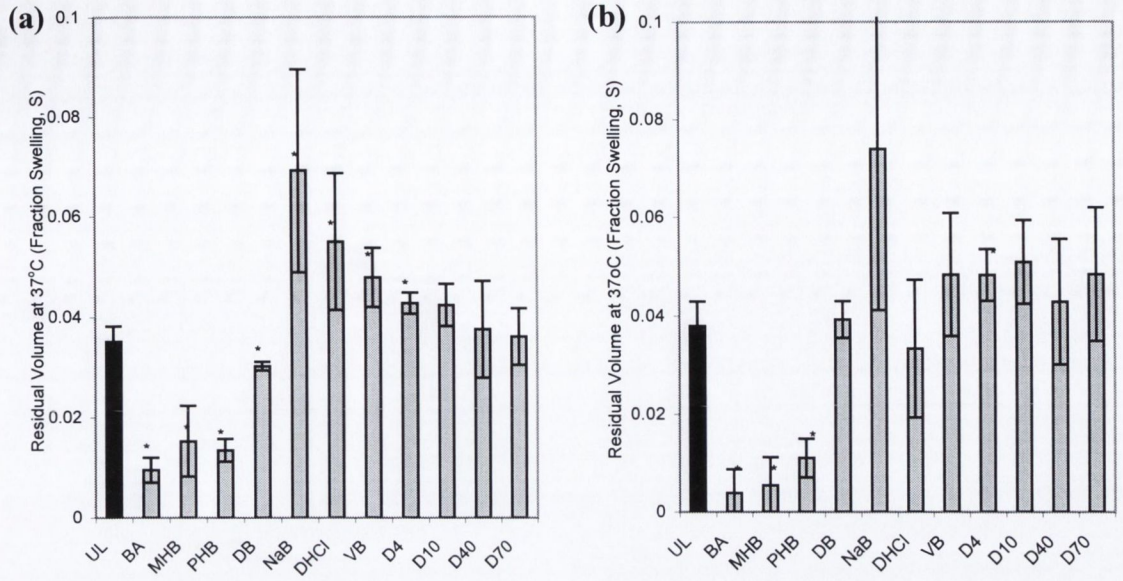

Fig. 7.5: Influence of model drugs on residual volume at 37°C after (a) T=8 hours and (b) T=48 hours. UL = unloaded PNIPA-H1 hydrogel (black bar). Asterisk indicates statistically significant difference ($p<0.05$) from corresponding unloaded hydrogel (UL).

7.3.2 Hydrophilic drugs

Loading of the hydrogel with the hydrophilic drugs resulted in an increase in the rate of swelling of the hydrogel at 25°C (Table 7.2), contrasting with the decrease observed with the hydrophobic drugs. The effect was particularly pronounced with NaB and DHCl, which would exert the greatest osmotic effect of the series as was described in chapter 5. The apparent diffusion coefficients of water (D_{app}) into the hydrogel also increased (Table 7.2).

At 37°C, a similar pattern was seen where the presence of NaB and DH caused an increased rate of swelling (Table 7.2), with no significant change in the swelling rate with the other hydrophilic drugs. The presence of the hydrophilic drugs within the hydrogel also affected the residual volume at 37°C as shown in Fig. 7.5. After 8 hours, a pattern can be seen where the smaller the hydrophilic drug, the higher the osmotic pressure exerted by the drug and as a result the greater the residual volume at that time point. By the 48-hour timepoint, the residual volume at 37°C for each loaded hydrogel was not statistically significant ($p > 0.05$) from the unloaded system. The osmotic effect therefore resulted in a transient, increased level of swelling at 37°C for the smaller, hydrophilic drugs. Similar transient swelling effects were shown by Lee (1985) during swelling of pHEMA beads loaded with the water-soluble drug thiamine HCl.

7.4 MODEL DRUG RELEASE

Release of the various model drugs from PNIPA-H1 was examined at both 25°C and 37°C in 900ml PB over 48 hours.

7.4.1 Hydrophobic Drugs

The fraction released over time of the benzoates from PNIPA-H1 at 25°C and at 37°C is shown in Fig. 7.6a and Fig. 7.6b respectively. The fraction released at both temperatures was plotted against the square root of time (Equation 2.12, *Higuchi*) to give the release rate constants k_{d25} and k_{d37} (Table 7.3).

Table 7.3: Release rate constants at 25°C and 37°C calculated using Equation 2.12 (*Higuchi*) along with associated coefficients of determination (CD). Also shown are diffusional exponents (*n*) calculated using Equation 2.11 (*Peppas*). *Values of NaB also calculated when diffusional exponent set as unity ($min^{-1} X10^3$)

25°C	**k_{d25} ($min^{-0.5}$)($X10^3$)**	**CD**	**k_{d37}:k_{d25}**	***n***
BA	3.461 ± 0.034	0.9978	0.41:1	0.523 ± 0.009
MHB	1.399 ± 0.093	0.9872	0.61:1	0.577 ± 0.002
PHB	0.607 ± 0.041	0.9852	0.74:1	0.586 ± 0.009
DB	2.742 ± 0.069	0.9942	0.18:1	0.551 ± 0.002
NaB	8.188 ± 2.187	0.8602	0.31:1	0.970 ± 0.086
	11.692 ± 3.009*	0.9950*	0.15:1*	1.0*
DH	4.485 ± 0.477	0.9930	0.57:1	0.557 ± 0.029
VB12	4.047 ± 0.567	0.9614	--	0.521 ± 0.014
D4	3.762 ± 0.318	0.9321	--	0.763 ± 0.048
D10	4.065 ± 0.366	0.9768	--	0.625 ± 0.026
D40	5.366 ± 1.273	0.5371	--	0.227 ± 0.061
D70	4.369 ± 0.587	0.9433	--	0.363 ± 0.023
37°C	**k_{d37} ($min^{-0.5}$)($X10^3$)**	**CD**		***n***
BA	1.424 ± 0.203	0.9938		0.442 ± 0.004
MHB	0.850 ± 0.138	0.9957		0.495 ± 0.017
PHB	0.452 ± 0.032	0.9946		0.533 ± 0.013
DB	0.486 ± 0.080	0.9702		0.401 ± 0.016
NaB	2.578 ± 0.951	0.7615		1.234 ± 0.179
	1.774 ± 0.691*	0.9545*		1.0*
DH	2.553 ± 0.305	0.9699		0.623 ± 0.127
VB12	0	--		--
D4	0	--		--
D10	0	--		--
D40	0	--		--
D70	0	--		--

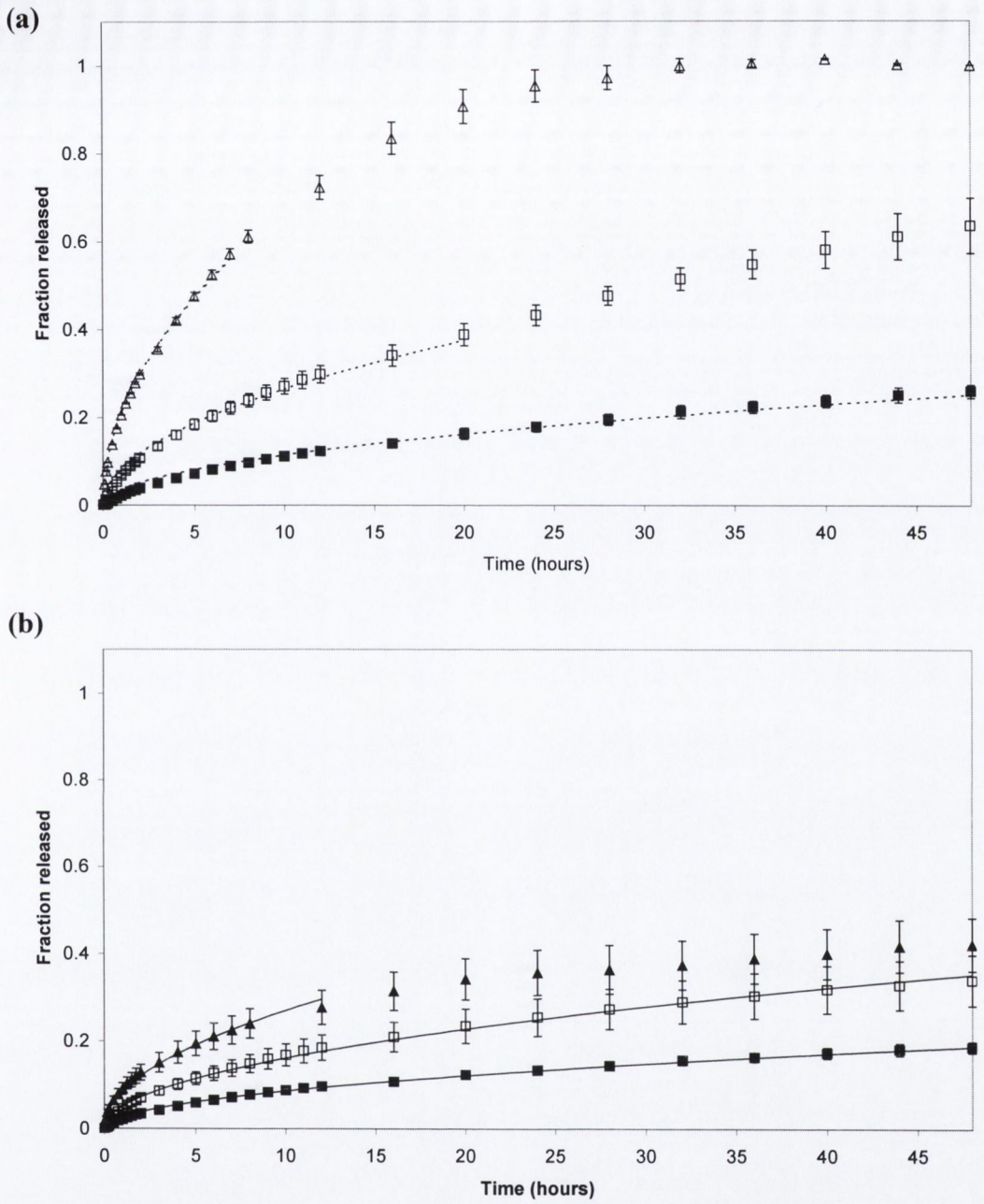

Fig. 7.6: Plot of fraction drug released over time in PB, fitted to the square root of time (Equation 2.12, *Higuchi*) at (a) 25°C (dashed lines) and at (b) 37°C (solid lines) [BA(▲), MHB (□) , PHB (■)]

Sustained release of the drugs was achieved at both temperatures with the lack of swelling at 37°C significantly slowing the diffusion of the model drugs, despite the increase in temperature. The release rate constants (k_d) of the benzoates were proportional to the square root of drug solubility (Fig. 7.7a) and to the dissolution rate constants (k_c) (Fig. 7.7b) at both temperatures. Also shown in Fig. 7.7 are the corresponding values for DB.

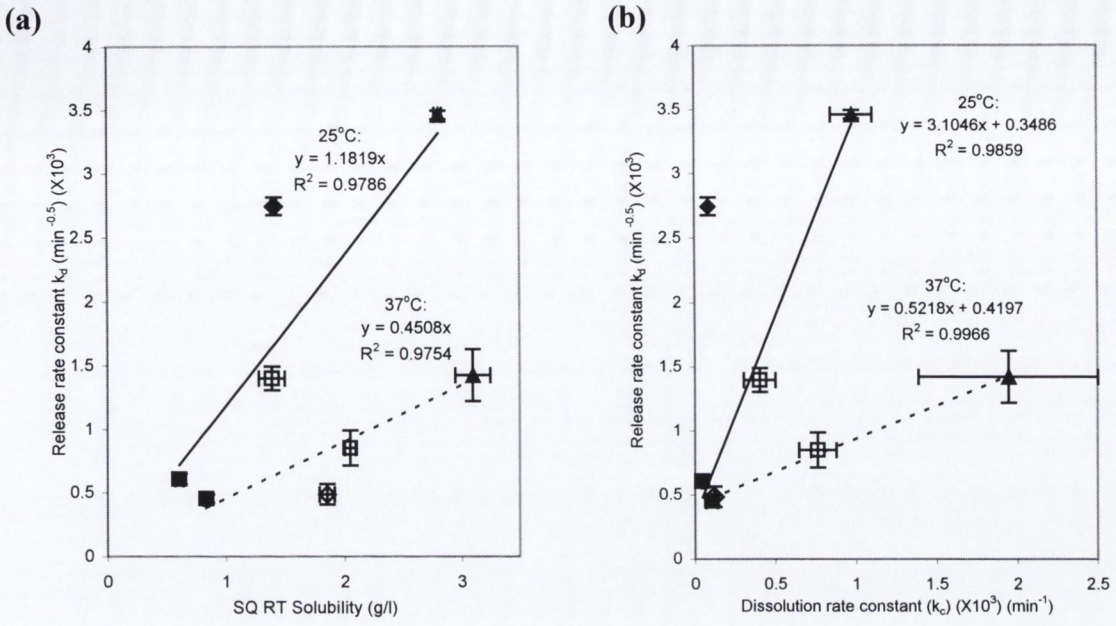

Fig. 7.7: Linear relationships for the benzoates between the release rate constants (k_{d25}/k_{d37}) and

(a) square root of solubility

(b) dissolution rate constants (k_{c25}/k_{c37})

at 25°C (solid line) and 37°C (dashed line)

[BA(▲), MHB (□) , PHB (■)].

Also shown are DB values at 25°C (♦) and 37°C (◊) for comparison.

The ratios between k_{d37} and k_{d25} are also shown in Table 7.3 and increased towards unity as the solubility of the benzoate series decreased. The ability to thermally control the release of drug therefore decreased as solubility of the series decreased. The estimated time taken for 50% release at each temperature was calculated using the release rate constants obtained and compared to the time taken for 50% dissolution of the pure drug discs. An effective 4-fold (PHB) to 12-fold (BA) reversal in thermal control of drug diffusion characteristics was achieved, where the higher release rate was at 25°C. The extent of this control was solubility dependent, with least control of the release rate of PHB. The lack of thermal control of PHB, the largest benzoate of the series, was consistent with the pulsed release data in Chapter 5. Significant binding between PHB and PNIPA prevented swelling of the hydrogel at 25°C, therefore resulting in a system similar to that at 37°C. Only a relatively small difference in release rates resulted in the current study with no control of the pulsatile release in Chapter 5.

The fraction released over time of DB and DHCl at 25°C and 37°C are shown in Fig. 7.8.

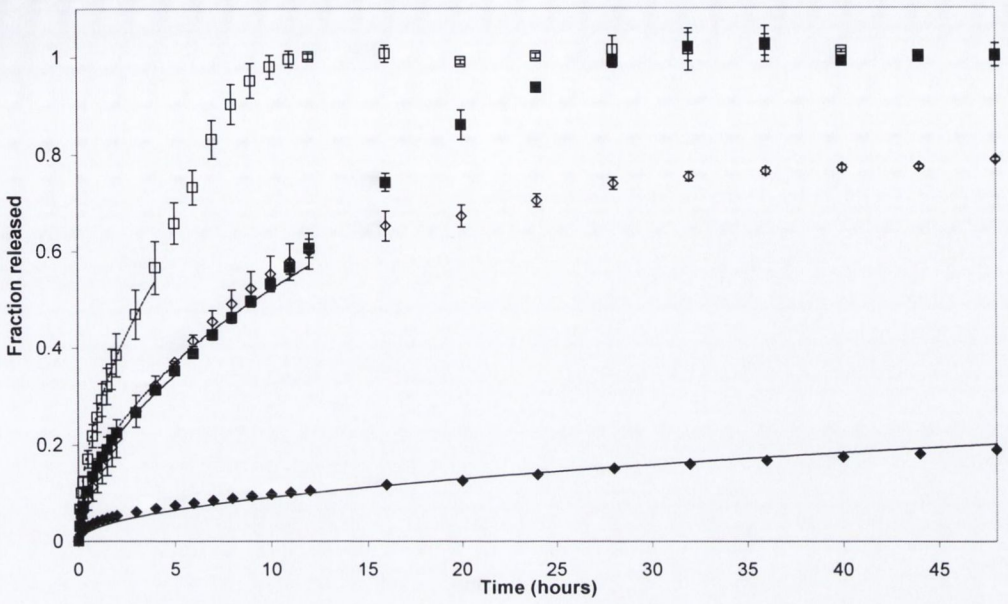

Fig. 7.8: Plot of fraction drug released over time in PB, fitted to the square root of time (Equation 2.1) at 25°C (□/■, dashed lines) and at 37°C (◊/♦, solid lines) [DH (open symbols), DB (closed symbols)].

Due to its solubility and size, DB would be expected to have a slower release rate from this hydrogel than MHB, and possibly even PHB. Fig. 7.7b plots the release rate constants (k_{d25},k_{d37}) against the corresponding dissolution rate constants (k_{c25},k_{c37}), with linear relationships for the benzoate series at both temperatures. As can be seen from Fig. 7.7(a/b), DB had a much larger k_{d25} value than expected from the benzoate series at 25°C. Such an effect can again be attributed to the drug-polymer binding apparent with the benzoates (section 6.2) but absent in the case of DB (section 6.3). The benzoates were shown in Fig 7.3 to influence the rate of swelling of the hydrogel to a much greater extent than DB, with this effect also slowing the rate of release of the benzoates from the gel. The release rate of the benzoates was therefore slower than expected due to the physical binding process but also through the secondary effect of decreasing effective pore size available for diffusion from the hydrogel, reflected in the slower rate of hydrogel swelling.

At 37°C, the influence of the drug on the swelling rate was not as significant as at 25°C due to the low swelling rate and residual level of swelling reached by the hydrogel at this temperature. The rate of release of DB at 37°C did not deviate to the same extent from the benzoate series as occurred at 25°C (Fig. 7.7b). The smaller pore size (~10Å) would have had a much greater influence on the release rate of DB (8.19Å) at this temperature than it would on the smaller benzoates (~4 to 6Å). The linear relationship for the benzoates at 37°C in Fig. 7.7b may be lower due to polymer binding directly influencing the rate of release and indirectly through lowering the

rate and extent of swelling. Based on the time taken for 50% release of DB compared to drug dissolution, an effective 44-fold reversal in thermal control of drug diffusion characteristics was achieved, where the higher release rate was at 25°C. Greater thermal control of drug release was achieved compared to the benzoate series, mainly due to molecular size differences.

Over longer time periods, the release rate of BA at 37°C started to level off with only about 40% of the loading released, perhaps due to the impact of drug-polymer binding in the collapsed state effectively limiting the release of the benzoate. Assuming binding of the remaining 60% of the BA loading, a binding value of 0.22moles BA per mole of NIPA was obtained, which can be compared to the k_{H2} value of 0.41 moles unionised BA/mole NIPA (Chapter 6, Table 6.1).

The drug release from the hydrogels at 25°C and 37°C was also examined using the power law equation (Equation 2.11, *Peppas*), where the diffusional exponent, n, was estimated. This equation, requiring two parameters, gave a better fit to the data compared with Equation 2.12 (*Higuchi*) (Table 7.3) and reflects the contribution of swelling to the overall release mechanism.

Similar to the data in Chapter 5, there was a decrease in the exponent at 25°C towards Fickian diffusion as the solubility of the series increased (Fig. 7.9). At 37°C, a decrease in the diffusional exponent also occurred with increasing solubility. The diffusional exponents at 25°C were higher than at 37°C due to a greater contribution from the swelling process to the release profiles.

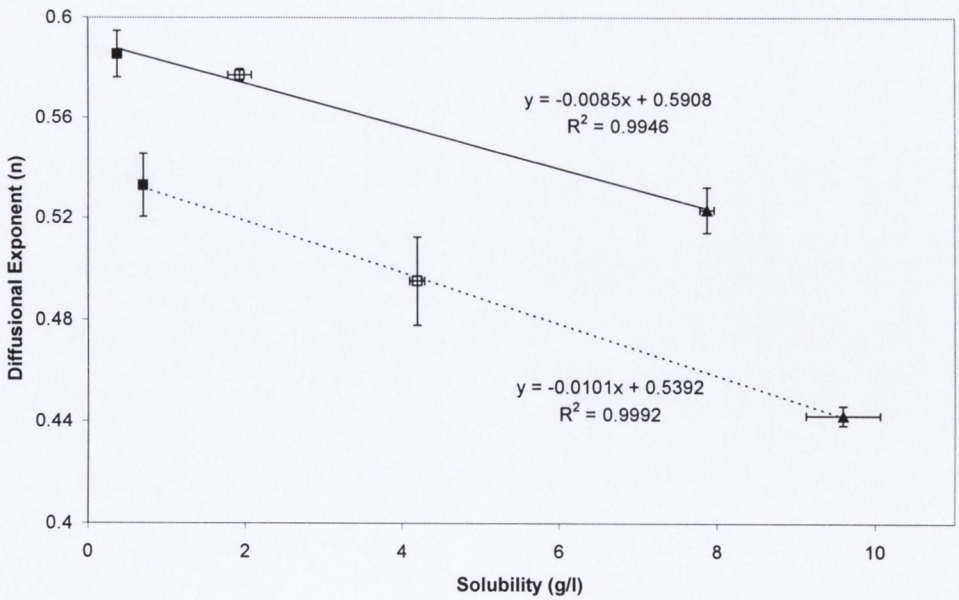

Fig. 7.9: Plot of diffusional exponent (*n*, Equation 2.11 *Peppas*) at 25°C (solid line) or 37°C (dashed line) against drug solubility [BA(▲), MHB (□) , PHB (■)].

Since little or no hydrogel swelling was apparent in the benzoate loaded hydrogels at 37°C, the pattern of an increase in the diffusional exponent with increasing hydrophobicity can be attributed to the benzoate-polymer binding, which also increases with increasing hydrophobicity. The most soluble benzoate of the series, BA, with less binding tendency, showed release profiles approaching Fickian diffusion.

7.4.2 Hydrophilic Drugs

The fraction released over time of NaB at 25°C and 37°C is shown in Fig. 7.10. The release profiles of NaB at both temperatures gave relatively poor fits when plotted against the square root of time (Table 7.3). When the diffusional exponent, n (Equation 2.11, *Peppas*), was allowed to vary, better fits resulted (Table 7.3), where the release profile was approximately zero-order in the early time-period ($F < 0.6$). Release at 25°C was rapid compared to the less soluble acid and complete within 5 hours. Release at 37°C was more sustained than at 25°C and reached a maximum of about 90% of drug released over 48 hours due to entrapment/binding of the drug within the collapsed meshwork. Some drug-polymer binding of the ionised species in the solid state may also have been possible as indicated by the FTIR data in Chapter 6, although binding appears to be dominant in the unionised state. The remainder of the loading was only released on lowering the temperature.

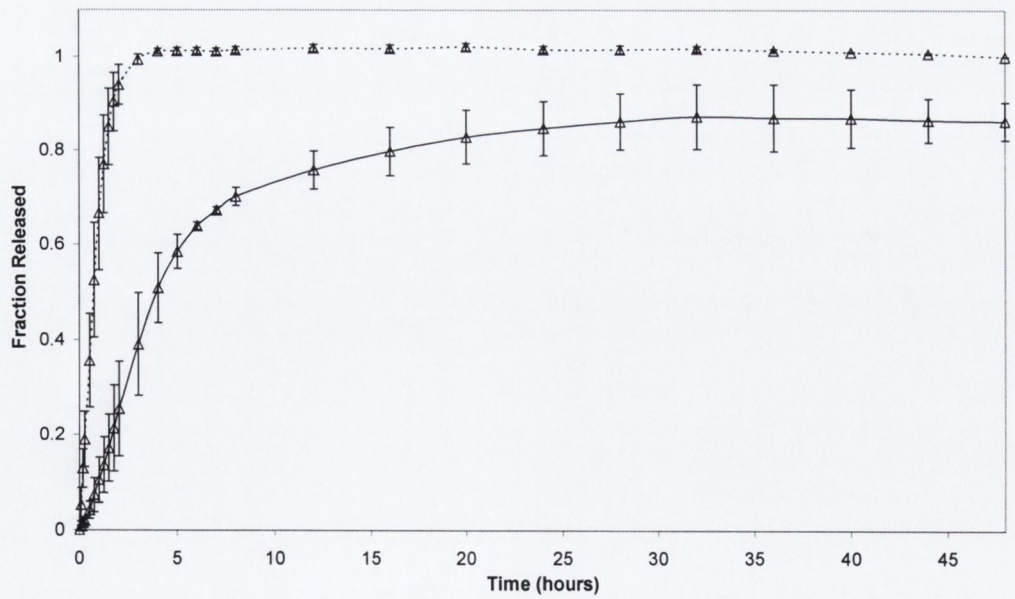

Fig. 7.10: Plot of fraction sodium benzoate released over time in PB at 25°C (dashed line) and 37°C (solid line)

The ratio between the release rate constants k_{d37}:k_{d25} was 0.15:1. While the effect of temperature on the dissolution rates of the pure NaB discs could not be shown due to the rapid dissolution of the highly soluble salt, sustained release of the salt was shown at both temperatures with an

approximate 6-fold decrease in the release rate at the higher temperature. Difficulty in controlling the release by change of temperature was, however, shown in Fig. 5.9 (Chapter 5) due to the rapid rate of release from the system of this small soluble compound.

The release characteristics of this model drug substance from PNIPA-H1 were further examined at different loadings in section 7.5 below.

The fraction released over time of DHCl at 25°C and 37°C was shown in Fig. 7.8. DHCl is highly soluble and a larger molecule than NaB and was completely released at 25°C over approximately 10 hours, longer than the time taken for complete release of NaB. At 37°C, only 80% of the loading was released over the first 36 hours, with no subsequent release at that temperature. There was no evidence of binding between diltiazem and the polymer in section 6.3. The 80% release of DHCl at this temperature was consistent with the pore size distribution of the gel as described using the solute exclusion technique (section 4.4.5.3). Using this technique, DHCl was shown to be accessible to ~80% of the pores of PNIPA-H1 in the collapsed state at 37°C (Fig. 4.30). 80% of the loaded drug was therefore able to diffuse from the hydrogel, with the remaining 20% trapped in pores inaccessible to the outside media. The molecular size of DHCl (~8Å) was near the estimated average pore size of PNIPA-H1 at 37°C of ~10Å.

Comparison of the release mechanisms of NaB and DHCl from PNIPA-H1 showed that NaB showed approximately zero-order release kinetics ($n \sim 1.0$), compared to the near Fickian diffusion ($n \sim 0.5$) of the bulkier DHCl. The release of NaB was controlled by penetration of the medium into the hydrogel, which was the rate-limiting factor in this case. A combination of high solubility, osmotic influence on hydrogel swelling and small molecular size in relation to the swollen region resulted in zero-order release profiles. The bulkier drugs were influenced to a greater extent by the hydrogel meshwork and release was controlled by diffusion of the drug through the meshwork. Peppas and co-workers (Davidson and Peppas, 1986; Brannon-Peppas and Peppas, 1989; Brazel and Peppas, 1999b) showed that if the diffusion coefficient of the drug in the swollen phase is increased in comparison to the penetrating swelling front and time dependent thickness of the swollen phase, zero-order drug release might be expected. In the present context, decreasing the size of the drug from DHCl to NaB, assuming all other factors equal, is consistent with the above hypothesis. Similarly, Shah *et al.* (1991) showed that the diffusion mechanism of bulkier drugs from a hydrogel could be shown to approach zero-order if the level of hydration was increased. The meshwork would therefore have less of an influence on the bulkier drug and release may be controlled by penetration of the media.

The fraction released over time of VB12 at 25°C and 37°C is shown in Fig. 7.11. Release at 25°C was approximately proportional to the square root of time (Table 7.3) and was complete after approximately 20 hours. VB12 is a larger molecule and less soluble than NaB or DHCl with a slower release rate as a result. Release of VB12 at 37°C was negligible.

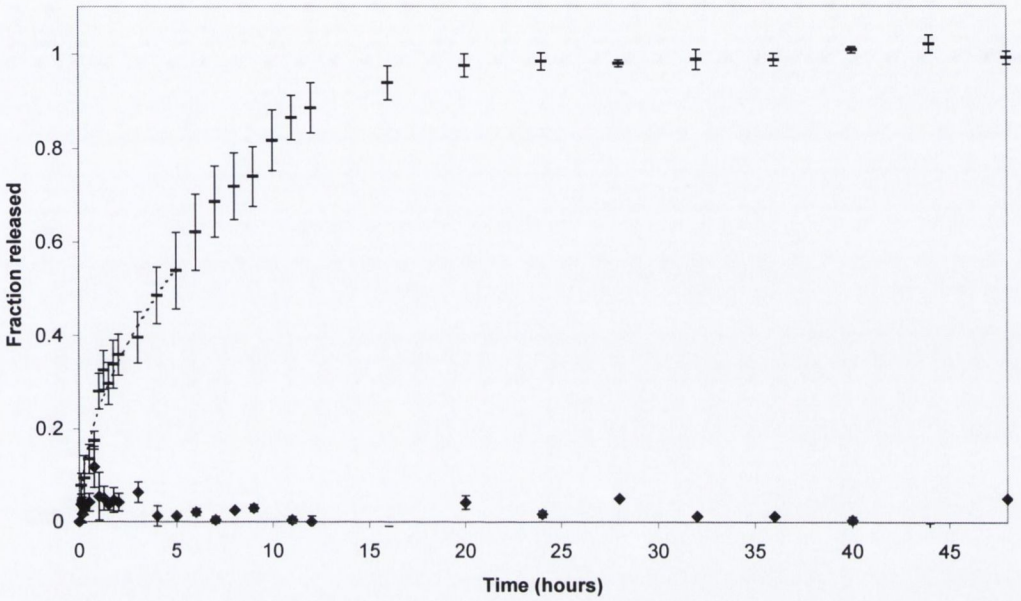

Fig. 7.11: Plot of fraction VB12 released over time in PB, fitted to the square root of time (Equation 2.12, *Higuchi*) at 25°C (dashed lines) and at 37°C (♦).

The hydrogel pore size at 37°C appeared to prevent diffusion of the molecule. From the solute exclusion technique in section 4.4.5.3, it was estimated that VB12 could access ~40% of the pores and its molecular size (~11.75Å) was above the ~10Å average pore size of PNIPA-H1 at 37°C. Diffusion out from the dense collapsed hydrogel of a relatively large molecule such as VB12 involves a tortuous route where the accessible pores must be interconnected for release to occur. This may have resulted in little or no drug release being detected.

The fraction released over time of the dextrans at 25°C and the corresponding release rates are shown in Fig. 7.12a and Fig 7.12b respectively. The fraction of dextran released over time at 37°C is shown in Fig. 7.12c.

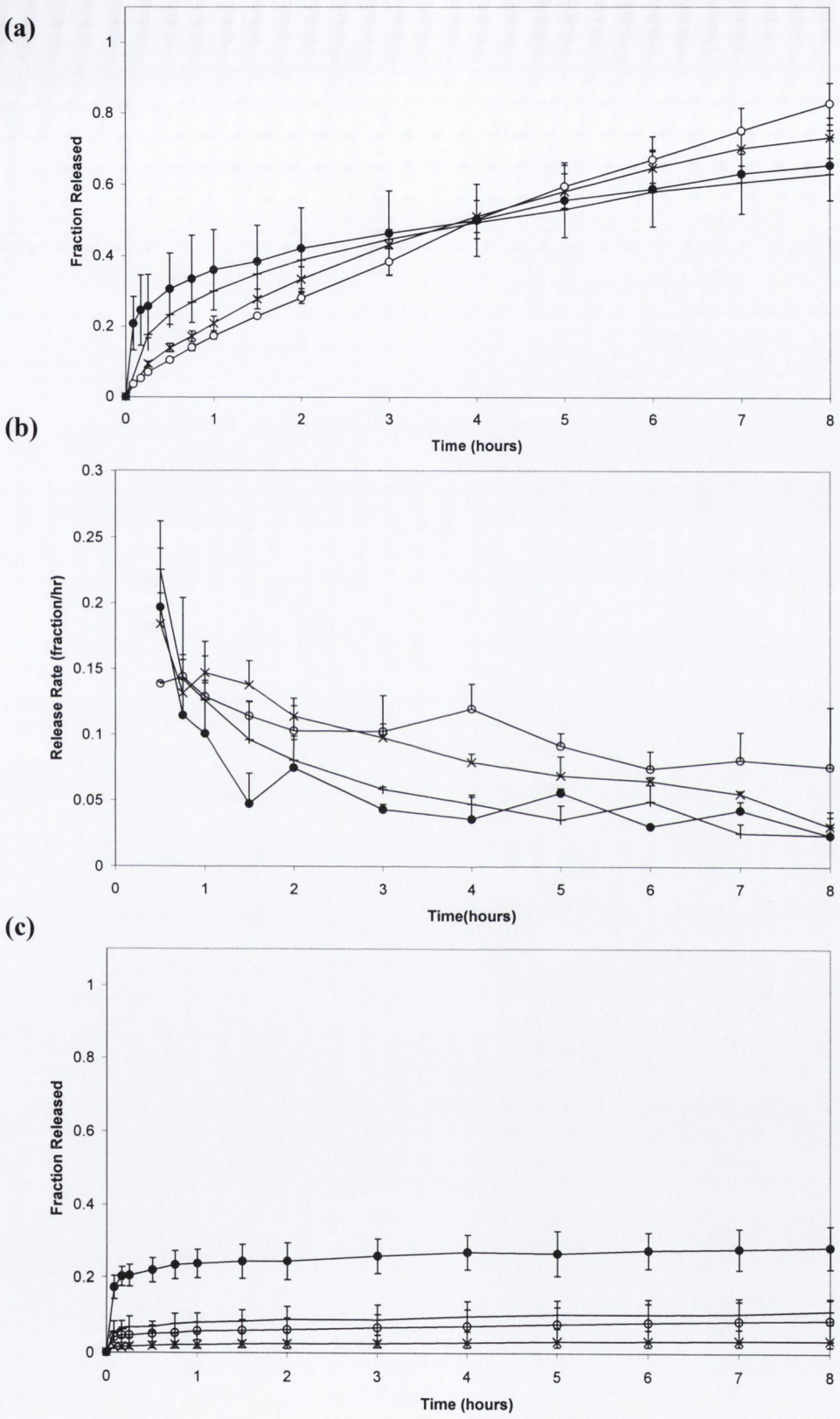

Fig. 7.12: Plot of (a) fraction dextran released over time at 25°C and (b) corresponding release rate at 25°C and (c) fraction dextran released over time at 37°C [D4 (○), D10 (x), D40 (●) D70 (+)].

The release profiles in Fig. 7.12a at 25°C were plotted against the square root of time and the fits obtained for the higher molecular weight dextrans did not adequately account for the early time-period (Table 7.3). D4 is a more soluble but larger molecule than VB12 and the release rate was slower at 25°C (Table 7.3). The higher molecular weight dextrans may expect to have slower release rates than D4 from this hydrogel due to lower diffusion coefficients and greater hindrance of release. The higher molecular weight dextrans, however, gave higher, more variable release rates. Examination of the release rate profiles (Fig. 7.12b) reveals no trends over the first hour. After this timeperiod, however, the release rate decreased with increasing molecular weight as expected. A lag phase may have been expected to be observed in the release profile of a molecule larger than the available mesh size as described by am Ende *et al.* (1995). Coupled to the unexpected molecular size dependent profile seen with the same dextrans in the pulsed release (Chapter 5, Fig. 5.11), a molecular size dependent gradient appears to have formed during drug loading, particularly with the larger dextrans. As described in Chapter 5, a molecular size dependent gradient may be expected considering that the higher molecular weight dextrans were not accessible to all the available pores at 25°C.

At 37°C (Fig. 7.12c), a sharp "burst" was seen at the first timepoint, particularly for D40, and can be attributed to surface drug, again possibly caused by the outer edges of this molecular weight gradient. There was no diffusion-controlled release of the dextrans at 37°C due to the hydrogel pore size being smaller (~10Å) than the molecular diameter of the dextrans (25Å to 98Å). The effect of smaller pore size cancelled out the increased diffusion rate due to the increase in temperature. Despite the gradient being formed, the effect of the higher temperature was to completely stop the release of these relatively large, highly soluble dextrans.

Comparisons between swelling and release profiles of all the model drugs can be made. The swelling rates at 25°C were all approximately proportional to the square root of time, with an increased rate of swelling due to the osmotic effect of small hydrophilic model drug such as NaB and DHCl and a decreased rate in the presence of hydrophobic drugs such as DB and the benzoate esters. In the present context, release of drugs of MW~500 and greater were diffusion controlled as the meshwork had a significant influence on release. The release rate constant at 25°C decreased as expected in the series of NaB to D4 due to increased hindrance to diffusion. The higher molecular weight dextrans did not show a trend over the first hour, attributed to the molecular size gradient apparent from drug loading of the high molecular weight compounds.

The effect of benzoate binding decreased the swelling rate even further than may have been expected from a non-binding drug such as DB, with binding tendency increasing with increasing hydrophobicity of the series. Release of BA and its esters from the hydrogel was also diffusion

controlled, in contrast to the zero-order release of the sodium salt of BA. Binding of the benzoate to the polymer decreased the effective pore size available and diffusion controlled release resulted. Fig.7.9 showed a trend of an increase in the release exponents of the benzoates at both temperatures with increasing size/decreasing hydration level. This trend is opposite to what may be expected from the study of Shah *et al.* (1991) and predicted from the equations of Peppas and co-workers (Davidson and Peppas, 1986; Brannon-Peppas and Peppas, 1989, Brazel and Peppas, 1999b) as described above. Increased binding with increased hydrophobicity (and size) can account for this pattern with stronger binding resulting in a more anomalous release mechanism. The rate of release from this series increased with increasing solubility, in proportion to square root of drug solubility as predicted by diffusion equations (Equation 2.6). Since the extent of binding was directly proportional to a decrease in drug solubility of the series as described in section 6.2, the relationship between release rate and drug solubility still held. The actual release rates, however, were lower than may be expected from a non-binding hydrophobic drug such as DB.

Transient increases in swelling rate and extent were seen at 37°C in the presence of the small, hydrophilic drugs, again attributed to the osmotic effect. The release rates of NaB and DHCl were, however, decreased significantly at this temperature compared to 25°C. The complete drug loading was also not being released at this temperature, attributable to physical entrapment in the case of DHCl. The model drugs with molecular size greater than ~10Å showed no release at this temperature due to the relationship between drug molecular size and micropore size.

7.5 INFLUENCE OF DRUG LOADING ON SWELLING/RELEASE

The influence of various loadings of sodium benzoate and benzoic acid on the swelling of, and release pattern from, PNIPA-H1 at 25°C was examined.

7.5.1 Benzoic Acid

The swelling pattern of PNIPA-H1 at 25°C containing various loadings of BA is shown in Fig. 7.13a. The amount of BA released and fraction released over time are shown in Fig. 7.13b/c. In each case, the swelling and release profiles were approximately proportional to the square root of time (Equation 2.12, *Higuchi*) (Table 7.4) and the fitted profiles are shown in Fig. 7.13a and Fig 7.13c. In addition, the diffusional exponent was allowed to vary (Equation 2.11, *Peppas*) and the values of n are also given in Table 7.4.

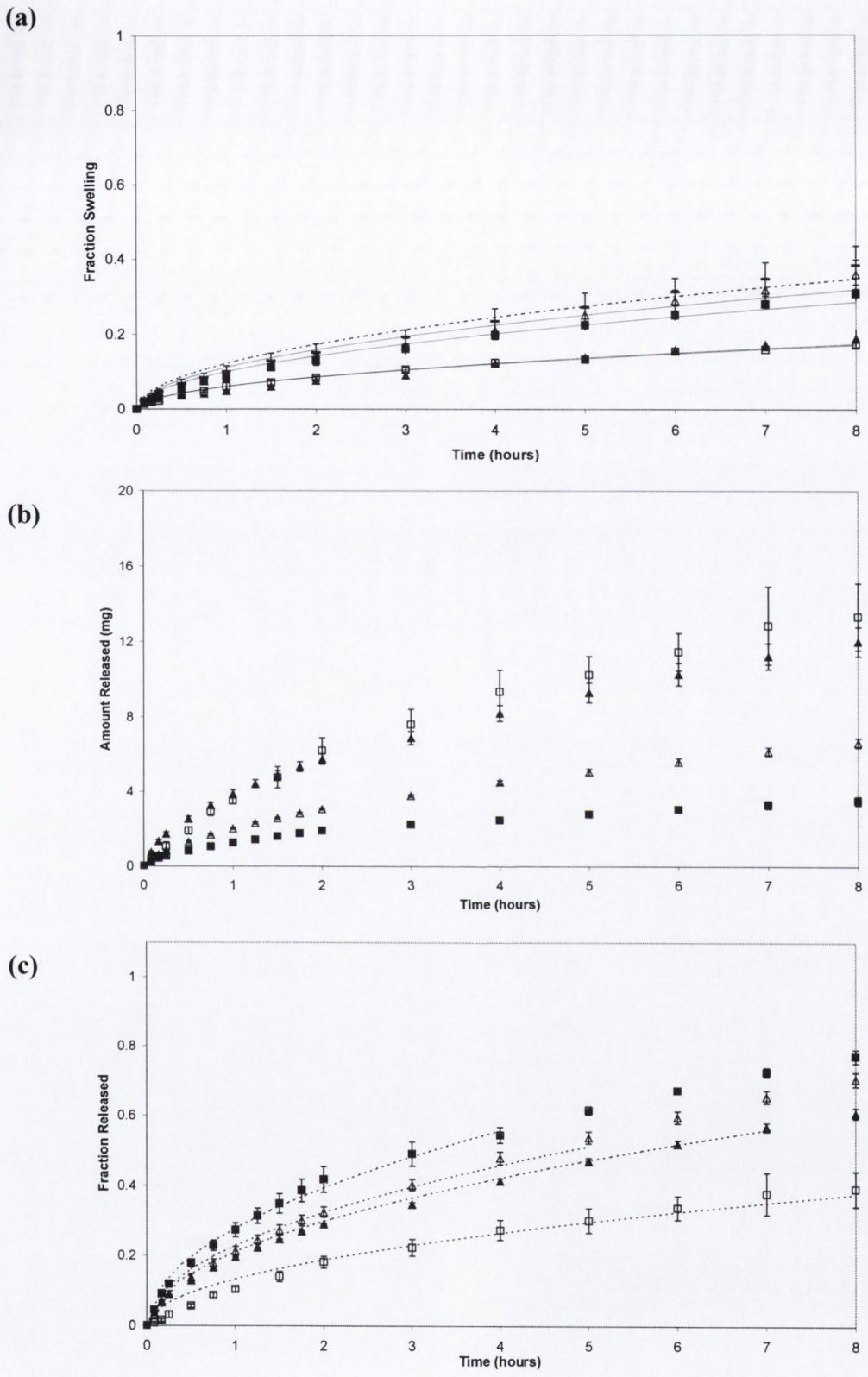

Fig. 7.13: (a) Fraction swelling of PNIPA-H1 at 25°C containing various loadings of benzoic acid in comparison to unloaded PNIPA-H1 (- dashed line). (b) Amount released and (c) fraction released of BA from same systems [■ 5mg (9.1% w/w), Δ 10mg (16.7% w/w), ▲ 20mg (28.6% w/w), □ 40mg (44.4% w/w)]. Lines shown represent fit of data to the square root of time.

The swelling profiles of PNIPA-H1 containing various loadings of BA (Fig. 7.13a) were all approximately proportional to the square root of time. There was no statistical difference ($p>0.05$) in the swelling rate of the hydrogel in the presence of up to 17% w/w BA (5-10mg). Higher loadings (>28% w/w, >20mg) decreased the rate of swelling, although the highest loading (40mg) had no further effect on the swelling rate.

Table 7.4: Swelling (k_s) of BA loaded PNIPA-H1 and release rate constants (k_d) for BA calculated using Equation 2.12 (*Higuchi*), where S is the fraction swelling (25°C equilibrium) and F is the fraction released. Diffusional exponent, *n*, also estimated using Equation 2.11 (*Peppas*). The coefficients of determination (CD) shown in each case.

Swelling	$S = k_s t^{0.5}$		$S = k_s t^n$	
(%w/w BA)	k_s $(min^{-0.5})(X10^3)$	CD	n	CD
0%	2.047 ± 0.268	0.9762	0.639 ± 0.008	0.9981
9.10%	1.682 ± 0.074	0.9839	0.605 ± 0.022	0.9981
16.70%	1.873 ± 0.180	0.9649	0.673 ± 0.037	0.9957
28.60%	1.029 ± 0.059	0.9721	0.626 ± 0.032	0.9806
44.40%	1.012 ± 0.046	0.9916	0.536 ± 0.026	0.9942
Release	$F = k_d t^{0.5}$		$F = k_d t^n$	
(%w/w BA)	k_d $(min^{-0.5})(X10^3)$	CD	n	CD
9.10%	4.668 ± 0.367	0.9816	0.624 ± 0.014	0.9987
16.70%	3.688 ± 0.181	0.9802	0.613 ± 0.028	0.9974
28.60%	3.461 ± 0.034	0.9978	0.523 ± 0.009	0.9989
44.40%	2.217 ± 0.253	0.9664	0.648 ± 0.024	0.9918

The drug release rate was also approximately proportional to the square root of time with no apparent pattern in the diffusional exponents when the loading of BA was varied (Table 7.4a). The release rate constants (k_d) decreased linearly with increasing drug loading (Fig. 7.14). According to the equations of *Higuchi* (Equations 2.5-2.6), an increase in the diffusional rate of release from a non-swellable system would have been expected by increasing the total concentration of drug available, with the rate increase proportional to the square root of drug concentration. A decrease in the release rate was proportional to the loading in the current study and can be attributed to the influence of the BA on hydrogel swelling due to drug-polymer binding. Binding between BA and the polymer not only directly slowed the release rate of BA due to the binding with the polymer but also indirectly affected the release rate by decreasing local swelling and therefore pore size.

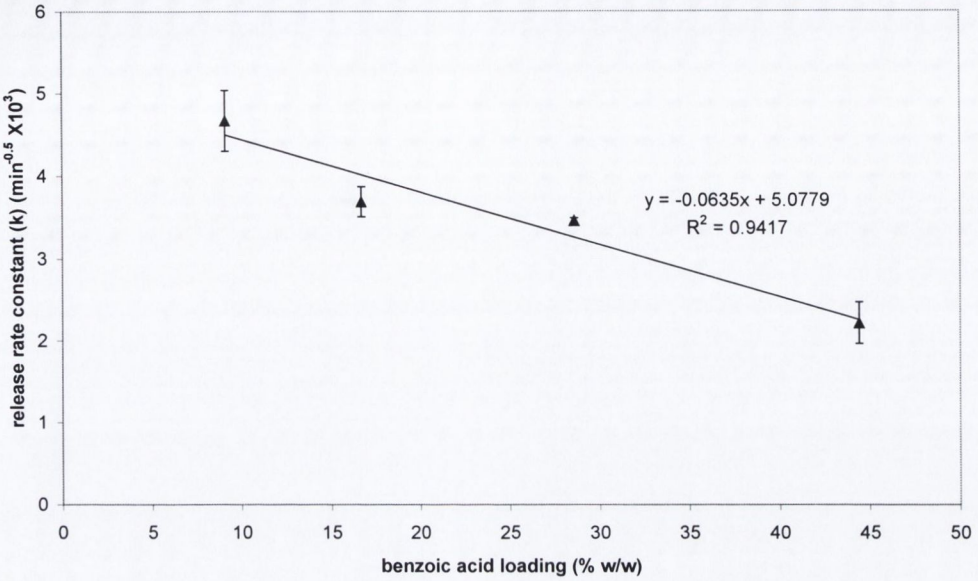

Fig. 7.14: Plot of diffusional release rate constants (k_d) against benzoic acid loading.

Fig. 7.15 shows a picture of PNIPA-H1, loaded with BA (28.6% w/w), in various stages of swelling at 25°C. At T = 12 hours and T = 24 hours, a clear boundary exists between the swollen exterior and the collapsed interior. At T = 24 hours, the hydrogel system was deformed, possibly due to the weight difference between the swollen exterior and the drug interior where swelling was prevented due to binding. The boundary had disappeared and the hydrogel had regained its normal shape by T = 48 hours.



Fig. 7.15: Pictures of swelling of a benzoic acid loaded hydrogel at various time points at 25°C From left to right, T = 0, T = 12hrs, T = 24hrs, T = 48hrs [loading 20mg (28.6% w/w)].

7.5.2 Sodium Benzoate

The swelling patterns of PNIPA-H1 at 25°C containing various loadings of NaB are shown in Fig. 7.16a. The amount of NaB released and fraction released over time are shown in Fig. 7.16b/c. In each case, the swelling and release profiles were plotted against the square root of time (Equation 2.12, *Higuchi*) (Table 7.5) and also against the power law equation (Equation 2.11, *Peppas*). The release profiles were also directly plotted against time and shown on Fig. 7.16c.

The swelling profiles of PNIPA-H1 loaded with NaB were all approximately proportional to the square root of time. The presence of NaB in the hydrogel at all concentrations studied resulted in an increase in the swelling rate constant (k_s) due to the high solubility of the salt and the resulting osmotic effect as previously described. There was no apparent pattern in the swelling rate constants (k_s, Table 7.5) with increasing loading of NaB.

Table 7.5: Swelling (k_s) of NaB loaded PNIPA-H1 and release rate constants (k_d) for NaB calculated using Equation 2.12 (*Higuchi*) and Equation 2.11 (*Peppas*), where S is the fraction swelling (25°C equilibrium) and F is the fraction released. Estimates of $k_{d'}$ also obtained when value of *n* set as unity.

Swelling	$S = kt^n$		$S = k_s t^{0.5}$		$S = kt$	
(%w/w NaB)	n	CD	k_s $(min^{-0.5})(X10^3)$	CD		
	0.639 ± 0.008	0.9981	2.047 ± 0.268	0.9762	--	--
9.10%	0.660 ± 0.046	0.9983	4.136 ± 0.400	0.9751	--	--
16.70%	0.650 ± 0.009	0.9984	4.874 ± 0.520	0.9788	--	--
28.60%	0.463 ± 0.011	0.9933	3.341 ± 0.108	0.9903	--	--
44.40%	0.526 ± 0.041	0.9951	5.362 ± 0.932	0.9905	--	--
Release	$F = kt^n$		$F = k_d t^{0.5}$		$F = k_{d'} t$	
(%w/w NaB)	n	CD	k_d $(min^{-0.5})(X10^3)$	CD	$k_{d'}$ $(min^{-1})(X10^3)$	CD
9.10%	1.410 ± 0.277	0.9948	3.839 ± 1.960	0.7712	3.647 ± 1.717	0.9628
16.70%	1.282 ± 0.016	0.9952	4.747 ± 2.319	0.7883	5.349 ± 2.629	0.9785
28.60%	0.970 ± 0.086	0.9976	8.188 ± 2.187	0.8602	11.692 ± 3.009	0.9950
44.40%	0.627 ± 0.124	0.9978	14.034 ± 0.566	0.9755	23.482 ± 1.334	0.8755

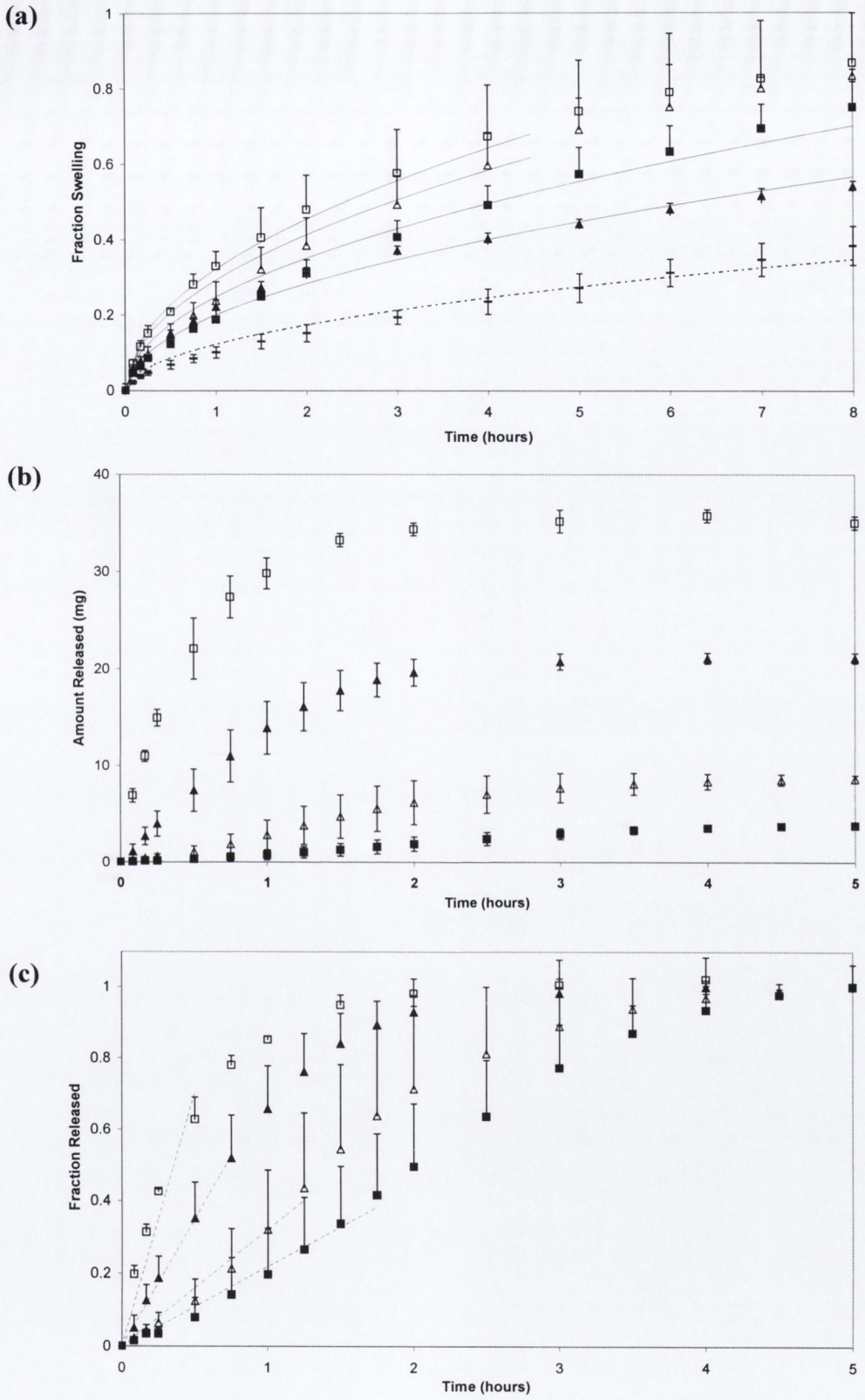

Fig. 7.16: (a) Fraction swelling of PNIPA-H1 at 25°C containing various loadings of sodium benzoate in comparison to unloaded PNIPA-H1 (dashed line). (b) Amount released and (c) fraction released of NaB from same systems [■ 5mg (9.1% w/w), Δ 10mg (16.7% w/w), ▲ 20mg (28.6% w/w), □ 40mg (44.4% w/w)]. Lines shown represent fit of release data directly against time.

Release of various loadings of sodium benzoate cannot be described as being proportional to the square root of time as shown in Table 7.5. Better fits were obtained when the diffusional exponent, *n*, was allowed to vary or when the value of n was set as unity. When the diffusional exponent was allowed to vary, the values of *n* obtained were linearly proportional to loading (Fig. 7.17a). At low loading levels, a value of $n > 1.0$ was obtained, resulting in a sigmoidal type release pattern at these loadings. As the loading increased, the diffusional exponent approached 0.5. The swelling therefore appears to have a greater influence on the release profile at the lower loadings, resulting in approximately zero-order release. Studies by Lee (1985) and Lee and Kim (1991) also reported that fractional release of water-soluble drugs from pHEMA and solvent front penetration into pHEMA behaved more Fickian as the loading level increased, attributable to a change of relative importance of the diffusion process versus the polymer relaxation as a function of drug loading.

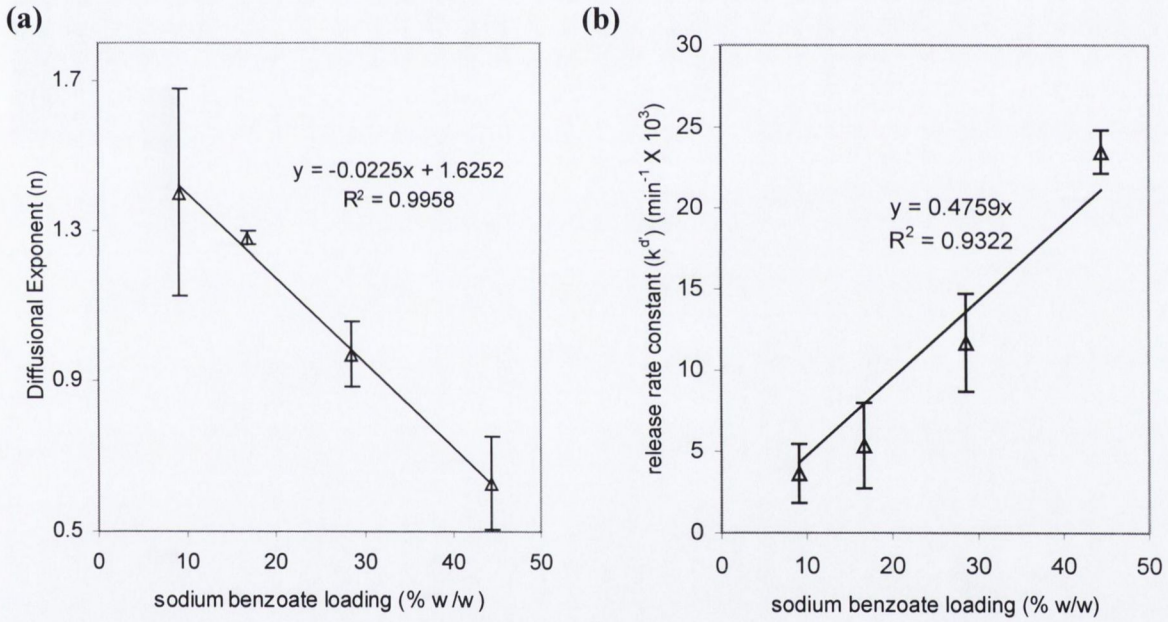

Fig. 7.17:

(a) Influence of loading of NaB on diffusional exponent, n (Equation 2.11, *Peppas*)

(b) Plot of release rate constant ($k_{d'}$), calculated when diffusional exponent set as unity, against sodium benzoate loading

In order to compare the rates of release, the release profiles were plotted against time and the zero-order release rate constants obtained ($k_{d'}$) are given in Table 7.4. There was a linear relationship between the loading level and the release rate constant, which increased in proportion to the loading (Fig. 7.17b). Higher loading resulted in a faster release rate due to the greater concentration difference between the gel and the release medium. A similar increase in release rate from non-thermoresponsive hydrogels with increasing loading has previously been described (Lee, 1985; am

Ende *et al.*, 1995). The increase in the release rate with increasing loading was in contrast with the decrease in release rate with increasing loading of BA, attributable to the effect of BA-PNIPA binding. As described in chapter 6, binding of the benzoate appears to mainly occur when the species was unionised, and was not significant in the case of NaB. Pictures of PNIPA-H1 loaded with NaB (28.6% w/w) in various stages of swelling at 25°C are shown in Fig. 7.18.

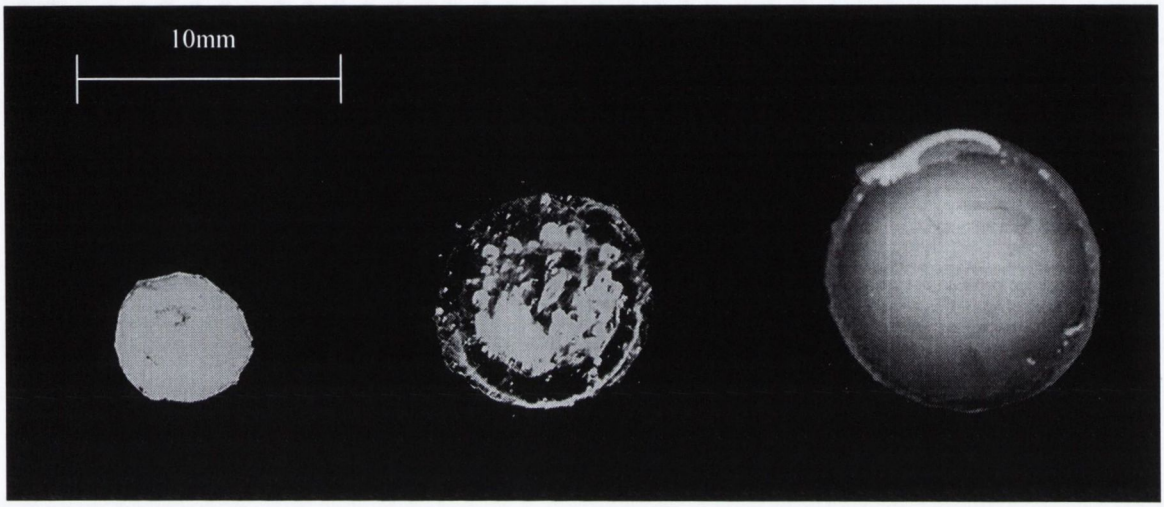

Fig. 7.18: Pictures of swelling of a sodium benzoate loaded hydrogel at various time points at 25°C From left to right, T=0, T=1.5 hrs, T=24 hrs [loading 20mg (28.6% w/w)].

A change in the drug loading will therefore have an effect on the release rate from these systems, whether the drug interacts with the hydrogel or not. The effect of loading of a drug, which exerts a significant osmotic pressure or slows the swelling rate, will influence the rate of swelling and therefore the magnitude of deswelling/contraction as described in Chapter 5. The swelling/contraction cycle will in turn influence the release pattern and the ability to thermally control release. The fraction of loaded drug available for the drug pulse will also be significant, influencing the magnitude of that pulse.

Apart from hydrophobic binding of BA and its esters, two other types of drug-hydrogel interactions were described in Chapter 6. NaB was shown to cause a salting out effect, which lowered the phase transition temperature of the hydrogel and therefore the swelling level at a particular temperature. This salting out effect was not as strong as the binding effect seen with the other benzoates, quantified by the slope of the k_{H2} value (Table 6.1) and the k_L values (Table 6.2). The salting out effect caused by a loaded hydrophilic drug did not appear to significantly affect the rate of swelling and the release profile, where the osmotic effect was more significant. Similarly, the studies shown in Chapter 6, which showed that high concentrations of the hydrophilic drugs decreased the ability of the hydrogel to swell, did not appear to be significant in the current study. The osmotic effect of the hydrophilic drugs on the swelling rate was more important. The two types

of interactions would, however, have implications if smaller volumes of media were used for release studies from these hydrogels.

7.6 CONCLUSIONS

The present study showed that the release rate and mechanism of drug release from a thermoresponsive hydrogel depended on the temperature; type of model drug used and on the drug loading. From these experiments, predictions of the release rate and extent of other model drugs could be made at both temperatures, with implications for the ability to predict the pattern of pulsatile release as described in Chapter 5.

Increasing the temperature increased both the solubility and intrinsic dissolution rate of the drug substances as expected. In contrast, increasing the temperature decreased the ability of the hydrogel to swell and decreased the diffusion coefficient of the drug from the system. In thermo-responsive systems, these two temperature effects counteracted one another and an effective reversal of thermal control resulted. The magnitude of this reversal was particularly dependent on drug size, where drugs of molecular diameter >10Å were not released at the higher temperature. The ability to thermally control the drug was consistent with the results from the pulsed release study in Chapter 5 and indicated that pore size was the controlling mechanism for release in those systems. In the case of smaller drugs such as DHCl, the fraction released at 37°C was consistent with the fraction of pores of that size accessible to the outside media. Interconnection of pores to enable the drug to diffuse from the system was also suggested as being important when the drug size was "borderline", such as the case of VB12 (molecular diameter 11.75Å).

The hydrophobic drugs were shown to decrease the rate of swelling with the influence of the drugs chemical nature on swelling and release patterns clarified in the present study in terms of hydrophobic binding of the benzoates. The binding was detailed in the previous chapter and was shown to be of influence in the swelling and release profiles. Binding of the benzoates further decreased the swelling rate at 25°C and both the rate and extent at 37°C, where the release rate of BA effectively stopped. Binding also influenced the mechanism of diffusion from these systems.

The quantity of loaded drug affected the swelling rate depending on the hydrophilicity of the drug and other related effects such as binding with the hydrogel and osmotic effects. Such a loading effect has implications for swelling/deswelling patterns and pulsatile drug release studies.

CHAPTER 8

An Investigation into the Effect of Crosslinking Content on Release from PNIPA Hydrogels

8.1 INTRODUCTION

The swelling and drug release studies presented in Chapters 5 and 7 were preformed using PNIPA-H1, containing 1.15mol% crosslinker (N,N'-methylenebisacrylamide, MBA). Three other hydrogels were also prepared, containing higher percentage crosslinker, designated as PNIPA-H2 (2.22mol% MBA), PNIPA-H3 (5.68mol% MBA) and PNIPA-H4 (11.17mol% MBA) (Table 4.6).

Studies by Peppas and coworkers (Peppas, 1986; Canal and Peppas, 1989; am Ende *et al.,* 1995) have shown the importance of crosslinking in controlling the mesh size and therefore the rate of drug release from swellable systems. As the crosslinking ratio increased, the mesh size decreased at the molecular level, therefore decreasing the free volume available for solute transport. A reduction in the rate of drug release has been shown due to a reduction in the solute diffusion coefficient (e.g. am Ende *et al.*, 1995; Yu and Grainger, 1995). In most cases, the crosslinking agents were incorporated in small amounts (~1 %w/w, Peppas and Lustig, 1985) and differences in swelling rates were not apparent (e.g. am Ende *et al.*, 1995; Yu and Grainger, 1995; Brazel and Peppas, 1999a). Increasing the level of crosslinker, however, is potentially a useful method of increasing the mechanical strength of the gel (Johnson *et al.*, 2004) and altering the swelling kinetics of the gel (Omidian *et al.,* 1998). The swelling study presented at 25°C in Chapter 4 (Fig. 4.18) and other recent studies on acrylate hydrogels (Omidian *et al.,* 1998; Kabiri *et al.*, 2003) have shown an increase in the swelling rate with increasing concentration of crosslinker. In addition to a difference in swelling rate, a higher equilibrium swelling level was seen at 37°C with PNIPA-H4 than with the other hydrogels, with greater effective macropore size as a result shown by SEM (Chapter 4). The SEM and nitrogen desorption data also showed differences in macro- and mesopore sizes within the hydrogel series at 37°C, even when differences in equilibrium swelling levels were undetectable (PNIPA-H3 versus PNIPA-H1 and H2). The effective pore size therefore increased with increasing levels of crosslinker above the polymer LCST, in contrast to an expected decrease in the pore size at a molecular level as previously shown by several authors in non-thermoresponsive hydrogels (e.g. Peppas and Lustig, 1985; am Ende *et al.*, 1995).

The present chapter examines the influence of the small model drugs benzoic acid and sodium benzoate on the swelling profiles of, and release patterns from, the series of thermoresponsive hydrogels at 25°C and 37°C.

8.2 SWELLING

The hydrogels (Table 4.6) were characterised in Chapter 4 based on their glass transition temperature, equilibrium swelling levels at particular temperatures and swelling kinetics over time.

The percentage crosslinker was shown to significantly influence the equilibrium swelling at a particular temperature (section 4.4.1) and the swelling rate over time (section 4.4.3). At 25°C, the equilibrium swelling level decreased and the swelling rate increased with increasing percentage crosslinker (Fig. 4.18). The fraction swelling of the various hydrogels over time at 25°C and 37°C, loaded with NaB and BA, are shown in Figs 8.1 to 8.4. The swelling rate constants were calculated using Equation 2.12 (*Higuchi*) and are shown in Table 8.1 along with the apparent diffusion coefficient (D_{app}) of water into the hydrogel calculated using Equation 2.5a. Since the four gels had different equilibrium swelling levels (Fig. 4.18a), the swelling rate constants were normalised with respect to the equilibrium swelling level of PNIPA-H1 at 25°C. The swelling rate constants of the different gels could then be compared. The swelling profiles were also fitted to Equation 2.11 (*Peppas*) to estimate the diffusional exponent, *n*, and the values of *n* are also shown in Table 8.1.

Table 8.1: Swelling rate constants calculated using the fraction swelling (Equation 2.12, *Higuchi*) at 25°C and 37°C along with associated coefficients of determination (CD). Swelling constants normalised with respect to equilibrium swelling level of PNIPA-H1 at 25°C. Diffusional exponents, *n*, were estimated using Equation 2.11 (*Peppas*). Also shown are apparent diffusion coefficients (D_{app}) of water into the hydrogels estimated using the amount of media absorbed per unit surface area (Equation 2.5a).

	Swelling rate constant (k_s) ($min^{-0.5}$)($X10^3$)	**CD**	**D_{app} (cm^2/s) ($X10^{-6}$)**	**Diffusional exponent (*n*)**
25°C	**k_{s25}**			
PNIPA-H1	2.047 ± 0.268	0.9762	1.437 ± 0.309	0.639 ± 0.008
PNIPA-H2	2.735 ± 0.298	0.9490	2.701 ± 0.409	0.730 ± 0.081
PNIPA-H3	2.988 ± 0.375	0.9390	2.295 ± 1.581	0.666 ± 0.198
PNIPA-H4	6.566 ± 1.307	0.9734	14.062 ± 2.418	0.654 ± 0.105
H1 (NaB)	3.341 ± 0.108	0.9903	3.754 ± 0.301	0.463 ± 0.011
H2 (NaB)	4.171 ± 0.498	0.9810	3.122 ± 2.73	0.591 ± 0.001
H3 (NaB)	6.547 ± 0.671	0.8058	8.930 ± 0.989	1.174 ± 0.066
H4 (NaB)	6.290 ± 0.220	0.8784	15.716 ± 3.249	0.917 ± 0.035
H1 (BA)	1.029 ± 0.059	0.9721	0.299 ± 0.030	0.626 ± 0.032
H2 (BA)	1.226 ± 0.251	0.9725	0.465 ± 0.029	0.653 ± 0.021
H3 (BA)	1.089 ± 0.017	0.9889	0.208 ± 0.024	0.586 ± 0.009
H4 (BA)	0.660 ± 0.003	0.9683	0.066 ± 0.058	0.665 ± 0.001
37°C	**k_{s37}**			
PNIPA-H1	0.456 ± 0.009	0.9036	0.067 ± 0.002	0.260 ± 0.191
PNIPA-H2	0.387 ± 0.013	0.8013	0.057 ± 0.004	0.250 ± 0.043
PNIPA-H3	0.574 ± 0.023	0.8715	0.058 ± 0.005	0.293 ± 0.012
PNIPA-H4	3.740 ± 0.323	0.9742	3.558 ± 0.588	0.679 ± 0.080
H1 (NaB)	1.368 ± 0.118	0.9254	0.500 ± 0.074	0.352 ± 0.077
H2 (NaB)	0.527 ± 0.264	0.7373	0.109 ± 0.068	0.309 ± 0.124
H3 (NaB)	0.634 ± 0.107	0.8168	0.059 ± 0.019	0.337 ± 0.088
H4 (NaB)	4.340 ± 0.581	0.8396	3.576 ± 0.172	0.977 ± 0.094
H1 (BA)	0.194 ± 0.048	0.6060	0.011 ± 0.005	0.237 ± 0.099
H2 (BA)	0.088 ± 0.037	0.8155	0.005 ± 0.003	0.532 ± 0.339
H3 (BA)	0.306 ± 0.038	0.7668	0.013 ± 0.003	0.258 ± 0.031
H4 (BA)	1.191 ± 0.113	0.9786	0.251 ± 0.080	0.589 ± 0.021

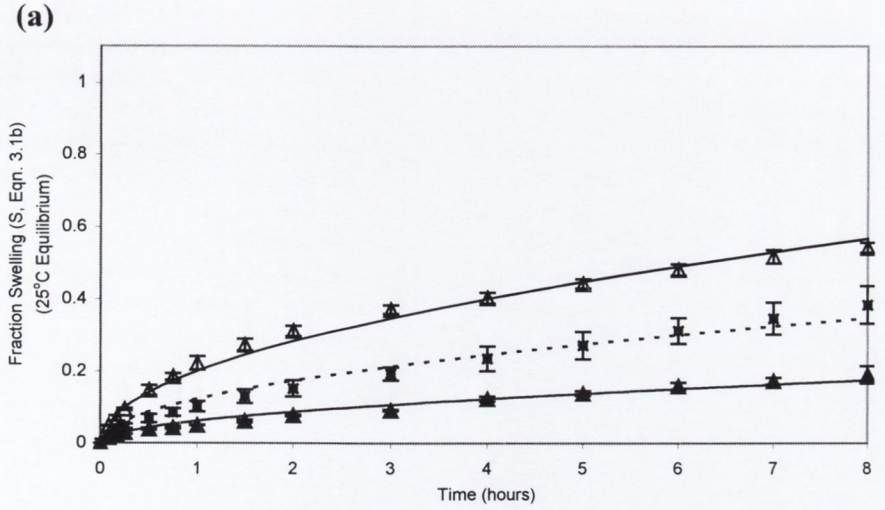

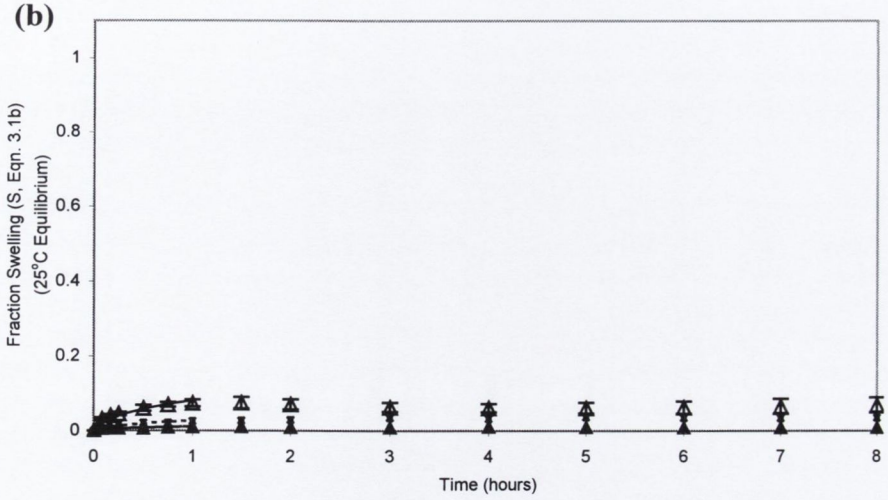

Fig 8.1: Plot of fraction swelling of **PNIPA-H1** over time at 25°C (a) and 37°C (b) [unloaded (■), loaded with 28.6%w/w BA (▲)/NaB (Δ)]. Data fitted to Equation 2.12 (*Higuchi*)

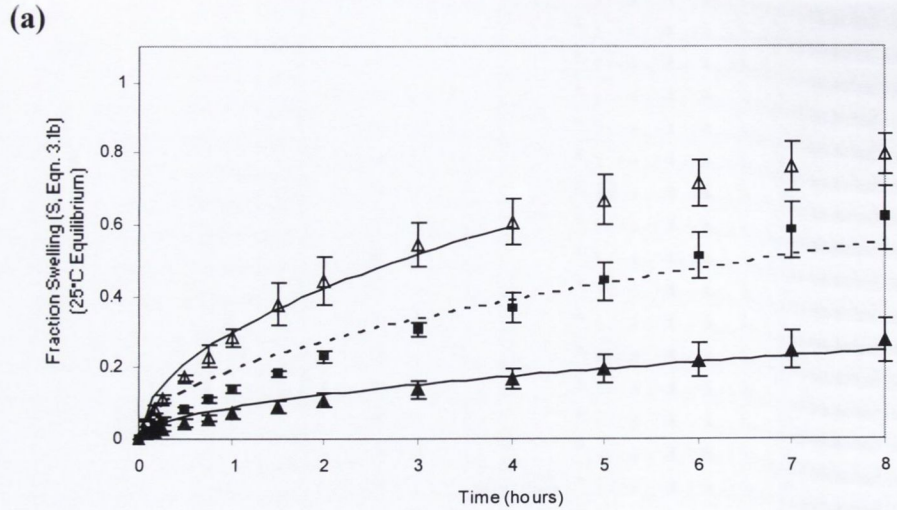

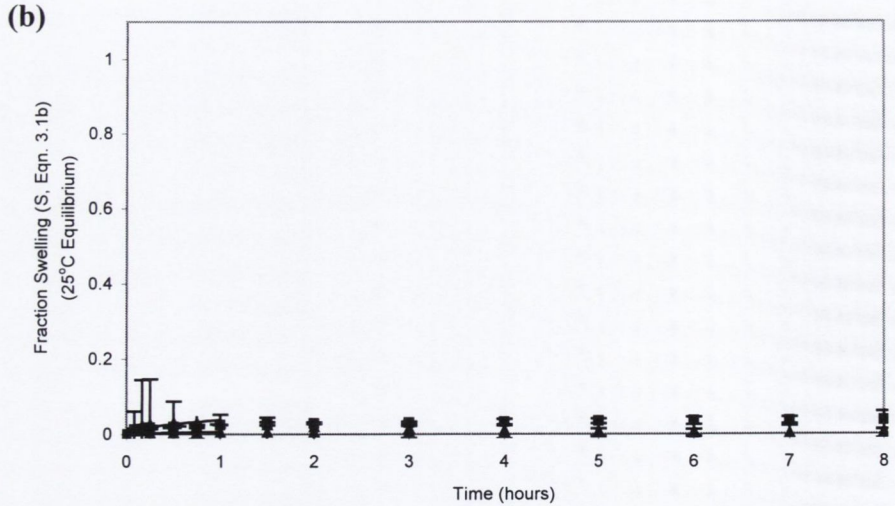

Fig 8.2: Plot of fraction swelling of **PNIPA-H2** over time at 25°C (a) and 37°C (b) [unloaded (■), loaded with 28.6%w/w BA (▲)/NaB (Δ)]. Data fitted to Equation 2.12 (*Higuchi*).

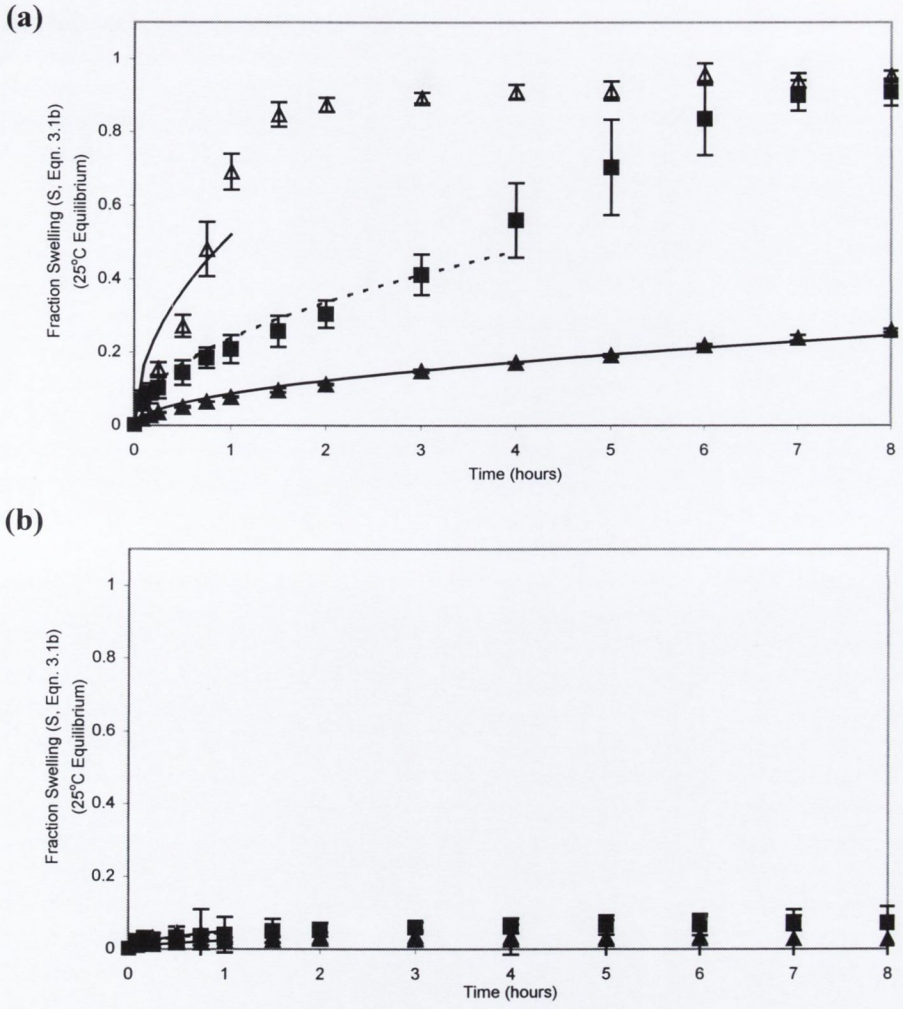

Fig 8.3: Plot of fraction swelling of **PNIPA-H3** over time at 25°C (a) and 37°C (b) [unloaded (■), loaded with 28.6%w/w BA (▲)/NaB (Δ)]. Data fitted to Equation 2.12 (*Higuchi*).

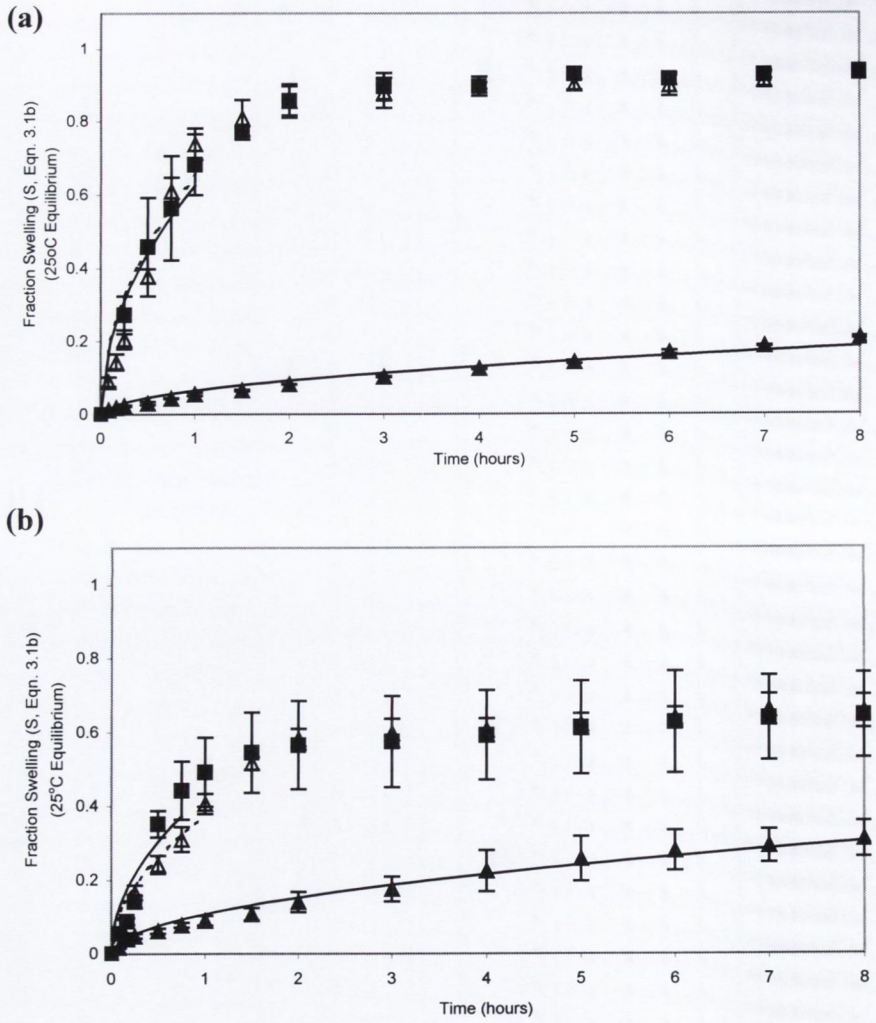

Fig 8.4: Plot of fraction swelling of **PNIPA-H4** over time at 25°C (a) and 37°C (b) [unloaded (■), loaded with 28.6%w/w BA (▲)/NaB (Δ)]. Data fitted to Equation 2.12 (*Higuchi*).

At 25°C, the diffusional exponent (n) in each case was approximately proportional to the square root of time (Table 8.1), except where the more highly crosslinked systems were loaded with NaB. In that case, the diffusional exponent approached unity. A pattern of an increase in the diffusional exponent with increasing crosslinking ratio was seen with the NaB loaded hydrogels, similar to the crosslinker dependent pattern recently shown by Brazel and Peppas (1999a) in hydrophilic glassy polymers. At 37°C, values of $n<0.5$ were generally observed where swelling was minimal. In the case of PNIPA-H4 loaded with NaB at 37°C, there was an increase in the value of n towards unity, similar to the trend seen at 25°C.

The diffusional exponents in each case were set at 0.5 to estimate the swelling rate constants (k_{s25}, k_{s37}) in Table 8.1. The swelling rate constants at 25°C (k_{s25}) were plotted against the percentage crosslinker in the hydrogel in Fig. 8.5. There was a linear increase in the swelling rate constant of the unloaded systems at 25°C with increasing crosslinker as described in Chapter 4 (Fig. 4.17). In this case the rate constants were calculated using the normalised swelling data.

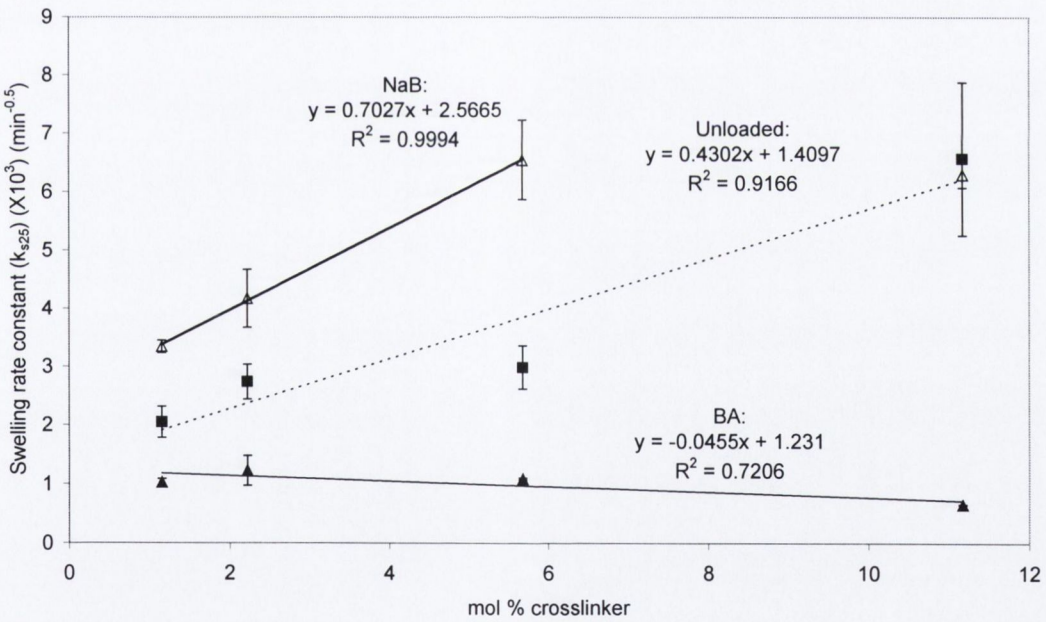

Fig. 8.5: Plot of swelling rate constants at 25°C against mol% crosslinker (MBA) of hydrogel in the absence (■, dashed line) and presence of loaded drug [BA (▲), NaB (Δ), loading 28.6%w/w]

The presence of NaB in the hydrogel increased the swelling rate for the series PNIPA-H1 to H3, with the resulting linear relationship ($R^2 = 0.9994$) approximately parallel to the unloaded system (Fig. 8.5). The osmotic effect of NaB (28.6%w/w loading) on swelling of PNIPA hydrogels therefore resulted in an average of a 1.5-fold increase in the swelling rate of the hydrogels in the series PNIPA-H1 to H3. NaB did not influence the swelling rate of PNIPA-H4 at 25°C, although an increase in the diffusional exponent was apparent. In the case of PNIPA-H4, the diffusional exponent of swelling ($n \sim 1.0$) indicated that the media influx was controlled by the rate of polymer

relaxation as opposed to the media diffusion process. The osmotic effect of NaB did not affect the polymer relaxation process, with no significant influence on the swelling rate of PNIPA-H4 as a result.

The effect of BA on hydrogel swelling was to lower the rate of swelling at 25°C significantly in each case. The presence of BA caused between a 2-fold and 10-fold decrease in the swelling rate of the hydrogels, depending on the rate of swelling of the unloaded system. The resulting swelling profiles showed no trend with increasing level of crosslinking (Fig. 8.5). The swelling rate of the BA loaded PNIPA hydrogels at 25°C was therefore effectively independent of the level of crosslinking in the system. Swelling was diffusion controlled, with binding between BA and PNIPA, as described in Chapters 6-7, controlled the swelling rate of the PNIPA hydrogels studied.

Fig. 8.6 plots the swelling rate constants at 37°C against the percentage crosslinker in the hydrogel, shown on the same scale as in Fig. 8.5. Only a residual swelling level and rate was observed in the PNIPA-H1 to H3 series of hydrogels at 37°C. An increase in the swelling rate constant was seen with PNIPA-H4 as described in chapter 4 and resulted in the pattern seen in Fig. 8.6 (dashed line).

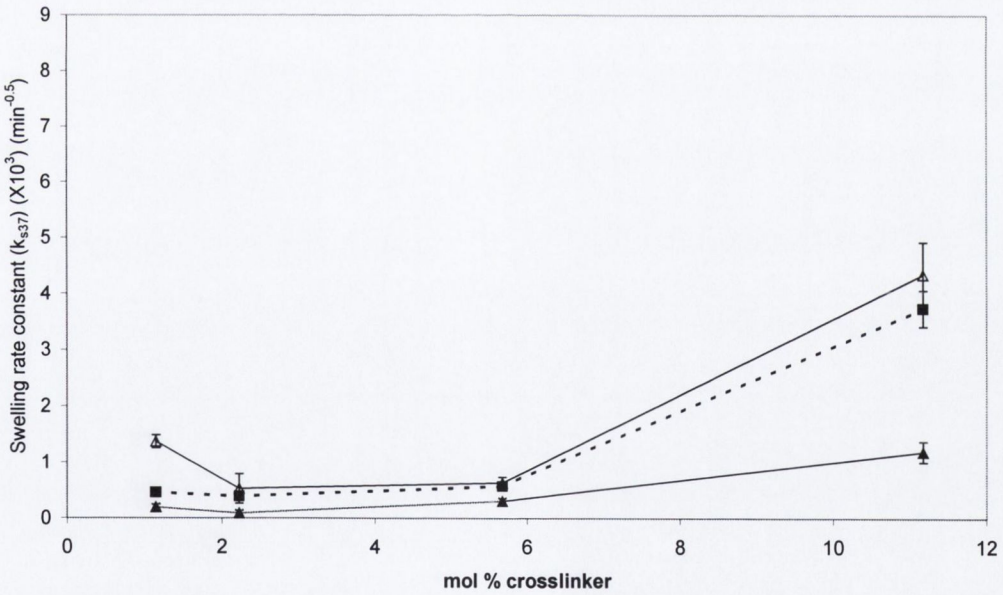

Fig. 8.6: Plot of swelling rate constants at 37°C against mol% crosslinker (MBA) of hydrogel in the absence (■, dashed line) and presence of loaded drug [BA (▲), NaB (Δ), loading 28.6%w/w]

The presence of NaB in the hydrogel at 37°C resulted in a significant increase in the swelling rate of PNIPA-H1 with no apparent effect on the swelling of the other hydrogels. The presence of BA caused between a 2-fold and 4-fold decrease in the swelling rate constant (k_s) of each of the hydrogels, depending on the swelling rate constant of the unloaded system. The swelling rate

constant (k_s) of PNIPA-H4 loaded with BA was significantly higher ($p<0.05$) than the other hydrogels at 37°C, with a resulting larger decrease in swelling rate due to the presence of BA.

The effect of NaB on PNIPA hydrogel swelling therefore appears to be osmotic in nature, increasing the swelling rate by about 50% at 25°C. The effect at 37°C was less significant due to a lack of swelling at that temperature. The swelling rate of PNIPA-H4 was not affected by NaB at either temperature where the rapid swelling was controlled by the relaxation of the polymer. BA was shown to control the swelling rate of the PNIPA hydrogels at both temperatures, attributable to benzoate-PNIPA binding.

The rate of swelling of the hydrogels in the presence of BA can be divided into two distinct groups, depending on whether the unloaded hydrogel showed significant swelling at the temperature of the experiment. Above the LCST (37°C) where only residual swelling occurred (in the series PNIPA-H1 to H3), the swelling rate and extent was further reduced by about 2-fold. In cases where a reasonable level of swelling occurred (i.e. for all the hydrogels at 25°C and in the case of PNIPA-H4 at 37°C), the swelling rate was reduced in proportion to the swelling rate of the unloaded hydrogel. In addition to the binding effect, drug dissolution, experimental temperature and polymer relaxation also played a limited role in the swelling of BA loaded PNIPA hydrogels. The influence of BA on swelling will be discussed further in the context of drug release.

8.3 DRUG RELEASE

The release of sodium benzoate and benzoic acid from the four hydrogels was examined at 25°C and 37°C.

The fraction released of NaB over time at both 25°C and 37°C is shown in Fig. 8.7. The fraction released was fitted to Equation 2.11 (*Peppas*) (Table 8.2) and there was a linear decrease in the diffusional exponents (n) with increasing percentage crosslinker at both 25°C (Fig. 8.8a) and 37°C (Fig. 8.8b). The lower the level of crosslinker, the more anomalous the release pattern, deviating from Fickian diffusion behaviour and resulting in a near zero-order release pattern. Fig. 8.8 also compares the swelling exponents of the four hydrogels loaded with NaB with the release exponents of NaB at 25°C (Fig. 8.8a) and 37°C (Fig. 8.8b) from the relevant hydrogel. Swelling of PNIPA-H1 and PNIPA-H2 at both temperatures was approximately diffusion controlled ($n \sim 0.5$), with concomitant release of the small, highly soluble, NaB controlled by penetration of the media ($n \sim 1.0$). In contrast, swelling of PNIPA-H4 was faster and was relaxation controlled ($n \sim 1.0$). Release of NaB from PNIPA-H4 was therefore diffusion controlled ($n \sim 0.5$) since the swelling front advanced faster than the drug could diffuse out.

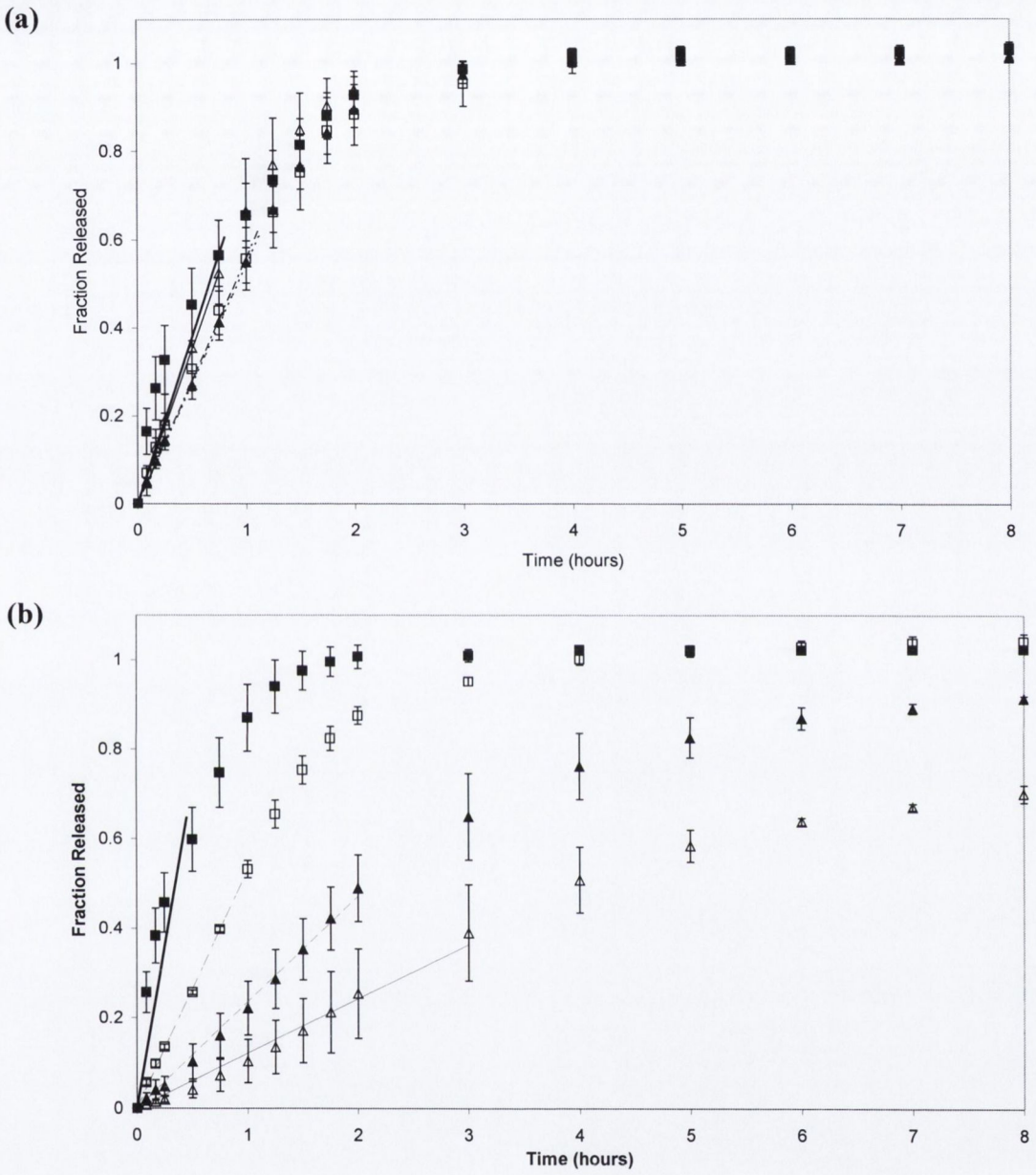

Fig. 8.7: Fraction released over time of NaB from PNIPA hydrogels containing various percentage crosslinker at 25°C (a) and 37°C (b) [PNIPA-H1 (Δ, solid line), PNIPA-H2 (▲, dashed), PNIPA-H3 (□, dash-dot line), PNIPA-H4 (■, bold line); loading 28.6%w/w] {profiles fitted to equation of form F=kt).

Table 8.2: Release rate constants (k_d) of BA or NaB from various hydrogels at 25°C and 37°C calculated using Equation 2.12 (*Higuchi*). Diffusional exponent *n* estimated using Equation 2.11 (*Peppas*). Release rate of NaB also estimated ($k_{d'}$) when value of n set as unity. Also shown are associated coefficients of determination (CD).

	$F=k_dt^{0.5}$		$F=kt^n$	$F=k_{d'}t$		
	Release rate constant ($min^{-0.5}$)($X10^3$)	**CD**	**Diffusional exponent (*n*)**	**Release rate constant (min^{-1})($X10^3$)**	**CD**	
25°C	**(k_{d25})**			**($k_{d'25}$)**		**k_{d37}: k_{d25}**
H1 (NaB)	8.188 ± 2.187	0.8602	0.970 ± 0.086	11.692 ± 3.009	0.9950	--
H2 (NaB)	8.230 ± 0.768	0.8738	0.967 ± 0.054	9.071 ± 0.807	0.9985	--
H3 (NaB)	8.583 ± 1.085	0.9213	0.823 ± 0.017	9.323 ± 1.164	0.9853	--
H4 (NaB)	10.819 ± 1.715	0.9905	0.535 ± 0.085	12.620 ± 1.826	0.7931	--
H1 (BA)	3.461 ± 0.034	0.9978	0.523 ± 0.009	--	--	0.40:1
H2 (BA)	2.998 ± 0.183	0.9674	0.560 ± 0.031	--	--	0.45:1
H3 (BA)	2.860 ± 0.053	0.9798	0.568 ± 0.044	--	--	0.48:1
H4 (BA)	3.274 ± 0.200	0.9958	0.476 ± 0.014	--	--	0.90:1
37°C	**(k_{d37})**			**($k_{d'37}$)**		**$k_{d'37}$: $k_{d'25}$**
H1 (NaB)	2.223 ± 0.910	0.7231	1.338 ± 0.220	1.774 ± 0.691	0.9545	0.15:1
H2 (NaB)	4.479 ± 0.783	0.8314	1.140 ± 0.335	3.940 ± 0.665	0.9765	0.43:1
H3 (NaB)	7.168 ± 0.184	0.8668	0.978 ± 0.038	8.851 ± 0.236	0.9980	0.95:1
H4 (NaB)	14.712 ± 2.021	0.9920	0.447 ± 0.032	23.949 ± 3.168	0.6918	1.90:1
H1 (BA)	1.371 ± 0.193	0.9888	0.442 ± 0.004	--	--	--
H2 (BA)	1.364 ± 0.406	0.9420	0.632 ± 0.104	--	--	--
H3 (BA)	1.373 ± 0.252	0.9750	0.546 ± 0.016	--	--	--
H4 (BA)	2.941 ± 0.149	0.9975	0.515 ± 0.018	--	--	--

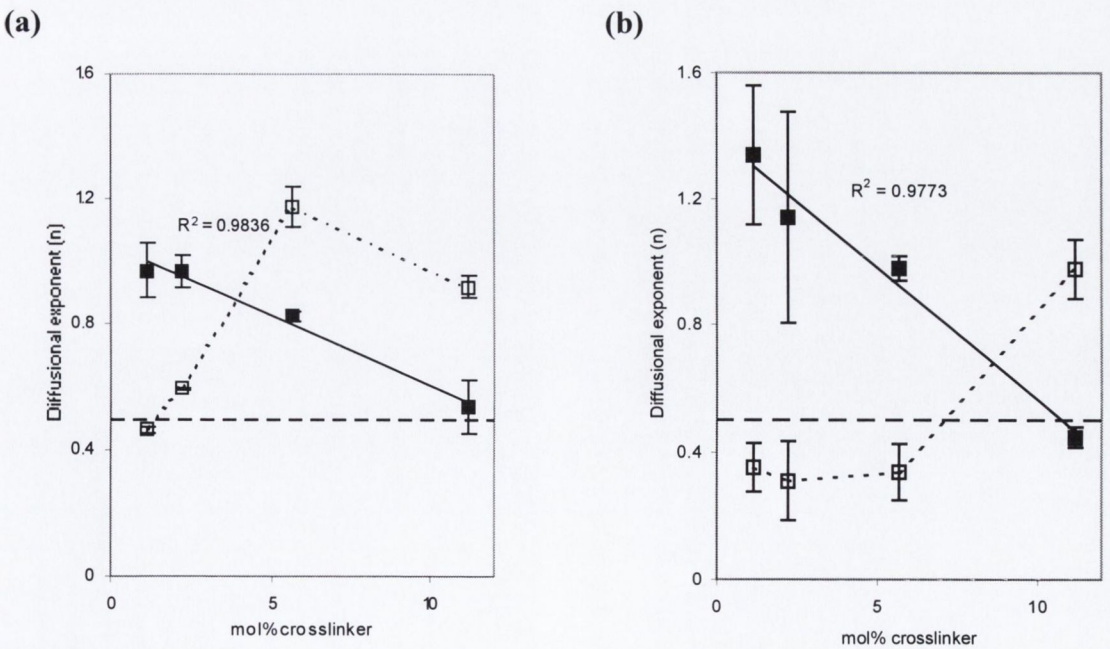

Fig. 8.8: Plot of diffusional exponents (*n*) obtained against percentage crosslinker in the hydrogel at (a) 25°C and (b) 37°C when the fraction of NaB released from the hydrogel was fitted to Equation 2.11 (*Peppas*) [Release exponents (■, solid line), Swelling exponents (□, dashed line)].

In order to compare the release rates, the release exponents were fixed as unity and reasonable fits were obtained as shown in Fig. 8.7b and Table 8.2. The release rate constants are given in Table 8.2 and a plot of the release constants against percentage crosslinker is shown in Fig. 8.9. At 25°C, release of NaB from each hydrogel was rapid and complete within about 3 hours (Fig. 8.7). Despite the differences in swelling rates between the NaB loaded hydrogels (Table 8.1), there was no apparent crosslinker dependent release pattern at 25°C (Fig. 8.9). The macropore size at equilibrium swelling was shown by SEM to decrease as the percentage crosslinker increased (Fig. 4.23). The swelling rate, however, increased at higher crosslinking levels (Fig. 8.5). The lack of a crosslinker dependent release pattern on the release rate of this small, highly soluble compound may be due to a balance of faster swelling rate/smaller average pore size with higher level of crosslinking, and slower swelling rate/larger pore size with lower levels of crosslinking.

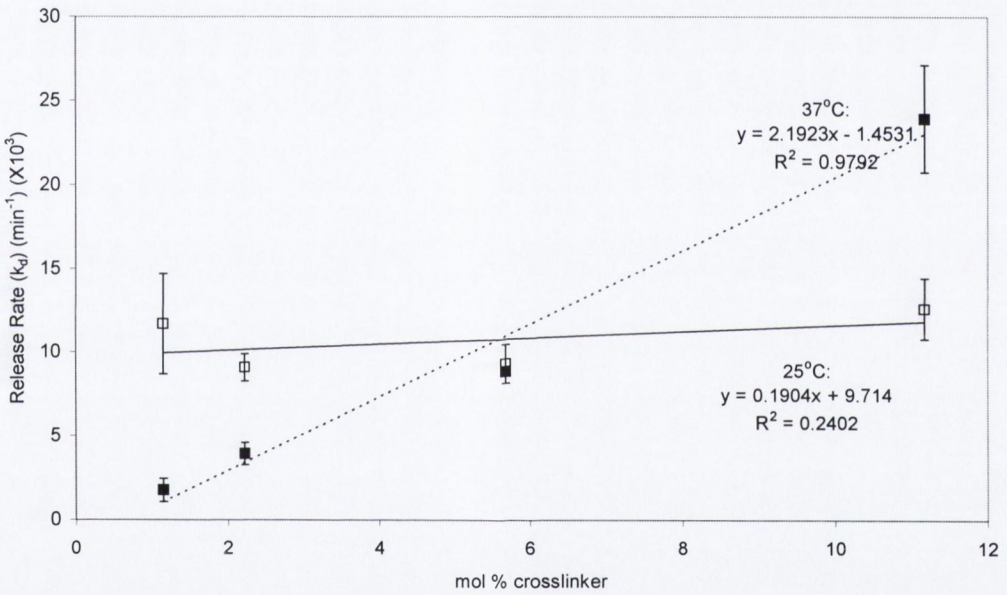

Fig. 8.9: Plot of change in release rate constant of NaB with percentage crosslinker in PNIPA-hydrogels at 25°C (■, solid line) and 37°C (□, dashed line).

Release of NaB at 37°C was highly dependent on the percentage crosslinker (Fig. 8.9). As the percentage crosslinker increased, the ability of the system to sustain drug release decreased. An increased rate of release is shown with increasing level of crosslinker, opposite to what may be expected and the patterns previously reported of crosslinker dependent release from hydrogels (e.g. Peppas and Lustig, 1985; am Ende *et al.*, 1995). In the case of PNIPA-H4, the relatively high level of crosslinker resulted in an influence of the water-soluble crosslinker on the hydrophilicity of the hydrogel, preventing a shrunken state at 37°C (Fig. 4.15a). A greater effective macropore size resulted as shown by SEM (Fig. 4.24) due an increase in the level of swelling, resulting in a greater free volume for solute transport. As a result, faster and more complete release of sodium benzoate was apparent than with the less highly crosslinked systems due to a larger effective pore size. In the

series PNIPA-H1 to PNIPA-H3, the equilibrium residual levels reached at this temperature were not significantly different from one another when media uptake was measured by gravimetric analysis (Fig. 4.15a) and there was no apparent pattern in the swelling rates (Table 8.1). In this series it may have been expected that the release rate would decrease with increasing percentage crosslinker due to increased hindrance to diffusion. The present study, however, suggested that pore size at the molecular level increases with increasing crosslinker in the series from PNIPA-H1 to PNIPA-H3, corresponding to an increase in the release rate of NaB. The SEM and nitrogen desorption data in Chapter 4 indicated an increase in the macro- and mesopore size with increasing crosslinking level in the hydrogel series. This pattern appeared to reflect the relative micropore size at the molecular level in the hydrogel series. The higher level of crosslinking may be acting in these systems to prevent complete hydrophobic collapse of the thermoresponsive polymer, resulting in greater effective pore sizes as the crosslinker content increased.

The data in Chapter 4 showed that the crosslinker had the effect of decreasing the thermosensitivity of the system, as measured by the magnitude of the phase transition detected by DSC. The decrease in thermosensitivity was also shown by the swelling patterns (Fig. 4.14), where the chemical nature of the crosslinker was significant in PNIPA-H4, preventing a shrunken state being achieved at 37°C. Larger effective pores resulted with PNIPA-H4 at 37°C, despite the higher percentage crosslinker. The ability of the hydrogels to thermally control the release rate of NaB therefore decreased with increasing crosslinker, as shown by the ratio between the release constants $k_{d'37}$:$k_{d'25}$ in Table 8.2. The ratio between the release constants ($k_{d'37}$:$k_{d'25}$) was 0.15:1 for PNIPA-H1, compared to a ratio of 1.90:1 for PNIPA-H4. The temperature responsiveness of PNIPA-H4 appeared to be negligible in controlling the release of the small, highly soluble salt. A significant increase in the release rate of NaB from PNIPA-H4 occurs when the temperature was increased (Fig. 8.5), due to the effect of temperature on the diffusion coefficient of the drug being greater than the effect of any decrease in swelling rate.

Over longer time-periods, the rate of release of NaB from PNIPA-H1 at 37°C effectively stopped at approximately 90% release (Fig. 7.10), with further release only apparent on dropping the temperature. Some physical entrapment of even this small molecule within the collapsed meshwork may therefore be a possibility as described in section 7.4.2. The complete loading of NaB was released from the other hydrogels at 37°C within the time period, where the effective pore sizes were larger.

Changing the crosslinking content of these thermoresponsive hydrogels could therefore alter the mechanism and rate of release of the small, highly soluble NaB. The release mechanisms were dependent on the percentage crosslinking, with relaxation-controlled swelling and diffusion-

controlled release at higher percentage crosslinking and diffusion-controlled swelling and relaxation-controlled release at lower percentage crosslinking.

The fraction released of BA with time at both temperatures is shown in Fig. 8.10.

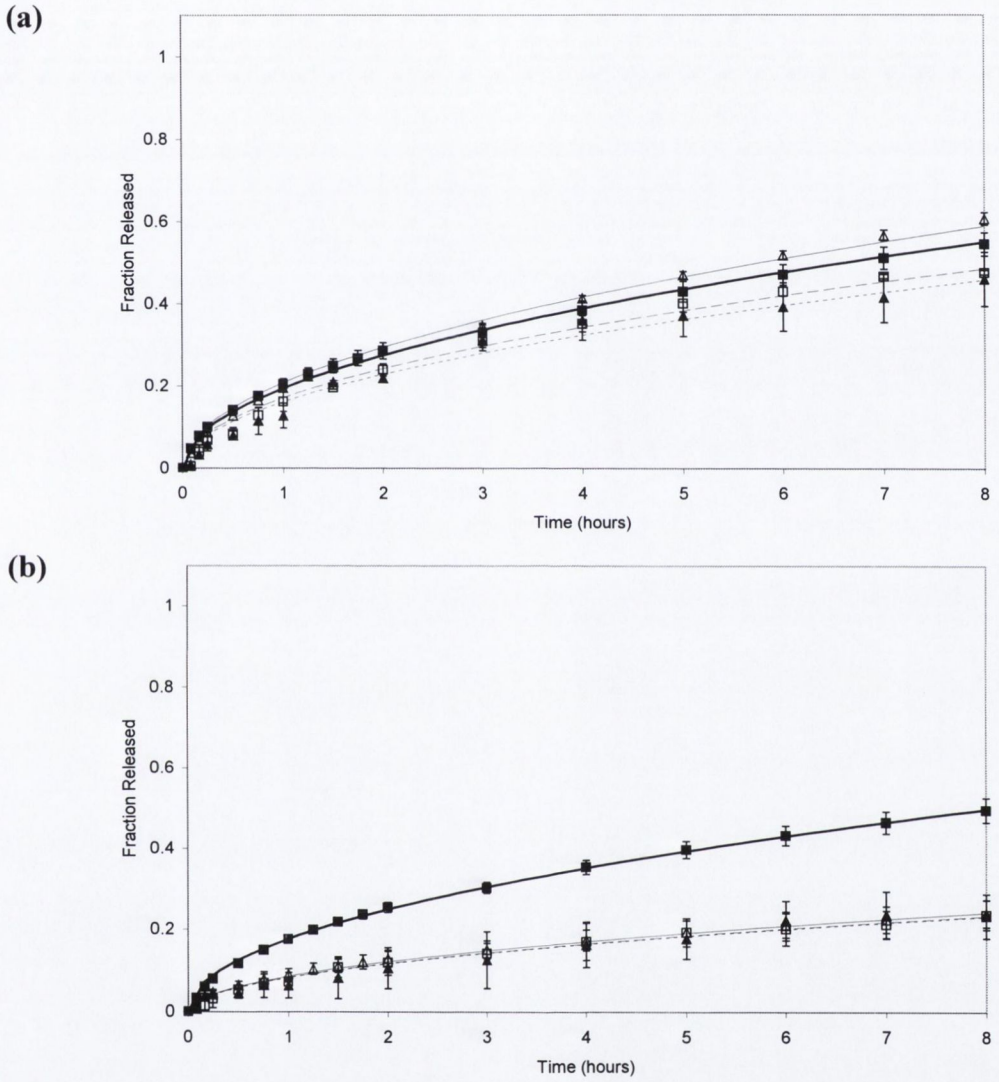

Fig. 8.10: Fraction released over time of BA from PNIPA hydrogels containing various percentage crosslinker at 25°C (a) and 37°C (b) [PNIPA-H1 (Δ, solid line), PNIPA-H2 (▲, dashed), PNIPA-H3 (□, dash-dot line), PNIPA-H4 (■, bold line); loading 28.6%w/w]

The release rate in each case was approximately proportional to the square root of time (Table 8.2). Hydrogel swelling and BA release was therefore diffusion controlled in all the systems, in contrast with the crosslinker dependent patterns seen with NaB (Fig. 8.8). A plot of the release rate constant (k_d) against percentage crosslinker is shown in Fig. 8.11. At 25°C, similar release rates were obtained in each case with no crosslinker dependent pattern apparent (Fig 8.11). The results obtained were consistent with the swelling profiles of the hydrogels in the presence of BA (Fig. 8.5), where there was no crosslinker dependent pattern seen. Benzoate-polymer binding influenced

the swelling rate and therefore the effective pore size of the systems, resulting in diffusion-controlled release of this small model compound from each of the hydrogels. As a consequence, the rate of release from the systems at 25°C was self-controlled by the drug (BA) and was essentially independent of the swelling kinetics of the PNIPA hydrogel used.

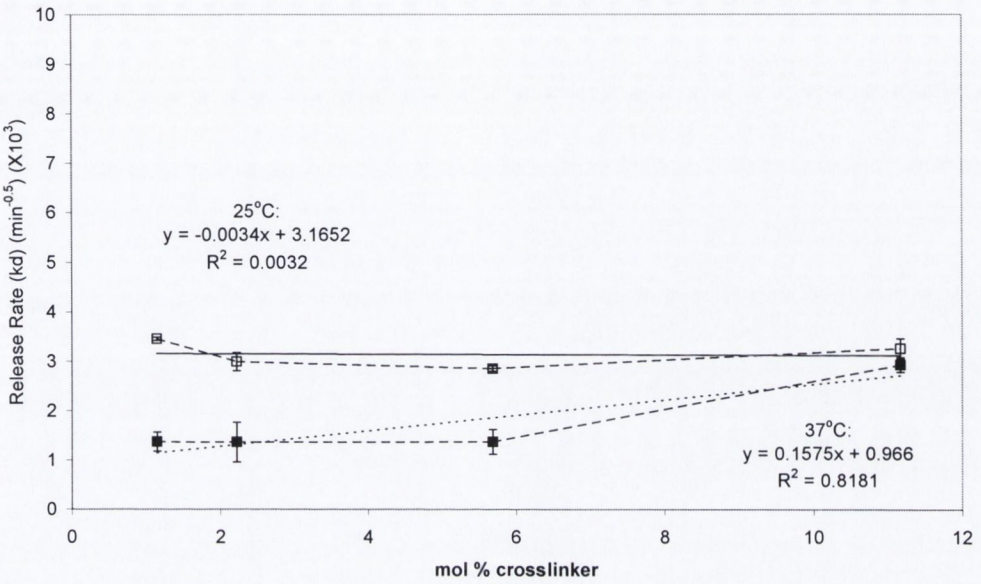

Fig. 8.11: Plot of BA release rate constant (k_d) from PNIPA hydrogels with various percentage crosslinker at 25°C (■) and 37°C (□).

At 37°C, the release rates of BA from PNIPA-H1 to H3 were not statistically different from each other ($p < 0.05$) but were lower than the release rate from PNIPA-H4. The patterns of release rates of BA from the hydrogels at 37°C corresponded to the pattern of hydrogel swelling in the presence of BA (Fig. 8.6). Fig. 8.12 plots the swelling rate constants of the gels loaded with BA against the release rate constants of BA at both 25°C (open symbols) and 37°C (closed symbols).

The systems can be divided into two distinct groups (indicated in Fig. 8.12), depending on whether the unloaded hydrogel showed significant swelling at the temperature of the experiment. The BA release rates followed the same pattern as the swelling rates, with the release rate from PNIPA-H4 at 37°C similar to the systems at 25°C.

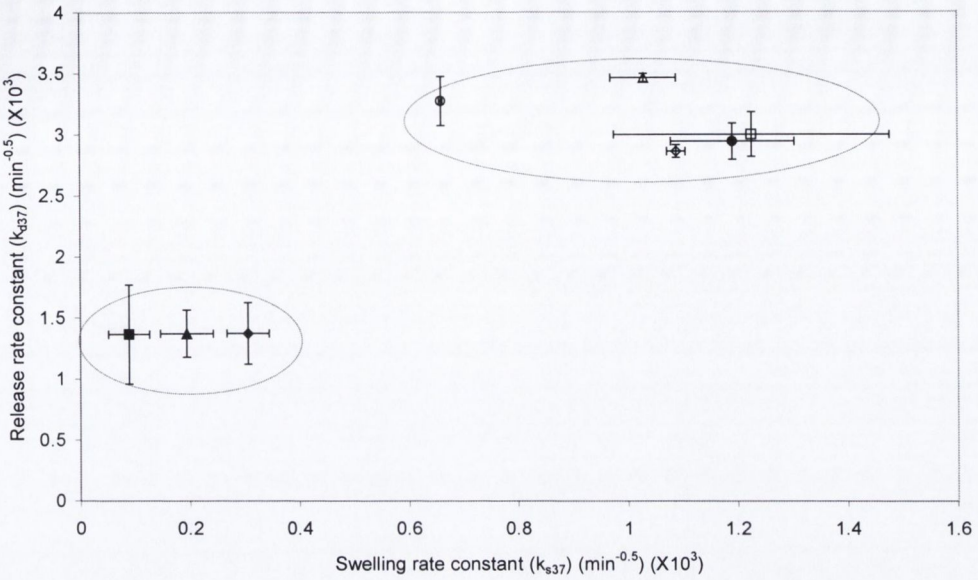

Fig. 8.12: Plot of BA release rate constant (k_d) from PNIPA hydrogels against the corresponding swelling rate constants (k_s) at 25°C (open symbols) and at 37°C (closed symbols) [PNIPA-H1 (Δ/▲), PNIPA-H2 (□/■), PNIPA-H3 (◊/♦), PNIPA-H4 (○/●)]

The swelling rate of the unloaded system was not seen as an important factor as the BA controlled the swelling of the hydrogel. The ability of the BA to control swelling resulted in control of pore size and therefore release rate. PNIPA-H4 was the only hydrogel of the series to show significant swelling at 37°C, with the swelling rate reduced in the presence of BA to a rate similar to that shown by all four BA loaded hydrogels at 25°C. The release rate of BA from PNIPA-H4 at 37°C was not statistically significant ($p < 0.05$) from the release rates of BA from PNIPA-H4 at 25°C.

8.4 CONCLUSIONS

Two contrasting thermoresponsive swelling/release systems were therefore shown in the present chapter using the same series of hydrogels with increasing crosslinking content.

The study of the release of NaB from thermoresponsive hydrogels showed a correlation between the type of swelling mechanism and type of release mechanism, both of which were dependent on the extent of crosslinking. Thermo-control of NaB decreased as the percentage crosslinker increased, opposite to previous crosslinker dependent release patterns reported in the literature. This effect was due to an increase in the effective pore size above the phase transition at higher levels of crosslinking. The mechanism and rate of release of the small, highly soluble NaB could therefore be altered by changing the crosslinking content of these thermoresponsive hydrogels.

The effectiveness of thermocontrol of larger water-soluble molecules would therefore also be affected by the percentage crosslinker present, depending on molecular size, and the choice of crosslinking content was shown to be useful as a method of altering the release kinetics of a drug. The different swelling rates and thermosensitivity of the systems would also impact on pulsed release, in particular on the rate and extent of hydrogel contraction and therefore the magnitude of the drug pulse.

The swelling and release patterns of BA loaded PNIPA hydrogels were completely different to the sodium salt due to the effect of binding to the hydrogel. Local concentration of the acid at the dissolving front would be sufficiently high to depress the phase transition temperature and therefore swelling of the hydrogel. There was no apparent pattern in the release rates with increasing level of crosslinker. The release rate of BA was therefore effectively self-controlled, with the only major difference depending on whether the hydrogel could obtain a collapsed state or not. Binding to these hydrogels would appear to be a unique method of controlling the swelling pattern of a hydrogel, which otherwise would show vastly different rates of relaxation and swelling.

CHAPTER 9

Molecular Modelling of Poly (N-isopropylacrylamide) and Drug-Polymer Interactions

9.1 INTRODUCTION

The use of computer simulations in the modelling and design of drug delivery systems has recently received some attention. Computer simulations have been used to model drug release studies (Zygourakis and Markenscoff, 1996; Jacobson, 1999) and have also been examined in other related areas such as the prediction of drug pharmacokinetic profiles (Plontke and Salt, 2003). Such studies are often carried out with the aim of using computer simulation to predict system properties, usually in conjunction with experimental studies. Molecular modelling of the diffusion properties of small molecules in polymers has also been performed with the aim of understanding the relationship between local atomic organization and molecular transport (Gee and Boyd, 1995; Li *et al.*, 1997; Muller-Plathe, 1998; Hadgett *et al.*, 2000; Hofmann *et al.*, 2000). Computer simulations of drug delivery devices are potentially useful for elucidating transport mechanisms and for designing new systems with desirable properties for the release of a particular drug.

Computer modelling of PNIPA in the literature is limited. Molecular dynamic simulation of poly(N-isopropylacrylamide) was attempted by Tamai *et al.* (1996a and 1996b) who examined water-polymer interactions with various thermoresponsive polymers. They showed that water-water hydrogen bonds were enhanced around hydrophobic methyl groups in the side chain of PNIPA and stabilised around hydrophilic groups of PNIPA. Longhli *et al.* (2004) recently examined the conformations of PNIPA at 300K and 310K, either side of the LCST. They found a more compact conformation at the higher temperature, in qualitative agreement with experiments.

Simulation studies in the literature examining the interactions between drugs and delivery devices are also limited. Poupaert and Couvreur (2003) recently reported a molecular simulation study of doxorubicin interacting with n-butyl polycyanoacrylate in an attempt to explore cohesion forces operating in the drug-polymer matrix. The cohesion was attributed to a blend of dipole-charge interaction, H-bonds and hydrophobic forces.

The studies carried out in chapter 6 indicated the presence of hydrophobic benzoate-PNIPA interactions. Such interactions were shown to influence the swelling of the hydrogel as well as the release rate and mechanism. The current study uses a commercial molecular modelling software package (Accelrys' Materials Studio® Version 2.1.5) to simulate PNIPA in the presence of water molecules and the three benzoates: BA, MHB and PHB. The ability to simulate the thermoresponsive nature of PNIPA is first examined. The presence of the three benzoates in the simulation is then examined in section 9.3.

9.2 PNIPA-WATER SYSTEMS

A preliminary investigation was performed on the polymer in the absence and presence of water molecules, in an attempt to simulate the physical characteristics of the system, in particular the glass transition temperature (Tg) and the thermoresponsive nature of the polymer. Model periodic cells were constructed in triplicate (section 3.6.2) containing a 20mer NIPA fragment in vacuo (Simulation A) and in the presence of 20 water molecules (Simulation B) or 100 water molecules (Simulation C).

9.2.1 Simulation of transition temperatures

Molecular dynamic simulations have previously been used to estimate the glass transition temperature (Tg) of amorphous synthetic polymers such as polyethylene (Han *et al.*, 1994) and poly(methyl methacrylate) (Tsige and Taylor, 2002) and of carbohydrates (Momany and Willett, 2002; Yoshioka *et al.*, 2003). A previous attempt has also been made to simulate the phase transition temperature of PNIPA by examination of polymer-water interactions (Tami *et al.*, 1996a and 1996b).

In the present study, isothermal-isobaric (NPT) molecular dynamic simulations were performed on the constructed periodic systems as described in section 3.6.2 over a series of temperatures from 500K to 250K, at intervals of 10K. In this simulation mode, the number of molecules (N), pressure (P) and temperature (T) were defined and remained constant while the cell volume was allowed to fluctuate in order to equilibrate the system. A sample input file in this mode is given in Appendix V(c). An average density value was obtained at each temperature (n = 3) as described in section 3.6.2 and plotted against the temperature value (Fig. 9.1a-c).

Discontinuities in the slope of the density vs. temperature plot were seen in Simulation A at approximately 320K and 420K (Table 9.1), attributable to the phase transition temperature (LCST) and glass transition temperature (Tg) of the polymer respectively. Simulation B also showed two discontinuities at slightly higher temperature values (Fig. 9.1b). The plasticising effect of water on the Tg of a polymer would be expected to decrease the Tg, although such an effect was not observed. There were no observed discontinuities in the density vs. temperature plot when the water content was increased further (Simulation C, Fig. 9.1c). As expected, the density of the system decreased as the number of molecules present increased.

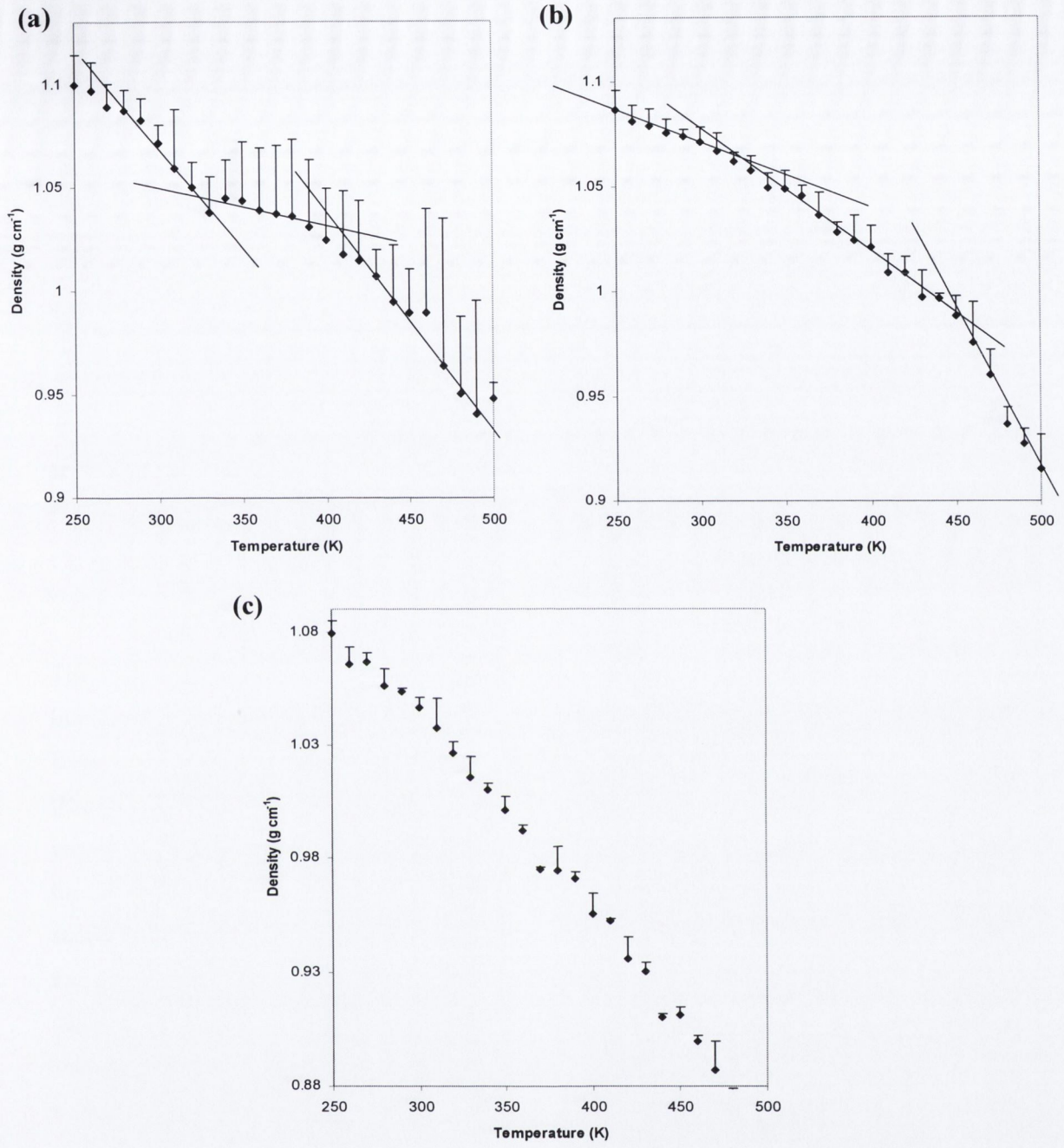

Fig. 9.1: Plot of density (n = 3; mean ± s.d.) of simulated systems at various temperatures. [Simulation A- PNIPA (MW 2265) (0 mol% water); Simulation B- 13.72mol% water; Simulation C- 44.40mol% water].

Density change at the LCST may be due to destruction of the polymer-water bonds caused by the raised temperature, resulting in volume increase and therefore density decrease at the higher temperature (Tamai *et al.*, 1996). An increase in the number of water molecules appears to influence the ability to detect such density fluctuations caused by specific polymer-water interactions. Apart from examining density changes, other authors have previously simulated the glass transition temperature of a polymer by examining changes in the temperature dependence of

the diffusivity of atoms (Tsige and Taylor, 2002; Yoshioka *et al.*, 2003). In contrast to the present study, studies by Yoshioka *et al.* (2003) and Momany and Willett (2002) showed difficulty estimating the Tg in the absence of moisture by this diffusivity method.

Table 9.1: Composition of various simulations and estimated glass transition temperatures (Tg) and phase transition temperatures (LCST). Experimental systems also shown. ND = Not Detectable

Simulation	**mol %**			**Tg (K)**	**LCST (K)**
	NIPA	Water	BA	**(Sim ± 10K)**	**(Sim ± 10K)**
Simulation A	100	0	0	420	320
Simulation B	86.28	13.72	0	440	310
Simulation C	55.7	44.3	0	ND	ND
Experimental	100	0	0	413 to 418[(a)]	---
Experimental	0.22	99.78	0	---	306 to 308 [(b)]
Literature	---	---	---	---	305 to 308[(c)]

[(a)] analysed by DSC at heating rates from 5 to 30°C/min

[(b)] corresponded to range 33.3°C-34.7°C using various concentrations of PNIPA in water and heating rates of 1°C to 6°C/min

[(c)] Schild (1992)

The experimentally determined Tg and LCST values of PNIPA-L3 (MW ~1.3 X10^6), as well as literature values, compared favourably with the simulated values (MW 2265) (Table 9.1). Experimentally determined Tg values depend on polymer molecular weight and heating rate (Rosen, 1993). Yoshioka *et al.* (2003), using the present software, demonstrated a simulated increase in Tg with increase in polymer fragment size. The choice of cooling rate would also affect the simulated Tg (Yoshioka *et al.*, 2003). The experimentally determined LCST of PNIPA is also susceptible to the method of determination, the heating rate (Schild and Tirrell, 1990) and possibly the polymer molecular weight (Schild, 1992). The use of density measurements in the present study to determine both the LCST and the Tg of a thermoresponsive polymer was shown to be susceptible to the water content of the system. Computer simulation would, however, appear to be a useful method for determining the transition temperatures of thermoresponsive polymers.

9.2.2 Diffusivity

The diffusivity of the polymer oxygen atoms (D_p) and the water oxygen atoms (D_w) was simulated at a temperature below (i.e. 300K) and above (i.e. 350K) the LCST as well as above (i.e. 450K) the Tg of the polymer. Isothermal molecular dynamics simulations at a constant volume (NVT) were performed on the equilibrated systems at each of these temperatures as described in section 3.6.3. A sample input file is shown in Appendix V (d). Mean square displacements (MSD) were calculated for oxygen atoms in both the polymer and the water molecules at each temperature (Appendix V (e)). The MSD is a measure of the average distance a molecule travels. If the molecule encountered no other molecules then the distance travelled would be proportional to the

time interval and the MSD would increase quadratically with time. Beyond this time, the motion is better described as a random walk, for which the MSD increases only linearly with time. The rate of growth of the MSD depends on how often the molecule suffers collisions. The limiting slope of MSD (t) is related to the self-diffusion constant D by the Einstein relation (Allen and Tildesley, 1987)

$$D = \lim_{t\to\infty} \frac{1}{6n} \sum_{i=1}^{n} \left\langle [x_i(t) - x_i(0)]^2 \right\rangle$$

Equation 9.1

where n is the number of molecules of a given type and x is the position of the centre of mass as a function of time. The broken brackets denote averaging over all choices of time origin, which in the current situation was the saved trajectory files (section 3.6.3). The motion of the atom should be considered for a sufficiently long time period for it to be in the linear regime. The linearity of log-log plots can be used to confirm that the calculation had converged. In the current study, the diffusion coefficients were determined from the linear portion of a log-log plot of the mean square displacement of the oxygen atoms as described by Yoshioka *et al.* (2003) and shown in Appendix V(e).

The estimated diffusion coefficients of water (D_w) and of the polymer (D_p) based on the three constructed and equilibrated configurations at each temperature are given in Table 9.2.

Table 9.2: Estimated diffusion coefficients of water (D_w) and polymer (D_p) oxygen atoms

		300K **D ($cm^2\ s^{-1}$)** **($\pm$ s.d.)**	**350K** **D ($cm^2\ s^{-1}$)** **($\pm$ s.d.)**	**450K** **D ($cm^2\ s^{-1}$)** **($\pm$ s.d.)**
Simulation A (100mol% NIPA)	D_p	1.47 (0.24) $X10^{-8}$	3.46 (1.34) $X10^{-8}$	6.59 (2.15) $X10^{-8}$
Simulation B (86.28 mol% NIPA)	D_p	1.89 (0.59) $X10^{-8}$	4.33 (2.30) $X10^{-8}$	8.34 (4.39) $X10^{-8}$
Simulation C (55.70 mol% NIPA)	D_p	4.92 (0.89) $X10^{-8}$	7.41 (0.75) $X10^{-8}$	27.60 (7.45) $X10^{-8}$
100mol% water	D_w	1.48 (0.59) $X10^{-6}$	2.26 (0.54) $X10^{-6}$	6.97 (1.36) $X10^{-6}$
Simulation C (44.3 mol% water)	D_w	0.21 (0.08) $X10^{-6}$	0.31 (0.10) $X10^{-6}$	0.96 (0.22) $X10^{-6}$
Simulation B (13.72 mol% water)	D_w	0.14 (0.06) $X10^{-6}$	0.27 (0.02) $X10^{-6}$	1.31 (0.51) $X10^{-6}$

Fig. 9.2(a) and (b) show plots of D_p and D_w respectively in the different simulations. The diffusion coefficients showed temperature dependence: at a fixed concentration they increased with increasing temperature in each system. The polymer had a relatively small diffusion constant due to its large size and the values of D may not be reasonable due to limited trajectory time used. The diffusion coefficients (D_p) obtained may therefore be caused by local motion within a void and not by diffusive transport (Jacobson, 1999). The values estimated for the D_w of pure water were lower than the self-diffusion coefficient of water at 298K ($D_w \sim 2.2 \times 10^{-5}$) (Angell *et al.*, 1976; Tyrrell and Harris, 1984), possibly due to the relatively short timescale used.

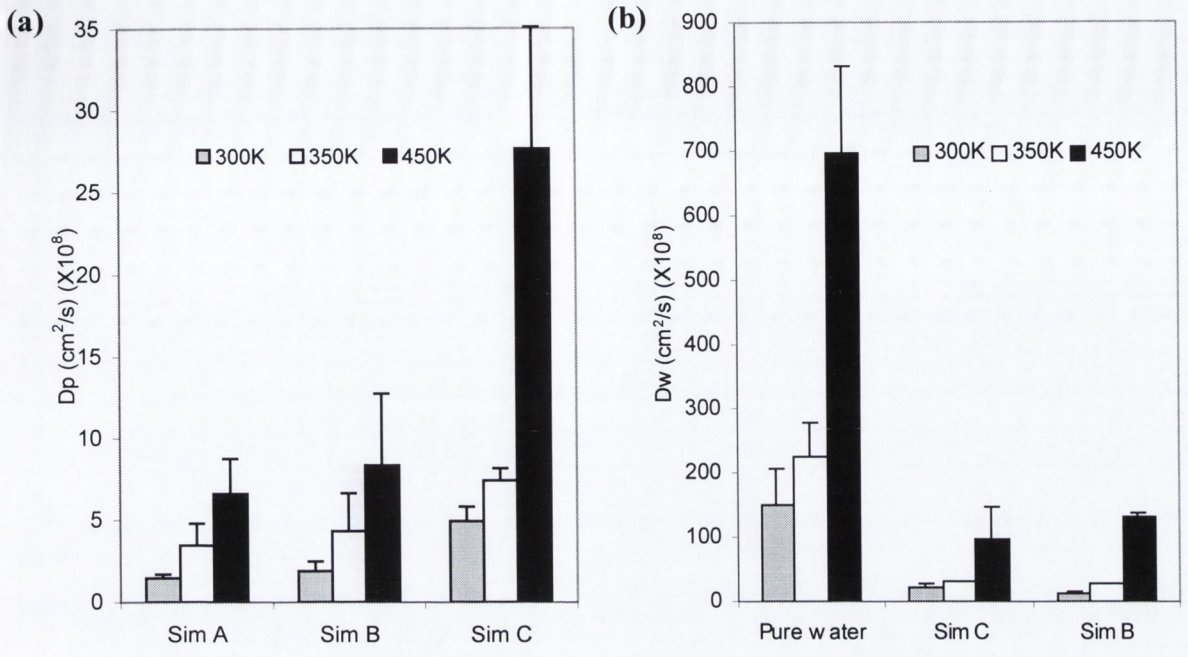

Fig. 9.2: Bar chart showing the estimated diffusion coefficients of (a) the polymer (D_p) in the three simulated systems at 300K, 350K and 450K and (b) water (D_w) in Simulations B and C at 300K, 350K and 450K in comparison to the pure water system

At a particular temperature, the simulated values of D_p and D_w were dependent on the presence of the other molecules. The diffusion coefficient of water decreased with increasing polymer content at each temperature, similar to the result obtained by Muller-Plathe (1998) using poly(vinyl alcohol). At 300K, there was an approximate 10-fold decrease in the diffusion coefficient of water from the pure water system to the system containing 13.7 mol% water (simulation B). The hydrogels examined in Chapter 4, containing up to 5.7 mol% crosslinker (PNIPA-H1 to H3), also slowed the diffusion coefficient of water during swelling at 298K by approximately 10-fold. Above the phase transition temperature, there was an increase in the simulated D_w due to the effect of the increase in temperature. The thermoresponsive polymer did not significantly decrease the diffusion coefficient of water with increase of temperature, as seen with the hydrogels used in Chapter 4. The simulations, however, do not represent water uptake by the polymer but rather diffusion in the presence of the polymer. A decrease in the diffusion coefficient with increasing temperature may not therefore be expected.

9.2.3 Bonding interactions

The influence of temperature and polymer concentration on the interactions of PNIPA and water molecules was examined using Simulation B and Simulation C. The various functional groups of PNIPA and water were labelled as shown in Fig. 9.3.

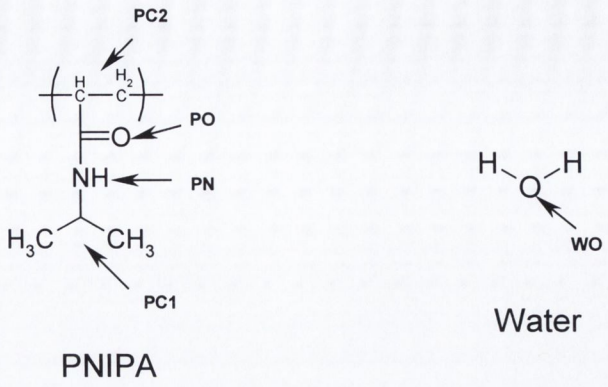

Fig. 9.3: Structure of PNIPA and water with relevant atoms/groups labelled [PO = polymer oxygen atom, PN = polymer nitrogen atom, PC1 = polymer isopropyl group, PC2 = polymer carbon backbone, WO = water oxygen atom].

The radial distribution function, also known as the pair correlation function g(r), is commonly used in computer simulations for the study of specific interactions between molecules e.g. hydrogen bonding (Ladanyi and Skaf, 1993). The g(r) describes fluctuations in density around a given atom. The function is essentially a measure of the average number of atoms found at a given distance in all directions. The peaks in the g(r) indicate where the atoms spend the most time. A typical g(r) is zero up until a certain distance and then has a peak, corresponding to the average number of atoms at that distance in the simulation. The g(r) of water (at 300K, 350K and 450K) is shown in Fig. 9.4a and is a typical radial distribution function indicating hydrogen bonding.

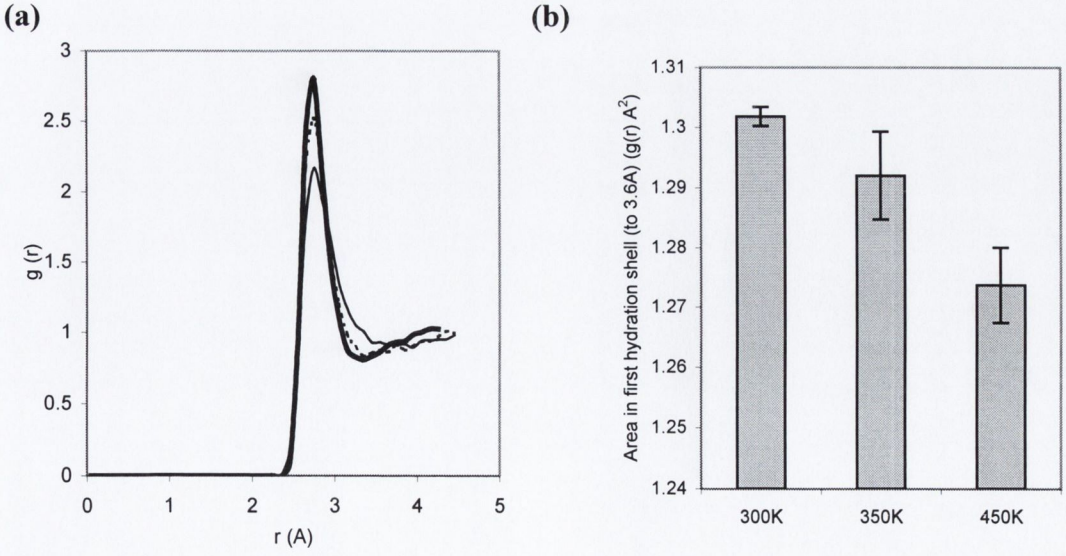

Fig 9.4: (a) Radial distribution function of water oxygen atoms at 300K (bold line); 350K (dashed line); 450K (solid line) (b) Area under curves in first hydration shell, defined as area up to 3.6Å.

Tamai *et al.* (1996a) described a pair of water molecules as being hydrogen bonded if the distance between the oxygen atoms is less than 3.60Å, the distance between one oxygen atom and the hydrogen atom is less than 2.45Å and the angle between one oxygen atom and an oxygen-hydrogen pair is less than 30°. Simulations and experimental data on water show a peak in g(r) near 2.8Å, followed by a local minimum near 3.5Å (Ladanyi and Skaf, 1993), similar to the data in Fig. 9.4a. These values define the average radius of the first hydration shell. The area under the curves up to a distance of 3.6Å was therefore calculated by integration of the curves and is shown in Fig. 9.4b. The peaks become less intense and the valleys are raised with increasing temperature resulting in a decrease in the area under the curve.

The g(r) between the various functional groups of aqueous mixtures can also be calculated at different temperatures. The radial distribution function between water oxygen atoms (WO) and the various functional groups of the polymer are shown in Fig 9.4 for Simulation B.

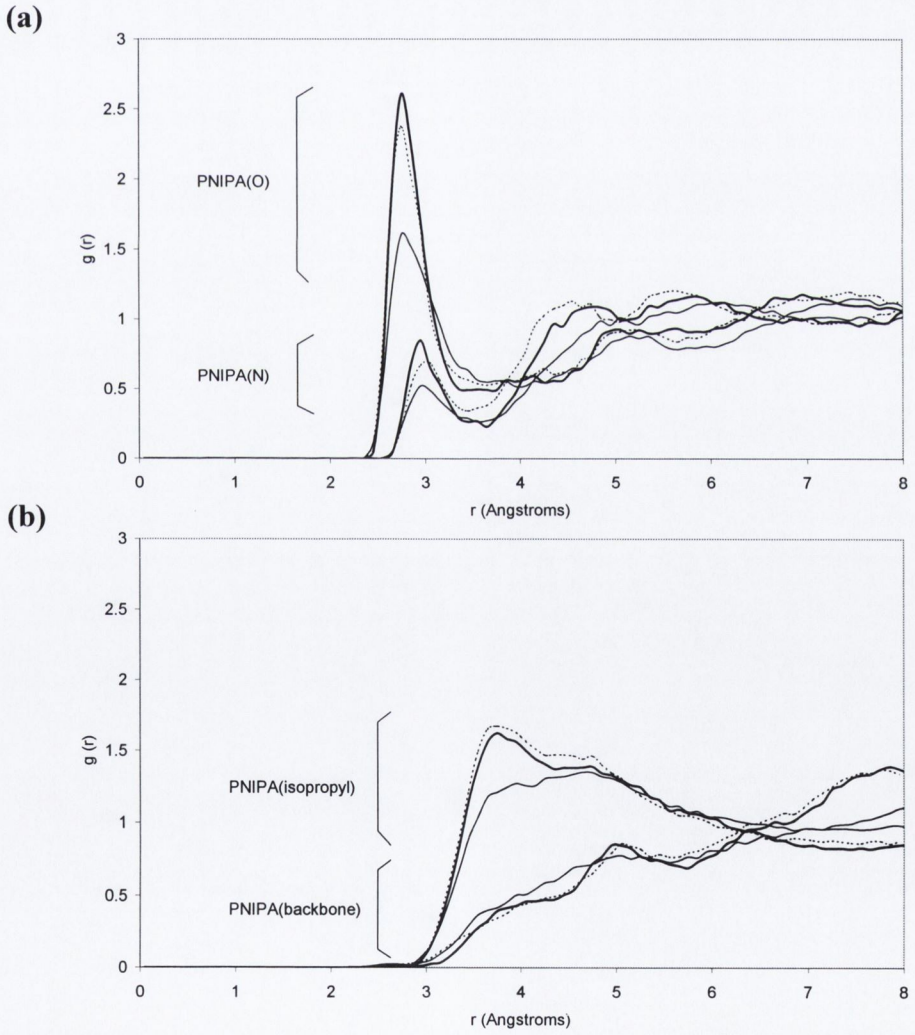

Fig. 9.4: Water-PNIPA radial distribution function g(r) of Simulation B at 300K (bold lines), 350K (dashed lines) and 450K (solid lines) between water oxygen (WO) and polymer functional groups [(a) polymer oxygen (PO), polymer nitrogen (PN); (b) polymer isopropyl (PC1), polymer backbone (PC2)].

Fig. 9.4a shows the g(r) function for Simulation B between the water molecules and the hydrophilic groups of the polymer, namely the oxygen atom (PO) and the nitrogen atom (PN). Large peaks were found at a distance of ~3Å between the WO and the hydrophilic polymer groups, indicating the presence of hydrogen bonds as described by the definition of Tamai *et al.* (1996a). The peaks were integrated around the hydrophilic groups (PN, PO) up to 3.6Å and around the hydrophobic groups (PC1, PC2) up to 6Å (Table 9.3). The resulting areas give an indication of the relative position of the water molecules in relation to each functional group, with the greater the area, the smaller the average distance between the two atoms.

Table 9.3: Areas under the g(r) curves involving the water or polymer groups shown at 300K, 350K and 450K

Water (W) and PNIPA(P) groups involved	**Cutoff**	**300K Area (± s.d.)**	**350K Area (± s.d.)**	**450K Area (± s.d.)**
W(oxygen)-P(oxygen)	3.6Å	1.26 ± 0.11	1.20 ± 0.17	1.04 ± 0.08
W(oxygen)-P(nitrogen)	3.6Å	0.45 ± 0.10	0.44 ± 0.12	0.30 ± 0.03
W(oxygen)-P(isopropyl grp)	6Å	3.64 ± 0.28	3.62 ± 0.27	3.26 ± 0.10
W(oxygen)-P(carbon backbone)	6Å	2.23 ± 0.54	2.15 ± 0.40	2.22 ± 0.40

Hydrogen bonding was particularly prominent around the carbonyl group in the polymer, indicated by the magnitude of the peak shown. Some hydrogen bonding between water molecules and PN was also apparent although of less significance. The influence of increasing temperature on the peak size was also shown. With increasing temperature, the heights of the peaks were reduced, indicating a decrease in the hydrogen-bonding tendency of the polymer. Tamai *et al.* (1996b) and Yoshioka *et al.* (2003) also found that the height of the peaks as measured by g(r) decreased with increasing temperature.

Broader peaks at ~4Å were seen between WO and the isopropyl groups of the polymer (PC1) (Fig. 9.4b) where hydrogen bonding was absent. The presence of a peak around the isopropyl group in the polymer side chain did, however, indicate that the water molecules were structured in this region as previously indicated by Tamai *et al.* (1996b). The height of the peaks also decreased slightly with increasing temperature. The effect of increasing temperature was therefore to decrease the number of water molecules in the hydrophilic and hydrophobic regions around the polymer, with a corresponding increase in the bulk water region. The desolvation of the polymer at higher temperatures can therefore account for the thermoresponsive nature of the polymer. Tamai *et al.* (1996b) also showed that the water molecules associated with non-thermoresponsive polymers showed more tendency to remain in the hydration shell at high temperatures.

The radial distribution function of WO around the polymer functional groups in Simulation C was also examined. Simulation C contained a greater number of water molecules (Table 9.1) than

Simulation B and there were no observed discontinuities in the density vs. temperature plot (Fig. 9.1c). Similar peaks to those shown in Simulation B (Fig 9.4) were seen in the radial distribution function plots, although at a lower intensity as indicated in Table 9.4.

Table 9.4: Comparison of magnitude of pair correlation functions in simulation B and simulation C at 300K

Water (W) and Polymer(P) groups involved		**Simulation B 13.72mol% water Area (± s.d.)**	**Simulation C 44.30mol% water Area (± s.d.)**	**100mol% water Area (± s.d.)**
W(oxygen)-W(oxygen)	3.6Å	4.64 ± 0.24	2.37 ± 0.01	1.30 ± 0.01
W(oxygen)-P(oxygen)	3.6Å	1.26 ± 0.11	0.63 ± 0.04	--
W(oxygen)-P(nitrogen)	3.6Å	0.45 ± 0.10	0.18 ± 0.02	--
W(oxygen)-P(isopropyl grp)	6Å	3.64 ± 0.28	2.49 ± 0.06	--
W(oxygen)-P(carbon backbone)	6Å	2.23 ± 0.54	1.26 ± 0.21	--

There was a decrease in the intensity of the first peak in the water g(r) with decreasing polymer concentration (Fig. 9.5).

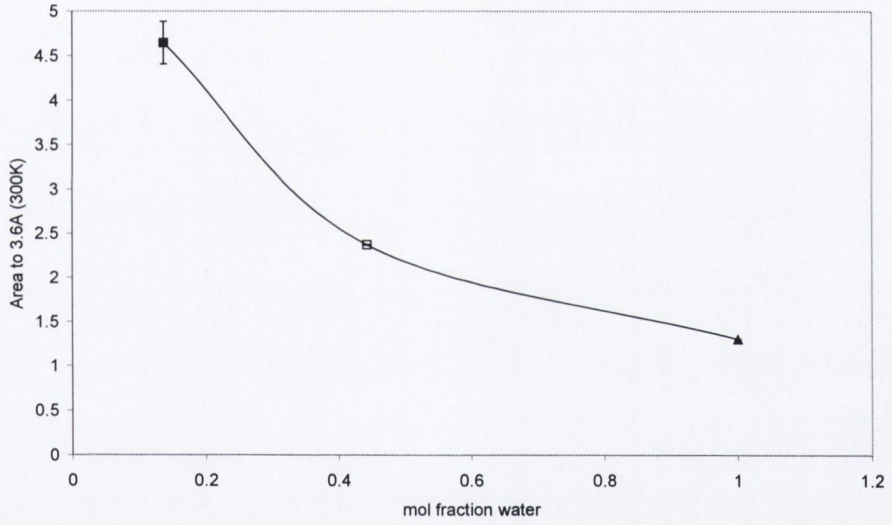

Fig. 9.5: Area in first hydration shell (to 3.6Å) of water oxygen-oxygen (WO-WO) pair correlation function with increasing mole fraction of water in the presence of PNIPA. [Simulation B (■), Simulation C (□), pure water (▲)].

Ladanyi and Skaf (1993) also described a decrease in the intensity of the first peak in the solvent water g(r) with decreasing solute concentration, similar to the present study. The decreased height of the pair distribution was ascribed to the dimished structural state of the water species (Ladanyi and Skaf, 1993), but may also be due to an increase in the solvent (water) average density when solute concentration decreased (Vaisman and Berkowitz, 1992).

The molecular modelling software therefore successfully characterised the phase transition temperatures of the polymer and described the relative positioning of water molecules around the

functional groups of the polymer. The diffusivity values of water were lower than expected from experimental data, although the expected trends with temperature change were shown.

9.3 POLYMER-BENZOATE-WATER SYSTEMS

Two sets of experiments were performed to examine benzoate-polymer interactions. The effect of the benzoates on the Tg/LCST of the polymer was estimated using density versus temperature measurements. In addition, simulations were performed between the benzoates and the polymer in the presence and absence of water molecules and the diffusivity of the atoms as well as the pair correlation function between the various groups were determined.

9.3.1 Simulation of transition temperatures

In order to examine the effect of the benzoates on the polymer, simulations containing different polymer/water/BA concentrations as shown in Table 9.5 were prepared and equilibrated over a range of temperatures as described in section 3.6.2. Plots of density values against temperature are shown in Fig. 9.6. Lines of best fit are also shown for each temperature segment to reveal approximations of the polymer Tg/LCST, given in Table 9.5.

Table 9.5: Composition of various simulations and estimated glass transition temperatures (Tg) and phase transition temperatures (LCST). Experimental systems also shown

Simulation	**mol %**			**Tg (K)**	**LCST (K)**
	NIPA	Water	BA	**(± 10K)**	**(± 10K)**
Simulation D	82.26	0	17.74	360	290
Simulation E	82.44	13.11	4.45	380	310
Simulation F	78.93	12.55	8.52	ND	310
Simulation G	69.99	11.13	18.88	~390	ND
Experimental	90.66	0	9.34	$381.47 \pm 0.69^{(a)}$	---
Experimental	81.19	0	18.81	$367.07 \pm 0.77^{(a)}$	---
Experimental	71.57	0	28.43	$355.08 \pm 1.87^{(a)}$	---
Experimental	0.22	99.75	0.015	---	$304.27 \pm 0.03^{(b)}$

[(a)] heating rate 10°C/min; [(b)] heating rate 2°C/min; ND = not detectable

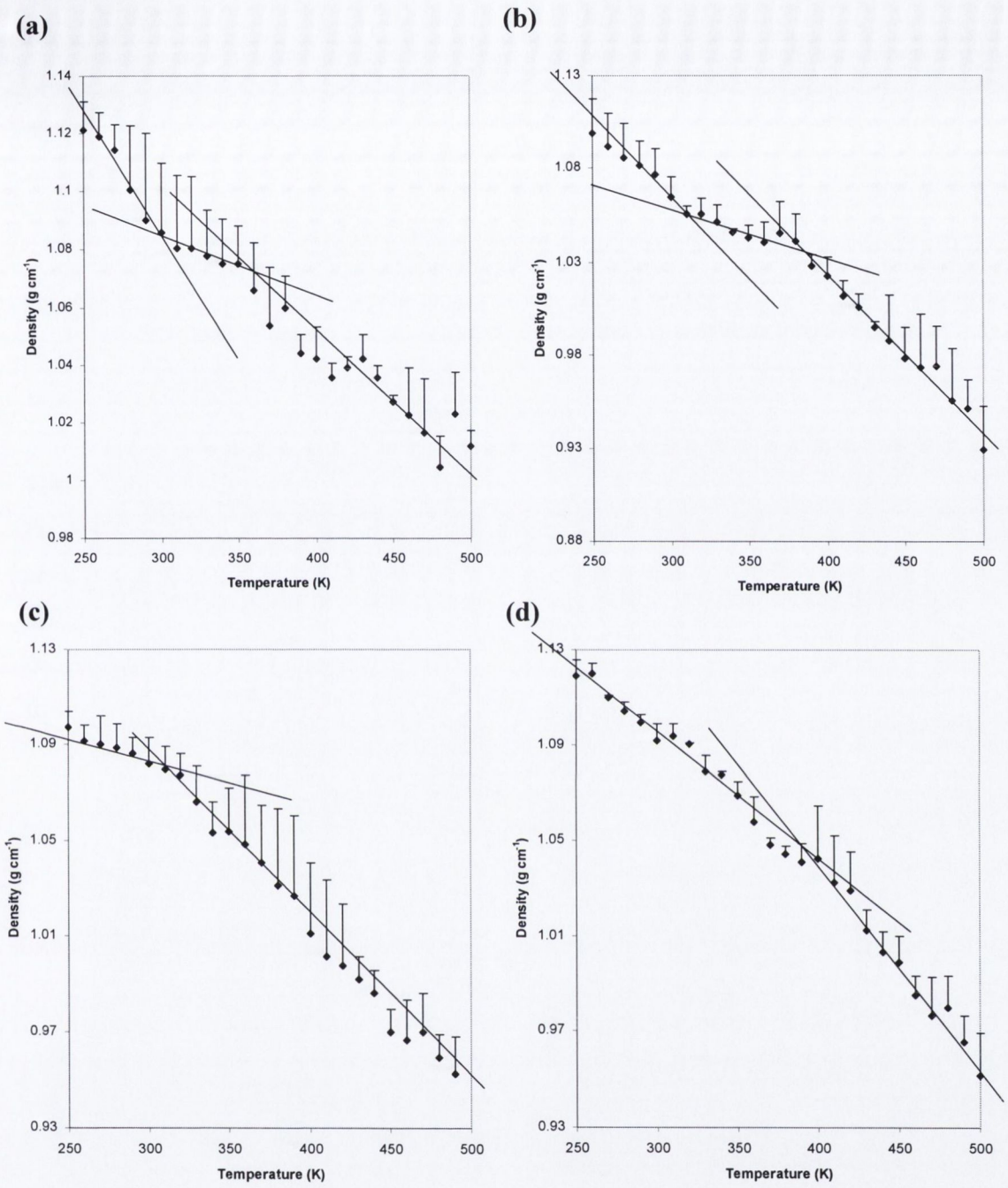

Fig. 9.6: Plot of density (n=3) of simulated systems at different temperatures containing PNIPA and various percentages of water and BA [(a) Simulation D (0 mol% water, 17.74 mol% BA); (b) Simulation E (13.11 mol% water, 4.45 mol% BA); (c) Simulation F (12.55 mol% water, 8.52 mol% BA); (d) Simulation G (11.13 mol% water, 18.88 mol% BA)]

As can be seen in Fig. 9.6, at higher water/BA concentrations the phase transitions of the polymer were more difficult to observe, similar to the result shown in Fig. 9.1 where the transitions could not be detected at higher aqueous concentrations. A decrease in the estimated Tg (Table 9.5) was observed in each simulation to values of 360-390K compared to the system without drug where the

Tg was in the range 420-440K. A concentration dependent pattern could not, however, be shown. The effect of BA on the Tg can possibly be attributed to the plasticising effect of the small substance, although such a plasticising effect was not observed in the pure polymer-water systems described in section 9.2 above (Table 9.1). Contributions from hydrophobic binding interactions, as described in section 6.2, are another possible reason. The present simulations were not sensitive to drug concentrations and so a similar effect on the Tg was observed in each system.

Discontinuities in the slope of the density versus temperature plot were also seen around 300K, attributed to the LCST of the polymer. The LCST was apparent in the current simulations, although a significant shift in the position of the LCST was not observed.

The study in Chapter 6 showed that MHB and PHB also decreased the Tg and LCST of PNIPA. Further simulations were performed containing the 20mer polymer and 5 benzoate molecules in the presence and absence of 20 water molecules (Table 9.6). Fig. 9.7 shows the effect of MHB (5 molecules, 21.20 mol%) and PHB (5 molecules, 24.16 mol %) on the Tg of PNIPA as measured by density change. Estimated Tg and LCST values are shown in Table 9.6 together with estimates from the polymer simulations and the BA-polymer simulations.

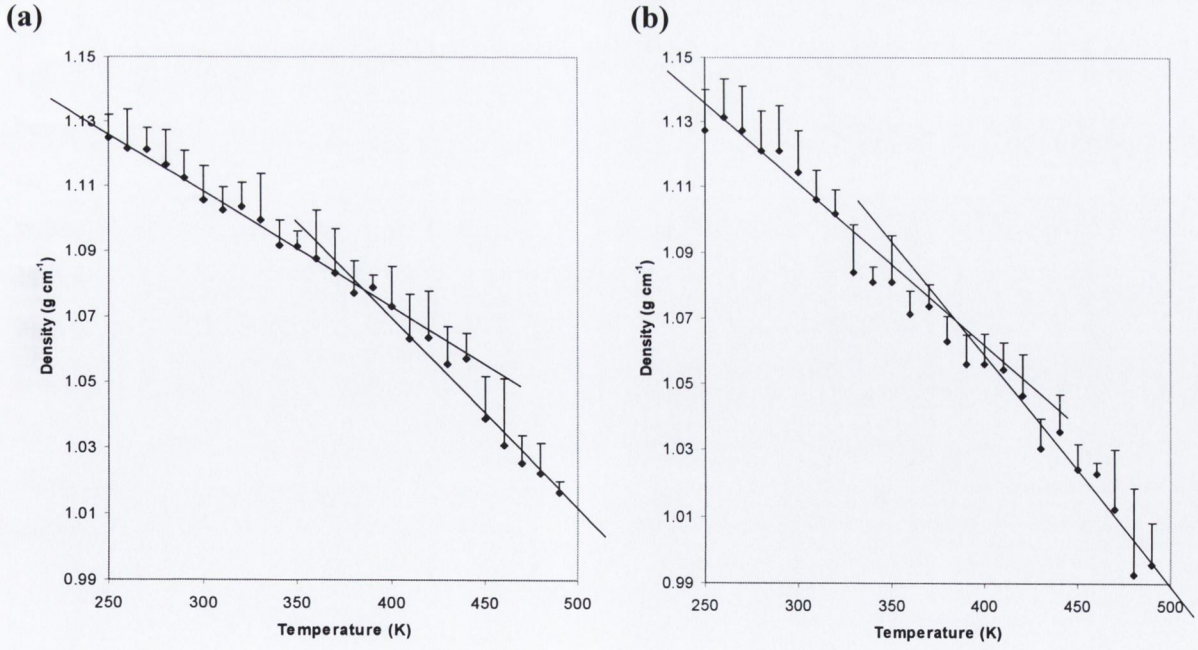

Fig. 9.7: Plot of density (n = 3; mean ± s.d.) of simulated systems at different temperatures containing PNIPA and (a) MHB (5 molecules, 21.20 mol%) and (b) PHB (5 molecules, 24.16 mol %).

Table 9.6: Composition of various simulations and estimated glass transition temperatures (Tg) and phase transition temperatures (LCST).

Simulation	Number of molecules			Tg (K) (± 10K)	LCST (K) (± 10K)
	NIPA	H_2O	Drug		
Sim A	20	0	0	420	320
Sim B	20	20	0	440	310
Sim D	20	0	5 BA	360	290
Sim E	20	20	5 BA	380	310
Sim H	20	0	5 MHB	380	ND
Sim J	20	20	5 MHB	380	ND
Sim K	20	0	5 PHB	370	ND
Sim L	20	20	5 PHB	380	ND

The discontinuity seen with temperature change was not as clear in the presence of these larger molecules. The simulations showed a Tg at approximately 380K with no apparent LCST detectable in the temperature range examined. A decrease in Tg in comparison to the pure polymer simulations (Simulation A, B) was still apparent, although no correlation could be seen between drug size/hydrophobicity and simulated Tg.

9.3.2 Diffusivity

The diffusivity of the three benzoates in the presence of the polymer was also examined and the values obtained are shown in Table 9.7. Due to the relatively large size of the polymer and benzoate molecules and the limited simulation times used, the observed values shown may correspond to diffusion within a void. As a result, error bars were relatively large. Some trends were, however, observed. The diffusivity of the polymer, benzoates and water all increased with increasing temperature. The ability of the polymer to decrease the diffusion rate of the drugs at higher temperatures was not shown, possibly due to the size of the simulated system and length of simulation (20mer polymer over 50ps). Longhi *et al.* (2004) recently simulated a 50mer PNIPA in 20,211 water molecules over 4,400ps and showed a more compact configuration at 310K than at 300K, in qualitative agreement with experiments. Such a system may potentially influence the diffusion of a drug molecule at higher temperature as shown experimentally in Chapter 7.

Table 9.7: Estimated diffusion coefficients of polymer (D_p), drug (D_d) and water (D_w)

	Number of molecules				300K D ($cm^2 s^{-1}$) ($X10^{-8}$)($\pm$ s.d.)	350K D ($cm^2 s^{-1}$) ($X10^{-8}$)($\pm$ s.d.)	450K D ($cm^2 s^{-1}$) ($X10^{-8}$)($\pm$ s.d.)
	NIPA	H_2O	Drug				
Sim D	20	0	5BA	D_p	1.68 $\pm$ 0.47	3.94 $\pm$ 2.08	6.68 $\pm$ 0.25
				D_d	6.24 $\pm$ 3.27	17.74 $\pm$ 8.31	38.02 $\pm$ 24.31
Sim E	20	20	5BA	D_p	2.06 $\pm$ 0.22	4.58 $\pm$ 2.13	9.36 $\pm$ 0.83
				D_d	8.84 $\pm$ 1.80	23.49 $\pm$ 10.46	40.99 $\pm$ 7.08
				D_w	14.45 $\pm$ 3.12	44.40 $\pm$ 14.25	160.38 $\pm$ 22.58
Sim H	20	0	5 MHB	D_p	2.55 $\pm$ 1.35	3.94 $\pm$ 1.23	8.51 $\pm$ 2.17
				D_d	5.24 $\pm$ 1.58	13.07 $\pm$ 2.70	28.22 $\pm$ 5.66
Sim J	20	20	5 MHB	D_p	2.26 $\pm$ 0.64	4.39 $\pm$ 3.71	10.76 $\pm$ 3.50
				D_d	5.02 $\pm$ 1.26	12.84 $\pm$ 10.53	30.22 $\pm$ 6.72
				D_w	14.83 $\pm$ 2.08	47.67 $\pm$ 13.25	130.07 $\pm$ 6.22
Sim K	20	0	5 PHB	D_p	1.71 $\pm$ 0.69	3.66 $\pm$ 1.43	6.54 $\pm$ 2.15
				D_d	2.26 $\pm$ 0.43	7.61 $\pm$ 3.00	22.48 $\pm$ 9.26
Sim L	20	20	5 PHB	D_p	2.86 $\pm$ 1.11	7.02 $\pm$ 3.09	15.14 $\pm$ 9.86
				D_d	5.10 $\pm$ 3.12	12.18 $\pm$ 1.59	20.64 $\pm$ 4.10
				D_w	23.78 $\pm$ 17.04	34.07 $\pm$ 8.67	162.08 $\pm$ 50.74

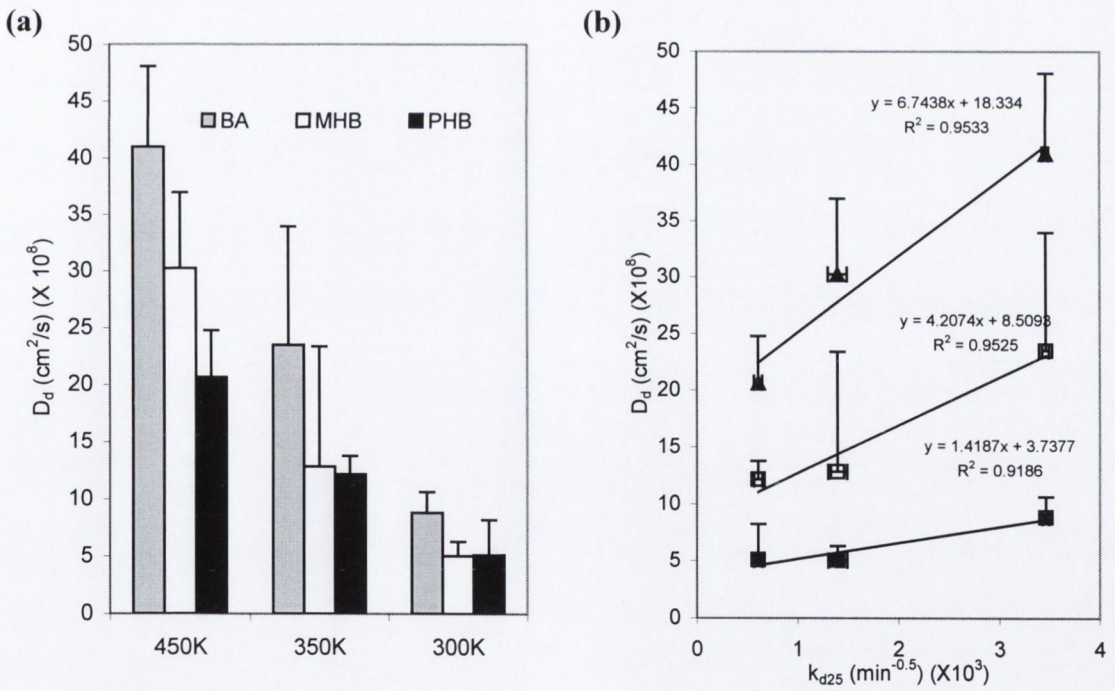

Fig. 9.8: Simulated diffusion coefficient of model drugs (D_d) in presence of polymer and water (Sim E, J and L) (a) at 300K, 350K and 450K and (b) plotted against the release rate constants (k_{d25}) at 25°C (298K) from PNIPA-H1 [300K (■), 350K(□) and 450K(▲)].

There was a decrease in the diffusion coefficient of the benzoates (D_d) with increasing size in both the presence (Fig. 9.8a) and absence of water molecules. The simulated values were linearly proportional to the diffusional release rate constants (k_d) from PNIPA-H1 at 25°C (Fig. 9.8b). The

simulated diffusion coefficients obtained were therefore useful in predicting the relative release rate of a series of molecules from the polymer.

9.3.3 Bonding interactions

The functional groups of the polymer and benzoates in the simulated systems shown in Table 9.7 were further examined to investigate potential interactions. The various functional groups were labelled as shown in Fig. 9.9.

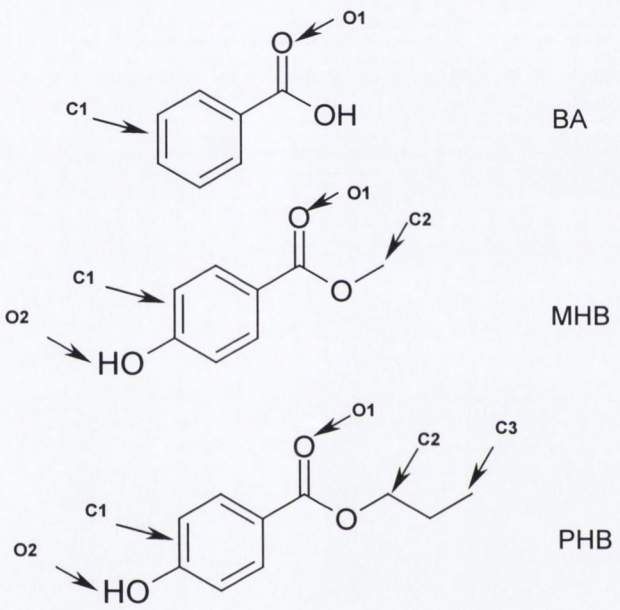

Fig. 9.9: Structure of BA, MHB and PHB with relevant atoms and groups labelled [C1 = benzene ring, O1 = side chain carboxyl atom, O2 = para hydroxy group, C2/C3 = side chain ester carbons as shown]

Potential interactions between PNIPA and the benzoates may occur between the hydrophilic groups (PO, PN, O1, O2) in the form of hydrogen bonding or between the hydrophobic groups (PC1, PC2, C1, C2, C3) in the form of hydrophobic binding. Hydrophobic binding between the benzene ring of the benzoates and the polymer groups was shown in Chapter 6 using FTIR. Binding also increased with increasing length of the side-chain ester.

Potential hydrogen bonding between the polymer amide group (PO, PN) and the benzoate oxygen groups (O1, O2) was examined at 300K in the presence (Simulations E, J, L) and absence (Simulations D, H, K) of water molecules. The curves obtained were integrated up to 3.6Å and the areas obtained are shown in Table 9.8. Also shown are the areas obtained on integration of the g(r) curves between the hydrophobic groups up to 6Å.

Table 9.8: Area obtained on integration of g(r) function up to 3.6Å for hydrophilic groups and up to 6Å for hydrophobic groups

	Polymer functional group	Benzoate functional group	BA Area at 300K	MHB Area at 300K	PHB Area at 300K
Hydrophilic groups (3.6Å)					
Vacuum	PN	O1	0.71 ± 0.46	0.62 ± 0.48	0.71 ± 0.33
Water	PN	O1	0.70 ± 0.11	0.24 ± 0.03	0.04 ± 0.04
Vacuum	PO	O1	1.09 ± 0.22	0.27 ± 0.18	0.40 ± 0.18
Water	PO	O1	0.40 ± 0.15	0.53 ± 0.13	0.69 ± 0.10
Vacuum	PO	O2	--	1.93 ± 0.31	2.28 ± 0.24
Water	PO	O2	--	0.54 ± 0.27	1.03 ± 0.40
Hydrophobic groups (6Å)					
Vacuum	PC1	C1	2.98 ± 0.12	2.68 ± 0.20	2.67 ± 0.16
Water	PC1	C1	2.99 ± 0.35	3.08 ± 0.29	2.62 ± 0.18
Vacuum	PC2	C1	1.43 ± 0.38	1.88 ± 0.09	1.98 ± 0.55
Water	PC2	C1	1.82 ± 0.55	1.98 ± 1.04	1.25 ± 0.52
Vacuum	PC1	C2	--	3.09 ± 0.52	2.74 ± 0.43
Water	PC1	C2	--	3.49 ± 0.42	2.95 ± 0.48
Vacuum	PC2	C2	--	1.60 ± 0.78	1.98 ± 0.54
Water	PC2	C2	--	1.74 ± 0.36	1.13 ± 0.37
Vacuum	PC1	C3	--	--	3.48 ± 0.26
Water	PC1	C3	--	--	3.23 ± 0.51
Vacuum	PC2	C3	--	--	1.42 ± 0.47
Water	PC2	C3	--	--	1.52 ± 0.58

There was a general decrease in the areas obtained in the presence of water due to structural and/or density effects as previously described (Ladanyi and Skaf, 1993; Vaisman and Berkowitz, 1992). Several trends were, however, observed firstly between the different benzoates and secondly with the different functional groups of a given benzoate.

In the presence of water, the extent of hydrogen bonding between the benzoate carboxyl group (O1) and the nitrogen of the polymer amide (PN) depended on the esterification of the side chain. Fig. 9.10 (a) shows the g(r) between PN and the benzoate carboxyl group (O1) in the presence of water molecules, where the carboxyl is present as an acid in BA and esterified in the case of MHB and PHB. The areas obtained in the hydrophilic region are shown in Fig 9.10(b) along with the corresponding areas between the oxygen of the polymer amide (PO) and O1. Hydrogen bonding was apparent between the polymer nitrogen (PN) and the acid group of BA and between the polymer oxygen (PO) and the carboxyl group (O1) of the three benzoates. The pattern shown in Fig. 9.10b revealed a decrease in area of the PN-O1 pair correlation curve with increasing length of the side chain ester, with a corresponding increase in the area under the PO-O1 curve.

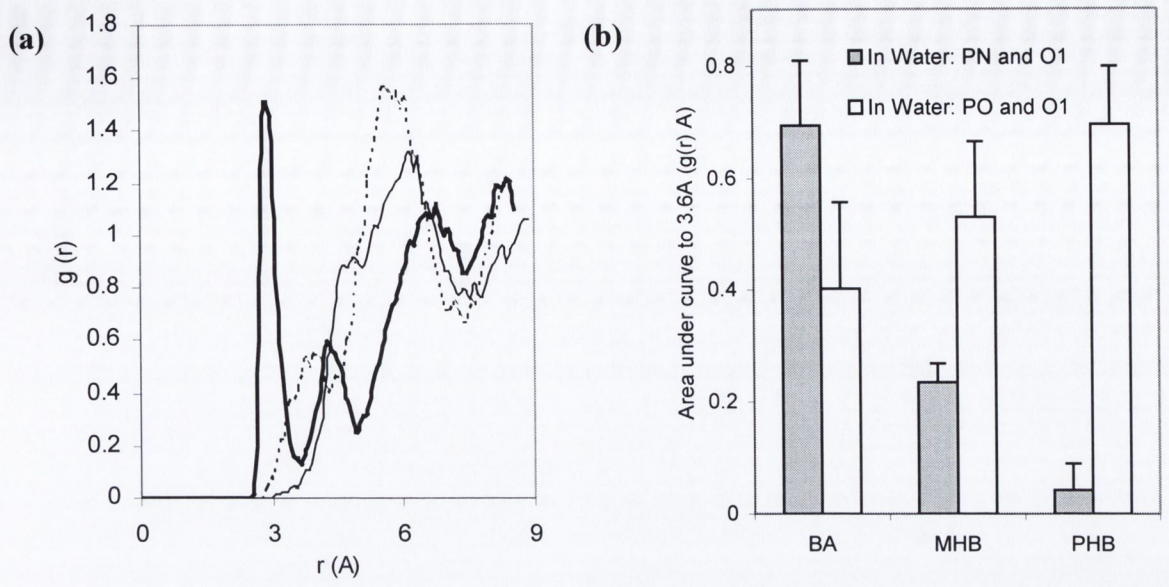

Fig. 9.10: (a) Radial distribution function g(r) between nitrogen atom of polymer amide (PN) and oxygen atom of benzoate (O1) at 300K in the presence of water molecules. [BA, (bold lines); MHB (dashed lines) and PHB (solid lines)]. (b) Areas under the PN-O1 and PO-O1 g(r) curves for each drug molecule in water.

Esterification therefore hindered hydrogen bonding at PN in the case of MHB and PHB. Consequently hydrogen-bonding of O1 to the polymer oxygen atom (PO) was favoured in the case of the esters. Such a pattern suggested a difference in orientation of BA and the esters around the polymer and will be discussed in more detail below.

In the absence of water molecules, the importance of hydrogen bonding appeared to change in this region. Hydrogen bonding peaks between PN and O1 were observed at ~3Å with all three benzoates, with no statistical difference in the area under the curve ($p>0.05$) (Table 9.8). The presence of hydrogen bonding water molecules may decrease the available sites of hydrogen bonding between the drugs and the polymer, resulting in slightly different interactions in the solid state.

The two esters used in the present study also contain a hydrophilic para-hydroxy group. Hydrogen bonding between the p-hydroxy group of MHB and PHB (O2) and the polymer amide was also apparent. The peaks obtained for MHB in the absence and presence of water are shown in Fig. 9.11a along with the areas obtained on integration for both MHB and PHB (Fig. 9.11b)

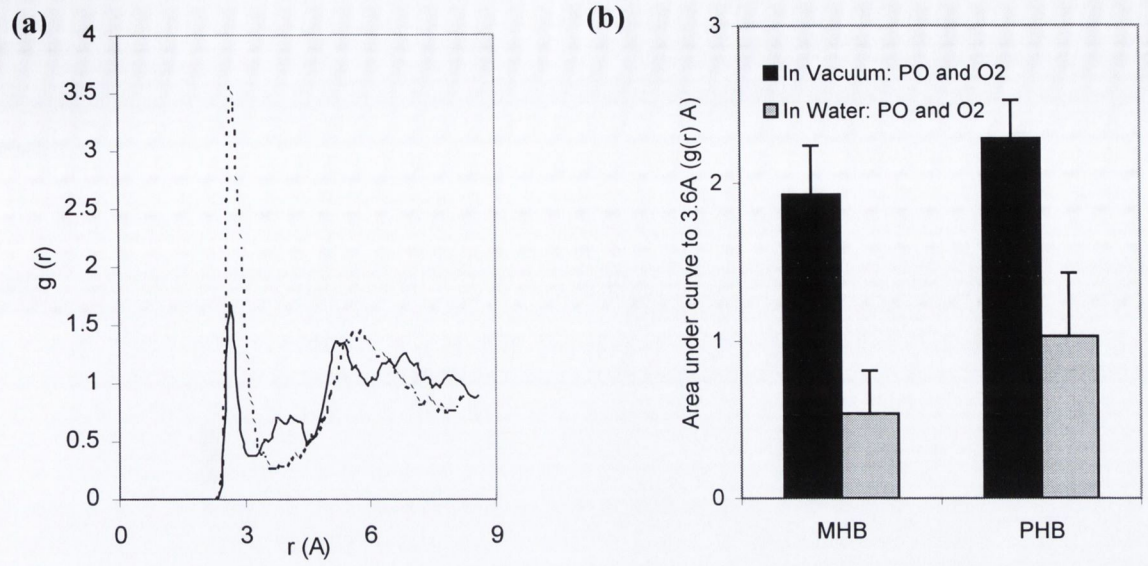

Fig. 9.11: (a) Radial distribution function g(r) between oxygen atom of polymer amide (PO) and MHB oxygen in the para position (O2) at 300K in the presence (solid line) and absence (dashed line) of water molecules. (b) Areas obtained on integration of same g(r) functions for MHB and PHB in the absence (black bars, simulations H,K) and presence (grey bars, simulation J,L) of water molecules.

The magnitude of the peaks in the para-hydroxy position (O2) were greater than for the carboxyl group (O1) (Table 9.8), indicating that the esters preferentially hydrogen bond in the para-hydroxy position, both with adjacent water molecules and also with hydrophilic groups of the polymer.

Examination of the hydrophilic groups in the polymer and benzoates therefore revealed potential hydrogen bonding between the molecules. BA hydrogen bonded with the polymer through its acidic group while the esters preferentially hydrogen bonded through the para-hydroxy group, particularly with the longer chained PHB. The presence of moisture also appeared to change the nature and extent of the interactions, suggesting competition with the water molecules for binding sites on the polymer.

Potential hydrophobic bonding between the carbon groups of the polymer (PC1, PC2) and benzoates (C1, C2, C3) were also examined (Table 9.8). Fig. 9.12 shows the g(r) obtained between the isopropyl group (PC1) or carbon backbone (PC2) of PNIPA and the benzene ring of BA (C1). Similar graphs were obtained with the other benzoates. A peak was observed at ~4Å around the isopropyl side chain (PC1), suggesting that the benzoate molecules were structured in this region, similar to the structuring of water molecules in this region described above and also by Tamai *et al.* (1996b). No peaks and hence smaller areas were apparent between the backbone carbons (PC2)

and the benzene ring. Similar patterns were also apparent (Table 9.8) between the hydrophobic polymer groups and the ester carbon atoms (C2 and C3). The lack of a peak and the smaller areas obtained between the backbone carbons and the benzoates reveal that any interactions with the backbone carbons were not as significant as those with the isopropyl group.

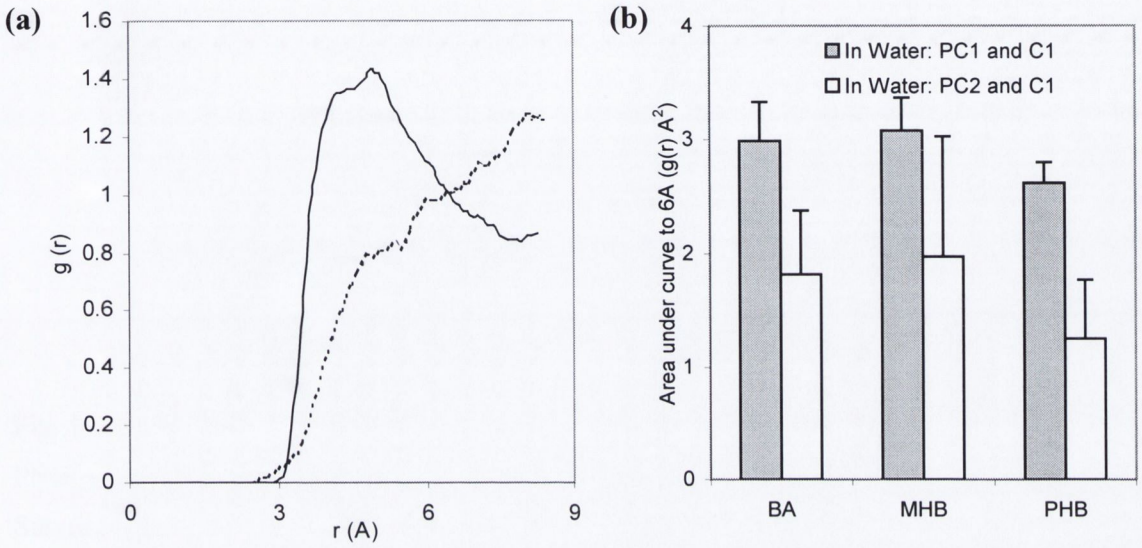

Fig. 9.12: (a) Example of the g(r) function between hydrophobic groups of polymer [PC1 (isopropyl side chain) (solid line); PC2 (carbon backbone) (dashed line)] and benzene ring of BA (C1) (b) corresponding area under curves for BA (simulation E), MHB (simulation J) and PHB (simulation L) in the presence of water molecules.

While there were no apparent differences or patterns between the different benzoates, the results obtained give some insight into the orientation of the benzoates relative to the N-isopropylacrylamide monomer units. Fig. 9.13 shows differences in area under the g(r) curves (and therefore also in the average distance) between the polymer isopropyl group (PC1) and the hydrophobic groups of PHB.

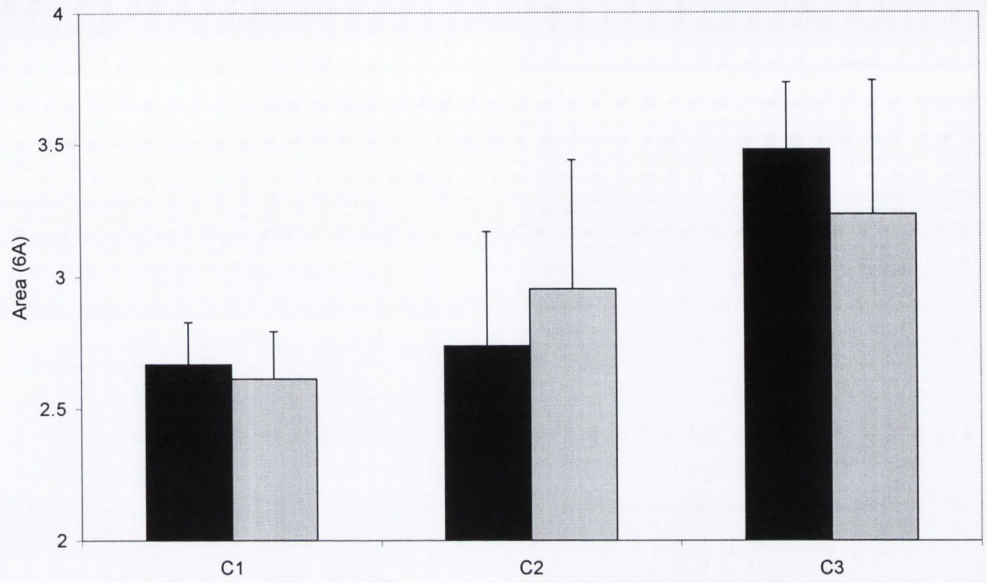

Fig. 9.13: Area obtained on integration of g(r) curves (to 6Å) between the isopropyl group of PNIPA (PC1) and the various carbon groups of PHB (C1, C2 and C3) in the absence (black bars, Simulation K) and presence (grey bars, simulation L) of water molecules.

The greater the area, the shorter the average distance between the functional groups. PHB was therefore orientated with the side chain ester towards the isopropyl group while the benzene ring, containing a hydrophilic hydroxy group, was orientated away from the isopropyl group. The same pattern was also seen with MHB (Table 9.8).

The results obtained can be compared to the experimental results in previous chapters. The isopropyl group of the polymer was clarified as being the main site of hydrophobic interaction with the benzoates, with access to the carbon backbone less likely. Direct binding between the benzene rings of the three benzoates and the polymer was confirmed in Chapter 6 by FTIR. The alkyl side chain of the esters was also shown by secondary methods in Chapter 6 to contribute to binding, with a significant increase in the binding effect as the length of the ester increased. Combining the molecular modelling results in the hydrophilic and hydrophobic regions with the binding data from Chapter 6 leads to two probable orientations of the benzoates used towards PNIPA shown graphically in Fig. 9.14. The experimental and simulation results suggest that BA binds to the polymer in a different orientation than the benzoate esters as shown.

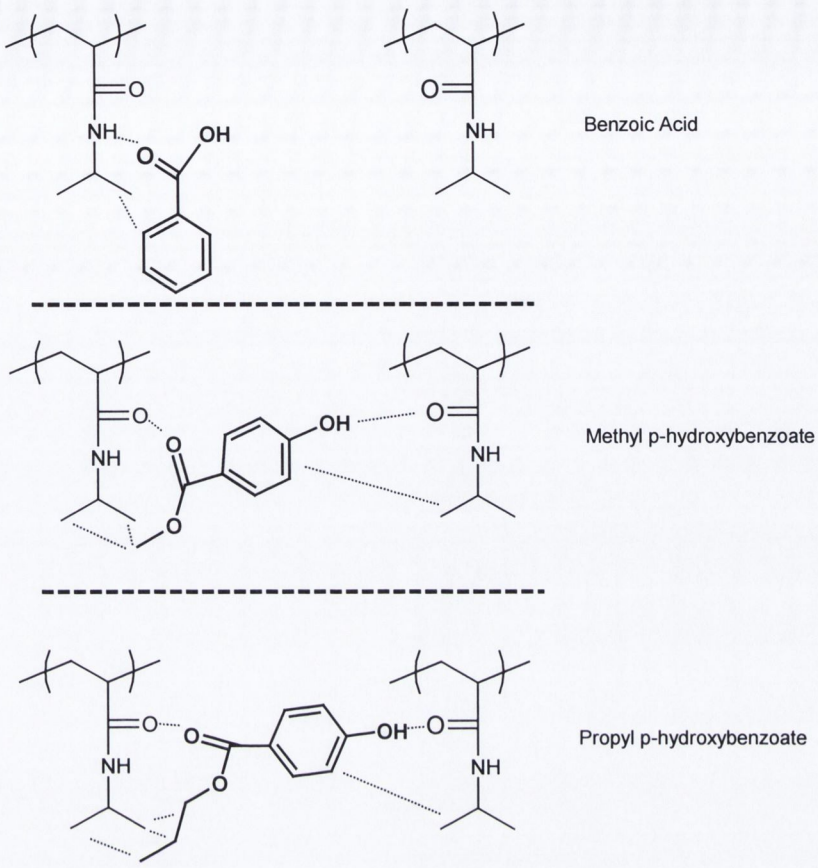

Fig 9.14: Possible 2-dimensional orientation of BA, MHB and PHB relative to two PNIPA chains in water from binding studies (Chapter 6) and molecular modelling. Dashed lines indicate interaction/binding sites.

BA (Fig 9.14a) binds to the isopropyl group in an unionised form by hydrophobic interactions with its benzene ring. Some hydrogen bonding of the acid with the nitrogen atom (PN) adjacent to the isopropyl group was also apparent from the simulations (Fig. 9.10).

In the case of MHB (Fig. 9.14b) and PHB (Fig. 9.14c), the simulations predicted that the alkyl ester chain was in closest proximity to the isopropyl group with the main hydrophilic interaction site on the polymer for O1 switching from PN, in the case of BA, to PO in the case of MHB and PHB. Greater interaction could occur between PO and O1 as the ester side chain increased in length and these two groups come into closer proximity. Binding of the ester group with the polymer isopropyl group was consistent with the increase in binding with increasing ester side chain length seen experimentally. The binding of the benzene ring would therefore appear to be of less importance in the esters, shown both by simulation and by experiment. The presence of a hydrophilic p-hydroxy group on the ring would decrease the binding ability of the benzene group. Hydrogen bonding of

the p-hydroxy group with PO may occur with an adjacent PNIPA chain as shown where the benzene ring can also interact to some extent with a polymer isopropyl group and/or a backbone carbon. The esters were therefore orientated with the alkyl side chain nearer the isopropyl group than the benzene ring, effectively reversing the orientation shown by BA.

9.4 CONCLUSIONS

Molecular dynamics simulation was shown to be a useful method for determination of the glass transition temperature and phase transition temperature of a thermoresponsive poly(N-isopropylacrylamide) segment. A significant downwards shift in the Tg was observed in the presence of the model benzoates, with no observable plasticising effect in the presence of water molecules.

Using short simulation times, useful information on the relative diffusion coefficients of the model benzoates was obtained. A linear relationship of the relevant diffusion coefficient coefficients with the release rates from a lightly crosslinked poly(N-isopropylacrylamide) hydrogel (PNIPA-H1) was observed.

The molecular modelling simulations also gave further insights into the nature of the PNIPA-benzoate binding interactions discussed in previous chapters. The modelling software, while not explicitly predicting the presence of hydrophobic binding, did suggest a difference in orientation within the benzoate series in the presence of the polymer due to different functional groups on the model drugs. Such information could potentially be useful in modifying the binding interaction for desirable hydrogel swelling/drug release characteristics.

CHAPTER 10

General Discussion

10.1 INTRODUCTION

The influence of drug physicochemical properties on the *in vitro* release characteristics from poly(N-isopropylacrylamide) hydrogels was examined in the course of this thesis. The effect of temperature change on the release profiles of a range of model drugs was examined. The influence of drug loading on release characteristics was also investigated as well as the effect of changing the hydrogel crosslinker content. Binding between the benzoates and the hydrogel was a significant finding of the present work and the release characteristics of these benzoates from the PNIPA hydrogels will be discussed separately.

10.2 SWELLING AND RELEASE STUDIES

Temperature responsive hydrogels were shown to be useful to sustain the release of a model drug or to pulse the release between an *"on"* state and an *"off"* state. Drug release from thermoresponsive hydrogels can potentially be controlled by utilisation of the drug diffusion process below the LCST (e.g. Okano *et al.*, 1990) or by use of the pulse of drug release on temperature switch above the LCST (e.g. Yoshida *et al.*, 1994a). In Chapter 7, the drug diffusion process above the LCST was also shown to sustain release of the drug if the drug size was less than hydrogel pore size at this temperature.

From the results obtained it was clear that drug release from these hydrogels, either at a single temperature or by switching the temperature, was dependent on the properties of the model drug. Diffusion controlled release depends on the factors described in the equation of Higuchi (Equation 2.6) such as drug loading, solubility and the diffusion coefficient of the drug in the matrix (related to drug size and shape and temperature of experiment). These and additional factors concerning the PNIPA hydrogels have been discussed including hydrogel swelling, temperature effects, solute size and the effect of drug-polymer binding

10.2.1 Hydrogel swelling and diffusional drug release

Swelling of non-thermoresponsive hydrogels has been shown by several authors to influence the release kinetics of drugs, with deviation from diffusion-controlled release due to the effect of swelling on the release pattern (Ritger and Peppas, 1987b; Lee, 1985; Shah *et al.*, 1991). However, the influence of the model drug on the hydrogel swelling rate and mechanism has often not been clarified in the literature along with the subsequent implications for the drug release profile.

The effect of a temperature rise from 25°C to 37°C was shown in Chapter 7 to increase both the solubility and intrinsic dissolution rate of the pure drugs as expected. The environmental temperature, however, also significantly affected the PNIPA hydrogels with a decrease in both the rate and extent of hydrogel swelling at the higher temperature. The net effect of a temperature rise on release of the drugs from the hydrogel was a decrease in the release rate due to influence of the hydrogel mesh size on the diffusion of the drugs. Table 10.1 shows a semi-quantitative comparison between the ability of PNIPA-H1 to prevent the release of the hydrophilic drugs at the constant temperature of 37°C (Chapter 7) and the ability of the same hydrogel to stop release after a temperature "switch" to 37°C (Chapter 5).

Table 10.1: Comparison of fraction of hydrophilic drug release at 37°C after 48 hours (Chapter 7) with achievement of an "*off*" state after temperature switch as measured by k_{ss} values (Chapter 5)

	Fraction released at 37°C after 48hours*	"Off" state achieved as measured by k_{ss} values
NaB (~4Å)	~0.9	No
DHCl (~ 8Å)	~0.8	Yes
VB12 (~ 12Å)	0	Yes
D4 (~ 25Å)	0	Yes
D10 (~ 38Å)	0	Yes
D40 (~ 78Å)	0	Yes
D70 (~ 98Å)	0	Yes

*Excluding any surface drug effects

The hydrogel used (PNIPA-H1) was shown to contain a range of pore sizes in the swollen state, from macropores (>500Å) to micropores (<20Å). The pores at the molecular level (micropores) controlled the ability of the model drugs to diffuse from the hydrogel and the solute exclusion technique (section 4.4.5.3) was useful in determining the extent to which the pores present were accessible to the drugs at a particular level of swelling. The average size of pores which influenced the drug diffusion were determined to be ~60Å at 25°C and ~10Å at 37°C. The magnitude of thermal control was particularly dependant on drug size in the case of the water-soluble drugs, where release of compounds of molecular diameter ~12Å was completely prevented at 37°C due to the relationship between molecular size and pore size. The release of the smaller drugs was prevented to a limited extent and in the case of DHCl (~8Å) was related to the fraction of pores of that size accessible to the outside media. The ability to thermally control the drug was consistent with the results from the pulsed release study in Chapter 5 and confirmed that pore size was the controlling mechanism for release in those systems. Pulsatile release has previously been explained by the formation of a dense, less permeable surface layer of gel, described as a "skin-type barrier". The length of the alkyl side chain was shown to control the thickness and density of the surface skin layer (Yoshida *et al.*, 1991,1994b; Okano *et al.*, 1990; Gutowska, *et al.*, 1992). The current systems, without the alkyl side chain, did not show any evidence of a skin-type barrier. A surface layer of polymer may still form in the initial stages of shrinkage caused by the collapsing of

the desolvated polymer chains from the outside of the system (Hoffman, 1986). This desolvated layer did not stop release of the small model drugs (NaB and other benzoates), suggesting that pore size was still the most important factor controlling release in these systems and the "skin layer" mechanism of stopping release was not significant in PNIPA hydrogels. The "skin layer" mechanism of controlling release may be a specific effect due to the presence of the long chain hydrophobic comonomers used in the studies of Okano and co-workers (Bae *et al.,* 1987, 1991b; Okano *et al.,* 1990; Yoshida *et al.*, 1991a, 1991b, 1992, 1994a). A possible reason for the enhanced skin layer described by these authors is discussed later.

The model drug, DHCl, appeared to be of a "borderline" size (~8Å) for thermal control from PNIPA-H1. Despite 80% release over time at 37°C, an apparent *"off"* phase during the pulsatile release studies was still shown. In contrast, the slightly larger VB12 (~12Å) was not released at 37°C.

The use of the PNIPA hydrogels as sustained release systems will therefore depend on the size of the drug and the temperature of the experiment. In addition, use of these hydrogels as *"on-off"* thermoresponsive systems where the *"on"* phase is caused by drug diffusion below the LCST will depend on loading of a drug of sufficient hydrophilicity and size (e.g. >8Å in the case of PNIPA-H1). The chemical nature of the drug may be important if such a factor influences the rate of swelling. Since the release rate was shown to decrease between consecutive *"on"* phases, the time interval would have to be lengthened to achieve delivery of the same dose. This time interval below the LCST would have to be lengthened further in the case of drugs of relatively high molecular weight, where release by diffusion is slow due to the physical size of the drug.

The ability to alter the swelling kinetics and pore size of the PNIPA hydrogel by increasing the crosslinker content was shown in Chapter 8. Below the LCST, techniques such as SEM and nitrogen desorption revealed a decrease in macropore and mesopore size respectively with increasing percentage crosslinker. Above the LCST, an effective increase in pore size was apparent from these techniques. An increase in release rate of NaB with increasing crosslinker above the LCST also showed that pores at the molecular level were influenced in the same way by the presence of the crosslinker, with a resulting effect on the drug release profiles.

Apart from influencing the release rate, the hydrogel swelling properties and the drug size was also shown to influence the release mechanism from these systems. A zero-order release mechanism is often required where the drug is released proportional to time. The swelling of a drug-loaded system has previously been shown to cause deviations of the release mechanism from the square root of time diffusional relationship (Ritger and Peppas, 1987b; Lee, 1985; Shah *et al.,* 1991). The

current work showed that the release mechanism of a small hydrophilic compound (NaB) from the various PNIPA hydrogels (Chapter 8) depended on the swelling characteristics. The release mechanism from a single hydrogel (Chapter 7) was shown to depend on the drug size, similar to previous studies, which used non-thermoresponsive swellable systems (Vyavahare *et al.,* 1990; Shah *et al.,* 1991). The possibility therefore exists of designing a thermoresponsive hydrogel system with desirable swelling kinetics and pore sizes to achieve a particular mechanism and rate of release during the swelling phase.

The loaded drug also influenced the hydrogel swelling, depending on the hydrophilicity of the drug and other related effects such as binding with the hydrogel and osmotic effects. Increasing the loading of NaB increased the release rate of the drug, similar to the predictions of Higuchi (Equation 2.6). The increase in release rate was, however, directly proportional to loading (Fig. 7.17b) due to the effect of swelling on the release rate.

The influence of drug solubility on hydrogel swelling was also explored. Assuming no binding occurs between the drug and hydrogel, the solubility of the model drug was shown to affect the ability of the dissolving front to penetrate into the hydrogel. Drugs that have relatively low solubility such as DB slowed the rate of swelling, but only to a limited degree compared to the benzoates. DB showed no interactions with the hydrogel and only slowed the swelling rate during the first swelling cycle shown in Chapter 5, thus indicating that the swelling was slowed by the presence of a drug diffusion front. The benzoates would also have slowed the swelling rate if binding did not occur, with an enhanced effect due to the binding to the polymer. The study of Yoshida *et al.* (1991a) described a decrease in the rate of swelling of an indomethacin loaded PNIPA-co-BMA hydrogel. The release of DB from PNIPA-H1 showed, however, that the presence of a "hydrophobic" drug does not necessarily mean that hydrophobic interactions between the drug and the hydrogel will occur.

In contrast to the hydrophobic drugs, the hydrophilic drugs (e.g. NaB, DHCl) increased the swelling rate, attributable to the osmotic effect of the loaded drug on the swelling rate. A 50% increase in the rate of swelling of the hydrogel series PNIPA-H1 to H3 was shown with NaB (loading 28%w/w). The size and concentration of the solute influenced the osmotic effect exerted and therefore the swelling rate of the hydrogel.

10.2.3 Hydrogel contraction and drug pulse

An important consequence of the influence of the drugs on the swelling rate is the subsequent change in the magnitude of hydrogel contraction following temperature switch above the LCST.

The use of the drug pulse caused by hydrogel contraction can potentially control the drug release from a thermoresponsive hydrogel (Yoshida *et al.,* 1994a; Zhang *et al.,* 2002; Gutowska *et al.,* 1997; Shin *et al.,* 2001). Brazel and Peppas (1996) also showed a drug pulse from a pH/temperature responsive system.

In the case of hydrophobic, non-binding drugs, the proportion of the drug loading in the dissolved state will determine the magnitude of the pulse. The pulse of hydrophobic drugs can therefore potentially be altered by knowledge of the extent of drug dissolution prior to temperature switch. The subsequent diffusion rate from systems that use the drug pulse to switch on release (e.g. Yoshida *et al.,* 1994a) could therefore be predicted.

Hydrophilic drugs of MW > ~500 (diameter > ~8Å) appeared to be the best candidates for producing a consistent magnitude of drug pulse from PNIPA-H1. The drug pulse of the even larger hydrophilic compounds (MW>4,000) appears to have been affected by the method of loading, resulting in a molecular size gradient and therefore a molecular size dependent pulse. Previous studies have also reported a drug pulse using a similar loading method (Yoshida *et al.,* 1994a, Brazel and Peppas 1996; Gutowska *et al.,* 1997; Shin *et al.,* 2001; Zhang *et al.,* 2002). The studies mentioned, however, did not attempt to quantify the magnitude of the pulse and the same effect may have been present depending on the relationship between drug size and molecular pore size in the particular system used. Quantification of the effect of the gradient on the magnitude of pulse, could however, be useful in changing the magnitude of the pulse in a given system to meet particular requirements. In addition, the slow and often negligible diffusion of the higher molecular weight drugs below the LCST can be countered by the use of this drug pulse to turn *"on"* release by increase of temperature (positive thermosensitive release). Such a system would not need an impermeable membrane with a releasing orifice (Yoshida *et al.,* 1994a; Zhang *et al.,* 2002; Gutowska *et al.,* 1997; Shin *et al.,* 2001) to achieve short-term positive pulsatile release.

10.2.3 Effect of drug-polymer binding

A significant finding of the present work was binding between the benzoates and poly(N-isopropylacrylamide). The binding effect was investigated by FTIR, swelling studies, spectroscopic studies and thermal analysis and the evidence suggested that it was of the hydrophobic type between the unionised form of the benzoates and the polymer. Binding occurred between both the benzene ring/ester side chain of the benzoate and the isopropyl group of the polymer.

Studies to establish binding isotherms have previously been carried out to investigate binding involving drugs and polymers (e.g. Connors, 1987; Peppas and Wright, 1998; Alvarez-Lorenzo and Concheiro, 2002; Rodriguez *et al*, 2003; Porcar *et al.,* 2004) or involving proteins (Elbary *et al.,* 1982; Nour and Vallner, 1984; Santhanalakshmi and Balaji, 2001). Most previous studies showed ionic binding between the relevant substituents (e.g. am Ende *et al.,* 1995; Peppas and Wright, 1998; Alvarez-Lorenzo and Concheiro 2002; Rodriguez *et al.*, 2003). Alvarez-Lorenzo and Concheiro (2002) studied adsorption of a divalent molecule to a NIPA hydrogel copolymerised with a pH-ionisable component. Adsorption was attributed in this case to ionic interactions between the molecule and the ionisable comonomer. Studies by Peppas and coworkers have previously shown ionic bonding between drugs and polymers (am Ende *et al.,* 1995; Peppas and Wright, 1998). For example, am Ende *et al.* (1995) showed that that the cationic solute oxyprenolol HCl strongly interacted with ionic hydrogels and showed increased hindrance in solute transport of the drug from an anionic solute at high pH (pH >5). Some studies (e.g. Yu and Grainger 1995; Pina *et al.*, 1999) also mention possible hydrophobic binding between the substituents used. Yu and Grainger (1995) synthesised a hydrogel containing PNIPA and a hydrophobic comonomer, n-N-alkylacrylamide, and hydrophobic interactions were proposed between the peptides released (insulin or interferon) and alkylated regions of the gel network. Direct hydrophobic binding data was, however, not presented in conjunction with the above drug release studies.

The investigations in Chapter 6 indicated that binding occurs between PNIPA and the benzoates, in particular benzoic acid and its esters. In the 1950's to 1970's, several authors reported the binding of benzoic acid derivatives to non-ionic surfactants (Goodhart and Martin, 1962; Patel and Romanowski, 1970; Blanchard *et al.,* 1977), thus decreasing the preservative activity of the benzoate. Patel and Romanowski (1970) showed that the magnitude of this inactivation increased from MHB to PHB, due to higher binding of PHB. The benzoates were also shown to bind to other compounds. Higuchi and Zuch (1953) showed that benzoic acid and sodium benzoate formed soluble complexes with caffeine. Patel and Nagabhushan (1970) showed that a plastic nylon, capran polyamide, reduced the antimicrobial activity of MHB and PHB due to a sorption effect. The later study is particularly relevant in the context of this thesis as binding was shown between the esters and the plastic polyamide. The thermoresponsive polymer used in our investigations is also a polyamide derivative.

In the studies presented (Chapters 5, 7 and 8), the hydrophobic binding affected the swelling of the hydrogels and concomitant release pattern of the benzoates. Hydrophobic binding between the drug and the polymer increased the hydrophobicity of the polymer, resulting in a decrease in the phase transition temperature (LCST) of the thermoresponsive system (section 6.2.2.4). At a certain

concentration of each benzoate, the LCST of the polymer was reduced to the temperature of the experiment and polymer precipitation or hydrogel collapse occurred. The reverse was also true, in that a high local drug concentration prevented hydrogel swelling until a critical level or minimum concentration was reached and swelling could occur. The net result was a further decrease in the swelling rate, more than would have been expected from a non-binding drug like DB.

The effect of binding between the model drug and the hydrogel on the release profile was two-fold. Drug-polymer binding directly slowed the release rate by increasing the hindrance to solute transport. A second, indirect, effect was also apparent as the effect of binding slowed the water uptake and therefore the effective pore size available for diffusion from the system.

Binding between the benzoates and PNIPA therefore resulted in a new type of swelling front in PNIPA-hydrogels. Fig. 10.1(a) shows a diagram of hydrogel swelling and concomitant non-binding drug (*D*) release. Schematics of a drug loaded hydrogel at time zero and the swollen hydrogels after time *t* in aqueous media, *A*, are shown in Fig 10.1(i) and 10.1(ii) respectively and were explained in section 2.3.2 (Chapter 2). Also shown are theoretical concentration profiles of the solvent (*A*) diffusing into the hydrogel (Fig. 10.1(iii)) and the drug diffusing out of the hydrogel (Fig. 10.1(iv)), both also after time, t.

The influence of the benzoates (*B*) on PNIPA hydrogel swelling is shown in Fig. 10.1b and is compared to a non-binding drug (*D*, Fig. 10.1a). The solubility and size of the two "drugs" were assumed to be the same and the swelling and diffusion fronts were also assumed to coincide for clarity. A new type of swelling front is observed during swelling of PNIPA hydrogels in the presence of the benzoates, designated as front *B'*. The front *B'* represented the boundary at which the local concentration of the diffusing benzoate decreased below a critical level (C_{crit}) to allow hydrogel swelling. This boundary between the hydrophobically collapsed interior and the swollen exterior was shown in Chapter 7 (Fig. 7.15). At local drug concentrations above the critical level, binding between the benzoate and the polymer suppressed the LCST of the local polymer chains below the temperature of the experiment (25°C), as described in Chapter 6. The extent of swelling was lower and the position of the swollen front (S') less advanced at time *t* than with the non-binding drug. A sharp change in the ability of the hydrogel to swell occured at this front as the LCST of the hydrogel reached the temperature of the swelling medium as shown in Fig. 6.8. The concomitant drug release profile was therefore slower than expected from a non-binding drug (Fig. 10.1(iv)).

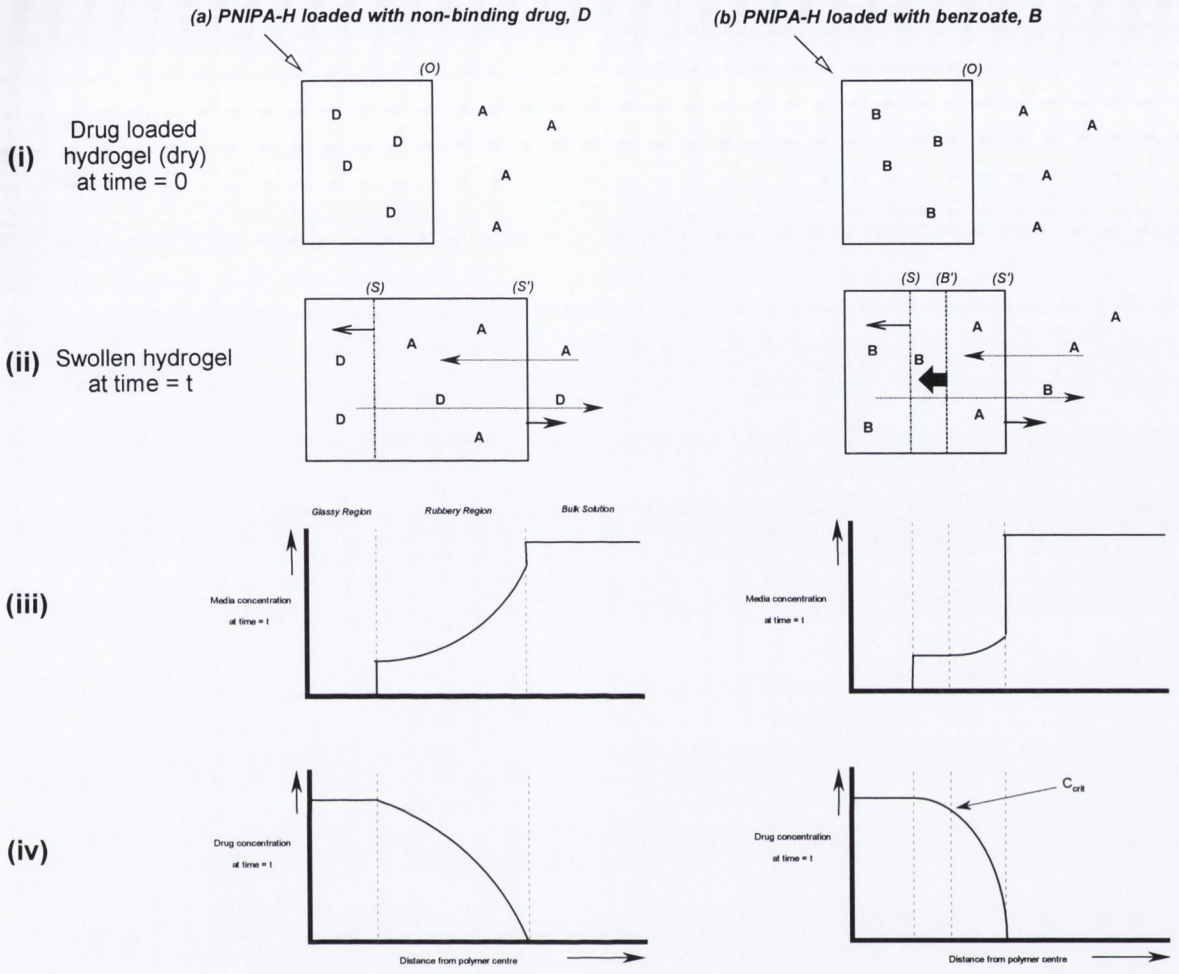

Fig. 10.1: Hydrogel swelling/drug release profiles of a (a) non-binding drug, ***D***, and (b) a benzoate, ***B*** from a PNIPA hydrogel placed in aqueous media, ***A***. Desolvated hydrogel containing drug **D/B**, placed into aqueous medium, ***A*** (i) at time zero and (ii) after time, t. Also shown are theoretical concentration profiles at time t of (iii) water during the swelling controlled release process (iv) of drug during the swelling controlled release process.

[Boundaries: ***(S)*** swelling front/drug diffusion front between drug core and rubbery hydrated hydrogel, ***(O)*** original polymer/penetrant interface at T=0, ***(S')*** interface between rubbery hydrogel and bulk solution, ***(B')*** binding front]

The position of this critical level (C_{crit}) depended on several factors, namely drug binding properties, other drug physicochemical properties and hydrogel/system properties. Firstly, drug binding properties such as the hydrophobicity of the benzoate was of importance; the greater the hydrophobicity of the benzoate the greater the strength of binding as described in section 6.2. The length of the ester side chain increased the extent of binding. In addition, for ionisable drugs (e.g.

BA) the state of ionisation would be important and is influenced by the pH of the swelling media with binding only apparent with the unionised species.

Secondly, other drug physicochemical properties such as drug solubility and size would influence the rate of drug diffusion from the system, and therefore the time taken for the critical level to be reached. The drug loading was also shown in the present study to influence the swelling and release rate (section 7.5.1). The higher the loading, the longer it would take for the local drug concentration to drop below the critical level described, allowing the LCST to rise above 25°C and swelling to occur. As a result, the higher the loading, the greater the influence of the drug on the effective pore size available for diffusion and therefore the greater influence on its own release rate. The release rate of BA decreased with increasing loading (Fig.7.14), in contrast to an increase in release rate seen with NaB (Fig. 7.17b) and expected from matrix-controlled release systems.

The third factor that affects the position of this critical level is hydrogel/system properties such as the LCST of the hydrogel relative to the temperature of the experiment. The difference between the LCST of the hydrogel and the temperature of the experiment dictates the drop in temperature required through binding to prevent swelling. Conversely, the rise in the drug bound polymer LCST required for swelling to commence would depend on the temperature of the experiment. If the temperature was already above the polymer LCST, then swelling may not occur at all as was the case in Chapter 7 at 37°C. The drug release kinetics from such systems were therefore essentially independent of the swelling process.

Some other points are worth considering in relation to the effect of binding on swelling and release profiles. Firstly, it was shown in Fig. 7.9 that there was a linear increase in the release exponents (n) of the benzoates at both temperatures with increasing size/decreasing hydration level. The present study with the hydrophilic drugs and previous studies from non-thermoresponsive swellable systems (Shah *et al.*, 1991; Davidson and Peppas, 1986; Brannon-Peppas and Peppas, 1989, Brazel and Peppas, 1999b) have shown that an increase in the diffusional exponent is more likely with smaller drug substances, since the drug is less likely to be diffusion controlled due to its small size. The trend seen in the present study would therefore appear to be a consequence of the binding contributing to the diffusion controlled release. Swelling also played a role in the release patterns at 25°C, further increasing the diffusional exponents of all three benzoates.

Based on the ability of the benzoates to bind to PNIPA, the binding of other substances, including other drugs, would also appear possible. It has been suggested, although not conclusively established, that the mechanism by which surfactants increase the LCST of thermoresponsive polymers is also through a binding process (Schild and Tirrell, 1991; Saito *et al.*, 1992; Kokufta *et*

al., 1993; Eeckman *et al.,* 2001). Binding between the hydrophobic segments was thought to increase the overall hydrophilicity of the system due to the resulting complex being more hydrophilic than before.

In addition it can be postulated from the binding shown in this thesis that the "enhanced skin layer" described by Okano and coworkers (Yoshida *et al.,* 1991, 1994b; Okano *et al.,* 1990; Gutowska, *et al.*, 1992) and attributed to the length of the alkyl side chain may be due to the alkyl side chain hydrophobically binding to adjacent thermoresponsive monomers. The structure of PHB is compared to poly(butylmethacrylate) in Fig. 10.2.

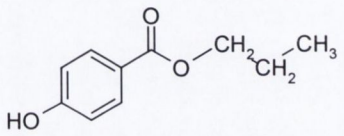

Propyl (4-hydroxybenzoate)

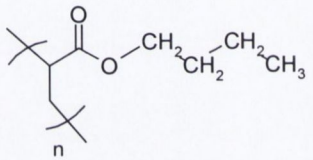

Poly (butyl methacrylate)

Fig. 10.2: Comparison of structure of PHB and poly(butyl methacrylate), both showing a side alkyl group

The alkyl side chain is common to both the benzoate esters and the alkyl methacrylates. The length of the alkyl side chain was shown to control the thickness and density of the surface skin layer (Yoshida *et al.,* 1994b), similar to the increase in binding shown in the present thesis with increase in the length of the side chain ester. The "skin layer" described was formed on hydrogel contraction where the polymer chains reverted to a hydrophobic state and as a result the effect of hydrophobic binding may be more visible during this process. The same authors sometimes incorporated hydrophilic comonomers to prevent the formation of the enhanced skin layer (e.g. Yoshida *et al.*, 1994c). Hydrophilic comonomers would interfere with the hydrophobic binding between the alkyl side chain units and the NIPA units. The release studies previously described from PNIPA-co-alkyl methacrylate gels (Bae *et al.,* 1987, 1991b; Okano *et al.,* 1990; Yoshida *et al.*, 1991a, 1991b, 1992, 1994a) may therefore be strongly influenced by this internal binding, which would influence effective pore size available for drug diffusion.

In Chapter 8, it was also shown that the binding process was able to control the swelling rate of the four different PNIPA hydrogels, each with vastly different swelling kinetics. The release profiles of the drug from these systems were therefore self-controlled. The factors described above affecting the critical level may therefore be altered to achieve a required swelling rate for a

hydrogel. Possible implications of the binding include the use of the binding to control the swelling rate and therefore pore size of a hydrogel that also contained a second, larger drug. Release of this second drug could be then pre-programmed to only occur after a certain time interval when the pore size reached a critical level e.g. programmed release of theophylline. Changing the hydrophobicity of the benzoate will alter the strength of binding and the time taken for swelling and therefore release to occur.

The fact that the transition temperature and volume changes are dependent on the readily controlled properties of the benzoates could be useful in other areas of drug delivery research. The binding may be useful for molecular sensing as described by Kokufuta *et al.* (1993), where the system can directly recognise a particular molecule and converts the interaction between the molecule and the system into an observable change in the system (i.e. a change in the level of swelling). The sharp binding properties of the benzoates to the hydrogel could also be useful in the area of flow control in drug delivery devices as reviewed recently by Eddington and Beebe (2004). This involves responsive hydrogels being used in controlling the flow of media and drug substances from drug delivery devices. Changes in the concentration or type of benzoate can be converted into mechanical energy in the form of a change in shape or size of the system, resulting in an increase in flow from the system due to an increased area for diffusion. The systems described would not require a temperature change since the benzoate is controlling the position of the LCST relative to the temperature of the study. The increased concentration of benzoate can subsequently be diluted in order to reverse the effect on the hydrogel.

10.3 MOLECULAR MODELLING

The use of computer modelling in the design of drug delivery devices is a relatively new area as described in Chapter 9. The ability to realistically simulate a particular system by molecular modelling will still depend on the computational power and time available to obtain reasonable results. In addition, the forcefield used will also only parameterise well-understood molecule-molecule interactions known in the scientific literature. The simulations described in Chapter 9, however, successfully characterised the glass transition temperature and phase transition temperature of poly(N-isopropylacrylamide) using a relatively short simulation time. A decrease in the glass transition temperature was also shown in the presence of the benzoates, similar to the experimental work. Useful information on the relative diffusion coefficients of the model benzoates was obtained, with a linear relationship between the simulated diffusion coefficients and the release rate constants of the same drugs from PNIPA-H1.

The software used (Accelrys' Materials Studio® Version 2.1.5) did not directly predict the presence of hydrophobic binding between the benzoates and poly(N-isopropylacrylamide). In contrast to hydrogen bonding interactions, hydrophobic interactions between functional groups may not be as well parameterised using current forcefields in molecular modelling packages. The simulations, however, correlated well with the experimental results and gave further insights into the nature of the PNIPA-benzoate binding interactions. Experimental results showed binding between PNIPA and the unionised form of benzoic acid. In addition, the strength of binding was greater with the esters, which had an alkyl side chain as well as a hydrophilic para-hydroxy group in their structures. Since binding increased when the alkyl side chain was lengthened, the experiments suggested that the alkyl side chain was the primary binding site for binding of the esters, in contrast to the benzene ring being the primary binding site for benzoic acid. The trends shown by the simulations supported the hypothesis that two orientations were possible to obtain binding and that a longer side chain would aid the binding process (Fig. 9.14). Hydrogen bonding with the polymer amide also appeared to anchor the relevant molecules into the two different positions and the para-hydroxy group was important in causing such an effect. The simulations also suggested that the isopropyl groups rather than the backbone carbons were the primary binding site on the polymer.

The simulations therefore showed the usefulness of computer modelling in understanding drug-polymer interactions observed experimentally. Such information could potentially be useful in modifying the binding interaction for desirable hydrogel swelling/drug release characteristics.

10.4 CONCLUSIONS

- The presence of a loaded drug influenced the swelling of poly(N-isopropylacrylamide) hydrogels, with the rate and extent of swelling also depending on the temperature and the crosslinker content. Small hydrophilic drugs increased the swelling rate due to an osmotic effect while hydrophobic drugs slowed the swelling rate. The resulting magnitude and rate of hydrogel contraction after switching the temperature above the LCST was proportional to this drug-dependent magnitude of swelling.

- Binding occurred between the unionised benzoates and poly(N-isopropylacrylamide). Such binding was shown to be hydrophobic in nature between the polymer isopropyl group and the benzene ring/ester side chain of the benzoate and resulted in a detectable decrease in the LCST of the hydrogel. Molecular modelling, in conjunction with the techniques such as DSC, FTIR and phase solubility studies, suggested two different benzoate-polymer binding orientations depending on the functional groups present on the benzoate molecule.

The main binding position of the unionised form of BA was through its benzene ring, while the para hydroxy group present on MHB and PHB hindered such an interaction with the ester side chain being the main site of interaction with these molecules. The hydrophobic binding slowed the swelling rate even further than would be expected from a non-binding hydrophobic drug such as DB.

- Release of most of the model drugs used was approximately proportional to the square root of time below the LCST, with the swelling having a significant influence on the release mechanism of the small, highly soluble NaB. Altering the swelling rate of the hydrogel by changing the amount of crosslinker was also shown to influence the release kinetics of NaB. The effect of binding was to decrease the release rate of the hydrophobic benzoates even further than expected from a non-binding drug due to the direct binding effect and the indirect effect on pore size and therefore volume available for diffusion.

- Increasing the drug loading of NaB decreased the release diffusional exponent (n) and increased the release rate from the hydrogel. In contrast, increasing the loading of BA caused a decrease in the release rate of the drug, attributable to the binding effect of the unionised species.

- Release of the model drugs above the LCST depended on the molecular size of the drug in solution relative to the pore size available for diffusion. The increase in temperature decreased the release rate of the model drugs where smaller drugs could diffuse out while the larger molecules remained trapped in the hydrogel with no release over time.

- A temperature switch above the LCST caused a drug pulse in most cases, which was solubility dependent in the hydrophobic benzoate series. The drug pulse was attributed in the hydrophobic series to the presence of dissolved drug in the swollen hydrogel region surrounding the drug core prior to temperature increase. The magnitude of pulse of hydrophilic drug release on hydrogel contraction increased with molecular diameter, attributed to a molecular size dependent gradient formed with the larger molecules during the loading/drying process.

- The release rates of the model drugs were dependent on the pore size available for diffusion. From the present study, the "enhanced skin layer" mentioned in the literature, which was said to control the drug release on hydrogel contraction, was probably due to a binding effect between the long alkyl side chain of the alkyl methacrylates used in these studies and poly(N-isopropylacrylamide).

10.5 FUTURE WORK

The current thesis revealed a potential molecular sensing system involving the binding of the benzoates to the polymer, with a resulting physical change in the system. An interesting continuation of the work would be to investigate potential applications of such a system in drug delivery devices. The hydrophobic binding process could also be further examined to obtain, with the aid of molecular modelling studies, structure-activity relationships in order to be able to predict such drug-polymer hydrophobic binding and its effect on drug release.

In addition, future work could examine in more detail the size-dependent drug gradient formed within the hydrogel with the larger drug molecules. Knowledge of such a gradient and the ability to predict its effect on release characteristics would be useful for the controlled delivery of relatively large drug substances.

References

Akala, E.O., Kopeckova, P., Kopecek, J., Novel pH-sensitive hydrogels with adjustable swelling kinetics. *Biomaterials* 19 (1998) 1037-1047.

Akerman, S., Viinikka, P., Svarfvar, B., Putkonen, K., Jarvinen, K., Kontturi, K., Nasman, J., Urtti, A., Paronen, P., Drug permeation through a temperature-sensitive poly(N-isopropylacrylamide) grafted poly(vinylidene fluoride) membrane. *Int. J. Pharm.* 164 (1998) 29-36.

Alexander, C., Twaites, B., Cunliffe, D., de las Heras, C., Smith, J.R., Gorecki, D., Pysicochemical investigations into thermoresponsive synthetic polymer-DNA complexes. *UKICRS Symposium* 10 (2004).

Allen, M.P., Tildesley, D.J., *Computer simulation of liquids*. Oxford: Clarendon Press, 1987.

Alvarez-Lorenzo, C., Concheiro, A., Reversible adsorption by a pH- and temperature sensitive acrylic hydrogel. *J. Cont. Rel.* 80 (2002) 247-257.

Andersson, M., Axelsson, A., Zacchi, G., Diffusion of glucose and insulin in a swelling N-isopropylacrylamide gel. *Int. J. Pharm.* 157 (1997) 199-208.

Angell, C.A., Finch, E.D., Woolf, L.A., Bach, P., Spin-echo diffusion coefficients of water to 2380 bar and –20°C. *J. Chem. Phys.*, 65 (1976) 3036-3066.

Aoki, T., Nakamura, K., Sanui, K., Ogata, N., Kikuchi, A., Okano, T., Sakurai, Y., Temperature responsive drug release polymeric hydrogels based on 6-(acryloyloxymethyl)uracil in physiological solution. *Proceed. Intern. Symp. Control. Rel. Bioact. Mater.* 23 (1996) 767-768.

Aoki, T., Nishimura, T., Sanui, K., Ogata, N., Phase-transition changes of poly(N-(S)-*sec*-butylacrylamide-*co*-N-isopropylacrylamide) in response to amino acids and its chiral recognition. *Reactive & Functional Polymers* 37 (1998) 299-303.

Ashraf, M., Iuorno, V.L., Coffin-Beach, D., Evans, C.A., Augsburger, L.L., A novel nuclear magnetic resonance (NMR) imaging method for measuring the water front penetration rate in hydrophilic polymer matrix capsule plugs and its role in drug release. *Pharm. Res.* 11 (1994) 733-737.

Ataman, M., Properties of aqueous salt solutions of poly(ethylene oxide) cloud point, theta temperature. *Colloid Polm. Sci.* 265 (1987) 19-25.

Bae, Y.H., Okano, T., Hsu, R., Kim, S.W., Thermosensitive polymers as on-off switches for drug release. *Makromol. Chem., Rapid Commun.* 8 (1987) 481-485.

Bae, Y.H., Okano, T., Kim, S.W., "On-off" Thermocontrol of solute transport. I. Temperature dependence of swelling of N-isopropylacrylamide networks modified with hydrophobic components in water. *Pharm. Res.* 8 (1991a) 531-537.

Bae, Y.H., Okano, T., Kim, S.W., "On-off" Thermocontrol of solute transport. II. Solute release from thermosensitive hydrogels. *Pharm. Res.* 8 (1991b) 624-628.

Banga, A.K., Chien, Y.W., Iontophoretic delivery of drugs: fundamentals, developments and biomedical applications. *J. Cont. Rel.* 7 (1988) 1-24.

Beltran, S., Baker, J.P., Hooper, H.H., Blanch, H.W., Prausnitz, J.M., Swelling Equilibria for weakly ionizable, temperature-sensitive hydrogels. *Macromolecules* 24 (1991) 549-551.

Blanchard, J., Fink, W.T., Duffy, J.P., Effect of sorbitol on interaction of phenolic preservatives with polysorbate 80. *J. Pharm. Sci.* 66 (1977) 1470-1473.

Brannon-Peppas, L., Peppas, N.A., Solute and penetrant diffusion in swellable polymers. IX. The mechanisms of drug release from pH-sensitive swelling-controlled systems. *J. Cont. Rel.* 8 (1989) 267-274.

Brazel, C.S., Peppas, N.A., Pulsatile local delivery of thrombolytic and antithrombotic agents using poly(N-isopropylacrylamide-co-methacrylic acid) hydrogels. *J. Cont. Rel.* 39 (1996) 57-64.

Brazel, C.S., Peppas, N.A., Mechanisms of solute and drug transport in relaxing, swellable, hydrophilic glassy polymers. *Polymer* 40 (1999a) 3383-3398.

Brazel, C.S., Peppas, N.A., Dimensionless analysis of swelling of hydrophilic glassy polymers with subsequent drug release from relaxing structures. *Biomaterials* 20 (1999b) 721-732.

Brazel, C.S., Peppas, N.A., Modeling of drug release from swellable polymers. *Eur. J. Pharm Biopharm.* 49 (2000) 47-58 .

Bromberg, L.E., Ron, E.S., Temperature-responsive gels and thermogelling polymer matrices for protein and peptide delivery. *Adv. Drug Del. Rev.* 31 (1998) 197-221.

Brownlee, M., Cerami, A., A glucose-controlled insulin-delivery system: semisynthetic insulin bound to lectin. *Science* 206 (1979) 1190-1191.

Büchi, V.J., Hansen, J.B., Tammilehto, S.A., Physikalisch-chemische Eigenschaften und antimikrobielle Wirksamkeit einiger 4-Hydroxybenzoeaureester. *Pharm. Acta. Helv.* 46 (1971) 620-626.

Bustamante, P., Pena, M.A., Barra, J., The modified extended Hansen method to determine partial solubility parameters of drugs containing a single hydrogen bonding group and their sodium derivatives: benzoic acid/Na and ibuprofen/Na. *Int. J. Pharm.* 194 (2000) 117-124.

Canal, T., Peppas, N., Correlation between mesh size and equilibrium degree of swelling of polymeric networks. *J. Biomed. Mater. Res.* 23 (1989) 1183-1193.

Chilkoti, A., Dreher, M.R., Meyer, D.E., Raucher, D., Targeted drug delivery by thermally responsive polymers. *Adv. Drug Del. Rev.* 54 (2002) 613-630.

Chiou, W.L., Kyle, L.E., Differential thermal, solubility, and aging studies on various sources of digoxin and digitoxin powder: biopharmaceutical implications. *J. Pharm. Sci.* 10 (1979) 1224-1229.

Chun, S-W., Kim, J-D., A novel hydrogel-dispersed composite membrane of poly(N-isopropylacrylamide) in a gelatin matrix and its thermally actuated permeation of 4-acetamidophen. *J. Cont. Rel.* 38 (1996) 39-47.

Colombo, P., Swelling-controlled release in hydrogel matrices for oral route. *Adv. Drug Del. Rev.* 11 (1993) 37-57.

Colombo, P., Bettini, R., Massimo, G., Catellani, P.L., Santi, P., Peppas, N.A., Drug diffusion front movement is important in drug release control from swellable matrix tablets. *J. Pharm. Sci.* 84 (1995) 991-997.

Colombo, I., Grassi, M., Fermeglia, M., Lapasin, R., Pricl, S., Modeling phase transitions and sorption desorption kinetics in thermo-sensitive gels for controlled drug delivery systems. *Fluid Phase Equilibria* 116 (1996) 148-161.

Connors, K.A., *Binding Constants:* The measurement of molecular complex stability. John Wiley & sons, New York, 1987

Corrigan O.I., Stanley, C.T., Dissolution properties of phenobarbitone-ß-cyclodextran systems. *Pharm. Acta. Helv.* 56 (1981) 204-208.

Costo, P., Lobo J.M.S., Modeling and comparison of dissolution profiles. *Eur. J. Pharm. Sci.* 13 (2001) 123-133.

Crank, J., *The mathematics of diffusion*, 2nd ed., Clarendon Press, Oxford, 1975

David, G., Alupei, V., Simionescu, B.C., Dincer, S., Piskin, E., Poly(N-isopropylacrylamide)/poly[(N-acetylimino)ethylene] thermosensitive block and graft copolymers. *European Polymer Journal* 39 (2003) 1209-1213.

Davidson III, G.W.R., Peppas, N.A., Solute and penetrant diffusion in swellable polymers VI. The Deborah and swelling interface numbers as indicators of the order of biomolecule release. *J. Cont. Rel.* 3 (1986) 259-271.

D'Emanuele, A., Dinarvand, R., Preparation, characterization, and drug release from thermoresponsive microspheres. *Int. J. Pharm.* 118 (1995) 237-242.

Desai, S.J., Simonelli, A.P., Higuchi, W.I., Investigation of factors influencing release of solid drug dispersion inert matrices. *J. Pharm. Sci.* 54 (1965) 1459-1464.

Dinarvand, R., D'Emanuele, A., The use of thermoresponsive hydrogels for on-off release of molecules. *J. Cont. Rel.* 36 (1995) 221-227.

Dittgen, M., Durrani, M., Lehmann, K., Acrylic polymers. A review of pharmaceutical applications. *S.T.P. Pharma. Sci.* 7 (1997) 403-457.

Dong, L.C., Hoffman, A.S., Thermally reversible hydrogels III. Immobilization of enzymes for feedback reaction control. *J. Cont. Rel.* 4 (1986) 223-227.

Dong, L-C., Hoffman, A.S., A novel approach for preparation of pH-sensitive hydrogels for enteric drug delivery. *J. Cont. Rel.* 15 (1991) 141-152.

Dong, L-C., Hoffman, A.S., Yan, Q.I. Dextran permeation through poly(N-isopropylacrylamide) hydrogels. *J. Biomater. Sci. Polymer Edn.* 5 (1994) 473-484.

am Ende, M.T., Hariharan, D., Peppas, N.A., Factors influencing drug and protein transport and release from ionic hydrogels. *Reactive polymers* 25 (1995) 127-137.

Eddington, D.T., Beebe, D.J., Flow control with hydrogels. *Adv. Drug Del. Rev.* 56 (2004) 199-210.

Eeckman, F., Amighi, K., Moes, A.J., Effect of some physiological and non-physiological compounds on the phase transition temperature of thermoresponsive polymers intended for oral controlled-drug delivery. *Int. J. Pharm.* 222 (2001) 259-270

Elbary, A.A., Vallner, J.J., Whitworth, C.W., Effect of albumin conformation on the binding of phenylbutazone and oxyphenbutazone to human serum albumin. *J. Pharm. Sci.* 71 (1982) 241-244.

Feil, H., Bae, Y.H., Feijen, J., Kim, S.W., Effect of comonomer hydrophilicity and ionisation on the lower critical solution temperature of N-isopropylacrylamide copolymers. *Macromolecules* 26 (1993) 2496-2500.

Forster, A., Hempenstall, J., Tucker, I., Rades, T., Selection of excipients for melt extrusion with two poorly water-soluble drugs by solubility parameter calculation and thermal analysis. *Int. J. Pharm.* 226 (2001) 147-161.

Gangakhedkar, N.S., Namjoshi, A.V., Tamhane, P.S., Chaudhuri, N.K., Polarization study of electronic transitions in molecules in a stretched PVA matrix using their projected three dimensional vibrational space. *J. Chem. Phys.* 60 (1974) 2584-2593.

Gee, R.H., Boyd, R.H., Small penetrant diffusion in polybutadiene: a molecular dynamics simulation study. *Polymer* 36 (1995) 1435-1440.

Gehrke, S.H., Uhden, L., Schiller, M.E., Enhanced loading and activity retention of proteins in hydrogel delivery systems. *Proceed. Inter. Symp. Cont. Rel. Bio. Mat.* 22 (1995) 145-146.

Goodhart, F.W., Martin, A.N., Solubilization of benzoic acid derivatives by polyoxyethylene stearates. *J. Pharm. Sci.* 51 (1962) 50-54.

Gordon, M., Taylor, J.S., Ideal copolymers and the second-order transitions of synthetic rubbers. I. Non-crystalline copolymers. *J. Appl. Chem.* 2 (1952) 493-500.

Grassi, M., Lapasin, R., Pricl, S., Modeling of drug release from a swellable matrix. *Chem. Eng. Comm.* 169 (1998) 79-109.

Greenhalgh, D.J., Williams, A.C., Timmins, P., York, P., Solubility parameters as predictors of miscibility in solid dispersions. *J. Pharm Sci.* 88 (1999) 1182-1190.

Grodzinsky, A.J., Grimshaw, P.E., Electrically and chemically controlled hydrogels for drug delivery, in: I. Kost (Ed), *Pulsed and Self-Regulated Drug Delivery*, CRC Press, Boca Raton, FL, 1990, 47-64.

Gupta, A.K., Madan, S., Majumdar, D.K., Maitra, A., Ketorolac entrapped in polymeric micelles: preparation, characterisation and ocular anti-inflammatory studies. *Int. J. Pharm.* 209 (2000) 1-14.

Gupta, K.C., Khandekar, K., Temperature-responsive cellulose by ceric(IV) ion-initiated graft copolymerisation of N-isopropylacrylamide. *Biomacromolecules* 4 (2003) 758-765.

Gupta, P., Vermani, K., Garg, S., Hydrogels: from controlled release to pH responsive drug delivery. *Drug Discovery Today* 7 (2002) 569-579.

Gutierrez-Roca, J.C., McGinity, J.W., Influence of water soluble and insoluble plasticizers on the physical and mechanical properties of acrylic resin copolymers. *Int. J. Pharm.* 103 (1994) 293-301.

Gutowska, A., Bae, Y.H., Feijen, J., Kim, S.W., Heparin release from thermosensitive hydrogels. *J. Cont. Rel.* 22 (1992) 95-104.

Gutowska, A., Bae, Y.H., Jacons, H., Feijen, J., Kim, S.W., Thermosensitive interpenetrating polymer networks: synthesis, characterisation, and macromolecular release. *Macromolecules* 27 (1994) 4167-4175.

Gutowska, A., Bark, J.S., Kwon, I.C., Bae, Y.H., Cha, Y., Kim, S.W., Squeezing hydrogels for controlled oral drug delivery. *J. Cont. Rel.* 48 (1997) 141-148.

Hadgett, P.M., Goldbeck-Wood, G., Windle, A.H., Lattice modelling of penetrant diffusion through heterogeneous polymers. *Polymer* 41 (2000) 6151-6160.

Han, J., Gee, R.H., Boyd, R.H., Glass transition temperatures of polymers from molecular dynamics simulations. *Macromolecules* 27 (1994) 7781-7784.

Han, M-H., Kim, J-W., Kim, J., Ko, J.Y., Magda, J.J., Han, I.S., Temperature-dependent transparency of poly(HPMA-co-DMA) hydrogels: effect of synthesis parameters. *Polymer* 44 (2003) 4541-4546.

Hancock, B.C., York, P., Rowe, R.C., The use of solubility parameters in pharmaceutical dosage form design. *Int. J. Pharm.* 148 (1997) 1-21.

Havemeyer, R.N., Higuchi, T., The complexing tendencies of cyanocobalamin with inorganic compounds. *J. Am. Pharm. Assoc.* 49 (1960) 356-360.

Hassan, C.M., Doyle, F.J.I., Peppas, N.A., Dynamic behavior of glucose-responsive poly(methacrylic acid-g-ethyleneglycol) hydrogels, *Macromolecules* 30 (1997) 6166-6173.

Hayashi, S., Umemura, J., Disappearances of COOH infrared bands of benzoic acid *J. Chem. Phys.* 60 (1974) 2630-2633.

Higuchi, T., Connors, K.A., "*Phase solubility techniques*" In Advances in Analytical Chemistry and Instrumentation. New York: Reilly, C.N., (1965) 117-211.

Higuchi, T., Lach, J.L., Investigation of some complexes formed in solution by caffeine IV. Interactions between caffeine and sulfathiazole, sulfadiazine, p-aminobenzoic acid, benzocaine, phenobarbitol, and barbitol. *J. Am. Pharm. Assoc.* 43 (1954) 349-354.

Higuchi, T., Zuck, D.A., Investigation of some complexes formed in solution by caffeine. II Benzoic acid and benzoate ion. *J. Am. Pharm. Ass.* 42 (1953) 132-137.

Higuchi, W.I., Rate of release of medicaments from ointment bases containing drugs in suspension. *J. Pharm. Sci.* 50 (1961) 874-875.

Higuchi, W.I., Analysis of data on the medicament release from ointments. *J. Pharm. Sci.* 51 (1962) 802-804.

Hinrichs, W.L.J., Schuurmans-Nieuwenbroek, N.M.E., van de Wetering, Hennink, W.E., Thermosensitive polymers as carriers for DNA delivery. *J Cont. Rel.* 60 (1999) 249-259.

Hixson, A.W., Crowell, J.H., Dependence of reaction velocity upon surface and agitation, *Ind. Eng. Chem.* 23 (1931) 923-931.

Hoffman, A.S., Application of thermally reversible polymers and hydrogels in therapeutics and diagnostics. *J Cont. Rel.* 6 (1987) 297-305.

Hoffman, A.S., Afrassiabi, A., Dong, L.C., Thermally reversible hydrogels: II. Delivery and selective removal of substances from aqueous solutions. *J. Cont. Rel.* 4 (1986) 213-222.

Hoffman, A.S., Chen, G., Kaang, S., Priebe, D.T., New bioadhesive polymer compositions for prolonged drug release in the eye. *Proceed. Intern. Symp. Control. Rel. Bioact. Mater.* 22 (1995) 159-160.

Hofmann, D., Fritz, L., Ulbrich, J., Schepers, C., Bohning, M., Detailed-atomistic molecular modelling of small molecule diffusion and solution processes in polymeric membrane materials. *Macromol. Theory Simul.* 9 (2000) 293-327.

Horne, R.A., Almeida, J.P., Day, A.F., Yu, N.-T., Macromolecular hydration and effect of solutes on the cloud point of aqueous solutions of polyvinyl-methyl-ether: a possible model for protein denaturation and temperature control in homeothermic animals. *J. Colloid Surfaces Sci.* 35 (1971) 77-84.

Hovgaard, L., Brondsted, H., Dextran hydrogels for colon specific drug delivery, *J. Cont. Rel.* 36 (1995) 159-166.

Hsiue, G-H., Hsu, S., Yang, C-C., Lee, S-H., Yang, I-K, Preparation of controlled release ophthalmic drops, for glaucoma therapy using thermosensitive poly-N-isopropylacrylamide. *Biomaterials* 23 (2002) 457-462.

Hsiue, G-H., Chang, R-W., Wang, C-H., Lee, S-H., Development of in situ thermosensitive drug vehicles for glaucoma therapy. *Biomaterials* 24 (2003) 2423-2430.

Huglin, M.B., Velada, J.L., Thermoreversible swelling behaviour of hydrogels based on N-isopropylacrylamide with acidic comonomers. *Polymer* 38 (1997) 5785-5791.

Ichikawa, H., Fukumori, Y., New applications of acrylic polymers for thermosensitive drug release. *S.T.P. Pharma Sciences* 7 (1997) 529-545.

Ichikawa, H., Fukumori, Y., A novel positively thermosensitive controlled-release microcapsule with membrane of nano-sized poly(N-isopropylacrylamide) gel dispersed in ethylcellulose matrix. *J. Cont. Rel.* 63 (2000) 107-119.

Ishikiriyama, K., Sakamoto, A., Todoki, M., Tayama, T., Tanaka, K., Kobayashi, T., Pore size distribution measurements of polymer hydrogel membranes for artificial kidneys using differential scanning calorimetry. *Thermochimica Acta* 267 (1995) 169-180.

Ito, Y., Casolaro, M., Kono, I., Yukio, I., An insulin-releasing system that is responsive to glucose. *J. Cont. Rel.* 10 (1989) 195-203.

Iza, M., Woerly, S., Danumah, C., Kaliaguine, S., Bousmina, M., Determination of pore size distribution for mesoporous materials and polymeric gels by means of DSC measurements: thermoporometry. *Polymer* 41 (2000) 5885-5893.

Jacobson, S.H., Molecular modelling studies of polymeric transdermal adhesives: structure and transport mechanisms. *Pharmaceutical Technology* (1999) 120-130

Jeong, B., Bae, Y.H., Lee, D.S., Kim, S.W., Biodegradable block copolymers as injectible drug delivery systems. *Nature* 388 (1997) 860-862.

Jeong, B., Kim, S.W., Bae, Y.H., Thermosensitive sol-gel reversible hydrogels. *Adv. Drug Del. Rev.* 54 (2002) 37-51.

Johnson, S.L., Rumon, K.A., Infrared spectra of solid 1:1 pyridine-benzoic acid complexes; the nature of the hydrogen bond as a function of the acid-base levels in the complex. *J. Phys. Chem.* 69 (1965) 74-86.

Johnson, B.D., Beebe, D.J., Crone, W.C., Effects of swelling on the mechanical properties of a pH-sensitive hydrogel for use in microfluidic devices. *Materials Science and Engineering C* 24 (2004) 575-581.

Juodkazis, S., Mukai, N., Wakaki, R., Yamaguchi, A., Matsuo, S., Misawa, H., Reversible phase transitions in polymer gels induced by radiation forces. *Nature* 408 (2000) 178-181.

Kabiri, K., Omidian, H., Hashemi, S.A., Zohuriaan-Mehr, M.J., Synthesis of fast-swelling superabsorbent hydrogels: effect of crosslinker type and concentration on porosity and absorption rate. *European Polymer Journal* 39 (2003) 1341-1348.

Kabra, B.G., Akhtar, M.K., Gehrke, S.H., Volume change kinetics of temperature-sensitive poly(vinyl methyl ether) gel. *Polymer* 33 (1992) 990-995.

Kajiwara, K., Ross-Murphy, S.B., Synthetic gels on the move. *Nature* 355 (1992) 208-209.

Katime, I., Novoa, R., Zuluaga, F., Swelling kinetics and release studies of theophylline and aminophylline from acrylic acid/n-alkyl methacrylate hydrogels. *Eur. Poly. J.* 37 (2001) 1465-1471.

Katono, H., Maruyama, A., Sanui, K., Ogata, N., Okano, T., Sakurai, Y., Thermoresponsive swelling and drug release switching of interpenetrating polymer networks composed of poly(acrylamide-co-butylmethacrylate) and polyacrylic acid. *J. Cont. Rel.* 16 (1991) 215-228

Kerč, J., Srčič, S., Thermal analysis of glassy pharmaceuticals. *Thermochimica Acta* 248 (1995) 81-95.

Kim, S.W., Pai, C.M., Makino, K., Seminoff, L.A., Holmberg, D.L., Gleeson, J.M., Wilson, D.E., Mack, E.J., Self-regulated glycosylated insulin delivery. *J. Cont. Rel.* 11 (1990) 193-201.

Kim, S.W., Bae, Y.H., Okano, T., Hydrogels: swelling, drug loading, and release. *Pharm. Res.* 9 (1992) 283-290.

Kim, I.S., Jeong, Y-I., Cho, C-S., Kim, S-H., Core-shell type polymeric nanoparticles composed of poly(L-lactic acid) and poly(N-isopropylacrylamide). *Int. J. Pharm.* 211 (2000) 1-8.

Kim, Y-H., Bae, Y.H., Kim, S.W., pH/temperature-sensitive polymers for macromolecular drug loading and release. *J. Cont. Rel.* 28 (1994) 143-152.

Kitano, S., Koyama, Y., Kataoka, K., Okano, T., Sakurai, Y., A novel drug delivery system utilizing a glucose responsive polymer complex between poly(vinyl alcohol) and poly(N-vinyl-2-pyrrolidone) with a phenyl boronic acid moiety. *J. Cont. Rel.* 19 (1992) 162-170.

Kohori, F., Sakai, K., Aoyagi, T., Yokoyama, M., Sakurai, Y., Okano, T., Preparation and characterization of thermally responsive block copolymer micelles comprising poly(N-isopropylacrylamide-b-DL-lactide). *J. Cont. Rel.* 55 (1998) 87-98.

Kokufuta, E., Zhang, Y-Q., Tanaka, T., Mamada, A., Effects of surfactants on the phase transition of poly(N-isopropylacrylamide) gel. *Macromolecules* 26 (1993) 1053-1059.

Kono, K., Hayashi, H., Takagishi, T., Temperature-sensitive liposomes: liposomes bearing poly(N-isopropylacrylamide). *J. Cont. Rel.* 30 (1994) 69-75.

Kono, K., Henmi, A., Takagishi, T., Temperature-controlled interaction of thermosensitive polymer-modified cationic liposomes with negatively charged phospholipid membranes. *Biochimica et Biophysica Acta* 1421 (1999) 183-197.

Kono, K., Thermosensitive polymer-modified liposomes. *Adv. Drug. Del. Rev.* 53 (2001) 321-339.

Korsmeyer, R.W., Peppas, N.A., Solute and penetrant diffusion in swellable polymers. III. Drug release from glassy poly(HEMA-co-NVP) copolymers. *J Cont. Rel.* 1 (1984) 89-98.

Kost, J., Wolfrum, J., Langer, R., Magnetically enhanced insulin release in diabetic rats. *J. Biomed. Mater. Res.* 21 (1987) 1367-1373.

Kost, J., Langer, R., Magnetically and ultrasonically modulated drug delivery systems, in: J. Kost (ed), *Pulsed and self-regulated drug delivery*, CRC Press, Boca Raton, FL, (1990) 3-16.

Kost, J., Langer, R., Responsive polymeric delivery systems. *Adv. Drug Del. Rev.* 6 (1991) 19-50.

Kost, J., Langer, R., Responsive polymeric systems for controlled delivery of therapeutics. *Trends in Biotechnology* 10 (1992) 127-131.

Kown, I.C., Bae, Y.H., Okano, T., Kim, S.W., Drug release from electric current sensitive polymers. *J. Cont. Rel.* 17 (1991) 149-156.

Kugita, H., Inoue, H., Ikezaki, M., Konda, M., Takeo, S., Synthesis of 1,5-benzothiazepine derivatives III. *Chem Pharm Bull* 19 (1971) 595-602.

Kurisawa, M., Matsuo, Y., Yui, N., Modulated degradation of hydrogels with thermoresponsive network in relation to their swelling behavior. *Macromol. Chem. Phys.* 199 (1998) 705-709.

Kurisawa, M., Yokoyama, M., Okano, T., Gene expression control by temperature with thermo-responsive polymeric gene carriers. *J. Cont. Rel.* 69 (2000) 127-137.

Ladanyi, B.M., Skaf, M.S., Computer simulation of hydrogen-bonding liquids. *Annu. Rev. Phys. Chem.* 44 (1993) 335-368.

Lau, A.C., Wu, C., Thermally sensitive and biocompatible poly(N-vinylcaprolactam): synthesis and characterization of high molar mass linear chains. *Macromolecules* 32 (1999) 581-584.

Lee, P.I., Kinetics of drug release from hydrogel matrices. *J. Cont. Rel.* 2 (1985) 277-288.

Lee, P.I., Kim, C-J., Probing the mechanisms of drug release from hydrogels. *J. Cont. Rel.* 16 (1991) 229-236.

Lee, S.C., Kim, C., Kwon, I.C., Kim, Y-H., Thermosensitive hydrogels based on poly(2-ethyl-2-oxazoline)/poly(ε-caprolactone) multiblock copolymers. *Proceed. Int. Symp. Control. Rel. Bioact. Mater.* 25 (1998) 717-718.

Lee, S.B., Song, S-C., Jin, J-I., Sohn, Y.S., Solvent effect on the lower critical solution temperature of biodegradable thermoresponsive poly(organophosphazenes). *Polymer Bulletin* 45 (2000) 389-396.

Li, T., Kildsig, D.O., Park, K., Computer simulation of molecular diffusion in amorphous polymers. *J. Cont. Rel.* 48 (1997) 57-66.

Lin, J.K., Ladisch, M.R., Patterson, J.A., Noller, C.H., Determining pore size distribution in wet cellulose by measuring solute exclusion using a differential refractometer. *Biotechnology and bioengineering* 29 (1987) 976-981.

Lin, W., Hu, M., Hsieh, Y-L., Kurth, M.J., Krochta, J.M., Thermosensitive lactitol-based polyether polyol (LPEP) hydrogels. *J. Poly. Sci. A, Pol. Chem.* 36 (1998) 979-984.

Lin-Vien, D., Colthup, N.B., Fateley, W.G., Grasselli, J.G., The handbook of infrared and raman characteristic frequencies of organic molecules. Academic Press, New York, 1991.

Liu, W., Zhang, B., Lu, W.W., Li, X., Zhu, D., Yao, K.D., Wang, Q., Zhao, C., Wang, C., A rapid temperature-responsive sol-gel reversible poly(N-isopropylacrylamide)-g-methylcellulose copolymer hydrogel. *Biomaterials* 25 (2004) 3005-3012.

Longhi, G., Lebon, F., Abbate, S., Fornili, S.L., Molecular dynamics simulation of a model oligomer for poly(N-isopropylamide) in water. *Chemical Physics Letters* 386 (2004) 123-127.

Lowe, T.L., Nayak, B.R., Huang, X., Engineering biodegradable-co-responsive hydrogels for drug delivery. *Proceed. Int. Symp. Control. Rel. Bioact. Mater.* 30 (2003) 707-708.

Makino, K., Hiyoshi, J., Ohshima, H., Effects of thermosensitivity of poly (N-isopropylacrylamide) hydrogel upon the duration of a lag phase at the beginning of drug release from the hydrogel. *Colloids and Surfaces B: Biointerfaces* 20 (2001) 341-346.

Mamada, A., Tanaka, T., Kungwachakun, D., Irie, M., Photo-induced phase transition of gels. *Macromolecules* 23 (1990) 1517-1519.

Mandal, T.K., Swelling-controlled release system for the vaginal delivery of miconazole. Eur. J. Pharm. Biopharm. 50 (2000) 337-343.

Markland, P., Zhang, Y.H., Amidon, G.L., Yang, V.C., A pH- and ionic strength-responsive polypeptide hydrogel: Synthesis, characterization and preliminary protein release studies. *J Biomed. Mat. Res.* 47 (1999) 595-602.

Martin, A., *Physical Pharmacy*, 4th Edition, Lea & Febiger, Philadelphia (1993).

Martindale The Extra Pharmacopoeia, Thirty–first Edition, Reynolds, J.E.F. (Ed.), The Pharmaceutical Press, London, 1996.

Meyer, D.E., Shin, B.C., Kong, G.A., Dewhirst, M.W., Chilkoti, A., Drug targeting using thermally responsive polymers and local hyperthermia. *J. Cont. Rel.* 74 (2001) 213-224.

Miyajima M., Yoshida M., Sato H., Omichi H., Katakai R., Higuchi W.I., Controlled release of 9-β-D-arabinofuranosyladenine from thermo-responsive devices based on acryloyl-L-proline methyl ester. *Int. J. Pharm.* 95 (1993) 153-160.

Miyata, T., Asami, N., Uragami, T., A reversibly antigen-responsive hydrogel. *Nature* 399 (1999) 766-769.

Miyata, T., Uragami, T., Nakamae, K., Biomolecule-sensitive hydrogels. *Adv. Drug Del. Rev.* 54 (2002) 79-98.

Miyazaki, S., Hou, W.M., Takada, M., Controlled drug release by ultrasound irradiation, *Chem. Pharm. Bull.* 33 (1985) 428-431.

Momany, F.A., Willett, J.L., Molecular dynamics calculations on amylose fragments. I. Glass transition temperatures of maltodextrose at 1,5,10 and 15.8% hydration. *Biopolymers* 63 (2002) 99-110.

Muller-Plathe, F., Diffusion of water in swollen poly(vinyl alcohol) membranes studied by molecular dynamics simulation. *J. Membrane Sci.* 141 (1998) 147-154.

Nair, R., Nyamweya, N., Gonen, S., Martinez-Miranda, L.J., Hoag, S.W., Influence of various drugs on the glass transition temperature of poly(vinylpyrrolidone): a thermodynamic and spectroscopic investigation. *Int. J. Pharm.* 225 (2001) 83-96.

Nernst, W., Brunner, E., Theorie der reaktionsgeschwindigkeit in heterogenen systemen, Z . *Phys. Chem.,* 47 (1904) 52-55; 47 (1904) 56-102.

Ni, C., Zhu, X-X., Synthesis and swelling behavior of thermosensitive hydrogels based on N-substituted acrylamides and sodium acrylate. *Eur. Poly. J.* 40 (2004) 1075-1080.

Nour, S., Vallner, J.J., An ultraviolet difference spectrophotometric method for determination of drug-binding parameters. *Analytica Chimica Acta* 162 (1984) 323-331.

NovaWin2 Version 2.1 Operation Manual, Quantachrome Instruments, 2003.

Ogata, T., Nonaka, T., Kurihara, S., Permeation of solutes with different molecular size and hydrophobicity through the poly(vinyl alcohol)-graft-N-isopropylacrylamide copolymer membrane. *J. Membrane Sci.* 103 (1995) 159-165.

Oguchi, T., Tozuka, Y., Hanawa, T., Mizutani, M., Sasaki, N., Limmatvapirat, S., Yamamoto, K., Elucidation of solid-state complexation in ground mixtures of cholic acid and guest compounds. *Chem. Pharm. Bull.* 50 (2002) 887-891.

Oh, J.S., Kim, J.M., Lee, K.J., Bae, Y.C., Swelling behavior of N-isopropylacrylamide gel particles with degradable crosslinker. *Eur. Poly. J.* 35 (1999) 621-630.

Okabe, K., Yamaguchi, H., Kawai, Y., New iontophoretic transdermal administration of the beta-blocker metoprolol. *J. Cont. Rel* 4 (1986) 79-86.

Okahata, Y., Noguchi, H., Seki, T., Thermoselective permeation from a polymer-grafted capsule membrane. *Macromolecules* 19 (1986) 493-494.

Okano, T., Bae, Y.H., Jacobs, H., Kim, S.W., Thermally on-off switching polymers for drug permeation and release. *J. Cont. Rel.* 11 (1990) 255-265.

Okhamafe, A., York, P., Thermal characterization of drug/polymer and excipient/polymer interactions in some film coating formulations. *J. Pharm. Pharmacol.* 41 (1989) 1-6.

Okuyama, Y., Yoshida, R., Sakai, K., Okano, T., Sakurai, Y., Swelling controlled zero order and sigmoidal drug release from thermoresponsive poly(N-isopropylacrylamide-co-butyl methacrylate) hydrogel. *J. Biomater. Sci. Polymer Edn.* 4 (1993) 545-556.

Omidian, H., Hashemi, S.A., Sammes, P.G., Meldrum, I., A model for the swelling of superabsorbent polymers. *Polymer* 39 (1998) 6697-6704.

Osada, Y., Okuzaki, H., Hori, H., A polymer gel with electrically driven motility. *Nature* 355 (1992) 242-244.

Otake, K., Inomata, H., Konno, M., Saito, S., Thermal analysis of the volume phase transition with N-isopropylacrylamide gels. *Marcomolecules* 23 (1990) 283-289.

Owen, C., James, K., Sampson, L., Ahmed, S., Synthesis and biochemical evaluation of some novel benzoic acid based esters as potential inhibitors of oestrone sulphatase. *J. Pharm. Pharmacol.* 55 (2003) 85-93.

Painter, P.C., Graf, J.F., Coleman, M.M., Effect of hydrogen bonding on the enthalpy of mixing and the composition dependence of the glass transition temperature of polymer blends. *Macromolecules* 24 (1991) 5630-5638.

Panomsuk, S.P., Hatanaka, T., Aiba, T., Katayama, K., Koizumi, T., A study of the hydrophilic cellulose matrix: effect of indomethacin and a water-soluble additive on swelling properties. *Int. J. Pharm.* 126 (1995) 147-153.

Park, T.G., Hoffman, A.S., Estimation of temperature-dependent pore size in poly(N-isopropylacrylamide) hydrogel beads. *Biotechnol. Prog.* 10 (1994) 82-86.

Patel, N.K., Nagabhushan, N., Drug-plastic interactions II: Sorption of p-hydroxybenzoic acid acid esters by capran polyamide and in vitro biologic activity. *J. Pharm. Sci.* 59 (1970) 264-266.

Patel, N.K., Romanowski, J.M., Heterogeneous systems II: Influence of partitioning and molecular interactions on in vitro biologic activity of preservatives in emulsions. *J. Pharm. Sci.* 59 (1970) 372-376.

Patel, V.R., Amiji, M.M., Preparation and characterization of freeze-dried chitosan-poly(ethylene oxide) hydrogels for site-specific antibiotic delivery in the stomach. *Pharm. Res.* 13 (1996) 588-593.

Peppas, N.A., *Hydrogels in medicine and Pharmacy.* Vol. I. Fundamentals. CRC Press, Inc. Boca Raton, Florida 1986.

Peppas, N.A., Lustig, S.R., The role of cross-links, entanglements, and relaxations of the macromolecular carrier in the diffusional release of biologically active materials. Conceptual and scaling relationships. *Annals of New York Academy of Sciences* 446 (1985) 26-40.

Peppas, N.A., Wright, S.L., Drug diffusion and binding in ionisable interpenetrating networks from poly(vinyl alcohol) and poly (acrylic acid). *Eur. J. Pharm. Biopharm.* 46 (1998) 15-29.

Pina, A., Nakache, E., Feret, B., Depraetere, P., Copolymer polyelectrolyte adsorption onto titanium dioxide. *Colloids and Surfaces A: Physicochemical and Engineering Aspects* 158 (1999) 375-384.

Plontke, S.K.R., Salt, A.N., Quantitative interpretation of corticosteroid pharmacokinetics in inner fluids using computer simulations. *Hearing Research* 182 (2003) 34-42.

Porcar, I., Codoner, A., Gomez, C.M., Abad, C., Campos, A., Interactions of quinine with polyacrylic and poly-L-glutamic acids in aqueous solutions. *Eur. Poly. J.* 40 (2004) 819-828.

Poupaert, J.H., Couvreur, P., A computationallty derived structural model of doxorubicin interacting with oligomeric polyalkylcyanoacrylate in nanoparticles. *J. Cont. Rel.* 92 (2003) 19-26.

Qui, Y., Park, K., Environment-sensitive hydrogels for drug delivery. *Adv. Drug Del. Rev.* 53 (2001) 321-339.

Ramkisoon-Ganorkar, C., Liu, F., Baudys, M., Kim, S.W., Effect of molecular weight and polydispersity on kinetics of dissolution and release from pH/temperature-sensitive polymers. *J. Biomater. Sci. Polymer Edn.* 10 (1999) 1149-1161.

Ranjha, N.M., Doelker, E., pH-sensitive hydrogels for site-specific drug delivery II. Drug release behaviour from crosslinked alkyl acrylates/methacrylic acid copolymers. *S.T.P. Pharma Sci.* 9 (1999) 341-349.

Ritger, P.L., Peppas, N.A., A simple equation for description of solute release I. Fickian and non-fickian release from non-swellable devices in the form of slabs, spheres, cylinders or discs. *J. Cont. Rel.* 5 (1987a) 23-36.

Ritger, P.L., Peppas, N.A., A simple equation for description of solute release II. Fickian and anomalous release from swellable devices. *J. Cont. Rel.* 5 (1987b) 37-42.

Rodriguez, R., Alvarez-Lorenzo, C., Concheiro, A., Influence of cationic cellulose structure on its interactions with sodium dodecylsulfate: implications on the properties of the aqueous dispersions and hydrogels. *Eur. J. Pharm. Biopharm.* 56 (2003) 133-142.

Rosen, S.L., *Fundamental properties of polymeric materials*. 2nd Ed., Wiley-Interscience Pub., New York, 1993.

Rost, M., Quist, P-O., Dissolution of USP predisone calibrator tablets. Effects of stirring conditions and particle size distribution. *J. Pharm. & Biomed. Anal.* 31 (2003) 1129-1143.

Rowe, R.C., Interaction of lubricants with microcrystalline cellulose and anhydrous lactose-a solubility parameter approach. *Int. J. Pharm.* 41 (1988) 223-226.

Saito, S., Konno, M., Inomata, H., Volume phase transition of N-alkylacrylamide gels. *Adv. Poly. Sci.* (1992) 207-232.

Santhanalakshmi, J., Balaji, S., Binding studies of crystal violet on proteins. *Colloids and Surfaces A: Physicochemical and Engineering Aspects* 186 (2001) 173-177.

Sasase, H., Aoki, T., Katona, H., Sanui, K., Ogata, N., Ohta, R., Kondo, T., Okano, T., Sakurai, Y., Regulation of temperature-response swelling behavior of interpenetrating networks composed of hydrogen bonding polymers. *Makromol. Chem., Rapid Commun.* 13 (1992) 577-581.

Saslawski, O., Couvreur, P., Peppas, N., Alginate magnetic release systems: crosslinked structure, Swelling and release studies. *Proceed. Int. Symp. Cont. Rel. Bioact. Mat.* 15 (1988) 26-27.

Sawahata, K., Hara, M., Yasunaga, H., Osada, Y., Electrically controlled drug delivery system using polyelectrolytes gels. *J. Cont. Rel.* 14 (1990) 253-262.

Scherer, G.W., Freezing gels. *Journal of non-crystalline solids* 155 (1993) 1-25.

Schild, H.G., Tirrell, D.A., Microcalorimetric detection of lower critical solution temperatures in aqueous polymer solutions. *J. Phys. Chem.* 94 (1990) 4352-4356.

Schild, H.G., Tirrell, D.A., Interaction of poly(N-isopropylacrylamide) with sodium n-alkyl sulfates in aqueous solution. *Langmuir* 7 (1991) 665-671.

Schild, H.G., Poly(N-isopropylacrylamide): experiment, theory and application. *Prog. Polym. Sci.* 17 (1992) 163-249.

Scientist Handbook, Micromath Scientific Software, Utah, U.S.A (1995).

Seminoff, L.A., Olsen, G.B., Kim, S.W., A self-regulating insulin delivery system. I. Characterisation of a synthetic glycosylated insulin derivative. *Int. J. Pharm.* 54 (1989) 241-249.

Sen, M., Uzun, C., Safrany, A., Kantoglu, O., Guven, O., Changing of network characteristics of acrylamide/maleic acid hydrogels by alteration of irradiation dose rate. *Radiation physics and chemistry* 67 (2003) 371-374.

Shah, S.S., Kulkarni, M.G., Mashelkar, R.A., pH Dependent zero-order release from glassy hydrogels: penetration vs. diffusion control. *J. Cont. Rel.* 15 (1991) 121-132.

Shamblin, S.L., Taylor, L.S., Zografi, G., Mixing behavior of colyophilized binary systems. *J. Pharm. Sci.* 87 (1998) 694-701.

Shin, Y., Chang, J.H., Liu, J., Williford, R., Shin, Y-K., Exarhos, G.J., Hybrid nanogels for sustainable positive thermosensitive drug release. *J. Cont. Rel.* 73 (2001) 1-6.

Siddiqui, O., Sun, Y., Liu, J.C., Chien, Y.W., Facilitated transdermal transport of insulin. *J. Pharm. Sci.* 76 (1987) 341-345.

Siegel, R.A., Falamarzian, B.A., Firestone, B.C., Moxley, B.C., pH-controlled release from hydrophobic/polyelectrolyte copolymer hydrogels. *J. Cont. Rel.* 8 (1988) 179-182.

Siepmann, J., Podual, K., Sriwongjanya, M., Peppas, N.A., Bodmeier, R., A new model describing the swelling and drug release kinetics from hydroxypropyl methylcellulose tablets. *J. Pharm. Sci.* 88 (1999) 65-72.

Sihma, R., Boyer, R.F., On a general relation involving the glass temperature and coefficients of expansion of polymers. *J. Chem. Phys.* 37 (1962) 1003-1007.

Sousa, R.G., Magalhaes, W.F., Freitas, R.F., Glass transition and thermal stability of poly(N-isopropylacrylamide) gels and some of their copolymers with acrylamide. *Polymer Degradation and Stability* 61 (1998) 275-281.

Stone, J.E., Scallan, A.M., A structural model for the cell wall of water-swollen wood pulp fibres based on their accessibility to macromolecules. *Cellulose Chem.. Technol.* 2 (1968) 343-358.

Suzuki, A., Tanaka, T., Phase transition in polymer gels induced by visible light. *Nature* 346 (1990) 345-347.

Tachibana, Y., Kurisawa, M., Uyama, H., Kakuchi, T., Kobayashi, S., Biodegradable thermoresponsive poly(amino acid)s. *Chem Commun.* (2003) 106-107.

Takayama, K., Nambu, N., Nagai, T., Interaction of sulfonamides with cyclic polyether 18-crown-6 in solution and in solid state. *Chem. Pharm. Bull.* 25 (1977) 2608-2612.

Tamai, Y., Tanaka, H., Nakanishi, K., Molecular dynamics study of water in hydrogels. Hydrogen-bond structure. *Molecular Simulation* 16 (1996a) 359-374.

Tamai, Y., Tanaka, H., Nakanishi, K., Molecular dynamics study of polymer-water interaction in hydrogels. 1. Hydrogen-bond structure. *Macromolecules* 29 (1996b) 6750-6760.

Tanaka, T., Inoue, H., Date, T., Okamura, K., Aoe, K., Takeda, M., Hiroshi, K., Murata, S., Yamaguchi, T., Kikkawa, K., Nakajima, S., Nagao, T., Synthesis of the optically active trans-isomers of diltiazem and their cardiovascular effects and Ca-antagonistic activity. *Chem. Pharm. Bull.* 40 (1992) 1476-1480.

Taylor, L.S., Zografi, G., Sugar-polymer hydrogen bond interactions in lyophilised amorphous mixtures. *J. Pharm. Sci.* 87 (1998) 1615-1621.

Tong, P., Zografi, G., Solid-state characterization of amorphous sodium indomethacin relative to its free acid. *Pharm. Res.* 16 (1999) 1186-1192.

Tong, P., Taylor, L.S., Zografi, G., Influence of alkali metal counterions on the glass transition temperature of amorphous indomethacin salts. *Pharm. Res.* 19 (2002) 649-654.

Tsige, M., Taylor, P.L., Simulation study of the glass transition temperature in poly(methyl methacrylate). *Phys. Rev. E.* 65 (2002) 1-8.

Tyle, P., Iontophoretic devices for drug delivery. *Pharm. Res.* 3 (1986) 318-345.

Tyrrell, H.J.V., Harris, K.R., *Diffusion in Liquids:* A theoretical and experimental study. Butterworths and Co., 1984.

Uludag, H., Norrie, B., Kousinioris, N., Gao, T., Engineering temperature-sensitive poly(N-isopropylacrylamide) polymers as carriers of therapeutic proteins. *Biotechnology and Bioengineering.* 73 (2001) 510-521.

United States Pharmacopoeia XXIV, United States Pharmacopoeial Convention, Rockville, Maryland, 2000.

Vaisman, I.I., Berkowitz, M.L., Local structural order and molecular associations in water-DMSO mixtures. Molecular dynamics study. *J. Am. Chem. Soc.* 114 (1992) 7889-7896.

Vakkalanka, S.K., Brazel, C.S., Peppas, N.A., Temperature- and pH-sensitive terpolymer for modulated delivery of streptokinase. *J. Biomater. Sci. Polymer Edn.* 8 (1996) 119-129.

Van Krevelen, D., *Properties of polymers*: Their correlation with chemical structure. Elsevier, New York (1990) 189-224.

Vyavahare, N.R., Kulkarni, M.G., Mashelkar, R.A., Zero-order release from glassy hydrogels: enigma of the swelling interface number. *J. Membrane Sci.* 49 (1990) 207-222.

Walther, D.H., Sin, G.H., Blanch, H.W., Prausnitz, J.M., Pore-size distributions of cationic 2-hydroxyethyl methacrylate (HEMA) hydrogels. *Polymer gels and networks* 3 (1995) 29-45.

Wang, L-Q., Tu, K., Li, Y., Zhang, J., Jiang, L., Zhang, Z., Synthesis and characterisation of temperature responsive graft copolymers of dextran with poly(N-isopropylacrylamide). *Reactive & Functional Polymers* 53 (2002) 19-27.

Weidner, J., Drug delivery and drug targeting. *Drug Discovery Today* 6 (2001) 1239-1241.

Wolkers, W.F., Oliver, A.E., Tablin, F., Crowe, J.H., A Fourier-transform infrared spectroscopy study of sugar glasses. *Carbohydrate research* 339 (2004) 1077-1085.

Wu, J.Y., Yang, Y.Y., Heng, P.W.S., Moochhala, S., Evaluating protein release and interactions with thermosensitive PNIPAAm hydrogels. *Proceed. Intern. Symp. Control. Rel. Bioact. Mater. 30* (2003) 696-697.

Wu, X.S., Hoffman, A.S., Yager, P., Synthesis and characterization of thermally reversible macroporous poly(N-isopropylacrylamide) hydrogels. *J. Polym. Sci., Part A* 30 (1992a) 2121-2129.

Wu, X.S., Hofman, A.S., Yager, P., Conjugation of phosphatidylethanolamine to poly(N-isopropylacrylamide) for potential use in liposomal drug delivery systems. *Polymer* 33 (1992b) 4659-4662.

Xiao, C., Zhou, G., Synthesis and properties of degradable poly(vinyl alcohol) hydrogel. *Polymer degradation and stability* 81 (2003) 297-301.

Xue, W., Champ, S., Huglin, M.B., Network and swelling parameters of chemically crosslinked thermoreversible hydrogels. *Polymer* 42 (2001) 3665-3669.

Xue, W., Hamley, I.W., Thermoreversible swelling behaviour of hydrogels based on N-isopropylacrylamide with a hydrophobic comonomer. *Polymer* 43 (2002) 3069-3077.

Yildiz, B., Isik, B., Kis, M., Synthesis and characterization of thermoresponsive isopropylacrylamide-acrylamide hydrogels. *Eur. Poly. J.* 38 (2002) 1343-1347.

Ying, L., Kang, E.T., Neoh, K.G., Characterization of membranes prepared from blends of poly(acrylic acid)-graft-poly(vinylidene fluoride) with poly(N-isopropylacrylamide) and their temperature- and pH-sensitive microfiltration. *J. Membrane Sci.* 224 (2003) 93-106.

Yokoyama, M., Miyazaki, T., Chung, J.E., Nakayama, M., Okano, T., Temperature responsive polymeric micelles for double targeted drug delivery. *Inter. Symp. Microencapsulation* 14 (2003) 7-8.

Yoshida, M., Asano, M., Kumakura, M., A new temperature-sensitive hydrogel with α-amino acid group as side chain of polymer. *Eur. Polym. J.* 25 (1989) 1197-1202.

Yoshida R., Sakai K., Okano T., Sakurai, Y., A new model for zero-order drug release I. Hydrophobic drug release from hydrophilic polymeric matrices. *Polymer Journal* 23 (1991a) 1111-1121.

Yoshida R., Sakai K., Okano T., Sakurai, Y., Bae, Y.H., Kim, S.W., Surface modulated skin layers of thermal responsive hydrogels as on-off switches: I. Drug release. *J. Biomater. Sci. Polymer Edn.*, 3 (1991b) 155-162.

Yoshida M., Asano M., Kumakura M., Kataki R., Mashimo, T., Yuasa, H., Yamanaka, H., Thermoresponsive hydrogels based on acryloyl-L-proline methyl ester and their use as long acting testosterone delivery systems. *Drug Design and Delivery* 7 (1991c) 159-174.

Yoshida, R., Sakai K., Okano T., Sakurai, Y., Drug release profiles in the shrinking process of thermoresponsive poly (N-isopropylacrylamide-co-alkyl methacrylate) gels. *Ind. Eng. Chem. Res.* 31 (1992) 2339-2345.

Yoshida, R., Okuyama, Y., Sakai, K., Okano, T., Sakurai, Y., Sigmoidal swelling profiles for temperature-responsive poly (N-isopropylacrylamide-co-butyl methacrylate) hydrogels. *J. Membrane Sci.* 89 (1994a) 267-277.

Yoshida, R., Sakai K., Okano T., Sakurai, Y., Modulating the phase transition temperature and thermosensitivity in N-isopropylacrylamide copolymer gels. *J. Biomater. Sci. Polymer Edn.* 6 (1994b) 585-598.

Yoshida, R., Kaneko, Y., Sakai K., Okano T., Sakurai, Y., Bae, Y.H., Kim, S.W., Positive thermosensitive pulsatile drug release using negative thermosensitive hydrogels. *J. Cont. Rel.* 32 (1994c) 97-102.

Yoshida, R., Uchida, K., Kaneko, Y., Sakai, K., Kikuchi, A., Sakurai, Y., Okano, T., Comb-type grafted hydrogels with rapid de-swelling response to temperature changes. *Nature* 374 (1995) 240-242.

Yoshioka, M., Hancock, B.C., Zografi, G., Inhibition of indomethacin crystallization in poly(vinylpyrrolidone) coprecipitates. *J. Pharm. Sci.* 84 (1995) 983-986.

Yoshioka, S., Aso, Y., Kojima, S., Prediction of glass transition temperature of freeze-dried formulations by molecular dynamics simulation. *Pharm. Res.* 20 (2003) 873-878.

Yu, H., Grainger, D.W., Modified release of hydrophilic, hydrophobic and peptide agents from ionised amphiphilic gel networks. *J. Cont. Rel.* 34 (1995) 117-127.

Yui, N., Okano, T., Skurai, Y., Photo-responsive degradation of heterogeneous hydrogels comprising crosslinked hyaluronic acid and lipid microspheres fro temporal drug delivery. *J. Cont. Rel.* 26 (1993) 141-145.

Zhang, J., Peppas, N.A., Morphology of poly(methacrylic acid)/poly(N-isopropylacrylamide) interpenetrating polymeric networks. *J. Biomater. Sci. Polymer Edn.* 13 (2002) 511-525.

Zhang, X., Li, Y., Hu, Z., Littler, C.L., Bending of N-isopropylacrylamide gel under the influence of infrared light. *J. Chem. Phys.* 102 (1995) 551-555.

Zhang, X-Z., Zhuo, R-X., Cui, J-Z., Zhang, J-T., A novel thermo-responsive drug delivery system with positive controlled release. *Int. J. Pharm.* 235 (2002) 43-50.

Zhang, R., Li, W., Liang, X., Wu, G., Lu, Y., Zhan, L., Lu, C., Ling, L., Effect of hydrophobic group in polymer matrix on porosity of organic and carbon aerogels from sol-gel polymerisation of phenolic resole and methylolated melamine. *Microporous and mesoporous materials.* 62 (2003) 17-27.

Zhong, X., Wang, Y-X., Wang, S-C., Pressure dependence of the volume phase transition of temperature sensitive gels. *Chem. Eng. Sci.* 51 (1996) 3235-3239.

Zygourakis, K., Markenscoff, P.A., Computer-aided design of bioerodible devices with optimal release characteristics: a cellular automata approach. *Biomaterials* 17 (1996) 125-135.

Appendix I:

Calibration Curves

(A) Calibration curves in form y = mx + c, where y is absorbance at given wavelength and x is concentration (mg/ml)

Drug Assays (UV):		
In phosphate buffer pH 6.8 (isotonic)		
NaB(224nm):	y = 55.087x + 0.009	R^2 = 0.9995
BA(224nm):	y = 63.451x + 0.0174	R^2 = 0.9993
MHB(256nm):	y = 91.275x + 0.0232	R^2 = 0.9988
PHB(256nm):	y = 76.488x +0.0106,	R^2 = 0.9998
DHCl(238nm):	y = 52.049x – 0.0209	R^2 = 0.9945
DB(238nm):	y = 55.791x + 0.010	R^2 = 0.9998
VB(362nm):	y = 18.394x +0.0053	R^2 = 0.9998
In 0.01M HCl (isotonic)		
BA(230nm):	y = 79.812x + 0.0357	R^2= 0.9976
MHB(256nm):	y = 86.085x + 0.0367	R^2 = 0.9988
PHB(256nm):	y = 77.829x +0.0209	R^2 = 0.9969

(B) Calibration curve obtained for GPC using polystyrene standards in DMF

Gel Permeation Chromatography (GPC):	
In DMF	
$Log_e^{(Molecular\ weight)}$ = -1.3906*(elution time) + 22.701	R^2 = 0.9933

Appendix II:

Glass Transition Temperature of Drug-Polymer Co-Precipitate Blends

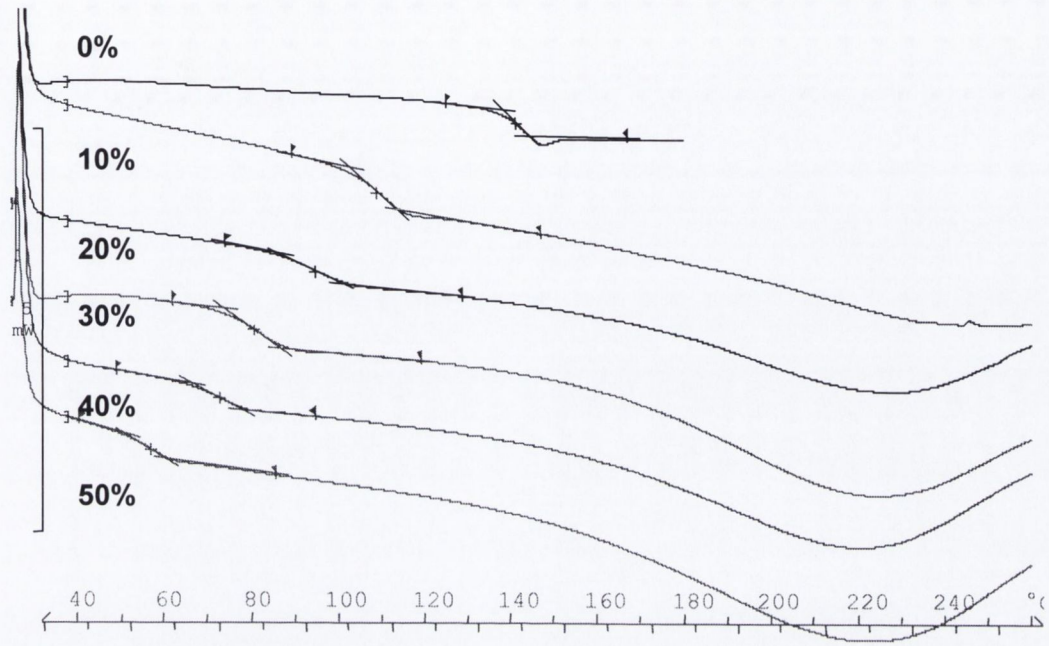

Fig. 1: Glass transition temperature of BA/PNIPA-L co-precipitate blends containing shown % w/w of BA (Heating rate 10°C/min)

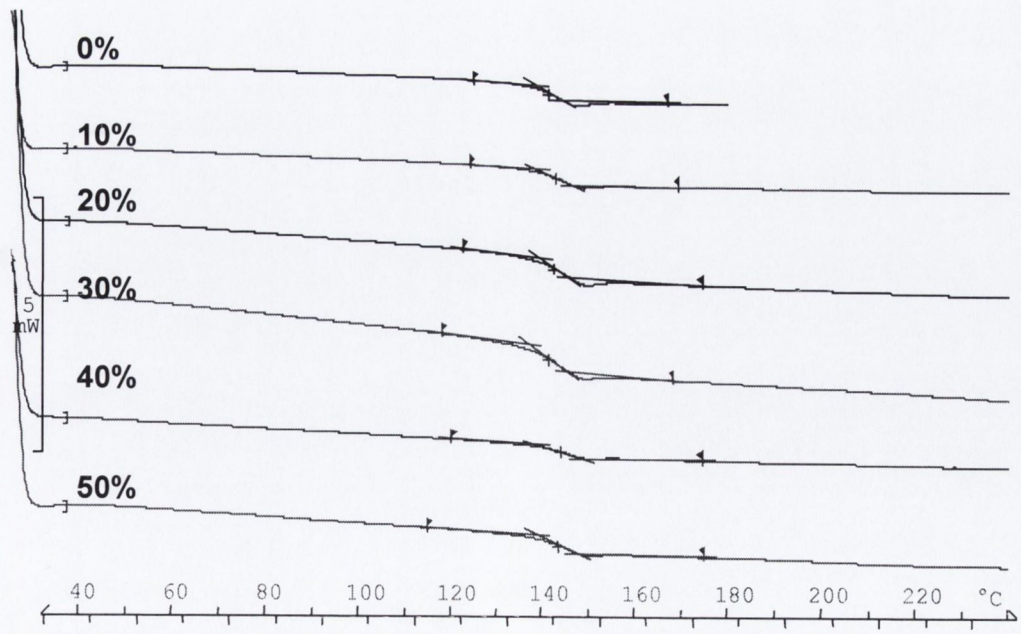

Fig. 2: Glass transition temperature of NaB/PNIPA-L co-precipitate blends containing shown % w/w of NaB (Heating rate 10°C/min)

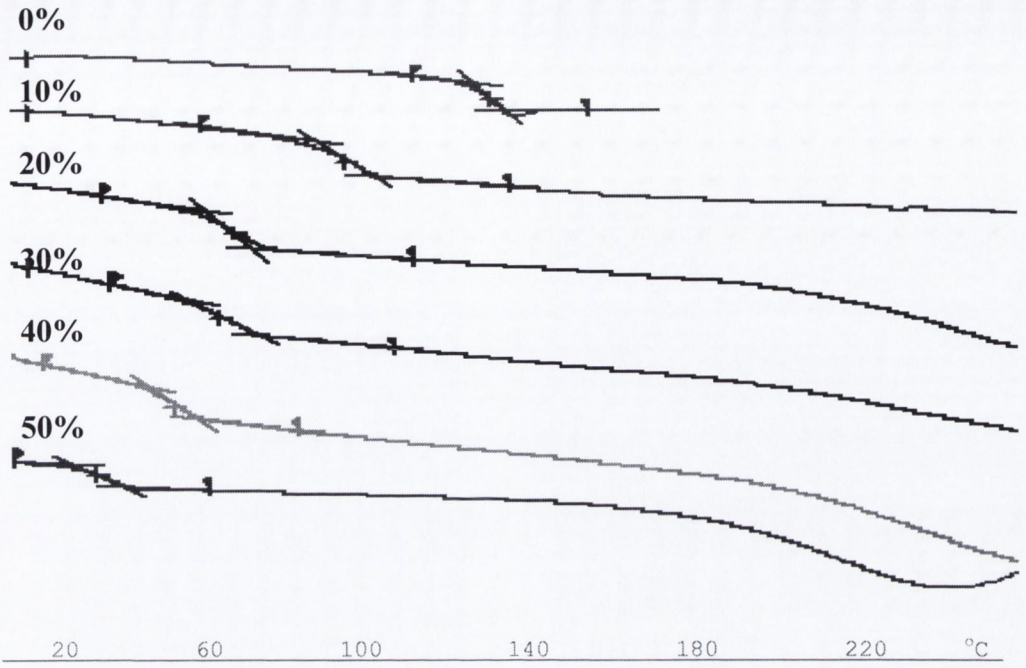

Fig. 3: Glass transition temperature of MHB/PNIPA-L co-precipitate blends containing shown % w/w of MHB (Heating rate 10°C/min)

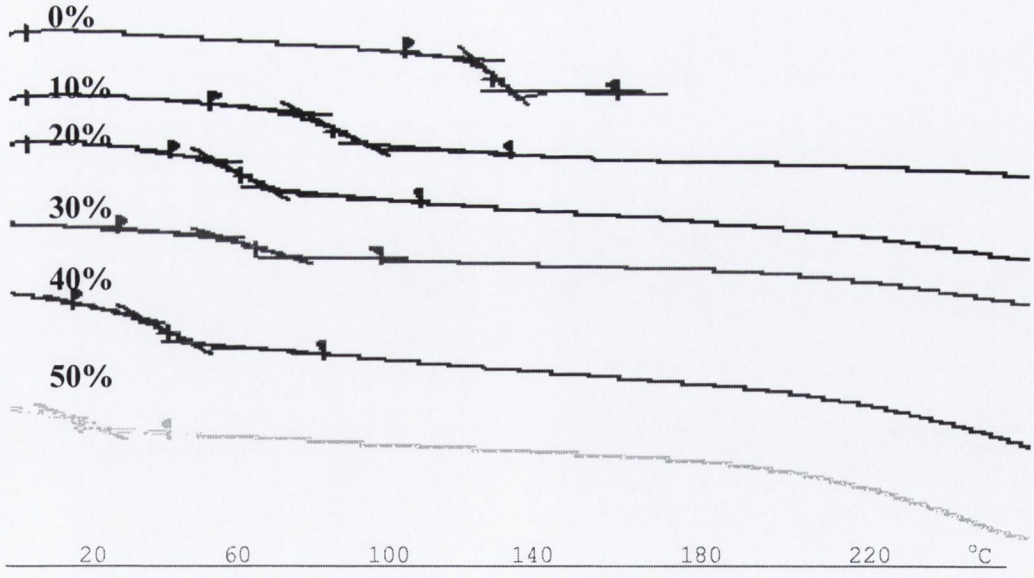

Fig. 4: Glass transition temperature of PHB/PNIPA-L co-precipitate blends containing shown % w/w of PHB (Heating rate 10°C/min)

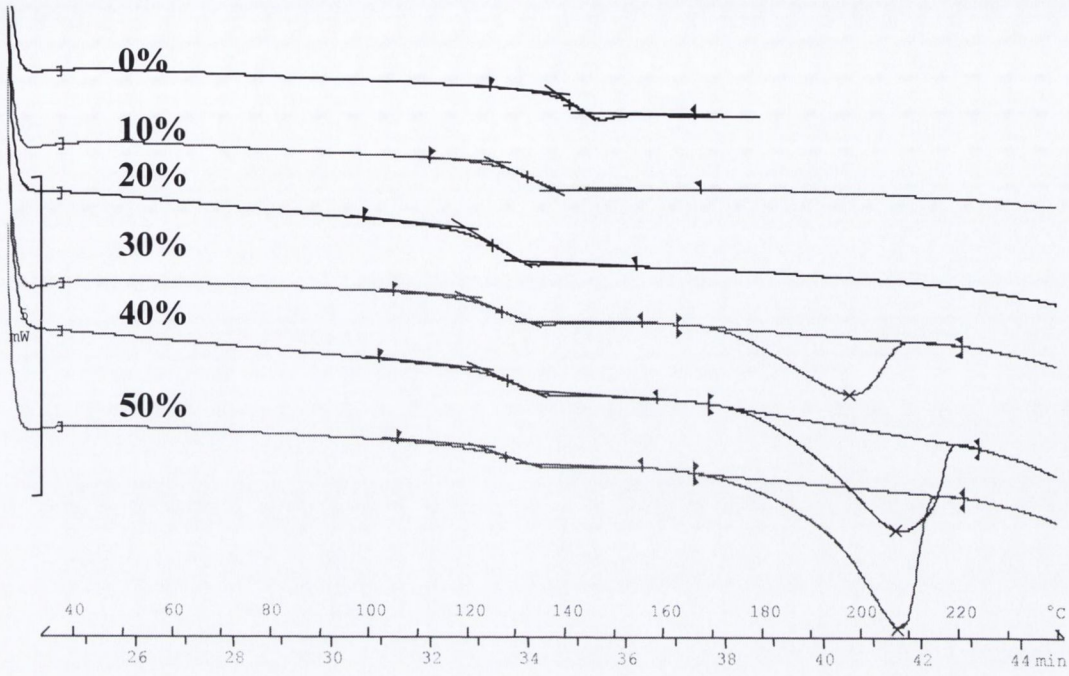

Fig. 5: Glass transition temperature of DHCl/PNIPA-L co-precipitate blends containing shown % w/w of DHCl (Heating rate 10°C/min)

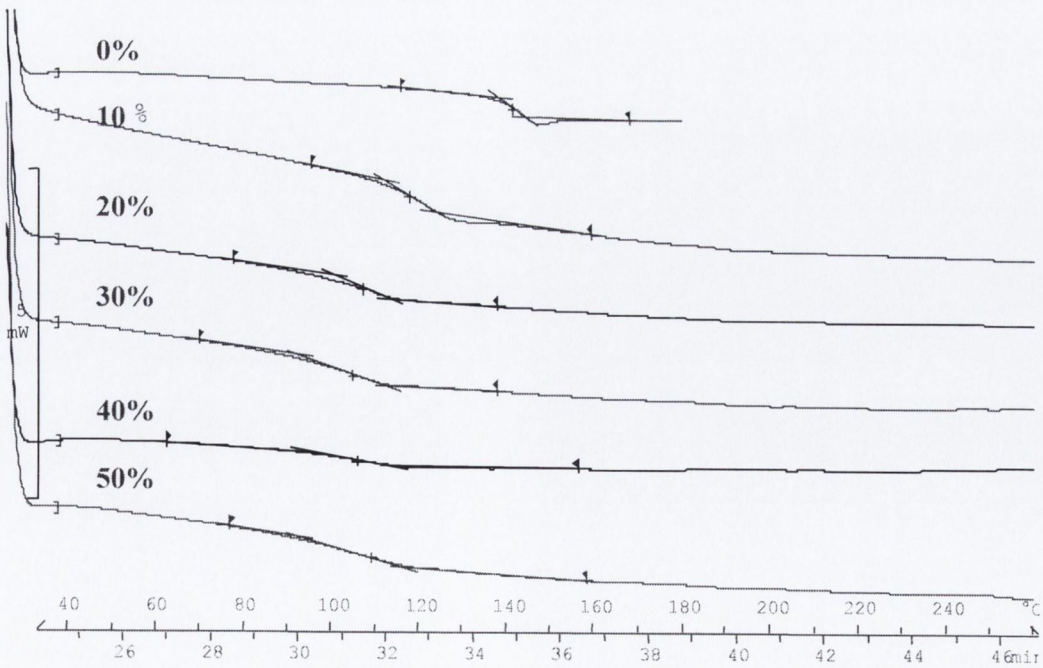

Fig. 6: Glass transition temperature of DB/PNIPA-L co-precipitate blends containing shown % w/w of DB (Heating rate 10°C/min)

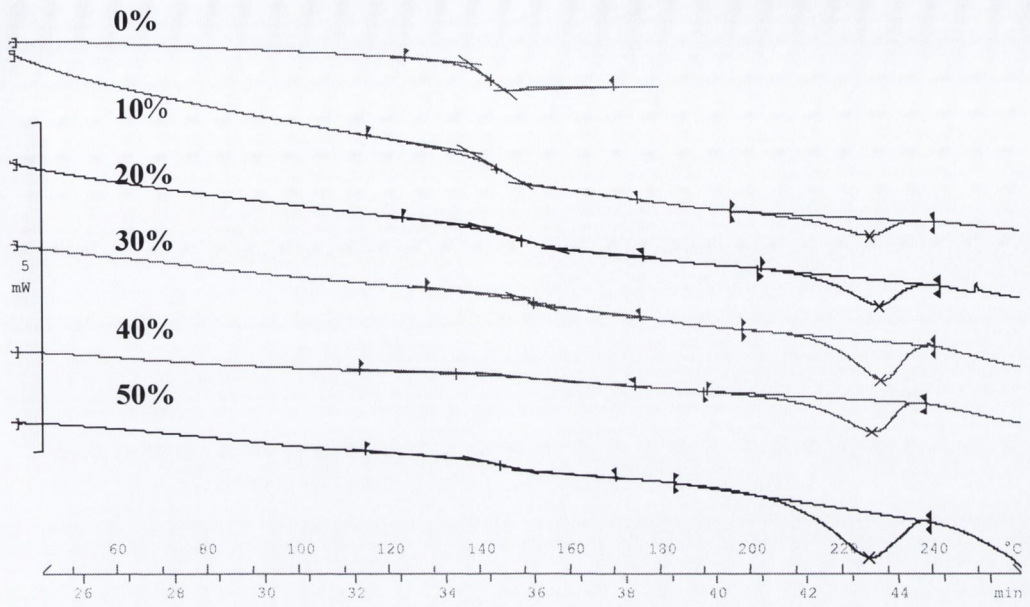

Fig. 7: Glass transition temperature of VB12/PNIPA-L co-precipitate blends containing shown % w/w of VB12 (Heating rate 10°C/min)

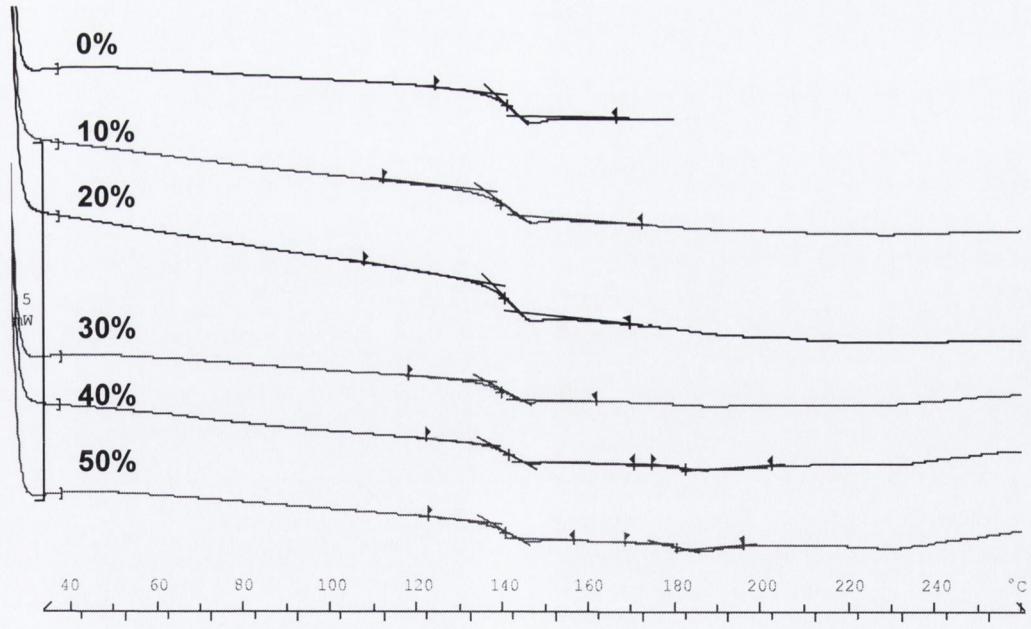

Fig. 8: Glass transition temperature of D4/PNIPA-L co-precipitate blends containing shown % w/w of D4 (Heating rate 10°C/min)

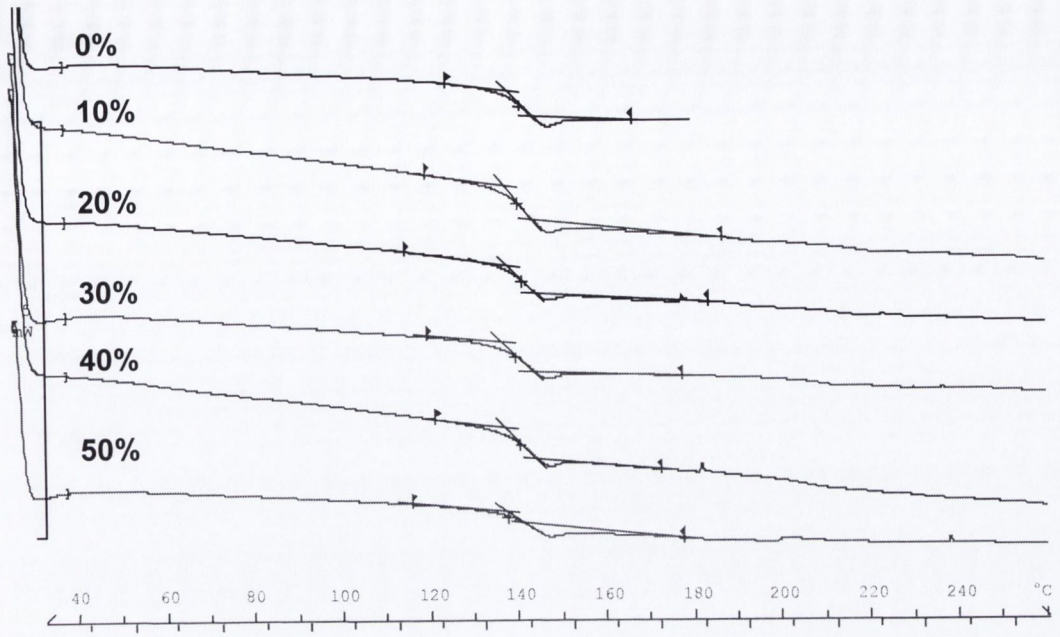

Fig. 9: Glass transition temperature of D10/PNIPA-L co-precipitate blends containing shown % w/w of D10 (Heating rate 10°C/min)

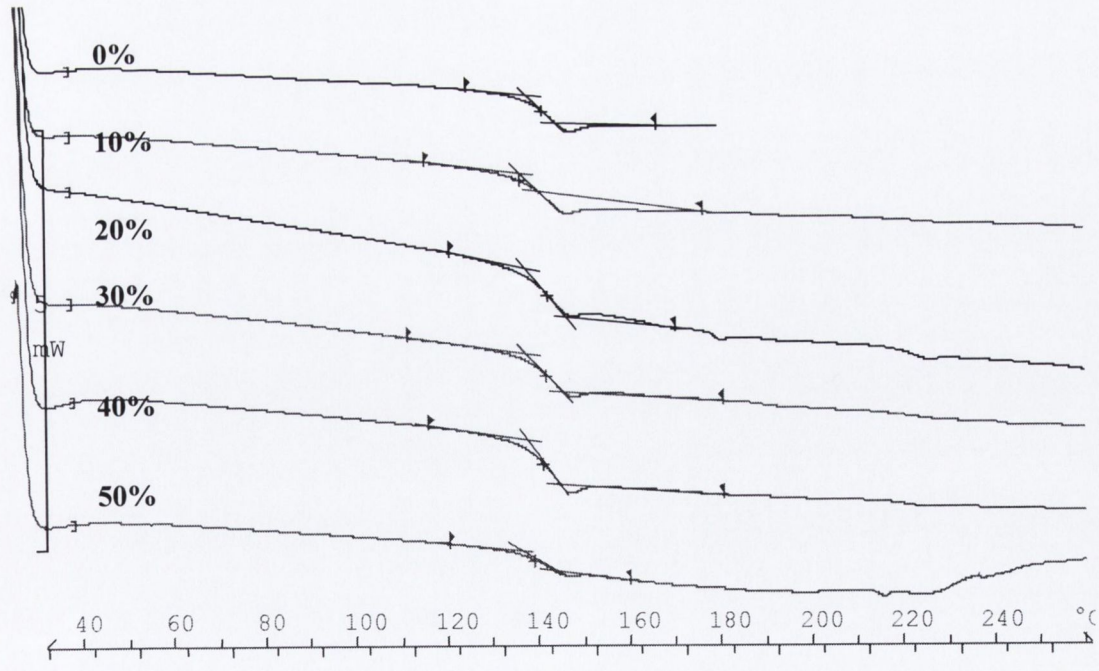

Fig. 10: Glass transition temperature of D40/PNIPA-L co-precipitate blends containing shown % w/w of D40 (Heating rate 10°C/min)

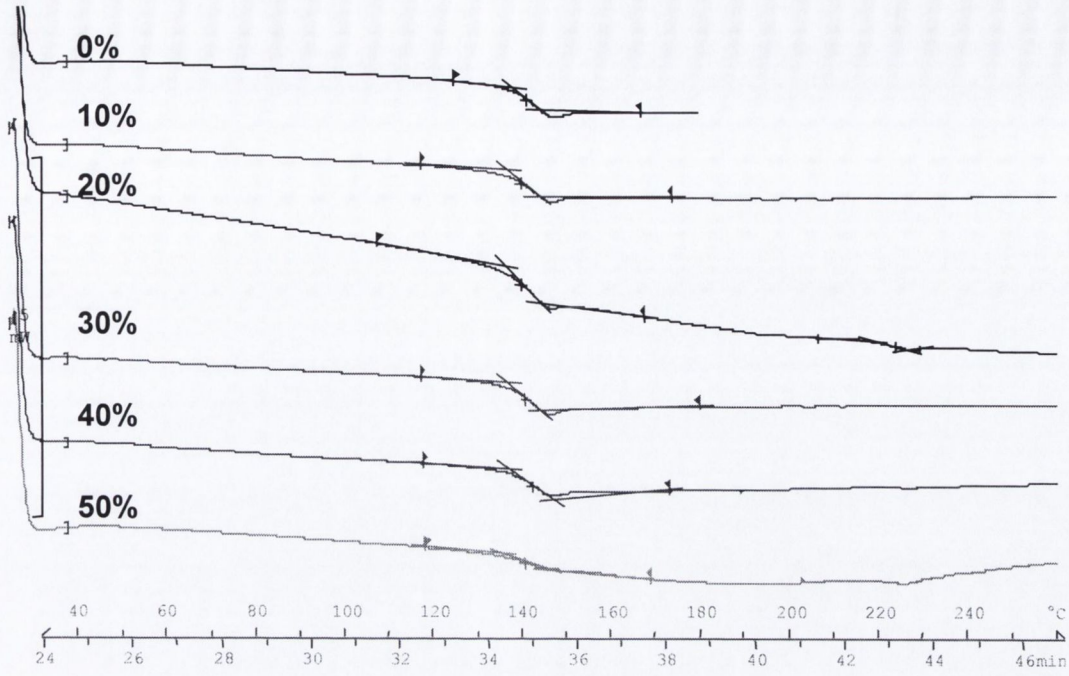

Fig. 11: Glass transition temperature of D70/PNIPA-L co-precipitate blends containing shown % w/w of D70 (Heating rate 10°C/min)

Appendix III:

FTIR Spectra of Drug-Polymer Co-Precipitate Blends

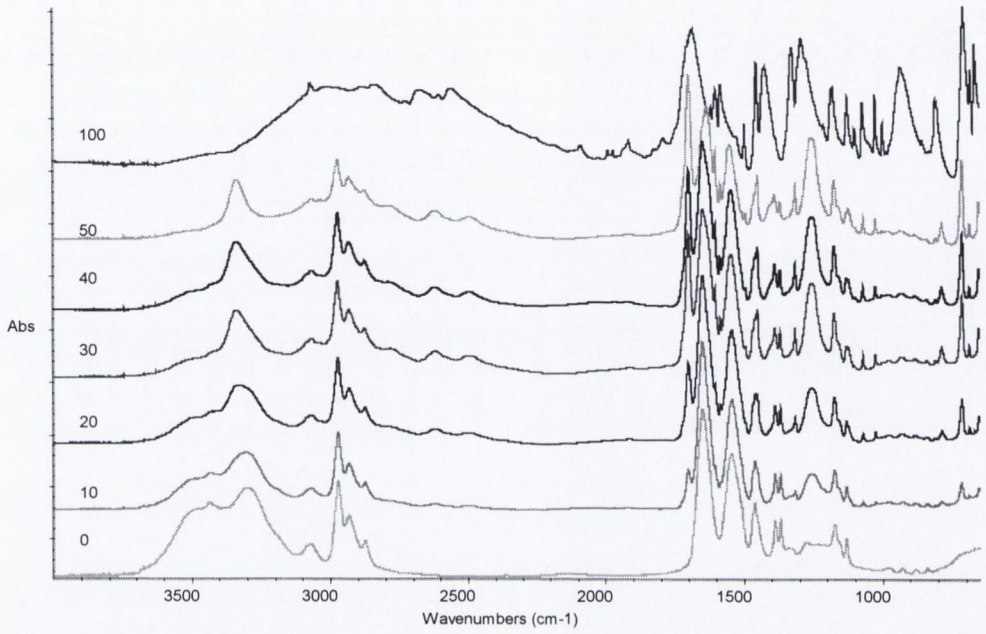

Fig. 1: FTIR of BA/PNIPA-L co-precipitate blends containing from bottom to top 0% w/w, 10% w/w, 20% w/w, 30% w/w, 40% w/w, 50% w/w and 100% w/w BA.

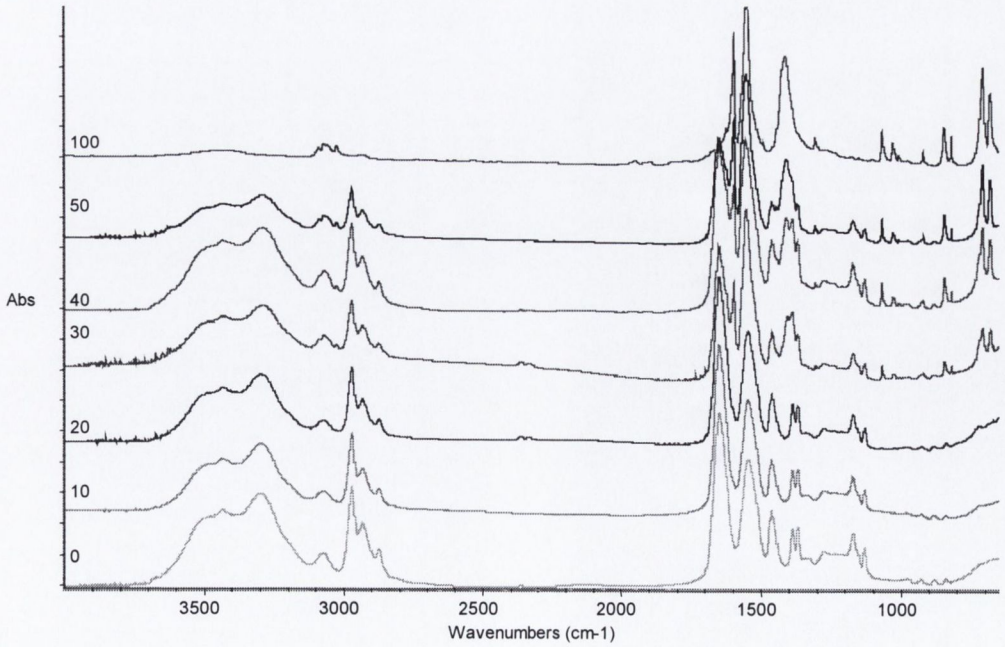

Fig. 2: FTIR of NaB/PNIPA-L co-precipitate blends containing from bottom to top 0% w/w, 10% w/w, 20% w/w, 30% w/w, 40% w/w, 50% w/w and 100% w/w NaB.

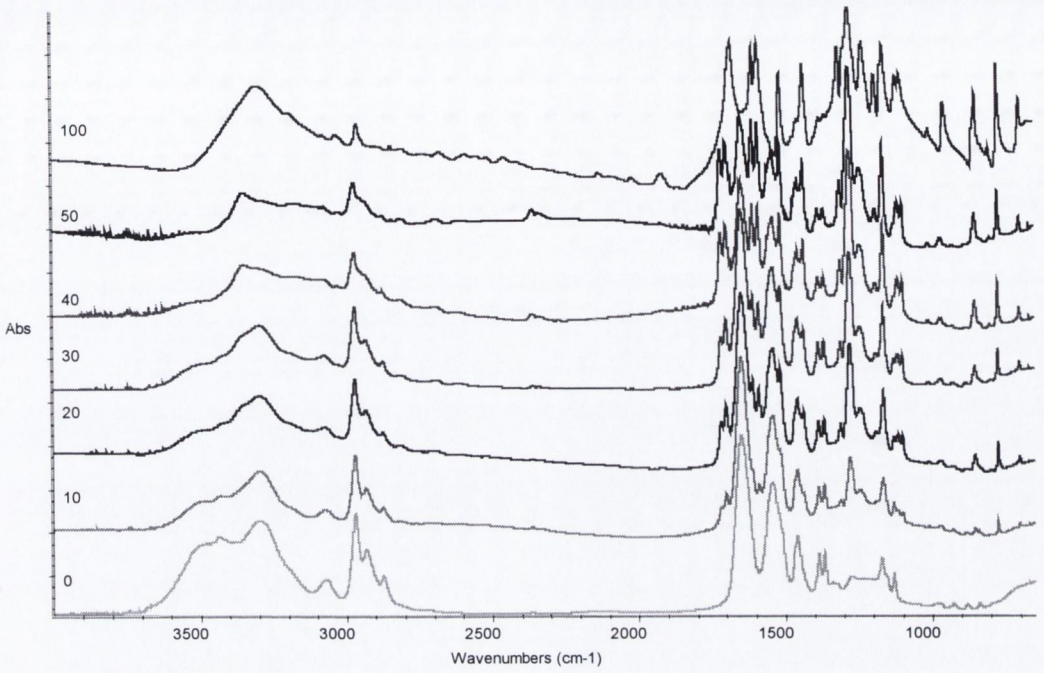

Fig. 3: FTIR of MHB/PNIPA-L co-precipitate blends containing from bottom to top 0% w/w, 10% w/w, 20% w/w, 30% w/w, 40% w/w, 50% w/w and 100% w/w MHB.

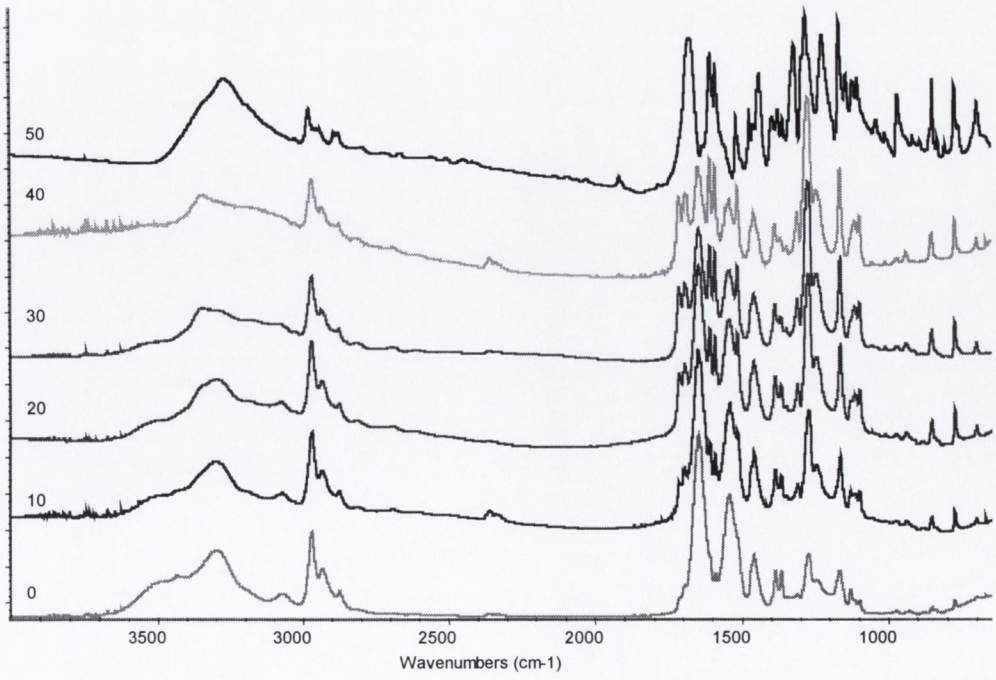

Fig. 4: FTIR of PHB/PNIPA-L co-precipitate blends containing from bottom to top 0% w/w, 10% w/w, 20% w/w, 30% w/w, 40% w/w, 50% w/w and 100% w/w PHB.

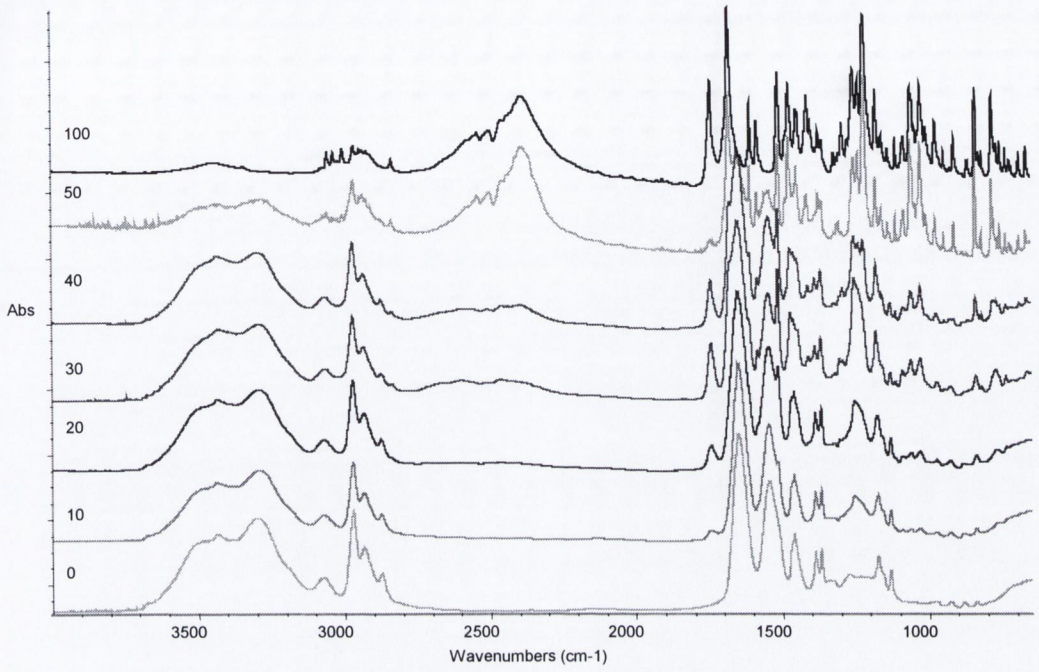

Fig. 5: FTIR of DHCl/PNIPA-L co-precipitate blends containing from bottom to top 0% w/w, 10% w/w, 20% w/w, 30% w/w, 40% w/w, 50% w/w and 100% w/w DHCl.

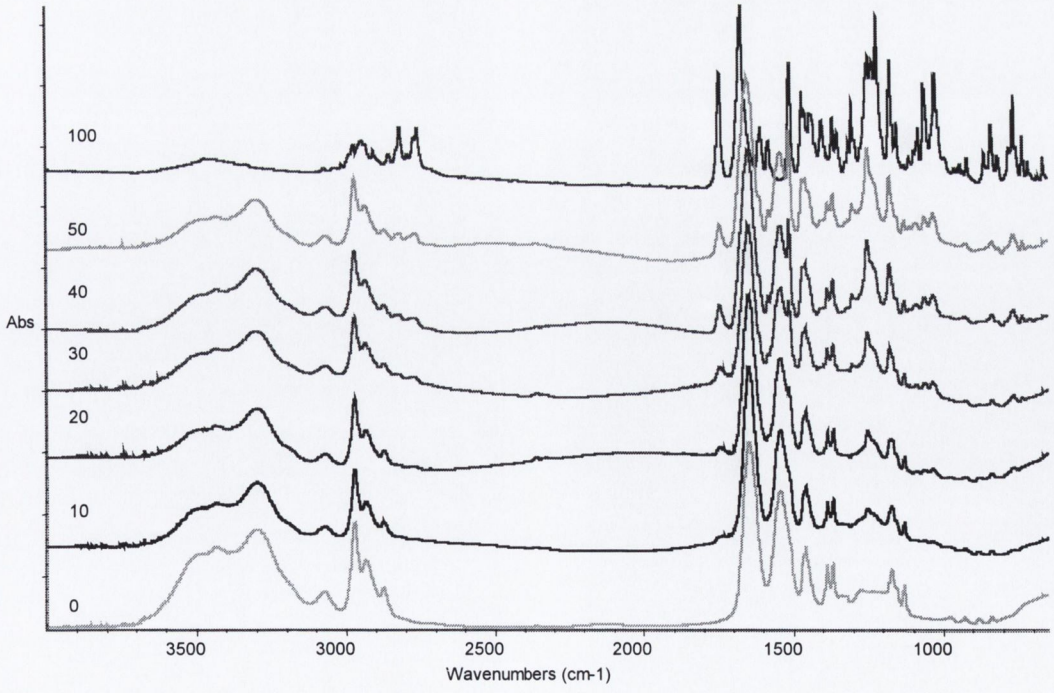

Fig. 6: FTIR of DB/PNIPA-L co-precipitate blends containing from bottom to top 0% w/w, 10% w/w, 20% w/w, 30% w/w, 40% w/w, 50% w/w and 100% w/w DB.

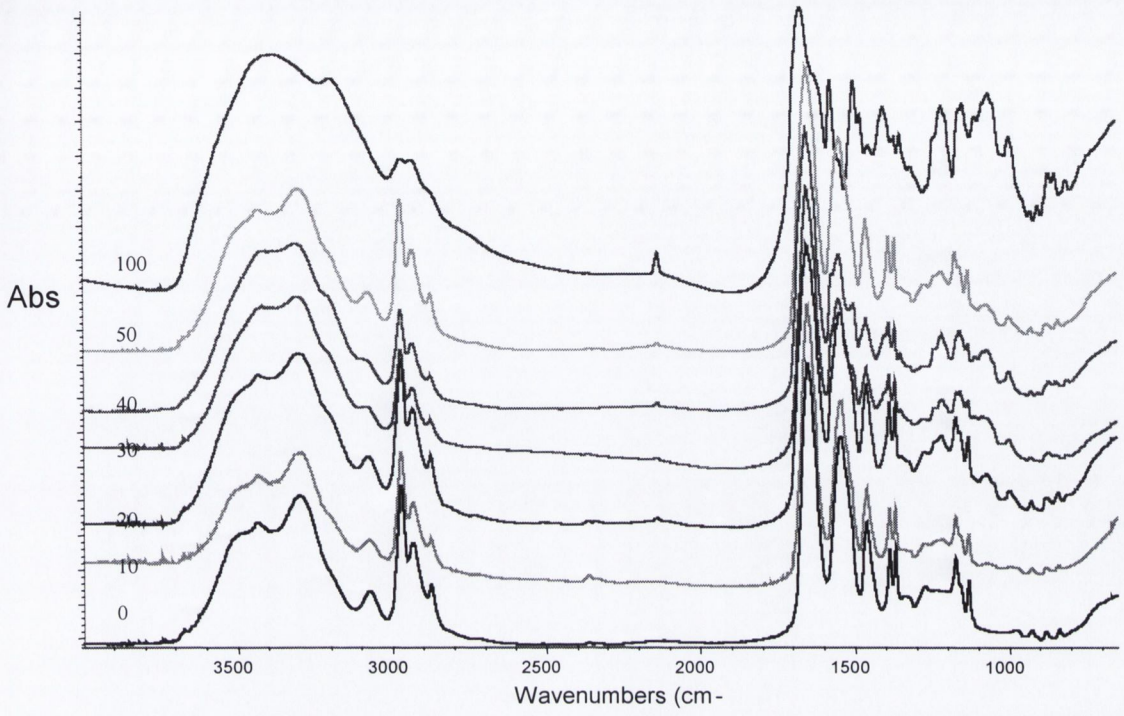

Fig. 7: FTIR of VB12/PNIPA-L co-precipitate blends containing from bottom to top 0% w/w, 10% w/w, 20% w/w, 30% w/w, 40% w/w, 50% w/w and 100% w/w VB12.

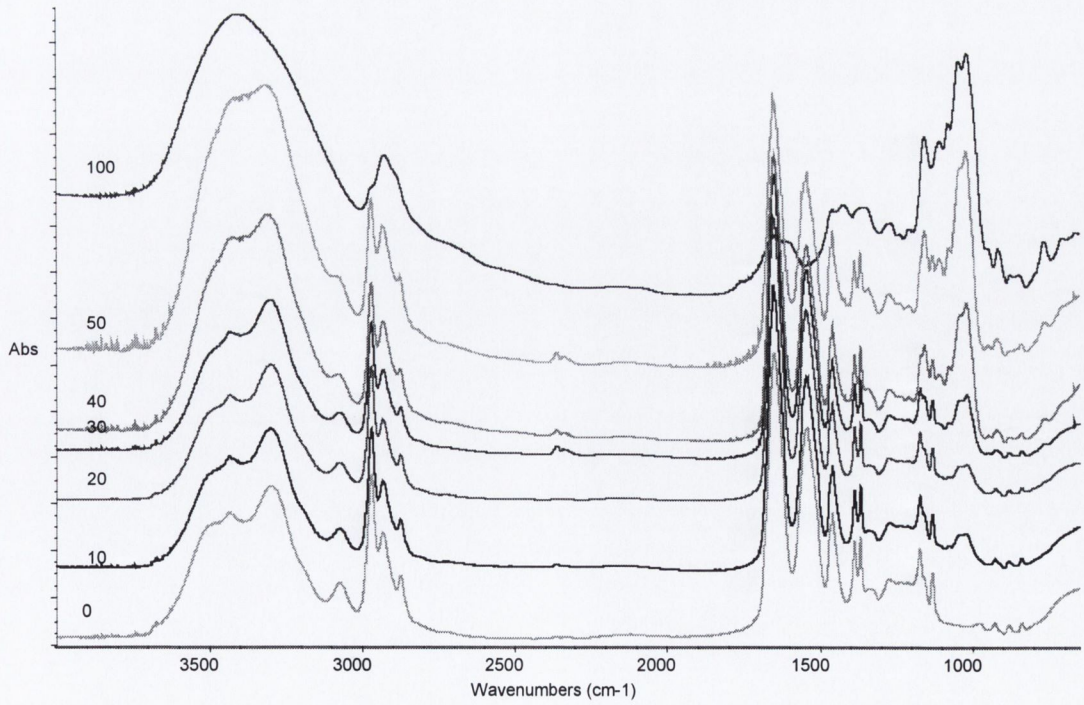

Fig. 8: FTIR of D4/PNIPA-L co-precipitate blends containing from bottom to top 0% w/w, 10% w/w, 20% w/w, 30% w/w, 40% w/w, 50% w/w and 100% w/w D4.

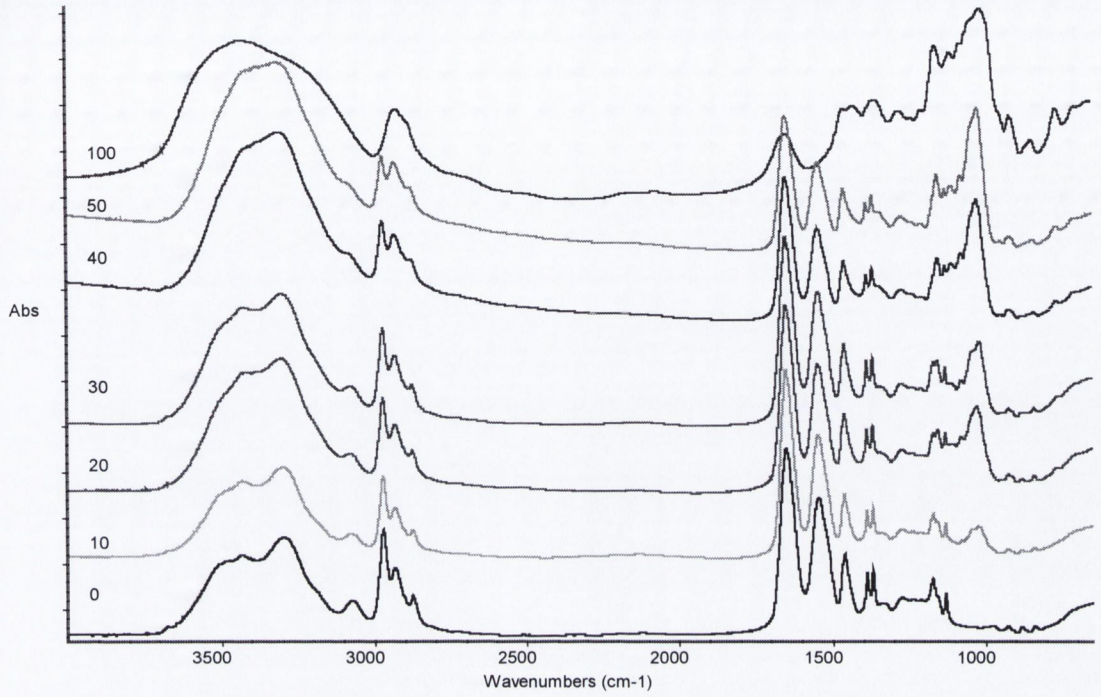

Fig. 9: FTIR of D10/PNIPA-L co-precipitate blends containing from bottom to top 0%w/w, 10% w/w, 20% w/w, 30% w/w, 40% w/w, 50% w/w and 100% w/w D10.

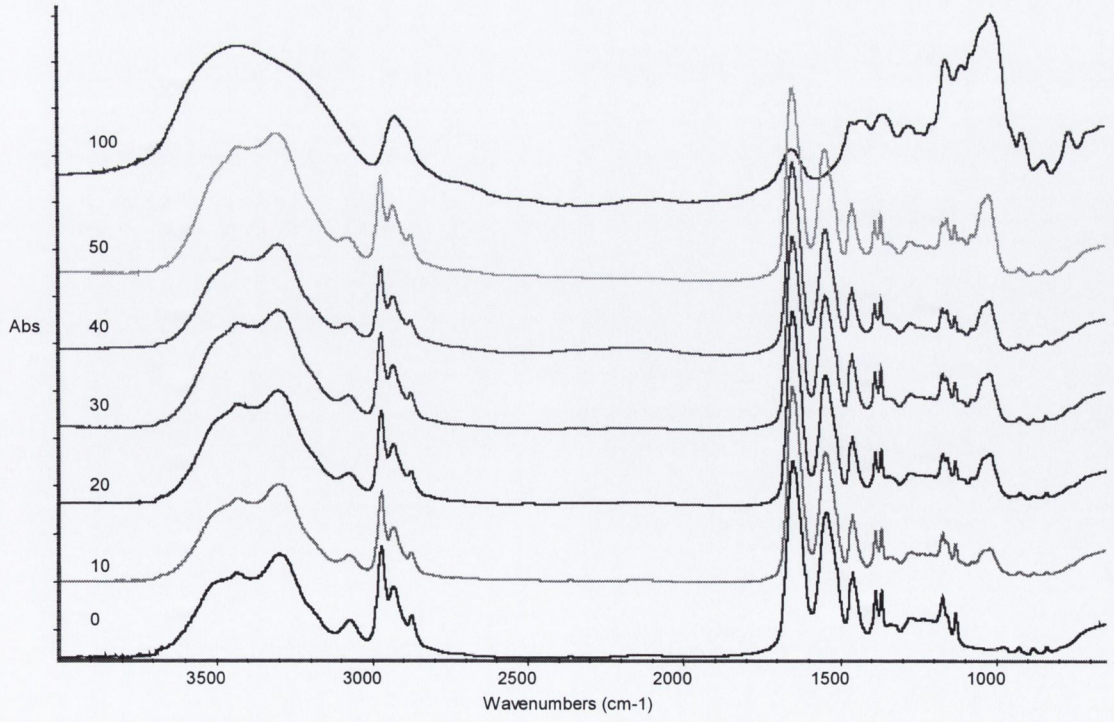

Fig. 10: FTIR of D40/PNIPA-L co-precipitate blends containing from bottom to top 0% w/w, 10% w/w, 20% w/w, 30% w/w, 40%w/w, 50% w/w and 100% w/w D40.

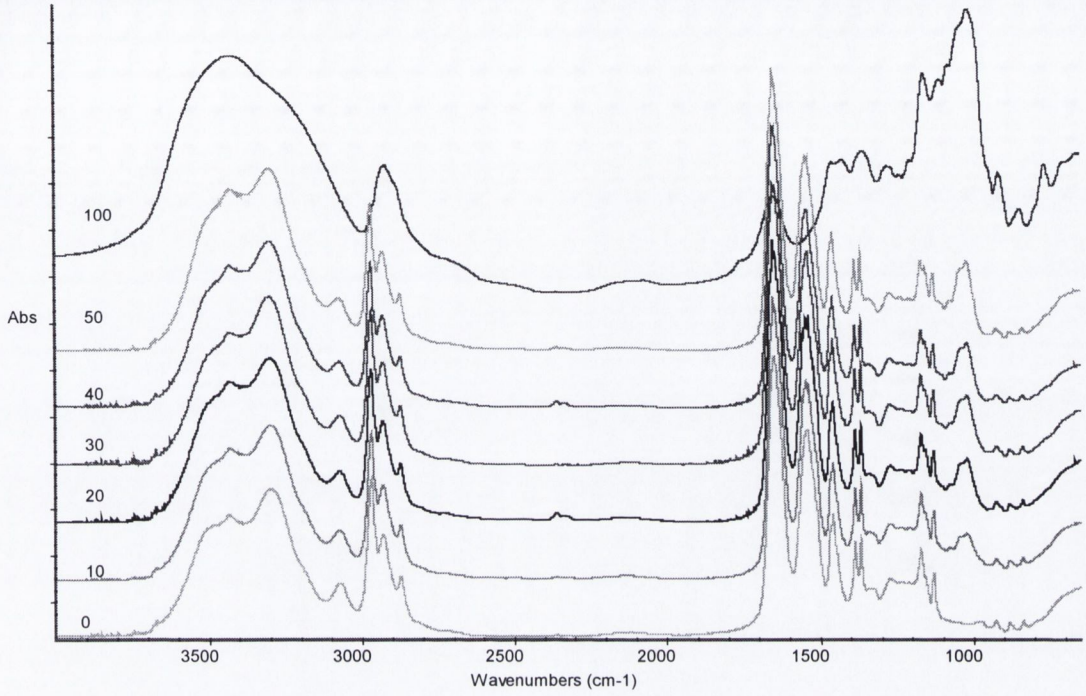

Fig. 11: FTIR of D70/PNIPA-L co-precipitate blends containing from bottom to top 0% w/w, 10% w/w, 20% w/w, 30% w/w, 40% w/w, 50% w/w and 100% w/w D70.

Appendix IV:

Phase Transition Temperature (LCST) Measurements

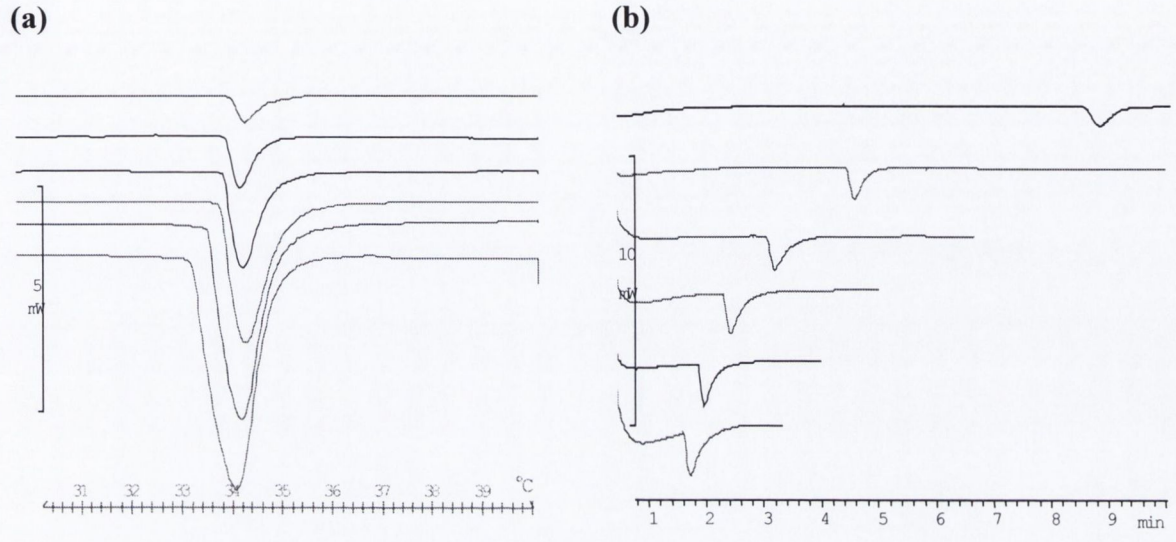

Fig. 1: DSC thermograms of PNIPA-L3 in deionised water showing the effect of
(a) polymer concentration [top to bottom: 0.5% w/v, 1.4% w/v, 3.0% w/v, 5.0% w/v, 10% w/v, 20% w/v] (heating rate 2°C/min)
(b) heating rate [top to bottom: 1°C/min, 2°C/min, 3°C/min, 4°C/min, 5°C/min, 6°C/min] (polymer concentration 1.4% w/w)

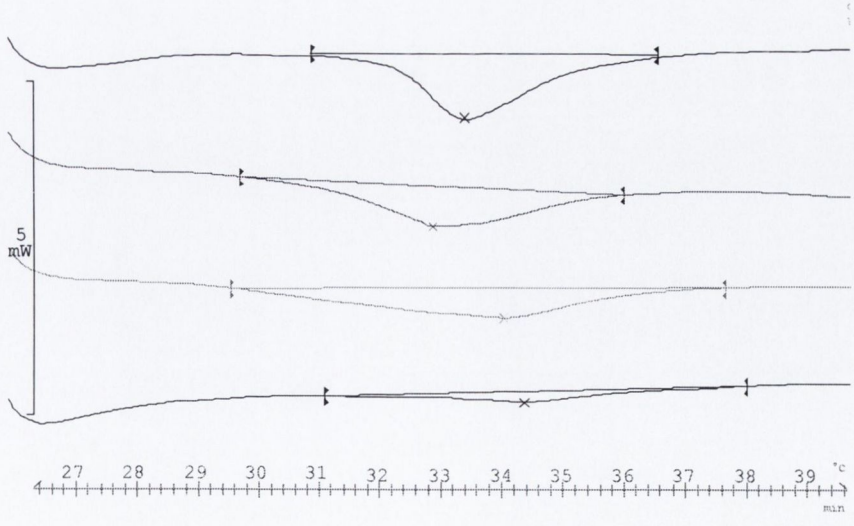

Fig 2: LCST determination of PNIPA hydrogels in water by DSC [from top to bottom, PNIPA-H1, PNIPA-H2, PNIPA-H3, PNIPA-H4] (heating rate 2°C/min)

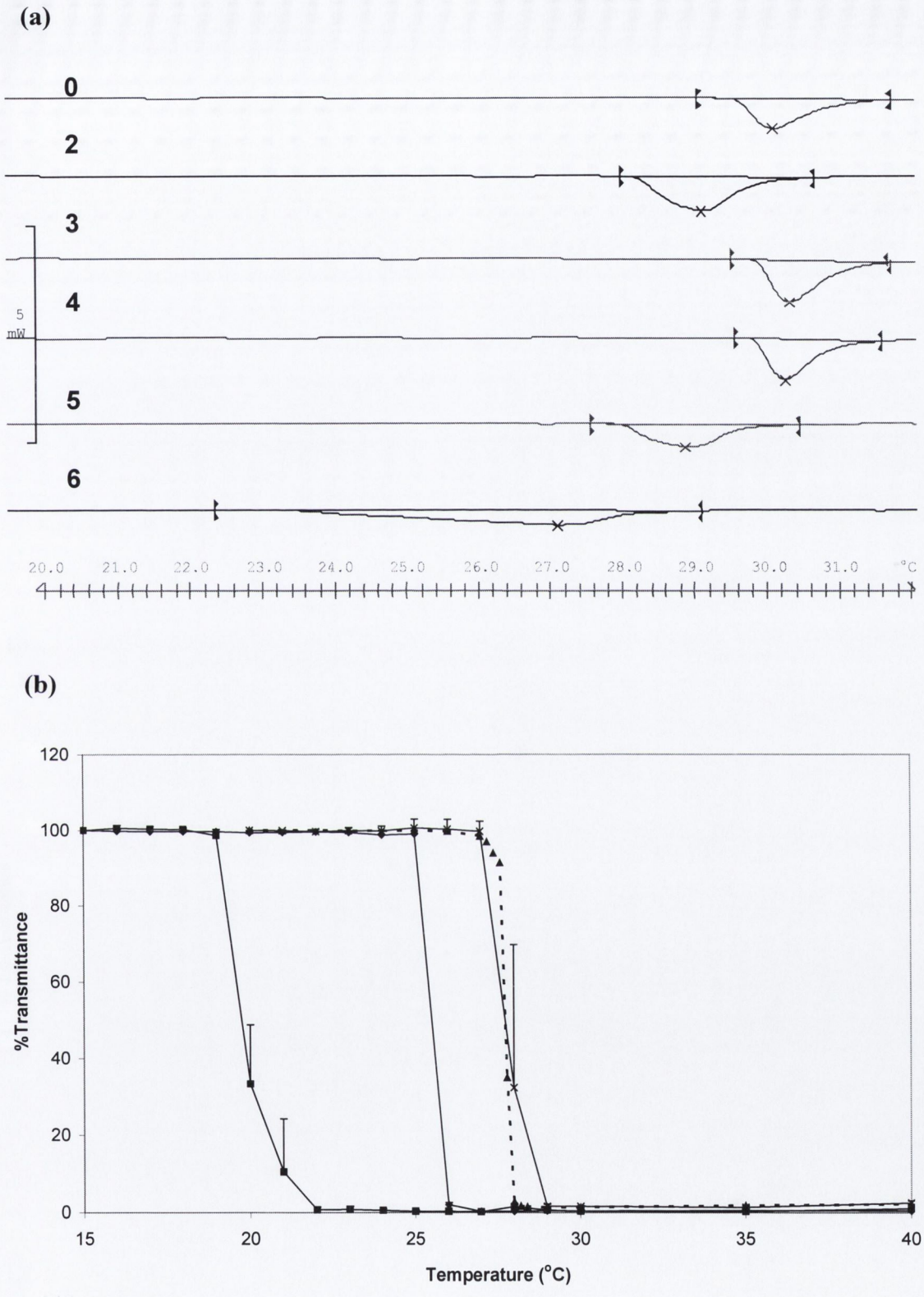

Fig. 3: Influence of various concentrations (shown in g/l) of **BA** on the phase transition temperature of a 1.4% w/w PNIPA-L3 solution in PB. (a) DSC (2°C/min) (b) Transmittance, from right to left (500nm, 0.5°C/min) 0g/l (dashed line) 4g/l, 5g/l, 6g/l

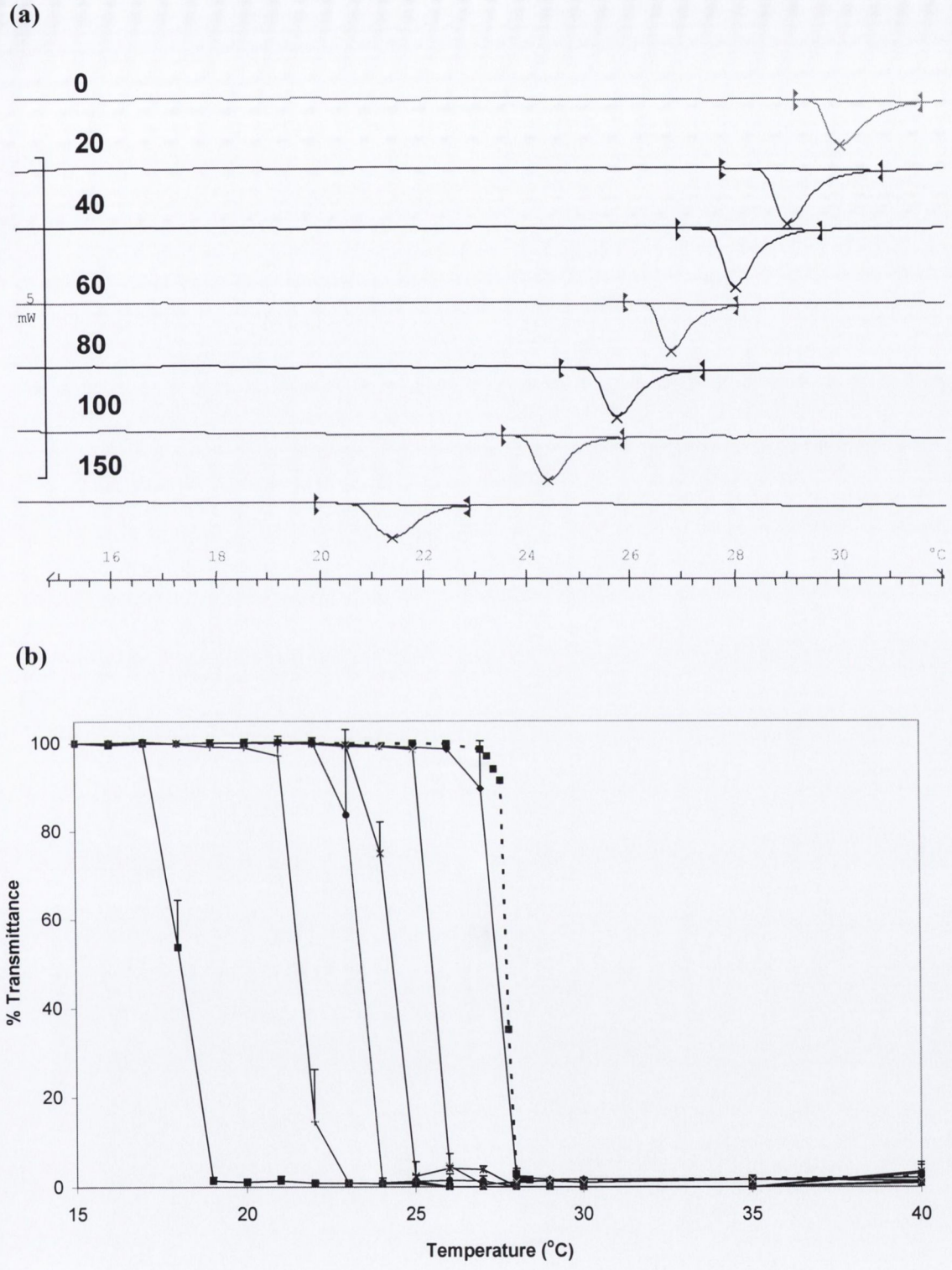

Fig. 4: Influence of various concentrations (shown in g/l) of **NaB** on the phase transition temperature of a 1.4% w/w PNIPA-L3 solution in PB (a) DSC (2°C/min) (b) Transmittance, from right to left (500nm, 0.5°C/min) 0g/l (dashed line), 20g/l, 40g/l, 60g/l, 80g/l, 100g/l, 150g/l

(a)

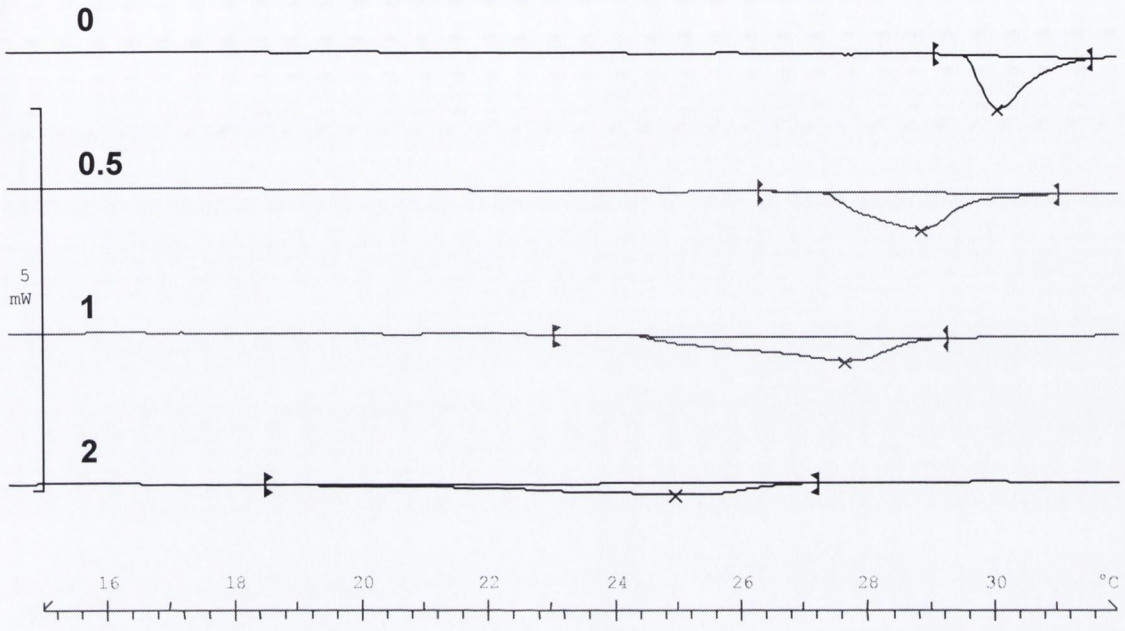

(b)

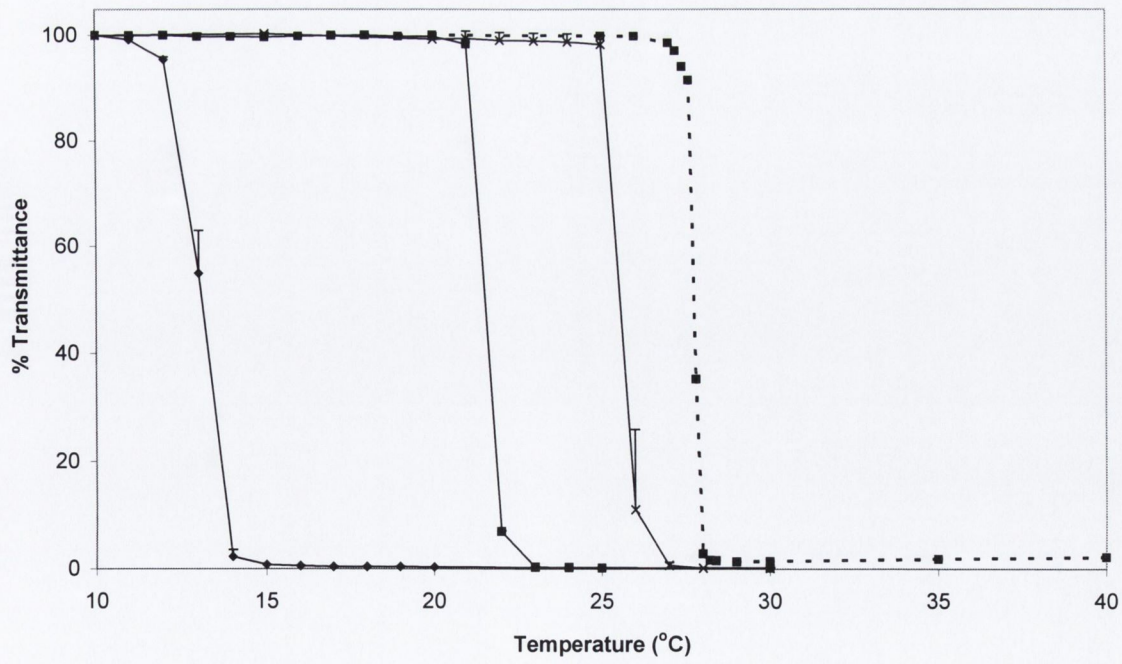

Fig. 5: Influence of various concentrations (shown in g/l) of **MHB** on the phase transition temperature of a 1.4% w/w PNIPA-L3 solution in PB. (a) DSC (2°C/min) (b) Transmittance, from right to left (500nm, 0.5°C/min) 0g/l (dashed line), 0.5g/l, 1g/l, 2g/l

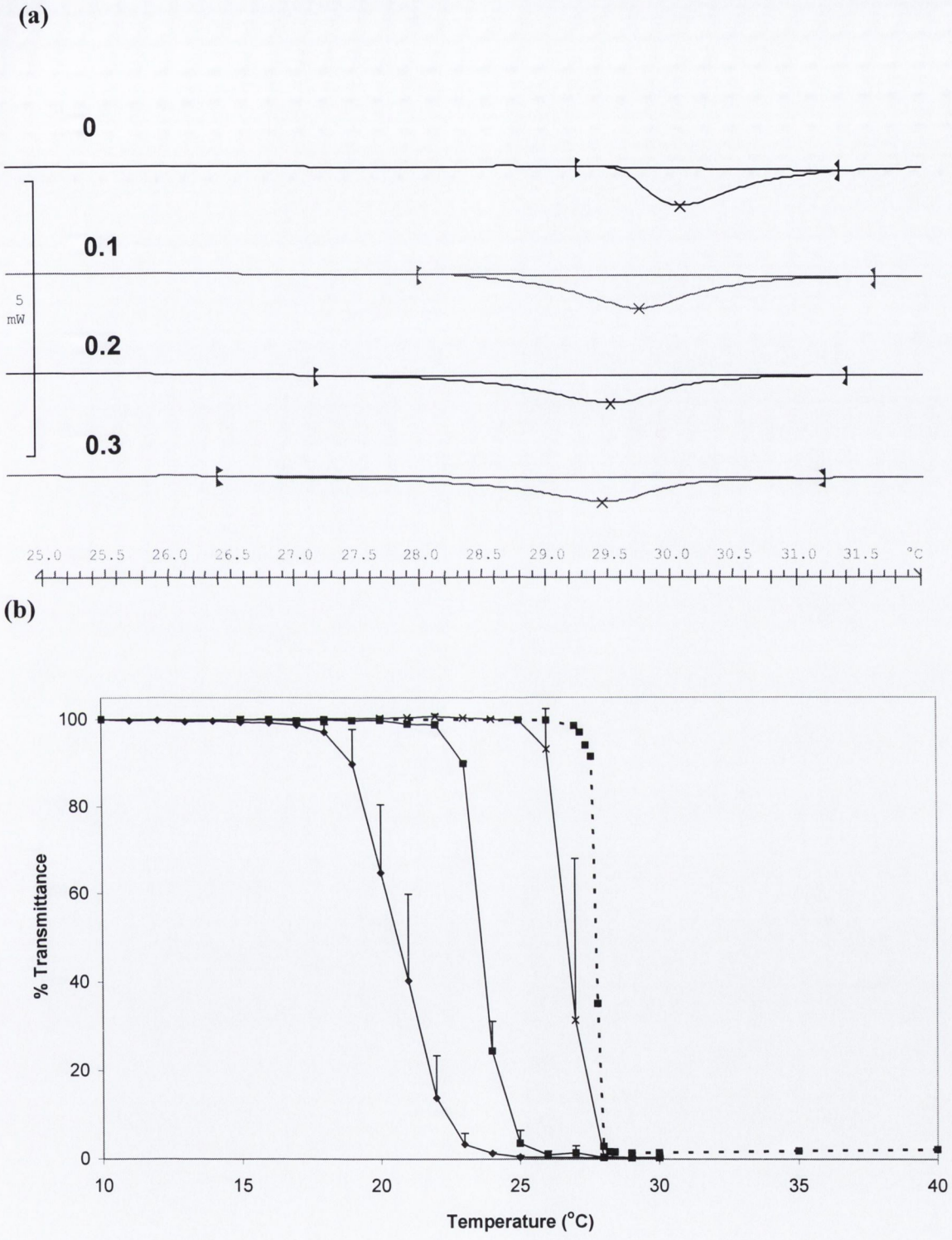

Fig. 6: Influence of various concentrations (shown in g/l) of **PHB** on the phase transition temperature of a 1.4% w/w PNIPA-L3 solution in PB. (a) DSC (2°C/min) (b) Transmittance, from right to left (500nm, 0.5°C/min) 0g/l (dashed line), 0.1g/l, 0.2g/l, 0.3g/l

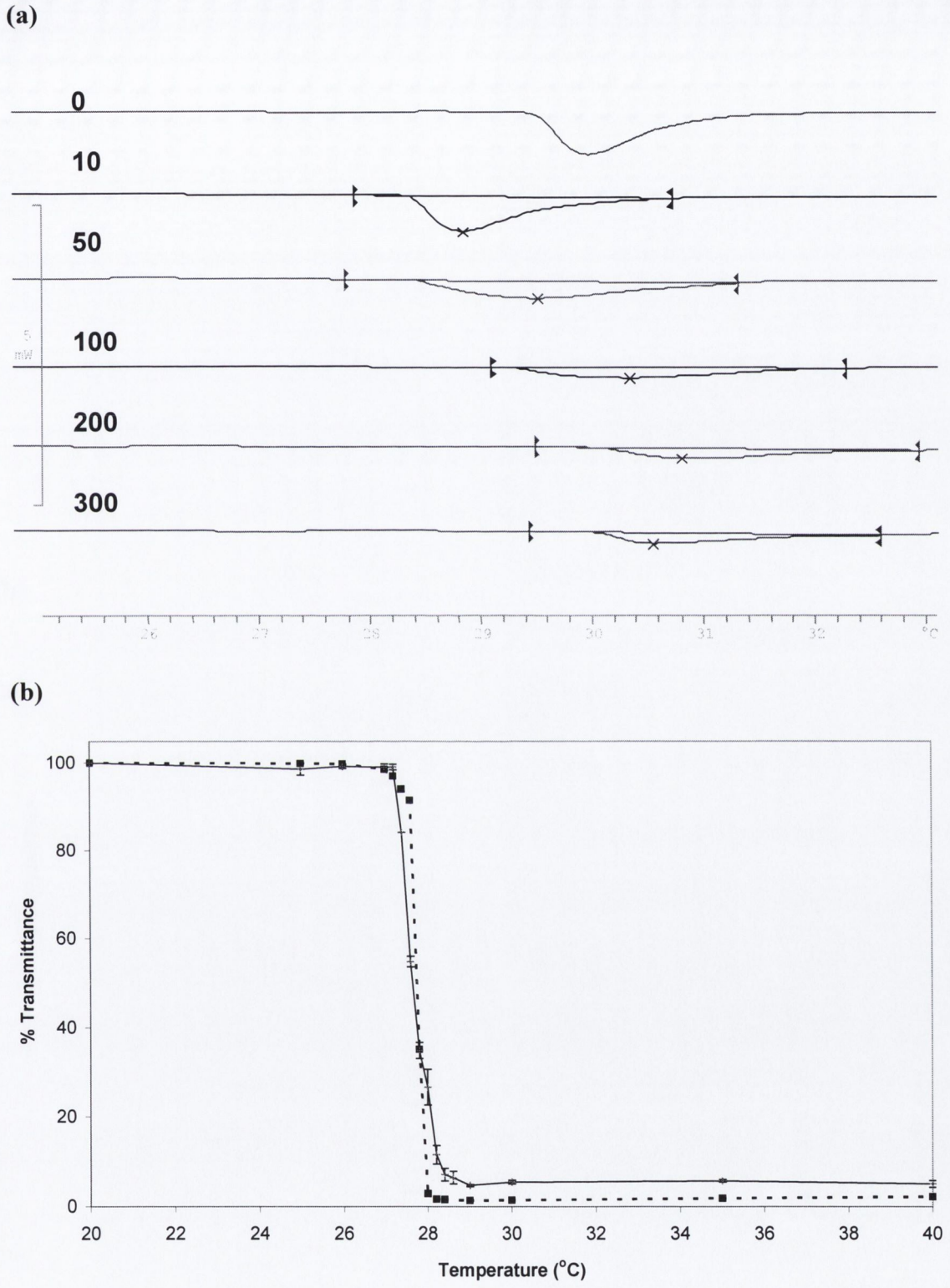

Fig. 7: Influence of various concentrations (shown in g/l) of **DHCl** on the phase transition temperature of a 1.4% w/w PNIPA-L3 solution in PB. (a) DSC (2°C/min) (b) Transmittance (500nm, 0.5°C/min) 0g/l (dashed line), 300g/l DHCl.

(a)

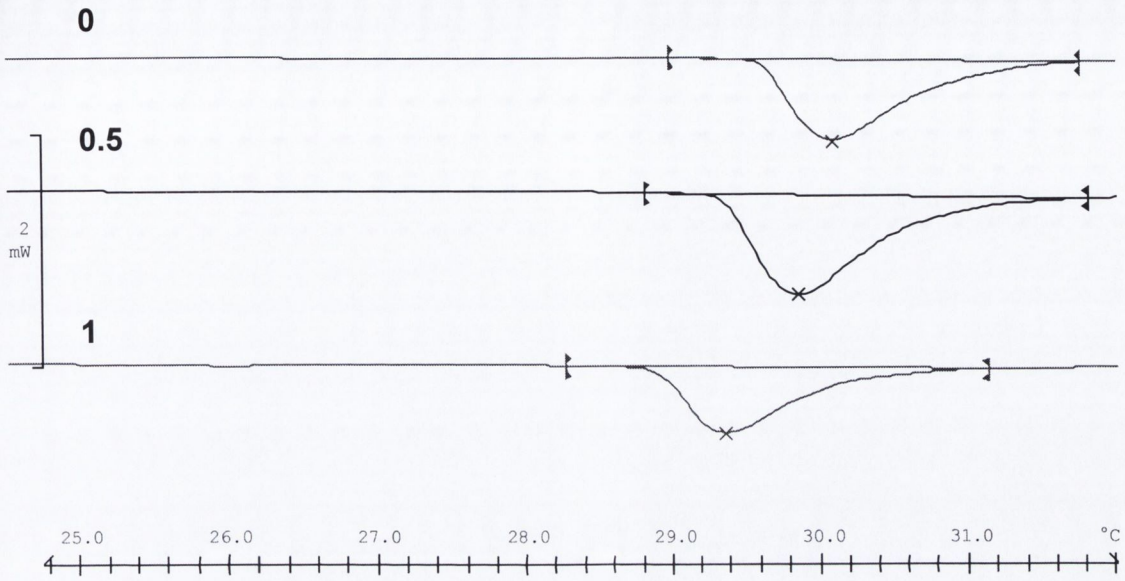

(b)

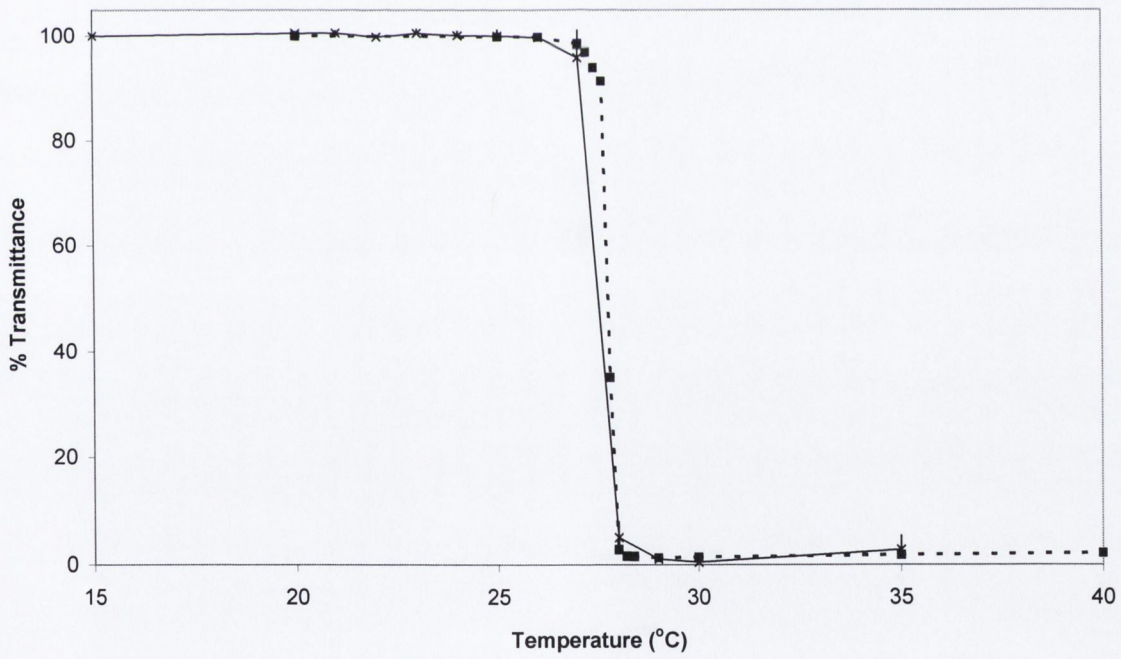

Fig. 8: Influence of various concentrations (shown in g/l) of **DB** on the phase transition temperature of a 1.4% w/w PNIPA-L3 solution in PB. (a) DSC (2°C/min) (b) Transmittance (500nm, 0.5°C/min) 0g/l (dashed line), 1g/l

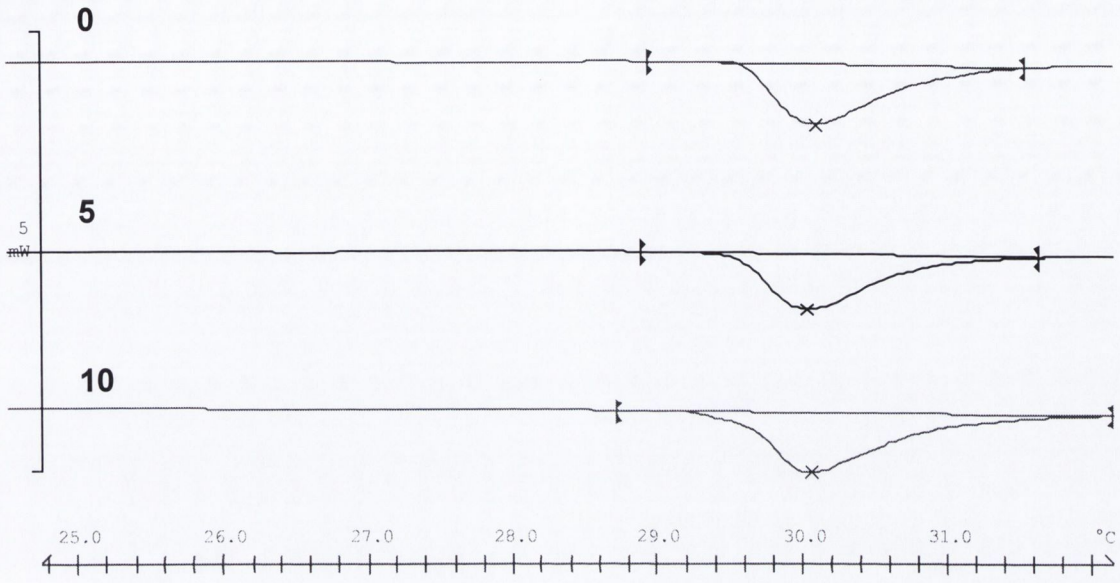

Fig. 9: Influence of various concentrations (shown in g/l) of **VB12** on the phase transition temperature of a 1.4% w/w PNIPA-L3 solution in PB. DSC (2°C/min)

(a)

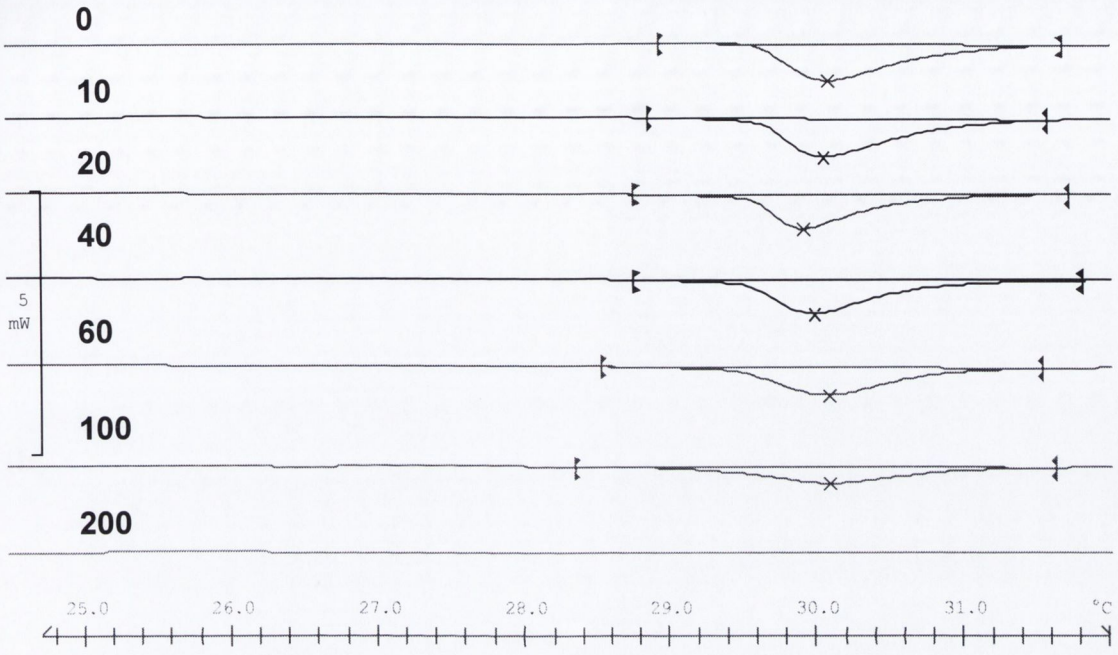

(b)

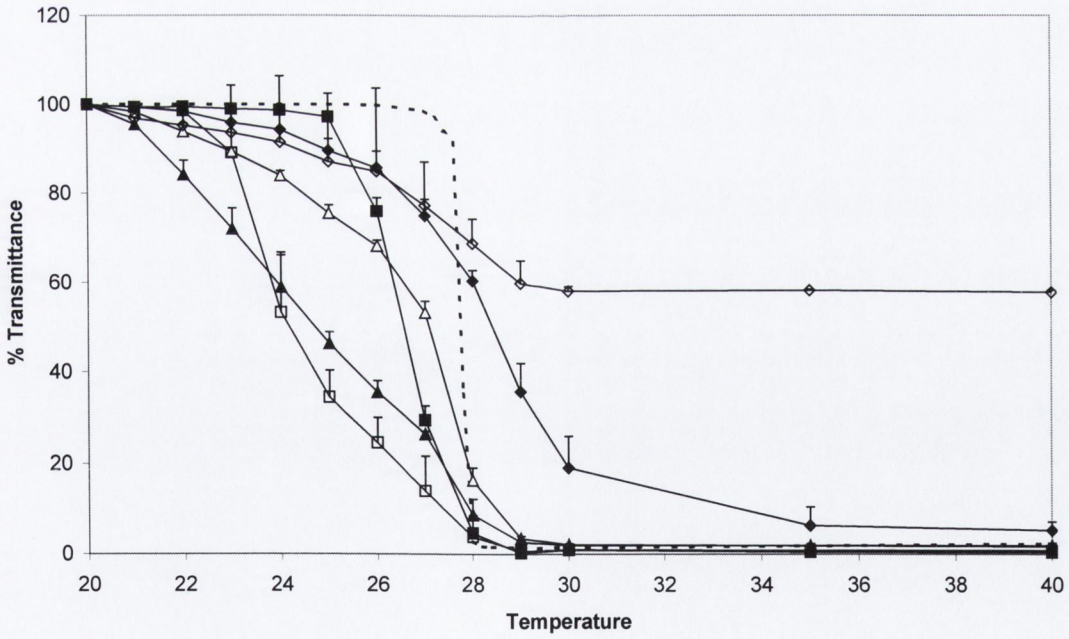

Fig. 10: Influence of various concentrations (shown in g/l) of **D40** on the phase transition temperature of a 1.4% w/w PNIPA-L3 solution in PB. (a) DSC (2°C/min) (b) Transmittance (500nm, 0.5°C/min) 0g/l (------), 10g/l (■); 20g/l (□); 40g/l (▲); 60g/l (Δ); 100g/l (♦); 200g/l (◊).

(a)

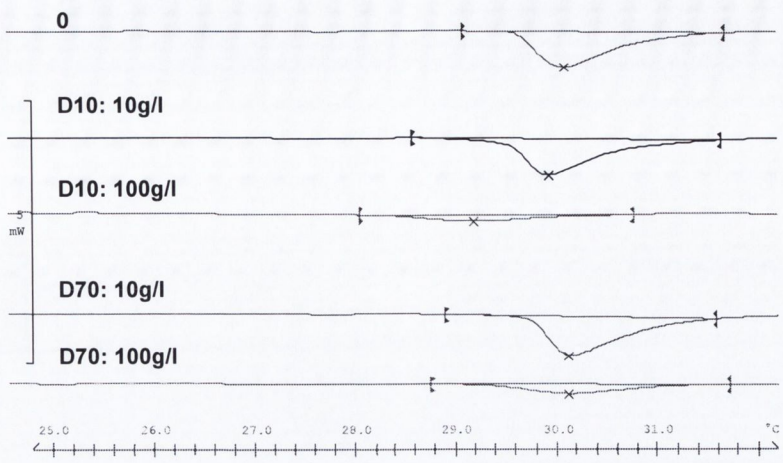

(b)

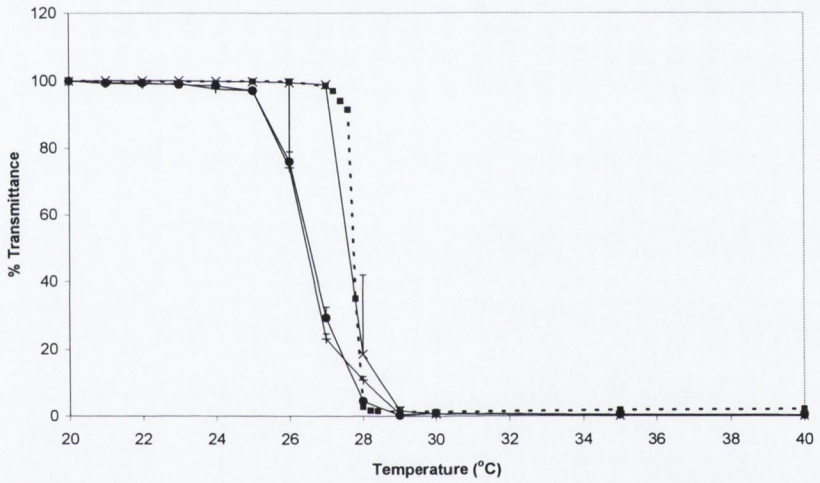

(c)

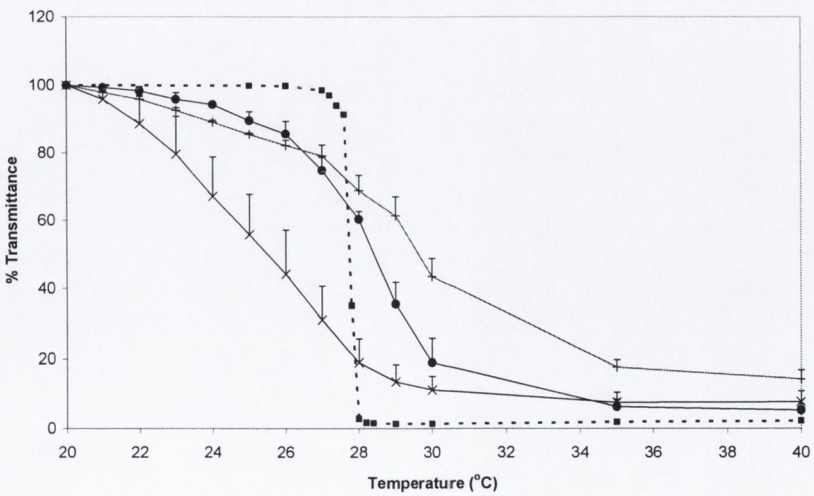

Fig. 11: Influence of various concentrations (shown in g/l) of **D10** and **D70** on the phase transition temperature of a 1.4% w/w PNIPA-L3 solution in PB. (a) DSC (2°C/min) (b) Transmittance (500nm, 0.5°C/min) 10g/l dextran (c) Transmittance 100g/l dextran [D10 (x), D40 (●) and D70 (+)]

Appendix V:

Molecular Modelling Software Input Files from Accelrys' Materials Studio® Version 2.1.5

(A) Typical input file for Temperature Cycle Protocol

```
#BIOSYM btcl 3
#
#  Input File For Discover Generated By Materials Studio
#  Input Client Model Document: C:\Documents and Settings\coughld\My Documents\Materials
Studio Projects\EXP040 Files\Documents\Poly13aD_glucose AC Constr\Poly13aD_glucose.xtd
#  Job: [45086] - Poly13aD_glucose AC Temp
#
  autoEcho off
#
# Begin Forcefield Section
  begin forcefield = compass
#
# Nonbond section:
  forcefield nonbond \
      -separate_coulomb \
    vdw \
    summation_method = group_based \
      cutoff = 8.50 \
      spline_width = 1.00 \
      buffer_width = 0.50 \
    coulomb \
    dielectric_value = 1.0000
#
# vdw long range energy correction
  vdwTailCorrection 8.50
# End Forcefield Section
#
    lappend auto_path $env(BIOSYM)/data/polymer/script

#-------------------------------------------------------------
#       Parameters for optional use by protocols
#-------------------------------------------------------------
          set construct_temp  300.000
          set default_cutoff 8.50
#
#-------------------------------------------------------------
#       List of frames to be refined
#-------------------------------------------------------------
        set config_list "  1 2 3 "
#
#-------------------------------------------------------------
#       Loop over structures in archive file
#-------------------------------------------------------------
        foreach iconfig $config_list {
          puts "\n*****************************"
          puts "Processing frame number $iconfig"
          puts "*****************************\n"
          readFile archive frame = $iconfig
#
          Temperature_Cycle 0.05 200 400 11 5000 400 100 1 1
          writeFile archive frame = $iconfig
         }
#
          convertTblToCsvTC [format "%s.csv" $PROJECT] [format "%s.tbl" $PROJECT]
#
#-------------------------------------------------------------
```

(B) Typical input file for Amorphous Cell Construction

```
#BIOSYM dsl 3
#
#  INPUT FILE FOR DISCOVER GENERATED BY THE AMORPHOUS CELL MODULE
#
      autoEcho off
#
      begin
#
#
#-------------------------------------------------------------
```

```
#       Nonbond setup
#-----------------------------------------------------------------------
        forcefield nonbond \
          -separate_coulomb \
          vdw \
            summation_method = group_based \
            cutoff = 8.5 \
            spline_width = 0.0 \
            buffer_width = 0.5
#
#-----------------------------------------------------------------------
#       Loop over structures in the archive file
#-----------------------------------------------------------------------
        for {$i = 1} {$i <= 3} {incr i 1} \
        {
          echo "\n*****************************"
          echo "Processing frame number $i"
          echo "*****************************\n"
          readFile archive frame = $i

#-----------------------------------------------------------------------
#       MD Stage
#-----------------------------------------------------------------------

        dynamics \
          time = 1000 timestep = 1.0 \
          initial_temperature = 500.00 +boltzmann \
          ensemble = NVT temperature_control_method = velocity_scaling \
          integration_method = Velocity_verlet \
          temperature = 500.00 temperature_window = 10 \
          deviation = 5000 \
          execute frequency = 1000 last_step = 0 \
            command = {print table +append \
            +average \
            +batch_average \
            +batch_sd \
            batch_size = 1000 \
            +total_energy \
            +kinetic_energy \
            +potential_energy \
            +temperature }
#
#-----------------------------------------------------------------------
#       Post-Minimization stage
#-----------------------------------------------------------------------
        minimize \
          iteration_limit = 5000 movement_limit = 0.200 \
           method = conjugate \
          cg convergence = 0.010000 sd convergence = 50 \
          final_convergence = 0.010000

           writeFile archive frame = $i
```

(C) Typical input file for NPT equilibration

```
BIOSYM btcl 3
#
#  Input File For Discover Generated By Materials Studio
#  Input Client Model Document: C:\Documents and Settings\coughld\My Documents\Materials
Studio Projects\Thermoresponsive Files\Documents\C\Frame 3 330\330\1\320\1\310\1\B1.xtd
#  Job: [saved] - B Disco Dynamics
#
  autoEcho off
#
# Begin Forcefield Section
  begin forcefield = compass
#
# Nonbond section:
  forcefield nonbond \
      -separate_coulomb \
    vdw \
    summation_method = group_based \
      cutoff = 9.50 \
      spline_width = 1.00 \
      buffer_width = 0.50 \
    coulomb \
    dielectric_value = 1.0000
#
# vdW long range energy correction
  vdWTailCorrection 9.50
# End Forcefield Section
#
# Dynamics Section:
  dynamics \
    time = 50000.00 \
    timestep = 1.00 \
    initial_temperature = 300.00 \
```

```
    ensemble = NPT \
    temperature_control_method = andersen \
    collision_ratio = 1.00 \
    temperature = 300.00 \
    pressure_control_method = andersen_cp \
    cell_mass = 20.00 \
    stress = {-0.10000 -0.10000 -0.10000 0.00000 0.00000 0.00000 } \
    deviation = 5000.00 \
execute frequency = 50.0 last_step = 0 \
     command = {print table \
     filename = density \
     +average \
     +batch_average \
     batch_size = 50 \
     +density} \
    execute frequency = 500.00 \
      command = {print history}
```

(D) Typical input file for NVT production run

```
BIOSYM btcl 3
#
#  Input File For Discover Generated By Materials Studio
#  Input Client Model Document: C:\Documents and Settings\coughld.bak\My
Documents\Materials Studio Projects\Thermoresponsive Files\Documents\C\Frame 2
330\330\1\320\1\310\1\300\1\B1.xtd
#  Job: [saved] - B Disco Dynamics
#
  autoEcho off
#
# Begin Forcefield Section
  begin forcefield = compass
#
# Nonbond section:
  forcefield nonbond \
      -separate_coulomb \
    vdw \
    summation_method = group_based \
      cutoff = 9.50 \
      spline_width = 1.00 \
      buffer_width = 0.50 \
    coulomb \
    dielectric_value = 1.0000
#
# vdw long range energy correction
  vdwTailCorrection 9.50
# End Forcefield Section
#
# Dynamics Section:
  dynamics \
    time = 50000.00 \
    timestep = 0.50 \
    initial_temperature = 300.00 \
    ensemble = NVT \
    temperature_control_method = nose \
    q_ratio = 1.00 \
    temperature = 300.00 \
    deviation = 5000.00 \
    execute frequency = 50.00 \
      command = {print history}
```

(E) Typical input file for calculation of mean square displacement

```
#BIOSYM btcl 3
#
#  Input File For Discover Generated By Materials Studio
#  Input Client Model Document: C:\Documents and Settings\coughld.bak\My
Documents\Materials Studio Projects\Thermoresponsive Files\Documents\A\A nvt\F1 nvt 300K\B
Disco Dynamics\B.his
#  Job: [MO16V] - B Disco  Mean squared displacement
#
  autoEcho off
#
# Begin Forcefield Section
  begin forcefield = compass
#
# Nonbond section:
  forcefield nonbond \
      -separate_coulomb \
    vdw \
    summation_method = group_based \
      cutoff = 9.50 \
      spline_width = 1.00 \
      buffer_width = 0.50 \
    coulomb \
    dielectric_value = 1.0000
```

```
#
# vdW long range energy correction
  vdWTailCorrection 9.50
# End Forcefield Section
#
analysis \
         method = Mean_Square_Displacement \
         subset = "wo"   \
         frame_definition = B.fdf \
         table = 1 \
         file = B.tbl
```

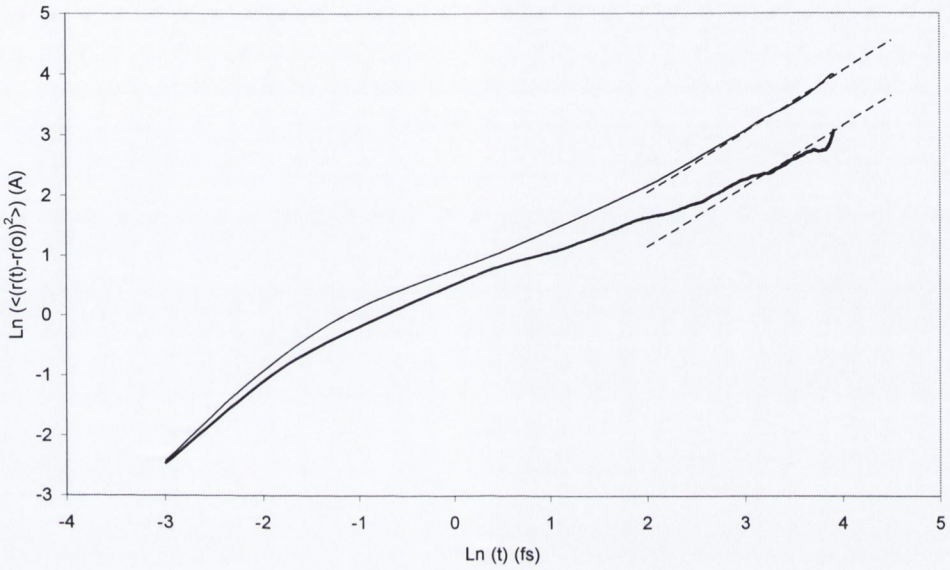

Fig. 1: Log-log plot of mean squared displacement vs. time for PNIPA ring oxygen (bold line) and water oxygen (solid line) in Simulation C at 300K. The dotted lines have a slope of unity and their intercept corresponds to ln(6nD).

(F) Typical input file for calculation of pair correlation function

```
#BIOSYM btcl 3
#
#  Input File For Discover Generated By Materials Studio
#  Input Client Model Document: C:\Documents and Settings\coughld.bak\My
Documents\Materials Studio Projects\Thermoresponsive Files\Documents\A\A nvt\F1 nvt 300K\B
Disco Dynamics\B.his
#  Job: [582KH] - B Disco  Pair correlation function
#
  autoEcho off
#
# Begin Forcefield Section
  begin forcefield = compass
#
# Nonbond section:
  forcefield nonbond \
      -separate_coulomb \
    vdw \
    summation_method = group_based \
      cutoff = 9.50 \
      spline_width = 1.00 \
      buffer_width = 0.50 \
    coulomb \
    dielectric_value = 1.0000
#
# vdW long range energy correction
  vdWTailCorrection 9.50
# End Forcefield Section
#
analysis \
         method = Pair_Correlation_Function  \
         subset = "w"   \
         subset2 = "p"   \
         frame_definition = B.fdf \
         table = 1 \
         file = B.tbl
```

Appendix VI:

Binding Isotherm

(A) UV spectroscopic study on effect of benzoate binding to PNIPA-H1

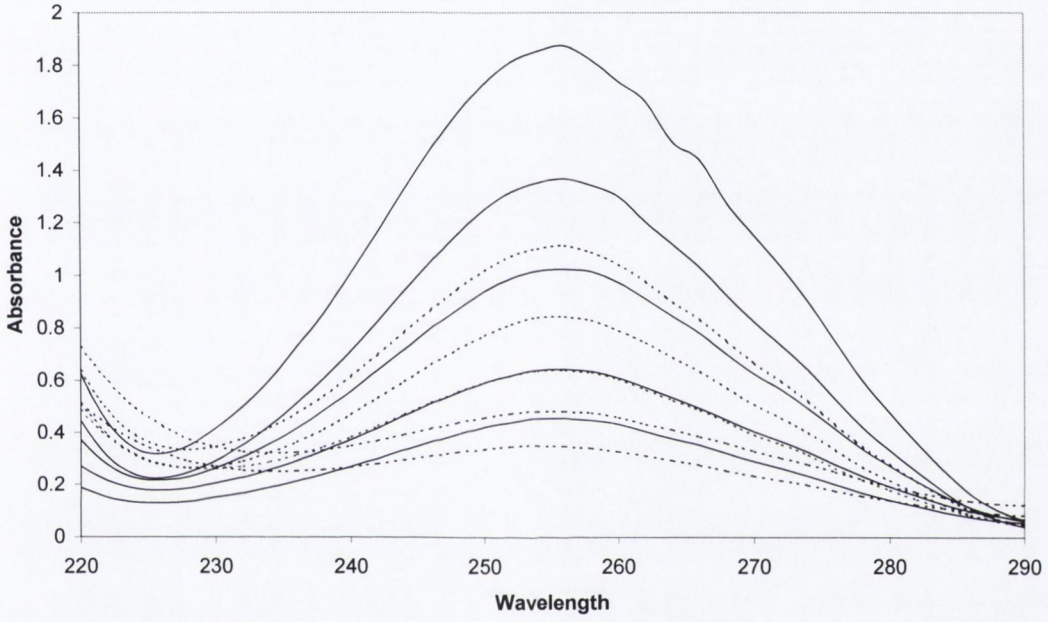

Fig.1: UV absorbance profile of various concentrations of MHB in 0.01M HCl (solid lines from top to bottom 0.02mg/ml, 0.014mg/ml, 0.010mg/ml, 0.006mg/ml, 0.004mg/ml). Dashed lines are profiles of same solutions in same order in the presence of 25mg/ml PNIPA-H1 (dried) at 37°C.

(B) Binding Isotherm Statistics

Table 1: Binding constants (k_b) calculated at 37°C (Equation 6.2) (n = 3)

	Binding constant (k_b) at 37°C M^{-1} (X 10^2)			
	PB pH 6.8		**0.01M HCl**	
	Ave	s.d.	Ave	s.d.
BA	ND	--	0.54	0.41
MHB	3.53	1.88	2.63	1.44
PHB	9.20	2.96	33.89	16.88

Appendix VII:

Dissolution of Pure Drug Discs

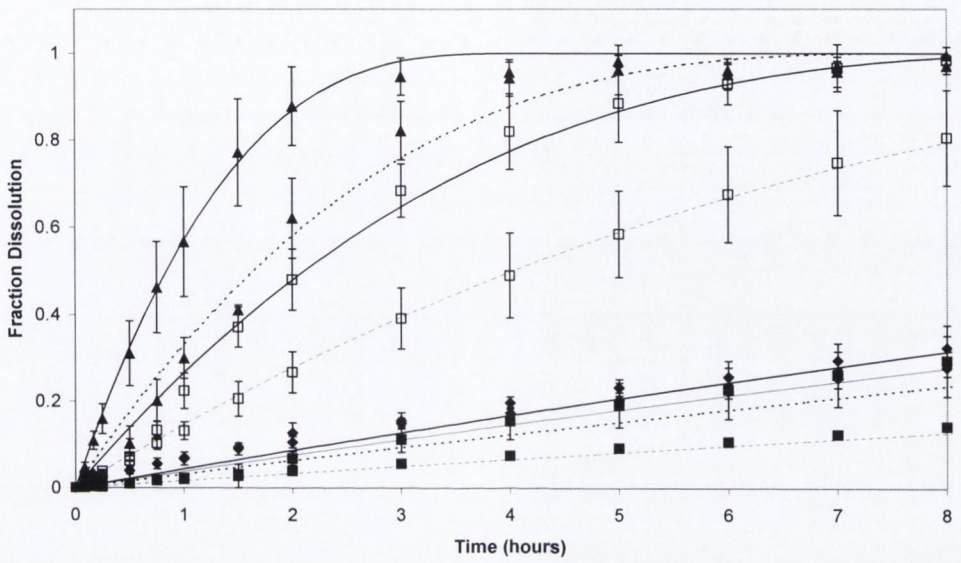

Fig. 1: Plot of dissolution of pure drug discs (100mg) over time in PB, fitted to the cube root law (Equation 2.4b) at 25°C (dashed lines) and at 37°C (solid lines) [BA(▲), MHB (□) , PHB (■), DB (♦)].

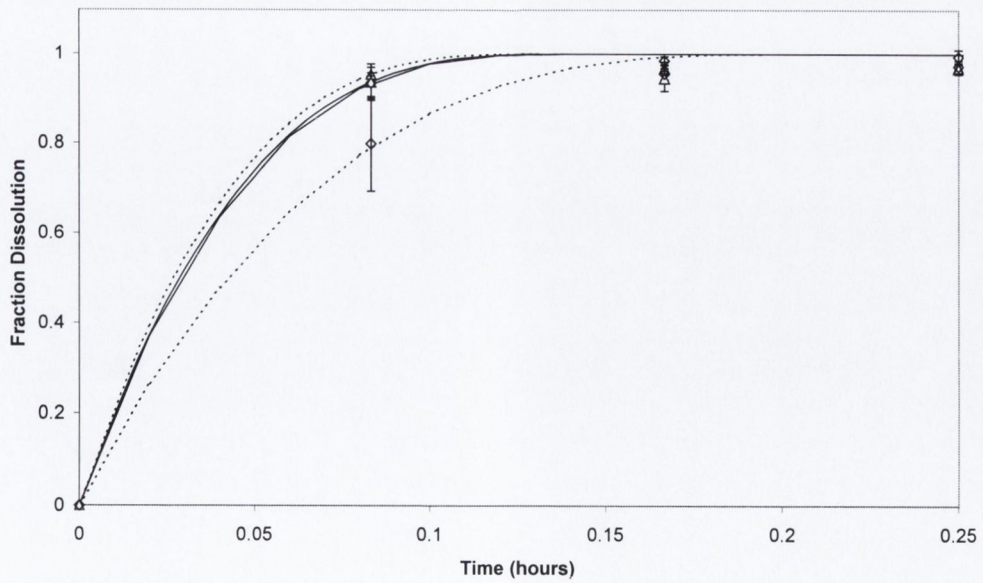

Fig. 2: Plot of dissolution of pure drug discs (100mg) in PB, fitted to the cube root law (Equation 2.4b) at 25°C (dashed lines) and at 37°C (solid lines) [NaB (Δ), DH (◊)].

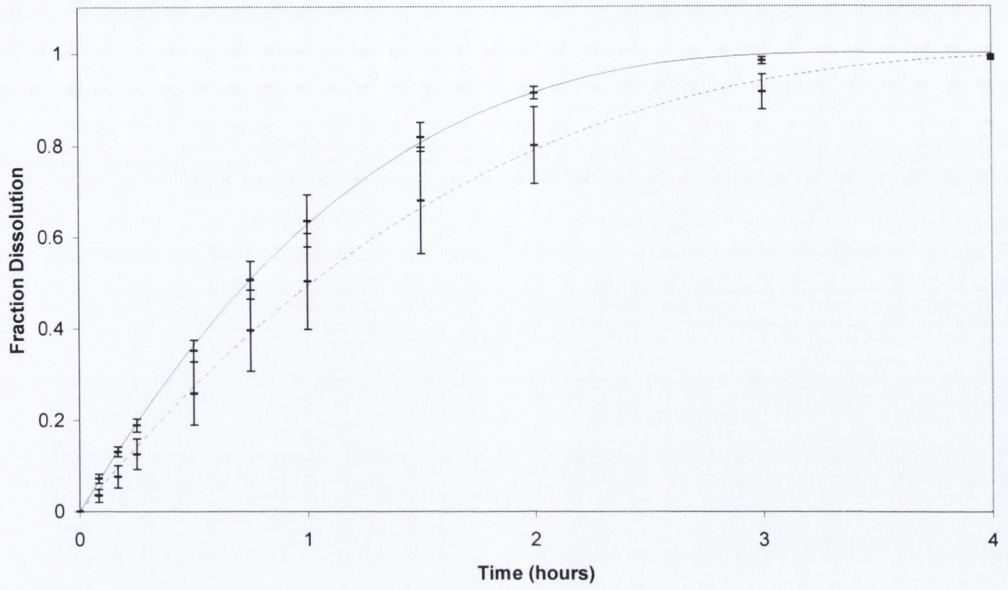

Fig. 3: Plot of dissolution of pure VB12 discs (100mg) in PB, fitted to the cube root law (Equation 2.4b) at 25°C (dashed line) and at 37°C (solid line)

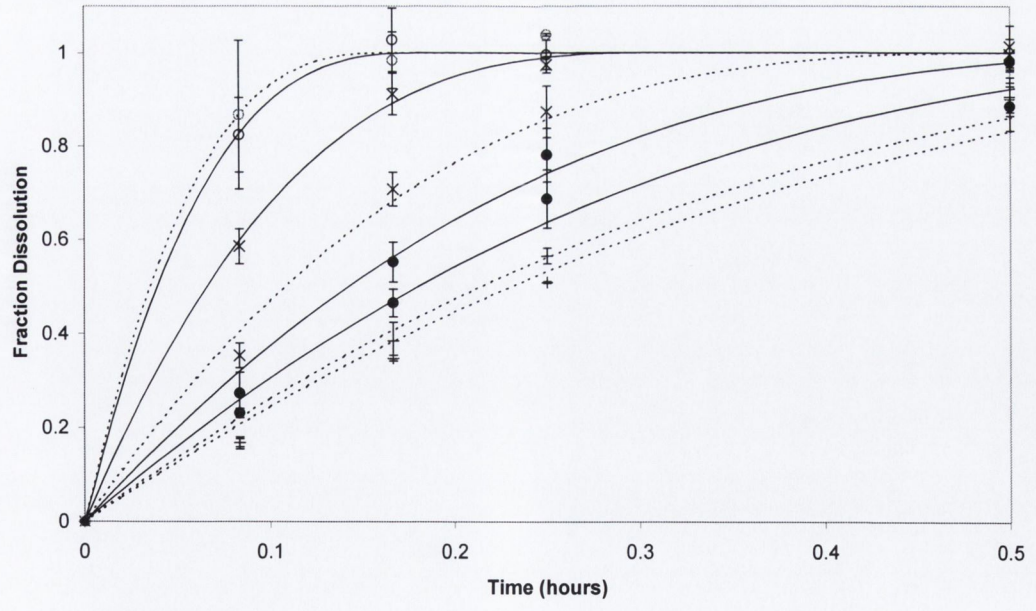

Fig. 4: Plot of dissolution of pure drug discs (100mg) in PB, fitted to the cube root law (Equation 2.4b) at 25°C (dashed lines) and at 37°C (solid lines) [D4 (○), D10 (x), D40 (●), D70 (+)].